

Gaspar Banfalvi *Editor*

Cellular Effects of Heavy Metals



 Springer

Cellular Effects of Heavy Metals

Gáspár Bánfalvi
Editor

Cellular Effects of Heavy Metals

 Springer

Editor

Dr. Gáspár Bánfalvi
Institute of Biology and Ecology
University of Debrecen
Egyetem Square 1,
4010 Debrecen
Hungary
bgaspar@delfin.klte.hu

ISBN 978-94-007-0427-5 e-ISBN 978-94-007-0428-2

DOI 10.1007/978-94-007-0428-2

Springer Dordrecht Heidelberg London New York

Library of Congress Control Number: 2011921316

© Springer Science+Business Media B.V. 2011

No part of this work may be reproduced, stored in a retrieval system, or transmitted in any form or by any means, electronic, mechanical, photocopying, microfilming, recording or otherwise, without written permission from the Publisher, with the exception of any material supplied specifically for the purpose of being entered and executed on a computer system, for exclusive use by the purchaser of the work.

Cover design: deblik, Berlin

Printed on acid-free paper

Springer is part of Springer Science+Business Media (www.springer.com)

Preface

Cellular lesions are related to macromolecular synthetic processes including the hierarchical flow of genetic information. Heavy metals generate oxidizing radicals through the Fenton and Haber-Weiss reactions leading to metal-induced carcinogenesis mediated primarily by the elevated levels of reactive oxygen species. Heavy metal-induced oxidative stress can lead to different types of cellular damages as a consequence of incomplete reduction of oxygen. Oxidative damage causes changes in DNA structure, the long term effects of which can lead to multiple mutations and malignant transformation. The detection of oxidative damages involves chromatographic, biochemical and immunochemical approaches. Early detection of cytotoxicity at structural and functional level of DNA combined with high sensitivity are the expected benefits of the approaches suggested in this book. The advantages of using cell cultures to measure the cellular toxicity of heavy metals are: controlled cell growth, known concentrations and time of exposure to metal ions.

The book summarizes the cellular effects of metals including in alphabetical order: Ag, As, Cd, Cr, Cu, Hg, Ni, Pb, Ta, U, W, Zn with respect to their impact on microbial, plant, yeast, insect and mammalian cells. Cellular effects of heavy metals involve: accumulation, mutagenesis, chromosomal changes, gene expression, activation of signal transduction pathways, apoptosis, transporters, protein binding, folding and degradation. These cellular changes affect not only the fate of cells but also our everyday life. The special website provides vivid performance of cellular movements of individual cells, cell division and how cellular etology is influenced by the presence of heavy metals.

Cells have evolved sophisticated defense mechanisms to protect themselves against heavy metal toxicity. At the genomic level many genes and regulatory pathways have been identified, but their implications on the higher order structure of the genetic material have not been investigated. To better define the impact of heavy metals on chromatin structure the effects of cadmium, nickel, chromium and silver in mammalian cells have been examined and compared with earlier studies on mercury and lead. Accumulating data suggest that the chemical properties of metal ions are the primary determinants in their biological effects. The three dimensional structures of heavy metal ions seem to influence their uptake by transporters into cells and their oxidation potential, mutagenicity and carcinogenicity. As these last two main

properties are different, the genotoxic effects of heavy metal ions are also variable and characteristic to individual metals. To distinguish among morphological changes, data of heavy metal treatments have been converted to graphical presentations allowing the detection of normal behavior, apoptotic or necrotic cell death.

The wealth of information provided in the book and the additional information in the website provide information for a wide spectrum of audience. Besides the experts, universities, schools and students, scientists involved in chemistry and biology, particularly in DNA research including cell biology, genetics, biochemistry, molecular biology will find new information in this book, which is expected to have an intellectually stimulating impact on their future research. The book does not go into details regarding the effect of heavy metals on organisms with the notable exceptions of blood lead levels and heavy metal-induced carcinogenicity caused by depleted uranium and heavy-metal tungsten alloy in human and animal populations. The long-term low-grade toxicity is in most of the cases more damaging on the long-term leading to chronic illness than a single acute heavy metal exposure which is rare. Due to the increasing concern of heavy metals pollutions world-wide, health service employees and non-professional readers will be equally attracted by the book.

Special Website

The reader will find a special Springer website; <http://extras.springer.com/> entitled: “Long-term scanning system to visualize the cellular toxicity of heavy metals” orchestrated by Gabor Nagy, Melinda Turani, Kinga Ujvarosi and Gáspár Bánfalvi. This site deals with cellular ethology, and follows the fate of individual cells upon heavy metal treatment. The heavy metal induced cellular changes have been compared with the cellular movement of normal healthy cells.

Acknowledgements

The contribution of authors representing different fields of heavy metal toxicology from several countries is gratefully acknowledged. The editor is especially indebted to members of the Cell Biology Group of the Department of Microbial Biotechnology and Cell Biology, University of Debrecen including PhDs, PhD students and student researchers.

In particular I wish to express my gratitude to the two reviewers, who focused on the chemical and biological aspects of the chapters, respectively:

Prof. Imre Sovago, Department of Inorganic and Analytical Chemistry, University of Debrecen,

Prof. Peter Nemeth, Institute of Immunology and Biotechnology, University of Pecs.

Contents

Part I Introduction	1
1 Heavy Metals, Trace Elements and Their Cellular Effects	3
Gáspár Bánfalvi	
Part II Heavy Metal Toxicity in Microbes	29
2 Toxic Metal/Metalloid Tolerance in Fungi—A Biotechnology-Oriented Approach	31
István Pócsi	
3 Interference of Chromium with Cellular Functions	59
Borut Poljsak, István Pócsi and Miklós Pesti	
4 <i>Saccharomyces cerevisiae</i> as a Model Organism for Elucidating Arsenic Tolerance Mechanisms	87
Robert Wysocki and Markus J. Tamás	
Part III Heavy Metal Induced Toxicity in Insect Cells	113
5 Heavy Metal Toxicity in an Insect Cell Line (Methyl-HgCl, HgCl₂, CdCl₂ and CuSO₄)	115
Bart P. Braeckman	
Part IV Genotoxic Effects of Heavy Metals	145
6 Cellular Changes in Mammalian Cells Induced by Cadmium	147
Gáspár Bánfalvi	
7 Chromatin Toxicity of Ni(II) Ions in K562 Erythroleukemia Cells	163
Gábor Nagy, Diána Laza, Kinga Ujvárosi and Gáspár Bánfalvi	

8 Genotoxic Chromatin Changes in <i>Schizosaccharomyces Pombe</i> Induced by Hexavalent chromium (CrVI) Ions	179
Gábor Papp, Gábor Nagy, István Pócsi, Miklós Pesti and Gáspár Bánfalvi	
9 Chromatin Changes upon Silver Nitrate Treatment in Human Keratinocyte HaCaT and K562 Erythroleukemia Cells	195
Gábor Nagy, Melinda Turáni, Katalin Éva Kovács and Gáspár Bánfalvi	
Part V Chemical Carcinogenesis Induced by Heavy Metals	219
10 Heavy Metal-Induced Carcinogenicity: Depleted Uranium and Heavy-Metal Tungsten Alloy	221
John F. Kalinich	
11 Role of Oxidative Damage in Metal-Induced Carcinogenesis	237
Kazimierz S. Kasprzak	
Part VI Cellular Responses to Heavy Metal Exposure	261
12 Non-native Proteins as Newly-Identified Targets of Heavy Metals and Metalloids	263
Sandeep K. Sharma, Pierre Goloubinoff and Philipp Christen	
13 Cellular Mechanisms to Respond to Cadmium Exposure: Ubiquitin Ligases	275
Karin Flick and Peter Kaiser	
14 Metals Induced Disruption of Ubiquitin Proteasome System, Activation of Stress Signaling and Apoptosis	291
Xiaozhong Yu, Rafael A. Ponce and Elaine M. Faustman	
Part VII Biomarkers	313
15 Blood Lead Level (BLL, B-Pb) in Human and Animal Populations: B-Pb as a Biological Marker to Environmental Lead Exposure	315
Nelly Mañay, Adriana Cousillas and Teresa Heller	
Part VIII Removal of Heavy Metals	331
16 Removal of Heavy Metal Sulfides and Toxic Contaminants from Water	333
Gábor Szalóki, Ildikó Czégény, Gábor Nagy and Gáspár Bánfalvi	
Index	347

Contributors

Gáspár Bánfalvi Department of Microbial Biotechnology and Cell Biology, University of Debrecen, 1 Egyetem Square, 4010 Debrecen, Hungary
Tel.: +36-52-512-900, Fax: +36-52-512-925
e-mail: bgaspar@delfin.klte.hu

Bart P. Braeckman Department of Biology, Ghent University, K.L. Ledeganckstraat 35, 9000 Gent, Belgium Tel.: +32-09-264-8744,
Fax: +32-9-264-5334
e-mail: bart.braeckman@ugent.be

Philipp Christen Department of Biochemistry, University of Zurich, Winterthurerstrasse 190, 8057 Zürich, Switzerland, Fax: +41-44-635-6805
e-mail: christen@bioc.uzh.ch

Adriana Cousillas Toxicology and Environmental Hygiene, Faculty of Chemistry, University of the Republic of Uruguay, Gral. Flores 2124, 11800 Montevideo, Uruguay

Idikó Czégény Hajdu-Bihar Municipality Waterworks Co., 4034 Debrecen, Hungary

Elaine M. Faustman Department of Environmental Health, University of Washington, 4225 Roosevelt Way NE, Suite 100, Seattle, WA 98105, USA
Fax: +1-206-685-4696
e-mail: faustman@uw.edu
Institute for Risk Analysis and Risk Communication, University of Washington, Seattle, WA 98105, USA
Center for Ecogenetics and Environmental Health and Institute for Risk Analysis and Risk, Seattle, WA 98105, USA

Karin Flick Department of Biological Chemistry, School of Medicine, University of California Irvine, 240D Med Sci I, Irvine, CA 92697-1700, USA

Pierre Goloubinoff Institute of Biochemistry, University of Zurich, Winterthurerstrasse 190, 8057 Zürich, Switzerland

Teresa Heller Toxicology and Environmental Hygiene, Faculty of Chemistry, University of the Republic of Uruguay, Gral. Flores 2124, 11800 Montevideo, Uruguay

Peter Kaiser Department of Biological Chemistry, School of Medicine, University of California Irvine, 240D Med Sci I, Irvine, CA 92697-1700, USA
Tel.: +1-949-824-9442, Fax: +1-949-824-2688
e-mail: pkaiser@uci.edu

John F. Kalinich Armed Forces Radiobiology Research Institute, 8901 Wisconsin Avenue, Bethesda, MD 20889-5603, USA
Tel.: +1-301-295-9242, Fax: +1-301-295-1731
e-mail: kalinich@afri.usuhs.mil

Kazimierz S. Kasprzak Laboratory of Comparative Carcinogenesis, National Cancer Institute at Frederick, Bldg. 538, Room 205E, Frederick, MD 21702-1201, USA, Tel.: +1-301-846-5738, Fax: +1-301-846-5946
e-mail: kasprzak@mail.nih.gov

Katalin Éva Kovács Department of Microbial Biotechnology and Cell Biology, University of Debrecen, 1 Egyetem Square, 4010 Debrecen, Hungary

Diána Laza Department of Microbial Biotechnology and Cell Biology, University of Debrecen, 1 Egyetem Square, 4010 Debrecen, Hungary

Nelly Mañay Toxicology and Environmental Hygiene, Faculty of Chemistry, University of the Republic of Uruguay, Gral. Flores 2124, 11800 Montevideo, Uruguay, Tel.: +598-2-9241-809, Fax: +598-2-9241-906
e-mail: nmanay@fq.edu.uy

Gábor Nagy Department of Microbial Biotechnology and Cell Biology, University of Debrecen, 1 Egyetem Square, 4010 Debrecen, Hungary

Gábor Papp Department of General and Environmental Microbiology, University of Pécs, 6 Ifjúság Street, 7624 Pécs, Hungary

Miklós Pesti Department of General and Environmental Microbiology, University of Pécs, 6 Ifjúság Street, 7624 Pécs, Hungary,
Tel.: +36-72-501-573, Fax: +36-72-501-573
e-mail: pmp@gamma.ttk.pte.hu

István Pócsi Department of Microbial Biotechnology and Cell Biology, University of Debrecen, 1 Egyetem Square, 4010 Debrecen, Hungary,
Tel.: +36-52-512-900, Fax: +36-52-512-925
e-mail: ipocsi@gmail.com

Borut Poljsak Environmental Health, Faculty of Health Studies, University of Ljubljana, Slovenia

Rafael A. Ponce Department of Environmental and Occupational Health Sciences, University of Washington, Seattle, WA 98195, USA
Amgen, Inc., Seattle, WA 98021, USA

Sandeep K. Sharma Department of Biochemistry, University of Zurich,
Winterthurerstrasse 190, 8057 Zürich, Switzerland

Gábor Szalóki Department of Microbial Biotechnology and Cell Biology,
University of Debrecen, 1 Egyetem Square, 4010 Debrecen, Hungary

Markus J. Tamás Department of Cell and Molecular Biology/Microbiology,
University of Gothenburg, 405 30 Gothenburg, Sweden,
Tel.: +46-31-786-2548, Fax: +46-31-786-2599
e-mail: markus.tamas@cmb.gu.se

Melinda Turáni Department of Microbial Biotechnology and Cell Biology,
University of Debrecen, 1 Egyetem Square, 4010 Debrecen, Hungary

Kinga Ujvárosi Department of Microbial Biotechnology and Cell Biology,
University of Debrecen, 1 Egyetem Square, 4010 Debrecen, Hungary

Robert Wysocki Department of Genetics and Cell Physiology,
University of Wrocław, 50-328 Wrocław, Poland

Xiaozhong Yu Department of Environmental and Occupational Health Sciences,
University of Washington, Seattle, WA 98195, USA
Fax: +1-206-685-4696
e-mail: yuxz@uw.edu
Institute for Risk Analysis and Risk Communication, University of Washington,
Seattle, WA 98105, USA

Abbreviations

<i>C. albicans</i>	<i>Candida albicans</i>
Cr	Chromium
Cr(VI)	Hexavalent chromium
Cr(III)	Trivalent chromium
EPR	Electron paramagnetic resonance
GSH	Glutathione
GSSG	Oxidized glutathione
GRd	Glutathione reductase
GPx	Glutathione peroxidase
ROS	Reactive oxygen species
<i>S. cerevisiae</i>	<i>Saccharomyces cerevisiae</i>
<i>S. pombe</i>	<i>Schizosaccharomyces pombe</i>
SOD	Superoxide dismutase
8-OHdG	8-oxo-7,8-dihydro-2'-deoxyguanosine
ATP	Adenosine-5'-triphosphate
BiP	Binding immunoglobulin protein
DIC	Differential interference contrast
EGTA	Ethylene glycol- <i>O,O'</i> -bis(2-aminoethyl)- <i>N,N,N',N'</i> -tetraacetic acid
FCS	Foetal calf serum
FITC	Fluorescein-5-isothiocyanate
Grp	Glucose-regulated protein
HSP	Heatshock protein
IC	Inhibitory concentration
LD	Lethal dose
MeHgCl	Methylmercuric chloride
MK	Modified Kitamura
NADH	Nicotinamide adenine dinucleotide (reduced)
PBS	Phosphate-buffered saline
RER	Rough endoplasmic reticulum
SDS-PAGE	Sodium dodecyl sulphate polyacrylamide gel electrophoresis
SER	Smooth endoplasmic reticulum
YE	Yeast extract

EDTA	Ethylenediaminetetraacetic acid
GSH	Glutathione, reduced form
HP2 ₁₋₁₅	RTHGQ-SHYRR-RHCSR-amide
NTA	Nitrilotriacetate

Part I
Introduction

Chapter 1

Heavy Metals, Trace Elements and Their Cellular Effects

Gáspár Bánfalvi

Abstract The book starts with the brief review of chapters. In this chapter heavy metals have been redefined as those trace elements that have $\geq 3 \text{ g/cm}^3$ densities and may cause harmful biological effects. The chapter arrived to this definition by clarifying first the light elements on the basis of their electronic configurations and compatibility with those of bioelements (CHNOPS group) in constructing biomolecules. As compatibility criteria the chemical bond formation between s - p electrons and p - p electrons were taken, allowing the tetrahedral three dimensional construction of biological compounds with four bonding partners. The compatibility range ended at $1s^2 2s^2 2p^6 3s^2 3p^6 4s^2$ electronic configuration corresponding to calcium, which is the 20th element in the periodic table. From element 21 (Sc) the wide range of redox behavior, high reactivity, rich coordination chemistry and complex formation of transition metals is due to the outer d and f electron subshells and explain their important catalytic role in enzyme reactions and toxicity at higher cellular concentrations. The chapter describes the most important cellular effects of heavy metals. The advantages of changing from *in vivo* to *in vitro* cellular systems have been pointed out. The methods for the detection and determination of heavy metals in cells are summarized.

Introduction

Why Another Book on Heavy Metals?

The short answer to this question is that cellular and subcellular functions of heavy metals have neither been described in any detail nor summarized in a book. To the contrary the effect of heavy metals on organs and organisms has been intensively

G. Bánfalvi (✉)

Department of Microbial Biotechnology and Cell Biology, University of Debrecen, 1 Egyetem Square, 4010 Debrecen, Hungary

Tel.: +36-52-512-900

Fax: +36-52-512-925

e-mail: bgaspar@delfin.klte.hu

studied. This is indicated by a fast search in PubMed by entering the words “heavy metals” and getting more than 338,000 publications (as of January 2011). After justifying the requirement of a book dealing with the cellular effects of heavy metals one can omit lengthy discussions of general toxic effects, comprehensive reviews of heavy metals dealing with the physiology, including nutrition, intestinal absorption, heavy metal poisoning, excretion, homeostasis and their role in the function of different organs (heart, muscle, liver, lung, brain, kidney etc.).

Brief Review of Chapters

Before going into the details of Chap. 1, a brief outline of Chaps. 2–16 is given.

Chapter 2. The aim of this chapter is the biotechnological evaluation of data accumulated in the last decade on the molecular background of the toxic metal/metalloid tolerance of fungi.

Chapter 3 describes that although, Cr(VI) reduction itself may proceed outside the cell, it is now generally accepted that Cr(VI)-induced DNA damage and genotoxicity takes place intracellularly. The extracellular reduction of Cr(VI) to Cr(III) is regarded as a detoxification process, as Cr(III) crosses the cell membrane at a much slower rate than Cr(VI). There are certain Cr(V) and Cr(III) complexes generated extracellularly that have high permeabilities and consequently may penetrate into the cell and cause intracellular damage. The reduction of Cr(VI) to Cr(III) with different antioxidants is not only a detoxification reaction, but also increases the viability of the budding yeast *Saccharomyces cerevisiae*.

Chapter 4. The arsenic tolerance mechanism of yeast cells is elucidated by reviewing the molecular biology of arsenic tolerance in budding yeast, focusing on arsenic sensing, signalling and detoxification mechanisms and how these pathways are regulated.

Chapter 5. Heavy metal toxicity of methyl-HgCl, HgCl₂ and CdCl₂ in the *Aedes albopictus* insect cell line is discussed. Short treatment of *Aedes albopictus* cells with sublethal doses of CdCl₂ and HgCl₂ induced abnormal microtubular polymerization giving the cells a neuron-like appearance, while MeHgCl was not able to induce such neurite-like processes. Viability and proliferation assays showed clear distinction among the toxicities of Cd, Hg and MeHg reflecting differences of their mechanisms of action.

Chapters 6–9. The effect of heavy metal ions (Cd²⁺, Ni²⁺, Cr⁶⁺, Ag⁺) on chromatin structure was a neglected field so far. Chromatin distortions are visualized in these chapters. These chapters confirm the notion that cells similarly to organisms die in many ways and the genotoxic cell death is dependent on the heavy metal or other toxic agent.

Chapter 6. Oxidative DNA damages of Cd have apoptotic biochemical and morphological consequences. Low concentrations of CdCl₂ (0.5–5 μM) cause biochemical (strand breaks, carcinogenic indicator, DNA replication, DNA repair) and morphological (chromatin) changes in CHO and murine preB cells.

In Chap. 7 chromatotoxicity was visualized by time-lapse video microscopy designed to follow the motility of single cells under physiological and genotoxic conditions. Ni-treated cells moved faster than control cells, but this motion was less intense than the so called “apoptotic dance” preceding cell death observed recently after Pb-treatment of HaCaT cells.

Chapter 8. With regard to carcinogenicity two heavy metals, chromium(VI) and arsenic(III) are considered human carcinogens sharing common properties. That chromium ions, especially Cr(VI) interfere with the chromatin structure and cellular functions of *Schistosaccharomyces pombe* are discussed in Chap. 8. Results show that subtoxic levels of Cr(VI) ($<1 \mu\text{M}$) did not cause significant chromatin changes in *S. pombe* cells. Early signs of apoptotic cytotoxicity were observed at $10 \mu\text{M}$ Cr(VI) concentration. Nuclear changes caused by 10 and $50 \mu\text{M}$ Cr(VI) were characterized by apoptosis seen as broken nuclei and apoptotic bodies. High concentration of Cr(VI) ions ($75\text{--}200 \mu\text{M}$) initiated necrotic nuclear changes. MIC_{50} values of Cr(VI) and Cr(III) show that Cr(VI) is ~ 15 -times more toxic than Cr(III).

Chapter 9. The most typical chromatin change upon AgNO_3 treatment of HaCaT and K562 cells was chromatin tail formation that could be accounted for by a decrease in chromatin supercoiling related to a dose dependent reduction of ATP content.

Chapter 10. In this chapter, two of the more recent additions to the weapons arena, depleted uranium and heavy metal tungsten-induced genotoxic and carcinogenic properties are detailed. The toxicological and genotoxic properties derived from *in vitro* and *in vivo* studies and the health effects of known human exposures are discussed.

Chapter 11. The possible role of oxidative damage in metal-induced carcinogenesis is reviewed in this chapter presenting evidence of the possible mechanistic involvement of oxidative DNA and protein damage in metal-induced carcinogenesis. The strongest association of oxidative damage with carcinogenesis comes from the mutagenicity of DNA. Oxidative damage to nuclear proteins affects chromatin structure, gene expression, whereas damage to regulatory proteins disturbs cell cycle and induces apoptosis.

Chapter 12. Proteins as targets of heavy metals and metalloids are discussed in this chapter. The interference of heavy metal ions (Cd^{2+} , Hg^{2+} and Pb^{2+}), metalloid arsenic(III) species inhibit the refolding of denatured proteins and may lead to the formation of proteotoxic aggregates of misfolded proteins.

Chapter 13 describes that ubiquitin ligases play a key role in the cadmium induced stress response. Murine embryonic fibroblast cells exposed to cadmium, methylmercury and arsenic induce oxidative stress, disrupt the ubiquitin proteasomal system, cell cycle regulation and may affect key cell stress pathways.

Chapter 14. The heavy metal-induced disruption of ubiquitin proteasomal system plays a critical role in cellular mechanisms such as cell cycle regulation and apoptosis.

Chapter 15: As far as the cellular effect of heavy metals is concerned lead poisoning is known to cause the formation of small red blood cells. As a consequence

of lead poisoning megaloblastic anemia/pernicious anemia may occur inducing elevated serum iron level. Blood level-Pb is regarded as a biological marker to environmental lead exposure.

Chapter 16: The best known way to inactivate heavy metals is by chelation, without removing them from the environment. The last chapter of the book provides a solution for the removal of heavy metals as their highly insoluble sulfides and the oxidation of toxic contaminants.

Definition of Heavy Metals

The term heavy metals has been generally used by referring to a group of metals and metalloids (semimetals), and to their contamination that is often causing toxicity and ecological problems. The available lists of heavy metals significantly differ from one another raising the question how heavy metals could be more precisely defined. Since there is no such clear definition, let us define first the light metals. Looking at the periodic table we see a gradual increase in the atomic number of elements starting from hydrogen. But which element should be the upper limit of the light elements. The electronic configurations is a reasonable orientation point. The basic principle is to go as far in the electronic configuration of elements as possible without disturbing the compatibility of the bioelements known as the CHNOPS group. In the mnemonic CHNOPS the letters stand for the symbols of carbon, hydrogen, nitrogen, oxygen, phosphorus and sulfur. Worthwhile to notice that the elements of the CHNOPS group belong to the first three periods and these elements contain exclusively *s* and *p* electrons, but no *d* or *f* electrons (Table 1.1). The *s* sublevel can hold two electrons, so *1s* in the first period is filled at helium ($1s^2$). The *p* sublevel in the second and third periods can hold six electrons, in the *d*-block the atoms of the elements have between 1 and 10 *d* electrons and the *f* sublevel 14 electrons. Periods four and five can hold 18, period six can hold 32 and period seven 16 elements.

Although, there are more than 30 elements that can be found in cells, the elements of the CHNOPS group are the most abundant. These six bioelements make up nearly 98% of humans. Although, calcium is not among the bioelements, it contributes to 1.5% body weight at least in humans. Most of the calcium is present as bones where Ca is in homeostatic equilibrium with the calcium level of the blood. In Table 1.1 the first 20 elements are indeed light, as their density is less than 3 g/cm³. The 21st element in the periodic table is scandium (Sc) with a density of nearly 3 g/cm³ and an electron configuration of $1s^2 2s^2 2p^6 3s^2 3p^6 4s^2 3d^1$. Its properties are intermediate between those of Al and Y, which are other eka-boron elements (lying under boron in the periodic table), similarly to the properties of Ca which is intermediate between those of Mg and Sr. There is also a diagonal relationship between Mg and Sc, just as there is between Be and Al. Scandium is not only a transition element, but also a rare earth element. The atoms of transition metals have incomplete *d*-sub-shells or can give rise to cations with incomplete *d*-sub-shells. Groups 3 through 12 of the periodic table are called “transition metals” with valence elec-

Table. 1.1 Electronic configuration of the light elements of the periodic table

Atomic number	Element Symbol	Orbital diagram									Electronic configuration	
		1s	2s	2p			3s	3p				4s
				x	y	z		x	y	z		
1	H	↑										1s
2	He	↑↓										1s ²
3	Li	↑↓	↑									1s ² 2s ¹
4	Be	↑↓	↑↓									1s ² 2s ²
5	B	↑↓	↑↓	↑								1s ² 2s ² 2p ¹
6	C	↑↓	↑↓	↑	↑							1s ² 2s ² 2p ²
7	N	↑↓	↑↓	↑	↑	↑						1s ² 2s ² 2p ³
8	O	↑↓	↑↓	↑↓	↑	↑						1s ² 2s ² 2p ⁴
9	F	↑↓	↑↓	↑↓	↑↓	↑						1s ² 2s ² 2p ⁵
10	Ne	↑↓	↑↓	↑↓	↑↓	↑↓						1s ² 2s ² 2p ⁶
11	Na	↑↓	↑↓	↑↓	↑↓	↑↓	↑					1s ² 2s ² 2p ⁶ 3s ¹
12	Mg	↑↓	↑↓	↑↓	↑↓	↑↓	↑↓					1s ² 2s ² 2p ⁶ 3s ²
13	Al	↑↓	↑↓	↑↓	↑↓	↑↓	↑↓	↑				1s ² 2s ² 2p ⁶ 3s ² 3p ¹
14	Si	↑↓	↑↓	↑↓	↑↓	↑↓	↑↓	↑↓				1s ² 2s ² 2p ⁶ 3s ² 3p ²
15	P	↑↓	↑↓	↑↓	↑↓	↑↓	↑↓	↑↓	↑			1s ² 2s ² 2p ⁶ 3s ² 3p ³
16	S	↑↓	↑↓	↑↓	↑↓	↑↓	↑↓	↑↓	↑	↑		1s ² 2s ² 2p ⁶ 3s ² 3p ⁴
17	Cl	↑↓	↑↓	↑↓	↑↓	↑↓	↑↓	↑↓	↑↓	↑		1s ² 2s ² 2p ⁶ 3s ² 3p ⁵
18	Ar	↑↓	↑↓	↑↓	↑↓	↑↓	↑↓	↑↓	↑↓	↑↓		1s ² 2s ² 2p ⁶ 3s ² 3p ⁶
19	K	↑↓	↑↓	↑↓	↑↓	↑↓	↑↓	↑↓	↑↓	↑↓	↑	1s ² 2s ² 2p ⁶ 3s ² 3p ⁶ 4s ¹
20	Ca	↑↓	↑↓	↑↓	↑↓	↑↓	↑↓	↑↓	↑↓	↑↓	↑↓	1s ² 2s ² 2p ⁶ 3s ² 3p ⁶ 4s ²

Light elements include twenty elements with atomic number from 1 to 20. The orbital diagram shows that only s and p electrons are involved in the covalent bond formation.

trons, or the electrons they use to combine with other elements, present in more than one shell. The three noteworthy elements in the transition metals family are iron, cobalt, and nickel, which are able to produce a magnetic field. Of the 38 transition elements here only those are mentioned which also belong to the microelements i.e. they have been found in cells or are frequently mentioned among toxic agents: Sc, Ti, V, Cr, Mn, Fe, Co, Ni, Cu, Zn, Zr, Mo, Ag, Cd, Hg, B. Post-transition metals are: Zn, Cd, Hg and Uub of group 12. The 30 rare earth elements that are special transition metals at the bottom of the periodic table belong to the lanthanide and actinide series found in group 3 of the periodic table and in the 6th and 7th periods. Some of the trans-uranium elements have been synthesized by man. Sixteen of the rare earth elements are not as rare as their name would suggest. They are found in nature in much higher quantities than the precious metals gold or platinum with a yearly rare earth element production of nearly 150,000 t. Actinides are all radioactive including the best known and most dangerous actinides of uranium (U), thorium (Th), neptunium (Np) and the transuranium plutonium (Pu, artificial). Environmental radioactivity and pollution is not limited solely to actinides. There are non-actinides such as radium (Ra) and radon (Rn) which is the radioactive daughter from the decay of uranium or cobalt-60 (Co⁶⁰) and strontium-90 (Sr⁹⁰).

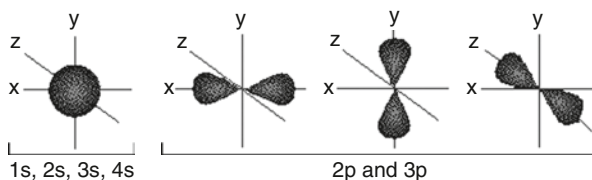
Due to the number of properties shared by the transition elements it is reasonable to classify them as heavy metals. But is it right to draw the dividing line between light and heavy metals at ~3 g/cm³? The term heavy metals was regarded as mean-

ingless as scientists were unable to come up with a consensus. Moreover, the term heavy metal has never been defined by IUPAC, thus it was suggested that any idea of defining heavy metals on the basis of density should be abandoned as it was yielding nothing but confusion (Duffus 2002). This conclusion came from definitions modified by various authors classifying heavy metals with different specific gravity values (Bjerrum 1936; Van Nostrand 1964; Grant and Grant 1987; Parker 1989; Lozet and Mathieu 1991; Morris 1992; Streit 1994; Thornton 1995; Falbe and Regitz 1996; Srivastava and Majumder 2008). The general tendency in these earlier definitions was that the elemental specific gravity values of heavy metals decreased from ≥ 7 to ≥ 3.5 g/cm³ between 1936 and 1996. Heavy metal is meaningless in the sense that metals are available to plant and animal cells in solution and once such a chemical compound is formed the density of the metal is of less importance (Appenroth 2010). The main reason why the name “heavy metal” cannot be abandoned is that the term is associated with elements that have harmful biological effects or are expected to be toxic. In plant science, the term heavy metal is so widely accepted that it would be difficult to eliminate it (Appenroth 2010). As a typical example the accumulation of heavy metals in plants is mentioned. There is a significant difference in heavy metal accumulation in plant roots versus shoots between accumulator and nonaccumulator plants indicating that metal accumulation and tolerance is a complex trait, requiring the coordinated expression of specific metal transport-related genes in different cell types (Klein et al. 2008). Specific metal tolerance found at cellular level in hyperaccumulating plants reflected specific adaptations to heavy metals (Ni, Zn, Cd) not only in the whole plant but also in cells (Marquès et al. 2004). The metal/metalloid tolerance in fungi is discussed in the next chapter.

As we can neither abandon the use of “heavy metals” nor wait till this term becomes obsolete, it is better to redefine it. It is suggested to set the boundary between light and heavy metals at the lowest specific gravity value (≥ 3 g/cm³). The most important heavy metals include (in alphabetic order): antimony (Sb, atomic number 51), arsenic (As, 33), barium (Ba, 56), bismuth (Bi, 83), cadmium (Cd, 48), cerium (Ce, 58), chromium (Cr, 24), cobalt (Co, 27), copper (Cu, 29), gallium (Ga, 31), germanium (Ge, 32), gold (Au, 79), iron (Fe, 26), lead (Pb, 82), manganese (Mn, 25), mercury (Hg, 80), nickel (Ni, 28), platinum (Pt, 78), rubidium (Rb, 37) silver (Ag, 47), strontium (Sr, 38), tellurium (Te, 52), thallium (Th, 81), tin (Sn, 50), titanium (Ti, 22), uranium (U, 92), vanadium (V, 23), zinc (Zn, 30), zirconium (Zr, 40).

At 3 g/cm³ and higher density values the chemical properties of transition or *d*-metals have several features in common: most transition metals have variable valences, with more than one possible oxidation- or valence-state causing significant incompatibility with bioelements. The covalent bonding of bioelements requires the consideration of valence shell atomic orbitals. For second period elements such as carbon, nitrogen and oxygen, these orbitals have been designated $2s$, $2p_x$, $2p_y$ and $2p_z$. The spatial distribution of electrons occupying each of these orbitals is shown in the diagram below reflecting the axial symmetry of single bond formation between electrons and the tetrahedral geometry of *s*-*p* and *p*-*p* bond formation with a tetrahedral bond angle of 109.5° with four bonding partners (Fig. 1.1), trigonal configuration (120°) with three and linear arrangement (180°) with two bonding

Fig. 1.1 Atomic orbitals for the s electrons of the 1–4 period elements and tetrahedral orientation of p electrons of the second and third period elements



partners. The bond angles of water (H_2O , 104.5°) and ammonia (NH_3 , 107.3°) are somewhat distorted relative to the tetrahedral bond angle and make these molecules polar.

Due to the presence of *d* electrons the atoms of transition metals can form nine sp^3d hybrid bond orbitals either as neutral atoms (Co, Rh, Ir) or after taking up an electron (Fe, Ru, Os). To demonstrate how much such structures differ from the tetrahedral building blocks of the CHNOPS group, the involvement of enneacovalence (formation of nine covalent bonds) is taken as an example. In enneacovalent structures with nine hydrogens, these atoms lie at the corners of a trigonal prism with three lateral caps (Abrahams et al. 1964). Enneacovalence of iron can be achieved by transferring an electron to the iron atom. Enneacovalent iron and cobalt structures are compatible with the electroneutrality principle of covalent bonds, but their molecular shape is quite different. The electroneutrality principle states that the resultant electric charge on each atom is close to zero (in the range of ± 1).

If we would not consider their biological impact and would take only the specific gravity to define heavy metals, then all metals above 3 g/cm^3 would belong to the heavy metals. To come closer to an acceptable definition we have to make a selection and specify that heavy metals have higher than 3 g/cm^3 densities, have biological effects at low concentrations and are toxic when present in cells at higher than the tolerable physiological level.

Trace Metal Elements

Here only the analytical and biochemical meaning of trace metal elements is dealt with, while the geochemical composition of trace metals is neglected. To denote the relative proportions, a trace metal element is present in a sample of less than 100 parts per million (ppm, 10^{-6}) i.e. less than $100 \mu\text{g/g}$. Such minute quantities of trace metals are needed for the proper growth, development, and physiology of the cell or organism (Bowen 1976). Trace metal elements in nutrition are also referred to as micronutrients. Major criteria for a micronutrient trace element are: (a) its presence in healthy tissues, (b) appearance in fetus and newborns, (c) homeostatic control of uptake in the blood, (d) control of excretion, (e) known biological function. The essential microelements that meet all these criteria include cobalt (Co, atomic number 27), copper (Cu, 29), chromium (Cr, 24), fluorine (F, 9), iron (Fe, 26), iodine (I, 53), manganese (Mn, 25), molybdenum (Mo, 42), selenium (Se, 34) and zinc (Zn, 30).

H																	He
Li*	Be											B*	C	N	O	F*	Ne
Na	Mg*											Al*	Si*	P	S	Cl	Ar
K	Ca	Sc	Ti*	V*	Cr*	Mn*	Fe*	Co*	Ni*	Cu*	Zn*	Ga	Ge	As*	Se*	Br*	Kr
Rb	Sr*	Y	Zr*	Nb*	Mo*	Tc	Ru	Rh	Pd	Ag*	Cd*	In	Sn*	Sb*	Te*	I*	Xe
Cs	Ba		Hf	Ta	W	Re	Os	Ir	Pt	Au*	Hg*	Tl	Pb	Bi*	Po	At	Rn
Fr	Ra		Rf	Db	Sg	Bh	Hs	Mt	Uun	Uuu	Uub						
			La	Ce	Pr	Nd	Pm	Sm	Eu	Gd	Tb	Dy	Ho	Er	Tm	Yb	Lu
			Ac	Th	Pa	U	Np	Pu	Am	Cm	Bk	Cf	Es	Fm	Md	No	Lr

Fig. 1.2 Trace elements of the periodic table. These include elements from the 2nd to the 6th periods: Li, B, F, Mg, Al, Si, Ti, V, Cr, Mn, Fe, Co, Ni, Cu, Zn, Ga, Ge, As, Se, Br, Rb, Sr, Zr, Mo, Ag, Cd, Sn, I, Ba, Au, Hg, Pb, Bi (boxed and indicated by asterisk in the periodic table). The staircase-shaped dividing line between metalloids from boron to astatine is indicated by the white dotted line. In periods 1–4 only the noble gases (He, Ne, Ar, Kr) and scandium (Sc) have no known biological function

Less stringent criteria would allow the additional incorporation of nickel (Ni, 28), tin (Sn, 50), vanadium (V, 23), silicon (Si, 14), boron (B, 5) as important micronutrients, whereas aluminum (Al, 13), arsenic (As, 33), barium (Ba, 56), bismuth (Bi, 83), bromine (Br, 35), cadmium (Cd, 48), germanium (Ge, 32), gold (Au, 79), lead (Pb, 82), lithium (Li, 3), magnesium (Mg, 12), mercury (Hg, 80), rubidium (Rb, 37), silver (Ag, 47), strontium (Sr, 38), titanium (Ti, 22) and zirconium (Zr, 40) have been found in plant and animal tissues (Fig. 1.2), but their biological importance is still to be clarified. The comparison of heavy metals with trace elements shows that most of the heavy metals are trace elements some of them with known, others with unknown biological function. Trace elements which are not heavy metals i.e. their density is less than 3 g/cm^3 are: Li, B, Mg, Al and Si. Trace amounts of lithium are present in the oceans and in some marine organisms, without apparent vital biological function. Lithium, despite of its simple structure, has numerous biological effects. It was reported to have a therapeutic effect in the prophylactic treatment of manic depression (Shastry 2005). Boron is a plant nutrient, its lack causes boron deficiency, whereas high soil boron concentration is toxic to plants. It is regarded as an ultratrace element at least for rats, without known biological function. Magnesium ions play an important role in the chemical reactions of biological phosphate compounds such as ATP, DNA, and RNA. Many enzymes require magnesium ions in order to function. Magnesium is the metallic ion at the center of chlorophyll. Aluminum has no known biological function, but may play a role in pathology. Silicon is ingested with tap water as silicic acid. Silicon present in the body as silicic acid may

have a role in protection against aluminium toxicity (Parry et al. 1998). Looking at the periodic table we can see that in periods 1–4 only the noble gases (He, Ne, Ar, Kr) and scandium (Sc) have no biological function. In the right side of periods 5 and 6 we find primarily heavy metals belonging to transition metals (Ag, Au), post-transition metals (Cd and Hg), metals belonging to main group elements (Rb, Sr, Ba, Sn, Pb, Bi) and the metalloids along the stair-step line that distinguishes metals from non-metals drawn from between boron and aluminum to the border between polonium and astatine (Sb, Te, Po).

After reviewing briefly the trace elements, one can define heavy metals as:

1. metals that have $\geq 3 \text{ g/cm}^3$ density,
2. those trace metal elements that are found in cells and are known as microelements: including elements from the 2nd to the 6th periods: Ti, V, Cr, Mn, Fe, Co, Ni, Cu, Zn, Ga, Ge, As, Se, Br, Rb, Sr, Zr, Mo, Sn, I, Ba, Pb, Bi, with the exception of those trace elements which are not heavy, i.e. their density is less than 3 g/cm^3 : Li, B, Mg, Al and Si,
3. trace elements that may form amphoteric oxides (Al, Ga, In, Tl, Sn, Pb, Sb, Po), include metalloids (Ge, As, Te), that are transition metals (Ag, Au), post-transition metals (Al, Ga, In, Sn, Th, Pb, Bi), rare earth element (Sc),
4. transition metals mentioned among the trace elements.

As a conclusion of the introduction heavy metals are defined as trace elements with $\geq 3 \text{ g/cm}^3$ densities, have some biological functions at low concentration and cause toxic effects at higher than physiological concentrations.

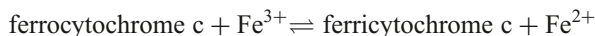
Cellular Effects of Heavy Metals

Biological toxicity may originate from inorganic (metals, metalloids, non-metal compounds) and organic (phosphorus, nitrogen, aldehyde containing) compounds, drugs, biological venoms, toxins, poisonous food, plant, fungi. Here only the cellular effects of inorganic compounds particularly those exerted by metals and metalloids will be dealt with. Minerals occurring in small quantities in cells are important for normal biological function. Minerals play a homeostatic role in organisms controlling nerve function, muscle contraction and metabolism, regulate electrolyte and hormone production. Among the heavy metals trace amounts of cobalt, copper, iron, manganese, molybdenum, vanadium, strontium, selenium and zinc are essential for cells.

Cobalt: The reactive C–Co bond of vitamin B12 (cyanocobalamin) participates in enzyme catalyzed reactions (Voet and Voet 1995).

Copper is found in the copper centers of cytochrome c oxidase, in the Cu–Zn containing enzyme superoxide dismutase and in the oxygen carrying pigment hemocyanin. More than a dozen enzymes have been found to contain copper.

Iron has two vital functions in the cells of all mammals: (1) hemoglobin is limited to oxygen transport in erythrocytes where it is in ferrous state (Fe^{2+}), and (2) the other cellular function of iron is mitochondrial oxidation where it is involved in iron-cytochrome-c reductase catalysing the chemical oxydoreduction of:



Cyanide is poisoning the cytochrome function, forming a stable complex with another cytochrome, namely the ferric form of cytochrome oxidase. This enzyme promotes the transfer of electrons in the mitochondria of cells during the synthesis of ATP. Without cytochrome oxidase function, cells cannot utilize the oxygen present in the blood, resulting in cytotoxic hypoxia or cellular asphyxiation, respiratory arrest and death.

Manganese is necessary for energy production, bone and blood formation, nerve function, protein, lipid, and glucose metabolism Mn is involved in the production of cholesterol in the metabolism of lipids and glucose.

Molybdenum as a trace element helps to regulate the iron stores and is involved in the carbohydrate, lipid and urine metabolism. Mo plays a crucial role in the catalytic activation of xanthine oxidase (uric acid synthesis) aldehyde and sulfite oxidation.

Vanadium seems to be essential to growth and is involved in lipid metabolism. Its deficiency may increase blood cholesterol and triglyceride levels.

Stroncium is promoting calcium uptake into bones at moderate supplementation, but contributes to rachitis at higher Sr levels (Nielsen 2004).

Selenium containing enzymes are involved in the hormonal effects of thyroid hormones (T_3 , T_4) and are efficient antioxidant peroxidases and in combination with antioxidant vitamins (vitamin C, E) help the production of antibodies, aid the function of pancreas and provide defence against oxidation. Over 70 metalloenzymes are known to require zinc for their functions. (<http://www.diagnose-me.com/cond/C15891.html#G368>).

Non-essential Harmful Heavy Metals

These metals include cadmium, antimony, chromium, mercury, lead, and arsenic, the last three of them being the most toxic. The toxicity of metals on multicellular organisms is not the subject of this book. Signs and symptoms of heavy metal poisoning are only mentioned but not discussed as they belong to the organismal level of toxicity. Heavy metals (Fe, Mn, Cd, Cu, Hg) originating from dental amalgams are suspicious of being implicated in the development of Parkinson's disease. Toxic exposure to heavy metals generating high blood and brain levels, is believed to play a role in the development of Alzheimer's disease. Heavy metals such as mercury, cadmium, lead and thallium poison the glucose metabolism resulting in hypoglycemia manifested as lack of concentration, hyperactivity, impulsive, unpredictable

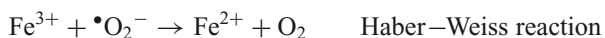
or depressive behavior. Arsenic and lead may cause neuritis accompanied by nerve pain (neuralgia).

Cellular Toxicity of Heavy Metals

As far as the cellular effects of heavy metals are concerned lead poisoning is known to cause the formation of small red blood cells. As a consequence of lead poisoning megaloblastic anemia/pernicious anemia may occur inducing elevated serum iron level. Blood level-Pb as a biological marker to environmental lead exposure will be detailed in Chap. 15.

At the cellular level the wide range of redox behavior, higher reactivity and complex formation of transition metals is based on the outer *d* electron subshell and explains their important catalytic role in enzyme reactions. It has been recently described that such pluridentate protein–metal complexes interfere severely with the formation of the native protein conformation (Sharma et al. 2008; Ramadan et al. 2009). That heavy metal ions (e.g. Cd^{2+} , Hg^{2+} and Pb^{2+}) and metalloid arsenic(III) species efficiently inhibit the refolding of chemically denatured proteins will be discussed in Chap. 12.

Cell injury is likely to be initiated by the formation of stable complex with a protein, receptor, cofactor, or via the formation of highly reactive species (Bridges et al. 2006). All ionic heavy metals significantly contribute to the production of free radicals. A free radical is an atom or a compound which has an odd number of electrons in its outer orbital, living this electron unpaired and reactive. Cells constantly encounter low levels of free radicals. These reactive species indiscriminately pick up electrons from other atoms in their neighborhood and convert those into secondary free radicals setting up a chain reaction causing random biological damage in the cell. This process is now considered a major cause of aging. One of the most reactive transition metal ions is iron, present at low levels in biological systems that catalyzes the Haber–Weiss reaction generating hydroxyl ($\bullet\text{OH}$) and superoxide ($\bullet\text{O}_2^-$) radicals. Iron catalyzed by hydrogen peroxide generates the production of hydroxy (OH^-) ions and hydroxyl radical ($\bullet\text{OH}$) known as the Fenton's reaction. The Haber–Weiss reaction and the following Fenton reaction have been widely postulated to account for the *in vivo* generation of hydroxyl radical, known as the most reactive oxygen species (Haber and Weiss 1932; Kehrer 2000; Koppenol 2001).



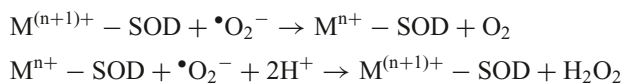
The reason why heavy metals entering cells multiply free radicals from thousand to million times is that when free radicals collide with toxic metals many new free radicals are generated initiating a chain-reaction. Environmental agents significant-

ly contribute to an increase of free radicals. Among them lead, cadmium, pesticides, ionizing radiation, alcohol and cigarette smoking initiate most frequently free radicals. Chapter 11 presents and discusses evidence of the involvement of oxidative DNA and protein damage in metal-induced carcinogenesis.

Detoxification of Heavy Metals

Known means in heavy metal detoxification include garlic and cilantro (coriander leaves), vegetables, fruits and their juices. Vegetable juice is an important source of raw food and has the advantage that it does not raise insulin levels like fruit juice. The loaded sugar content is a significant drawback to drinking soda and is even worse than fruit juicing resulting in weight gain. Antioxidants (e.g. vitamin C, vitamin E, beta carotene, coenzyme Q10) are able to prevent the formation of reactive oxygen species, but do not eliminate metals from cells. The best known way to remove toxic heavy metals is chelation using N-acetyl-cystein or EDTA. The removal of heavy metals from water as sulfides and toxic contaminants will be described in the last chapter of this book.

There are specific enzymes adapted to catalyze the detoxification of superoxide radicals to oxygen and peroxide. These superoxide dismutases provide an effective antioxidant defense mechanism in most of the cells exposed to molecular oxygen. The general chemical reactions catalyzed by dismutases:



where M is the metal (Cu, n=1; Mn, n=2; Fe, n=2; Ni, n=2), $\bullet\text{O}_2^-$ is the superoxide radical and SOD stands for superoxide dismutase.

Detection of Cellular Toxicity of Heavy Metals

Replacing In Vivo Animal Studies with In Vitro Systems

The classical approach to determine the toxicity of a compound aimed to predict whether a chemical could be harmful to man was done by using different animal species and increasing doses in short-term (acute) and long-term (chronic) toxicity tests. Long-term animal studies served as conclusive evidence for the carcinogenicity of a chemical. The lowest short-term toxic dose of a potential drug in the most sensitive animal was regarded as the highest applicable dose to be given to man. This approach has been abandoned as such a theoretical external dose could have significantly differed from the internal level measured in the blood or specific target organs due to adsorption, distribution, metabolization or elimination in the

organism. To bypass most of these possible influences it is advised to monitor toxic changes *in vitro* as in such contained systems it is easier to follow cellular and metabolic alterations. After this recognition many *in vitro* systems have been developed for testing purposes.

Bacterial, Fungal and Mammalian In Vitro Systems

The biological end points of *in vitro* systems for the assesment of the genotoxic potential of a compound include: induction of mutation, DNA damage, chromosomal and chromatin alterations. Mutations are detected mainly as phenotypic changes and structural alterations of DNA (deletion, insertion, substitution, frameshift, translocation). To measure such mutational changes bacteria and fungi turned out to be the most sensitive and easy to handle test organisms (Dunkel 2006). The best known and most widely accepted gene assay is the Ames test that uses *Salmonella typhimurium* to assess the mutagenic potential of a chemical (Ames 1971). As bacteria do not contain cytochromes, they are unable to metabolize and eventually convert procarcinogenic compounds to carcinogens, thus this test was complemented by the inclusion of an exogeneous mammalian metabolic activation system containing liver microsomal fraction (Ames et al. 1973). The microsomal fraction contains artifactual vesicles formed from the endoplasmic reticulum when cells are disrupted.

The problem with other less frequently used microbial systems utilizing *Escherichia coli*, *Bacillus subtilis*, *Saccharomyces cerevisiae* and *Neurospora crassa* is the impermeability of the cell wall preventing the entry of chemicals into these cells. Moreover, fungi require higher concentrations of mutagens than bacteria due to their more effective detoxification capability and repair systems (Dunkel 2006). The more effective detoxification and repair systems of mammalian cells is reflected by their mechanisms of recovery during early molecular changes before irreversible changes including cell death would occur (Bridges et al. 2006).

Mammalian Cell Cultures

When the toxic effects of heavy metals are studied in mammalian cells, cell cultures might be useful. In such cell culture systems cell viability and cellular growth data should be supported by additional metabolic parameters reflecting toxicity (De Ruiter et al. 1985). During the screening of toxic compounds including heavy metals in mammalian cell cultures, it turned out that most agents (~80%) had a similar toxicity *in vitro* and *in vivo*. This observation suggested an interference in man with basal functions common to all specialized human tissues as well as cultured cells. *In vitro* tests can be used: (a) to screen an unlimited number of chemicals and their extracts for potential basal cytotoxicity, (b) to supplement animal tests in acute toxicity examinations and (c) to study the mechanism of cytotoxicity of a wide variety

of chemicals (Ekwall 1983). However, this does not mean that the results of cytotoxicity tests are sufficient by themselves. They should be compared with toxicity data *in vivo* to evaluate the systemic cytotoxicity of chemicals (Ekwall 1980).

Permeability Changes Caused by Heavy Metals

Early observations of studies related to the cellular toxicity of heavy *metals* were reported back in 1936 and 1938. These experiments have shown that some heavy metals caused the loss of potassium from rabbit erythrocytes (Henriques and Orskov 1936; Davson and Danielli 1938). The slow exchange of K^+ between erythrocytes and the surrounding fluid was demonstrated with radioactive tracer experiments (Mullins et al. 1941). Heavy metals caused a net loss of K^+ from rabbit erythrocytes in the order of $Pb^{2+} > Au^+ > Hg^{2+}$ (Joyce et al. 1954). Passow and Rothstein found that Hg^{2+} treatment led to the complete loss of K^+ and that the mercury induced loss of K^+ from yeast cells was an all-or-none effect. Cu^{2+} caused loss of K^+ from baker's yeast, but similar concentration of Pb^{2+} or Zn^{2+} did not have any effect (Passow and Rothstein 1960). The comparison of heavy metal toxicity in an insect cell line (*Aedes albopictus*) made a further distinction among three metal species (organomercurial, mercury and cadmium chlorides) tested and decreased viability to different extents ($MeHgCl > HgCl_2 > CdCl_2$). Low concentrations of methylmercury chloride caused both cell death and inhibition of cell proliferation; $HgCl_2$ primarily disrupted the plasma membrane, whereas the primary effect of $CdCl_2$ was exerted on cell proliferation (Braeckman et al. 1997). Heavy metal toxicity of methyl-HgCl, $HgCl_2$ and $CdCl_2$ in the *Aedes albopictus* insect cell line will be the subject of Chap. 5.

In 1965 McBrien and Hassall studied the toxic effects of copper on respiration, photosynthesis and growth of the single-celled green alga, *Chlorella vulgaris* belonging to the *Chlorella* genus and the phylum Chlorophyta. They found that potassium normally low of permeability was released by the graded response of the barrier, due to increasing concentration of bound copper (McBrien and Hassall 1965). This increase of permeability of the cells was considered to be the primary toxic effect of copper. Potassium-depleted cells remained viable if subsequently transferred to a copper-free medium. This experiment can be regarded as one of the early attempts to reversibly permeabilize cells. With plant cells not only the loss of K^+ , but also the abolition of photosynthesis are among the known results of heavy metal poisoning (Overnell 1975). Reversible permeabilization is a technique for the introduction of nucleotides (Banfalvi et al. 1984) and oligonucleotides into cells (Lesh et al. 1995) or to induce nuclear reprogramming (Miyamoto et al. 2008).

In animal cells the rapid interaction of mercury or copper with the membrane could be followed by the penetration into the interior of the muscle cell (Demis and Rothstein 1955). A physiological function associated with the action of heavy metals on the membrane is the uptake of glucose (Passow and Rothstein 1960). Another function associated with the interior of the cell is respiration. It is likely that in different animal cells a similar sequence of events occurs. Some of the effects on mem-

brane function include: changes in the permeability to glycerol generated by copper (Jacobs 1950) and by mercury (Wilbrandt 1941); losses of K^+ from red blood cells produced by lead, mercury, gold, and silver (Joyce et al. 1954); inhibition of surface-bound invertase in the yeast cell by silver and mercury (Myrbäck 1957) and inhibitory effects on absorptive activities of kidney cells with organic mercurials. Effects of metals might include the inhibition of metabolic activities (respiration and glycolysis) and the block of cell division (Passow and Rothstein 1960). Mercury, cadmium, lead and thallium are known to poison glucose metabolism in cells.

Oxidative Damages Caused by Heavy Metals

Heavy metals generate oxidizing radicals through Fenton chemistry and by the Haber–Weiss reaction leading to the conclusion that metal carcinogenesis is mediated primarily by the elevated level of free radicals (Kasprzak 1995). When cells were exposed to mercury a sequence of interactions was observed starting at the cell membrane and proceeding inward. The first reaction was between the metal and the ligands of the cell membrane for which the metal possesses chemical affinity. In addition the metal passed through the membrane into the cytoplasm reacting with subcellular constituents the kinetics of which is governed by the rate of entry, mixing and chemical reactions (Passow and Rothstein 1960). The possible role of oxidative damage in metal-induced carcinogenesis will be reviewed in Chap. 11. That ubiquitin ligases play a key role in the cadmium induced stress response will be discussed in Chap. 13. The heavy metal-induced disruption of ubiquitin proteasomal system plays a critical role in cellular mechanisms such as cell cycle regulation and apoptosis (Chap. 14).

Lipid Peroxidation

Cell membranes made of unsaturated lipids are particularly susceptible to free radicals also referred to as reactive oxygen species (ROS) initiate uncontrolled chain reactions in cells. The oxidative damage by lipid peroxidation causes the hardening of lipids constituting the cell membrane. The damaged cell membrane changes the uptake of nutrients, the cell signaling system and many other cellular functions. Inside the cell informational macromolecules (DNA, RNA, proteins) are also susceptible to oxidative damage.

Oxidative DNA Damage

The most susceptible macromolecule in the eukaryotic cell is mitochondrial DNA. In mitochondria the citric acid cycle converts the energy of fuel carbon atoms of

acetate to CO_2 and reducing equivalents ($3 \text{ NADH} + \text{H}^+$ and 1 FADH_2) by hydrolytic oxidation using two molecules of water (Banfalvi 1991). In turn the increased reducing power represented by the reducing power is released in the mitochondrial respiratory chain producing water and ATP. As in the terminal oxidation of hydrogen to water in the presence of molecular oxygen (O_2) many steps are involved it is unavoidable to generate radicals. The other reason why most of the radicals affect mitochondrial DNA is that the mitochondrial DNA has no repair system. To the contrary cellular (nuclear) DNA damages are effectively removed. Oxidative DNA damages with apoptotic biochemical and morphological consequences induced by cadmium are dealt with in Chap. 6

Estimation of Toxic Effects of Heavy Metals

Tumorigenic Potential of Heavy Metals

With regard to carcinogenicity two heavy metals, chromium(VI) and arsenic(III) are considered human carcinogens sharing common properties. That chromium ions, especially Cr(VI) interfere with the cellular functions and chromatin structure of *Schisosaccharomyces pombe* are discussed in Chaps. 3 and 8. The arsenic tolerance mechanism of yeast cells will be elucidated in Chap. 4.

To estimate the tumorigenic potential of heavy metals, the ^{18}F FDG glucose analog uptake and the expression of facilitative glucose transporters have been suggested (Rastogi et al. 2007). Of the estimated twelve GLUT transporters the GLUT-1 and GLUT-3 take up more ^{18}F FDG than other GLUT transporters, suggesting that ^{18}F FDG uptake of cultured tumor cells is governed by GLUT expression, and is a distinct characteristic of the neoplastic process (Waki et al. 1998). Several lines of studies indicate that malignant cells with increased uptake of ^{18}F FDG have overexpressed GLUT-1 and/or GLUT-3 (Yamamoto et al. 1990; Nishioka et al. 1992; Brown and Wahl 1993; Waki et al. 1998; Rastogi et al. 2007). Increased expression of GLUT-1 and GLUT-3 has been reported in rat tumor cancers and is associated with poor survival (Trencsenyi et al. 2010). The heavy metal-induced toxicological changes depleted uranium and heavy metal tungsten-induced genotoxic and carcinogenic properties will be detailed in Chap. 10.

Metabolic Parameters

To support basal cytotoxicity data such as cell viability, growth and different staining methods have been developed. Biochemical changes in cells caused by the loss of total protein content can be measured by lactate dehydrogenase leakage, lowered lysosomal activity and succinate dehydrogenase activity. The production of nitric oxide (NO) plays multiple roles in defence reactions under abiotic stresses, including heavy metal load.

Beside the loss of ions and proteins heavy metal ions such as Cd^{2+} , Hg^{2+} and Pb^{2+} as well as metalloid arsenic(III) species inhibit efficiently the refolding of chemically denatured proteins. Proteins as targets of heavy metals and metalloids will be discussed in Chap. 12.

Cytoskeletal and Nucleoskeletal Changes

For the detection of the toxic effects of heavy metals on the cytoskeleton, fluorescein isothiocyanate (FITC)-labelled phalloidin is regularly used for staining F-actin, whereas conjugated monoclonal anti-tubulin antibody could be applied to stain tubulin.

Genotoxicity. There are two major cytogenetic endpoints applied for genotoxicity studies and biomonitoring purposes: chromosome aberrations and micronuclei (Mateuca et al. 2006). If the process of cell division is disturbed the distribution of the genetic material can be affected and DNA is not incorporated into a new nucleus but may form a small nucleus (“micronucleus”), visible under microscope. However, we have observed many times in different mammalian cells that during regular chromatin condensation the extruded chromatin turns around itself forming the head portion (micronucleus) seen during early S phase when chromatin structures are succeeded by linearly arranged, distinguishable chromosomes. Based on these observations the micronucleus is regarded as a regularly occurring element of chromatin condensation (Banfalvi, unpublished results).

Age related cytotoxicity of stannic chloride (SnCl_4) affected mitotic index, damaged cells, caused chromosome aberration, and micronuclei formation as endpoints (Ganguly 1993). Less attention has been paid to chromosomal changes taking place in the early stages of chromosome condensation in interphase nuclei of eukaryotic cells. Such chromatin changes will be visualized after Cd(II) , Ni(II) , Cr(VI) and Ag(I) treatment in Chaps. 6–9.

Chromosomal and Chromatin Changes Induced by Heavy Metals

Human lymphocytes treated for 3 h with lead, cadmium, and zinc acetate separately and in combinations of two or three metal salts between 10^{-3} and 10^{-8} M was followed by chromosome analysis and revealed higher incidences of chromatid-type aberrations and gaps only for cultures exclusively treated with cadmium (Gasiorek and Bauchinger 1981). The heavy metal load of small rodents increased the frequency of chromosomal aberrations and pathological changes in erythrocytes has shown that mercury is a strong damaging factor for chromosomes and red blood cell apparatus (Topashka-Ancheva et al. 2003).

Due to its diagnostic significance we have started to systematize the chromatin changes of toxic agents including heavy metals (Banfalvi 2009). The most characteristic changes caused by cadmium were large extensive disruptions and holes in the nuclear membrane, sticky and incompletely folded chromosomes

at the end of the S phase (Banfalvi et al. 2005, 2007). These alterations are in agreement with chromatid-type aberrations observed by others (Gasiorek and Bauchinger 1981).

Cellular changes of mercuric ions were characterized by their properties of causing reduced cellular motility (10–50 μM), and complete lack of cellular movement at higher concentrations (100–1,000 μM). In K562 erythroleukemia cells upon low concentration of mercuric acetate (≤ 1 μM): (a) chromatin changes were the earliest signs of cytotoxicity, (b) highly condensed supercoiled and decondensed veil-like chromatin appeared, (c) decondensed chromosomes were rejected as clustered puffs and (d) often the nuclear material was broken down to apoptotic bodies. In the concentration range between 10 and 50 μM of Hg(II) acetate chromatin changes were characterized by apoptosis seen as broken nuclei and apoptotic bodies. High concentration of Hg^{2+} ions (100 μM) initiated necrotic nuclear changes, with enlarged leaky or opened nuclei (Farkas et al. 2010).

Detection of Apoptotic and Necrogenic Chromatin Changes

Such changes can be detected by cytotoxic assays, staining methods, *in situ* end labeling, flow cytometry, light scattering flow cytometry, fluorescence activated cell sorting (FACS), TUNEL assay, comet assay, immunological detection of low molecular weight DNA, detection of mono- and oligonucleosomes, apoptotic proteins and enzymes (Banfalvi 2009).

Detection and Determination of Heavy Metals in Cells

Several instrumental methods have been used to determine heavy metals in aqueous samples, some of which needed preconcentration when the sensitivity of direct analysis was insufficient. For the selective solvent extraction of heavy metals (e.g. Ag, Cu, Hg) macrocyclic extractants have been applied. The separated heavy metals have been determined either by means of atomic absorption spectrometry, spectrometry, X-ray fluorescence analysis, thin layer chromatography in combination with visual or densitometric determination, protein based biosensors, isotope-labelled chelates, X-ray fluorescence, inductively coupled plasma atomic emission spectroscopy, indirect detection of heavy metals as unithiol complexes, disposable cuvette test.

Spectroscopy, Spectrometry

Atomic Absorption Spectrophotometry

The organic matter in samples can be digested by wet, dry or microwave digestion and the heavy metals (As, Cd, Pb, Hg) determined by using graphite furnace

atomic absorption spectrophotometer (GF-AAS) and flow injection analysis system-atomic absorption spectrophotometer (FIAS-AAS) (<http://www.aseansec.org/MRA-Cosmetic/Doc-3.pdf>).

Inductively Coupled Plasma Atomic Emission Spectroscopy (ICP-AES)

This turned out to be one of the most reliable analytical techniques for the determination of heavy metal (Cd, Co, Cr, Cu, Fe, Mn, Mo, Ni, Pb, and Zn) concentrations in plants after digestion in a closed microwave system using HNO₃, and ICP-AES was applicable to different environmental samples (Kos et al. 1996).

X-ray Fluorescence

Small amounts of heavy metals have been determined by the technique of X-ray fluorescence (XRF) in natural waters and pure salts (Eksperiandova et al. 1998).

Backscatter Electron (BSE) Imaging and Energy Dispersive Spectroscopy

Backscatter electron (BSE) imaging (20 kV) was used to discern metal particles within tissues. Energy dispersive spectroscopy (EDS) (15 kV) verified the specific elements present. This allowed for the spatial characterization of the nanoparticles within the tissues but quantification of the amount of metal was not possible (Ayers et al. 2007).

Amperometric Detection of Unithiol Complexes of Heavy Metals

Pb(II), Cd(II), Hg(II), Ni(II), Co(II), and Cu(II) were indirectly determined as their unithiol complexes by amperometric detection under static and HPLC conditions (Osipova et al. 2000).

Isotope Techniques

Isotope Dilution Mass Spectrometric Method (IDMS)

IDMS has been developed for the simultaneous determination of the complexes of heavy metals (Ag, Cd, Cu, Mo, Ni, Pb, Tl, U, W, Zn and Zr) by coupling high pressure liquid chromatography (HPLC) with inductively coupled plasma mass spectroscopy (ICP-MS) and applying the on-line isotope dilution technique (Vogl and Heumann 1997).

Tritium-Labelled Chelates

Such compounds have been used for the radiometric determination of Pb, Cd and Hg (Zolotov et al. 1987).

Whole-Cell-Sensing Systems

Protein Based Biosensors

These biosensors have been applied to detect femtomolar (10^{-15} M) levels of heavy metal ions. Heavy metal binding proteins were overexpressed in *Escherichia coli*, purified, and immobilized to a self-assembled thiol layer on a gold electrode placed as the working electrode in a potentiostatic arrangement in a flow analysis system (Bontidean et al. 1998).

Construction of Metal Detection Circuits in *E. coli*

Bacterial whole-cell biosensors are useful for toxicity measurements of various samples. Simple bacterial biosensors were constructed for the quantitative and rapid measurements of arsenite and arsenate in potable water. These biosensors are based on the natural resistance of *E. coli* against arsenite and arsenate, and on three reporter proteins: bacterial luciferase, beta-galactosidase and green fluorescent protein (GFP) (Stocker et al. 2003). The introduction of new reporter genes and refined detection equipment, could lead to the extensive use of stress-responsive biosensors for toxicity estimations (Sørensen et al. 2006).

Luminescence-Based Whole-Cell-Sensing Systems using Genetically Engineered Bacteria

Genetically engineered cells, tailored to respond by a dose-dependent signal to the presence of toxic chemicals, are useful tools for the environmental monitoring of toxic substances (Elad et al. 2008). Biosensing cells can be classified into two groups in terms of their biosensing mechanisms—constitutive expression and stress- or chemical-specific inducible expression (Gu et al. 2004). For the detection of heavy metals inducible gene promoters have been utilized. Systems responding to cadmium and lead ions have been designed and developed using genetically engineered bacteria. These systems take advantage of the ability of certain bacteria to survive in polluted environments. In *Escherichia coli* harboring two plasmids (pYSC1 and pYS2/pYSG1) the expression of the reporters beta-galactosidase and red-shifted green fluorescent protein (rs-GFP) was controlled by CadC, the regulatory protein of the cad operon. This heavy metal sensing bacterial systems responds

to cadmium, lead, and zinc ions, but has no significant response to nickel, copper, manganese, and cobalt (Shetty et al. 2003). A genetically engineered bacterial system was developed for the electrochemical sensing of antimonite and arsenite (Scott et al. 1997). Of the five cysteinyl residues of the cadCA operon in *Staphylococcus aureus* three (Cys-7, Cys-58, and Cys-60) are involved in sensing Pb(II), Cd(II), and Zn(II) by the plasmid pI258 CadC repressor and could be used for the detection of these soft metals (Sun et al. 2001).

Whole-Cell Heavy Metal Detecting Yeast System using Cadmium-Inducible Gene Promoter

The acquisition of metals (e.g. iron, copper, and zinc) by yeasts is tightly regulated. High affinity uptake systems are induced under metal-limiting conditions to maintain an adequate supply of these essential nutrients (Waters and Eide 2002). Metal-responsive transcription factors exist in yeast to modulate expression of genes that encode proteins involved in cellular uptake of iron, copper and zinc. These signal transduction pathways are involved in the homeostasis of the intracellular concentration of free metal ions. A second component of the equilibrium is the regulation of metal-ion binding through protein-mediated metallation (Winge et al. 1998). Fungi detect changes in metal ion levels using unique metallo-regulatory factors whose activity is responsive to the cellular metal ion status (Bird 2008). The genome-wide gene expression profiling of the methylotrophic yeast *Hansenula polymorpha* exposed to cadmium (Cd) allowed the identification of novel genes responsive to Cd treatment. The *HpSEO1* promoter of *H. polymorpha* as a bioelement in whole-cell biosensors is expected to monitor heavy metal contamination, particularly Cd (Park et al. 2007).

The detection of three heavy metals has been reported recently by the team KU_Seoul successfully applied metal detection circuits in *E. coli* and constructed a heavy metal detecting machine. Such machines are now commercially available. In the KU_Seoul instrument the integrated Zn detecting promoter used red fluorescence protein (RFP) as a reporter and worked at the range of 1~2 mM concentration. The arsenic detector applied green fluorescent protein (GFP) as a reporter and worked at the range of 0.15~1 mM concentration. Their cadmium detector utilized aryl acylamidase (AMD) as a reporter and worked in the range of 0.2~0.4 mM concentration (Ko et al. 2009).

Heavy Metal Toxicity Detected by Cardiac Cell-Based Biosensor

Among the many types of whole-cell bacterial biosensors that have been developed using recombinant DNA technology cardiac cell-based biosensors turned out to be of clinical importance (Yagi 2007). A novel biosensor for monitoring electrophysiological activity was developed by light-addressable potentiometric sensor (LAPS). After exposing cardiomyocytes to 10 μ M concentration of different heavy metal

ions (Hg, Pb, Cd, Fe, Cu, Zn) for 15 min the characteristic changes in beating frequency, amplitude and duration suggested that with physiological monitoring acute and chronic toxicities induced by heavy metals can be studied in a non-invasive way (Liu et al. 2007).

Antibody-Based Sensors for Heavy Metal Ions

Competitive immunoassays for Cd(II), Co(II), Pb(II) and U(VI) were developed using two different assay formats, a competitive microwell format and an immunosensor format (Blake et al. 2001).

Porphyrin Test

To measure mercury that was absorbed into the cells the Porphyrin Analysis test requires urine samples that are subjected to laboratory analysis. If Coproporphyrin III is high, this indicates that mercury is present. Altered porphyrin metabolism is a biomarker of mercury exposure and toxicity (Woods 1996).

Disposable Cuvette Test for the Enzymatic Determination of Heavy Metals

An optical cuvette test for the determination of total heavy metals was reported. The test is based on the inhibition of the enzyme urease by metals ions including silver(I), mercury(II), copper(II), nickel(II), cobalt(II), and cadmium(II) (Wolfbeis and Preininger 1995).

References

- Abrahams SC, Ginsberg P, Knox K (1964) Transition metal-hydrogen compounds. II. The crystal and molecular structure of potassium rhenium hydride, K_2ReH_9 . *Inorg Chem* 3:558–567
- Ames BN (1971) The detection of chemical mutagens with enteric bacteria. In: Hollaender A (ed) *Chemical mutagens, principles and methods for their detection*, vol 1. Plenum Press, New York, pp 267–282
- Ames BN, Durston WE, Yamasaki E, Lee FD (1973) Carcinogens are mutagens: a simple test system combining liver homogenates for activation and bacteria for detection. *Proc Natl Acad Sci U S A* 70:2281–2285
- Appenroth K-J (2010) Definition of “Heavy Metals” and their role in biological systems. In: Sherameti A, Verma A (eds) *Soil heavy metals*. Springer, Berlin, pp 19–29
- Ayers R, High W, Chandler J, Ranville J (2007) The detection and characterization of nanoparticulate heavy metals in epithelial tissues in patients with nephrogenic fibrosing dermopathy. MRS Fall Meeting. Symposium 00, 1063-0010-06. MRS Website: http://www.mrs.org/s_mrs/sec_subscribe.asp?CID=11306&DID=212403&action=detail
- Bánfalvi G (1991) Conversion of oxidation energy to reductive power in the citrate cycle. *Biochem Educ* 19:24–26
- Bánfalvi G (2009) Apoptotic chromatin changes. Springer, Holland, pp 269–293

- Banfalvi G, Sooki-Toth A, Sarkar N, Csuzi S, Antoni F (1984) Nascent DNA chains synthesized in reversibly permeable cells of mouse thymocytes. *Eur J Biochem* 139:553–559
- Banfalvi G, Gacsi M, Nagy G, Kiss ZB, Basnakian AG (2005) Cadmium induced apoptotic changes in chromatin structure and subphases of nuclear growth during the cell cycle in CHO cells. *Apoptosis* 10:631–642
- Banfalvi G, Ujvarosi K, Trencsenyi G, Somogyi C, Nagy G, Basnakian AG (2007) Cell culture density dependent toxicity and chromatin changes upon cadmium treatment in murine pre-B-cells. *Apoptosis* 12:1219–1228
- Bird AJ (2008) Metallosensors, the ups and downs of gene regulation. *Adv Microb Physiol* 53:231–267
- Bjerrum N (1936) Bjerrum's inorganic chemistry, 3rd Danish edn. Heinemann, London
- Blake DA, Jones RM, Blake RC II, Pavlov AR, Darwish IA, Yu H (2001) Antibody-based sensors for heavy metal ions. *Biosensors Bioelectronics* 16:799–809
- Bontidean I, Berggren C, Johansson G, Csöregi E, Mattiasson B, Lloyd JR, Jakeman KJ, Brown NL (1998) Detection of heavy metal ions at femtomolar levels using protein-based biosensors. *Anal Chem* 70:4162–4169
- Bowen HJM (1976) Trace elements in biochemistry, 2nd edn. Academic, London
- Braeckman B, Raes H, Van Hoye D (1997) Heavy-metal toxicity in an insect cell line. Effects of cadmium chloride, mercuric chloride and methylmercuric chloride on cell viability and proliferation in *Aedes albopictus* cells. *Cell Biol Toxicol* 13:389–397
- Bridges JW, Benford DJ, Hubbard SA (2006) Mechanism of toxic injury. *Ann N Y Acad Sci* 407:42–63
- Brown RS, Wahl RL (1993) Overexpression of GLUT-1 glucose transporter in human breast cancer. An immunohistochemical study. *Cancer* 72:2979–2985
- Davson H, Danielli JF (1938) Studies on the permeability of erythrocytes. Factors in cation permeability. *Biochem J* 32:991–1001
- De Ruiter N, Mailänder V, Kappus H (1985) Effect of heavy metals on cellular growth, metabolism and integrity of cultured Chinese hamster kidney cells. *Xenobiotica* 15:665–671
- Demis DJ, Rothstein A (1955) Relationship of the cell surface to metabolism. XII. Effect of mercury and copper on glucose uptake and respiration of rat diaphragm. *Am J Physiol* 180:566–574
- Duffus JH (2002) Heavy metals—a meaningless term? *Pure Appl Chem* 74:793–807
- Dunkel VC (2006) Biological significance of end points. *Ann N Y Acad Sci* 407:34–41
- Eksperiandova LP, Makarovska YN, Blank AB (1998) Determination of small quantities of heavy metals in water-soluble salts and natural water by X-ray fluorescence. *Anal Chim Acta* 371:1105–1108
- Ekwall B (1980) Screening of toxic compounds in tissue culture. *Toxicology* 17:127–142
- Ekwall B (1983) Screening of toxic compounds in mammalian cell cultures. *Ann N Y Acad Sci* 407:64–77
- Elad T, Benovich E, Magrisso S, Belkin S (2008) Toxicant identification by a luminescent bacterial bioreporter panel: application of pattern classification algorithms. *Environ Sci Technol* 42:8486–8491
- Falbe JM, Regitz M (eds) (1996) Roempp Chemie Lexikon, Georg Thieme, Weinheim
- Farkas E, Ujvarosi K, Nagy G, Posta J, Banfalvi G (2010) Apoptogenic and necrogenic effects of mercuric acetate on the chromatin structure of K562 human erythroleukemia cells. *Toxicol in vitro* 24:267–275
- Ganguly BB (1993) Cell division, chromosomal aberration, and micronuclei formation in human peripheral blood lymphocytes. *Biol Trace Elem Res* 38:55–62
- Gasiorek K, Bauchinger M (1981) Chromosome changes in human lymphocytes after separate and combined treatment with divalent salts of lead, cadmium, and zinc. *Environ Mutagen* 3:513–518
- Grant R, Grant C (eds) (1987) Grant and Hackh's chemical dictionary, 5th edn. McGraw-Hill, New York
- Gu MB, Mitchell RJ, Kim BC (2004) Whole-cell-based biosensors for environmental biomonitoring and application. *Adv Biochem Eng Biotechnol* 87:269–305
- Haber F, Weiss J (1932) On the catalysis of hydroperoxide. *Naturwissenschaften* 20:948–950

- Henriques V, Orskov SL (1936) Untersuchungen fiber die Schwankungen des Kationgehaltes der roten Blutkörperchen. *Skand Arch Physiol* 74:63–78
- Jacobs MH (1950) Surface properties of the erythrocyte. *Ann N Y Acad Sci* 50:824–834
- Joyce CRB, Moore H, Weatherall M (1954) The effects of lead, mercury, and gold on the potassium turnover of rabbit blood cells. *Br J Pharmacol Chemother* 9:463–470
- Kasprzak KS (1995) Possible role of oxidative damage in metal-induced carcinogenesis. *Cancer Invest* 13:411–430
- Kehrer JP (2000) The Haber–Weiss reaction and mechanisms of toxicity. *Toxicology* 149:43–50
- Klein MA, Sekimoto H, Milner MJ, Kochian LV (2008) Investigation of heavy metal hyperaccumulation at the cellular level: development and characterization of *Thlaspi caerulescens* suspension cell lines. *Plant Physiol* 147:2006–2016
- Ko H, Roh H, Kim S, Choi C, Jang J, Shin J, Byun YS, Choi I-G (2009) KU Seoul team: integrated heavy metal detection system. http://2009.igem.org/files/poster/KU_Seoul.pdf
- Koppenol WH (2001) The Haber–Weiss cycle—70 years later. *Redox Report* 6:229–234
- Kos V, Budie B, Hudnik V, Lobnik F, Zupan M (1996) Determination of heavy metal concentrations in plants exposed to different degrees of pollution using ICP-AES. *Fresenius J Anal Chem* 354:648–652
- Lesh RE, Somlyo AP, Owens GK, Somlyo AV (1995) Reversible permeabilization. A novel technique for the intracellular introduction of antisense oligodeoxynucleotides into intact smooth muscle. *Circ Res* 77:220–230
- Liu Q, Cai H, Xu Y, Xiao L, Yang M, Wang P (2007) Detection of heavy metal toxicity using cardiac cell-based biosensor. *Biosens Bioelectron* 22:3224–3229
- Lozet J, Mathieu C (1991) Dictionary of soil science, 2nd edn. Balkema, Rotterdam
- Marquès L, Cossegal M, Bodin S, Czernic P, Lebrun M (2004) Heavy metal specificity of cellular tolerance in two hyperaccumulating plants, *Arabidopsis halleri* and *Thlaspi caerulescens*. *New Phytologist* 164:289–295
- Mateuca R, Lombaert N, Aka PV, Decordier I, Kirsch-Volders M (2006) Chromosomal changes: induction, detection methods and applicability in human biomonitoring. *Biochimie* 88:1515–1531
- McBrien DCH, Hassal KA (1965) The effect of toxic doses of copper upon respiration, photosynthesis and growth of *Chlorella vulgaris*. *Physiol Plant* 20:113–117
- Miyamoto K, Yamashita T, Tsukiyama T, Kitamura N, Minami N, Yamada M, Imai H (2008) Reversible membrane permeabilization of mammalian cells treated with digitonin and its use for inducing nuclear reprogramming by *Xenopus* egg extracts. *Cloning Stem Cells* 10:535–542
- Morris C (ed) (1992) Academic press dictionary of science and technology. Academic Press, San Diego
- Mullins LJ, Fenn WO, Noonan TR, Haeghe L (1941) Permeability of erythrocytes to radioactive potassium. *Am J Physiol* 135:93–101
- Myrbäck K (1957) Inhibition of yeast invertase (saccharase) by metal ions. V. Inhibition by mercury compounds. *Ark Kemi* 11:471–479
- Nielsen SP (2004) The biological role of strontium. *Bone* 35:583–588
- Nishioka T, Oda Y, Seino Y, Yamamoto T, Inagaki N, Yano H, Imura H, Shigemoto R, Kikuchi H (1992). Distribution of the glucose transporters in human brain tumors. *Cancer Res* 52:3972–3979
- Osipova EA, Shapovalova EN, Ofitserova MN, Podlesnykh SV (2000) Amperometric detection of unithiol complexes of heavy metals in high-performance liquid chromatography. *J Anal Chem* 55:52–57
- Overnell J (1975) The effect of heavy metals on photosynthesis and loss of cell potassium in two species of marine algae, *Dunaliella tertiolecta* and *Phaeodactylum tricornutum*. *Mar Biol* 29:99–103
- Park JN, Sohn MJ, Oh DB, Kwon O, Rhee SK, Hur CG, Lee SY, Gellissen G, Kang HA (2007) Identification from transcriptome analysis and application to whole-cell heavy metal detection systems of the cadmium-inducible *Hansenula polymorpha* *SEO1* gene promoter. *Appl Environ Microbiol* 73:5990–6000

- Parker SP (ed) (1989) McGraw-Hill dictionary of scientific and technical terms, 4th edn. McGraw-Hill, New York
- Parry R, Plowman D, Delves HT, Roberts NB, Birchall JD, Bellia JP, Davenport A, Ahmad R, Fahal I, Altmann P (1998) Silicon and aluminium interactions in haemodialysis patients. *Nephrol Dial Transplant* 13:1759–1762
- Passow H, Rothstein A (1960) The binding of mercury by the yeast cell in relation to changes in permeability. *J Gen Physiol* 43:621–633
- Ramadan D, Rancy PC, Nagarkar RP, Schneider JP, Thorpe C (2009) Arsenic(III) species inhibit oxidative protein folding *in vitro*. *Biochemistry* 48:424–432
- Rastogi S, Banerjee S, Chellappan S, Simon GR (2007) GLUT-1 antibodies induce growth arrest and apoptosis in human cancer cell lines. *Cancer Lett* 257:244–251
- Scott DL, Ramanathan S, Shi W, Rosen BP, Daunert S (1997) Genetically engineered bacteria: electrochemical sensing systems for antimonite and arsenite. *Anal Chem* 69:16–20
- Sharma SK, Goloubinoff P, Christen P (2008) Heavy metal ions are potent inhibitors of protein folding. *Biochem Biophys Res Commun* 372:341–345
- Shastri BS (2005) On the functions of lithium: the mood stabilizer. *Bioessays* 19:199–200
- Shetty RS, Deo SK, Shah P, Sun Y, Rosen BP, Daunert S (2003) Luminescence-based whole-cell-sensing systems for cadmium and lead using genetically engineered bacteria. *Anal Bioanal Chem* 376:11–17
- Sørensen SJ, Burmølle M, Hansen LH (2006) Making bio-sense of toxicity: new developments in whole-cell biosensors. *Curr Opin Biotechnol* 17:11–16
- Srivastava NK, Majumder CB (2008) Novel biofiltration methods for the treatment of heavy metals from industrial wastewater. *J Hazard Mater* 151:1–8
- Stocker J, Balluch D, Gsell M, Harms H, Feliciano J, Daunert S, Malik KA, van der Meer JR (2003) Development of a set of simple bacterial biosensors for quantitative and rapid measurements of arsenite and arsenate in potable water. *Environ Sci Technol* 37:4743–4750
- Streit B (1994) *Lexikon der Okotoxikologie*. VCH, Weinheim
- Sun Y, Wong MD, Rosen BP (2001) Role of cysteinyl residues in sensing Pb(II), Cd(II), and Zn(II) by the plasmid pI258 CadC repressor. *J Biol Chem* 276:14955–14960
- Thornton I (1995) Metals in the global environment—facts and misconceptions. ICME, Ottawa
- Topashka-Ancheva M, Metcheva R, Teodorova S (2003) A comparative analysis of the heavy metal loading of small mammals in different regions of Bulgaria II: chromosomal aberrations and blood pathology. *Ecotoxicol Environ Saf* 54:188–193
- Trencsenyi G, Juhasz T, Bako F, Marian T, Pocsi I, Kertai P, Hunyadi J, Banfalvi G (2010) Comparison of the tumorigenic potential of liver and kidney tumors induced by N-nitrosodimethylamine. *Histol Histopathol* 25:309–320
- Van Nostrand's International Encyclopaedia of Chemical Science (1964) Van Nostrand, Princeton
- Voet JG, Voet D (1995) *Biochemistry*. Wiley, New York, p 675
- Vogl J, Heumann KG (1997) Determination of heavy metal complexes with humic substances by HPLC/ICP-MS coupling using on-line isotope dilution technique. *Fresenius J Anal Chem* 359:438–441
- Waki A, Kato H, Yano R, Sadato N, Yokoyama A, Ishii Y, Yonekura Y, Fujibayashi Y (1998). The importance of glucose transport activity as the rate-limiting step of 2-deoxyglucose uptake in tumor cells *in vitro*. *Nucl Med Biol* 25:593–597
- Waters BM, Eide DJ (2002) Combinatorial control of yeast FET4 gene expression by iron, zinc, and oxygen. *J Biol Chem* 277:33749–33757
- Wilbrandt W (1941) Die Wirkung von Schwermetallsalzen auf die Erythrocyten-permeabilität für Glycerin. *Arch Ges Physiol (Pflügers)*. 244:637–643
- Winge DR, Jensen LT, Srinivasan C (1998) Metal-ion regulation of gene expression in yeast. *Curr Opin Chem Biol* 2:216–221
- Wolfbeis OS, Preininger C (1995) Disposable cuvette test for enzymatic determination of heavy metals. In: Vo-Dinh T (ed) *Environmental monitoring and hazardous waste site remediation*, Proceedings SPIE, p 140

- Woods JS (1996) Altered porphyrin metabolism as a biomarker of mercury exposure and toxicity. *Can J Physiol Pharmacol* 74:210–215
- Yagi K (2007) Applications of whole-cell bacterial sensors in biotechnology and environmental science. *Appl Microbiol Biotechnol* 73:1251–1258
- Yamamoto T, Seino Y, Fukumoto H, Koh G, Yano H, Inagaki N, Yamada Y, Inoue K, Manabe T, Imura H (1990). Overexpression of facilitative glucose transporter genes in human cancer. *Biochem Biophys Res Commun* 170:223–230
- Zolotov YA, Malofeeva GI, Petrukhin OM, Timerbaev AR (1987) New methods for preconcentration and determination of heavy metals in natural water. *Pure Appl Chem* 59:497–504

Part II
Heavy Metal Toxicity in Microbes

Chapter 2

Toxic Metal/Metalloid Tolerance in Fungi—A Biotechnology-Oriented Approach

István Pócsi

Abstract This review aims at the biotechnological evaluation of the wealth of data accumulated in the last decade on the molecular background of the toxic metal/metalloid tolerance of fungi. Yeast-based models are highly applicable when metal/metalloid transport and compartmentalization processes are mapped in other fungal species or higher eukaryotes but this approach has limitations, which necessitates further fungal models evolutionarily closer to heavy metal exposed fungal taxons. In terms of biotechnology, the most promising targets in the genetic engineering of metal/metalloid tolerant fungi include (i) increased secretion of extracellular metal chelators, (ii) elimination of metal transporters facilitating the uptake of toxic metals/metalloids, (iii) overexpression of transporters pumping metals and/or their complexes out of the cells or into cellular organelles, (iv) overproduction of intracellular metal chelators, (v) overproduction of elements of the antioxidative defense system, (vi) genetic modification of the regulatory network of metal/metalloid stress defense, and (vii) interfering with the metal/metalloid-dependent initialization of apoptotic cell death. Owing to the wide-spread application of robust ‘-omics’ technologies, the biotechnologically exploitable data including potential future targets for genetic manipulation are accumulating fast. In contrast, today’s genetic modifications often result in unforeseeable or even paradox phenotypes in this field, which clearly indicates that a deeper understanding of the underlying molecular mechanisms of fungal toxic metal/metalloid tolerance is needed to improve the biotechnological performance of the genetically modified strains.

I. Pócsi (✉)

Department of Microbial Biotechnology and Cell Biology, University of Debrecen, 1 Egyetem Square, 4010 Debrecen, Hungary

Tel.: +36-52-512-900

Fax: +36-52-512-925

e-mail: ipocsi@gmail.com

Introduction

Metal pollutants are released into the environment in many ways at potentially harmful levels (Avery 2001). In addition to vast industrial and agricultural discharges, different metal compounds are also used to treat severe human diseases like promyelocytic leukemia {As(III)} and leishmaniasis {Sb(V)} (Tamás et al. 2005). In some areas, the origin of the heavy metals and/or metalloids appearing in the food chain is geological rather than anthropogenic (like the As contamination of drinking water). Because some toxic metals and metalloids are widely distributed in nature microorganisms developed (and are developing!) quite effective strategies to cope with the harmful consequences of metal/metalloid exposures (Tamás et al. 2005).

Today's knowledge on the molecular background of metal/metalloid toxicity in eukaryotes arises in great part from extensive genome, transcriptome, deletome, proteome, interactome and metabolome analyses having been done in baker's yeast cultures. *Saccharomyces cerevisiae* is an excellent model organism to address important biological questions because the available molecular biological, genetic and bioinformatic tools are unprecedentedly sophisticated and versatile with this hemiascomycete. As shown by numerous examples, knowledge obtained from yeast-based models, e.g. on the mechanism of action of and the tolerance against toxic metals, can be transferred with high efficiency to higher eukaryotes including humans (Tamás et al. 2005; Wysocki and Tamás 2010).

On the other hand, the wide evolutionary distances between hemiascomycetes and other major fungal taxons warn us that the applicability of yeast-based models to map metabolic and regulatory pathways in other fungi (even in ascomycetes!) may have some limitations (Miskei et al. 2009). In fact, some well-characterized metal/metalloid stress response pathways in baker's yeast, e.g. the Yap8p-dependent regulation of As(III) stress response, seem to be clearly hemiascomycete specific and, therefore, are not exploitable in other fungi (Wysocki and Tamás 2010). Suitable molecular tools and coordinated community efforts are eagerly needed to set up additional fungal models evolutionarily closer to the heavy metal exposed fungal taxons like the mycorrhizal species (Hildebrandt et al. 2007; González-Guerrero et al. 2009).

Considering the wealth of information accumulated on the toxic metal/metalloid tolerances of yeasts and filamentous fungi in the last decade, an applied microbiology/biotechnology-oriented researcher may feel a bit puzzled when she/he aims at the production of fungal strains with a significantly augmented toxic metal/metalloid tolerance and/or with enhanced metal/metalloid biosorption and bioaccumulation properties. For example, the overlap between the genome-wide screens for genes contributing to toxic metal/metalloid tolerance may be as low as 10–20% although the gene groups coming from different laboratories and surveys complement nicely each other in terms of physiological functions (Thorsen et al. 2009). Because excellent reviews are available in this field, which are summarizing today's yeast-based knowledge on toxic metals and metalloids in an easy-to-read and easy-to-understand way (Tamás et al. 2005; Wysocki and Tamás 2010), the focus of this

review is placed on the possible future targets of the genetic engineering of toxic metal/metalloid tolerant fungi. Moreover, the chapter incorporates the most relevant physiological and genetic data gained in toxic metal/metalloid exposed filamentous fungi as well as in yeast and filamentous fungus cultures exposed to essential micronutrient metals like Fe, Cu or Zn.

It is the hope of the author that a biotechnology-oriented evaluation and systematization of our current understanding of fungal metal/metalloid tolerance would help us to develop new, environmentally friendly and economically feasible technologies in the remediation of heavy metal contaminated soil (Gadd 2000, 2010; Schützendübel and Polle 2002; Gaur and Adholeya 2004; Khan 2005; Lebeau et al. 2008; Marques et al. 2009; Bothe et al. 2010; Hong-Bo et al. 2010; Purakayastha and Chhonkar 2010; Wu et al. 2010) and water (Baldrian 2003; Agrawal et al. 2006; Swami and Buddhi 2006; Wang and Chen 2006; Pan et al. 2009, More et al. 2010; Sankaran et al. 2010), in bioleaching of heavy metals from preservative-treated wood (Mai et al. 2004; Sierra-Alvarez 2007, 2009), and in the mining and recovery of metals (Mulligan et al. 2004; Fujii and Fukunaga 2008; Kuroda and Ueda 2010; Simate et al. 2010). Fungal toxic metal/metalloid resistance genes heterologously expressed in plants (Mejárez and Bülow 2001; Song et al. 2003; Wawrzyński et al. 2006; Guo et al. 2008) may enhance the efficiency of the available phytoremediation or phytomining technologies (Lasat 2002; Chaney et al. 2007; Sheoran et al. 2009).

Considering the structure of this review, after the presentation and discussion of the major elements of fungal metal/metalloid stress defense systems, readers' attention is called to some promising future targets and genetic tools to increase the metal/metalloid tolerance of fungi.

First Line of Defense: Extracellular Chelation and Binding to Cell Wall Constituents

Metal chelation by small molecular mass metabolites, peptides and proteins is a crucially important element of almost all metal/metalloid detoxification processes (Tamás et al. 2005; González-Guerrero et al. 2009; Wysocki and Tamás 2010) and, hence, the significance of extracellular and cytosolic chelation reactions cannot be overestimated. Glutathione (GSH) secretion is a very important element of the GSH-homeostasis in yeast under different environmental conditions (Perrone et al. 2005), and it is sensible that yeast cells intensify GSH-secretion under As(III)-exposures to relieve the intracellular detoxification pathways (Wysocki and Tamás 2010).

Oxalate secretion is well-documented in both brown-rot and white-rot fungi, and this process seems to be stimulated under Cu(II) and Cd(II) stress (Clausen and Green 2003; Jarosz-Wilkolazka et al. 2006). The bulk formation of water-insoluble metal-oxalate crystals is undoubtedly an efficient way to prevent toxic metal ions entering fungal cells (Jarosz-Wilkolazka and Gadd 2003). In addition, oxalate is

primarily important to maintain the lignolytic system of white rot basidiomycetes (Schlosser and Höfer 2002).

A wide range of fungi has been reported to produce extracellular mucilaginous materials (ECMM or “emulsifier”) with excellent toxic metal binding capabilities. As demonstrated by Paraszkievicz et al. (2007, 2009, 2010), Ni(II) {unlike Cu(II), Pb(II) and Zn(II)} did not trigger ECMM production by *Curvularia lunata*. These authors reported the saturation of cellular fatty acids, which is clearly attributable to Ni(II)-initiated lipid peroxidation processes. Importantly, the pullulan production by *Aureobasidium pullulans* was positively affected by Ni(II) and Cd(II) exposures (Breierová et al. 2004), and pullulan increased the Cd(II) tolerance of this industrially important species (Čertík et al. 2005). Vesentini et al. (2006) also reported elevated ratio of ECMM in the biomass in Cu(II) exposed *Trametes versicolor* and *Gloeophyllum trabeum* cultures.

Isolates of the arbuscular mycorrhizal fungi *Glomus* and *Gigaspora* species produce a soil glycoprotein called glomalin (Wright et al. 1996), which possesses a remarkable capability to sequester Cu(II) (González-Chávez et al. 2004; Cornejo et al. 2008; Ferrol et al. 2009). Glomalin is located mainly in the cell wall (Purin and Rilling 2008; Ferrol et al. 2009). Besides glomalin, other cell wall polymers like chitin and melanin can also take part in metal biosorption (González-Guerrero et al. 2009). As demonstrated by Lanfranco et al. (2002a, 2004), Zn(II) exposures affected chitin synthase gene expression patterns and chitin deposition in an ericoid mycorrhizal fungus.

Although decreasing the bioavailability of the toxic metals/metalloids through extracellular complexation, precipitation, and binding to cell wall constituents represents a reasonable and straightforward strategy in strain developments the genetic tools to approach this aim are still in a premature stage. The lack of yeast systems suitably modeling extracellular toxic metal/metalloid detoxification pathways obviously represents a major handicap especially when it is compared to the abundance of models and information available on the organization and regulation of intracellular detoxification pathways.

Second Line of Defense: Transport, Intracellular Chelation and Compartmentalization

Heavy metals enter cells through channels and transporters, which normally facilitate the uptake of essential transition metal micronutrients like Fe, Mn and Zn, anions including phosphate and sulphate as well as sugars (glucose) and sugar derivatives (glycerol) (Tamás et al. 2005; Wysocki and Tamás 2010). In theory, one of the most simple and most effective way to keep off toxic metals/metalloids outside the cell is to eliminate the channel or transporter responsible for the uptake of a given toxic metal/metalloid ion. Unfortunately, these ions may be channeled through multiple transporters into the cytoplasm and, aggravating the situation, the absence of even one of these transport routes may disturb the normal metabolism of the cells.

The elimination of the following plasma membrane channels and transporters has been demonstrated to confer metal tolerance to metal/metalloid exposed *S. cerevisiae* cells (Tamás et al. 2005; Wysocki and Tamás 2010):

- As(V): Pho84p high-affinity and Pho87p low-affinity phosphate transporters (Bun-ya et al. 1996),
- As(III) and Sb(III): Fps1p aquaglyceroporin channel (Wysocki et al. 2001),
- Cd(II): Zrt1p Zn(II) and Smf1p and Smf2p Mn(II) transporters (Gomes et al. 2002; Gitan et al. 2003; Ruotolo et al. 2008),
- Cr(VI) and Se(VI): Sul1p and Sul2p sulphate transporters (Cherest et al. 1997).

Importantly, yeast cells lacking either Pho86p, which is required in trafficking Pho84p from the ER to the cytoplasmic membrane, or Gtr1p, a cytoplasmic GTP binding protein, a regulator of phosphate transport through Pho84p, displayed As(V)-tolerant phenotypes (Bun-ya et al. 1992, 1996; Yompakdee et al. 1996). Furthermore, the elimination of *BSD2* encoding an ER protein trafficking Smf1p and Smf2p transporters to the vacuoles for degradation resulted in Cd(II) and Cu(II) hypersensitivities (Liu et al. 1997; Liu and Culotta 1999). All these observations suggest that intracellular protein trafficking systems represent relevant and promising targets for engineering new fungal strains with an altered toxic metal/metalloid tolerance.

The heavy metal influx through micronutrient metal transporters can be blocked by supplementing the culture media with high concentrations of the essential ions like Zn(II), which leads to the elimination of the zinc-transporter Zrt1p (Gitan et al. 1998, 2003). In the biotechnologist's point of view, the variation of the metal content of the culture media to hinder toxic metal/metalloid uptake is always an attractive alternative to any kind of genetic manipulations of the transport processes themselves.

Nevertheless, overexpression of transporters pumping toxic metals/metalloids and/or their chelates out of the cells or into subcellular organelles (primarily into the vacuoles) may represent a distinguished tool in the genetic engineering of metal resistant fungal strains. Potential targets include:

- As(III): Acr3p plasma membrane transporter (Wysocki et al. 1997) and, somewhat paradoxically, Fps1p aquaglyceroporin channel, which is likely to perform As(III) and Sb(III) export as well (Maciaszczyk-Dziubinska et al. 2010),
- Cd(II) and Cu(II): Pca1p plasma membrane P-type ATPase (Adle et al. 2007),
- Co(II), Rh(II) and Zn(II): Cot1p vacuolar Zn(II) transporter (Conklin et al. 1992; MacDiarmid et al. 2000),
- Fe(II) and Mn(II): Ccc1p vacuolar transporter (Li et al. 2001),
- Se(IV): Ssu1p plasma membrane sulphite pump (Pinson et al. 2000),
- Zn(II) and Co(II): Zrc1p vacuolar membrane Zn(II) transporter (Conklin et al. 1994),
- GSH complexes of Cd(II), As(III), Hg(II), Pb(II): Ycf1p ATP-binding cassette family vacuolar GSH S-conjugate transporter, a strong induction of which can be achieved by overexpressing Yap1p, the master regulator transcription factor

of oxidative stress response (Wemmie et al. 1994; Sharma et al. 2002; Song et al. 2003); Yor1p plasma membrane ABC transporter (Nagy et al. 2006),

- phytochelatin complexes of Cd(II): HMT1 vacuolar membrane transporter of ATP-binding cassette-type (*S. pombe*; Ortiz et al. 1995), although HMT1 is likely to be a GSH S-conjugate transporter in *S. pombe* according to most recent data published by Prévéral et al. (2009).

Importantly, vacuolar Zn(II) (GintZnT1; González-Guerrero et al. 2005) and Cd(II)/Cu(II) (GintABC1; González-Guerrero et al. 2009, 2010a) transporters have been characterized in the endomycorrhizal fungus *Glomus intraradices* with high homology and functional orthology to well-characterized baker's yeast proteins, which clearly demonstrates the applicability of yeast-based heavy metal sequestration models in this case. Not surprisingly, the expression of *GintABC1* was up-regulated when the fungus was exposed to Cd(II) and Cu(II) (González-Guerrero et al. 2010a).

In terms of biotechnology, overexpression of fungal metal/metalloid transporters in transgenic plants is a viable option when new-type phytoremediators with increased metal/metalloid bioaccumulation and tolerance are engineered. A notable example comes from the work published by Song et al. (2003) when the Ycf1p transporter of *S. pombe* was heterologously expressed in *Arabidopsis thaliana* resulting in increased Cd(II) and Pb(II) tolerances.

One may tackle the cytosolic metal toxicity problem solely by increasing the biosynthesis of metal chelators. GSH is a key player in both heavy metal tolerance and oxidative stress defense (Wu and Moye-Rowley 1994; Stephen and Jamieson 1997; Westwater et al. 2002; Pócsi et al. 2004; Mendoza-Cózatl et al. 2005; Tamás et al. 2005; Hegedűs et al. 2007; Wysocki and Tamás 2010), and its overexpression increases the toxic metal/metalloid tolerance. When yeast γ -glutamylcysteine synthetase *GSH1* and garlic phytochelatin synthase *AsPCS1* were expressed either alone or simultaneously in *Arabidopsis thaliana* the transgenic plants accumulated and tolerated Cd and As remarkably well (Guo et al. 2008). Moreover, transgenic tobacco (*Nicotiana tabacum* cv. LA Burley 21) plants harboring *E. coli* serine acetyltransferase (Cys biosynthesis), *E. coli* γ -glutamylcysteine synthetase (GSH biosynthesis) and *S. pombe* phytochelatin synthase genes showed an increased non-protein thiol production and an elevated Cd(II) accumulation in the roots but not in the shoots (Wawrzyński et al. 2006). It is worth noting that recombinant GSH-overproducing yeast strains have also been engineered using self-cloning modules containing the *GSH1* gene (*S. cerevisiae*; Wang et al. 2007, 2009) or an intracellular expression vector with *GSH1* and *GSH2* biosynthesis genes (*Pichia pastoris*; Fei et al. 2009). Intracellular GSH levels can also be elevated considerably in baker's yeast by overexpressing the Hgt1p GSH-transporter (Srikanth et al. 2005) but resulted in some GSH-induced cell toxicity (Srikanth et al. 2005), indicating the limitation of this approach.

Considering GSH turnover, vacuolar γ -glutamyltranspeptidase and aminopeptidase are needed to recycle GSH-derived amino acids into the cytoplasm (Pócsi et al. 2004). Interestingly, a yeast strain with *LAP4* mutation accumulated three

times more Cd(II) than the control strain with an unexpected decrease in the Cd(II)-elicited oxidative stress (Adamis et al. 2009)—an observation with the potential of biotechnological application.

Overexpression of phytochelatin or even implant the phytochelatin biosynthetic pathway into fungi without any capability to synthesize this kind of highly efficient chelating molecules could improve profoundly the metal/metalloid tolerance of the recipient fungal strains. In fact, heterologous expression of either *S. pombe*, plant, red alga or nematode phytochelatin synthases conferred Cd(II), Cu(II), As(III) and Sb(III) resistance to the yeast *S. cerevisiae* (Clemens et al. 1999; Vatamaniuk et al. 2001; Wysocki et al. 2003; Rea et al. 2004; Ramos et al. 2007; Osaki et al. 2008) It were definitely worth seeing the heavy metal tolerance of good GSH-producer ectomycorrhizal fungi like *Paxillus involutus* (Ott et al. 2002; Courbot et al. 2004; Hegedűs et al. 2007) after the phytochelatin synthase biosynthetic capability had been implanted!

Interestingly, *S. pombe* deposits Cd(II) in the form of vacuolar high molecular mass phytochelatin-Cd(II) aggregates with CdS crystallites in their cores (Dameron et al. 1989; Mendoza-Cózatl et al. 2005). These semiconductor nanoparticles can be used in the fabrication of diodes (Kowshik et al. 2002), and genetically engineered *E. coli* cell lines (Kang et al. 2008; Chen et al. 2009) as well as *Lactobacillus* sp. and *S. cerevisiae* based systems (Prasad and Jha 2010) are now also available to produce CdS nanocrystals. In terms of metal/metalloid detoxification, S²⁻-overproduction seems to be beneficial in yeast in general. This can be achieved in several ways including the construction of *MET2* (encoding homoserine *O*-acetyltransferase) or *MET17/MET15/MET25* (encoding *O*-acetylserine and *O*-acetylhomoserine sulfhydrylase) mutations (Ono et al. 1991). Alternatively, *via* the ubiquitination of the Met4p transcriptional regulator by overexpressed Cdc34p ubiquitin-conjugating enzyme could result in a reduced expression of *MET17/MET15/MET25* (Hwang et al. 2007).

Metallothioneins are low molecular mass metal chelator proteins with high affinity towards Cu(II), Zn(II) and Cd(II) (Ecker et al. 1986; Borrelly et al. 2002; Zhang et al. 2003; Kumar et al. 2005; Wysocki and Tamás 2010). *S. cerevisiae* may contain tandem repeats of the *CUP1* metallothionein gene, and the number of the gene copies correlates with the Cu(II) and Zn(II) binding capacities and the Cu(II)-tolerance of the yeast cells (Stroobants et al. 2009). Heterologously expressed yeast metallothionein Cup1p promoted successfully the uptake of Cu(II) from contaminated soils by transgenic tobacco plants (Thomas et al. 2003). Furthermore, metallothionein PiMT1 found in *P. involutus* complemented the Cu(II) and Cd(II) hypersensitivity of metallothionein deficient yeast strains and even increased the Cu(II) tolerance of the ectomycorrhizal fungus *Hebeloma cylindrosporum* (Bellion et al. 2007). Most recently, the functional characterization of *H. cylindrosporum* metallothioneins HcMT1 and HcMT2 took place (Ramesh et al. 2009). Considering the fact that metallothioneins of taxonomically distant arbuscular mycorrhizal fungi, *e.g.* GmarMT1 (*Gigaspora margarita*; Lanfranco et al. 2002b) and GintMT1 (*G. intraradices*; González-Guerrero et al. 2007), share common features with yeast metallothioneins, *e.g.* Cu(II) and Cd(II) sequestering capabilities, we can conclude

that yeast-based metal tolerance models are highly applicable for taxonomically distant fungal species in this case.

Intriguingly, one of the centerpieces of the antioxidative defense systems of fungi, Cu,Zn-superoxide dismutase (Cu/Zn-SOD), may also play a pivotal role in buffering intracellular Cu(II) concentrations *via* incorporating superfluous (and redox active!) free Cu(II) under both aerobic and anaerobic conditions (Culotta et al. 1995; Avery 2001). Genetic engineers may take advantage of the Cu(II) {and Zn(II)?} binding potential of Cu,Zn-superoxide dismutases in the future when Cu(II) and Zn(II) tolerant fungal strains are required for different technological purposes like in water or soil bioremediation programs (Vallino et al. 2009; Villegas et al. 2009).

Similar to copper, the redox active iron is also an essential metal and needs a proper uptake, intracellular transport and storage to avoid the deleterious consequences of the appearance of free iron in either the cytosol or the cell organelles. In filamentous fungi, intracellular siderophores like ferricrocin and hydroxyferricrocin have been reported to keep excess iron in a thermodynamically inert state (Eisendle et al. 2003, 2006; Schrettl et al. 2007, 2008; Johnson 2008). The iron regulon including the siderophore biosynthetic pathways are tightly and negatively regulated by the GATA factor SreA in *Aspergillus fumigatus* (Schrettl et al. 2008). The complex forming ability of hexadentate hydroxamate fungal siderophores with heavy metals other than Fe(III) is relatively weak (Enyedy et al. 2004; Farkas et al. 2008) and, as a consequence, their potential in heavy metal detoxification technologies does not seem to be significant. On the other hand, these Fe(III)-complexing compounds reduce the free Fe-dependent steps in the pathogenesis of atherosclerosis *in vitro* and one of them, desferricoprogen is absorbed effectively in the gastrointestinal tract of rats (Pócsi et al. 2008). These observations point to a novel role of fungal iron chelators, *e.g.* in the field of food biotechnology in the development of functional foods and food additives (Pócsi et al. 2008; Tóth et al. 2009).

In baker's yeast, iron homeostasis is balanced by the Aft1p and Aft2p transcriptional activators (Yamaguchi-Iwai et al. 1995; Blaiseau et al. 2001; Johnson 2008). The yeast frataxin Yfh1p may play a crucial role in the coordination of mitochondrial iron use in basically important mitochondrial metabolic processes like heme biosynthesis and [Fe-S] cluster assembly and stabilization. Yeast strains defective in frataxin synthesis represent applicable models of a well-known human iron metabolic disorder called Friedreich's ataxia (De Freitas et al. 2003). The self-assembly of yeast frataxin is iron-dependent and is leading to multimers (up to 60 subunits), which can sequester >3,000 atoms of iron (Adamec et al. 2000). In addition, it is highly reasonable to assume that Yfh1p is an iron chaperone with primary function in mitochondrial iron detoxification (Bulteau et al. 2004; Gakh et al. 2006, 2008). In good accordance with this, the expression of the human iron storage protein ferritin in frataxin-deficient yeast cells rescued the majority of the mitochondrial functions deteriorated in the absence of Yfh1p and extended the lifespan of the mutant (Campanella et al. 2004; Desmyter et al. 2008). However, frataxin overexpression in yeast affected iron-dependent metabolic processes ambiguously (increased heme synthesis *vs.* defective [Fe-S] cluster assembly/stability; Seguin et al. 2009), but did

not alter the soluble-to-insoluble iron ratio in mitochondria (Seguin et al. 2010). These observations necessitate further studies to clarify the exact physiological functions of these important mitochondrial proteins, and their potential biotechnological application.

Vacuoles represent the primary sites of intracellular metal/metalloid sequestration and storage in fungi (Tamás et al. 2005; Wysocki and Tamás 2010). It is noteworthy that under the depletion of essential metals vacuolar metal deposits can be mobilized including Zn(II) (Zrt3p, MacDiarmid et al. 2000), Cu(II) (Ctr2p, Rees et al. 2004) and Fe(II) (Smf3p; Portnoy et al. 2000; Fet5p-Fth1p complex, Urbanowski and Piper 1999). Due to the high turnover of redox active essential metals, the redox milieu of the vacuoles has to be fairly stable to avoid the generation of highly fragmented and damaged organelles (Corson et al. 1999).

As discussed by Ferrol et al. (2009), the vacuolar metal binding activity shows an uneven distribution in arbuscular mycorrhizal fungi mycelia with clear-cut maxima in the intraradical vesicles and extraradical spores (Weiersbye et al. 1999; González-Guerrero et al. 2008; Orłowska et al. 2008). In a spectacular study performed by González-Guerrero et al. (2008), high Cu(II)-accumulating vacuoles were clearly concentrated in the blue-green colored spores of *G. intraradices*.

Third Line of Defense: The Antioxidative Defense System

Fungi exposed to toxic metal/metalloid stress commonly face oxidative cell injuries caused by reactive oxygen species (Avery 2001). Fungal cells possess a wide array of antioxidants to cope with different kinds of oxidative stress. For example, GSH-independent and GSH-dependent enzyme activities are able to neutralize reactive oxygen species with remarkable efficiency (Pócsi et al. 2004).

As mentioned above, Cu/Zn-superoxide dismutases buffer redox active Cu(II) levels within the cytosol (Culotta et al. 1995) but also catalyze superoxide \rightarrow peroxide + O₂ conversions. The elimination of this type of enzyme results in a metal sensitive phenotype in fungi (Sumner et al. 2005), elevation in the intracellular “free iron” concentrations (Srinivasan et al. 2000), fragmenting vacuoles (Corson et al. 1999) and, as a consequence, reorganization of the iron metabolic network (De Freitas et al. 2000). As demonstrated by González-Guerrero et al. (2010b), the endomycorrhizal fungus *G. intraradices* also has a Cu(II)-inducible Cu,Zn-superoxide dismutase (GintSOD1). Interestingly, the Zn(II)-tolerant ericoid mycorrhizal fungus *Oidiodendron maius* Zn releases a Cu,ZnSOD into the extracellular environment, which may contribute to the metal tolerance of the plant symbiont as well (Vallino et al. 2009). It is reasonable to assume that the overexpression of Cu/Zn-superoxide dismutase in fungal cells would provide them with an improved metal and oxidative stress tolerance. But increased oxidative stress tolerance and chronological life span were only observable in yeast cells when Sod1p was co-expressed with the Cu(II)-chaperone Ccs1p (Brown et al. 2004) and the culture medium was supplemented with high Cu(II) concentrations (Harris et al. 2005). In the absence of

either Ccs1p overexpression or high-dose Cu(II)-supplementation the cells showed the symptoms of emerging oxidative stress and a shortened chronological life span (Harris et al. 2005).

For the biotechnologist, one of the most attractive options to improve the performance of Cu/Zn-superoxide dismutases in any engineered fungi is the replacement of the wild-type enzyme with a Cu/Zn-superoxide dismutase with superior enzymological parameters. For example, the Cu/Zn-superoxide dismutase cloned and characterized in the deep-sea yeast *Cryptococcus liquifaciens* strain N6 possessed four-fold higher activity than baker's yeast's Sod1p and was functional in *S. cerevisiae* (Kanamasa et al. 2007).

The overexpression of the mitochondrial flavohemoglobin 2, which has a role in nitric oxide detoxification, resulted in an unexpected H₂O₂-hypersensitive phenotype in *Aspergillus oryzae* (Zhou et al. 2010). This observation warns us that the overproduction of any antioxidants in fungal cells may turn up unforeseeable or even disadvantageous physiological consequences especially when the antioxidants are not well-characterized or when their overproduction is not controlled satisfactorily.

Paradoxically, a tight control of glutathione reductase activity may result in a Cr(VI)-tolerant phenotype in fungi because this central element of the GSH-dependent antioxidative defense system catalyzes Cr(VI)→Cr(V) conversion giving rise to harmful redox species and cycling reactions in yeasts (Pesti et al. 2002; Gazdag et al. 2003; Koósz et al. 2008; Poljšak et al. 2010).

It is worth mentioning that heterologous expression of *E. coli* GSH biosynthetic enzymes in Indian mustard (*Brassica juncea* L.) plants increased the toxic metal/metalloid tolerance of the plant (Zhu et al. 1999a, b; Reisinger et al. 2008)—a promising strategy, which might be exploitable in fungi as well.

Antioxidants, such as ascorbic acid can reduce transition metals giving these compounds a pro-oxidant character (Poljšak et al. 2005). Therefore any overload of fungal cells with antioxidants (e.g. Tempol, Trolox, melatonin) might exacerbate oxidative cell damages in the presence of redox active metals/metalloids (Lewinska and Bartosz 2007). In accordance with these observations, deletion of sulphite reductases (*MET10* and *MET5*) in the sulphate assimilation pathway, which is basically important in the *de novo* synthesis of S-containing amino acids and the antioxidant GSH, prevents Te(III)→Te(0) conversion and results in an enhanced metalloid tolerance in baker's yeast (Wysocki and Tamás 2010). All these observations indicate that any modulation of the antioxidative defense systems of fungi to increase metal/metalloid tolerance should be done by extreme care because of the unforeseeable impacts on the pro-oxidant/antioxidant status of the cells.

Another option to gain metal/metalloid tolerant fungal strains is the overexpression of elements of the signal transduction and regulatory pathways, which are normally operating in metal/metalloid stress exposed wild-type strains (Avery 2001; Haugen et al. 2004; Tamás et al. 2005; Rodrigues-Pousada et al. 2010; Wysocki and Tamás 2010).

The master regulator, which orchestrates metal/metalloid stress responses in baker's yeast {e.g. under Cd(II), As(III), Sb(III), Se(III) and Hg exposures;

(Wysocki and Tamás 2010)} is the bZIP-type transcriptional factor Yap1p. As demonstrated by Wemmie et al. (1994), wild type yeast cells harboring multiple copies of *YAP1* possessed an increased Cd(II)-tolerance. Another bZIP-type factor, Yap2p, suppressed the Cd(II)-sensitive phenotype of a *YAP1* disruptant although the *YAP2* disruptant itself was not characterized with any increased Cd(II)-sensitivity (Hirata et al. 1994). According to Azevedo et al. (2007), Yap1p and Yap2p transcription factors share a common Cd(II)-sensing domain. Considering other bZIPs, Yap5p is involved in the regulation of the Fe-homeostasis *via* the regulation of *CCC1* encoding the vacuolar iron transporter Ccc1p (Li et al. 2008), and Yap8p plays a pivotal role in the regulation of As(III)-detoxification (Haugen et al. 2004; Wysocki et al. 2004).

The appearance of high quantities of damaged, non-functional, mistranslated or even aggregated proteins is a common symptom of metal/metalloid toxicity (Holland et al. 2007; Medicherla and Goldberg 2008). Proteasomes are in the first line of the removal and degradation of such proteins, and this activity is regulated positively by the transcriptional factor Rpn4p (Haugen et al. 2004; Thorsen et al. 2007, 2009; Medicherla and Goldberg 2008). One may speculate that a constitutively high-level expression or even the overexpression of Rpn4p would lead to the development of metal/metalloid tolerant fungal strains but, again, the outcome of such genetic modifications may be quite different. As demonstrated by Wang et al. (2010), both the availability and the proteasomal degradation of Rpn4p are equally important factors to maintain cell viability under various types of stress conditions!

The mitogen-activated protein kinase Hog1p also plays an indispensable role in metal/metalloid stress defense in yeasts (Wysocki and Tamás 2010). The Hog1p of *S. cerevisiae* downregulates As(III) transport activity *via* Fps1p (Thorsen et al. 2006; Dilda et al. 2008), controls cell cycle progression (Migdal et al. 2008) meanwhile the orthologous *S. pombe* (Sty1/Spc1) and *C. albicans* (Ca-Hog1) kinases are transported to the nuclei upon Cd(II) and As(III) exposures and reprogram global transcription (Enjalbert et al. 2006; Kennedy et al. 2008). On the other hand, the hyperactivation of Hog1p is deleterious for yeasts (Wurgler-Murphy et al. 1997; Warmka et al. 2001).

Not surprisingly, the major nutrient-responsive signal transduction pathways TOR (target of rapamycin) and PKA (protein kinase A) also contribute to the regulation of general stress responses in yeast (Wysocki and Tamás 2010). Under nutrient abundance, these pathways stimulate physiological processes maintaining a high growth rate including the down-regulation of stress defense systems. Under nutrient limitation or toxic metal/metalloid exposures, Msn2p/Msn4p transcription factors are activated and they stimulate the expression of a wide array of antioxidant enzymes (Gasch et al. 2000; Hosiner et al. 2009). Interestingly, the elimination of *MSN2* and *MSN4* resulted in an As(III)-tolerant phenotype in *S. cerevisiae*, which might be indicative of an exaggerated expression of stress-defense genes (Hosiner et al. 2009). Another transcription factor, Sfp1p is removed from DNA when TOR activity is inhibited by metal/metalloid stress and this detachment leads to the downregulation of ribosomal protein synthesis (Marion et al. 2004; Hosiner et al. 2009). Unexpectedly, deletion of *SFP1* resulted in an increased As(III)-tolerance (Hosiner et al. 2009).

Metal/metalloid stress response regulatory elements do not work independently of each other (Salin et al. 2008). For example, Yap1p (redox homeostasis), Rpn4p (protein degradation), Hsf1p (protein folding), Pdr1p, Pdr3p, Yrr1p (multidrug resistance), Aft2 (iron homeostasis) and Cin5p (osmotic stress tolerance) transcription factors join in a highly interconnected regulatory network including transcriptional loops to orchestrate Se(III) stress response in the most efficient way (Salin et al. 2008). Obviously, the elimination or modification of any element of the network may trigger unpredictable physiological changes and the appearance of unforeseeable phenotypes, which makes the genetic engineering of the regulatory network itself to develop metal/metalloid tolerant mutants risky, and still largely empirical with some unexpected consequences.

Screening for Future Targets to Engineer Heavy Metal Tolerant Fungi

Genome, transcriptome, deletome, proteome, metabolome and interactome analyses have been performed and are in progress to learn how different fungi respond to versatile toxic metal/metalloid exposures. To become familiar with the elements and the regulation of the metal/metalloid stress response networks may provide us with suitable tools to augment the metal/metalloid tolerance of selected fungi with potential applications in a wide spectrum of environmental technologies. This subchapter summarizes the most promising pieces of information extracted from the abundant experimental data having been generated in the last decade using robust “-omics” techniques.

In their substantial work, Jin et al. (2008) compared the transcriptome profiles of baker's yeast exposed to Ag(I), As(III), Cd(II), Cr(VI), Co(II), Hg(II) and Zn(II), and they found that the chemical properties of the metals/metalloids basically determined the pattern of the genome-level transcriptional response. Not surprisingly, principal component analysis and hierarchical clustering of the expression data by treatment conditions grouped Ag(I)-Zn(II), Cd(II)-Hg(II) and As(III)-Cu(II) metal/metalloid pairs close together meanwhile Cr(VI) was separated from other metals—a valuable piece of information when fungal strains with multiple metal resistances should be developed. Jin et al. (2008) managed to identify the group of CRM (Common Metal Responsive) genes, which may provide us with the possibility to construct fungal strains with a general metal/metalloid tolerance! Overexpressions of genes encoding *e.g.* polyamine and iron transporters, proteins maintaining ion homeostasis and iron transport as well as elements of the antioxidant defense system, or elimination of genes encoding *e.g.* protein kinase subunits and transition metal and carbohydrate transporters (Jin et al. 2008) can be among the most promising targets of future genetic engineering technologies. On the other hand, deletome analysis performed concomitantly by Jin et al. (2008) indicated that the metal-resistance and metal-sensitivity genes were basically metal-specific. As a consequence, the

metal/metalloid-responsive transcriptome and deletome datasets shared as few as 22 genes in overlapping regions including *CYS3* {cystathionine γ -lyase; essential for survival in the presence of As(III), Cd(II) and Cu(II)}, *ADH1* {alcohol dehydrogenase; important in As(III) and Cu(II) tolerances} and *RNR1* {ribonucleotide-diphosphate reductase; with pivotal importance in Cd(II) and Cr(VI) tolerances}. Furthermore, sulphur amino acid transport and biosynthesis were essential under As(III), Cd(II), Cr(VI) and Cu(II) stress conditions.

In accordance with and partly supplementary to the observations of Jin et al. (2008), Ruotolo et al. (2008) demonstrated by deletome and interactome analyses that tolerance against both Cd(II) and Ni(II) exposures relied on the concerted action of several functional subnetworks including proteasome, vacuolar fusion, cell wall integrity pathway, v-ATPase assembly/regulation, essential ion homeostasis, ERG pathway, nuclear pore complex, Ccr4p and other mRNA processing enzymes and chromatin remodeling. Another yeast deletome analysis performed by Thorsen et al. (2009) with As(III) and Cd(II) indicated that metal/metalloid tolerance required sulphur and glutathione biosynthesis, environmental sensing, mRNA synthesis and transcription as well as vacuolar/endosomal transport and sorting. The importance of the sulphur assimilation pathway in Cd(II)-exposed *S. cerevisiae* cells was also emphasized by several other authors performing transcriptome (Momose and Iwahashi 2001; Haugen et al. 2004) and proteome (Vido et al. 2001) studies. Sulphur starvation caused by Cr(VI) exposures was also demonstrated in baker's yeast by Pereira et al. (2008) at transcriptome level, and the channeling of sulphur towards GSH synthesis by stimulating the transcription of sulphur-poor isoenzymes (the sulphur-sparing response) was shown in *S. cerevisiae* treated with Cd(II) and Cr(VI) (Fauchon et al. 2002; Pereira et al. 2008). Overlapping oxidative stress responses were also recorded in the yeast *Hansenula polymorpha* exposed to Cu(II) or V(V) (Mannazzu et al. 2000).

Further interesting metal-specific stress-responsive cell biological, metabolic and regulatory pathways, which are necessary to gain metal/metalloid tolerance in *S. cerevisiae*, are also presented here, and the data are grouped according to the toxic metals/metalloids:

- Al(III): retrograde endosome-to-Golgi vesicle transport, signal transduction (Pkc1p, cell integrity signaling serine/threonine protein kinase), protein mannosylation (cell wall architecture) (deletome, Kakimoto et al. 2005),
- As(III): shikimate and serine, threonine, glutamate biosynthesis (deletome; Haugen et al. 2004), cytoskeleton, DNA repair, secretory pathway and vacuole function, osmoregulation (deletome; Dilda et al. 2008), cell cycle regulation, spindle body and microtubule formation, mitochondrion biogenesis and function, lipid and fatty acid metabolism, cytoskeleton (deletome; Thorsen et al. 2009),
- Cd(II): DNA repair and replication (*RAD27* and *DNA2*, deletome, Serero et al. 2008), ESCRT and retromer complexes in the carboxypeptidase Y (CPY) Golgi-to-vacuole transport route, DNA repair (deletome, interactome; Ruotolo et al. 2008), ion homeostasis and transport, sugar/carbohydrate metabolism (deletome; Thorsen et al. 2009), ER stress response (transcriptome; Gardarin et al. 2010),

- Co(II): iron regulon (transcriptome; Stadler and Schweyen 2002),
- Cu(II): metallothionein production, iron transport (transcriptome; Gross et al. 2000), transportation into the late endosomes *via* the carboxypeptidase Y Golgi-to-vacuole transport route (CPY, deletome; Jo et al. 2008), tryptophan biosynthetic pathway (deletome; Jo et al. 2008), metallothionein production, lipid, fatty acid metabolism, methionine metabolism (transcriptome; Yasokawa et al. 2008),
- Fe(II): transportation into the vacuoles through the alkaline phosphatase Golgi-to-vacuole transport route (ALP, deletome; Jo et al. 2008),
- Ni(II): transportation into the vacuoles through the alkaline phosphatase Golgi-to-vacuole transport route, nucleocytoplasmic transport (ALP, deletome, interactome; Ruotolo et al. 2008),
- Se(III): iron deprivation, oxidative stress and protein degradation responses (transcriptome; Salin et al. 2008),
- Zn(II): low-oxygen response, iron metabolism (transcriptome; Lyons et al. 2004), vacuolar assembling and biogenesis, chaperones for protein folding and targeting, some components of the iron regulon (deletome; Pagani et al. 2007).

Deprivation of essential metals like Zn and Fe, may also lead to the reorganization of the metabolic networks in yeasts, and these processes are well-characterized by transcriptome analyses (Lyons et al. 2000, 2004; Shakoury-Elizeh et al. 2004, 2010; Dainty et al. 2008; Wu et al. 2008). Importantly, iron-deficiency stimulates riboflavin overproduction in *Pichia guilliermondii*, which may possess biotechnological significance (Boretsky et al. 2007; Pynyaha et al. 2010).

Cd(II)-stress related “-omics” studies performed with *S. pombe* (Chen et al. 2003; Bae and Chen 2004; Kennedy et al. 2008), *C. albicans* (Enjalbert et al. 2006), *Blastocladiella emersonii* (Georg and Gomes 2007), *Ganoderma lucidum* (Chuang et al. 2009) and *Cadophora finlandica* (Gorfer et al. 2009) also provided a wealth of information on the organization and regulation of fungal metal stress defense systems. Cd(II) stress responses of different fungi share many common features. Nonetheless, the same studies revealed some species-specific responses as well, *e.g.* deletome analysis of *S. pombe* by Kennedy et al. (2008) pointed to the important role of ubiquinone (coenzyme Q10) biosynthesis in the Cd(II)-tolerance. In addition, fission yeast but not budding yeast harbors *CNT5*, encoding a member of the centaurin ADP ribosylation factor GTPase activating protein family, which may contribute to As(III)/Cd(II) tolerance through the maintenance of membrane integrity and the modulation of membrane trafficking (Vashisht et al. 2009), and a Cd(II)-regulated centaurin-type protein was also identified in the genome of *C. finlandica* (Gorfer et al. 2009). In the aquatic fungi *B. emersonii* (Georg and Gomes 2007), transcriptome analysis revealed six glutathione S-transferases and six metacaspases, which were induced by Cd(II) exposures. In the ectomycorrhizal basidiomycete *Suillus luteus*, the production of heat shock proteins, a metal transporter, a hydrophobin and proteins with function in ubiquitin-dependent proteolysis were related to Zn(II) detoxification and tolerance (Muller et al. 2007). Mycorrhizal symbioses with *Suillus* spp. is considered now as a suitable tool to cultivate pine trees on Cd(II), Cu(II) and Zn(II) contaminated soils (Adriaensen et al. 2005, 2006; Krznanic et al. 2009).

It is worth noting that *Aspergillus* spp. possess a robust and delicately regulated stress defense system (Pócsi et al. 2005; Miskei et al. 2009), and data on the molecular background of the high heavy metal tolerance of this genus are also accumulating (Fraser et al. 2002; Cánovas et al. 2003, 2004, 2007; Bučková et al. 2005; Odon et al. 2007; Todorova et al. 2008; Mukherjee et al. 2010). Considering the remarkably wide array of molecular genetic tools available for the genetic engineering of this genus it is reasonable to assume that genetically modified *Aspergillus* strains will appear in the future in versatile metal removal technologies. It is remarkable that the number of publications on *Aspergillus*-based water and soil remediation technologies is already rocketing up owing to the abundance of biotechnological experience with this group of fungi (e.g. Price et al. 2001; Rajendran et al. 2002; Katsifas et al. 2004; Mulligan et al. 2004; Deepa et al. 2006; Sandana Mala et al. 2006; Srivastava and Thakur 2006; Fukuda et al. 2008; Coreño-Alonso et al. 2009; Maheswari and Murugesan 2009; Ren et al. 2009; Sharma et al. 2009; Sun et al. 2010; Taştan et al. 2010). In addition, further spectacular technological progress is clearly foreseeable, e.g. in aspergilli-based nanocrystal producing technologies (Bhainsa and D'Souza 2006; Binupriya et al. 2010; Verma et al. 2010).

Fungi can undergo metal/metalloid induced/controlled apoptosis (Borghouts et al. 2001; Georg and Gomes 2007; Liang and Zhou 2007; Nargund et al. 2008; Azevedo et al. 2009; Chatterjee and Luo 2010). Exposures to toxic metals change the morphology and physiology of mitochondria (Yang and Pon 2003; Liang and Zhou 2007) and, as a consequence, may lead to the initialization of cell death programs (Eisenberg et al. 2007). It is worth mentioning that mitochondria, besides many important cellular functions, play a pivotal role in the control of the iron homeostasis of the cells (Foury and Talibi 2001). Mitochondrial and cellular integrity (and life-span!) can be engineered now by the construction of longevity mutants as demonstrated in *Podospora anserina*, e.g. by the overexpression of *O*-methyltransferase, carotenoid biosynthesis enzymes, misfolded-protein-degrading mitochondrial protease, or by the deletion of the “dynamamin-related protein 1”, which regulates mitochondrial division (Scheckhuber et al. 2009). It remains to be seen whether or not such mutations would give the fungal cells an increased resistance against the metal/metalloid-initiated apoptosis as well. Importantly, deletion of *PaMTH1* encoding *O*-methyltransferase resulted in a decreased Cu(II)-tolerance (Kunstmann and Osiewacz 2009).

Finally it remains to be mentioned that “-omics” data are also accumulating on both the plant and the fungus sides of plant-mycorrhizal associations under toxic metal exposures (Ouziad et al. 2005; Aloui et al. 2009), leading to a deeper understanding of the combined plant-fungus metal/metalloid stress responses (Schützendübel and Polle 2002). Undoubtedly, this is the prerequisite of the development of new end effective biotechnologies to combat the increasing toxic metal load of our environment.

Acknowledgement The author is indebted to Dr. M. J. Tamás, University of Gothenburg, for reading critically the manuscript.

References

- Adamec J, Rusnak F, Owen WG, Naylor S, Benson LM, Gacy AM, Isaya G (2000) Iron-dependent self-assembly of recombinant yeast frataxin: implications for Friedreich ataxia. *Am J Hum Genet* 67:549–562
- Adamis PD, Mannarino SC, Riger CJ, Duarte G, Cruz A, Pereira MD, Eleutherio EC (2009) Lap4, a vacuolar aminopeptidase I, is involved in cadmium-glutathione metabolism. *Biometals* 22:243–249
- Adle DJ, Sinani D, Kim H, Lee J (2007) A cadmium-transporting P1B-type ATPase in yeast *Saccharomyces cerevisiae*. *J Biol Chem* 282:947–955
- Adriaensen K, Vrålstad T, Noben JP, Vangronsveld J, Colpaert JV (2005) Copper-adapted *Suillus luteus*, a symbiotic solution for pines colonizing Cu mine spoils. *Appl Environ Microbiol* 71:7279–7284
- Adriaensen K, Vangronsveld J, Colpaert JV (2006) Zinc-tolerant *Suillus bovinus* improves growth of Zn-exposed *Pinus sylvestris* seedlings. *Mycorrhiza* 16:553–558
- Agrawal A, Kumar V, Pandey BD (2006) Remediation options for the treatment of electroplating and leather tanning effluent containing chromium—a review. *Mineral Proc Extr Metall Rev* 27:99–130
- Aloui A, Recorbet G, Gollotte A, Robert F, Valot B, Gianinazzi-Pearson V, Aschi-Smiti S, Dumas-Gaudot E (2009) On the mechanisms of cadmium stress alleviation in *Medicago truncatula* by arbuscular mycorrhizal symbiosis: a root proteomic study. *Proteomics* 9:420–433
- Avery SV (2001) Metal toxicity in yeasts and the role of oxidative stress. *Adv Appl Microbiol* 49:111–142
- Azevedo D, Nascimento L, Labarre J, Toledano MB, Rodrigues-Pousada C (2007) The *S. cerevisiae* Yap1 and Yap2 transcription factors share a common cadmium-sensing domain. *FEBS Lett* 581:187–195
- Azevedo MM, Almeida B, Ludovico P, Cássio F (2009) Metal stress induces programmed cell death in aquatic fungi. *Aquat Toxicol* 92:264–270
- Bae W, Chen X (2004) Proteomic study for the cellular responses to Cd²⁺ in *Schizosaccharomyces pombe* through amino acid-coded mass tagging and liquid chromatography tandem mass spectrometry. *Mol Cell Proteomics* 3:596–607
- Baldrian P (2003) Interactions of heavy metals with white-rot fungi. *Enzyme Microb Technol* 32:78–91
- Bellion M, Courbot M, Jacob C, Guinet F, Blaudez D, Chalot M (2007) Metal induction of a *Paxillus involutus* metallothionein and its heterologous expression in *Hebeloma cylindrosporum*. *New Phytol* 174:151–158
- Bhainsa KC, D'Souza SF (2006) Extracellular biosynthesis of silver nanoparticles using the fungus *Aspergillus fumigatus*. *Colloids Surf B Biointerfaces* 47:160–164
- Binupriya AR, Sathishkumar M, Vijayaraghavan K, Yun SI (2010) Bioreduction of trivalent aurum to nano-crystalline gold particles by active and inactive cells and cell-free extract of *Aspergillus oryzae* var. *viridis*. *J Hazard Mater* 177:539–545
- Blaiseau PL, Lesuisse E, Camadro JM (2001) Aft2p, a novel iron-regulated transcription activator that modulates, with Aft1p, intracellular iron use and resistance to oxidative stress in yeast. *J Biol Chem* 276:34221–34226.
- Boretsky YR, Protchenko OV, Prokopiv TM, Mukalov IO, Fedorovych DV, Sibirny AA (2007) Mutations and environmental factors affecting regulation of riboflavin synthesis and iron assimilation also cause oxidative stress in the yeast *Pichia guilliermondii*. *J Basic Microbiol* 47:371–377
- Borghouts C, Werner A, Elthon T, Osiewicz HD (2001) Copper-modulated gene expression and senescence in the filamentous fungus *Podospora anserina*. *Mol Cell Biol* 21:390–399
- Borrelly GP, Harrison MD, Robinson AK, Cox SG, Robinson NJ, Whitehall SK (2002) Surplus zinc is handled by Zym1 metallothionein and Zhf endoplasmic reticulum transporter in *Schizosaccharomyces pombe*. *J Biol Chem* 277:30394–30400

- Bothe H, Regvar M, Turnau K (2010) Arbuscular mycorrhiza, heavy metal, and salt tolerance. In: Sherameti I, Varma A (eds) Soil heavy metals. Springer, Berlin, pp 87–111
- Breierová E, Gregor T, Juršiková P, Stratilová E, Fišera M (2004) The role of pullulan and pectin in the uptake of Cd²⁺ and Ni²⁺ ions by *Aureobasidium pullulans*. *Ann Microbiol* 54:247–255
- Brown NM, Torres AS, Doan PE, O'Halloran TV (2004) Oxygen and the copper chaperone CCS regulate posttranslational activation of Cu, Zn superoxide dismutase. *Proc Natl Acad Sci U S A* 101:5518–5523
- Bučková M, Godočíková J, Šimonovičová A, Polek B (2005) Production of catalases by *Aspergillus niger* isolates as a response to pollutant stress by heavy metals. *Curr Microbiol* 50: 175–179
- Bulteau AL, O'Neill HA, Kennedy MC, Ikeda-Saito M, Isaya G, Szveda LI (2004) Frataxin acts as an iron chaperone protein to modulate mitochondrial aconitase activity. *Science* 305:242–245
- Bun-ya M, Harashima S, Oshima Y (1992) Putative GTP-binding protein, Gtr1, associated with the function of the Pho84 inorganic phosphate transporter in *Saccharomyces cerevisiae*. *Mol Cell Biol* 12:2958–2966
- Bun-ya M, Shikata K, Nakade S, Yompakdee C, Harashima S, Oshima Y (1996) Two new genes, *PHO86* and *PHO87*, involved in inorganic phosphate uptake in *Saccharomyces cerevisiae*. *Curr Genet* 29:344–351
- Campanella A, Isaya G, O'Neill HA, Santambrogio P, Cozzi A, Arosio P, Levi S (2004) The expression of human mitochondrial ferritin rescues respiratory function in frataxin-deficient yeast. *Hum Mol Genet* 13:2279–2288
- Cánovas D, de Lorenzo V (2007) Osmotic stress limits arsenic hypertolerance in *Aspergillus* sp. P37. *FEMS Microbiol Ecol* 61:258–263
- Cánovas D, Mukhopadhyay R, Rosen BP, de Lorenzo V (2003) Arsenate transport and reduction in the hyper-tolerant fungus *Aspergillus* sp. P37. *Environ Microbiol* 5:1087–1093
- Cánovas D, Vooijs R, Schat H, de Lorenzo V (2004) The role of thiol species in the hypertolerance of *Aspergillus* sp. P37 to arsenic. *J Biol Chem* 279:51234–51240
- Čertík M, Breierová E, Juršiková P (2005) Effect of cadmium on lipid composition of *Aureobasidium pullulans* grown with added extracellular polysaccharides. *Int Biodeter Biodegr* 55:195–202
- Chaney RL, Angle JS, Broadhurst CL, Peters CA, Tappero RV, Sparks DL (2007) Improved understanding of hyperaccumulation yields commercial phytoextraction and phytomining technologies. *J Environ Qual* 36:1429–1443
- Chatterjee N, Luo Z (2010) Cr(III)-organic compounds treatment causes genotoxicity and changes in DNA and protein level in *Saccharomyces cerevisiae*. *Ecotoxicology* 19:593–603
- Chen D, Toone WM, Mata J, Lyne R, Burns G, Kivinen K, Brazma A, Jones N, Bähler J (2003) Global transcriptional responses of fission yeast to environmental stress. *Mol Biol Cell* 1:214–229
- Chen YL, Tuan HY, Tien CW, Lo WH, Liang HC, Hu YC (2009) Augmented biosynthesis of cadmium sulfide nanoparticles by genetically engineered *Escherichia coli*. *Biotechnol Prog* 25:1260–1266
- Cherest H, Davidian JC, Thomas D, Benes V, Ansorge W, Surdin-Kerjan Y (1997) Molecular characterization of two high affinity sulfate transporters in *Saccharomyces cerevisiae*. *Genetics* 145:627–635
- Chuang HW, Wang IW, Lin SY, Chang YL (2009) Transcriptome analysis of cadmium response in *Ganoderma lucidum*. *FEMS Microbiol Lett* 293:205–213
- Clausen CA, Green F (2003) Oxalic acid overproduction by copper-tolerant brown rot basidiomycetes on southern yellow pine treated with copper-based preservatives. *Int Biodeter Biodegr* 51:139–144
- Clemens S, Kim EJ, Neumann D, Schroeder JI (1999) Tolerance to toxic metals by a gene family of phytochelatin synthases from plants and yeast. *EMBO J* 18:3325–3333
- Conklin DS, McMaster JA, Culbertson MR, Kung C (1992) *COT1*, a gene involved in cobalt accumulation in *Saccharomyces cerevisiae*. *Mol Cell Biol* 12:3678–3688
- Conklin DS, Culbertson MR, Kung C (1994) Interactions between gene products involved in divalent cation transport in *Saccharomyces cerevisiae*. *Mol Gen Genet* 244:303–311

- Coreño-Alonso A, Acevedo-Aguilar FJ, Reyna-López GE, Tomasini A, Fernández FJ, Wrobel K, Gutiérrez-Corona JF (2009) Cr(VI) reduction by an *Aspergillus tubingensis* strain: role of carboxylic acids and implications for natural attenuation and biotreatment of Cr(VI) contamination. *Chemosphere* 76:43–47
- Cornejo P, Meier S, Borie G, Rillig MC, Borie F (2008) Glomalin-related soil protein in a Mediterranean ecosystem affected by a copper smelter and its contribution to Cu and Zn sequestration. *Sci Total Environ* 406:154–160
- Corson LB, Folmer J, Strain JJ, Culotta VC, Cleveland DW (1999) Oxidative stress and iron are implicated in fragmenting vacuoles of *Saccharomyces cerevisiae* lacking Cu,Zn-superoxide dismutase. *J Biol Chem* 274:27590–27596
- Courbot M, Díez L, Ruotolo R, Chalot M, Leroy P (2004) Cadmium responsive thiols in the ectomycorrhizal fungus *Paxillus involutus*. *Appl Environ Microbiol* 70:7413–7417
- Culotta VC, Joh HD, Lin SJ, Slekar KH, Strain J (1995) A physiological role for *Saccharomyces cerevisiae* copper/zinc superoxide dismutase in copper buffering. *J Biol Chem* 270:29991–29997
- Dainty SJ, Kennedy CA, Watt S, Bähler J, Whitehall SK (2008) Response of *Schizosaccharomyces pombe* to zinc deficiency. *Eukaryot Cell* 7:454–464
- Dameron CT, Reese RN, Mehra RK, Kortan AR, Carroll PJ, Steigerwald ML, Brus LE, Winge DR (1989) Biosynthesis of cadmium-sulfide quantum semiconductor crystallites. *Nature* 338:696–697
- De Freitas JM, Liba A, Meneghini R, Valentine JS, Gralla EB (2000) Yeast lacking Cu-Zn superoxide dismutase show altered iron homeostasis. Role of oxidative stress in iron metabolism. *J Biol Chem* 275:1645–11649
- De Freitas J, Wintz H, Kim JH, Poynton H, Fox T, Vulpe C (2003) Yeast, a model organism for iron and copper metabolism studies. *Biometals* 16:185–197
- Deepa KK, Sathishkumar M, Binupriya AR, Murugesan GS, Swaminathan K, Yun SE (2006) Sorption of Cr(VI) from dilute solutions and wastewater by live and pretreated biomass of *Aspergillus flavus*. *Chemosphere* 62:833–840
- Desmyter L, Dewaele S, Reekmans R, Nystrom T, Contreras R, Chen C (2008) Expression of the human ferritin light chain in a frataxin mutant yeast affects ageing and cell death. *Exp Gerontol* 39:707–715
- Dilda PJ, Perrone GG, Philp A, Lock RB, Dawes IW, Hogg PJ (2008) Insight into the selectivity of arsenic trioxide for acute promyelocytic leukemia cells by characterizing *Saccharomyces cerevisiae* deletion strains that are sensitive or resistant to the metalloid. *Int J Biochem Cell Biol* 40:1016–1029
- Ecker DJ, Butt TR, Sternberg EJ, Neep MP, Debouck C, Gorman JA, Crooke ST (1986) Yeast metallothionein function in metal ion detoxification. *J Biol Chem* 261:16895–16900
- Eisenberg T, Büttner S, Kroemer G, Madeo F (2007) The mitochondrial pathway in yeast apoptosis. *Apoptosis* 12:1011–1023
- Eisendle M, Oberegger H, Zadra I, Haas H (2003) The siderophore system is essential for viability of *Aspergillus nidulans*: functional analysis of two genes encoding L-ornithine N⁵-monooxygenase (*sidA*) and a non-ribosomal peptide synthetase (*sidC*). *Mol Microbiol* 49:359–375
- Eisendle M, Schrettl M, Kragl C, Müller D, Illmer P, Haas H (2006) The intracellular siderophore ferricrocin is involved in iron storage, oxidative-stress resistance, germination, and sexual development in *Aspergillus nidulans*. *Eukaryot Cell* 5:1596–1603
- Enjalbert B, Smith DA, Cornell MJ, Alam I, Nicholls S, Brown AJ, Quinn J (2006) Role of the Hog1 stress-activated protein kinase in the global transcriptional response to stress in the fungal pathogen *Candida albicans*. *Mol Biol Cell* 17:1018–1032
- Enyedy EA, Pócsi I, Farkas E (2004) Complexation of desferricoprogen with trivalent Fe, Al, Ga, In and divalent Fe, Ni, Cu, Zn metal ions: effects of the linking chain structure on the metal binding ability of hydroxamate based siderophores. *J Inorg Biochem* 98:1957–1966
- Farkas E, Bátka D, Kremper G, Pócsi I (2008) Structure-based differences between the metal ion selectivity of two siderophores desferrioxamine B (DFB) and desferricoprogen (DFC): why DFC is much better Pb(II) sequestering agent than DFB? *J Inorg Biochem* 102:1654–1659

- Fauchon M, Lagniel G, Aude JC, Lombardia L, Soularue P, Petat C, Marguerie G, Sentenac A, Werner M, Labarre J (2002) Sulfur sparing in the yeast proteome in response to sulfur demand. *Mol Cell* 9:713–723
- Fei L, Wang Y, Chen S (2009) Improved GSH production by gene expression in *Pichia pastoris*. *Bioproc Biosyst Eng* 32:729–735
- Ferrol N, González-Guerrero M, Valderas A, Benabdellah K, Azcón-Aguilar C (2009) Survival strategies of arbuscular mycorrhizal fungi in Cu-polluted environments. *Phytochem Rev* 8:551–559
- Foury F, Talibi D (2001) Mitochondrial control of iron homeostasis. A genome wide analysis of gene expression in a yeast frataxin-deficient strain. *J Biol Chem* 276:7762–7768
- Fraser JA, Davis MA, Hynes MJ (2002) A gene from *Aspergillus nidulans* with similarity to *URE2* of *Saccharomyces cerevisiae* encodes a glutathione S-transferase which contributes to heavy metal and xenobiotic resistance. *Appl Environ Microbiol* 68:2802–2808
- Fujii K, Fukunaga S (2008) Isolation of highly copper-tolerant fungi from the smelter of the Nanobori copper mine, an historic mine in Japan. *J Appl Microbiol* 105:1851–1857
- Fukuda T, Ishino Y, Ogawa A, Tsutsumi K, Morita H (2008) Cr(VI) reduction from contaminated soils by *Aspergillus* sp. N2 and *Penicillium* sp. N3 isolated from chromium deposits. *J Gen Appl Microbiol* 54:295–303
- Gadd GM (2000) Bioremediation potential of microbial mechanisms of metal mobilization and immobilization. *Curr Opin Biotechnol* 11:271–279
- Gadd GM (2010) Metals, minerals and microbes: geomicrobiology and bioremediation. *Microbiology* 156:609–643
- Gakh O, Park S, Liu G, Macomber L, Imlay JA, Ferreira GC, Isaya G (2006) Mitochondrial iron detoxification is a primary function of frataxin that limits oxidative damage and preserves cell longevity. *Hum Mol Genet* 15:467–479
- Gakh O, Smith DY 4th, Isaya G (2008) Assembly of the iron-binding protein frataxin in *Saccharomyces cerevisiae* responds to dynamic changes in mitochondrial iron influx and stress level. *J Biol Chem* 283:31500–31510
- Gardarin A, Chédin S, Lagniel G, Aude JC, Godat E, Catty P, Labarre J (2010) Endoplasmic reticulum is a major target of cadmium toxicity in yeast. *Mol Microbiol* 76:1034–1048
- Gasch AP, Spellman PT, Kao CM, Carmel-Harel O, Eisen MB, Storz G, Botstein D, Brown PO (2000) Genomic expression programs in the response of yeast cells to environmental changes. *Mol Biol Cell* 11:4241–4257
- Gaur A, Adholeya A (2004) Prospects of arbuscular mycorrhizal fungi in phytoremediation of heavy metal contaminated soils. *Curr Sci* 86:528–534
- Gazdag Z, Pócsi I, Belágyi J, Emri T, Blaskó A, Takács K, Pesti M (2003) Chromate tolerance caused by reduced hydroxyl radical production and decreased glutathione reductase activity in *Schizosaccharomyces pombe*. *J Basic Microbiol* 43:96–103
- Georg RC, Gomes SL (2007) Transcriptome analysis in response to heat shock and cadmium in the aquatic fungus *Blastocladiella emersonii*. *Eukaryot Cell* 6:1053–1062
- Gitan RS, Luo H, Rodgers J, Broderius M, Eide D (1998) Zinc-induced inactivation of the yeast ZRT1 zinc transporter occurs through endocytosis and vacuolar degradation. *J Biol Chem* 273:28617–28624
- Gitan RS, Shababi M, Kramer M, Eide DJ (2003) A cytosolic domain of the yeast Zrt1 zinc transporter is required for its post-translational inactivation in response to zinc and cadmium. *J Biol Chem* 278:39558–39564
- Gomes DS, Fragoso LC, Riger CJ, Panek AD, Eleutherio EC (2002) Regulation of cadmium uptake by *Saccharomyces cerevisiae*. *Biochim Biophys Acta* 1573:21–25
- González-Chávez MC, Carrillo-Gonzalez R, Wright SF, Nichols KA (2004) The role of glomalin, a protein produced by arbuscular mycorrhizal fungi, in sequestering potentially toxic elements. *Environ Pollut* 130:317–323
- González-Guerrero M, Azcón-Aguilar C, Mooney M, Valderas A, MacDiarmid CW, Eide DJ, Ferrol N (2005) Characterization of a *Glomus intraradices* gene encoding a putative Zn transporter of the cation diffusion facilitator family. *Fungal Genet Biol* 42:130–140

- González-Guerrero M, Cano C, Azcón-Aguilar C, Ferrol N (2007) *GintMT1* encodes a functional metallothionein in *Glomus intraradices* that responds to oxidative stress. *Mycorrhiza* 17:327–335
- González-Guerrero M, Melville LH, Ferrol N, Lott JN, Azcón-Aguilar C, Peterson RL (2008) Ultrastructural localization of heavy metals in the extraradical mycelium and spores of the arbuscular mycorrhizal fungus *Glomus intraradices*. *Can J Microbiol* 54:103–110
- González-Guerrero M, Benabdellah K, Ferrol N, Azcón-Aguilar C (2009) Mechanisms underlying heavy metal tolerance in arbuscular mycorrhizas. In: Azcón-Aguilar C, Barea JM, Gianinazzi S, Gianinazzi-Pearson V (eds) *Mycorrhizas—Functional Processes and Ecological Impacts*. Springer, Berlin, pp 107–122
- González-Guerrero M, Benabdellah K, Valderas A, Azcón-Aguilar C, Ferrol N (2010a) *GintABC1* encodes a putative ABC transporter of the MRP subfamily induced by Cu, Cd, and oxidative stress in *Glomus intraradices*. *Mycorrhiza* 20:137–146
- González-Guerrero M, Oger E, Benabdellah K, Azcón-Aguilar C, Lanfranco L, Ferrol N (2010b) Characterization of a CuZn superoxide dismutase gene in the arbuscular mycorrhizal fungus *Glomus intraradices*. *Curr Genet* 56:265–274
- Gorfer M, Persak H, Berger H, Brynda S, Bandian D, Strauss J (2009) Identification of heavy metal regulated genes from the root associated ascomycete *Cadophora finlandica* using a genomic microarray. *Mycol Res* 113:1377–1388
- Gross C, Kelleher M, Iyer VR, Brown PO, Winge DR (2000) Identification of the copper regulon in *Saccharomyces cerevisiae* by DNA microarrays. *J Biol Chem* 275:32310–32316
- Guo J, Dai X, Xu W, Ma M (2008) Overexpressing *GSH1* and *AsPCSI* simultaneously increases the tolerance and accumulation of cadmium and arsenic in *Arabidopsis thaliana*. *Chemosphere* 72:1020–1026
- Harris N, Bachler M, Costa V, Mollapour M, Moradas-Ferreira P, Piper PW (2005) Overexpressed Sod1p acts either to reduce or to increase the lifespans and stress resistance of yeast, depending on whether it is Cu²⁺-deficient or an active Cu,Zn-superoxide dismutase. *Aging Cell* 4:41–52
- Haugen AC, Kelley R, Collins JB, Tucker CJ, Deng C, Afshari CA, Brown JM, Ideker T, Van Houten B (2004) Integrating phenotypic and expression profiles to map arsenic-response networks. *Genome Biol* 5:R95
- Hegedűs N, Emri T, Szilágyi J, Karányi Zs, Nagy I, Penninckx MJ, Pócsi I (2007) Effect of heavy metals on the GSH status in different ectomycorrhizal *Paxillus involutus* strains. *World J Microbiol Biotechnol* 23:1339–1343
- Hildebrandt U, Regvar M, Bothe H (2007) Arbuscular mycorrhiza and heavy metal tolerance. *Phytochemistry* 68:139–146
- Hirata D, Yano K, Miyakawa T (1994) Stress-induced transcriptional activation mediated by *YAP1* and *YAP2* genes that encode the Jun family of transcriptional activators in *Saccharomyces cerevisiae*. *Mol Gen Genet* 242:250–256
- Holland S, Lodwig E, Sideri T, Reader T, Clarke I, Gkargkas K, Hoyle DC, Delneri D, Oliver SG, Avery SV (2007) Application of the comprehensive set of heterozygous yeast deletion mutants to elucidate the molecular basis of cellular chromium toxicity. *Genome Biol* 8:R268
- Hong-Bo S, Li-Ye C, Cheng-Jiang R, Hua L, Dong-Gang G, Wei-Xiang L (2010) Understanding molecular mechanisms for improving phytoremediation of heavy metal-contaminated soils. *Crit Rev Biotechnol* 30:23–30
- Hosiner D, Lempiäinen H, Reiter W, Urban J, Loewith R, Ammerer G, Schweyen R, Shore D, Schüller C (2009) Arsenic toxicity to *Saccharomyces cerevisiae* is a consequence of inhibition of the TORC1 kinase combined with a chronic stress response. *Mol Biol Cell* 20:1048–1057
- Hwang GW, Furuchi T, Naganuma A (2007) Ubiquitin-conjugating enzyme Cdc34 mediates cadmium resistance in budding yeast through ubiquitination of the transcription factor Met4. *Biochem Biophys Res Commun* 363:873–878
- Jarosz-Wilkolazka A, Gadd GM (2003) Oxalate production by wood-rotting fungi growing in toxic metal-amended medium. *Chemosphere* 52:541–547

- Jarosz-Wilkolazka A, Graz M, Braha B, Menge S, Schlosser D, Krauss GJ (2006) Species-specific Cd-stress response in the white rot basidiomycetes *Abortiporus biennis* and *Cerrena unicolor*. *Biomaterials* 19:39–49
- Jin YH, Dunlap PE, McBride SJ, Al-Refai H, Bushel PR, Freedman JH (2008) Global transcriptome and deletome profiles of yeast exposed to transition metals. *PLoS Genet* 4:e1000053
- Jo WJ, Loguinov A, Chang M, Wintz H, Nislow C, Arkin AP, Giaever G, Vulpe CD (2008) Identification of genes involved in the toxic response of *Saccharomyces cerevisiae* against iron and copper overload by parallel analysis of deletion mutants. *Toxicol Sci* 101:140–151
- Johnson L (2008) Iron and siderophores in fungal-host interactions. *Mycol Res* 112:170–183
- Kakimoto M, Kobayashi A, Fukuda R, Ono Y, Ohta A, Yoshimura E (2005) Genome-wide screening of aluminum tolerance in *Saccharomyces cerevisiae*. *Biomaterials* 18:467–474
- Kanamasa S, Sumi K, Yamuki N, Kumasaka T, Miura T, Abe F, Kajiwara S (2007) Cloning and functional characterization of the copper/zinc superoxide dismutase gene from the heavy-metal-tolerant yeast *Cryptococcus liquefaciens* strain N6. *Mol Genet Genomics* 277:403–412
- Kang SH, Bozhilov KN, Myung NV, Mulchandani A, Chen W (2008) Microbial synthesis of CdS nanocrystals in genetically engineered *E. coli*. *Angew Chem. Int Ed Engl* 47:5186–5189
- Katsifas EA, Giannoutsou E, Lambraki M, Barla M, Karagouni AD (2004) Chromium recycling of tannery waste through microbial fermentation. *J Ind Microbiol Biotechnol* 31:57–62
- Kennedy PJ, Vashisht AA, Hoe KL, Kim DU, Park HO, Hayles J, Russell P (2008) A genome-wide screen of genes involved in cadmium tolerance in *Schizosaccharomyces pombe*. *Toxicol Sci* 106:124–139
- Khan AG (2005) Role of soil microbes in the rhizospheres of plants growing on trace metal contaminated soils in phytoremediation. *J Trace Elem Med Biol* 18:355–364
- Koós Z, Gazdag Z, Miklós I, Benko Z, Belágyi J, Antal J, Meleg B, Pesti M (2008) Effects of decreased specific glutathione reductase activity in a chromate-tolerant mutant of *Schizosaccharomyces pombe*. *Folia Microbiol* 53:308–314
- Kowshik M, Deshmukh N, Vogel W, Urban J, Kulkarni SK, Paknikar KM (2002) Microbial synthesis of semiconductor CdS nanoparticles, their characterization, and their use in the fabrication of an ideal diode. *Biotechnol Bioeng* 78:583–588
- Krzarnic E, Verbruggen N, Wevers JH, Carleer R, Vangronsveld J, Colpaert JV (2009) Cd-tolerant *Suillus luteus*: a fungal insurance for pines exposed to Cd. *Environ Pollut* 157:1581–1588
- Kumar KS, Dayananda S, Subramanyam C (2005) Copper alone, but not oxidative stress, induces copper-metallothionein gene in *Neurospora crassa*. *FEMS Microbiol Lett* 242:45–50
- Kunstmann B, Osiewacz HD (2009) The S-adenosylmethionine dependent O-methyltransferase PaMTH1: a longevity assurance factor protecting *Podospira anserina* against oxidative stress. *Aging (Albany NY)* 1:328–334
- Kuroda K, Ueda M (2010) Engineering of microorganisms towards recovery of rare metal ions. *Appl Microbiol Biotechnol* 87:53–60
- Lanfranco L, Balsamo R, Martino E, Perotto S, Bonfante P (2002a) Zinc ions alter morphology and chitin deposition in an ericoid fungus. *Eur J Histochem* 46:341–350
- Lanfranco L, Bolchi A, Ros EC, Ottonello S, Bonfante P (2002b) Differential expression of a metallothionein gene during the presymbiotic versus the symbiotic phase of an arbuscular mycorrhizal fungus. *Plant Physiol* 130:58–67
- Lanfranco L, Balsamo R, Martino E, Bonfante P, Perotto S (2004) Zinc ions differentially affect chitin synthase gene expression in an ericoid mycorrhizal fungus. *Plant Biosyst* 138:271–277
- Lasat MM (2002) Phytoextraction of toxic metals: a review of biological mechanisms. *J Environ Qual* 31:109–120
- Lebeau T, Braud A, Jézéquel K (2008) Performance of bioaugmentation-assisted phytoextraction applied to metal contaminated soils: a review. *Environ Pollut* 153:497–522
- Lewinska A, Bartosz G (2007) Protection of yeast lacking the Ure2 protein against the toxicity of heavy metals and hydroperoxides by antioxidants. *Free Radic Res* 41:580–590
- Li L, Chen OS, McVey Ward D, Kaplan J (2001) CCC1 is a transporter that mediates vacuolar iron storage in yeast. *J Biol Chem* 276:29515–29519

- Li L, Bagley D, Ward DM, Kaplan J (2008) Yap5 is an iron-responsive transcriptional activator that regulates vacuolar iron storage in yeast. *Mol Cell Biol* 28:1326–1337
- Liang Q, Zhou B (2007) Copper and manganese induce yeast apoptosis via different pathways. *Mol Biol Cell* 18:4741–4749
- Liu XF, Culotta VC (1999) Post-translation control of Nramp metal transport in yeast. Role of metal ions and the *BSD2* gene. *J Biol Chem* 274:4863–4868
- Liu XF, Supek F, Nelson N, Culotta VC (1997) Negative control of heavy metal uptake by the *Saccharomyces cerevisiae* *BSD2* gene. *J Biol Chem* 272:11763–11769
- Lyons TJ, Gasch AP, Gaitherm LA, Botstein D, Brown PO, Eide DJ (2000) Genome-wide characterization of the Zap1p zinc-responsive regulon in yeast. *Proc Natl Acad Sci U S A* 97:7957–7962
- Lyons TJ, Villa NY, Regalla LM, Kupchak BR, Vagstad A, Eide DJ (2004) Metalloregulation of yeast membrane steroid receptor homologs. *Proc Natl Acad Sci U S A* 101:5506–5511
- MacDiarmid CW, Gaither LA, Eide D (2000) Zinc transporters that regulate vacuolar zinc storage in *Saccharomyces cerevisiae*. *EMBO J* 19:2845–2855
- Maciaszczyk-Dziubinska E, Migdal I, Migocka M, Bocser T, Wysocki R (2010) The yeast aquaglyceroporin Fps1p is a bidirectional arsenite channel. *FEBS Lett* 584:726–732
- Maheswari S, Murugesan AG (2009) Remediation of arsenic in soil by *Aspergillus nidulans* isolated from an arsenic-contaminated site. *Environ Technol* 30:921–926
- Mai C, Kües U, Miltitz H (2004) Biotechnology in the wood industry. *Appl Microbiol Biotechnol* 63:477–494
- Mannazzu I, Guerra E, Ferretti R, Pediconi D, Fatichenti F (2000) Vanadate and copper induce overlapping oxidative stress responses in the vanadate-tolerant yeast *Hansenula polymorpha*. *Biochim Biophys Acta* 1475:151–156
- Marion RM, Regev A, Segal E, Barash Y, Koller D, Friedman N, O’Shea EK (2004) Sfp1 is a stress- and nutrient-sensitive regulator of ribosomal protein gene expression. *Proc Natl Acad Sci U S A* 101:14315–14322
- Marques AP, Rangel AO, Castro PM (2009) Remediation of heavy metal contaminated soils: phytoremediation as a potentially promising clean-up technology. *Crit Rev Environ Sci Technol* 39:622–654
- Medicherla B, Goldberg AL (2008) Heat shock and oxygen radicals stimulate ubiquitin-dependent degradation mainly of newly synthesized proteins. *J Cell Biol* 182:663–673
- Mejäre M, Bülow L (2001) Metal-binding proteins and peptides in bioremediation and phytoremediation of heavy metals. *Trends Biotechnol* 19:67–73
- Mendoza-Cózatl D, Loza-Tavera H, Hernández-Navarro A, Moreno-Sánchez R (2005) Sulfur assimilation and glutathione metabolism under cadmium stress in yeast, protists and plants. *FEMS Microbiol Rev* 29:653–671
- Migdal I, Ilina Y, Tamás MJ, Wysocki R (2008) Mitogen-activated protein kinase Hog1 mediates adaptation to G1 checkpoint arrest during arsenite and hyperosmotic stress. *Eukaryot Cell* 7:1309–1317
- Miskei M, Karányi Z, Pócsi I (2009) Annotation of stress-response proteins in the aspergilli. *Fungal Genet Biol* 46:S105–S120
- Momose Y, Iwahashi H (2001) Bioassay of cadmium using a DNA microarray: genome-wide expression patterns of *Saccharomyces cerevisiae* response to cadmium. *Environ Toxicol Chem* 20:2353–2360
- More TT, Yan S, Tyagi RD, Surampalli RY (2010) Potential use of filamentous fungi for wastewater sludge treatment. *Bioresour Technol* 101:7691–7700
- Mukherjee A, Das D, Kumar Mondal S, Biswas R, Kumar Das T, Boujedaini N, Khuda-Bukhs AR (2010) Tolerance of arsenate-induced stress in *Aspergillus niger*, a possible candidate for bioremediation. *Ecotoxicol Environ Saf* 73:172–182
- Muller LA, Craciun AR, Ruytinx J, Lambaerts M, Verbruggen N, Vangronsveld J, Colpaert JV (2007) Gene expression profiling of a Zn-tolerant and a Zn-sensitive *Suillus luteus* isolate exposed to increased external zinc concentrations. *Mycorrhiza* 17:571–580
- Mulligan CN, Kamali M, Gibbs BF (2004) Bioleaching of heavy metals from a low-grade mining ore using *Aspergillus niger*. *J Hazard Mater* 110:77–84

- Nagy Z, Montigny C, Leverrier P, Yeh S, Goffeau A, Garrigos M, Falson P (2006) Role of the yeast ABC transporter Yor1p in cadmium detoxification. *Biochimie* 88:1665–1671
- Nargund AM, Avery SV, Houghton JE (2008) Cadmium induces a heterogeneous and caspase-dependent apoptotic response in *Saccharomyces cerevisiae*. *Apoptosis* 13:811–821
- Oddon DM, Diatloff E, Roberts SK (2007) A CLC chloride channel plays an essential role in copper homeostasis in *Aspergillus nidulans* at increased extracellular copper concentrations. *Biochim Biophys Acta* 1768:2466–2477
- Ono BI, Ishii N, Fujino S, Aoyama I (1991) Role of hydrosulfide ions (HS⁻) in methylmercury resistance in *Saccharomyces cerevisiae*. *Appl Environ Microbiol* 57:3183–3186
- Orłowska E, Mesjasz-Przybyłowicz J, Przybyłowicz W, Turnau K (2008) Nuclear microprobe studies of elemental distribution in mycorrhizal and non-mycorrhizal roots of Ni-hyperaccumulator *Berkheya coddii*. *XRay Spectrom* 37:129–132
- Ortiz DF, Ruscitti T, McCue KF, Ow DW (1995) Transport of metal-binding peptides by HMT1, a fission yeast ABC-type vacuolar membrane protein. *J Biol Chem* 270:4721–4728
- Osaki Y, Shirabe T, Tamura S, Yoshimura E (2008) A functional putative phytochelatin synthase from the primitive red alga *Cyanidioschyzon merolae*. *Biosci Biotechnol Biochem* 72:3306–3309
- Ott T, Fritz E, Polle A, Schützendübel A (2002) Characterisation of antioxidative systems in the ectomycorrhiza-building basidiomycete *Paxillus involutus* (Bartsch) Fr. and its reaction to cadmium. *FEMS Microbiol Ecol* 42:359–366
- Ouziad F, Hildebrandt U, Schmelzer E, Bothe H (2005) Differential gene expressions in arbuscular mycorrhizal-colonized tomato grown under heavy metal stress. *J Plant Physiol* 162:634–649
- Pagani MA, Casamayor A, Serrano R, Atrian S, Ariño J (2007) Disruption of iron homeostasis in *Saccharomyces cerevisiae* by high zinc levels: a genome-wide study. *Mol Microbiol* 65:521–537
- Pan R, Cao L, Zhang R (2009) Combined effects of Cu, Cd, Pb, and Zn on the growth and uptake of consortium of Cu-resistant *Penicillium* sp. A1 and Cd-resistant *Fusarium* sp. A19. *J Hazard Mater* 171:761–766
- Paraszkiewicz K, Długoński J (2009) Effect of nickel, copper, and zinc on emulsifier production and saturation of cellular fatty acids in the filamentous fungus *Curvularia lunata*. *Int Biodeter Biodegr* 63:100–105
- Paraszkiewicz K, Frycie A, Słaba M, Długoński J (2007) Enhancement of emulsifier production by *Curvularia lunata* in cadmium, zinc and lead presence. *Biometals* 20:797–805
- Paraszkiewicz K, Bernat P, Naliwajski M, Długoński J (2010) Lipid peroxidation in the fungus *Curvularia lunata* exposed to nickel. *Arch Microbiol* 192:135–141
- Pereira Y, Lagniel G, Godat E, Baudouin-Cornu P, Junot C, Labarre J (2008) Chromate causes sulfur starvation in yeast. *Toxicol Sci* 106:400–412
- Perrone GG, Grant CM, Dawes IW (2005) Genetic and environmental factors influencing GSH homeostasis in *Saccharomyces cerevisiae*. *Mol Biol Cell* 16:218–230
- Pesti M, Gazdag Z, Emri T, Farkas N, Koósz Z, Belágyi J, Pócsi I (2002) Chromate sensitivity in fission yeast is caused by increased glutathione reductase activity and peroxide overproduction. *J Basic Microbiol* 42:408–419
- Pinson B, Sagot I, Daignan-Fornier B (2000) Identification of genes affecting selenite toxicity and resistance in *Saccharomyces cerevisiae*. *Mol Microbiol* 36:679–687
- Pócsi I, Prade RA, Penninckx MJ (2004) GSH, altruistic metabolite in fungi. *Adv Microb Physiol* 49:1–76
- Pócsi I, Miskei M, Karányi Z, Emri T, Ayoubi P, Pusztahelyi T, Balla G, Prade RA (2005) Comparison of gene expression signatures of diamide, H₂O₂ and menadione exposed *Aspergillus nidulans* cultures-linking genome-wide transcriptional changes to cellular physiology. *BMC Genomics* 6:182
- Pócsi I, Jeney V, Kertai P, Pócsi I, Emri T, Gyémánt G, Fésüs L, Balla J, Balla G (2008) Fungal siderophores function as protective agents of LDL oxidation and are promising anti-atherosclerotic metabolites in functional food. *Mol Nutr Food Res* 52:1434–1447

- Poljšak B, Gazdag Z, Jenko-Brinovec Š, Fujs Š, Pesti M, Bélagyi J, Plesničar S, Raspor P (2005) Pro-oxidative vs antioxidative properties of ascorbic acid in chromium(VI)-induced damage: an *in vivo* and *in vitro* approach. *J Appl Toxicol* 25:535–548
- Poljšak B, Pócsi I, Raspor P, Pesti M (2010) Interference of chromium with biological systems in yeasts and fungi: a review. *J Basic Microbiol* 50:21–36
- Portnoy ME, Liu XF, Culotta VC (2000) *Saccharomyces cerevisiae* expresses three functionally distinct homologues of the nramp family of metal transporters. *Mol Cell Biol* 20:7893–7902
- Prasad K, Jham AK (2010) Biosynthesis of CdS nanoparticles: an improved green and rapid procedure. *J Colloid Interface Sci* 342:68–72
- Prévéral S, Gayet L, Moldes C, Hoffmann J, Mounicou S, Gruet A, Reynaud F, Lobinski R, Verbatz JM, Vavasseur A, Forestier C (2009) A common highly conserved cadmium detoxification mechanism from bacteria to humans: heavy metal tolerance conferred by the ATP-binding cassette (ABC) transporter SpHMT1 requires GSH but not metal-chelating phytochelatin peptides. *J Biol Chem* 284:4936–4943
- Price MS, Classen JJ, Payne GA (2001) *Aspergillus niger* absorbs copper and zinc from swine wastewater. *Bioresour Technol* 77:41–49
- Purakayastha TJ, Chhonkar PK (2010) Phytoremediation of heavy metal contaminated soils. In: Sherameti I, Varma A (eds) *Soil heavy metals*. Springer, Berlin, pp 389–429
- Purin S, Rillig MC (2008) Immuno-cyto-localization of glomalin in the mycelium of the arbuscular mycorrhizal fungus *Glomus intraradices*. *Soil Biol Biochem* 40:1000–1003
- Pynyaha YV, Boretskym YR, Fedorovych DV, Fayura LR, Levkiv AI, Ubivovk VM, Protchenko OV, Philpott CC, Sibirny AA (2010) Deficiency in frataxin homologue YFH1 in the yeast *Pichia guilliermondii* leads to misregulation of iron acquisition and riboflavin biosynthesis and affects sulfate assimilation. *Biometals* 22:1051–1061
- Rajendran P, Ashokkumar B, Muthukrishnan J, Gunasekaran P (2002) Toxicity assessment of nickel using *Aspergillus niger* and its removal from an industrial effluent. *Appl Biochem Biotechnol* 102–103:201–206
- Ramesh G, Podila GK, Gay G, Marmeisse R, Reddy MS (2009) Different patterns of regulation for the copper and cadmium metallothioneins of the ectomycorrhizal fungus *Hebeloma cylindrosporum*. *Appl Environ Microbiol* 75:2266–2274
- Ramos J, Clemente MR, Naya L, Loscos J, Pérez-Rontomé C, Sato S, Tabata S, Becana M (2007) Phytochelatin synthases of the model legume *Lotus japonicus*. A small multigene family with differential response to cadmium and alternatively spliced variants. *Plant Physiol* 143:1110–1118
- Rea PA, Vatamaniuk OK, Rigden DJ (2004) Weeds, worms, and more. Papain's long-lost cousin, phytochelatin synthase. *Plant Physiol* 136:2463–2474
- Rees EM, Lee J, Thiele DJ (2004) Mobilization of intracellular copper stores by the ctr2 vacuolar copper transporter. *J Biol Chem* 279:54221–54229
- Reisinger S, Schiavon M, Terry N, Pilon-Smits EA (2008) Heavy metal tolerance and accumulation in Indian mustard (*Brassica juncea* L.) expressing bacterial γ -glutamylcysteine synthetase or glutathione synthetase. *Int J Phytoremediation* 10:440–454
- Ren WX, Li PJ, Geng Y, Li XJ (2009) Biological leaching of heavy metals from a contaminated soil by *Aspergillus niger*. *J Hazard Mater* 167:164–169
- Rodrigues-Pousada C, Menezes RA, Pimentel C (2010) The Yap family and its role in stress response. *Yeast* 27:245–258
- Ruotolo R, Marchini G, Ottonello S (2008) Membrane transporters and protein traffic networks differentially affecting metal tolerance: a genomic phenotyping study in yeast. *Genome Biol* 9:R67
- Salin H, Fardeau V, Piccini E, Lelandais G, Tanty V, Lemoine S, Jacq C, Devaux F (2008) Structure and properties of transcriptional networks driving selenite stress response in yeasts. *BMC Genomics* 9:333
- Sandana Mala JG, Unni Nair B, Puvanakrishnan R (2006) Bioaccumulation and biosorption of chromium by *Aspergillus niger* MTCC 2594. *J Gen Appl Microbiol* 52:179–186
- Sankaran S, Khanal SK, Jasti N, Jin B, Pometto III AL, Van Leeuwen JH (2010) Use of filamentous fungi for wastewater treatment and production of high value fungal byproducts: a review. *Crit Rev Environ Sci Technol* 40:400–449

- Scheckhuber CQ, Mitterbauer R, Osiewacz HD (2009) Molecular basis of and interference into degenerative processes in fungi: potential relevance for improving biotechnological performance of microorganisms. *Appl Microbiol Biotechnol* 85:27–35
- Schlosser D, Höfer C (2002) Laccase-catalyzed oxidation of Mn^{2+} in the presence of natural Mn^{3+} chelators as a novel source of extracellular H_2O_2 production and its impact on manganese peroxidase. *Appl Environ Microbiol* 68:3514–3521
- Schrettl M, Bignell E, Kragl C, Sabiha Y, Loss O, Eisendle M, Wallner A, Arst HN Jr, Haynes K, Haas H (2007) Distinct roles for intra- and extracellular siderophores during *Aspergillus fumigatus* infection. *PLoS Pathog* 3:1195–1207
- Schrettl M, Kim HS, Eisendle M, Kragl C, Nierman WC, Heinekamp T, Werner ER, Jacobsen I, Illmer P, Yi H, Brakhage AA, Haas H (2008) SreA-mediated iron regulation in *Aspergillus fumigatus*. *Mol Microbiol* 70:27–43
- Schützendübel A, Polle A (2002) Plant responses to abiotic stresses: heavy metal-induced oxidative stress and protection by mycorrhization. *J Exp Bot* 53:1351–1365
- Seguin A, Bayot A, Dancis A, Rogowska-Wrzesinska A, Auchère F, Camadro JM, Bulteau AL, Lesuisse E (2009) Overexpression of the yeast frataxin homolog (Yfh1): contrasting effects on iron-sulfur cluster assembly, heme synthesis and resistance to oxidative stress. *Mitochondrion* 9:130–138
- Seguin A, Sutak R, Bulteau AL, Garcia-Serres R, Oddou JL, Lefevre S, Santos R, Dancis A, Camadro JM, Latour JM, Lesuisse E (2010) Evidence that yeast frataxin is not an iron storage protein *in vivo*. *Biochim Biophys Acta* 1802:531–538
- Serero A, Lopes J, Nicolas A, Boiteux S (2008) Yeast genes involved in cadmium tolerance: identification of DNA replication as a target of cadmium toxicity. *DNA Repair (Amst)* 7:1262–1275
- Shakoury-Elizeh M, Tiedeman J, Rashford J, Ferea T, Demeter J, Garcia E, Rolfes R, Brown PO, Botstein D, Philpott CC (2004) Transcriptional remodeling in response to iron deprivation in *Saccharomyces cerevisiae*. *Mol Biol Cell* 15:1233–1243
- Shakoury-Elizeh M, Protchenko O, Berger A, Cox J, Gable K, Dunn TM, Prinz WA, Bard M, Philpott CC (2010) Metabolic response to iron deficiency in *Saccharomyces cerevisiae*. *J Biol Chem* 285:14823–14833
- Sharma KG, Mason DL, Liu G, Rea PA, Bachhawat AK, Michaelis S (2002) Localization, regulation, and substrate transport properties of Bpt1p, a *Saccharomyces cerevisiae* MRP-type ABC transporter. *Eukaryot Cell* 1:391–400
- Sharma S, Malik A, Satya S (2009) Application of response surface methodology (RSM) for optimization of nutrient supplementation for Cr (VI) removal by *Aspergillus lentulus* AML05. *J Hazard Mater* 164:1198–1204
- Sheoran V, Sheoran AS, Poonia P (2009) Phytomining: A review. *Minerals Eng* 22:1007–1019
- Sierra-Alvarez R (2007) Fungal bioleaching of metals in preservative-treated wood. *Proc Biochem* 42:798–804
- Sierra-Alvarez R (2009) Removal of copper, chromium and arsenic from preservative-treated wood by chemical extraction-fungal bioleaching. *Waste Manag* 29:1885–1891
- Simate GS, Ndlovu S, Walubita LF (2010) The fungal and chemolithotrophic leaching of nickel laterites—challenges and opportunities. *Hydrometallurgy* 103:150–157
- Song WY, Sohn EJ, Martinoia E, Lee YJ, Yang YY, Jasinski M, Forestier C, Hwang I, Lee Y (2003) Engineering tolerance and accumulation of lead and cadmium in transgenic plants. *Nat Biotechnol* 21:914–919
- Srikanth CV, Vats P, Bourbouloux A, Delrot S, Bachhawat AK (2005) Multiple cis-regulatory elements and the yeast sulphur regulatory network are required for the regulation of the yeast GSH transporter, Hgt1p. *Curr Genet* 47:345–358
- Srinivasan C, Liba A, Imlay JA, Valentine JS, Gralla EB (2000) Yeast lacking superoxide dismutase(s) show elevated levels of “free iron” as measured by whole cell electron paramagnetic resonance. *J Biol Chem* 275:29187–29192
- Srivastava S, Thakur IS (2006) Isolation and process parameter optimization of *Aspergillus* sp. for removal of chromium from tannery effluent. *Bioresour Technol* 97:1167–1173
- Stadler JA, Schweyen RJ (2002) The yeast iron regulon is induced upon cobalt stress and crucial for cobalt tolerance. *J Biol Chem* 277:39649–39654

- Stephen DW, Jamieson DJ (1997) Amino acid-dependent regulation of the *Saccharomyces cerevisiae* *GSH1* gene by hydrogen peroxide. *Mol Microbiol* 23:203–210
- Stroobants A, Delroisse JM, Delvigne F, Delva J, Portetelle D, Vandenberg M (2009) Isolation and biomass production of a *Saccharomyces cerevisiae* strain binding copper and zinc ions. *Appl Biochem Biotechnol* 157:85–97
- Summer ER, Shanmuganathan A, Sideri TC, Willetts SA, Houghton JE, Avery SV (2005) Oxidative protein damage causes chromium toxicity in yeast. *Microbiology* 151:1939–1948
- Sun YM, Horng CY, Chang FL, Cheng LC, Tian WX (2010) Biosorption of lead, mercury, and cadmium ions by *Aspergillus terreus* immobilized in a natural matrix. *Pol J Microbiol* 59:37–44
- Swami D, Buddhi D (2006) Removal of contaminants from industrial wastewater through various non-conventional technologies: a review. *Int J Environ Pollut* 27:324–346
- Tamás MJ, Labarre J, Toledano MB, Wysocki R (2005) Mechanisms of toxic metal tolerance in yeast. In: Tamás MJ, Martinoia E (eds) *Molecular biology of metal homeostasis and detoxification: from microbes to man*. Springer, Heidelberg, pp 395–454
- Taştan BE, Ertuğrul S, Dönmez G (2010) Effective bioremoval of reactive dye and heavy metals by *Aspergillus versicolor*. *Bioresour Technol* 101:870–876
- Thomas JC, Davies EC, Malick FK, Endreszl C, Williams CR, Abbas M, Petrella S, Swisher K, Perron M, Edwards R, Osenkowski P, Urbanczyk N, Wiesend WN, Murray KS (2003) Yeast metallothionein in transgenic tobacco promotes copper uptake from contaminated soils. *Biotechnol Prog* 19:273–280
- Thorsen M, Di Y, Tängemo C, Morillas M, Ahmadpour D, Van der Does C, Wagner A, Johansson E, Boman J, Posas F, Wysocki R, Tamás MJ (2006) The MAPK Hog1p modulates Fps1p-dependent arsenite uptake and tolerance in yeast. *Mol Biol Cell* 17:4400–4410
- Thorsen M, Lagniel G, Kristiansson E, Junot C, Nerman O, Labarre J, Tamás MJ (2007) Quantitative transcriptome, proteome, and sulfur metabolite profiling of the *Saccharomyces cerevisiae* response to arsenite. *Physiol Genomics* 30:35–43
- Thorsen M, Perrone GG, Kristiansson E, Traini M, Ye T, Dawes IW, Nerman O, Tamás MJ (2009) Genetic basis of arsenite and cadmium tolerance in *Saccharomyces cerevisiae*. *BMC Genomics* 10:105
- Todorova D, Nedeva D, Abrashev R, Tsekova K (2008) Cd(II) stress response during the growth of *Aspergillus niger* B 77. *J Appl Microbiol* 104:178–184
- Tóth V, Antal K, Gyémánt G, Miskei M, Pócsi I, Emri T (2009) Optimization of coprogen production in *Neurospora crassa*. *Acta Biol Hung* 60:321–328
- Urbanowski JL, Piper RC (1999) The iron transporter Fth1p forms a complex with the Fet5 iron oxidase and resides on the vacuolar membrane. *J Biol Chem* 274:38061–38070
- Vallino M, Martino E, Boella F, Murat C, Chiapello M, Perotto S (2009) Cu,Zn superoxide dismutase and zinc stress in the metal-tolerant ericoid mycorrhizal fungus *Oidiodendron maius* Zn. *FEMS Microbiol Lett* 293:48–57
- Vashisht AA, Kennedy PJ, Russell P (2009) Centaurin-like protein Cnt5 contributes to arsenic and cadmium resistance in fission yeast. *FEMS Yeast Res* 9:257–269
- Vatamaniuk OK, Bucher EA, Ward JT, Rea PA (2001) A new pathway for heavy metal detoxification in animals. Phytochelatin synthase is required for cadmium tolerance in *Caenorhabditis elegans*. *J Biol Chem* 276:20817–20820
- Verma VC, Kharwar RN, Gange AC (2010) Biosynthesis of antimicrobial silver nanoparticles by the endophytic fungus *Aspergillus clavatus*. *Nanomedicine (Lond)* 5:33–40
- Vesentini D, Dickinson DJ, Murphy RJ (2006) Fungicides affect the production of fungal extracellular mucilaginous material (ECMM) and the peripheral growth unit (PGU) in two wood-rotting basidiomycetes. *Mycol Res* 110:1207–1213
- Vido K, Spector D, Lagniel G, Lopez S, Toledano MB, Labarre J (2001) A proteome analysis of the cadmium response in *Saccharomyces cerevisiae*. *J Biol Chem* 276:8469–8474
- Villegas LB, Amoroso MJ, de Figueroa LI, Sñeriz F, Sñeriz F (2009) Cu(II) removal by *Rhodotorula mucilaginosa* RCL-11 in sequential batch cultures. *Water Sci Technol* 60:1225–1232

- Wang J, Chen C (2006) Biosorption of heavy metals by *Saccharomyces cerevisiae*: a review. *Biotechnol Adv* 24:427–451
- Wang ZY, He XP, Zhang BR (2007) Over-expression of *GSH1* gene and disruption of *PEP4* gene in self-cloning industrial brewer's yeast. *Int J Food Microbiol* 119:192–199
- Wang ZY, Wang JJ, Liu XF, He XP, Zhang BR (2009) Recombinant industrial brewing yeast strains with *ADH2* interruption using self-cloning *GSH1+CUPI* cassette. *FEMS Yeast Res* 9:574–581
- Wang X, Xu H, Ha SW, Ju D, Xie Y (2010) Proteasomal degradation of Rpn4 in *Saccharomyces cerevisiae* is critical for cell viability under stressed conditions. *Genetics* 184:335–342
- Warmka J, Hanneman J, Lee J, Amin D, Ota I (2001) Ptc1, a type 2C Ser/Thr phosphatase, inactivates the HOG pathway by dephosphorylating the mitogen-activated protein kinase Hog1. *Mol Cell Biol* 21:51–60
- Wawrzyński A, Kopera E, Wawrzyńska A, Kamińska J, Bal W, Sirko A (2006) Effects of simultaneous expression of heterologous genes involved in phytochelatin biosynthesis on thiol content and cadmium accumulation in tobacco plants. *J Exp Bot* 57:2173–2182
- Weiersbye IM, Straker CJ, Przybyłowicz WJ (1999) Micro-PIXE mapping of elemental distribution in arbuscular mycorrhizal roots of the grass, *Cynodon dactylon*, from gold and uranium mine tailings. *Nucl Instrum Methods Phys Res Sec B* 158:335–343
- Wemmie JA, Szczyпка MS, Thiele DJ, Moye-Rowley WS (1994) Cadmium tolerance mediated by the yeast AP-1 protein requires the presence of an ATP-binding cassette transporter-encoding gene, *YCF1*. *J Biol Chem* 269:32592–32597
- Westwater J, McLaren NF, Dormer UH, Jamieson DJ (2002) The adaptive response of *Saccharomyces cerevisiae* to mercury exposure. *Yeast* 19:233–239
- Wright SF, Franke-Snyder M, Morton JB, Upadhyaya A (1996) Time-course study and partial characterization of a protein on hyphae of arbuscular mycorrhizal fungi during active colonization of roots. *Plant Soil* 181:193–203
- Wu AL, Moye-Rowley WS (1994) *GSH1*, which encodes γ -glutamylcysteine synthetase, is a target gene for yAP-1 transcriptional regulation. *Mol Cell Biol* 14:5832–5839
- Wu CY, Bird AJ, Chung LM, Newton MA, Winge DR, Eide DJ (2008) Differential control of Zap1-regulated genes in response to zinc deficiency in *Saccharomyces cerevisiae*. *BMC Genomics* 9:370
- Wu G, Kang H, Zhang X, Shao H, Chu L, Ruan C (2010) A critical review on the bio-removal of hazardous heavy metals from contaminated soils: issues, progress, eco-environmental concerns and opportunities. *J Hazard Mater* 174:1–8
- Wurgler-Murphy SM, Maeda T, Witten EA, Saito H (1997) Regulation of the *Saccharomyces cerevisiae* HOG1 mitogen-activated protein kinase by the PTP2 and PTP3 protein tyrosine phosphatases. *Mol Cell Biol* 17:1289–1297
- Wysocki R, Tamás MJ (2010) How *Saccharomyces cerevisiae* copes with toxic metals and metalloids. *FEMS Microbiol Rev* 34:925–951
- Wysocki R, Bobrowicz P, Ułaszewski S (1997) The *Saccharomyces cerevisiae* *ACR3* gene encodes a putative membrane protein involved in arsenite transport. *J Biol Chem* 272:30061–30066
- Wysocki R, Chéry CC, Wawrzycka D, Van Hulle M, Cornelis R, Thevelein JM, Tamás MJ (2001) The glycerol channel Fps1p mediates the uptake of arsenite and antimonite in *Saccharomyces cerevisiae*. *Mol Microbiol* 40:1391–1401
- Wysocki R, Clemens S, Augustyniak D, Golik P, Maciaszczyk E, Tamás MJ, Dziadkowiec D (2003) Metalloid tolerance based on phytochelatin is not functionally equivalent to the arsenite transporter Acr3p. *Biochem Biophys Res Commun* 304:293–300
- Wysocki R, Fortier PK, Maciaszczyk E, Thorsen M, Leduc A, Odhagen A, Owsianik G, Ułaszewski S, Ramotar D, Tamás MJ (2004) Transcriptional activation of metalloid tolerance genes in *Saccharomyces cerevisiae* requires the AP-1-like proteins Yap1p and Yap8p. *Mol Biol Cell* 15:2049–2060
- Yamaguchi-Iwai Y, Dancis A, Klausner RD (1995) AFT1: a mediator of iron regulated transcriptional control in *Saccharomyces cerevisiae*. *EMBO J* 14:1231–1239

- Yang HC, Pon LA (2003) Toxicity of metal ions used in dental alloys: a study in the yeast *Saccharomyces cerevisiae*. *Drug Chem Toxicol* 26:75–85
- Yasokawa D, Murata S, Kitagawa E, Iwahashi Y, Nakagawa R, Hashido T, Iwahashi H (2008) Mechanisms of copper toxicity in *Saccharomyces cerevisiae* determined by microarray analysis. *Environ Toxicol* 23:599–606
- Yompakdee C, Bun-ya M, Shikata K, Ogawa N, Harashima S, Oshima Y (1996) A putative new membrane protein, Pho86p, in the inorganic phosphate uptake system of *Saccharomyces cerevisiae*. *Gene* 171:41–47
- Zhang B, Georgiev O, Haggmann M, Günes C, Cramer M, Faller P, Vasák M, Schaffner W (2003) Activity of metal-responsive transcription factor 1 by toxic heavy metals and H₂O₂ *in vitro* is modulated by metallothionein. *Mol Cell Biol* 23:8471–8485
- Zhou S, Fushinobu S, Kim SW, Nakanishim Y, Wakagi T, Shoun H (2010) *Aspergillus oryzae* flavohemoglobins promote oxidative damage by hydrogen peroxide. *Biochem Biophys Res Commun* 394:558–561
- Zhu YL, Pilon-Smits EA, Jouanin L, Terry N (1999a) Overexpression of glutathione synthetase in indian mustard enhances cadmium accumulation and tolerance. *Plant Physiol* 119:73–80
- Zhu YL, Pilon-Smits EA, Tarun AS, Weber SU, Jouanin L, Terry N (1999b) Cadmium tolerance and accumulation in Indian mustard is enhanced by overexpressing γ -glutamylcysteine synthetase. *Plant Physiol* 121:1169–1178

Chapter 3

Interference of Chromium with Cellular Functions

Borut Poljsak, István Pócsi and Miklós Pesti

Abstract Cr(VI) reduction may proceed outside the cell, but most of the Cr(VI)-induced genotoxic and membrane damages are accounted for by the reductive metabolism taking place intracellularly. The uptake of chromium ions by fungi is a biphasic process. The first step is known as biosorption, a metabolic energy-independent process that takes only a few minutes, but hinges on cellular parameters. The second, bioaccumulation step is much slower, also a metabolism-dependent process depending among others on pH, temperature, the ratio of the initial metal ion concentration and the presence of metabolic inhibitors. The bioaccumulation of heavy metals provided a useful means to remove heavy metal pollutants from water. Noticeable differences in absorption activity of different yeast species initiated further investigations to optimize relevant parameters for Cr biosorption. These studies focused on the transport of Cr(VI) and Cr(III) through non-selective and selective ion channels and yeast chromium mutants that are able to take up very low concentrations of chromium. This uptake-reduction model helps to explain the generation of reactive oxygen species (ROS), which are primarily responsible for the cytotoxicity and explain mutagenic and cancerogenic effect of Cr(VI).

Introduction

Chromium and Environment

Chromium (Cr) is abundant in the environment, occurring naturally in soils, rocks and living organisms. Cr exists primarily in either two valent (Cr(II)), trivalent (Cr(III)) and hexavalent (Cr(VI)) states, the latter being primarily produced by an-

M. Pesti (✉)

Department of General and Environmental Microbiology, University of Pécs,

6 Ifjúság Street, 7624 Pécs, Hungary

Tel.: +36-72-501-573

Fax: +36-72-501-573

e-mail: pmp@gamma.ttk.pte.hu

trophogenic sources (O'Brien et al. 2003). Cr(III) and Cr(VI) are generated by many different industries including welding, chrome plating, chrome pigmenting, ferrochrome industry and leather tanning (Fishbein 1981). Because of its wide industrial use, environmental contamination is an additional source of human exposure to this metal. It is estimated that several thousand workers are potentially exposed to high levels of Cr(VI) (IARC 1997). Occupational exposure to Cr (Cr(III), Cr(VI)) by inhalation depends on the job function and type of industry, but can reach several hundred micrograms per cubic meter (IARC 1997). These estimated exposures have been significantly lowered in the past few decades as industrial hygiene practices and worker protection have been implemented. Non-occupational exposure to Cr results from automobile emissions and cigarette smoke. It has been estimated by the International Agency for Research on Cancer (IARC) that on the average, cigarettes produced in United States contain 0.24–6.3 mg Cr/kg (IARC 1997). In the environment, elevated levels of Cr have been reported in areas near landfills, hazardous waste disposal sites, chromate industries and highways (O'Brien et al. 2003).

It is estimated that the atmospheric concentration of particulate chromates in rural or residential areas of the US ranges from 0.2 to 9 ng/m³ (O'Brien et al. 2003). In urban areas, especially in the vicinity of ferrochrome industries, Cr concentrations can easily be 10–100 times higher (O'Brien et al. 2003). If we assume that an urban dweller in a city with a ferrochrome production receives an inhalation of 20 m³ of 90 ng/m³ Cr per day, then the daily lung intake is 1.8 µg per day. As previously mentioned, this dose of particulates is not distributed evenly throughout the lungs but concentrates at major bifurcations (O'Brien et al. 2003). Although, much more information of public health significance of environmental Cr(VI) exposure is needed, the possibility exists that adverse health effects are not exclusively restricted to occupational Cr(VI) exposure. Since chromium is still a significant environmental pollutant with potential impact on human health, this chapter will review basic chromium chemistry; the uptake of chromium by yeast and fungi- as models to investigate and explain the ROS generation and chromium induced cito-, geno- and carcinogenic effects; chromium human health risk assessment versus chromium essentiality; as well as strategies to prevent or repair Cr-induced damage.

Many mammalian cell line studies have already been used to investigate chromium induced toxicity. On the other hand, we would like to review the significance and applicability of yeast-based models to map the molecular background of Cr(VI) toxicity because it is important in many aspects, also in relation to human risk assessment due to chromium exposure. Yeasts are relatively simple, genetically and biochemically well characterized and easy-to-handle microorganisms. Yeasts have been favorite eukaryotic organisms in the past years due to wide range of genetic approaches available. Yeast cells have remarkable similarities to mammalian cells at the macromolecular and organelle level, and a number of yeast proteins have been shown to be functionally interchangeable with highly homologous human proteins. Thus, it is not surprising that yeast cells were used as model organisms with relevant contribution to understand the molecular mechanisms underlying oxidative stress resistance (Costa and Moradas-Ferreira 2001). The application of yeasts as model organisms has shed considerable light on the mechanisms by which higher

eukaryotes cope with Cr(VI) toxicity, in consequence of high degree of functional conservation among *Saccharomyces cerevisiae*, *Schizosaccharomyces pombe* and human oxidative stress protection gene products (Hohmann and Mager 2003), allowing the results to be extrapolated to humans. Additionally, tumour cells, which are frequently used in toxicological studies, generally exhibit an abnormal redox balance and are prone to both ROS production and apoptotic cell death (Jackson and Loeb 2001), which may lead to misleading results when any kind of oxidative stress is being studied. Additionally, genes from higher eukaryotes can be functionally expressed in yeasts, suggesting that structural and functional conservation during evolution has occurred. For this reasons, experiments involving the use of yeasts as model organisms could have important advantages. Much of what we learned from the oxidative stress induced responses of microbes will undoubtedly have an important influence on our understanding of the mechanisms by which mammals and other higher eukaryotes cope with oxidative stress and oxidative damage. However, there are also differences between yeast and higher eukaryotes, especially when it comes to cell envelope. Yeast cells are surrounded by a thick cell wall built from glucans, chitin and mannoproteins (Klis et al. 2002; Lipke and Ovalle 1998). It serves to maintain cell shape and integrity (Cid et al. 1995) but it can pose problems when yeasts are used for research because data obtained on yeast cells cannot be simply extrapolated on higher eukaryotes since cell wall can influence the intracellular transport of investigated compounds.

Extracellular Reduction of Chromate

The reduction of Cr(VI) by sulphate-reducing bacteria has been reported (Smith 2001; Shakoory and Makhdoom 2000; Schmieman et al. 2000; Rahman et al. 2000, 2007). Various other research groups (Wang et al. 1989; Kvasuikova et al. 1984; Ishibishi et al. 1990; Fude and Shigui 1992) have demonstrated that bacterial strains such as *Pseudomonas* sp., *Enterobacter* sp. and *Desulfovibrio* sp. also have the ability to transform Cr(VI) to Cr(III). Acevedo-Aguilar et al. (2006) studied the reduction of Cr(VI) by a Cr(VI)-resistant strain of the filamentous fungus Ed8 (an *Aspergillus* sp.), indigenous to contaminated industrial wastes. This strain has the capability to reduce Cr(VI) present in the growth medium without accumulating it in the biomass, but the reduced Cr end-products have not been characterized.

The central tenet of Cr(VI)-induced DNA damage and genotoxicity is that a reductive metabolism must take place intracellularly (EPA 1998; Katz and Salem 1994; Kirpnick-Sobol et al. 2006). However, Cr(VI) reduction may also proceed outside the cell. The extracellular reduction of Cr(VI) to Cr(III) is regarded as a detoxification process because Cr(III) crosses the cell membrane at a much slower rate than Cr(VI). However, certain Cr(V) and Cr(III) complexes generated extracellularly may have high permeabilities and consequently may penetrate into the cell and cause intracellular damage. The possible incorporation of such species from the environment and their genotoxicity have been analysed by means of the SOS test in *Salmonella typhimurium* (Nakamura et al. 1987). The SOS test is based on the

ability of genotoxic chemicals to induce *umu* gene expression in the tester strain of *S. typhimurium* TA 1535/pSK1002, in which an *umuC-lacZ* fusion gene has been introduced. Thus the potentials of chemicals to induce SOS response and, hence, their genotoxicity can be quantified by measuring β -galactosidase activity spectrophotometrically. However, the extracellular reduction of Cr(VI) with different antioxidants did not increase the β -galactosidase activity, which led to the conclusion that reduction of Cr(VI) to Cr(III) with different antioxidants is a detoxification reaction (Poljsak et al. 2005). Similarly, the extracellular reduction of Cr(VI) with antioxidants increased the viability of *S. cerevisiae* (Poljsak 2004).

Metal Ion Uptake by Yeasts and Fungi

The uptake of metal ions by fungi is in general a biphasic process. The first step, frequently referred to as biosorption, is a metabolism-, and metabolic energy-independent process that requires only a few minutes, but depends considerably on parameters such as pH, temperature, the ratio of the initial metal ion and the initial biomass concentrations, the culturing conditions, and the presence of various ligands and competitive metal ions in solution. The microbial cell wall, the outer surface of the plasma membrane and, sometimes, extracellular polymers are involved in this process, via interactions with functional groups situated on the surface of the cells, such as carboxyl, phosphate, hydroxy, amino, thio, thiolo, *etc.* The processes of passive biosorption involve coordination, complexation, physical adsorption (*e.g.* electrostatic or London-van der Waals forces), ion-exchange, inorganic precipitation and redox reactions. The second step, bioaccumulation, is a slower, metabolism-dependent process that hinges on the temperature and the presence of metabolism inhibitors. However, the two steps of uptake cannot be exactly separated from each other in *in vivo* experiments (for reviews, see Wang and Chen 2006; Blackwell et al. 1995; White and Gadd 1995; Rosen 2002).

Biosorption of Chromium

Bacterial and fungal biosorption is a technique that can be used for removal of metal pollutants from water (see for reviews Kapoor and Viraraghavan 1995; Wang and Chen 2006; Viraraghavan and Yun 2008). The biosorption of Cr(VI) by differently dehydrated yeast species displays noticeable differences. *Candida utilis* demonstrates the highest biosorption activity, with the intact cells exhibiting less activity in sorption. The kinetics of the process depends on the temperature and the initial concentration of Cr(VI). The initial, rapid biosorption step takes place within 10 min (Pesti et al. 2000). This step is similar in *S. pombe* Cr(VI)-tolerant and parental mutant strains, but 4 times more Cr(VI) is taken up by the Cr(VI)-sensitive mutant, which reveals the difficulty in separating the biosorption and bioaccumulation processes in living cells (Czakó-Vér et al. 1999). A combination of Pb(II) or Cu(II) and CrO_4^{2-} displays a synergistic effect for Cr(VI) sorption,

whereas Cd(II) and Zn(II) inhibit Cr(VI) sorption by *C. utilis* cells (Mutter et al. 2002). The distribution of Cr(VI) between the cell wall and the spheroplast of a 12 h culture of *Candida intermedia* was 4.3 ± 0.6 ($\mu\text{g g}^{-1}$ dry cell mass) and 14.9 ± 3.0 ($\mu\text{g g}^{-1}$ dry cell mass), respectively, demonstrating the bioabsorption capacity of actively growing intact cells (Pas et al. 2004). The effect of pH on biosorption has been investigated in detail in tests on a variety of different types of biomasses. The optimum removal of Cr(VI) was reported at pH 2.0 and 1.0 for *Rhizopus nigricans* and *S. cerevisiae*, respectively (Özer and Özer 2003). Yeast cells modified by a cationic surfactant achieved maximum Cr(VI) removal at pH 5.5 (Bingol et al. 2004). Mapoleno and Torto (2004) demonstrated that the optimum pH for Cr(III) removal with budding yeast is 5.2. The temperature influences biosorption via the ion-exchange mechanism, but the results related to the biosorption of Cr(VI) in *S. cerevisiae* are controversial. Özer and Özer (2003) reported the optimum temperature to be 25°C, whereas Goyal et al. (2003) found that Cr(VI) sorption increased with increasing temperature in the range between 25 and 45°C. The results with dead fungal biomass (*Aspergillus niger*, *Rhizopus oryzae*, *Penicillium chrysogenum* and *S. cerevisiae*) suggested that the mechanism of Cr(VI) removal involved a redox reaction (Park et al. 2005; Sag and Kutsal 1996). The biosorption of Cr(VI) by *Mucor hiemalis* biomass has been reported to follow pseudo-second-order kinetics (Tewari et al. 2005).

These findings clearly demonstrate that it is highly desirable to investigate and optimize all relevant parameters related to the available fungal biomass when its application for Cr biosorption is considered.

Bioaccumulation of Chromium

Biological membranes are practically impermeable for Cr(III). On the other hand, Cr(III) readily forms complexes in aqueous solution with most biologically relevant ligand molecules, and these complexes may be taken up by cells. Cr(III) within cells participates in DNA–DNA cross-linking (Snow and Xu 1989), DNA–protein cross-linking (Kortenkamp et al. 1992), DNA condensation, and decreases DNA replication fidelity (Bridgewater et al. 1994). Cr(III) species have low toxicity, in part because their bioavailability is limited by their low solubility and by the tendency of dissolved Cr(III) to be adsorbed by organic carbon (Cohen et al. 1993; Batic and Raspor 1998). Cr(VI) exists mainly as the tetrahedral CrO_4^{2-} , analogous to physiological anions such as SO_4^{2-} and PO_4^{2-} . They enter cells through the same non-selective and oxidative state-sensitive anion channel via facilitated diffusion (Borst-Pauwells 1981). Not surprisingly, sulphate transport mutants of *Neurospora crassa* exhibit Cr(VI) resistance, and Cr(VI) toxicity against *Candida* and *Saccharomyces* species is modulated by inorganic and organic sulphur species (Marzluf 1970; Pepi and Baldi 1992). Recently, Pereira et al. (2008) found that chromate enters the cells mainly through sulfate transporters and competitively inhibits sulfate uptake in yeast *S. cerevisiae*. Also consistent with a competition between the two substrates, sulfate supplementation relieves chromate toxicity. Additionally, authors

show that chromate causes a strong decrease of sulfate assimilation and sulfur metabolite pools suggesting that cells experience sulfur starvation. As a consequence, nearly all enzymes of the sulfur pathway are highly induced as well as enzymes of the sulfur-sparing response.

Cr(VI) is rapidly reduced to Cr(III) inside cells (Corbett et al. 1998; Arslan et al. 1987) and the concentration of Cr in the Cr(VI) oxidation state will therefore never be equal on the two sides of a plasma membrane (as long as the cells have a satisfactory reducing capacity). Practically all Cr(VI) anions will be taken up by the cells from their surroundings (Kortenkamp et al. 1992; Mutter et al. 2001; Ksheminska et al. 2005), that explains why even a very low Cr(VI) concentration can cause the death of a cell population (Czakó-Vér et al. 2004), and why Cr-containing media cannot be used for the direct selection of chromium mutants and transformants at a single cell level (Koósz et al. 2008). Consequently, the reduction capacity of the cells is the main power of Cr(VI) bioaccumulation.

The uptake-reduction model was proposed by Wetterhahn and Hamilton (1989) to explain Cr(VI) carcinogenicity. After entering cell, Cr(VI) is reduced to Cr(III) by antioxidative enzymes and small molecular mass antioxidants such as GSH, ascorbate, vitamin E, cysteine, NADPH, saccharides, hydroxylic acids, *etc.*, with the concomitant formation of Cr(V/VI) complexes and various organic radicals, all of which are potentially DNA-damaging agents (Cieslak-Golonka 1995). A number of *in vitro* experiments have demonstrated that the reactive intermediates Cr(V) and Cr(IV), and also Cr(III), can generate harmful ROS quite effectively during their re-oxidation processes through the Fenton and Haber–Weiss reactions. The reaction products include H_2O_2 , superoxide anion ($O_2^{\bullet-}$) and hydroxyl radical ($\bullet OH$), which are primarily responsible for the cyto- and genotoxicity of Cr(VI). These processes proved to be valid for all living cell types (O'Brien and Kortenkamp 1996; Cieslak-Golonka and Daszkiewicz 2005; Codd et al. 2001; Shi et al. 1998, 1999). Cr(VI) accumulates mainly in the cytosolic compartment of cells (Ksheminska et al. 2005; Ghareb and Gadd 1998) and causes morphological changes in the cell surface (Mutter et al. 2001). As far as the genomic responses to the oxidative stress generated by Cr(VI) are concerned, the consequences are not known.

Cellular Interactions of Chromium

Interactions of Chromium with Plasma Membrane

Plasma membrane damage is one of the key factors in metal ion cytotoxicity. It generally involves a sudden alteration of membrane biophysical parameters (e.g. order parameter, phase transition temperature, etc.), increase in membrane permeability, resulting in a rapid loss of intracellular ions or, just the opposite, an enhanced accumulation of extracellular ions. Loss of building blocks of macromolecules (e.g. amino acids, nucleic acid basis etc.) or even intracellular enzymes can

be detected (Pesti et al. 2000). Membrane damages may also arise from changes in the activities of important membrane-bound enzymes, these activities being markedly dependent on their membrane-lipid environments (Pesti et al. 1981). The peroxidation of polyunsaturated fatty acids and the oxidation of membrane components (e.g. ergosterol, and proteins) may also contribute to the increased membrane permeability and by this way to the cytotoxicity of heavy metal ions. All these alterations may induce an array of signal transduction pathways (Cieslak-Golonka and Daszkiewicz 2005). However, the mechanism of action of the metal ion in question depends essentially on its chemical nature, the pH alteration caused by the metal ion, the membrane composition of the tested organism, and the experimental conditions employed.

In aqueous solution and at physiological pH (~7.4), Cr(VI) exists predominantly (~96%) as its tetrahedral anion CrO_4^{2-} . Before Cr(VI) enters cells, it is partly reduced by the biomolecules of the cell wall (e.g. polysaccharides and manno-proteins) and the plasma membrane (e.g. S-containing organic ligands) (Cieslak-Golonka and Daszkiewicz 2005). It has been proven in *in vitro* experiments that, unlike Cr(III), Cr(VI) does not form complexes with biologically relevant molecules (Corbett et al. 1998). The biosorption of Cr(VI) in yeasts and fungi by the cell wall and surface molecules of the plasma membrane may also be accompanied by the reduction of Cr(VI). Membrane-associated Cr(VI) reductase has been identified in *Bacillus megaterium*, *Pseudomonas putida*, and *Escherichia coli* (Cheung and Gu 2007), but corresponding data are not available for yeasts or fungi.

The effects of Cr(VI) on the plasma membrane have been investigated by electron paramagnetic resonance (EPR) spectroscopy in Cr-sensitive and -tolerant mutants of *S. pombe*. In all cases, treatment of the cell wall-free protoplast membranes with Cr(VI) increased the rotation mobility of the spin labels and decreased the phase-transition temperatures of the structural changes, clearly indicating an increased membrane fluidity in the strains studied. 5-Doxylstearic acid (5-SASL) and 3-doxylbutyric acid (HO-185) spin probes were used to label the membranes. A more pronounced effect of Cr(VI) was detected on HO-185-labelled membranes than on 5-SASL-labelled membranes. This observation furnished evidence that Cr(VI)-elicited membrane perturbations are mostly localized at the lipid-water interfaces. Although, the primary target of Cr(VI) and its reduced derivatives is the plasma membrane in yeasts, the interactions between the Cr and membrane constituents are not determinative in Cr toxicity processes (Belágyi et al. 1999; Farkas et al. 2003).

Importantly, Cr(III) significantly increased the fluidity of spin-labelled membranes of a *Candida albicans* ergosterol-producing (*33erg⁺*) strain and its ergosterol-deficient (*erg-2*) mutant, but the increased fluidity did not result in any visible changes in the plasma membrane structure, as revealed by freeze-etch electron microscopy (Pesti et al. 2000). It seems that the Cr(III) cation has preferred localization in the negatively charged regions of the membranes, and tends to create bridges between the phospholipids molecules and the side-chains of negatively charged amino acid residues. These interactions reduce the stability of the head group regions of the membranes, decrease rotational energy barriers for spin probes, and possibly affect the bound layer of phospholipids around the mem-

brane proteins. The absence of ergosterol in the *erg-2* mutant led to significantly increased levels of polyunsaturated fatty acids (16:3 and 18:3) (Pesti et al. 1985). This way, the heavy metal stress-induced lipid peroxidation might contribute to both the fluidification and the decreased membrane barrier function in Cr(III)-treated cells, which is in accord with the findings of Howlett and Avery (1997). Cr(III) treatment at the minimal inhibitory concentration (MIC=100 mM) caused a loss of metabolites absorbing at 260 nm, which amounted to 40 and 60% in the *33erg⁺* and *erg-2* strains, respectively. This decryptification process may be the main cause of growth inhibition and cell killing by Cr(III) ions in *C. albicans* (Pesti et al. 2000).

In general, the rapid and metabolism-independent biosorption step of chromate ion uptake by fungi is associated with the generation of reactive Cr(V) and Cr(IV) intermediates and complex-forming Cr(III) ions. Cr(V) and Cr(IV) species and Cr(III) complexes induce lipid peroxidation, and also effective and irreversible inhibition of the enzymes localized in the plasma membrane (e.g. Ca²⁺-ATPase and phosphatase). All these physiological changes together will lead to fluidization of the plasma membrane, loss of the plasma membrane barrier function and/or cell death (Al-Asheh and Duvjak 1995; Blackwell et al. 1995; Rapaport and Muter 1995; Moreira et al. 2005; Wang and Chen 2006).

ROS Formation During Intracellular Cr(VI) Metabolism

The chemistry of intracellular reduction of chromium and the role of oxygen species have been the subjects of intense debates for over 20 years (reviewed by O'Brien and Kortenkamp 1996). Cr(VI) compounds are highly toxic and carcinogenic compared to Cr(III) because Cr(VI), in contrast to Cr(III) (octahedral form), can cross cellular membranes via nonspecific anion carriers, such as SO₄²⁻ and PO₄³⁻ (Wenbo et al. 2000). The chromate anion (CrO₄²⁻) (which is the form of tetrahedral chromate anion) is structurally similar to the sulfate (SO₄²⁻) and hydrogen phosphate (HPO₄³⁻) anions, which are actively transported through cell membranes. Due to this similarity, chromate can easily penetrate the plasma membrane by normal cell anion transport system. Cr(III) ions can cross the membranes only very slowly via simple diffusion or phagocytosis. As already mentioned, once Cr(VI) enters the cell, it is reduced by certain molecules such as ascorbic acid (Connett and Wetterhahn 1983; Goodgame and Joy 1988), glutathione (Cupo and Wetterhahn 1985; O'Brien et al. 1985; Shi and Dalal 1988; Kitagawa et al. 1988), cysteine (Kitagawa et al. 1988), hydrogen peroxide (Kawanishi et al. 1986), riboflavin (Sugiyama et al. 1989), and flavoenzymes (De Flora et al. 1985; Banks and Cooke 1986) such as glutathione reductase (Koutras et al. 1964, 1965; Shi and Dalal 1989), to generate Cr(V). During this reduction process, molecular oxygen is reduced to superoxide (O₂^{•-}), which generates hydrogen peroxide (H₂O₂) via dismutation (Stearns and Wetterhahn 1994). The resultant Cr(V) reacts with H₂O₂ to generate the hydroxyl radical (OH[•]) via the Fenton-like reaction (Shi and Dalal 1990a, b). Among chromium species inside cells the Cr(V) species have been

shown to be long-lived reactive intermediates (Goodgame and Joy 1988; Jennette 1982) and to cause DNA breaks (Kawanishi et al. 1986; Rodney et al. 1989) *in vitro* as well as mutation in bacterial cells (Kawanishi et al. 1986). Thus, during the stepwise one-electron reduction of Cr(VI) to the final stable product Cr(III), a whole spectrum of reactive oxygen species (ROS) is generated. Any of these species could potentially target the DNA molecule. Through ROS-mediated reactions, Cr(VI) is able to cause oxidative damage to the DNA molecule. Many types of DNA damage caused by Cr(VI) have been observed *in vivo* and *in vitro*, including interstrand cross-links, DNA–protein cross-links (Borges and Wetterhahn 1989; Zhitkovich et al. 1996), single strand breaks (Kortenkamp et al. 1992, Aiyar et al. 1990), Cr-DNA adducts (Klein et al. 1998), and radical DNA adducts, most notably 8-hydroxydeoxy-guanosine (8-OHdG) (Tsou et al. 1996). This wide spectrum of DNA damage suggests that multiple mechanisms are necessary to adequately account for all of the observed lesions. The “ultimate” lesion, or lesions, responsible for the initiation or promotion of cancer by this metal is likewise unknown, and selection of one specific mechanism over another has primarily been researcher-dependent. The determination of a mechanistic pathway of cancer by Cr(VI) has been further complicated by multiple ROS generated during intracellular metabolism (reduction) of the metal complex.

Mechanisms of Chromium Sensitivity and Resistance

All cell types have the ability to respond to undesirable environmental changes in the concentrations of toxic metal ions which induce stress response. These responses involve sensing and signal transduction, leading to adaptation of the cells to adjustments of the gene expression profile, metabolic activities and other features (Hohmann and Mager 2003; Chen and Shi 2002; Harris and Shi 2003). Significant differences can be observed between naturally-occurring yeast species belonging in various taxonomic groups as regards their sensitivity and resistance (or tolerance) to Cr(VI), Cr(III) and other metal ions. This can be explained in terms of the diversity in genetic background during evolution. Organisms have devised two major strategies to protect themselves against heavy metal ion toxicity. The first one is avoidance, by restricting metal ion entry into the cell, either by a reduced uptake/active efflux or by the formation of complexes outside the cells. The second strategy is sequestration, to reduce the levels of free ions in the cytosol, either by the synthesis of ligands to achieve intracellular chelation/reduction or by compartmentalization into vacuoles (Ksheminska et al. 2005; Nies 1992; Tomsett 1993; Ksheminska et al. 2006). A number of genes, gene products and metabolites, and also regulatory processes, have already been identified and described in detail for various heavy metals, including Cd, Cu, *etc.* (for reviews, see Pócsi et al. 2004; Liu and Thiele 1997; Perego and Howell 1997; Chen et al. 2003; Mendoza-Cózatl et al. 2005; Hildebrand et al. 2007).

To investigate the mode of action of metal ions and their detoxification processes, mutants with altered metal ion sensitivity have been generated and widely used.

The first Cr-resistant mutants of the fungus *Neurospora crassa* were obtained by induced mutagenesis. Mutants resistant to Cr(VI) displayed deficiencies in sulphate transport and parallel losses in Cr(VI) uptake (Marzluf 1970; Roberts and Marzluf 1971). Slightly reduced rates of Cr(VI) uptake were also detected in Cr(VI)-resistant mutants of *S. cerevisiae* by Ono and Weng (1982). The Baldi group selected *Candida* sp. and *Rhodospiridium toruloides* strains from Cr-contaminated industrial wastes (Baldi et al. 1990). Three Cr(VI)-resistant strains exhibited significantly reduced bioaccumulation of Cr(VI) but their resistance was modified by the facilitation of sulphate transport (Pepi and Baldi 1992, 1995; Baldi et al. 1990). Increased Cr(VI), selenite and tellurite sensitivities were detected in vacuole mutants of *S. cerevisiae*, emphasizing the importance of functionally active vacuoles in heavy metal resistance (Ghaireb and Gadd 1998).

Cr(VI)-tolerant (*chr1-66T*) and -sensitive (*chr-51S*) mutants of *S. pombe* heterothallic strains (h^+ , h^-) have been obtained by induced mutagenesis. In contrast with earlier findings, these mutants demonstrated various patterns of cross-sensitivity to Cd^{2+} , Cu^{2+} , Ni^{2+} and VO_4^3 . The rapid transport of $^{51}Cr(VI)$ and high bioaccumulation ability of chromium with a dry biomass of $810 \mu g g^{-1}$ after 30 min were detected in the sensitive *chr-51S* mutant, in contrast with its parental *chr6^+* strain and the tolerant *chr1-66T* mutant (Czakó-Vér et al. 1999, 2004). The chromate tolerant *chr1-66T* mutant was sensitive to oxidative stress-generating agents such as H_2O_2 , menadione, *tert*-butyl hydroperoxide and Cd^{2+} . Both the Cr(VI) tolerance and the oxidative stress sensitivity were attributed to decreased specific glutathione reductase (GR) and mitochondrial superoxide dismutase (Mn-SOD) activities (Pesti et al. 2002; Gazdag et al. 2003). As expected, the mutant cells were characterized by significantly decreased GSH and elevated intracellular superoxide concentrations. When the chromium tolerant *chr1-66T* mutant was transformed with a GR-expressing non-integrative vector the chromium tolerance was lost (Koósz et al. 2008). No difference was detected in the sequences of the *pgr1^+* that codes the enzyme GR (Lee et al. 1997) and *pap1^+*, a transcriptional regulatory gene of GR (Ikner and Shiozaki 2005) genes in comparison with the parental strain *chr6^+*. These observations indicate that downregulation of the GR activity in the Cr(VI)-tolerant mutant might be a consequence of a mutation in the mitogen-activated protein kinase signal transduction system (Koósz et al. 2008).

In spite of the decreased GSH concentration, the Cr(VI)-sensitive *chr-51S* mutant exhibited an elevated Cr(V)-reducing activity together with increased intracellular superoxide and peroxide concentrations, suggesting that its Cr(VI) sensitivity was a consequence of an increased Cr(VI) uptake catalysed by an enhanced GR activity and, hence, an increased OH-producing ability (Pesti et al. 2002).

It is reasonable to assume that the Cr(VI) sensitivity/resistance (tolerance) of a given strain would be changed if the genes responsible for Cr(VI) uptake, GSH metabolism or intracellular peroxide and superoxide production are altered, whereby the oxido-reduction system of the cell will be overbalanced (Pesti et al. 2000, 2002; Gazdag et al. 2003; Pócsi et al. 2004). A global “uptake-reduction” model has been established by Wetterhahn et al. (1989), that is a generally accepted description of chromate transport into cells and induction of DNA damage. Recently,

a single, novel pathway mediating the toxicity of chromate was elucidated. Holland et al. (2007) demonstrated that mRNA mistranslation is a primary cause of cellular Cr toxicity of yeast mutants. Results of their study indicate that proteasomal (protein degradation) activity is crucial for cellular chromium (Cr) resistance. Further investigations showed that Cr causes the accumulation of insoluble and toxic protein aggregates, which predominantly arise from proteins synthesized during Cr exposure. A protein-synthesis defect provoked by Cr was identified as mRNA mistranslation, which was oxygen-dependent. Additionally, it was confirmed that Cr-induced S starvation is the cause of mRNA mistranslation (Holland et al. 2010).

The ability of Cr(VI) to oxidize biomolecules with the formation of Cr(III) complexes is believed to be responsible for the mutagenicity and carcinogenicity of Cr(VI) (Lay and Levina 1998). However, neither Cr(VI) nor Cr(III) alone cause significant DNA damage (which is a necessary but not a sufficient first step *en route* to cancer (Lay and Levina 1998). Wetterhahn and co-workers were the first to propose that reactive Cr(V) and Cr(IV) intermediates, formed during the course of Cr(VI) reactions with intracellular reductants, may be the DNA-damaging species (Connett and Wetterhahn 1983). Indeed, treatments of isolated DNA with Cr(VI) in the presence of reductants (ascorbic acid and GSH) led to various kinds of DNA damage. Liu and Thiele (1997) showed that Cr(V) complexes were generated in living organisms exposed to Cr(VI), supporting the hypothesis about the role of Cr(V) and possibly Cr(IV) intermediates in Cr(VI)-induced genotoxicities (Lay and Lavina 1998). One of the experimental evidences that favours the idea that molecular oxygen plays a role in Cr-induced genotoxicity was the finding that Cr(VI) induced mutations in certain strains of *Salmonella* only in the presence of O₂ (Sugden et al. 1990). Kortenkamp et al. (1996; Lay and Levina 1998) have shown that the absence of O₂ (or the presence of catalase) strongly reduces the *in vitro* DNA damage induced by the Cr(VI)+ascorbic acid or GSH system. Zhang and Lay (1996) and Lay and Levina (1998) provided electron paramagnetic resonance (EPR) spectroscopic evidence for the formation of Cr(V)-peroxo and peroxo-ascorbato complexes during the Cr(VI) reduction by ascorbic acid in aerated aqueous media. Maximal concentrations of Cr(V) peroxo species correlated with the conditions of maximal DNA damage *in vitro* in Cr(VI)+ascorbic acid system. Contrary to all these developments, the oxidation state of chromium and the radical species responsible for the formation of DNA damage upon reduction is unknown (Sugden and Stearns 2000). The elucidation of these mechanisms and species responsible for the formation of oxidative DNA lesions upon Cr(VI) treatment remains to be solved.

At physiological pH level, Cr(VI) reduction is controlled kinetically rather than thermodynamically. In general, there are two pathways for Cr(VI) reduction. First, a series of one electron reductions may occur, predominately at rather low relative levels of reductants, producing the intermediate Cr(V) and Cr(IV) species and, ultimately, Cr(III) (Stearns et al. 1995a). In contrast, when the intracellular reductant level is higher than that of Cr(VI), the initial step involves a two electron reduction to Cr(IV), followed by one electron reduction to Cr(III). During the reductive metabolism of Cr(VI), the oxidation of reductants can lead to ROS and produce

secondary toxicological effects (e.g. DNA strand breakage, DNA adducts) (Stearns et al. 1994, 1995a).

In contrast to Cr(VI) classified as a toxic element, some compounds of chromium are essential micronutrients (Mertz 1969; Katz and Salem 1993). Dietary deficiency of chromium has been associated with impaired growth and fertility, a diabetic-like state connected to impaired glucose tolerance, hyperinsulinemia, hypercholesterolemia and enhanced atherogenesis (Katz and Salem 1993). In experimental animals, chromium deficiency decreased their life-spans (Katz and Salem 1993).

Interactions of Chromium with Biomolecules

Cr in its hexavalent state (Cr(VI)) exhibits very little biological activity (i.e. interaction with cellular macromolecules) in toxicologically relevant concentrations. The interactions of Cr in different oxidation states with metabolites (biological reductants) and biopolymers (proteins, nucleic acids) were studied in numerous *in vitro* and *in vivo* systems (reviewed by Codd et al. 2001). At physiological pH, Cr(VI) interacts with GSH, normally present in eukaryotic cells in millimolar concentrations (Codd et al. 2001; Pócsi et al. 2004). GSH is regarded as an intramolecular stabilizer of Cr(VI) via the formation of thiolate esters in a rapid equilibrium step, followed by a slow reduction of Cr(VI) to highly reactive Cr(V) species (Connett and Wetterhahn 1983; Borges et al. 1991). Cr(VI) may also form thiolate esters with other low molecular mass thiols, including γ -glutamylcysteine, *N*-acetylcysteine and L-cysteine (Brauer et al. 1996). Additionally, a wide range of other biomolecules are capable of reducing Cr(VI).

The oxidation state of Cr(V), Cr(V)-diolato bindings between Cr(V) species and the *cis*-diolato group of ribose in single ribonucleotides (e.g. NAD(P)H) are of biological relevance in stabilizing the highly reactive Cr(V) species under physiological conditions (Goodgame and Joy 1986; Liu and Thiele 1997).

Whereas our knowledge on possible interactions of Cr(IV) species with biomolecules is rather limited (Codd et al. 2001), there is an increasing body of evidence related to the bulk formation of reductant-Cr(III)-DNA and amino acid-Cr(III)-DNA adducts during the intracellular reduction of Cr(VI) species (Kortenkamp et al. 1991, 1992; Zhitkovich et al. 1996; Quievryn et al. 2001).

Mechanism of Chromium Toxicity

Many lines of research have suggested the involvement of ROS and, in particular, the hydroxyl radical in the DNA damage promoted by Cr(VI) reduction. Much of the evidence for ROS-induced intracellular DNA damage is based on either (1) formation of oxidized DNA products, (2) *in vitro* formation of ROS during Cr(VI) reduction with a cellular reductant and hydrogen peroxide, and (3) formation of cellular oxidative stress as measured by oxidant-sensitive intracellular dyes and

activation of oxidative damage inducible genes (Sugden and Stearns 2000). While there is a significant body of evidence for ROS formation during Cr(VI) reduction, an alternative to this radical mediated process of oxidative DNA damage is a metal-mediated mechanism. For example, the intracellular dye used to define intracellular ROS formation 2,7-dichlorofluorescein can be directly oxidized by high valent chromium complexes such as Cr(V) *in vitro* (Martin et al. 1998). On the other hand ROS associated oxidative damage may be incidental rather than a cause of toxicity (Avery 2001), and the principal causes of most metal toxicities remain to be resolved unequivocally (Holland and Avery 2009). Transport of chromate anions into cells is known to occur via plasma membrane sulfate transporters (Alexander and Aaseth 1995; Pereira et al. 2008). Resultant competition between chromate and sulfate for uptake can lead to sulfur starvation in yeast (Pereira et al. 2008). Thus, sulfur starvation would represent a ROS independent mechanism of Cr toxicity, alternative to DNA damage. Additionally, recent work of Holland and Avery (2009) on yeasts showed that actin-mediated endocytosis is required to limit intracellular Cr accumulation and to help resist Cr toxicity during chromate stress.

Risk Assessment in Human Exposure to Cr(VI)

Risk assessment is the process for the identification and quantification of the risk resulting from a specific use or occurrence of a chemical, taking into account possible harmful effects on individual people or society of using the chemical in the amount and manner proposed and all the possible routes of exposure. In the estimation of the risks, three or more steps are involved, including hazard identification, dose–response analysis, exposure quantification. Toxicity tests are integrated in risk estimation and are mainly obtained with experimental animals and *in vitro* models (e.g. acute test (LC-50 or LD-50), short-term test, semi-chronic test, chronic test (N.E.L. or N.O.E.L.), tests on special effects: eye and skin irritation, sensitization, reproduction, teratogenicity, mutagenicity and carcinogenicity. Problems arise from extrapolating results from experimental animals or cell lines to humans, and/or from high to lower doses. In addition, the differences between individuals due to genetics or other factors mean that the hazard may be higher for particular groups, called susceptible populations. For this reason, safety factors are considered, typically a factor of 10 for each unknown step. There are many chromium toxicity tests reported on different test organisms but such detailed information would exceed the scope of this chapter.

The general population is exposed to total chromium (generally chromium (III)) by eating food, drinking water, and inhaling air that contains the chemical. Regarding the scope of risk assessment, oral ingestion via drinking water is the main source of chromium(VI) intake; provided a 1 L/day of water consumption of children (15 kg b.w.) and 2 L/day water consumption of adults (60 kg b.w.).

While Cr(VI) is classified as a toxic element, some compounds of chromium are believed to be essential micronutrients (Mertz 1969 cited by Katz and Salem

1993). Chromium(VI) is widely known to cause allergic dermatitis as well as toxic and carcinogenic effects in animals and humans. Although, chromium(V) has been identified as an ultimate carcinogen, investigators have demonstrated that Cr(V) complexes, produced in the reduction of Cr(VI) by cellular reductants, generate hydroxyl radicals and cause DNA damage (Zafra-Stone 2007).

The biological effects associated with Cr exposure are diverse and depend upon metal speciation. Exposure to only certain Cr(VI)-containing compounds is associated with an increased risk of lung cancer. IARC classifies Cr(VI)-containing compounds as Group 1 human carcinogens as they are encountered in certain occupational settings (IARC 1997). Nevertheless, not all Cr(VI)-containing compounds are carcinogenic. As early as in the middle of the 20th century some epidemiologists noted that the relatively insoluble hexavalent Cr compounds presented the greatest carcinogenic risk (Machle and Gregorius 1948 cited by O'Brien et al. 2003). Levy et al. (1986) found that the most soluble chromates (i.e. potassium chromate (K_2CrO_4) and the most insoluble chromates (i.e. $PbCrO_4$) were the least carcinogenic, whereas chromates with intermediate solubility (i.e. $ZnCrO_4$) were the most carcinogenic. The majority of *in vitro* carcinogenesis experiments with soluble chromates show a negative outcome which has been attributed to the vast extracellular reducing capacity of Cr(VI) in mammals (O'Brien et al. 2003). In contrast, low solubility particles adhere to lung epithelial cells and slowly release high concentrations of Cr(VI) on the cell surface. Thus, it is generally accepted that Cr is specifically a respiratory tract carcinogen when particulate forms are inhaled at relatively high doses for long periods of time.

The toxicity of Cr(VI) via the inhalation and ingestion are the main routes of exposure and have been examined in several species, including humans with occupational, accidental or suicidal exposures (WHO 1997; Paustenbach 2002).

Inhalation

There might be an increased risk associated to Cr(VI) exposure through inhalation. This relates to neutral pH and limited reduction capacity of the mucous and lung fluids (EPA 1998).

Following inhalation exposure, animal studies have shown that 20–30% of the administered Cr(VI) is absorbed via the respiratory tract. Contrary to ingestion, inhalation route has low capacity defense mechanisms to protect the lung from Cr(VI) toxicity.

According to EPA (1998) a number of factors can influence the absorption of chromium following inhalation, including the size, oxidation state, and solubility of the chromium particles, the activity of alveolar macrophages and the interaction of chromium with biomolecules following deposition in the lung. Absorption of inhaled chromium following occupational exposure has been demonstrated by measurement of chromium in the serum, urine, and hair of workers in the chromium industry (EPA 1998).

Also when inhaled, a significant difference between Cr(VI) and Cr(III) toxicity is observed. When rats were exposed to potassium dichromate (VI) and Cr(III) trichloride by inhalation, Cr(VI) was absorbed more efficiently than Cr(III) (EPA 1998).

Another possible root of exposure is exposure to airborne aerosols produced from contaminated ground water. Finley et al. (1997, in Paustenbach 2002) made shower air measurement to evaluate the significance of Cr(VI) aerosol exposures during showering activities. Beside showers other usage of contaminated water in certain air conditioners, spray irrigation or washing activities and cooling towers is possible root of chromium intake via inhalation. Finley found that there is a linear relationship between Cr(VI) concentration in shower water and shower air. Shower air concentration in ng/m^3 corresponded to $28 \times \text{Cr(VI)}$ water concentration in mg/L (Paustenbach 2002).

Dermal Absorption

There is little evidence to suggest that dermal absorption contributes in any significant way to total body burden of Cr, especially as a result of environmental exposure. *In vitro* studies of Mali et al. (1966) indicated that none of the Cr compounds diffused passively through the intact, isolated epidermal membranes. Only limited dermal absorption took place through the intact skin, with 1–4% Cr(VI) from an aqueous solution crossing the skin in guinea pig studies. The skin is also a barrier against Cr(VI) uptake that limits the toxicity via dermal contact.

Oral Intake

The vast majority of chromium intake in the household comes from water, ingestion is by orders of magnitude higher in comparison to potential inhalation of Cr(VI) in aerosols or dermal penetration of Cr(VI). The acid–base chemistry of the gastrointestinal tract (GI), as well as the reductive capacity of the blood, creates a substantial barrier to absorption of Cr(VI) species beyond the stomach.

The amount of chromium absorbed from the GI tract depends on its valence state. Highly water-soluble Cr(VI) is poorly absorbed via the gastrointestinal tract (only 2–9% of the dose was absorbed in human studies) due to reduction to the relatively poorly absorbed Cr(III). Studies by Donaldson and Barreras (EPA 1998) in humans and rats indicate that the normal absorption of Cr(III) or Cr(VI) by the GI tract is low but is increased when Cr is administered directly to the intestines, bypassing the gastric juices.

The ingestion studies demonstrated that exposure to soluble chromates in drinking water at concentrations of 1,000 to 5,000 ppb are not well absorbed in normal adults and are probably absorbed into blood stream almost entirely in trivalent forms. Exposures in this range were not toxic following acute or subchronic ad-

ministration to normal adults. Further, it appears that steady-state conditions are reached rapidly for an individual upon drinking 2 L per day of 2,000 ppb Cr(VI) in water (Paustenbach et al. 1996), which suggests that long term exposures are unlikely to result in Cr(VI) accumulation in tissues.

Considering the conclusions from human risk assessment studies, the WHO (2006) guideline value is 0.05 mg/L for total chromium. The same values have been set by the European Council Directive 98/83/EC to secure the quality of water intended for human consumption (Council Directive 98/83/EC). Since 1991 EPA raised the federal maximum contaminant levels for total chromium in drinking water to 0.1 mg/L, California maintained the 0.05 mg/L level (California department of public health 2007). There is inadequate evidence whether or not ingestion of Cr(VI) at the current U.S. EPA MCL of 100 ppb poses cancer or non cancer hazard to humans.

Kinetics and Metabolism

According to DeFlora et al. (in EPA 1998) ingested hexavalent chromium is efficiently reduced to the trivalent form by the gastric juices. Hexavalent chromium can also be reduced to the trivalent form in the epithelial lining fluid of the lungs by ascorbate and glutathione. Once absorbed into the bloodstream, hexavalent chromium readily enters red blood cells through the phosphate and sulfate anion-exchange carrier pathway, though a portion may remain in plasma for an extended period. Different hexavalent chromium studies, published in the Toxicological Review of EPA (1998) explain chromium metabolism.

Cr(III) travels in the bloodstream largely bound to amino acids, other organic acids, and plasma proteins such as globulins. The complexes of Cr(III) formed with lower molecular weight ligands are most likely to be able to pass cell membranes. Studies summarized in the Toxicological Review of Chromium (EPA 1998) show a significant amount of absorbed chromium in the bone, concentrated in tissues of the liver, kidney, and spleen.

Based on human and animals studies from 2 to 10% of orally administered dose of Cr(VI) is absorbed. Most of the Cr(VI) which is not sequestered in the blood cells is subsequently transferred to other organs, with the greatest retention by the liver, spleen, and bone marrow.

At physiological pH level, Cr(VI) reduction is controlled kinetically rather than thermodynamically. As already referred to it above, there are two pathways for Cr(VI) reduction. First, a series of one electron reductions may occur, predominately at rather low relative levels of reductants, producing the intermediate Cr(V) and Cr(IV) species and, ultimately, Cr(III) (Stearns et al. 1995a). In contrast, when intracellular reductant levels are present in gross excess over Cr(VI), the initial step involves a two electron reduction to Cr(IV), followed by one electron reduction to Cr(III). During the reductive metabolism of Cr(VI), the oxidation of reductants can lead to the ROS (reactive oxygen species) and produce secondary toxicological effects (i.e. DNA strand breakage, DNA adducts) (Stearns et al. 1995a).

Excretion

The main routes for the excretion of chromium are via the kidneys/urine and the bile/feces; minor routes include milk, sweat, hair, and nails. Studies in humans and/or animals have shown that chromium administered orally or intravenously is excreted principally in the urine, whereas chromium administered by inhalation or intratracheal injection is excreted in both the urine and the feces (RAIS 1992).

Nutritional Practices and Assessment of Risk Involved in Human Exposure to Chromium(III)

In the previous sections chromium was regarded mostly as a toxic compound. However, Cr(III) is classified also as an essential trace element for humans, since it participates in the metabolism of glucose and lipids (Anderson 1997; Vincent 2004). On the other hand, Cr seems not to be required by microorganisms (Wong and Trevors 1988) or plants (Shanker et al. 2004). At the extracellular level, Cr(III) is relatively innocuous as a consequence of its insolubility and subsequent inability to cross cell membranes (Wong and Trevors 1988; Katz and Salem 1993). Considering that trivalent chromium molecules are scarcely able to penetrate nuclear membranes, only when the reduction is near the genetic material, potential interaction of chromium with DNA could occur (Jones 1990).

Dietary deficiency of chromium has been associated with impaired growth and fertility, a diabetic-like state connected to impaired glucose tolerance, hyperinsulinemia, hypercholesterolemia and enhanced atherogenesis (Katz and Salem 1993). In experimental animals, chromium deficiency decreased their life-spans (Schroeder et al. 1963 cited by Katz and Salem 1993).

In 1954, the first suggestion that chromium(III) may be biologically active emerged when it was reported that chromium enhanced the synthesis of cholesterol and fatty acids from acetate in rat liver (Curran 1954). In 1959, trivalent chromium was reported to be the glucose tolerance factor (GTF) (Nielsen 2007) that alleviated the 1955 discovery of impaired glucose tolerance in rats fed torula yeast-sucrose diets (Mertz and Schwarz 1955; Schwarz and Mertz 1959). Several reports claiming that chromium as GTF normalized insulin responses and improved glucose tolerance in some individuals with impaired glucose tolerance or mild diabetes appeared in the period between 1960 and 1970 (Nielsen 2007).

An estimated safe and adequate daily dietary intake (ESADDI) for chromium by the Food and Nutrition Board in 1980 was established. Later the nutritional essentiality of chromium was questioned anew when it was found that chromium analyses before 1980 were not valid and repeated efforts to definitively characterize a chromium-containing GTF were unsuccessful, which raised doubts about its existence (Nielsen 2007). In 1989 it was reported that chromium in the form of chromium picolinate increased lean muscle mass and decreased body fat in young

men participating in a weight-training program (Evans 1989). Chromium picolinate (CrPic) is one of the most commonly used chromium dietary supplements available in the United States, and it has been marketed to consumers for use in weight loss, increasing muscle mass, and lowering serum cholesterol. Chromium picolinate is a synthetic compound that provides a bioavailable form of Cr(III) that is claimed to be absorbed better than dietary chromium. In general, the knowledge about the toxicological profile of chromium picolinate is rather limited and the data that do exist are contradictory, especially when it comes to the potential genotoxicity of the compound. Ozawa and Hanaki (1990) demonstrated that Cr(III) can be reduced to Cr(II) by the biological reductants L-cysteine and NADH, and the newly formed Cr(II) reacts with hydrogen peroxide to generate hydroxyl radicals, which can be detected by erythrocyte sedimentation rate (ESR) and high performance liquid chromatography (HPLC). Inside the cell Cr(III) may generate toxic effects by its ability to cause ROS formation and DNA damage (Kortenkamp et al. 1991; Bridgewater et al. 1994; Plaper et al. 2002). Jenko-Brinovec et al. (unpublished results) found that Cr(III) compounds also take part in a redox cycle where in the presence of H₂O₂ they generate OH• radicals and DNA damages. In the case of CrPic there are several reports that it can have adverse effects, the major concern about the toxicity of CrPic has been its potential genotoxicity (Whittaker et al. 2005; Stearns et al. 1995b, 2002; Bagchi et al. 1997; Speetjens et al. 1999; Hepburn et al. 2003a, b). In other studies, CrPic has been reported to be without any genotoxic effects (McCarty 1996; Esber and Moreno 1997) or only under non-physiological conditions (Andersson et al. 2007). There are many mechanistic aspects of CrPic genotoxicity that remain to be understood, including what individual contributions the metal center and the picolinate ligand make to cytotoxicity and DNA damage in cells, and whether or not the observed DNA damage is mutagenic (Stearns et al. 2002). It has been shown to cause single strand breaks in plasmid DNA *in vitro* in the presence of ascorbic acid or hydrogen peroxide, presumably by a Fenton mechanism in which reactive oxygen species are produced as chromium cycles between oxidation states of Cr(II), Cr(III), and Cr(IV) (Speetjens et al. 1999).

Major controversies surround the proposed role of Cr(III) as an essential micronutrient, as well as its use in nutritional supplements (Levina et al. 2007). Such controversies are partially caused by the lack of a clear understanding of the chemical mechanisms by which Cr(III) acts as an anti-diabetic agent and due to limited epidemiological studies on humans. Whether a specific biochemical function for chromium has been identified is still questioned, as a clear set of consistent deficiency signs has not been established for higher animals or humans (Levina et al. 2007). Chromium picolinate is neither approved as a food additive nor listed as Generally Recognized as Safe (GRAS) by the food and Drug Administration (FDA). The FDA has established a Reference Daily Intake (RDI) for chromium of 120 µg to assist consumers in understanding the nutritional significance of the levels of this nutrient in the context of the total daily diet. As recommended by the Food and Nutrition Board of the National Research Council, the best assurance of adequate and safe chromium intake is consumption of a varied diet balanced with other essential nutrients (Food and Nutrition Board, Institute of Medicine 2002). Additionally, CrPic is available

over-the-counter and can be bought at health food stores, supermarkets, pharmacies and mail order companies in a variety of forms including pills, sport drinks, nutrition bars and chewing gums (Speetjens et al. 1999; Vincent 2001), thus a great number of individuals in the population are exposed to these type of compounds. There is also growing evidence of the involvement of Cr(III) in Cr(VI)-induced cancers (Stearns 2000; Zhitkovich et al. 2001). Therefore, till further epidemiologic studies will provide the answer regarding chromium(III) toxicity, caution against taking excessive doses of chromium picolinate for long periods of time is advised.

Prevention and Repair of Chromium-Induced Damage

Chromium(VI) is a strong oxidizing agent. Against oxidative stress cells possess three lines of endogenous antioxidant defense: enzymatic, non-enzymatic antioxidants and repair processes. If antioxidants fail to prevent oxidative damage there is still the third line of defense, including protein and DNA repair systems, which remove the damaged biomolecules before they can accumulate and before their presence result in altered cell metabolism or viability. These mechanisms mainly involve the induced expression of components of the DNA repair machinery, and systems related to the homeostasis of iron and sulphur (Ozawa and Hanaki 1990). Oxidatively damaged nucleic acids are repaired by specific enzymes, oxidized proteins are removed by proteolytic systems and oxidized lipids are repaired by phospholipases, peroxidases and acyl transferases.

Although, the contribution of Cr(III) to the genotoxicity of Cr(VI) has not been well-established, the formation and significance of stable DNA–Cr(III)–protein and DNA–Cr(III)–DNA adducts has been discussed (Codd et al. 2001). Cr(III) is capable of binding to the phosphate moieties of the sugar–phosphate backbone in DNA (Kortenkamp et al. 1991; Bridgewater et al. 1994; Plaper et al. 2002). Not surprisingly, Cr(VI) has long been known to induce the *Escherichia coli* SOS DNA-repair system that protects DNA from oxidative damage (Llagostera et al. 1986). We have observed a lower degree of 8-OHdG formation in cells exposed to 0.1 mM Cr(VI) than in cells treated with 1 mM ascorbic acid (Poljsak et al. 2005). Obviously, the increased 8-OHdG concentrations in the ascorbic acid-treated cells were likely to trigger the induction of the yeast DNA-repair system (Cooke et al. 1998). Indeed, the exposure to the mild stress induced by ascorbic acid pretreatment evoked an improved resistance to the more severe stress induced by Cr(VI) (Poljsak et al. 2005). Pro-oxidative reactions induced by antioxidants could paradoxically exert a protective effect against DNA damage in yeast *in vivo* by intensifying the formation of 8-OHdG, which triggers an increased DNA-repair activity and enhanced antioxidant defense (Poljsak et al. 2005; Halliwell 1999). One reason why eukaryotic organisms have compartmentalized DNA in the nucleus well away from the sites of redox cycling reactions may be to avoid or minimize oxidative DNA damage. Indeed, when the concentrations of Cr are sufficient to saturate the reducing capacity of the cell, the harmful products of these redox reactions may reach the DNA.

Two comprehensive sets of metal-responsive genomic profiles were generated following exposure to equi-toxic concentrations of metal. One that provides information on the transcriptional changes associated with metal exposure (transcriptome), and a second that provides information on the relationship between the expression of approximately 4,700 non-essential genes and sensitivity to metal exposure (deletome). Approximately 22% of the genome was affected by exposure to chromium (Jin et al. 2008).

Pretreatment of *S. cerevisiae* cells with exogenous antioxidants such as ascorbic acid (vitamin C) or Trolox (a water-soluble analogue of vitamin E) demonstrated the positive effect of the increased reduction capacity of the cytosol on the modulation of Cr(V) formation, the accumulation of Cr, and the ability of the cells to scavenge superoxide anions and hydrogen peroxide. As a consequence, the pretreatment of yeast cells with reductants resulted in a decreased cytotoxicity and genotoxicity of Cr(VI) (Poljsak et al. 2005; Poljsak et al. 2006). O'Brien and Kortenkamp (1996) observed that the intracellular reduction of Cr(VI) has a toxifying effect, and the rate of Cr(VI) reduction influences the kinetics and extent of cellular damage. In general, the slower the reduction of Cr(VI), the more ROS are formed and, consequently, the greater the DNA damage (Kortenkamp and O'Brien 1994). When intracellular reductants are present in excess over Cr(VI), the initial reduction step involves a two-electron transfer to Cr(VI), which results in the generation of Cr(IV). In the next step, Cr(IV) is subjected to a one-electron reduction to Cr(III) (O'Brien et al. 2003). Thus, an increased cellular reduction capacity is expected to diminish the concentration of the highly reactive and long-lived Cr(V) intermediate. As a result, less Cr(V) can react directly with DNA or with H_2O_2 in a Fenton-like reaction leading to the formation of deleterious $\bullet OH$ radicals.

Conclusions

The fact that chromium is both, a chemical carcinogen, and an essential micronutrient, appears to be a paradox. Resolution to this paradox was provided by Katz and Salem (1993). These authors claimed that the paradox lies with the chemical speciation of chromium. The essentiality of chromium is associated with the glucose tolerance factor, a complex of trivalent chromium. The carcinogenicity of chromium, on the other hand, appears to reside with some of the hexavalent chromium compounds of limited solubility.

The essentiality of chromium is associated with the glucose tolerance factor, a complex of trivalent chromium. The carcinogenicity of chromium, on the other hand, appears to reside with some of the hexavalent chromium compounds of limited solubility. However, Jenko-Brinovec et al. (unpublished results) found that also Cr(III) compounds take part in a redox cycle and in the presence of H_2O_2 produce $OH\bullet$ and DNA damage. Any long-term impact of Cr exposure in organisms requires a full understanding of Cr biochemistry. In this aspect, chromium remains an interesting metal for further research regarding its toxicity and essentiality.

References

- Acevedo-Aguilar FJ, Espino-Saldaña AE, León-Rodríguez IL, Rivera-Cano ME, Avila-Rodríguez M et al (2006) Hexavalent chromium removal *in vitro* and from industrial wastes, using chromate-resistant strains of filamentous fungi indigenous to contaminated wastes. *Can J Microbiol* 52:809–815
- Aiyar J, Berkovits HJ, Floyd RA, Wetterhahn KE (1990) Reaction of chromium (VI) with hydrogen peroxide in the presence of glutathione: reactive intermediates and resulting DNA damage. *Chem Res Toxicol* 3:595–603
- Al-Asheh S, Duvnjak Z (1995) Absorption of copper and chromium by *Aspergillus carbonarius*. *Biotechnol Prog* 11:638–642
- Alexander J, Aaseth J (1995) Uptake of chromate in human red blood cells and isolated rat liver cells: the role of the anion carrier. *Analyst* 120:931–933
- Anderson RA (1997) Chromium as an essential nutrient for humans. *Regul Toxicol Pharmacol* 26:535–541
- Andersson MA, Petersson Grawé KV, Karlsson OM, Abramsson-Zetterberg LA, Hellman BE (2007) Evaluation of the potential genotoxicity of chromium picolinate in mammalian cells *in vivo* and *in vitro*. *Food Chem Toxicol* 45:1097–1106
- Arslan P, Beltrame M, Tomasi A (1987) Intracellular chromium reduction. *Biochim Biophys Acta* 931:10–15
- Avery SV (2001) Metal toxicity in yeasts and the role of oxidative stress. *Adv Appl Microbiol* 49:111–142
- Bagchi D, Bagchi M, Balmoori J, Ye X, Stohs SJ (1997) Comparative induction of oxidative stress in cultured J774A.1 macrophage cells by chromium by chromium picolinate and chromium nicotinate. *Res Commun Mol Pathol* 97:335–346
- Baldi F, Vaughan AM, Olson GA (1990) Chromium(VI)-resistant yeast isolated from a sewage treatment plant receiving tannery wastes. *Appl Environ Microbiol* 56:913–918
- Banks RB, Cooke RT (1986) Chromate reduction by rabbit liver aldehyde oxidase. *Biochem Biophys Res Commun* 137:8–14
- Batic M, Raspor P (1998) Uptake and bioaccumulation of Cr(III) in yeast *Saccharomyces cerevisiae*. *Food Technol Biotechnol* 36:291–297
- Belágyi J, Pas M, Raspor P, Pesti M, Páli T (1999) Effect of hexavalent chromium on eukaryotic plasma membrane studied by EPR spectroscopy. *Biochim Biophys Acta* 1421:175–182
- Bingol A, Uzun H, Bayhan YK, Karaguanduz A, Cakici A, Keskinler B (2004) Removal of chromate anions from aqueous stream by a cationic surfactant-modified yeast. *Biores Technol* 94:245–249
- Blackwell KJ, Singleton I, Tobin JM (1995) Metal cation uptake by yeast. *Appl Microbiol Biotechnol* 43:579–584
- Borges KM, Wetterhahn KE (1989) Chromium cross-links glutathione and cysteine to DNA. *Carcinogenesis* 10:2165–2168
- Borges KM, Boswell JS, Liebross RH, Wetterhahn KE (1991) Activation of chromium(VI) by thiols results in chromium(V) formation, chromium binding to DNA and altered DNA conformation. *Carcinogenesis* 12:551–561
- Borst-Pauwells GWFH (1981) Ion transport in yeast. *Biochem Biophys Acta* 650:88–127
- Brauer SL, Hneihen SA, Mcbridge JS, Wetterhahn KE (1996) Chromium(VI) forms thiolate complexes with gamma-glutamylcysteine, N-acetylcysteine, cysteine, and the methyl ester of N-acetylcysteine. *Inorg Chem* 35:373–381
- Bridgewater LC, Manning FC, Woo ES, Patierno SR (1994) DNA polymerase arrest by adducted trivalent chromium. *Mol Carcinog* 9:122–133
- California department of public health (2007) Chromium-6 in drinking water: regulation update. <http://www.cdph.ca.gov/CERTLIC/DRINKINGWATER/Pages/Chromium6.aspx>. Accessed 22 Oct 2008

- Chen F, Shi X (2002) Intracellular signal transduction of cells in response to carcinogenic metal. *Crit Rev Oncol Hematol* 42:105–121
- Chen D, Toone WM, Mata J, Lyne R, Burns G et al (2003) Global transcriptional responses of fission yeast to environmental stress. *Mol Biol Cell* 14:214–229
- Cheung KH, Gu J-D (2007) Mechanism of hexavalent chromium detoxification by microorganisms and bioremediation application potential. *Int Biodeterio Biodegrad* 59:8–15
- Cid VJ, Duran A, del Rey F, Snyder MP, Nombela C, Sanchez M (1995) Molecular basis of cell integrity and morphogenesis in *Saccharomyces cerevisiae*. *Microbiol Rev* 59:345–386
- Cieslak-Golonka M (1995) Toxic and mutagenic effects of chromium(VI). *Polyhedron* 15:3667–3689
- Cieslak-Golonka M, Daszkiewicz M (2005) Coordination geometry of Cr(VI) species: structural and spectroscopic characteristics. *Coord Chem Rev* 249:2391–2407
- Codd R, Rillon CT, Levina A, Lay PA (2001) Studies on the genotoxicity of chromium: from the test tube to the cell. *Coord Chem Rev* 216–217:537–582
- Chen MD, Kargacin B, Klein CB, Costa M (1993) Mechanism of chromium carcinogenicity and toxicity. *CRC Rev Toxicol* 13:255–281
- Connett PH, Wetterhahn KE (1983) Metabolism of the carcinogen chromate by cellular constituents. *Struct Bonding* 54:93–124
- Cooke MS, Evans MD, Podmore ID, Herbert KE, Mistry N et al (1998) Novel repair action of vitamin C upon *in vivo* oxidative DNA damage. *FEBS Lett* 439:363–367
- Corbett GE, Dodge GDO, Flaherty E, Liang J, Throop L et al (1998) *In vitro* reduction kinetics of hexavalent chromium in human blood. *Environ Res* 78:7–11
- Costa V, Moradas-Ferreira P (2001) Oxidative stress and signal transduction in *Saccharomyces cerevisiae*: insights into ageing, apoptosis and diseases. *Mol Aspects Med* 22:217–246
- Council Directive 98/83/EC of 3 November 1998 on the quality of water intended for human consumption (1998). Official J L 330, 05/12/1998, p 0032–0054
- Cupo DY, Wetterhahn KE (1985) Modification of chromium (VI)-induced DNA damage by glutathione and cytochromes P-450 in chicken embryo hepatocytes. *Proc Natl Acad Sci U S A* 82:6755–6759
- Curran GL (1954) Effect of certain transition group elements on hepatic synthesis of cholesterol in the rat. *J Biol Chem* 210:765–770
- Czakó-Vér K, Batic M, Raspor P, Sipiczki M, Pesti M (1999) Hexavalent chromium uptake by sensitive and tolerant mutants of *Schizosaccharomyces pombe*. *FEMS Microbiol Lett* 178:109–115
- Czakó-Vér K, Koósz Zs, Antal J, Rác T, Sipiczki M, Pesti M (2004) Characterization of chromate-sensitive and -tolerant mutants of *Schizosaccharomyces pombe*. *Folia Microbiol* 49:31–36
- De Flora S, Morelli A, Basso C, Romano M, Serra D, De Flora A (1985) Prominent role of DT-diaphorase as a cellular mechanism reducing chromium(VI) and reverting its mutagenicity. *Cancer Res* 45:3188–3196
- EPA (1998) Toxicological review of hexavalent chromium (CAS No. 18540-29-9); In support of summary information on the Integrated Risk Information System (IRIS)
- Esber H, Moreno V (1997) Evaluation of chromium picolinate in the rat *in vivo* chromosomal aberration assay. *Environ Mol Mutagen* 29:15
- Evans GW (1989) The effect of chromium picolinate on insulin controlled parameters in humans. *Int J Biosoc Med Res* 11:163–180
- Farkas N, Pesti M, Belágyi J (2003) Effect of hexavalent chromium on the plasma membrane of sensitive and tolerant mutants of *Schizosaccharomyces pombe*. An EPR study. *Biochim Biophys Acta* 1611:217–222
- Finley BL, Kerger BD, Katona MW, Gargas ML, Corbett GC, Paustenbach DJ (1997) Human ingestion of chromium (VI) in drinking water: pharmacokinetics following repeated exposure. *Toxicol Appl Pharmacol* 142:151–159
- Fishbein L (1981) Sources, transport and alteration of metal compounds: an overview. Arsenic, beryllium, cadmium, chromium and nickel. *Environ Health Perspect* 40:43–65

- Food and Nutrition Board, Institute of Medicine (2002) Chromium. Dietary reference intakes for vitamin A, vitamin C, arsenic, boron, chromium, copper, iodine, iron, manganese, molybdenum, nickel, silicon, vanadium, and zinc. National Academy Press, Washington
- Fude L, Shigui L (1992) Microbial removal and recovery of chromium(VI) from electroplating waste water. *J Sichuan Univ Nat Sci Ed* 2:266–273
- Gazdag Z, Pócsi I, Belágyi J, Emri T, Blaskó Á, Takács K, Pesti M (2003) Chromate tolerance caused by reduced hydroxyl radical production and decreased glutathione reductase activity in *Schizosaccharomyces pombe*. *J Basic Microbiol* 43:96–103
- Ghahrebb MM, Gadd GM (1998) Evidence for the involvement of vacuolar activity in metal(loid) tolerance: vacuolar-lacing and -defective mutants of *Saccharomyces cerevisiae* display higher sensitivity to chromate, tellurite and selenite. *BioMetals* 11:101–106
- Goodgame DM, Joy AM (1986) Relatively long-lived chromium(V) species are produced by the action of glutathione on carcinogenic chromium(VI). *J Inorg Biochem* 26:219–224
- Goodgame DM, Joy AM (1988) ESR study of the Cr(V) and radical species produced in the reduction of Cr(VI) by ascorbate. *Inorg Chim Acta* 135:115–118
- Goyal N, Jain SC, Banerjee UC (2003) Comparative study on the microbial adsorption of heavy metals. *Adv Environ Res* 7:311–319
- Halliwell B (1999) Vitamin C: poison, prophylactic or panacea? *Trends Biochem Sci* 24:255–259
- Harris GK, Shi X (2003) Signaling by carcinogenic metals and metal-induced reactive oxygen species. *Mut Res* 533:183–200
- Hepburn DD, Xiao J, Bindom S, Vincent JB, O'Donnell J (2003a) Nutritional supplement chromium picolinate causes sterility and lethal mutations in *Drosophila melanogaster*. *Proc Natl Acad Sci U S A* 100:3766–3771
- Hepburn D, Burney M, Wosky S, Vincent J (2003b) The nutritional supplement chromium picolinate generates oxidative DNA damage and peroxidized lipids *in vivo*. *Polyhedron* 22:455–463
- Hildebrand U, Regvar M, Bothe H (2007) Arbuscular mycorrhiza and heavy metal tolerance. *Phytochemistry* 68:139–146
- Hohmann S, Mager WU (eds) (2003) Yeast stress responses. Springer, Berlin
- Holland S, Lodwig E, Sideri T, Reader T, Clarke I, Gkargkas K, Hoyle DC, Delneri D, Oliver SG, Avery SV (2007) Application of the comprehensive set of heterozygous yeast deletion mutants to elucidate the molecular basis of cellular chromium toxicity. *Genome Biol* 8:R268
- Holland SL, Ghosh E, Avery SV (2010) Chromate-induced sulfur starvation and mRNA mistranslation in yeast are linked in a common mechanism of Cr toxicity. *Toxicol in vitro*. doi:10.1016/j.tiv.2010.07.006
- Holland SL, Avery SV (2009) Actin-mediated endocytosis limits intracellular Cr accumulation and Cr toxicity during chromate stress. *Toxicol Sci* 111(2):437–446
- Howlett NG, Avery SV (1997) Induction of lipid peroxidation during heavy metal stress in *Saccharomyces cerevisiae* and influence of plasma membrane fatty acid unsaturation. *Appl Environ Microbiol* 63:2971–2976
- IARC, International Agency for Research on Cancer, World Health Organization (1997) IARC monographs on the evaluation of carcinogenic risks to humans, vol 49. Chromium, nickel and welding. Summary of data reported and evaluation. Last updated: 5 Nov 1997
- Ikner A, Shiozaki K (2005) Yeast signalling pathways in the oxidative stress responses. *Mutat Res* 569:13–27
- Ishibishi Y, Cervantes CK, Silver S (1990) Chromium reduction in *Pseudomonas putida*. *Appl Environ Microbiol* 56:2268–2270
- Jackson AL, Loeb LA (2001) The contribution of endogenous sources of DNA damage to the multiple mutations in cancer. *Mutat Res* 477:7–21
- Jennette KW (1982) Microsomal reduction of the carcinogenic chromate produces chromium(V). *J Am Chem Soc* 104:874–875
- Jin YH, Dunlap PE, McBride SJ, Al-Refai H, Bushel PR, Freedman JH (2008) Global transcriptome and deletome profiles of yeast exposed to transition metals. *PLoS Genet* 25(4):e1000053
- Jones RE (1990) Hexavalent chrome: threshold concept for carcinogenicity. *Biomed Environ Sci* 3:20–34

- Kapoor A, Viraraghavan T (1995) Fungal biosorption—an alternative treatment option for heavy metal bearing wastewaters. *Bioresour Technol* 53:195–206
- Katz S, Salem H (1994) The biological and environmental chemistry of chromium. VCH, New York
- Katz SA, Salem H (1993) The toxicology of chromium with respect to its chemical speciation: a review. *J Appl Toxicol* 13:217–224
- Kawanishi S, Inoue S, Sano S (1986) Mechanism of DNA cleavage induced by sodium chromate(VI) in the presence of hydrogen peroxide. *J Biol Chem* 261:5952–5958
- Kirpnick-Sobol Z, Reliene R, Schiestl RH (2006) Carcinogenic Cr(VI) and the nutritional supplement Cr(III) induce DNA deletions in yeast and mice. *Cancer Res* 66:3480–3884
- Kitagawa S, Seki H, Kametani F, Sakurai H (1988) ESR study on the interaction of hexavalent chromium with glutathione or cysteine: production of pentavalent chromium and its stability. *Inorg Chim Acta* 152:251–255
- Klein CB, Snow ET, Frenkel K (1998) Molecular mechanisms in metal carcinogenesis: role of oxidative stress. In: Aruoma O, Halliwell B (eds) *Molecular biology of free radicals in human diseases*. OICA International, London, pp 79–117
- Klis FM, Mol P, Hellingwerf K, Brul S (2002) Dynamics of cell wall structure in *Saccharomyces cerevisiae*. *FEMS Microbiol Rev* 26:239–256
- Koós Z, Gazdag Z, Micros I, Benkő Z, Belágyi J, Antal J, Meleg B, Pesti M (2008) Downregulation of the specific glutathione reductase activity caused chromate tolerance in a mutant fission yeast. *Folia Microbiol* 53:308–314
- Kortenkamp A, O'Brien P (1994) The generation of DNA single-strand breaks during the reduction of chromate by ascorbic acid and/or glutathione *in vitro*. *Environ Health Perspect* 102:237–241
- Kortenkamp A, O'Brien P, Beyersmann D (1991) The reduction of chromate is a prerequisite of chromium binding to cell nuclei. *Carcinogenesis* 12:1143–1144
- Kortenkamp A, Curran B, O'Brien P (1992) Defining conditions for the efficient *in vitro* cross-linking of proteins to DNA by chromium(III) compounds. *Carcinogenesis* 13:307–308
- Kortenkamp A, Casadevall M, Faux SP, Jenner A, Shayer RO, Woodbridge N, O'Brien P (1996) A role for molecular oxygen in the formation of DNA damage during the reduction of the carcinogen chromium (VI) by glutathione. *Arch Biochem Biophys* 329:199–207
- Koutras GA, Hattori MJ, Schneider AS, Ebaugh FG, Valentine WN (1964) Studies on chromate erythrocytes. Effect of sodium chromate on erythrocyte glutathione reductase. *J Clin Invest* 43:323–331
- Koutras GA, Schneider AS, Hattori M, Valentine WN (1965) Studies on chromate erythrocytes. Effect of sodium chromate on erythrocyte glutathione reductase. *Br J Haematol* 2:360–369
- Ksheminska H, Fedorovych D, Babyak L, Yanovych D, Kaszycky P, Koloczek H (2005) Chromium(III) and (VI) tolerance and bioaccumulation in yeast: a survey of cellular chromium content in selected strains of representative genera. *Process Biochem* 40:1565–1572
- Ksheminska HP, Honchar TM, Gayda GZ, Gonchar MV (2006) Extra-cellular chromate-reducing activity of the yeast cultures. *Central Eur J Biol* 1:137–149
- Kvasuikova EI, Stepanyuk VV, Klyushnidova TM et al (1984) A new chromium reducing, gram variable bacterium with mixed type of flagellation. *Mikrobiologia* 54:83–88
- Lay PA, Levina A (1998) Activation of molecular oxygen during the reactions of Chromium(VI/V/IV) with biological reductants: Implications for chromium-induced genotoxicities. *J Am Chem Soc* 120:6704–6714
- Lee J, Dawes IW, Rhoe JH (1997) Isolation, expression and regulation of the *pgr1*⁺ gene encoding glutathione reductase absolutely required for growth of *Schizosaccharomyces pombe*. *J Biol Chem* 272:23042–23049
- Levina A, Mulyani I, Lay PA (2007) Redox chemistry and biological activities of chromium(III) complexes. In: Vincent J (ed) *The nutritional biochemistry of chromium(III)*. Elsevier, Amsterdam
- Levy LS, Martin PA, Bidstrup PL (1986) Investigation of the potential carcinogenicity of a range of chromium containing materials on rat lung. *Br J Ind Med* 43:243–256

- Lipke PN, Ovalle R (1998) Cell wall architecture in yeast: new structure and challenges. *J Bacteriol* 180:3735–3740
- Liu XD, Thiele DJ (1997) Yeast methallothionein gene expression in response to metals and oxidative stress. *Methods* 11:289–299
- Llagostera M, Garrido S, Guerrero R, Barbé J (1986) Induction of SOS genes of *Escherichia coli* by chromium compounds. *Environ Mutagen* 8:571–577
- Mali JWH, van Knoten WJ, Van Neer FCJ, Spruit D (1966) Quantitative aspects of chromium sensitization. *Acta Derm Venereol* 44:44–48
- Mapoleno M, Torto N (2004) Trace enrichment of metal ions in aquatic environments by *Saccharomyces cerevisiae*. *Talanta* 64:39–47
- Martin BD, Schoenhard JA, Sugden KD (1998) Hypervalent chromium mimics reactive oxygen species as measured by the oxidant-sensitive dyes 2,7-dichlorofluorescein and dihydrorhodamine. *Chem Res Toxicol* 11:1402–1410
- Marzluf GA (1970) Genetic and metabolic controls for sulphate metabolism in *Neurospora crassa*: isolation and study of chromate-resistant and sulphate transport-negative mutants. *J Bact* 102:716–721
- McCarty MF (1996) Chromium (III) picolinate. *FASEB J* 10:365–366
- Mendoza-Cózatl D, Loza-Tavera H, Hernández-Navarro A, Moreno-Sánchez R (2005) Sulfur assimilation and glutathione metabolism under cadmium stress in yeast, protist and plants. *FEMS Microbiol Rev* 29:653–671
- Mertz W (1969) Chromium occurrence and function in biological systems. *Physiol Rev* 49:163–239
- Mertz W, Schwarz K (1955) Impaired intravenous glucose tolerance as an early sign of dietaryneurotic liver degeneration. *Arch Biochem Biophys* 58:504–506
- Moreira OC, Rios PF, Barrabin H (2005) Inhibition of plasma membrane Ca^{2+} -ATPase by CrATP. LaATP but not CrATP stabilizes the Ca^{2+} -occluded state. *Biochem Biophys Acta* 1708:411–419
- Mutter O, Patmalnieks A, Rapoport A (2001) Interrelation of the yeast *Candida utilis* and Cr(VI): metal reduction and its distribution in the cell and medium. *Proc Biochem* 36:963–970
- Mutter O, Lubinga I, Millers D, Grigorjeva L, Ventinya E, Rapoport A (2002) Cr(VI) sorption by intact and dehydrated *Candida utilis* cells in the presence of other metals. *Process Biochem* 38:123–131
- Nakamura S, Oda Y, Shimada T, Oki I, Sugimoto K (1987) SOS-inducing activity of chemical carcinogens and mutagens in *Salmonella typhimurium* TA1535/pSK1002: examination with 151 chemicals. *Mutat Res* 192:239–246
- Nielsen FH (2007) The clinical and nutritional importance of chromium—still debated after 50 years of research. In: Vincent J (ed) *The nutritional biochemistry of chromium(III)*. Elsevier, Amsterdam
- Nies DH (1992) Resistance to cadmium, cobalt, zinc and nickel in microbes. *Plasmid* 2:17–28
- O'Brien P, Kortenkamp A (1996) The chemistry underlying chromate toxicity. *Transit Metal Chem* 20:636–642
- O'Brien P, Barrett J, Swanson F (1985) Chromium(V) can be generated in the reduction of chromium(VI) by glutathione. *Inorg Chim Acta* 108:19–20
- O'Brien TJ, Ceryak S, Patierno SR (2003) Complexities of chromium carcinogenesis: role of cellular response, repair and recovery mechanisms. *Mutat Res* 533:3–36
- Ono BI, Weng M (1982) Chromium resistant mutants of the yeast *Saccharomyces cerevisiae*. *Curr Genet* 6:71–77
- Ozawa T, Hanaki A (1990) Spin-trapping studies on the reactions of Cr(III) with hydrogen peroxide in the presence of biological reductants: is Cr(III) nontoxic? *Biochem Interact* 22:343–352
- Özer A, Özer D (2003) Comparative study of the biosorption of Pb(II), Ni(II) and Cr(VI) ions onto *S. cerevisiae*: determination of biosorption heats. *J Hazard Mater B* 100:219–229
- Park D, Yun YS, Park JM (2005) Use of dead fungal biomass for the detoxification of hexavalent chromium: screening and kinetics. *Process Biochem* 40:2559–2565

- Pas M, Milacic R, Draslar K, Pollak N, Raspor P (2004) Uptake of chromium (III) and chromium (VI) compounds in the yeast cell structure. *BioMetals* 17:25–33
- Paustenbach DJ, Hays SM, Brien BA, Dodge DG, Kerger BD (1996) Observation of steady state in blood and urine following human ingestion of hexavalent chromium in drinking water. *J Toxicol Environ Health* 49:453–461
- Paustenbach DJ (2002) Human and ecological risk assessment. Theory and practice. Wiley, New York
- Pepi M, Baldi F (1992) Modulation of chromium(VI) toxicity by organic and inorganic sulphur species in yeast from industrial waste. *BioMetals* 5:179–185
- Pepi M, Baldi F (1995) Chromate tolerance in strains of *Rhodospiridium toruloides* modulated by thiosulphate and sulfur amino acids. *BioMetals* 8:99–109
- Perego P, Howell SB (1997) Molecular mechanism controlling sensitivity to toxic metal ions in yeast. *Toxicol Appl Pharmacol* 147:312–318
- Pereira Y, Lagniel G, Godat E, Baudouin-Cornu P, Junot C, Labarre J (2008) Chromate causes sulfur starvation in yeast. *Toxicol Sci* 106(2):400–412
- Pesti M, Campbell JMcA, Peberdy JF (1981) Alteration of ergosterol content and chitin synthase activity in *Candida albicans*. *Curr Microbiol* 5:187–190
- Pesti M, Horváth L, Vigh L, Farkas F (1985) ESR determination of plasma membrane order parameter, lipid content and phase transition point in *Candida albicans* sterol mutants. *Acta Microbiol Hung* 32:305–313
- Pesti M, Gazdag Z, Belágyi J (2000) *In vivo* interaction of trivalent chromium with yeast plasma membrane, as revealed by EPR spectroscopy. *FEMS Microbiol Lett* 182:375–380
- Pesti M, Gazdag Z, Emri T, Farkas N, Koósz Z, Belágyi J, Pócsi I (2002) Chromate sensitivity in fission yeast is caused by increased glutathione reductase activity and peroxide overproduction. *J Basic Microbiol* 42:408–419
- Plaper A, Jenko-Brinovec S, Premzl A, Kos J, Raspor P (2002) Genotoxicity of trivalent chromium in bacterial cells. Possible effects on DNA topology. *Chem Res Toxicol* 15:943–949
- Pócsi I, Prade RA, Penninckx MA (2004) Glutathione, altruistic metabolite in fungi *Adv Microbial Physiol* 49:1–76
- Poljsak B (2004) Pro-oxidative vs. antioxidative properties of ascorbic acid and trolox in Cr(VI) induced damage. Doctoral Thesis, Nova Gorica Polytechnic, School of Environmental Science
- Poljsak B, Gazdag Z, Jenko-Brinovec S, Fujs S, Pesti M, Belagyi J, Plesnicar S, Raspor P (2005) Pro-oxidative vs. antioxidative properties of ascorbic acid in chromium(VI)-induced damage: an *in vivo* and *in vitro* approach. *J Appl Toxicol* 25:535–548
- Poljsak B, Gazdag Z, Pesti M, Jenko-Brinovec S, Belagyi J et al (2006) Pro-oxidative versus anti-oxidative reactions between trolox and Cr(VI): the role of H₂O₂. *Environ Toxicol Pharmacol* 22:15–19
- Quiévryn G, Goulart M, Messer J, Zhitkovich A (2001) Reduction of Cr (VI) by cysteine: significance in human lymphocytes and formation of DNA damage in reactions with variable reduction rates. *Mol Cell Biochem* 222:107–118
- Rahman M, Gul S, Din Z et al (2000) Removal of chromium by a consortium of bacteria isolated from domestic sewage Pak. *J Biol Sci* 3:2159–2162
- Rahman M, Gul S, Ul Haqu M (2007) Reduction of chromium(VI) by locally isolated *Pseudomonas* sp. C-171 Turk. *J Biol* 31:161–166
- Rapaport AI, Muter OA (1995) Biosorption of hexavalent chromium by yeast. *Process Biochem* 30:145–149
- Risk Assessment Information System—RAIS (1992) Toxicity summary for chromium. <http://rais.ornl.gov/index.shtml>. Accessed 22 Oct 2008
- Roberts KR, Marzluf GA (1971) The specific interaction of chromate with the dual sulphate permease systems of *Neurospora crassa*. *Arch Biochem Biophys* 142:651–659
- Rodney PF, Robert JJ, Lay PA, Dixon NE, Raker RSU, Bonin AM (1989) Chromium (V)-induced cleavage of DNA: are chromium complexes the active carcinogens in chromium (VI)-induced cancer? *Chem Res Toxicol* 2:227–229
- Rosen BP (2002) Transport and detoxification system for transition metals, heavy metals and metalloids in eukaryotic and prokaryotic microbes. *Comp Biochem Physiol Part A Mol Integr Physiol* 133:689–693

- Sag Y, Kutsal T (1996) The selective biosorption of chromium(VI) and copper(II) ions from binary metal mixtures by *R. arrhizus*. *Process Biochem* 31:561–572
- Schmieman EA, Yonge DR, Petersen JN et al (2000) Kinetics of chromium reduction by mixed cultures during growth phase. *Water Environ Res* 72:523–529
- Schroeder HA, Vinton WH, Balassa JJ (1963) Effects of chromium, cadmium and lead on the growth and survival of rats. *J Nutr* 80:48–54
- Schwarz K, Mertz W (1959) Chromium (III) and glucose tolerance factor. *Arch Chem Biophys* 85:292–295
- Shakoori AR, Makhdoom M (2000) Hexavalent chromium reduction by a dichromate resistant gram-positive bacterium isolated from effluents of tanneries. *Appl Microbiol Biotechnol* 53:348–351
- Shanker A, Djanaguiraman M, Sudhagar R, Chandrashekar CN, Patmanabhan G (2004) Differential antioxidative response of ascorbate glutathione pathway enzymes and metabolites to chromium speciation stress in green gram (*Vigna radiata*) roots. *Plant Sci* 166:1035–1043
- Shi X, Dalal NS (1988) On the mechanism of the chromate reduction by glutathione: ESR evidence for the glutathionyl radical and an isolable Cr(V) intermediate. *Biochem Biophys Res Commun* 156:137–142
- Shi X, Dalal NS (1989) Chromium (V) and hydroxyl radical formation during the glutathione reductase-catalyzed reduction of chromium (VI). *Biochem Biophys Res Commun* 163:627–634
- Shi X, Dalal NS (1990a) Evidence for a Fenton-type mechanism for the generation of OH• radicals in the reduction of Cr(VI) in cellular media *Arch Biochem Biophys* 281:90–95
- Shi X, Dalal NS (1990b) On the hydroxyl radical formation in the reaction between hydrogen peroxide and biologically generated chromium(V) species. *Arch Biochem Biophys* 277:342–350
- Shi X, Leonard SS, Liu KJ, Zang L, Ganett PM, Rojanasakal Y, Castranova V, Vallyathan V (1998) Cr(III)-mediated hydroxyl radical generation via Haber-Weiss cycle. *J Inorg Biochem* 69:263–268
- Shi X, Chiu A, Chen CT, Halliwell B, Castranova V, Vallyathan V (1999) Reduction of Cr(VI) and its relationship to carcinogenesis. *J Toxicol Environ Health* 2(B):87–104
- Smith WL (2001) Hexavalent chromium reduction and precipitation by sulphate-reducing bacterial biofilms. *Environ Geochem Health* 23:297–300
- Snow ET, Xu LS (1989) Effect of chromium(III) on DNA replication *in vitro*. *Biol Trace Elem Res* 21:113–117
- Speetjens JK, Collins RA, Vincent JB, Woski SA (1999) The nutritional supplement chromium(III) tris(picolinate) cleaves DNA. *Chem Res Toxicol* 12:483–487
- Stearns DM (2000) Is chromium a trace essential metal? *Biofactors* 11:149–162
- Stearns DM, Wetterhahn KE (1994) Reaction of chromium(VI) with ascorbate produces chromium(V), chromium(IV), and carbon-based radicals. *Chem Res Toxicol* 7:219–230
- Stearns DM, Courtney KD, Giangrande PH, Phieffer LS, Wetterhahn KE (1994) Chromium(VI) reduction by ascorbate: role of reactive intermediates in DNA damage *in vitro*. *Environ Health Perspect* 102(Suppl 3):21–25
- Stearns DM, Kennedy LJ, Courtney KD, Giangrande PH, Phieffer LS, Wetterhahn KE (1995a) Reduction of chromium(VI) by ascorbate leads to chromium-DNA binding and DNA strand breaks *in vitro* *Biochemistry* 34(3):910–919
- Stearns DM, Wise JP, Patierna SR, Wetterhahn KE (1995b) Chromium(III) picolinate produces chromosome damage in Chinese hamster ovary cells. *FASEB J* 9:1643–1648
- Stearns DM, Silverira SM, Wolf KK, Luke AM (2002) Chromium(III) tris(picolinate) is mutagenic at the hypoxanthine(guanine) phosphoribosyltransferase locus in Chinese hamster ovary cells. *Mutat Res* 513:135–42
- Sugden KD, Stearns DM (2000) The role of chromium(V) in the mechanism of chromate-induced oxidative DNA damage and cancer. *J Environ Pathol Toxicol Oncol* 19:215–230
- Sugden KD, Burris RB, Rogers SJ (1990) An oxygen dependence in chromium mutagenesis. *J Mutat Res* 244:239–244
- Sugiyama M, Ando A, Ogura R (1989) Vitamin B2-enhancement of sodium chromate (VI)-Induced DNA single strand breaks: ESR study of the action of vitamin B2. *Biochem Biophys Res Commun* 159:1080–1085

- Tewari N, Vasudevan P, Guha BK (2005) Study on biosorption of Cr(VI) by *Mucor hiemalis*. *Biochem Eng J* 23:185–192
- Tomsett AB (1993) Genetics and molecular biology of metal tolerance in fungi. In: Jennings DH (ed) *Stress tolerance of fungi*. Marcel Dekker Inc., New York
- Tsou TC, Chen CL, Liu TY, Yang JL (1996) Induction of 8-hydroxydeoxy-guanosine in DNA by chromium(III) plus hydrogen peroxide and its prevention by scavengers. *Carcinogenesis* 17:103–108
- Viraraghavan K, Yun Y-S (2008) Bacterial biosorbents and biosorption. *Biotechnol Adv* 26:266–291
- Vincent JB (2001) The bioinorganic chemistry of chromium (III). *Polyhedron* 20:1–26
- Vincent JB (2004) Recent developments in the biochemistry of chromium (III). *Biol Trace Elem Res* 99:1–16
- Wang J, Chen C (2006) Biosorption of heavy metals by *Saccharomyces cerevisiae*. *Biotechnol Adv* 24:427–451
- Wang PC, Mori T, Komori K et al (1989) Isolation and characterization of an *Enterobacter cloacae* strain that reduces hexavalent chromium under anaerobic conditions. *Appl Environ Microbiol* 55:1665–1669
- Wenbo Q, Reiter R, Dun-Xian T (2000) Chromium(III)-induced 8-hydroxydeoxyguanosine in DNA and its reduction by antioxidants. *Environ Health Perspect* 108(5):399–402
- Wetterhahn KE, Hamilton JW (1989) Molecular basis of hexavalent chromium carcinogenicity: effect on gene expression. *Sci Total Environ* 86:113–129
- Wetterhahn KE, Hamilton JW, Aiyar J, Borges KM, Floyd R (1989) Mechanisms of chromium(VI) carcinogenesis. Reactive intermediates and effect on gene expression. *Biol trace Elem Res* 21:405–411
- White C, Gadd GM (1995) Determination of metals and metal fluxes in algae and fungi. *Sci Total Environ* 176:107–115
- Whittaker P, San RHC, Clarke JJ, Seifried HE, Dunkel VC (2005) Mutagenicity of chromium picolinate and its components in *Salmonella typhimurium* and L5178Y mouse lymphoma cells. *Food Chem Toxicol* 43:1619–1625
- WHO, international agency for research on cancer IARC (1997) Monographs on the evaluation of carcinogenic risks to humans volume 49. Chromium, nickel and welding, summary of data reported and evaluation
- Wong PT, Trevors JT (1988) Chromium toxicity to algae and bacteria. In: Nriagu JO, Nieboer E (eds), *Chromium in the natural and human environments*. Wiley, New York
- World Health Organization (2006) Guidelines for drinking-water quality (electronic resource): incorporating first addendum. Vol 1, Recommendations, 3rd edn. World Health Organization, Geneva
- Zafra-Stone S, Bagchi M, Preuss HG, Bagchi D (2007) Benefits of chromium(III) complexes in animal and human health. In: Vincent J (ed) *The nutritional biochemistry of chromium(III)*. Elsevier, Amsterdam
- Zhang L, Lay PA (1996) EPR spectroscopic studies of the reactions of Cr(VI) with L-ascorbic acid, Ldehydroascorbic acid, and 5,6-O-isopropylidene-L-ascorbic acid in water. Implications for chromium(VI) genotoxicity. *J Am Chem Soc* 118:12624–12637
- Zhitkovich A, Voitkun V, Costa M (1996) Formation of the amino acid-DNA complexes by hexavalent and trivalent chromium *in vitro*: importance of trivalent chromium and the phosphate group. *Biochemistry* 35:7275–7282
- Zhitkovich A, Song Y, Quievryn G, Voitkun V (2001) Nonoxidative mechanisms are responsible for the induction of mutagenesis by reduction of Cr(VI) with cysteine: role of ternary DNA adducts in Cr(III)-dependent mutagenesis. *Biochemistry* 16:549–560

Chapter 4

Saccharomyces cerevisiae as a Model Organism for Elucidating Arsenic Tolerance Mechanisms

Robert Wysocki and Markus J. Tamás

Abstract The budding yeast *Saccharomyces cerevisiae* is a powerful eukaryotic model organism for elucidating arsenic detoxification and tolerance acquisition mechanisms. The discovery of key yeast proteins involved in arsenite accumulation and efflux, arsenate reduction, and the use of complementation assays where a yeast protein is replaced by a homologous protein from another organism, has accelerated the identification of arsenic tolerance genes in fungi, plants, animals, and humans. In this chapter, we review the molecular biology of arsenic tolerance in budding yeast, focusing on arsenic sensing, signalling and detoxification mechanisms, how these pathways are regulated, and on the importance of yeast as a model for understanding fundamental aspects of arsenic tolerance in eukaryotes.

Introduction

The impact of arsenic on living organisms has for long been a scope of scientific studies because of its toxic and carcinogenic properties, its prevalence in the environment, and also because of a long history of usage as a therapeutic agent. About a decade ago, when the first reports showing a remarkable efficacy of arsenic trioxide in the treatment of acute promyelocytic leukaemia were published (Chen et al. 1997; Shen et al. 1997; Soignet et al. 1998), knowledge of arsenic tolerance mechanisms in eukaryotes was very limited. In contrast, pathways for arsenic detoxification had been thoroughly characterized in bacteria thanks to extensive studies on the *ars* operon originated in the lab of Barry Rosen (Xu et al. 1998; Rosen 1999, 2002). However, homologues of prokaryotic resistance determinants were not known in eukaryotes and specific eukaryotic tolerance pathways remained unknown for a long time. Since Bobrowicz et al. (1997) reported the isolation of the first arsenic

M. J. Tamás (✉)

Department of Cell and Molecular Biology/Microbiology, University of Gothenburg,

405 30 Gothenburg, Sweden

Tel.: +46-31-786-2548

Fax: +46-31-786-2599

e-mail: markus.tamas@cmb.gu.se

tolerance genes in *Saccharomyces cerevisiae* (budding yeast), a significant progress has been made in understanding tolerance mechanisms in eukaryotes, and budding yeast has turned out to be a powerful model system to study this phenomenon. This chapter describes our current understanding of arsenic tolerance in budding yeast. It includes the latest advances on arsenic sensing and signalling, on the regulation of detoxification pathways, and on the role of *S. cerevisiae* in elucidating tolerance mechanisms in eukaryotic species.

Impact of Arsenic on Yeast Cells

In nature, organisms are usually exposed to either pentavalent arsenate [AsO_4^{3-} or As(V)] or trivalent arsenite [$\text{As}(\text{OH})_3$ or As(III)]. High toxicity of arsenic is often attributed to induction of oxidative stress, enzyme inhibition, impairment of DNA repair, and disruption of the function of key proteins regulating fundamental processes including growth, cell cycle progression, apoptosis, or differentiation (Stohs and Bagchi 1995; Ercal et al. 2001; Chen and Shi 2002; Harris and Shi 2003; Beyersmann and Hartwig 2008). The arsenate oxyanion resembles phosphate and is able to interfere with phosphate transport as well as with metabolic and signalling pathways that depend on phosphate or phosphorylated intermediates. Many mitochondrial processes are targeted by arsenicals (Vujcic et al. 2007; Ralph 2008; Thorsen et al. 2009) and As(V) inhibits ATP synthesis in yeast mitochondria (Cortes et al. 2000). As(III) is considered more toxic and it affects protein structure and/or function either by direct binding to sulphhydryl groups or indirectly by causing oxidative modifications (Aposhian and Aposhian 2006; Kitchin and Wallace 2008). For example, As(III) disrupts the actin and tubulin cytoskeleton in yeast, and probably interferes with folding of *de novo* synthesised actin and tubulin monomers (Thorsen et al. 2009). As(III) also affects major signalling pathways in yeast; it inhibits the rapamycin-sensitive TORC1 (TOR complex 1) protein kinase (Hosiner et al. 2009), and it activates the MAP (mitogen-activated protein) kinase Hog1p (Sotelo and Rodriguez-Gabriel 2006; Thorsen et al. 2006). The toxicity of As(III) is often associated with increased production of reactive oxygen species (ROS), especially in mammals (Liu et al. 2001). Enhanced ROS production and lipid peroxidation can be detected in As(III)-exposed yeast mutants lacking detoxification systems, indicating that As(III) can stimulate ROS production also in yeast (Menezes et al. 2008). Finally, As(III) is believed to induce DNA damage indirectly by triggering accumulation of toxic levels of ROS or by inhibiting DNA repair proteins, especially in mammalian systems (Shi et al. 2004; Beyersmann and Hartwig 2008). However, yeast cells lacking DNA damage response proteins are not sensitive to As(III) (Haugen et al. 2004; Thorsen et al. 2009) and DNA double strand breaks do not increase in yeast upon As(III) treatment (Jo et al. 2009). Thus, the effect of arsenic on genomic stability in yeast requires further investigation. To sum up, arsenic is known to affect a wide array of cellular targets but the molecular mechanisms through which it triggers toxicity remain largely elusive.

Arsenic Uptake Routes in Yeast

Arsenic, like many other toxic metals and metalloids, enter cells through proteins developed for accumulation of essential metals and other nutrients. Interestingly, cells utilize several mechanisms to prevent influx of toxic metals/metalloids and actively acquire tolerance. Studies on arsenic influx in yeast provided basic insights into metalloid uptake pathways and their regulation. In turn, this knowledge proved to be crucial for understanding this phenomenon in other eukaryotes, including humans.

Arsenate Uptake

The As(V) oxyanion structurally resembles inorganic phosphate and is probably accumulated via phosphate transporters in all organism (Fig. 4.1). *S. cerevisiae* has two high-affinity (Pho84p and Pho89p) and two low-affinity (Pho87p and Pho90p) phosphate permeases (Persson et al. 1999; Wykoff and O'Shea 2001). As(V) uptake

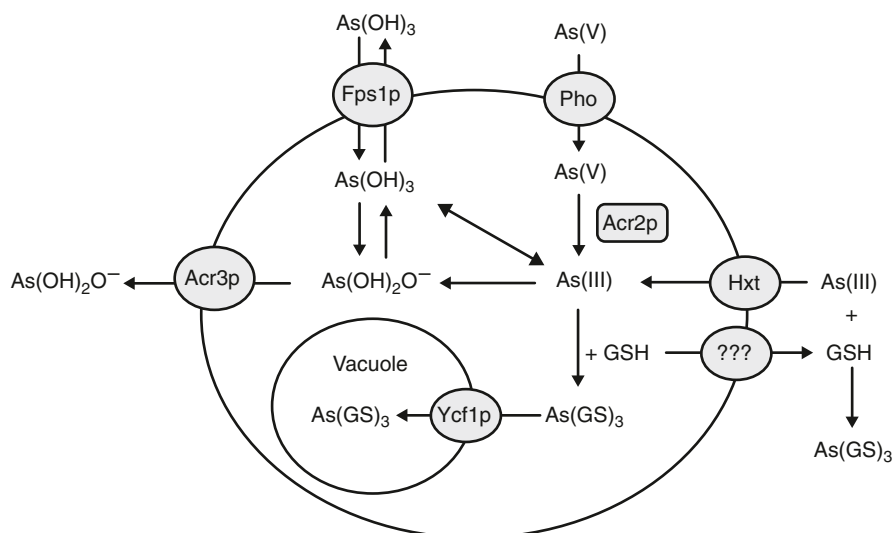


Fig. 4.1 Routes for arsenic uptake and detoxification in the yeast *Saccharomyces cerevisiae*. Pentavalent arsenic [As(V)] enters the yeast cell via phosphate transporters (Pho84p and Pho87p). In the cytoplasm As(V) is reduced to trivalent arsenic [As(III)], which is the only form of arsenic recognized by the detoxification systems. As(III) is taken up by the aquaglyceroporin Fps1p or by hexose permeases (Hxt1p-Hxt17p). As(III) is removed from the cytoplasm through export by the arsenite permease Acr3p or through transport into the vacuole by the ABC transporter Ycf1p as glutathione conjugates [As(GS)₃]. As(III) can also be extruded via Fps1p down the concentration gradient. In addition, the yeast cell actively exports glutathione to inactivate As(III) outside the cell and to prevent its accumulation. Fps1p recognizes arsenic in form of As(OH)₃ while Acr3p probably recognizes As(OH)₂O⁻

involves at least Pho84p and Pho87p, as deletion of *PHO84* or *PHO87* leads to As(V) tolerance (Bun-ya et al. 1996; Yompakdee et al. 1996b). As(V) influx into yeast cells can also be inhibited by disruption of *PHO86* or *GTRI*; *PHO86* encodes an endoplasmatic reticulum-localized protein involved in trafficking of Pho84p to the plasma membrane, and *GTRI* encodes a cytoplasmic GTPase regulating Pho84p-dependent phosphate transport (Bun-Ya et al. 1992, 1996; Yompakdee et al. 1996a; Lau et al. 2000). Hence, Pho84p and Pho87p are likely to mediate As(V) influx into yeast. Whether yeast can downregulate the phosphate transport systems to limit As(V) accumulation remains to be established.

Arsenite Uptake

While pathways of As(III) detoxification were well-known in bacteria and later also in yeast (see further), the routes for trivalent metalloid uptake escaped identification for a long time. Using random mutagenesis with the transposon TnphoA, Rosen and coworkers isolated a single *Escherichia coli* mutant with high-level tolerance to antimonite [Sb(OH)₃ or Sb(III)]. The transposon insertion was mapped to the *glpF* gene encoding an aquaglyceroporin involved in glycerol uptake. Based on this genetic data, it was proposed that GlpF serves as an uptake route for Sb(III) and that inactivation of the *glpF* gene results in Sb(III) tolerance due to reduced Sb(III) accumulation (Sanders et al. 1997). Later, direct transport assays confirmed that GlpF indeed mediates uptake of the related metalloids As(III) and Sb(III) into *E. coli* (Meng et al. 2004).

E. coli GlpF is homologous to the yeast aquaglyceroporin Fps1p which is a gated glycerol channel with an important role in osmoregulation (Luyten et al. 1995; Tamás et al. 1999). Since both proteins belong to the aquaporin (AQP) superfamily, we speculated that aqua(glycerol)porins may in fact be the long-sought As(III) uptake pathway. To test this hypothesis, we examined tolerance of the *FPS1* deletion mutant (*fps1Δ*) towards As(III) and Sb(III) (Wysocki et al. 2001). Indeed, *fps1Δ* cells showed high-level tolerance to both As(III) and Sb(III), and accumulated less As(III) than wild type cells. In addition, expression of a hyperactive *FPS1* allele with high transport activity resulted in increased sensitivity to both metalloids and higher intracellular content of As(III). Finally, increasing the osmolarity of the growth medium, a condition that inactivates Fps1p, rendered yeast cells more tolerant to As(III) and Sb(III) (Wysocki et al. 2001). These results clearly established the role of Fps1p in As(III) and Sb(III) transport, and was the first demonstration of a metalloid entry route in a eukaryotic organism (Fig. 4.1). Interestingly, AQPs are bidirectional channels and they may also mediate As(III) and Sb(III) efflux under certain conditions (see further). Importantly, the identification of Fps1p as a metalloid influx pathway paved the way for identifying and characterizing As(III)- and Sb(III)-transporting AQPs of plant and mammalian origin (Liu et al. 2002; Bienert et al. 2008; Isayenkov and Maathuis 2008). The findings that AQPs mediate As(III) and Sb(III) transport raised the question of how these metalloids are recognized as substrates. It was proposed that GlpF recognizes Sb(III) in the form of Sb(OH)₃,

which seems to be the dominant form of this metalloid at neutral pH (Sanders et al. 1997). It was later demonstrated that the main form of As(III) in solution is $\text{As}(\text{OH})_3$ (Ramirez-Solis et al. 2004) and that $\text{As}(\text{OH})_3$ and $\text{Sb}(\text{OH})_3$ are structurally very similar to glycerol as well as to each other (Porquet and Filella 2007). Hence, AQPs are likely to recognize $\text{As}(\text{OH})_3$ and $\text{Sb}(\text{OH})_3$ as glycerol analogues.

Hexose permeases constitute a second pathway of As(III) accumulation in yeast (Liu et al. 2004) (Fig. 4.1). It was noticed that cells lacking Fps1p accumulated significant amounts of As(III) in the absence of glucose, a condition that favours expression of many of the hexose permeases. A strain that lacks all hexose permeases accumulate less As(III) and is more tolerant than the wild type. Moreover, As(III) transport through individual hexose transporters is inhibited by glucose and *vice versa*, the presence of As(III) reduces sugar transport. The form of arsenic that is recognized by hexose transporters is not known but it was hypothesized that it may be a six-membered ring-structure consisting of three $\text{As}(\text{OH})_3$ molecules mimicking hexose sugars (Liu et al. 2004). Since the natural habitat of yeast mostly contains sugars, a condition that leads to repression of hexose permeases, Fps1p is probably the most relevant As(III)/Sb(III) entry pathway under physiological conditions. Importantly, the mammalian glucose permease GLUT1 catalyzes transport of $\text{As}(\text{OH})_3$ and a methylated form of arsenic (methylarsonous acid) when expressed in yeast or *Xenopus laevis* oocytes (Liu et al. 2006). The physiological relevance of this transport and whether GLUT1 has a role in arsenic-related diseases remains to be clarified.

One way for cells to avoid toxicity is to prevent uptake of the harmful agent. Yeast has been shown to acquire metal/metalloid tolerance by downregulating transporter activity or by removing transporter(s) from the plasma membrane by ubiquitin-mediated endocytosis followed by vacuolar degradation (reviewed in: Wysocki and Tamás 2010). Interestingly, Fps1p regulation involves both mechanisms depending on the condition that the cell encounters. In the presence of acetic acid, which also enters cells through Fps1p, Fps1p is rapidly removed from the plasma membrane and degraded to prevent influx and toxicity of this acid (Mollapour and Piper 2007). In contrast, in the presence of As(III)/Sb(III) Fps1p is regulated both at the level of transcription and transport activity but not at the level of degradation (Wysocki et al. 2001; Thorsen et al. 2006; Maciaszczyk-Dziubinska et al. 2010). First, transcription of *FPS1* rapidly decreases in response to As(III) and Sb(III), probably as a means to reduce metalloid influx and toxicity (Wysocki et al. 2001). Secondly, we demonstrated that Fps1p is phosphorylated on Thr231 by the MAP kinase Hog1p and that this modification reduces As(III) uptake through Fps1p (Thorsen et al. 2006) (Fig. 4.2). Phosphorylation of Thr231 may change the conformation of the cytosolic N-terminal tail that is important for Fps1p gating and transport activity (Tamás et al. 1999, 2003; Thorsen et al. 2006). Consequently, deletion of the N-terminal tail, changing Thr231 into Ala, or lack of Hog1p (*hog1Δ*) result in increased As(III) influx and metalloid sensitivity (Wysocki et al. 2001; Thorsen et al. 2006). Hog1p may also downregulate Fps1p activity indirectly by phosphorylating the pleckstrin homology (PH) domain proteins Rgc1p and Rgc2p, which are positive modulators of Fps1p (Beese et al. 2009). Interestingly, Rgc2p is phosphorylated in response to As(III), while disruption of *RGCI* and/or *RGC2* results in high-level As(III) tolerance (Beese et al. 2009), probably due to inhibi-

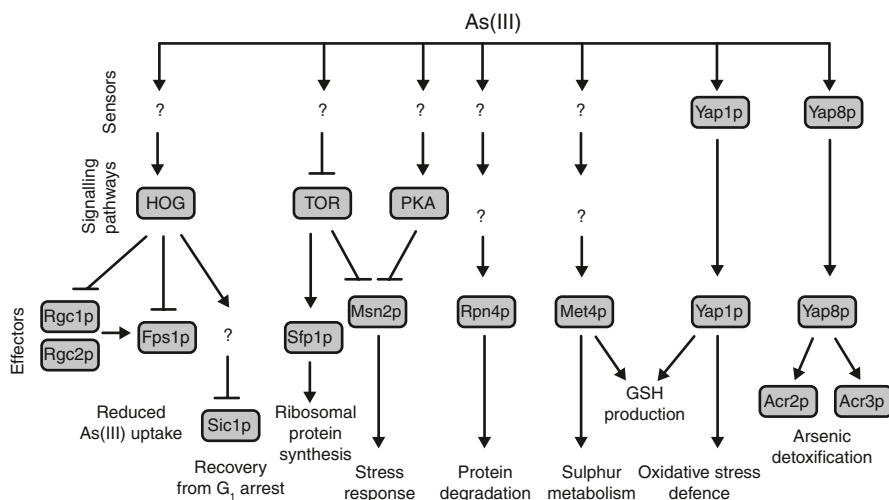


Fig. 4.2 Overview of arsenic sensing, signalling and adaptation mechanisms in budding yeast. See the text for details

tion of As(III) influx via Fps1p (Fig. 4.2). Importantly, Hog1p itself is activated by As(III) and Sb(III) and it contributes to metalloid tolerance through additional targets besides Fps1p (see further).

Arsenic Detoxification Systems in Yeast

ACR Gene Cluster—A Major Determinant of Arsenic Tolerance in Yeast

When studies on arsenic tolerance in *S. cerevisiae* were initiated in the Ulaszewski lab in 1996, knowledge of this phenomenon in eukaryotes was very limited. At that time, it was known that overexpression of the human ABC transporter MRP1 in HeLa cells enhanced their tolerance to anticancer drugs and also to As(V) and As(III), suggesting that MRP1 mediates efflux of arsenic in mammals (Cole et al. 1994). Moreover, the amplification of an at that time unknown efflux system was shown to confer high-level As(III) tolerance in *Leishmania tarentolae* (Dey et al. 1994). To isolate arsenic tolerance genes, Ulaszewski and coworkers took a classical genetic approach and screened a yeast genomic library for genes conferring hyper-tolerance to arsenic as a result of gene-copy amplification (Bobrowicz et al. 1997). Surprisingly, all arsenic tolerant clones contained multiple copies of three adjacent open reading frames of unknown function. Subsequent analyses revealed that each gene in this cluster is required for arsenic tolerance, and they were named *ACR1* (Arsenical Compound Resistance), *ACR2* and *ACR3* (Fig. 4.3). Based on the bacterial mode of metalloid tolerance, *in silico* analysis, and initial genetic char-

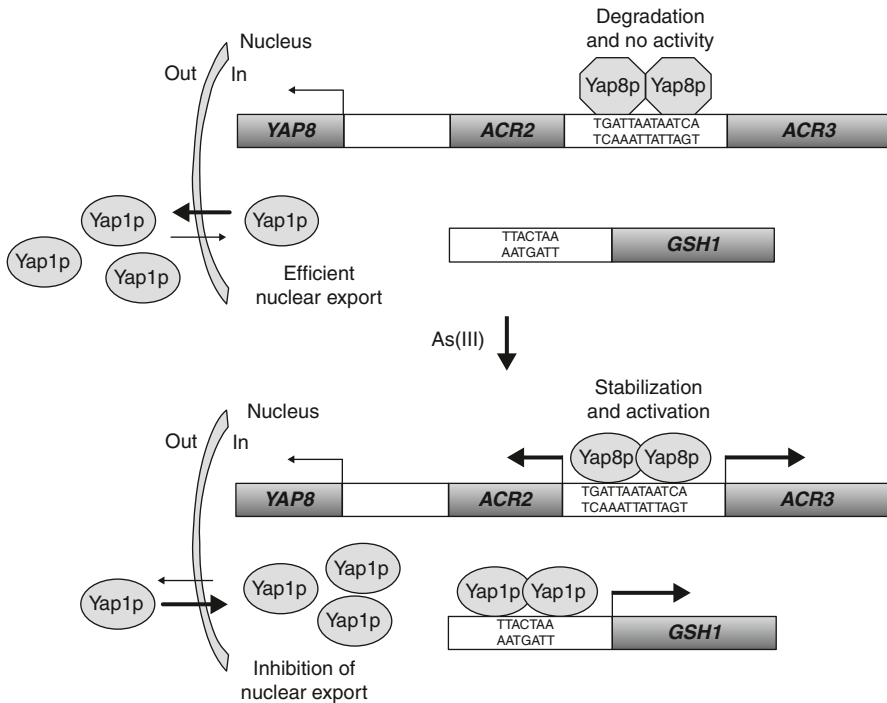


Fig. 4.3 Mechanisms of activation of gene transcription in response to arsenic by the yeast AP-1 factors Yap1p and Yap8p (also called Acr1p or Arr1p). In the absence of stress, Yap1p is maintained in the cytoplasm by promoting its nuclear export. Yap8p resides in the nucleus bound to the *ACR2-ACR3* promoter as a homodimer. In the absence of As(III), Yap8p shows no transcriptional activity and low stability. Upon addition of As(III), Yap1p quickly accumulates in the nucleus and triggers transcription of several stress defence genes, like the glutathione synthetase (*GSH1*) gene. Yap8p is stabilized and activated in the presence of As(III), probably by direct binding of As(III) to conserved cysteine residues. The exact details of As(III) sensing and target-gene activation by these proteins, remain to be elucidated

acterization of the *ACR* gene cluster, it was proposed that arsenic detoxification in yeast involves activation of the putative transcription factor Acr1p followed by Acr1p-dependent induction of *ACR2* and *ACR3* gene expression. Acr2p was proposed to reduce As(V) to As(III), and Acr3p was suggested to act as a plasma membrane As(III) export protein (Bobrowicz et al. 1997). Later, this model was confirmed by several research teams (see below).

As(III)-responsive Transcription Factor Yap8p/Acr1p

Acr1p, later called Yap8p or Arr1p, belongs to the fungal family of AP-1 like transcription factors of which Yap1p is the best characterized member (see further). These proteins contain a conserved basic leucine-zipper (bZIP) DNA-binding do-

main and conserved cysteine residues, and they activate gene expression under various environmental stress conditions (Fernandes et al. 1997; Toone and Jones 1999; Tan et al. 2008). Yap8p is indispensable for induced expression of *ACR2* and *ACR3* in response to arsenic and antimony (Fig. 4.3). In fact, *ACR2* and *ACR3* appear to be the sole gene-targets of Yap8p (Bobrowicz and Ulaszewski 1998; Wysocki et al. 2004; Ilina et al. 2008). Deletion of *YAP8* sensitizes cells to As(V) and As(III) to the same level as deletion of the genes encoding the arsenate reductase *Acr2p* and the arsenite permease *Acr3p*, respectively (Bobrowicz et al. 1997; Wysocki et al. 1997). Overexpression of *YAP8* by itself does not confer high-level metalloid tolerance, instead overexpression of the whole *YAP8(ACR1)-ACR2-ACR3* gene cluster is required to reach maximum level of tolerance (Bobrowicz et al. 1997). An interesting feature of the *ACR* gene cluster is that *ACR2* and *ACR3* share a common promoter (Bobrowicz et al. 1997; Bobrowicz and Ulaszewski 1998; Wysocki et al. 2004). This promoter contains an extended pseudopalindromic TGATTAA/TTAATCA sequence (Wysocki et al. 2004; Ilina et al. 2008), which differs from the canonical Yap1p-response element (YRE) with the TT/GAC/GTTA consensus sequence (Fernandes et al. 1997). We have shown that the TGATTAA/TTAATCA element is recognized by Yap8p and not by Yap1p, and that mutation of this pseudopalindromic sequence results in loss of As(III)-induced *ACR2* and *ACR3* expression and metalloid sensitivity (Wysocki et al. 2004; Ilina et al. 2008) (Fig. 4.3).

How Yap8p senses and is regulated by metalloids is not fully understood. *YAP8* is not regulated at the level of transcription; instead Yap8p is controlled at the level of protein stability (Wysocki et al. 2004; Di and Tamás 2007). In unexposed cells, Yap8p levels are low due to degradation via the ubiquitin-proteasome system. In response to As(III), Yap8p is stabilized and the protein level significantly increases. However, the purpose of this regulation is unclear since a dramatic increase in Yap8p protein levels only moderately enhances *ACR3* expression (Di and Tamás 2007). Yap8p resides in the nucleus where it binds to the *ACR2-ACR3* promoter as a homodimer, both in the absence as well as in the presence of As(III) (Wysocki et al. 2004; Di and Tamás 2007). Neither the presence of As(III), nor mutation of specific cysteines required for Yap8p activation (see below) affect its nuclear localization (Wysocki et al. 2004) or DNA binding-affinity (Yang and Rosen unpublished data). Importantly, three cysteine residues, Cys132, Cys137 and Cys274, which are conserved in all fungal AP-1 proteins, are required both for As(III)-induced Yap8p stabilization and for Yap8p-dependent induction of *ACR2* and *ACR3* gene expression (Menezes et al. 2004; Wysocki et al. 2004; Di and Tamás 2007). Based on these results, we hypothesized that Yap8p might sense As(III) by direct binding through the Cys132, Cys137 and Cys274 residues triggering Yap8p stabilization and activation of arsenic detoxification genes (Wysocki et al. 2004; Di and Tamás 2007). Indeed, analysis with X-ray spectroscopy revealed that As(III) binds to purified Yap8p with high affinity in an S_3 site pointing to the involvement of three cysteine residues. A Yap8p mutant lacking Cys132 and Cys274 shows dramatically reduced As(III) binding ability indicating that these are two of the three cysteines comprising the three-coordinate binding site (Yang and Rosen unpublished data). Hence, Yap8p seems to efficiently couple As(III) sensing to activation of detoxification systems.

However, how As(III)-binding alters the activity of Yap8p and how this in turn triggers induced gene expression remains to be elucidated.

Arsenate Reductase Acr2p

An arsenate reductase function for Acr2p was first inferred from the observation that the *ACR2* gene confers As(V) tolerance when co-amplified with the arsenite permease-encoding *ACR3* gene, assuming that As(V) needs to be reduced to As(III) before extrusion out of the cell (Bobrowicz et al. 1997) (Fig. 4.1). This function was later confirmed; *ACR2* deletion sensitizes cells only to As(V) (and not to As(III)) and purified Acr2p catalyzes the reduction of As(V) to As(III) with glutathione and glutaredoxin as electron donors (Mukhopadhyay and Rosen 1998; Mukhopadhyay et al. 2000). Interestingly, Acr2p uses a conserved protein tyrosine phosphatase signature HisCys(X)₅Arg motif as the catalytic centre for As(V) reduction (Mukhopadhyay and Rosen 2001). The phosphatase origin of Acr2p arsenate reductase is further supported by the evidence that Acr2p can acquire phosphatase activity by just three amino acid substitutions (Mukhopadhyay et al. 2003). Moreover, LmACR2 from *Leishmania major* displays both arsenate reductase and protein tyrosine phosphatase activities (Zhou et al. 2006). Similarly, the catalytic domains of the human protein tyrosine phosphatases Cdc25B and Cdc25C expressed and purified from *E. coli* also possess ability to reduce As(V) (Bhattacharjee et al. 2010). Importantly, characterization of yeast Acr2p as an arsenate reductase allowed the identification of similar enzymes in several plant species based on homology searches and complementation assays of the yeast *acr2Δ* mutant (Dhankher et al. 2002; Duan et al. 2005, 2007).

Arsenite Permease Acr3p

Acr3p is a plasma membrane protein that catalyzes As(III) export out of *S. cerevisiae* cells (Fig. 4.1). This protein is a major detoxification pathway not only in budding yeast (Wysocki et al. 1997; Ghosh et al. 1999) but also in several prokaryotic and fungal species (Aaltonen and Silow 2008; Fu et al. 2009). Acr3p-like proteins have 10 transmembrane domains (Aaltonen and Silow 2008; Fu et al. 2009) and constitute the arsenical resistance-3 (Acr3) family of transporters, which belongs to the bile/arsenite/riboflavin transporter (BART) superfamily (Mansour et al. 2007). Members of the Acr3 family are commonly present in prokaryotes and fungi, with so far few examples in lower plants (*Physcomitrella patens*, *Selaginella moellendorffii*, *Pteris vittata*) and one member in the animal kingdom (*Danio rerio*) (Wysocki et al. 1997; Maciaszczyk et al. 2004; Mansour et al. 2007). *ACR3* overexpression confers high-level As(III) tolerance whereas deletion of *ACR3* renders yeast cells highly sensitive due to impaired As(III) export (Bobrowicz et al. 1997; Wysocki

et al. 1997; Ghosh et al. 1999; Thorsen et al. 2006). These findings establish Acr3p as an arsenite export protein mediating tolerance. However, little is known about the mechanisms of As(III) extrusion via Acr3p and how this transporter is regulated. In analogy to the unrelated bacterial arsenite transporter ArsB (Rosen 1999), it has been hypothesized that Acr3p may facilitate transport of the arsenic anion $\text{As}(\text{OH})_2\text{O}^-$ coupled to the membrane potential and thus be classified as a uniporter (Fu et al. 2009). Interestingly, transport of As(III) through Acr3p probably involves thiol chemistry as mutated versions of Acr3 from *Alkaliphilus metalliredigens*, *Corynebacterium glutamicum* and *S. cerevisiae* lacking highly conserved cysteine residue in the fourth membrane-spanning helix are neither able to mediate As(III) export nor to confer metalloid tolerance (Fu et al. 2009); Maciaszczyk-Dziubinska, Sloma, Wysocki unpublished data). Regulation of Acr3p is well described at the transcriptional level and involves a robust Yap8p-dependent production of *ACR3* mRNA in response to metalloids (Bobrowicz and Ulaszewski 1998; Wysocki et al. 2004; Ilina et al. 2008). Whether Acr3p activity is regulated by other mechanisms remains to be determined.

Role of Fps1p in As(III) Efflux

Acr3p was initially thought to be the only way yeast could extrude As(III) (Wysocki et al. 1997; Ghosh et al. 1999). Paradoxically, we recently found that overexpression of the *FPS1* gene improved As(III) and Sb(III) tolerance, suggesting that it mediates both uptake and efflux of these metalloids (Maciaszczyk-Dziubinska et al. 2010) (Fig. 4.1). In line with this notion, we showed that the double *acr3Δfps1Δ* mutant is incapable of As(III) export while *acr3Δ* cells eventually decrease intracellular arsenic levels after prolonged exposure. Prolonged As(III) exposure triggers enhanced *FPS1* mRNA levels and more importantly, overexpression of *FPS1* reduces As(III) accumulation as a result of elevated efflux. The role of Fps1p in As(III) efflux is particularly evident during exposure to As(V) as *fps1Δ* cells are more sensitive to As(V) than the wild type (Maciaszczyk-Dziubinska et al. 2010). This dual role of Fps1p in As(III) toxicity and detoxification can be explained by the following model; immediately upon As(III) exposure, *FPS1* transcription and Fps1p transport activity are downregulated to reduce As(III) influx. During prolonged exposure, Fps1p is upregulated at the level of transcription and perhaps also at the level of activity, and the cell starts to release As(III) via Fps1p. Since Fps1p is a channel, it can only transport its substrates down a concentration gradient. We have found that yeast actively exports glutathione to form an arsenic-glutathione complex outside of cells during prolonged As(III) exposure (Thorsen, Jacobson, Vooijs, Schat and Tamás unpublished data). Formation of such arsenic-glutathione complexes would decrease the amount of free As(III) in the extracellular environment allowing diffusion of $\text{As}(\text{OH})_3$ out of cells via Fps1p down the concentration gradient. Similarly, when As(V) is reduced to As(III) by Acr2p, arsenic in the form of $\text{As}(\text{OH})_3$ may diffuse out of the cell via Fps1p down the concentration gradient,

while the $\text{As}(\text{OH})_2\text{O}^-$ anion is actively exported by Acr3p. Interestingly, AQPs from several organisms have been implicated in metalloid efflux and tolerance (Yang et al. 2005; Bienert et al. 2008; Carbrey et al. 2009; McDermott et al. 2010; Zhao et al. 2010). For instance, AqpS from the legume symbiont *Sinorhizobium meliloti* is present in an arsenic-resistance operon, and it functions as an efflux channel for As(III) that is generated by reduction of As(V) (Yang et al. 2005). Similarly, a number of plant aquaporins have been shown to be bidirectional channels mediating As(III) efflux from roots (Zhao et al. 2010), or conferring tolerance to As(V) when expressed in yeast (Bienert et al. 2008). Just recently, an important role for arsenic tolerance has been reported for the mammalian aquaglyceroporin Aqp9; human Aqp9 expressed in *Xenopus laevis* oocytes mediates export of methylated arsenic species (McDermott et al. 2010), and knockout mice lacking AQP9 shows increased sensitivity to As(III) due to impaired arsenic clearance into feces and urine (Carbrey et al. 2009). Thus, in addition to the well-established role in As(III) accumulation, aquaglyceroporins may also contribute to As(III) tolerance.

Vacuolar Sequestration of Metalloids

Transport of metals/metalloids into vacuoles or other internal organelles is a common detoxification mechanism in eukaryotes, and Ycf1p plays a central role in this process in yeast (reviewed in: (Paumi et al. 2009)). The *YCF1* gene (Yeast Cadmium Factor 1) was isolated in a screen for genes conferring cadmium tolerance to yeast cells when overexpressed (Szczyzka et al. 1994). Ycf1p shares a high degree of sequence similarity with the multidrug-associated protein MRP1, and it catalyzes ATP-dependent transport of endogenously produced toxins and of a range of glutathione-conjugated metals and xenobiotics into the vacuole (reviewed in Paumi et al. 2009). Ycf1p has been shown to contribute to the detoxification of As(III), Sb(III) and several other metals (Ghosh et al. 1999; Wysocki et al. 2001; Paumi et al. 2009). Cells lacking *YCF1* (*ycf1Δ*) are sensitive to As(III) and Sb(III) (Ghosh et al. 1999; Wysocki et al. 2001), Ycf1p catalyzes active transport of $\text{As}(\text{GS})_3$ into vacuoles *in vitro*, and Sb(III) inhibits Ycf1p-mediated transport of GSH conjugates (Ghosh et al. 1999; Gueldry et al. 2003). Together, these data establish the role of Ycf1p-mediated transport of metalloid-GSH conjugates for As(III)/Sb(III) tolerance (Fig. 4.1). Hence, Acr3p and Ycf1p represent two distinct and parallel yeast metalloid detoxification pathways with different specificities.

How Ycf1p is regulated by metals/metalloids is not well-understood. Expression of the *YCF1* gene is not induced to any large extent in wild type cells exposed to As(III) or Sb(III) (Wysocki et al. 2004). However, *YCF1* expression can be stimulated by overexpression of the transcriptional regulator Yap1p (Wemmie et al. 1994; Sharma et al. 2002) or in mutants that hyperaccumulate As(III) in the cytosol (Wysocki et al. 2004). In contrast, Ycf1p appears to be regulated at the level of proteolytic processing, intracellular trafficking, and phosphorylation (Mason and Michaelis 2002; Mason et al. 2003; Eraso et al. 2004; Paumi et al. 2008). Ycf1p transport activity is

positively affected by phosphorylation of Ser908 and Thr911, and by the guanine exchange factor Tus1p. However, mutation of these phosphorylated residues or deleting *TUS1* have only moderate effects on Ycf1p transport activity (Szczyepka et al. 1994; Eraso et al. 2004; Paumi et al. 2007). Phosphorylation of Ser251 has a negative effect on transport since mutation of Ser251 increases Ycf1p transport activity *in vitro* and enhances cadmium tolerance *in vivo* (Paumi et al. 2008). Recently, two kinases, Cka1p and Hal5p, were shown to interact with Ycf1p in an integrated membrane yeast two-hybrid screen (Paumi et al. 2008), but whether these kinases act as negative regulators of Ycf1p is not known. Further studies are required to establish how Ycf1p activity is modulated by As(III) and other metal(loid)s.

Glutathione Biosynthesis and the Role of Met4p

Glutathione (GSH) is a low-molecular-weight thiol molecule that is essential for viability of yeast and mammals. GSH is considered the main redox buffer of the cell, it serves as an electron donor for many enzymes, and is a key factor in the defence against oxidative stress and metal toxicity. GSH biosynthesis in *S. cerevisiae* involves sulphur uptake, reduction through the sulphur assimilation pathway and incorporation into the sulphur-containing amino acids methionine and cysteine, or into the low-molecular-weight thiol molecules S-adenosylmethionine and GSH. GSH contributes to metal/metalloid detoxification in several ways. First, it can bind to metals and the resulting complex is a substrate for proteins that mediate vacuolar sequestration (see above). Secondly, GSH protects cells against metal-induced oxidation. Thirdly, GSH may bind to reactive sulphhydryl groups on proteins (protein glutathionylation) thereby shielding them from irreversible metal binding and/or oxidative damage (Thomas and Surdin-Kerjan 1997; Grant 2001; Pompella et al. 2003). The first two mechanisms contribute to As(III) tolerance whereas the role of protein glutathionylation has not been investigated. As(III) exposed yeast cells strongly increase GSH biosynthesis and accumulate high levels of GSH in the cytosol (Thorsen et al. 2007). This is achieved by enhanced expression of basically all the genes in the sulphate assimilation and GSH biosynthesis pathways, as well as by elevated levels of the corresponding enzymes. Cells also boost sulphur metabolite pools, the GSH synthesis rate, as well as the flux in the GSH pathway. Interestingly, cells appear to redirect sulphur metabolism in response to As(III) by channelling a large part of the assimilated sulphur into GSH biosynthesis at the expense of sulphur incorporation into proteins (Thorsen et al. 2007). A similar response of the sulphur/GSH pathway occurs in cadmium-exposed cells (Momose and Iwahashi 2001; Vido et al. 2001; Fauchon et al. 2002; Lafaye et al. 2005). The importance of the sulphur assimilation/GSH biosynthesis pathways for As(III) tolerance is underscored by the fact that mutants lacking components or regulators of these pathways display As(III) sensitivity (Thorsen et al. 2007, 2009). An often cited mechanism of As(III) toxicity is GSH depletion (*e.g.* (Stohs and Bagchi 1995)). The observation that cytosolic GSH levels strongly increase in response to As(III) would argue against GSH deple-

tion as a major As(III) toxicity mechanism, at least in *S. cerevisiae* (Lafaye et al. 2005; Thorsen et al. 2007). We recently discovered a novel detoxification function for GSH involving extracellular chelation of As(III). During prolonged As(III) exposure, yeast cells export significant amounts of GSH to form a complex with As(III) outside cells. This complex does not readily enter cells; consequently, cells that produce and export GSH accumulate less arsenic in the cytosol and show improved tolerance (Thorsen, Jacobson, Vooijs, Schat and Tamás unpublished data) (Fig. 4.1).

The main regulator of the sulphur assimilation and GSH biosynthesis pathways is the bZIP transcriptional activator Met4p. The activity of Met4p is regulated by variations in the intracellular pool of an organic sulphur compound, possibly cysteine (Thomas and Surdin-Kerjan 1997; Hansen and Johannsen 2000; Menant et al. 2006) and by metal(loid)s like As(III) and cadmium (Fauchon et al. 2002, Yen et al. 2005, Thorsen et al. 2007). Met4p cannot bind to DNA itself but is recruited to target promoters by the DNA-binding proteins Met31p, Met32p and Cbf1p. Another co-factor, Met28p, stabilizes the DNA-bound Met4p-containing complexes (Thomas and Surdin-Kerjan 1997; Lee et al. 2009). Met4p regulation involves Met30p, the F-subunit of the SCF^{Met30} (Skp1/Cullin/F-box protein, where Met30p is the F-box protein) ubiquitin ligase complex that targets Met4p for ubiquitylation and inactivation. Interestingly, ubiquitylated Met4p can either be targeted by the 26S proteasome for degradation or it can be maintained in an oligo-ubiquitylated (one to four ubiquitin moieties) form without degradation (Kaiser et al. 2000; Rouillon et al. 2000; Kuras et al. 2002; Chandrasekaran et al. 2006; Flick et al. 2006). Cadmium has been shown to inhibit SCF^{Met30} activity by triggering dissociation of Met30p from the ubiquitin ligase complex. This is followed by a deubiquitylation step that removes ubiquitin moieties from Met4p, thereby fully restoring Met4p activity and expression of Met4p-dependent genes (Barbey et al. 2005; Yen et al. 2005). Similar effects on Met4p ubiquitylation have been observed with As(III) (Yen et al. 2005), which is consistent with the importance of Met4p for As(III)-induced expression of sulphur/GSH genes and As(III) tolerance (Thorsen et al. 2007) (Fig. 4.2). However, it is not known how cadmium and As(III) trigger dissociation of Met30p from the ubiquitin ligase complex, nor is the identity of the deubiquitylating enzyme that acts on Met4p known. Interestingly, fully activated Met4p triggers a cell cycle arrest (Patton et al. 2000; Su et al. 2005). The observations that As(III)-treated cells activate Met4p (Yen et al. 2005; Thorsen et al. 2007), enhance sulphur/GSH metabolism (Thorsen et al. 2007), and arrest cell cycle progression (Migdal et al. 2008) suggest a link between sulphur metabolism and cell cycle regulation, and a possible role for Met30p-Met4p in this control.

Oxidative Stress Defence and Yap1p

As(III) can induce enhanced ROS production leading to oxidative damage of proteins and other macromolecules (Liu et al. 2001; Menezes et al. 2008). In line with this, cells induce expression of genes and proteins with antioxidant functions in

response to As(III) exposure (Haugen et al. 2004; Thorsen et al. 2007). Yap1p, one of eight *S. cerevisiae* AP-1-like transcription factors (Yap1p to Yap8p), plays a central role in oxidative stress defence and metal tolerance. Yap1p regulates expression of genes encoding proteins that maintain a favourable redox balance in the cell, enzymes involved in detoxification of ROS, and proteins conferring metal and drug resistance (Lee et al. 1999; Gasch et al. 2000; Haugen et al. 2004; Thorsen et al. 2007). Cells lacking *YAP1* (*yap1Δ*) fail to properly induce expression of its gene-targets and display sensitivity to various oxidants and metals including As(III) and Sb(III) (Wysocki et al. 2004; Thorsen et al. 2007). Yap1p binds to the so-called Yap1p recognition element (YRE) with the consensus sequence TT/GAC/GTAA (Kuge and Jones 1994; Wu and Moye-Rowley 1994; Fernandes et al. 1997; Harbison et al. 2004; Tan et al. 2008), but it may also trigger gene expression through alternative YRE sequences (He and Fassler 2005).

Yap1p is activated by a broad range of stress agents including many oxidants, metals and the metalloids As(III) and Sb(III) (reviewed in: (Tamás et al. 2005; D'Autreaux and Toledano 2007)). Importantly, all these agents control Yap1p through regulated nuclear export by stress-induced post-translational modifications. Yap1p is mainly localized to the cytosol in the absence of stress due to rapid nuclear export mediated by the nuclear export receptor Crm1p that interacts with a nuclear export signal (NES) within Yap1p (Kuge et al. 1997, 1998; Yan et al. 1998) (Fig. 4.3). Exposure to stress signals triggers redox- or chemical-dependent modifications of Yap1p cysteines, loss of the Yap1p-Crm1p interaction, and nuclear accumulation of Yap1p (Kuge et al. 1998; Yan et al. 1998). In response to H₂O₂, disulphide bonds are formed between conserved N- and C-terminal cysteines (Delaunay et al. 2000; Wood et al. 2003). This disulphide linkage triggers a conformational change within Yap1p which masks the NES and results in its nuclear accumulation. Conversely, reduction of these disulphide bonds causes structural modifications that lead to NES exposure and redistribution of Yap1p to the cytosol (Wood et al. 2004). Yap1p activation by H₂O₂ involves Gpx3p that acts as the actual H₂O₂ sensor (Delaunay et al. 2002; Paulsen and Carroll 2009) and a second protein Ybp1p (Veal et al. 2003; Gulshan et al. 2004) whose function is not understood. The Gpx3p-Yap1p H₂O₂ sensor operates as a cysteine-redox relay where Gpx3p senses the H₂O₂ signal and transduces this signal to Yap1p (Delaunay et al. 2002; D'Autreaux and Toledano 2007; Paulsen and Carroll 2009). Metals and chemicals also activate Yap1p by regulating its nuclear export, but sensing of these compounds does not involve disulphide linkage between N- and C-terminal cysteines or Gpx3p (Kuge et al. 1997; Delaunay et al. 2000; Azevedo et al. 2003; Veal et al. 2003; Gulshan et al. 2004). For example, the electrophile N-ethylmaleimide activates Yap1p by covalent modification of C-terminal cysteines (Azevedo et al. 2003) whilst Yap1p activation by diamide involves formation of disulphide bonds between either one of the C-terminal cysteines Cys598, Cys620 and Cys629 (Kuge et al. 2001). How Yap1p senses As(III) is not completely understood. Yap1p mutants with modified C-terminal cysteines or N-terminal cysteines together with modified Cys620 displayed perturbed nuclear retention and reduced ability to confer As(III) tolerance (Wysocki et al. 2004). Whether these cysteines directly interact with As(III),

whether As(III) activates Yap1p through oxidative modifications, and whether those modifications disrupt the Yap1p-Crm1p interaction, remain to be revealed.

Hog1p and Cell Cycle Regulation in Response to As(III) Exposure

The p38 MAP kinase is a major stress-responsive signal transduction pathway in mammalian cells that is activated by As(III) (Cuenda and Rousseau 2007). As(III)-induced activation of p38 results in cell cycle arrest, differentiation, or induction of mitochondrial apoptotic cell death. In agreement with these findings, suppression of p38 activity attenuates growth inhibition and apoptosis of several malignant cell lines treated with As(III) (Kim et al. 2002; Li and Yang 2007). On the other hand, p38 shows a survival function in leukaemia cells by downregulating As(III)-induced apoptosis and increased activation of p38 is observed in As(III)-resistant myeloma cells (Wen et al. 2008). Hence, pharmacological inhibition of p38 greatly sensitizes leukaemia cells to As(III) treatment (Elbirt et al. 1998; Verma et al. 2002; Giafis et al. 2006). Similarly, the yeast p38 homologue Hog1p is also activated by As(III), while deletion of *HOG1* results in metalloid sensitivity (Thorsen et al. 2006) (Fig. 4.2). Importantly, under mild osmotic stress, Hog1p delays cell cycle progression by negatively regulating the activity of cyclin-dependent kinase complexes through a number of different mechanisms (Escoté et al. 2004; Clotet et al. 2006; Yaakov et al. 2009). Having established that Hog1p contributes to metalloid tolerance in yeast (Thorsen et al. 2006), we decided to examine the kinetics of yeast cell cycle progression and a possible role of Hog1p in regulating cell cycle checkpoints during As(III) stress (Migdal et al. 2008). Wild type cells exposed to As(III) display a transient growth delay in all phases of the cell cycle, indicating activation of cell cycle checkpoints followed by growth resumption. In contrast, *hog1Δ* cells permanently arrest in the G₁ phase suggesting that Hog1p promotes recovery from As(III)-induced cell cycle delay in G₁. We found that the observed cell cycle arrest in G₁ is associated with accumulation of Sic1p, an inhibitor of S phase cyclin-dependent kinase complexes. Moreover, the cell cycle defect of *hog1Δ* is fully suppressed by deleting the *SIC1* gene. Thus, Hog1p has a G₁-specific adaptation role by targeting Sic1p for degradation to allow entry into S phase after As(III)-induced cell cycle arrest (Migdal et al. 2008) (Fig. 4.2). However, the molecular mechanism of Hog1p-dependent degradation of Sic1p during As(III) stress remains to be revealed.

Other Detoxification and Tolerance Systems

Global Analysis of Tolerance Factors in Yeast

Recent screenings of genome-wide yeast knock-out mutant collections revealed a wide array of cellular functions that contribute to arsenic tolerance. Processes

required for tolerance acquisition include sulphur and GSH metabolism, environmental sensing and signalling, transcriptional regulation, and the cytoskeleton. Importantly, many of the arsenic-sensitive yeast genes have human orthologues and similar processes are associated with arsenic toxicity in various mammalian systems (Haugen et al. 2004; Dilda and Hogg 2007; Vujcic et al. 2007; Dilda et al. 2008; Jin et al. 2008; Jo et al. 2008; Ralph 2008; Thorsen et al. 2009). Hence, similar systems may act in yeast and humans to prevent arsenic toxicity. However, although many gene-products are associated with arsenic tolerance, the mechanisms by which they mediate tolerance acquisition are largely unknown.

Proteasomal Degradation of Damaged Proteins

As(III) interferes with enzyme/protein folding and activity (Aposhian and Aposhian 2006; Kitchin and Wallace 2008), and exposure may lead to accumulation of damaged proteins. The ubiquitin-proteasome pathway provides a mechanism to remove damaged or non-functional proteins (Goldberg 2003) and expression of proteasomal genes is induced by As(III). Enhanced expression of proteasomal genes requires the transcription factor Rpn4p, and cells lacking *RPN4* are highly As(III)-sensitive (Haugen et al. 2004; Thorsen et al. 2007, 2009) (Fig. 4.2). These data suggest that cells may increase the number of proteasomes and/or proteasome activity, and that enhanced protein degradation is important for As(III) tolerance. The latter is supported by the observation that mutants defective in the ubiquitin-proteasome pathway display severe As(III)-sensitivity (Di and Tamás 2007). Hence, As(III)-treated cells may accumulate damaged proteins that need to be removed for optimal tolerance.

TOR- and PKA-Pathway: Regulation of General Stress Responses and Ribosomal Proteins

Recent findings implicate two nutrient sensing and signalling pathways, the TOR (target of rapamycin) and PKA (Protein Kinase A) pathways (Santangelo 2006; Wullschleger et al. 2006; Soulard et al. 2009), in As(III) tolerance by modulating expression of genes involved in stress protection and protein biosynthesis (Hosiner et al. 2009) (Fig. 4.2). As(III) inhibits the TORC1 (TOR complex 1) protein kinase causing down-regulation of ribosomal protein-gene expression due to deactivation and nuclear exit of the TOR-regulated transcription factor Sfp1p. As(III) also triggers translocation of the redundant 'general stress responsive' transcription factors Msn2p and Msn4p from the cytosol to the nucleus leading to stimulation of target-gene expression (Hosiner et al. 2009). The activity of Msn2p/Msn4p is regulated by growth conditions and the nutritional status of cells, and involves the PKA and TOR pathways (Görner et al. 1998; Beck and Hall 1999). Interestingly, deletion of both *MSN2* and *MSN4* (*msn2Δ msn4Δ*) results in increased As(III) tolerance whereas their overexpression enhances sensitivity (Hosiner et al. 2009). Based on these data, it was suggested that As(III) toxicity might be a consequence of chronic activation

of stress responsive genes via Msn2p/Msn4p (Hosiner et al. 2009). In line with this notion, hyperactivation of these proteins has a negative effect on cell growth (Durchschlag et al. 2004). Curiously, while *tor1Δ* cells are As(III) sensitive, *SFP1* deletion results in enhanced As(III) tolerance. Moreover, *SFP1* overexpression sensitizes cells to As(III) (Hosiner et al. 2009). Currently, it is not completely clear how these apparently contradictory views on the role of Sfp1p and TORC1 can be reconciled into a coherent model.

Yeast as a Model System for Elucidating the Molecular Biology of Arsenic Toxicity and Tolerance

There are many examples of the power of yeast as a model to elucidate fundamental biological mechanisms. The examples below illustrate and underscore the impact that research on yeast has had for advancing our understanding of the molecular details of arsenic toxicity and tolerance in eukaryotic cells.

Aquaporins, Metalloid Transport and Human Health

Arsenic trioxide (As₂O₃) is currently used as a treatment for acute promyelocytic leukaemia, and arsenic- and antimony-containing drugs are used to treat diseases caused by the protozoan parasites *Leishmania* and *Trypanosoma*. To understand the action of these drugs, it is important to elucidate the pathways of drug uptake, factors that modulate their uptake, as well as regulation of drug uptake pathways (reviewed in Bhattacharjee et al. 2009). The finding that Fps1p mediates As(III)/Sb(III) uptake into yeast cells (Wysocki et al. 2001) has been important for identifying metalloid transporting aqua(glycerol)porins of mammalian and plant origin. For example, heterologous expression of rat rAQP9 and several plant AQPs in yeast lacking influx and detoxification pathways (*acr3Δ ycf1Δ fps1Δ*) reversed metalloid resistance and restored As(III) uptake in those cells (Liu et al. 2002; Bienert et al. 2008; Isayenkov and Maathuis 2008). Additional studies in bacteria, *Leishmania* and crop plants (e.g. rice) have confirmed that AQPs are metalloid entry pathways in probably most organisms (Gourbal et al. 2004; Meng et al. 2004; Ma et al. 2008). Importantly, this knowledge has been instrumental for exploring toxicity mechanisms and drug action. First, overexpression of specific AQPs sensitizes human leukaemia cells to metalloids due to increased accumulation (Bhattacharjee et al. 2004) and As₂O₃ sensitivity has been found to be proportional to AQP9 expression in leukemia cells (Leung et al. 2007). Similarly, *Leishmania major* takes up As(III) and Sb(III) through LmAQP1 and this aquaporin appears to play a major role in drug resistance (Gourbal et al. 2004). Secondly, our finding that phosphorylation of the aquaglyceroporin Fps1p by the p38-like MAP kinase Hog1p reduces uptake of As(III) and Sb(III) into yeast cells (Thorsen et al. 2006) suggests that down-regulation of MAP kinase activity may be an effective way to sensitize cells by increasing metalloid influx. In this way, malignant cell growth may be inhibited or

drug resistance may be reversed. Finally, As(III) uptake into crop plants, especially into rice, may be a major route for human exposure to this toxic agent. Hence, identification of As(III)-transporting plant aquaporins (Bienert et al. 2008; Isayenkov and Maathuis 2008; Ma et al. 2008) opens the way for modulating their activity and potentially reducing As(III) accumulation in crop plants.

ACR-Proteins in Plants

The prospect of using plants to clean contaminated soils (phytoremediation) as well as the development of 'safe crops' that do not accumulate arsenic, has recently attracted considerable attention. Nevertheless, to develop safe crop plants and plants for phytoremediation requires detailed understanding of arsenic toxicity and detoxification processes (Tripathi et al. 2007; Zhu and Rosen 2009). The identification of Acr2p and Acr3p homologues in *Pteris vittata* (Chinese brake fern) indicates that arsenic detoxification involving enzymatic reduction of As(V) to As(III) followed by As(III) export is conserved from bacteria to plants (Ellis et al. 2006; Salt and Norton 2008). Importantly, *P. vittata* is capable of hyperaccumulating arsenic in the fronds without toxicity and can therefore potentially be used for phytoremediation of contaminated soils (Ma et al. 2001). The exact role of *P. vittata* Acr2p and Acr3p in this process remains to be revealed.

Conclusions

It is clear that yeast is a very valuable tool and model system for elucidating As(III) toxicity and tolerance mechanisms. Indeed, from what was first learned in *S. cerevisiae*, we now know that metalloid uptake involves aqua(glycerol)porins probably in all organisms, and that several yeast detoxification systems also exist in higher eukaryotes. Nevertheless, although many systems appear to be conserved from yeast to man, more research is needed before we fully appreciate their roles in human health and diseases.

Acknowledgements The work in the Tamás lab is supported by the Swedish Research Council and the foundations Magnus Bergvalls Stiftelse and Stiftelsen Olle Engkvist Byggmästare. Work in the Wysocki lab is supported by grants from the Polish Ministry of Science and Higher Education.

References

- Aaltonen EK, Silow M (2008) Transmembrane topology of the Acr3 family arsenite transporter from *Bacillus subtilis*. *Biochim Biophys Acta* 1778:963–973
- Aposhian HV, Aposhian MM (2006) Arsenic toxicology: five questions. *Chem Res Toxicol* 19:1–15

- Azevedo D, Tacnet F, Delaunay A, Rodrigues-Pousada C, Toledano MB (2003) Two redox centers within Yap1 for H₂O₂ and thiol-reactive chemicals signaling. *Free Radic Biol Med* 35:889–900
- Barbey R, Baudouin-Cornu P, Lee TA, Rouillon A, Zarzov P, Tyers M, Thomas D (2005) Inducible dissociation of SCF^{Met30} ubiquitin ligase mediates a rapid transcriptional response to cadmium. *EMBO J* 24:521–532
- Beck T, Hall MN (1999) The TOR signalling pathway controls nuclear localization of nutrient-regulated transcription factors. *Nature* 402:689–692
- Beese SE, Negishi T, Levin DE (2009) Identification of positive regulators of the yeast Fps1 glycerol channel. *PLoS Genet* 5:e1000738
- Beyersmann D, Hartwig A (2008) Carcinogenic metal compounds: recent insight into molecular and cellular mechanisms. *Arch Toxicol* 82:493–512
- Bhattacharjee H, Carbrey J, Rosen BP, Mukhopadhyay R (2004) Drug uptake and pharmacological modulation of drug sensitivity in leukemia by AQP9. *Biochem Biophys Res Commun* 322:836–841
- Bhattacharjee H, Rosen BP, Mukhopadhyay R (2009) Aquaglyceroporins and metalloids transport: implications in human diseases. *Handb Exp Pharmacol* 309–325
- Bhattacharjee H, Sheng J, Ajees AA, Mukhopadhyay R, Rosen BP (2010) Adventitious arsenate reductase activity of the catalytic domain of the human Cdc25B and Cdc25C phosphatases. *Biochemistry* 49:802–809
- Bienert GP, Thorsen M, Schussler MD, Nilsson HR, Wagner A, Tamás MJ, Jahn TP (2008) A subgroup of plant aquaporins facilitate the bi-directional diffusion of As(OH)₃ and Sb(OH)₃ across membranes. *BMC Biol* 6:26
- Bobrowicz P, Ulaszewski S (1998) Arsenical-induced transcriptional activation of the yeast *Saccharomyces cerevisiae* *ACR2* and *ACR3* genes requires the presence of the *ACR1* gene product. *Cell Mol Biol Lett* 3:13–20
- Bobrowicz P, Wysocki R, Owsiński G, Goffeau A, Ulaszewski S (1997) Isolation of three contiguous genes, *ACR1*, *ACR2* and *ACR3*, involved in resistance to arsenic compounds in the yeast *Saccharomyces cerevisiae*. *Yeast* 13:819–828
- Bun-Ya M, Harashima S, Oshima Y (1992) Putative GTP-binding protein, Gtr1, associated with the function of the Pho84 inorganic phosphate transporter in *Saccharomyces cerevisiae*. *Mol Cell Biol* 12:2958–2966
- Bun-ya M, Shikata K, Nakade S, Yompakdee C, Harashima S, Oshima Y (1996) Two new genes, PHO86 and PHO87 involved in inorganic phosphate uptake in *Saccharomyces cerevisiae*. *Curr Genet* 29:344–351
- Carbrey JM, Song L, Zhou Y, Yoshinaga M, Rojek A, Wang Y, Liu Y, Lujan HL, DiCarlo SE, Nielsen S, Rosen BP, Agre P, Mukhopadhyay R (2009) Reduced arsenic clearance and increased toxicity in aquaglyceroporin-9-null mice. *Proc Natl Acad Sci U S A* 106:15956–15960
- Chandrasekaran S, Deffenbaugh AE, Ford DA, Bailly E, Mathias N, Skowrya D (2006) Destabilization of binding to cofactors and SCF^{Met30} is the rate-limiting regulatory step in degradation of polyubiquitinated Met4. *Mol Cell* 24:689–699
- Chen F, Shi X (2002) Intracellular signal transduction of cells in response to carcinogenic metals. *Crit Rev Oncol Hematol* 42:105–121
- Chen GQ, Shi XG, Tang W, Xiong SM, Zhu J, Cai X, Han ZG, Ni JH, Shi GY, Jia PM, Liu MM, He KL, Niu C, Ma J, Zhang P, Zhang TD, Paul P, Naoe T, Kitamura K, Miller W, Waxman S, Wang ZY, de The H, Chen SJ, Chen Z (1997) Use of arsenic trioxide (As₂O₃) in the treatment of acute promyelocytic leukemia (APL): I. As₂O₃ exerts dose-dependent dual effects on APL cells. *Blood* 89:3345–3353
- Clotet J, Escote X, Adrover MA, Yaakov G, Gari E, Aldea M, de Nadal E, Posas F (2006) Phosphorylation of Hsl1 by Hog1 leads to a G₂ arrest essential for cell survival at high osmolarity. *EMBO J* 25:2338–2346
- Cole SP, Sparks KE, Fraser K, Loe DW, Grant CE, Wilson GM, Deeley RG (1994) Pharmacological characterization of multidrug resistant MRP-transfected human tumor cells. *Cancer Res* 54:5902–5910

- Cortes P, Castrejon V, Sampedro JG, Uribe S (2000) Interactions of arsenate, sulfate and phosphate with yeast mitochondria. *Biochim Biophys Acta* 1456:67–76
- Cuenda A, Rousseau S (2007) p38 MAP-kinases pathway regulation, function and role in human diseases. *Biochim Biophys Acta* 1773:1358–1375
- D’Autreaux B, Toledano MB (2007) ROS as signalling molecules: mechanisms that generate specificity in ROS homeostasis. *Nat Rev Mol Cell Biol* 8:813–824
- Delaunay A, Isnard AD, Toledano MB (2000) H₂O₂ sensing through oxidation of the Yap1 transcription factor. *EMBO J* 19:5157–5166
- Delaunay A, Pflieger D, Barrault MB, Vinh J, Toledano MB (2002) A thiol peroxidase is an H₂O₂ receptor and redox-transducer in gene activation. *Cell* 111:471–481
- Dey S, Papadopoulou B, Haimeur A, Roy G, Grondin K, Dou D, Rosen BP, Ouellette M (1994) High level arsenite resistance in *Leishmania tarentolae* is mediated by an active extrusion system. *Mol Biochem Parasitol* 67:49–57
- Dhankher OP, Li Y, Rosen BP, Shi J, Salt D, Senecoff JF, Sashti NA, Meagher RB (2002) Engineering tolerance and hyperaccumulation of arsenic in plants by combining arsenate reductase and gamma-glutamylcysteine synthetase expression. *Nat Biotechnol* 20:1140–1145
- Di Y, Tamás MJ (2007) Regulation of the arsenic-responsive transcription factor Yap8p involves the ubiquitin-proteasome pathway. *J Cell Sci* 120:256–264
- Dilda PJ, Hogg PJ (2007) Arsenical-based cancer drugs. *Cancer Treat Rev* 33:542–564
- Dilda PJ, Perrone GG, Philp A, Lock RB, Dawes IW, Hogg PJ (2008) Insight into the selectivity of arsenic trioxide for acute promyelocytic leukemia cells by characterizing *Saccharomyces cerevisiae* deletion strains that are sensitive or resistant to the metalloloid. *Int J Biochem Cell Biol* 40:1016–1029
- Duan GL, Zhu YG, Tong YP, Cai C, Kneer R (2005) Characterization of arsenate reductase in the extract of roots and fronds of Chinese brake fern, an arsenic hyperaccumulator. *Plant Physiol* 138:461–469
- Duan GL, Zhou Y, Tong YP, Mukhopadhyay R, Rosen BP, Zhu YG (2007) A CDC25 homologue from rice functions as an arsenate reductase. *New Phytol* 174:311–321
- Durchschlag E, Reiter W, Ammerer G, Schuller C (2004) Nuclear localization destabilizes the stress-regulated transcription factor Msn2. *J Biol Chem* 279:55425–55432
- Elbirt KK, Whitmarsh AJ, Davis RJ, Bonkovsky HL (1998) Mechanism of sodium arsenite-mediated induction of heme oxygenase-1 in hepatoma cells. Role of mitogen-activated protein kinases. *J Biol Chem* 273:8922–8931
- Ellis DR, Gumaelius L, Indriolo E, Pickering IJ, Banks JA, Salt DE (2006) A novel arsenate reductase from the arsenic hyperaccumulating fern *Pteris vittata*. *Plant Physiol* 141:1544–1554
- Eraso P, Martinez-Burgos M, Falcon-Perez JM, Portillo F, Mazon MJ (2004) Ycf1-dependent cadmium detoxification by yeast requires phosphorylation of residues Ser(908) and Thr(911). *FEBS Lett* 577:322–326
- Ercal N, Gurer-Orhan H, Aykin-Burns N (2001) Toxic metals and oxidative stress part I: mechanisms involved in metal-induced oxidative damage. *Curr Top Med Chem* 1:529–539
- Escoté X, Zapater M, Clotet J, Posas F (2004) Hog1 mediates cell-cycle arrest in G1 phase by the dual targeting of Sic1. *Nat Cell Biol* 6:997–1002
- Fauchon M, Lagniel G, Aude JC, Lombardia L, Soularue P, Petat C, Marguerie G, Sentenac A, Werner M, Labarre J (2002) Sulfur sparing in the yeast proteome in response to sulfur demand. *Mol Cell* 9:713–723
- Fernandes L, Rodrigues-Pousada C, Struhl K (1997) Yap, a novel family of eight bZIP proteins in *Saccharomyces cerevisiae* with distinct biological functions. *Mol Cell Biol* 17:6982–6993
- Flick K, Raasi S, Zhang H, Yen JL, Kaiser P (2006) A ubiquitin-interacting motif protects polyubiquitinated Met4 from degradation by the 26S proteasome. *Nat Cell Biol* 8:509–515
- Fu HL, Meng Y, Ordonez E, Villadangos AF, Bhattacharjee H, Gil JA, Mateos LM, Rosen BP (2009) Properties of arsenite efflux permeases (Acr3) from *Alkaliphilus metalliredigens* and *Corynebacterium glutamicum*. *J Biol Chem* 284:19887–19895
- Gasch AP, Spellman PT, Kao CM, Carmel-Harel O, Eisen MB, Storz G, Botstein D, Brown PO (2000) Genomic expression programs in the response of yeast cells to environmental changes. *Mol Biol Cell* 11:4241–4257

- Ghosh M, Shen J, Rosen BP (1999) Pathways of As(III) detoxification in *Saccharomyces cerevisiae*. Proc Natl Acad Sci U S A 96:5001–5006
- Giafais N, Katsoulidis E, Sassano A, Tallman MS, Higgins LS, Nebreda AR, Davis RJ, Platanius LC (2006) Role of the p38 mitogen-activated protein kinase pathway in the generation of arsenic trioxide-dependent cellular responses. Cancer Res 66:6763–6771
- Goldberg AL (2003) Protein degradation and protection against misfolded or damaged proteins. Nature 426:895–899
- Görner W, Durchschlag E, Martinez-Pastor MT, Estruch F, Ammerer G, Hamilton B, Ruis H, Schuller C (1998) Nuclear localization of the C₂H₂ zinc finger protein Msn2p is regulated by stress and protein kinase A activity. Genes Dev 12:586–597
- Gourbal B, Sonuc N, Bhattacharjee H, Legare D, Sundar S, Ouellette M, Rosen BP, Mukhopadhyay R (2004) Drug uptake and modulation of drug resistance in leishmania by an aquaglyceroporin. J Biol Chem 279:31010–31017
- Grant CM (2001) Role of the glutathione/glutaredoxin and thioredoxin systems in yeast growth and response to stress conditions. Mol Microbiol 39:533–541
- Guedry O, Lazard M, Delort F, Dauplais M, Grigoras I, Blanquet S, Plateau P (2003) Ycf1p-dependent Hg(II) detoxification in *Saccharomyces cerevisiae*. Eur J Biochem 270:2486–2496
- Gulshan K, Rovinsky SA, Moye-Rowley WS (2004) YBP1 and its homologue YBP2/YBH1 influence oxidative-stress tolerance by nonidentical mechanisms in *Saccharomyces cerevisiae*. Eukaryot Cell 3:318–330
- Hansen J, Johannsen PF (2000) Cysteine is essential for transcriptional regulation of the sulfur assimilation genes in *Saccharomyces cerevisiae*. Mol Gen Genet 263:535–542
- Harbison CT, Gordon DB, Lee TI, Rinaldi NJ, Macisaac KD, Danford TW, Hannett NM, Tagne JB, Reynolds DB, Yoo J, Jennings EG, Zeitlinger J, Pokholok DK, Kellis M, Rolfe PA, Takusagawa KT, Lander ES, Gifford DK, Fraenkel E, Young RA (2004) Transcriptional regulatory code of a eukaryotic genome. Nature 431:99–104
- Harris GK, Shi X (2003) Signaling by carcinogenic metals and metal-induced reactive oxygen species. Mutat Res 533:183–200
- Haugen AC, Kelley R, Collins JB, Tucker CJ, Deng C, Afshari CA, Brown JM, Ideker T, Van Houten B (2004) Integrating phenotypic and expression profiles to map arsenic-response networks. Genome Biol 5:R95
- He XJ, Fassler JS (2005) Identification of novel Yap1p and Skn7p binding sites involved in the oxidative stress response of *Saccharomyces cerevisiae*. Mol Microbiol 58:1454–1467
- Hosiner D, Lempiainen H, Reiter W, Urban J, Loewith R, Ammerer G, Schweyen R, Shore D, Schuller C (2009) Arsenic toxicity to *Saccharomyces cerevisiae* is a consequence of inhibition of the TORC1 kinase combined with a chronic stress response. Mol Biol Cell 20:1048–1057
- Ilina Y, Sloma E, Maciaszczyk-Dziubinska E, Novotny M, Thorsen M, Wysocki R, Tamás MJ (2008) Characterization of the DNA binding motif of the arsenic-responsive transcription factor Yap8p. Biochem J 415:467–475
- Isayenkov SV, Maathuis FJ (2008) The *Arabidopsis thaliana* aquaglyceroporin AtNIP7;1 is a pathway for arsenite uptake. FEBS Lett 582:1625–1628
- Jin YH, Dunlap PE, McBride SJ, Al-Refai H, Bushel PR, Freedman JH (2008) Global transcriptome and deletome profiles of yeast exposed to transition metals. PLoS Genet 4:e1000053
- Jo WJ, Loguinov A, Chang M, Wintz H, Nislow C, Arkin AP, Giaever G, Vulpe CD (2008) Identification of genes involved in the toxic response of *Saccharomyces cerevisiae* against iron and copper overload by parallel analysis of deletion mutants. Toxicol Sci 101:140–151
- Jo WJ, Loguinov A, Wintz H, Chang M, Smith AH, Kalman D, Zhang L, Smith MT, Vulpe CD (2009) Comparative functional genomic analysis identifies distinct and overlapping sets of genes required for resistance to monomethylarsonous acid (MMAIII) and arsenite (AsIII) in yeast. Toxicol Sci 111:424–436
- Kaiser P, Flick K, Wittenberg C, Reed SI (2000) Regulation of transcription by ubiquitination without proteolysis: Cdc34/SCF^{Met30}-mediated inactivation of the transcription factor Met4. Cell 102:303–314

- Kim JY, Choi JA, Kim TH, Yoo, YD, Kim JI, Lee YJ, Yoo SY, Cho CK, Lee YS, Lee SJ (2002) Involvement of p38 mitogen-activated protein kinase in the cell growth inhibition by sodium arsenite. *J Cell Physiol* 190:29–37
- Kitchin KT, Wallace K (2008) The role of protein binding of trivalent arsenicals in arsenic carcinogenesis and toxicity. *J Inorg Biochem* 102:532–539
- Kuge S, Jones N (1994) YAP1 dependent activation of *TRX2* is essential for the response of *Saccharomyces cerevisiae* to oxidative stress by hydroperoxides. *EMBO J* 13:655–664
- Kuge S, Jones N, Nomoto A (1997) Regulation of yAP-1 nuclear localization in response to oxidative stress. *EMBO J* 16:1710–1720
- Kuge S, Toda T, Iizuka N, Nomoto A (1998) Crm1 (Xpo1) dependent nuclear export of the budding yeast transcription factor yAP-1 is sensitive to oxidative stress. *Genes Cells* 3:521–532
- Kuge S, Arita M, Murayama A, Maeta K, Izawa S, Inoue Y, Nomoto A (2001) Regulation of the yeast Yap1p nuclear export signal is mediated by redox signal-induced reversible disulfide bond formation. *Mol Cell Biol* 21:6139–6150
- Kuras L, Rouillon A, Lee T, Barbey R, Tyers M, Thomas D (2002) Dual regulation of the met4 transcription factor by ubiquitin-dependent degradation and inhibition of promoter recruitment. *Mol Cell* 10:69–80
- Lafaye A, Junot C, Pereira Y, Lagniel G, Tabet JC, Ezan E, Labarre J (2005) Combined proteome and metabolite-profiling analyses reveal surprising insights into yeast sulfur metabolism. *J Biol Chem* 280:24723–24730
- Lau WT, Howson RW, Malkus P, Schekman R, O'Shea EK (2000) Pho86p, an endoplasmic reticulum (ER) resident protein in *Saccharomyces cerevisiae*, is required for ER exit of the high-affinity phosphate transporter Pho84p. *Proc Natl Acad Sci U S A* 97:1107–1112
- Lee J, Godon C, Lagniel G, Spector D, Garin J, Labarre J, Toledano MB (1999) Yap1 and Skn7 control two specialized oxidative stress response regulons in yeast. *J Biol Chem* 274:16040–16046
- Lee TA, Jorgensen P, Bogner AL, Peyraud C, Thomas D, Tyers M (2009) Systematic dissection of combinatorial control by the Met4 transcriptional complex. *Mol Biol Cell* 21:456–469
- Leung J, Pang A, Yuen WH, Kwong YL, Tse EW (2007) Relationship of expression of aquaglyceroporin 9 with arsenic uptake and sensitivity in leukemia cells. *Blood* 109:740–746
- Li JP, Yang JL (2007) Cyclin B1 proteolysis via p38 MAPK signaling participates in G2 checkpoint elicited by arsenite. *J Cell Physiol* 212:481–488
- Liu SX, Athar M, Lippai I, Waldren C, Hei TK (2001) Induction of oxyradicals by arsenic: implication for mechanism of genotoxicity. *Proc Natl Acad Sci U S A* 98:1643–1648
- Liu Z, Shen J, Carbrey JM, Mukhopadhyay R, Agre P, Rosen BP (2002) Arsenite transport by mammalian aquaglyceroporins AQP7 and AQP9. *Proc Natl Acad Sci U S A* 99:6053–6058
- Liu Z, Boles E, Rosen BP (2004) Arsenic trioxide uptake by hexose permeases in *Saccharomyces cerevisiae*. *J Biol Chem* 279:17312–17318
- Liu Z, Sanchez MA, Jiang X, Boles E, Landfear SM, Rosen BP (2006) Mammalian glucose permease GLUT1 facilitates transport of arsenic trioxide and methylarsonous acid. *Biochem Biophys Res Commun* 351:424–430
- Luyten K, Albertyn J, Skibbe WF, Prior BA, Ramos J, Thevelein JM, Hohmann S (1995) Fps1, a yeast member of the MIP family of channel proteins, is a facilitator for glycerol uptake and efflux and is inactive under osmotic stress. *EMBO J* 14:1360–1371
- Ma LQ, Komar KM, Tu C, Zhang W, Cai Y, Kennelley ED (2001) A fern that hyperaccumulates arsenic. *Nature* 409:579
- Ma JF, Yamaji N, Mitani N, Xu XY, Su YH, McGrath SP, Zhao FJ (2008) Transporters of arsenite in rice and their role in arsenic accumulation in rice grain. *Proc Natl Acad Sci U S A* 105:9931–9935
- Maciaszczyk E, Wysocki R, Golik P, Lazowska J, Ulaszewski S (2004) Arsenical resistance genes in *Saccharomyces douglasii* and other yeast species undergo rapid evolution involving genomic rearrangements and duplications. *FEMS Yeast Res* 4:821–832
- Maciaszczyk-Dziubinska E, Migdal I, Migocka M, Bocer T, Wysocki R (2010) The yeast aquaglyceroporin Fps1p is a bidirectional arsenite channel. *FEBS Lett* 584:726–732

- Mansour NM, Sawhney M, Tamang DG, Vogl C, Saier MH Jr (2007) The bile/arsenite/riboflavin transporter (BART) superfamily. *FEBS J* 274:612–629
- Mason DL, Michaelis S (2002) Requirement of the N-terminal extension for vacuolar trafficking and transport activity of yeast Ycf1p, an ATP-binding cassette transporter. *Mol Biol Cell* 13:4443–4455
- Mason DL, Mallampalli MP, Huyer G, Michaelis S (2003) A region within a luminal loop of *Saccharomyces cerevisiae* Ycf1p directs proteolytic processing and substrate specificity. *Eukaryot Cell* 2:588–598
- McDermott JR, Jiang X, Beene LC, Rosen BP, Liu Z (2010) Pentavalent methylated arsenicals are substrates of human AQP9. *Biometals* 23:119–127
- Menant A, Baudouin-Cornu P, Peyraud C, Tyers M, Thomas D (2006) Determinants of the ubiquitin-mediated degradation of the Met4 transcription factor. *J Biol Chem* 281:11744–11754
- Menezes RA, Amaral C, Delaunay A, Toledano M, Rodrigues-Pousada C (2004) Yap8p activation in *Saccharomyces cerevisiae* under arsenic conditions. *FEBS Lett* 566:141–146
- Menezes RA, Amaral C, Batista-Nascimento L, Santos C, Ferreira RB, Devaux F, Eleutherio EC, Rodrigues-Pousada C (2008) Contribution of Yap1 towards *Saccharomyces cerevisiae* adaptation to arsenic-mediated oxidative stress. *Biochem J* 414:301–311
- Meng YL, Liu Z, Rosen BP (2004) As(III) and Sb(III) uptake by GlpF and efflux by ArsB in *Escherichia coli*. *J Biol Chem* 279:18334–18341
- Migdal I, Ilina Y, Tamás MJ, Wysocki R (2008) Mitogen-activated protein kinase Hog1 mediates adaptation to G1 checkpoint arrest during arsenite and hyperosmotic stress. *Eukaryot Cell* 7:1309–1317
- Mollapour M, Piper PW (2007) Hog1 mitogen-activated protein kinase phosphorylation targets the yeast Fps1 aquaglyceroporin for endocytosis, thereby rendering cells resistant to acetic acid. *Mol Cell Biol* 27:6446–6456
- Momose Y, Iwahashi H (2001) Bioassay of cadmium using a DNA microarray: genome-wide expression patterns of *Saccharomyces cerevisiae* response to cadmium. *Environ Toxicol Chem* 20:2353–2360
- Mukhopadhyay R, Rosen BP (1998) *Saccharomyces cerevisiae* ACR2 gene encodes an arsenate reductase. *FEMS Microbiol Lett* 168:127–136
- Mukhopadhyay R, Rosen BP (2001) The phosphatase C(X)5R motif is required for catalytic activity of the *Saccharomyces cerevisiae* Acr2p arsenate reductase. *J Biol Chem* 276:34738–34742
- Mukhopadhyay R, Shi J, Rosen BP (2000) Purification and characterization of Acr2p, the *Saccharomyces cerevisiae* arsenate reductase. *J Biol Chem* 275:21149–21157
- Mukhopadhyay R, Zhou Y, Rosen BP (2003) Directed evolution of a yeast arsenate reductase into a protein-tyrosine phosphatase. *J Biol Chem* 278:24476–24480
- Patton EE, Peyraud C, Rouillon A, Surdin-Kerjan Y, Tyers M, Thomas D (2000) SCF(Met30)-mediated control of the transcriptional activator Met4 is required for the G(1)-S transition. *EMBO J* 19:1613–1624
- Paulsen CE, Carroll KS (2009) Chemical dissection of an essential redox switch in yeast. *Chem Biol* 16:217–225
- Paumi CM, Menendez J, Arnoldo A, Engels K, Iyer KR, Thaminy S, Georgiev O, Barral Y, Michaelis S, Stagljar I (2007) Mapping protein-protein interactions for the yeast ABC transporter Ycf1p by integrated split-ubiquitin membrane yeast two-hybrid analysis. *Mol Cell* 26:15–25
- Paumi CM, Chuk M, Chevelev I, Stagljar I, Michaelis S (2008) Negative regulation of the yeast ABC transporter Ycf1p by phosphorylation within its N-terminal extension. *J Biol Chem* 283:27079–27088
- Paumi CM, Chuk M, Snider J, Stagljar I, Michaelis S (2009) ABC transporters in *Saccharomyces cerevisiae* and their interactors: new technology advances the biology of the ABCC (MRP) subfamily. *Microbiol Mol Biol Rev* 73:577–593
- Persson BL, Petersson J, Fristedt U, Weinander R, Berhe A, Pattison J (1999) Phosphate permeases of *Saccharomyces cerevisiae*: structure, function and regulation. *Biochim Biophys Acta* 1422:255–272

- Pompella A, Visvikis A, Paolicchi A, De Tata V, Casini AF (2003) The changing faces of glutathione, a cellular protagonist. *Biochem Pharmacol* 66:1499–1503
- Porquet A, Filella M (2007) Structural evidence of the similarity of $\text{Sb}(\text{OH})_3$ and $\text{As}(\text{OH})_3$ with glycerol: Implications for their uptake. *Chem Res Toxicol* 20:1269–1276
- Ralph SJ (2008) Arsenic-based antineoplastic drugs and their mechanisms of action. *Met Based Drugs* 2008:260146
- Ramirez-Solis A, Mukopadhyay R, Rosen BP, Stemmler TL (2004) Experimental and theoretical characterization of arsenite in water: insights into the coordination environment of As-O. *Inorg Chem* 43:2954–2959
- Rosen BP (1999) Families of arsenic transporters. *Trends Microbiol* 7:207–212
- Rosen BP (2002) Biochemistry of arsenic detoxification. *FEBS Lett* 529:86
- Rouillon A, Barbey R, Patton EE, Tyers M, Thomas D (2000) Feedback-regulated degradation of the transcriptional activator Met4 is triggered by the SCF^{Met30} complex. *EMBO J* 19:282–294
- Salt DE, Norton GJ (2008) Arsenic-eaters: by accident or by design. *New Phytol* 180:8–11
- Sanders OI, Rensing C, Kuroda M, Mitra B, Rosen BP (1997) Antimonite is accumulated by the glycerol facilitator GlpF in *Escherichia coli*. *J Bacteriol* 179:3365–3367
- Santangelo GM (2006) Glucose signaling in *Saccharomyces cerevisiae*. *Microbiol Mol Biol Rev* 70:253–282
- Sharma KG, Mason DL, Liu G, Rea PA, Bachhawat AK, Michaelis S (2002) Localization, regulation, and substrate transport properties of Bpt1p, a *Saccharomyces cerevisiae* MRP-type ABC transporter. *Eukaryot Cell* 1:391–400
- Shen ZX, Chen GQ, Ni JH, Li XS, Xiong SM, Qiu QY, Zhu J, Tang W, Sun GL, Yan KQ, Chen Y, Zhou L, Fang ZW, Wang YT, Ma J, Zhang P, Zhang TD, Chen SJ, Chen Z, Wang ZY (1997) Use of arsenic trioxide (As_2O_3) in the treatment of acute promyelocytic leukemia (APL): II. Clinical efficacy and pharmacokinetics in relapsed patients. *Blood* 89:3354–3360
- Shi H, Shi X, Liu KJ (2004) Oxidative mechanism of arsenic toxicity and carcinogenesis. *Mol Cell Biochem* 255:67–78
- Soignet SL, Maslak P, Wang ZG, Jhanwar S, Calleja E, Dardashti LJ, Corso D, DeBlasio A, Gabrilove J, Scheinberg DA, Pandolfi PP, Warrell RP Jr (1998) Complete remission after treatment of acute promyelocytic leukemia with arsenic trioxide. *N Engl J Med* 339:1341–1348
- Sotelo J, Rodriguez-Gabriel MA (2006) Mitogen-activated protein kinase Hog1 is essential for the response to arsenite in *Saccharomyces cerevisiae*. *Eukaryot Cell* 5:1826–1830
- Soulard A, Cohen A, Hall MN (2009) TOR signaling in invertebrates. *Curr Opin Cell Biol* 21:825–836
- Stohs SJ, Bagchi D (1995) Oxidative mechanisms in the toxicity of metal ions. *Free Radic Biol Med* 18:321–336
- Su NY, Flick K, Kaiser P (2005) The F-box protein Met30 is required for multiple steps in the budding yeast cell cycle. *Mol Cell Biol* 25:3875–3885
- Szczyпка MS, Wemmie JA, Moye-Rowley WS, Thiele DJ (1994) A yeast metal resistance protein similar to human cystic fibrosis transmembrane conductance regulator (CFTR) and multidrug resistance-associated protein. *J Biol Chem* 269:22853–22857
- Tamás MJ, Luyten K, Sutherland FC, Hernandez A, Albertyn J, Valadi H, Li H, Prior BA, Kilian SG, Ramos J, Gustafsson L, Thevelein JM, Hohmann S (1999) Fps1p controls the accumulation and release of the compatible solute glycerol in yeast osmoregulation. *Mol Microbiol* 31:1087–1104
- Tamás MJ, Karlgren S, Bill RM, Hedfalk K, Allegrì L, Ferreira M, Thevelein JM, Rydström J, Mullins JG, Hohmann S (2003) A short regulatory domain restricts glycerol transport through yeast Fps1p. *J Biol Chem* 278:6337–6345
- Tamás MJ, Labarre J, Toledano MB, Wysocki R (2005) Mechanisms of toxic metal tolerance in yeast. In: Tamás MJ, Martinoia E (eds) *Molecular biology of metal homeostasis and detoxification: from microbes to man*. Springer, Heidelberg
- Tan K, Feizi H, Luo C, Fan SH, Ravasi T, Ideker TG (2008) A systems approach to delineate functions of paralogous transcription factors: role of the Yap family in the DNA damage response. *Proc Natl Acad Sci U S A* 105:2934–2939
- Thomas D, Surdin-Kerjan Y (1997) Metabolism of sulfur amino acids in *Saccharomyces cerevisiae*. *Microbiol Mol Biol Rev* 61:503–532

- Thorsen M, Di Y, Tangemo C, Morillas M, Ahmadpour D, Van der Does C, Wagner A, Johansson E, Boman J, Posas F, Wysocki R, Tamás MJ (2006) The MAPK Hog1p modulates Fps1p-dependent arsenite uptake and tolerance in yeast. *Mol Biol Cell* 17:4400–4410
- Thorsen M, Lagniel G, Kristiansson E, Junot C, Nerman O, Labarre J, Tamás MJ (2007) Quantitative transcriptome, proteome, and sulfur metabolite profiling of the *Saccharomyces cerevisiae* response to arsenite. *Physiol Genomics* 30:35–43
- Thorsen M, Perrone GG, Kristiansson E, Traini M, Ye T, Dawes IW, Nerman O, Tamás MJ (2009) Genetic basis of arsenite and cadmium tolerance in *Saccharomyces cerevisiae*. *BMC Genomics* 10:105
- Toone WM, Jones N (1999) AP-1 transcription factors in yeast. *Curr Opin Genet Dev* 9:55–61
- Tripathi RD, Srivastava S, Mishra S, Singh N, Tuli R, Gupta DK, Maathuis FJ (2007) Arsenic hazards: strategies for tolerance and remediation by plants. *Trends Biotechnol* 25:158–165
- Veal EA, Ross SJ, Malakasi P, Peacock E, Morgan BA (2003) Ybp1 is required for the hydrogen peroxide-induced oxidation of the Yap1 transcription factor. *J Biol Chem* 278:30896–30904
- Verma A, Mohindru M, Deb DK, Sassano A, Kambhampati S, Ravandi F, Minucci S, Kalvakolanu DV, Platanius LC (2002) Activation of Rac1 and the p38 mitogen-activated protein kinase pathway in response to arsenic trioxide. *J Biol Chem* 277:44988–44995
- Vido K, Spector D, Lagniel G, Lopez S, Toledano MB, Labarre J (2001) A proteome analysis of the cadmium response in *Saccharomyces cerevisiae*. *J Biol Chem* 276:8469–8474
- Vujcic M, Shroff M, Singh KK (2007) Genetic determinants of mitochondrial response to arsenic in yeast *Saccharomyces cerevisiae*. *Cancer Res* 67:9740–9749
- Wemmie JA, Szczypka MS, Thiele DJ, Moye-Rowley WS (1994) Cadmium tolerance mediated by the yeast AP-1 protein requires the presence of an ATP-binding cassette transporter-encoding gene, YCF1. *J Biol Chem* 269:32592–32597
- Wen J, Cheng HY, Feng Y, Rice L, Liu S, Mo A, Huang J, Zu Y, Ballon DJ, Chang CC (2008) P38 MAPK inhibition enhancing ATO-induced cytotoxicity against multiple myeloma cells. *Br J Haematol* 140:169–180
- Wood MJ, Andrade EC, Storz G (2003) The redox domain of the Yap1p transcription factor contains two disulfide bonds. *Biochemistry* 42:11982–11991
- Wood MJ, Storz G, Tjandra N (2004) Structural basis for redox regulation of Yap1 transcription factor localization. *Nature* 430:917–921
- Wu AL, Moye-Rowley WS (1994) GSH1, which encodes gamma-glutamylcysteine synthetase, is a target gene for yAP-1 transcriptional regulation. *Mol Cell Biol* 14:5832–5839
- Wullschlegel S, Loewith R, Hall MN (2006) TOR signaling in growth and metabolism. *Cell* 124:471–484
- Wykoff DD, O’Shea EK (2001) Phosphate transport and sensing in *Saccharomyces cerevisiae*. *Genetics* 159:1491–1499
- Wysocki R, Tamás MJ (2010) How *Saccharomyces cerevisiae* copes with toxic metals and metalloids. *FEMS Microbiol Rev* 34:925–951
- Wysocki R, Bobrowicz P, Ulaszewski S (1997) The *Saccharomyces cerevisiae* *ACR3* gene encodes a putative membrane protein involved in arsenite transport. *J Biol Chem* 272:30061–30066
- Wysocki R, Chéry CC, Wawrzycka D, Van Hulle M, Cornelis R, Thevelein JM, Tamás MJ (2001) The glycerol channel Fps1p mediates the uptake of arsenite and antimonite in *Saccharomyces cerevisiae*. *Mol Microbiol* 40:1391–1401
- Wysocki R, Fortier PK, Maciaszczyk E, Thorsen M, Leduc A, Odhagen A, Owsianik G, Ulaszewski S, Ramotar D, Tamás MJ (2004) Transcriptional activation of metalloid tolerance genes in *Saccharomyces cerevisiae* requires the AP-1-like proteins Yap1p and Yap8p. *Mol Biol Cell* 15:2049–2060
- Xu C, Zhou T, Kuroda M, Rosen BP (1998) Metalloid resistance mechanisms in prokaryotes. *J Biochem* 123:16–23
- Yaakov G, Duch A, Garcia-Rubio M, Clotet J, Jimenez J, Aguilera A, Posas F (2009) The stress-activated protein kinase Hog1 mediates S phase delay in response to osmotic stress. *Mol Biol Cell* 20:3572–3582
- Yan C, Lee LH, Davis LI (1998) Crm1p mediates regulated nuclear export of a yeast AP-1-like transcription factor. *EMBO J* 17:7416–7429

- Yang HC, Cheng J, Finan TM, Rosen BP, Bhattacharjee H (2005) Novel pathway for arsenic detoxification in the legume symbiont *Sinorhizobium meliloti*. *J Bacteriol* 187:6991–6997
- Yen JL, Su NY, Kaiser P (2005) The yeast ubiquitin ligase SCF^{Met30} regulates heavy metal response. *Mol Biol Cell* 16:1872–1882
- Yompakdee C, Ogawa N, Harashima S, Oshima Y (1996a) A putative membrane protein, Pho88p, involved in inorganic phosphate transport in *Saccharomyces cerevisiae*. *Mol Gen Genet* 251:580–590
- Yompakdee C, Bun-ya M, Shikata K, Ogawa N, Harashima S, Oshima Y (1996b) A putative new membrane protein, Pho86p, in the inorganic phosphate uptake system of *Saccharomyces cerevisiae*. *Gene* 171:41–47
- Zhao FJ, Ago Y, Mitani N, Li RY, Su YH, Yamaji N, McGrath SP, Ma JF (2010) The role of the rice aquaporin Lsi1 in arsenite efflux from roots. *New Phytol* 186:392–399
- Zhou Y, Bhattacharjee H, Mukhopadhyay R (2006) Bifunctional role of the leishmanial antimonate reductase LmACR2 as a protein tyrosine phosphatase. *Mol Biochem Parasitol* 148:161–168
- Zhu YG, Rosen BP (2009) Perspectives for genetic engineering for the phytoremediation of arsenic-contaminated environments: from imagination to reality? *Curr Opin Biotechnol* 20:220–224

Part III
Heavy Metal Induced Toxicity
in Insect Cells

Chapter 5

Heavy Metal Toxicity in an Insect Cell Line (Methyl-HgCl, HgCl₂, CdCl₂ and CuSO₄)

Bart P. Braeckman

Abstract We have analyzed the toxicity, uptake and intracellular effects of CdCl₂, HgCl₂, MeHgCl and CuSO₄ in a cell line of the Asian tiger mosquito *Aedes albopictus*. Cell proliferation was drastically inhibited by CdCl₂ and MeHgCl while HgCl₂ showed only a moderate effect. Acute toxicity tests showed that membrane integrity was severely affected in cells treated with low doses of HgCl₂ and MeHgCl. Uptake of both mercury species occurred via simple diffusion while cadmium entered the cells through mediated transport. CdCl₂, HgCl₂ and CuSO₄, but not MeHgCl induced microtubulesupported neurite-like extensions in the *Aedes* cells. The metals induced some general intracellular pathologies such as mitochondrial alterations, nuclear deformation and increased lysosomal profiles. Mitochondrial swelling and severe RER dilatation by proteinaceous material was most pronounced in cadmium-treated cells. These morphological features were accompanied by lactate production and induction of a 78-kDa protein (possibly Grp78/BiP). The latter may represent a stress defense system that leads to a positive shift of the cell viability curve. Unlike other treatments, CuSO₄-treated cells showed massive apoptosis characterized by nuclear chromatin condensation and DNA laddering.

Introduction

Many insect species accumulate heavy metals from the environment in their body. Therefore, their role in food webs as well as their potential to serve as bioindicators have been widely studied (McGeoch 1998). However, less is known about the fate of the heavy metals at the cellular level in insects. A major advantage of using insect cell cultures for this purpose is that this method allows for controlled exposure of cells to precise metal concentrations for a specific amount of time. In this chapter,

B. P. Braeckman (✉)

Department of Biology, Ghent University, K.L. Ledeganckstraat 35, 9000 Gent, Belgium

Tel.: +32-09-264-8744

Fax: +32-9-264-5334

e-mail: bart.braeckman@ugent.be

we will describe the general toxicity, uptake kinetics, subcellular distribution and physiological effects of several heavy metals in a cell line of the Asian tiger mosquito *Aedes albopictus*.

In a series of dye exclusion tests and cell proliferation assays on mercury-, methylmercury-, and cadmium-treated cells, we found that they showed widely different toxicity patterns. Sublethal doses of the tested heavy metals showed a profound effect on general cell morphology: long, neurite-like, microtubule-supported extensions were induced (except for MeHgCl-treated cells). At the subcellular level, many general, stress-related pathologies were found, such as nuclear chromatin clumping, indentation and dilatation of the perinuclear cisternae, increase of ribosomal density, and lysosomal and RER volume. Cd-treated cells specifically showed clear mitochondrial condensation and swelling, suggesting impairment of aerobic function which was confirmed by increased lactic acid levels in the culture medium. Proteinaceous substance that we found in the dilated RER cisternae may represent the ER stress protein Grp78/BiP. Cells exposed to MeHgCl showed particular cytoplasmic tube-like structures of unknown function and the appearance of blebs suggested microtubular disorganization. Autometallographical silverstaining allowed us to localize mercury accumulation in the lysosomes. The uptake of both HgCl₂ and MeHgCl is mainly by simple diffusion. CdCl₂ was taken up through mediated transport (partly by Ca²⁺ channels) and did not require metabolic energy. In a separate study, it was found that acute toxicity of CuSO₄ was much lower than that of CdCl₂, HgCl₂ and MeHgCl. Although Cu²⁺ also induced the typical microtubule-supported neurite-like extensions, it caused massive apoptosis that was not observed for any of the other metals tested.

Materials

Cell Culture

For our experiments we used a cell line of the Asian tiger mosquito *Aedes albopictus* (Diptera: Culicidae). The cells used in this study were derived from the C6/36 clone isolated by Igarashi (1978) from a mixed embryonic cell culture (Singh 1967). The cells were grown in monolayers in Modified Kitamura (MK) medium (132 mM NaCl, 8 mM KCl, 0.82 mM CaCl₂, 0.86 mM KH₂PO₄, 24 mM D-glucose, 0.77% lactalbumin hydrolysate, 0.57% yeast extract (YE), 5% fetal calf serum (FCS) and 50 µg/ml gentamicin), as described by Kitamura (1966). Lactalbumin hydrolysate, FCS, and gentamicin were from Gibco BRL (Paisley, Schotland), YE was from Oxoid (Unipath Ltd., Basingstoke, UK), and all other chemicals were purchased from Merck. All culture recipients were from Nunclon (Roskilde, Denmark). The pH of the medium was adjusted to 6.8 and cell cultures were kept in the dark under ambient atmosphere and at 27°C. Cultures were usually seeded at a density of 10⁵ cells/ml. Under these conditions, cell population doubling time was approximately 30 h. Experiments were carried out on 7-day-old cultures.

Metal Exposure

HgCl₂ and MeHgCl were purchased from Merck (Darmstadt, Germany) and CdCl₂ and CuSO₄·5H₂O were from Janssen Chimica (Geel, Belgium). MeHgCl is volatile and extremely toxic; it should be handled in a fume hood with care. The metal stock solutions were prepared daily in MK medium without FCS. This solution was filter sterilized and 5% FCS was added if necessary.

Viability and Proliferation Assays

Propidium iodide and Hoechst 33258 were purchased from Molecular Probes (Eugene, Oregon). These fluorescent probes bind to double stranded DNA and are carcinogenic. Fluorescence was quantified in 96-well plates with a Cytofluor 2350 (Millipore).

Light and Electron Microscopy

Cells were fixed by adding an equal volume of 2× fixation buffer containing 4% paraformaldehyde (Sigma, St. Louis, Missouri) and 4% glutaraldehyde in cacodylate buffer (100 mM (CH₃)₂AsO₂Na·3H₂O, 60 mM sucrose and 0.05% CaCl₂, pH 7.2). Glutaraldehyde, cacodylic acid, osmium tetroxide, lead acetate, uranyl acetate and cytochalasin B were products from Fluka (Buchs, Switzerland). Cells were observed with a Reichert-Jung Polyvar microscope equipped for Nomarski DIC. During fluorescent staining procedures, cells were washed with phosphate-buffered saline (PBS: 137 mM NaCl, 1.47 mM KH₂PO₄, 2.68 mM KCl, 8.10 mM Na₂HPO₄, pH 7.2). PBSAT was made by adding 5% BSA and 1.75% Triton X-100 to the PBS. BODIPY[®]-phalloidin was purchased at Molecular Probes (Eugene, Oregon) and the FITC-labeled rabbit anti-mouse antibody and the fluorescein-conjugated swine anti rabbit immunoglobulins were obtained from DAKO (Santa Barbara, California). Vectashield was a product from Vector Laboratories Inc. (Burlingame, California). Nomarski DIC and fluorescence pictures were taken on AGFA APX 100ASA black-and-white film and KODAK TMAX TMY 400ASA black-and-white film, respectively. Digitized pictures were analyzed by an image analysis system (IBAS Kontron). Digital images were printed with a Sony Video Graphic Printer UP850.

The epoxy resin kit was purchased from Agar Scientific Ltd. (Stansted, UK) and DePeX was a product from BDH (Poole, UK). For ultrastructural analysis, thin and ultrathin sections of embedded cells were made with a Reichert-Jung Ultracut E and the ultrathin sections were post-stained with a Reichert-Jung Ultrastainer. Electron micrographs were made with a JEOL 1200 EX II transmission electron microscope.

The autometallographical developer for mercury localization consists of 60 ml gum Arabic, 10 ml citrate buffer (1.2 M citric acid monohydrate and 0.8 M trisodium citric acid dehydrate), and 30 ml of 0.5 M hydroquinone. Immediately before use, 0.5 ml of AgNO₃ (0.75 M) was added to this mixture.

Atomic Absorption and Fluorescence Spectrometry

Intracellular Cd concentrations were quantified with atomic absorption spectrometry (Perkin-Elmer 4100 ZL) while mercury was quantified with a Merlin mercury detector (Model PS Analytical 10023). The EGTA (ethylene glycol-*O,O'*-bis(2-aminoethyl)-*N,N,N',N'*-tetraacetic acid), $\text{SnCl}_2 \cdot 2\text{H}_2\text{O}$ and HNO_3 (<0.0000005% Hg) used for the cadmium or mercury preparations were purchased from Fluka (Buchs, Switzerland). The cadmium atomic absorption standard solution was a product from Sigma (St. Louis, Missouri).

Biochemical Assays

2,4-Dinitrophenol (DNP) was obtained from BDH (Poole, UK) and the ATP Bioluminescence Assay Kit CLS II was from Boehringer Mannheim (Mannheim, Germany). The SDS-gel electrophoresis low- and high-molecular weight protein standard ladder and Lactate Diagnostics kit were from Sigma (St. Louis, Missouri). The protein sample buffer for SDS-PAGE consisted of 100 mM Tris-HCl, pH 8.8, 1% mercaptoethanol, 3% SDS, bromophenol blue, and 10% glycerol (final concentrations). Medium acidification was quantified with a Consort P600 pH meter and NADH was measured in a Shimadzu UV2401PC spectrophotometer. The lysis buffer used for analyzing DNA laddering contained 50 mM Tris-HCl (pH 8.75), 100 mM Na_2EDTA , 0.2 M NaCl, 1% SDS, 1.67 mg/ml proteinase K. TBE buffer consisted of 50 mM Tris, 45 mM boric acid, and 0.5 mM EDTA.

Methods

Viability Assays

Cell viability was assessed by a propidium iodide exclusion assay (Nieminen et al. 1992) adapted for *Aedes albopictus* cells and automated measurement during a 24-h period. This method is basically a test for membrane integrity as the fluorochrome propidium iodide, that specifically binds to DNA, is excluded from living cells. Due to its high DNA content, yeast extract was omitted from the medium (designated MK-YE) during the viability test. The background fluorescence of the other medium components was negligible. The viability tests were performed in a climatized room at 27°C. As the FCS may have a detoxifying effect by binding heavy metal ions, tests were performed with and without the addition of 5% FCS to the MK-YE medium.

The viability test was initiated by changing the MK medium to MK-YE in a 7-day-old cell culture. In each well of a 96-well microtiterplate 50 μl propidium iodide solution (60 μM in MK-YE) was added to 50 μl cell suspension. After a 10-min staining period, the initial background staining (*A*) representing 100% viability was measured

in the fluorimeter. Propidium fluorescence was measured using 530 nm (25 nm BP) excitation and 620 nm (40 nm BP) emission filters. Next, 100 µl of each metal solution (in MK-YE) was added per well and changes in fluorescence were recorded hourly over a 24-h time span (X_1, X_2, \dots, X_{24}). Finally, 100 µl of digitonin (375 µM in MK-YE) was added to each well and, after cell permeation, a final reading gave the value for 0% viability (B). Viability percentages were calculated as $100(B-X)/(B-A)$ after correction for the blanks. Although in theory, these values cannot exceed 100%, due to quenching or dilution effects of digitonin, the values may slightly exceed the 0–100% interval. Viability curves show averages of two experiments, each containing eight technical replicates. LD values were calculated by linear intrapolation or by using a four-parameter logistic function for best fit ($Y = \{(a-d)/[1+(x/c)^b] + d$) in which X , Y , a , b , c , and d represent the metal concentration, expected viability, upper viability limit, slope, point of inflection, and lower viability limit, respectively.

Growth Assays

Inhibition of cell proliferation by heavy metals was followed over an 18-day period by quantifying DNA content of the metal-treated cultures with the fluorescent dye Hoechst 33258 (Labarca and Paigen 1980). Cells were seeded in flat-sided test tubes at a density of 4×10^5 cells/ml in MK medium, supplemented with 5% FCS, and treated with the appropriate metal concentration. To estimate the cell density after a given incubation time, a subseries of growing cultures were sacrificed for DNA quantification. These tubes were vortexed and cells were pelleted by centrifugation after which the MK medium was replaced by distilled water. The cells were sonicated for 2 min at 100 W. Fifty µl of 0.1% Hoechst 33258 was added to 25 ml of a concentrated salt solution (final concentration: 2 M NaCl, 50 µM NaPO₄, pH 7.4 and stored at 55°C to prevent crystallization). The high salt concentration was used to eliminate DNA-bound proteins to improve fluorochrome accessibility. The fluorescence intensity of 100 µl cell sonicate and 100 µl Hoechst 33258 salt solution was measured using a 360 nm (40 nm BP) excitation and 460 nm (40 nm BP) emission filter. Calibration curves showed a linear relation between cell concentration and Hoechst fluorescence for cell concentrations not exceeding 5×10^6 cells/ml. Samples were taken on days 0, 1, 2, 3, 4, 5, 7, 9, 12, 15, and 18. Regression coefficients of each proliferation curve were calculated and expressed relative to the untreated control. The results are averages of two experiments with eight technical replicates each.

Light Microscopy and Cytoskeleton Staining

For light microscopy, cells were seeded (1.6×10^5 cells/well) on round coverslips (Assistent) in 4-well culture plates and allowed to settle for 24 h. They were treated with metal and inhibitors or MK medium as a control. All test solutions were added successively to the wells without any washing steps to prevent disturbance or dis-

lodgement of the cells. After treatment, double concentrated fixation buffer was added and cells were fixed for 1 h at room temperature. Consequently, the coverslips were mounted upside down with glycerin on a glass slide and evaluated by Normarski DIC microscopy.

For actin staining, cells were fixed as described in the materials section and washed with PBS. Cells were permeated with 0.1% Triton X-100 for 30 min and washed again with PBS. F-actin was stained for 2 h on ice with BODIPY[®]-phalloidin (66 μ M) followed by five washing steps in PBS to remove unbound stain. All preparations were carried out in the dark to prevent photobleaching.

For microtubule staining, cells were fixed in methanol at -20°C and rinsed in PBS. Next, they were permeated with PBSAT for 30 min, followed by a triple PBS rinse (15 min each). A 1/100 dilution of Anti- α -tubulin antibody (TAT, Woods et al. 1989) was added for 30 min and this was followed by another triple rinse with PBS. Consequently, the cells were incubated with FITC-labeled anti-mouse antibodies (1/50) for another 30 min. After an additional PBS rinse, the coverslips containing the cells were mounted with Vectashield. The slides were observed with epifluorescence microscopy using a G1 filter for BODIPY[®] (exc. BP 546 ± 12 nm/em. LP 590 nm) and a B1 filter for FITC (exc. BP 450–490 nm/em. LP 520 nm).

Cu-induced apoptosis was quantified by pelleting the cells (5 min at 800 rpm) and medium was replaced by MK-FCS to which (1:1) methanol/acetic acid (1:20) and 15 μ l/ml propidium iodide (1 mM) were added. Discrimination between apoptotic (apoptotic and secondary necrotic) and non-apoptotic nuclei (necrotic and live cells) was based on chromatin morphology using epifluorescence microscopy (exc. BP $546 \text{ nm} \pm 12 \text{ nm/em. LP } 590 \text{ nm}$).

Electron Microscopy

Cells were fixed for 1 h at room temperature in fixation buffer and successively pelleted. Post-fixation was done by treating the cells with OsO_4 (1% in cacodylate buffer) for 1 h. During the dehydration steps, cells were stained ‘en bloc’ with 2% uranyl acetate in 50% ethanol and secondly in saturated lead acetate in ethanol–acetone (1:1), both for 1 h (Kushida 1966). The cell pellets were embedded in Araldite. Ultrathin sections were post-stained with a Reichert-Jung Ultrastainer programmed for 30 min uranyl acetate (40°C) and 3 min lead citrate (20°C) staining.

Autometallography

Aedes cells were treated with HgCl_2 and MeHgCl and prior to fixation, the MeHgCl -exposed cells were treated for 40 min with a 40 μ g/ml $\text{Na}_2\text{SeO}_3 \cdot 5\text{H}_2\text{O}$ solution to obtain Hg–Se complexes that can initiate the autometallographical reaction (Baatrup and Danscher 1987). Samples were fixed for 1 h at room temperature with fixation buffer and pelleted. Next, the fixative was replaced by autometallographi-

cal developer in the dark room. After a 1-h developing time, the cells were washed twice with distilled water and prepared for light or electron microscopy.

Atomic Absorption and Fluorescence Spectrometry

Cd-treated cells were washed twice with 2 mM EGTA in MK-YE to remove most of the extracellular and non-specifically bound Cd (Blazka and Shaikh 1991). To prevent chemical matrix interference, the EGTA was removed in a final wash with MK-YE. Next, the cells were transferred to 1% HNO₃ and Cd was quantified in an atomic absorption spectrometer.

Mercury-treated cells were also washed twice with 2 mM EGTA in MK-YE followed by a final wash with MK-YE to remove the remaining EGTA. The cell pellet was decomposed with 0.9 ml HNO₃ to which 0.1 ml BrCl (approx. 50 mM) was added. The BrCl is the reaction product of 33.3 mM KBr and 16.7 mM KBrO₃ in 2.4 M HCl, stored at 4°C, protected from light. BrCl was used for the demethylation of MeHg⁺ (overnight at room temperature). Next, reduction of Hg²⁺ to metallic mercury vapor Hg⁰ was carried out in a reduction flask containing 15 ml of water and 1 ml of freshly prepared stannous chloride solution (1.33 M SnCl₂·2H₂O in 1.2 M HCl, aerated with N₂ for at least 1 h). During a 5-min reduction period, the reduction flask was aerated with mercury-free argon gas. The mercury vapor was passed along a strong alkaline solution (mixture of equal volumes of 20% SnCl₂·2H₂O and 20% KOH, boiled, and filtered) to neutralize acidic vapors. Mercury was pre-concentrated by amalgamation on gold-coated sand (gold trap) and subsequently thermally released for 1 min with a heat spiral. The mercury was then recollected on a standardized gold trap, released during 30 s, and finally detected and quantified with an atomic fluorescence spectrometer. The results show the average of two to three experimental replicates each consisting of three technical replicates.

Biochemical Assays

Lactate concentration in the culture medium was assayed in a 1-ml sample that was deproteinized with 2 ml perchloric acid (8%, w/v). This mixture was vortexed for 30 s, cooled on ice for 5 min and centrifuged at 1,500 g. Of the supernatant, 33 µl was added to 966 µl of a cocktail consisting of 4 ml NAD (2.5 mg/ml), 2 ml glycine buffer (0.6 M glycine, hydrazine, pH 9.2), and 0.1 ml lactate dehydrogenase (1,000 U/ml). After a 15-min incubation period at 37°C, the NADH content (which is a measure of lactate in the sample) was determined spectrophotometrically at 340 nm.

Metal-induced proteins were analysed by SDS-polyacrylamide gel electrophoresis. Total protein content was determined according to the Bradford method (Bradford 1976) using BSA as a standard. Cell samples to be submitted for electrophoresis were mixed with protein sample buffer and the proteins were separated on a 15 cm × 15 cm native polyacrylamide gradient gel (7–14%), run at 200 V and silver

stained according to Blum et al. (1987). In all lanes equal amounts of proteins were loaded and one lane was loaded with low- and high-molecular-weight protein standard series. Relative quantification of the proteins on the gel was done by image analysis (Ibas Kontron).

For analysis of Cu-induced DNA fragmentation, DNA was isolated using the SDS-proteinase K method: the cells were washed with PBS and lysed with 1 ml of lysis buffer at 55°C for 3 h. After extracting the samples with phenol and phenol/chloroform/isoamylalcohol (25:24:1), approximately 700 µl of the aqueous phase was transferred to a new tube and 70 µl 3 M NaAc and 750 µl isopropanol were added. After incubation at -20°C for at least 1 h, precipitated nucleic acid was pelleted at 1,000 rpm for 5 min, washed twice with 75% EtOH, dried and redissolved in 0.5× TBE buffer. RNA was completely degraded by incubation with DNase-free RNase A (1 mg/ml) for 1 h at 30°C. DNA fragmentation was analyzed by electrophoresis on 1% agarose gels.

Results and Discussion

Viability Tests

We used the *Aedes albopictus* C6/36 cell line to study the uptake, intracellular distribution and morphological and biochemical effects of cadmium and mercury in insect cells. Although this cell line has been used frequently in virological studies, its sensitivity to heavy metals was not investigated yet. Hence, we initiated this study by characterizing the acute and chronic toxicity of CdCl₂, HgCl₂, MeHgCl, and CuSO₄ in these cells. Short-term toxicity was assessed with the propidium iodide dye-exclusion method. As FCS in the medium may protect the cells from heavy metal toxicity by binding of metal ions to free thiol groups of the serum proteins (Fang and Fallin 1976; Corrigan and Huang 1981), these tests were carried out with and without 5% FCS in the medium. The toxicity of CdCl₂, HgCl₂ and MeHgCl was assessed in parallel while CuSO₄ toxicity was tested separately under slightly different conditions (2.5% FCS). For cadmium and both mercury species, a time and concentration-dependent decrease in viability was observed, but toxicity kinetics and lethal concentrations differed considerably among the metal species (Fig. 5.1). The protective effect of FCS in the MK medium is evident in the three metal species although the extent to which it decreased toxicity was widely different (Table 5.1). This effect was very strong in HgCl₂-treated cultures, fairly obvious in case of MeHgCl and almost negligible for CdCl₂. Fang and Fallin (1976) found that the association constant for Hg²⁺ to bovine serum albumin is higher than that of MeHg⁺, which is in accordance to the effects of FCS on mercury toxicity described here. Both mercury species disrupted membrane integrity at low concentrations while cadmium was less toxic (MeHgCl > HgCl₂ > CdCl₂), regardless of the presence of FCS in the medium. This is consistent with the findings of Nakada et al. (1978) that, in contrast to Hg²⁺ and MeHg⁺, Cd²⁺ does not readily permeate liposomes.

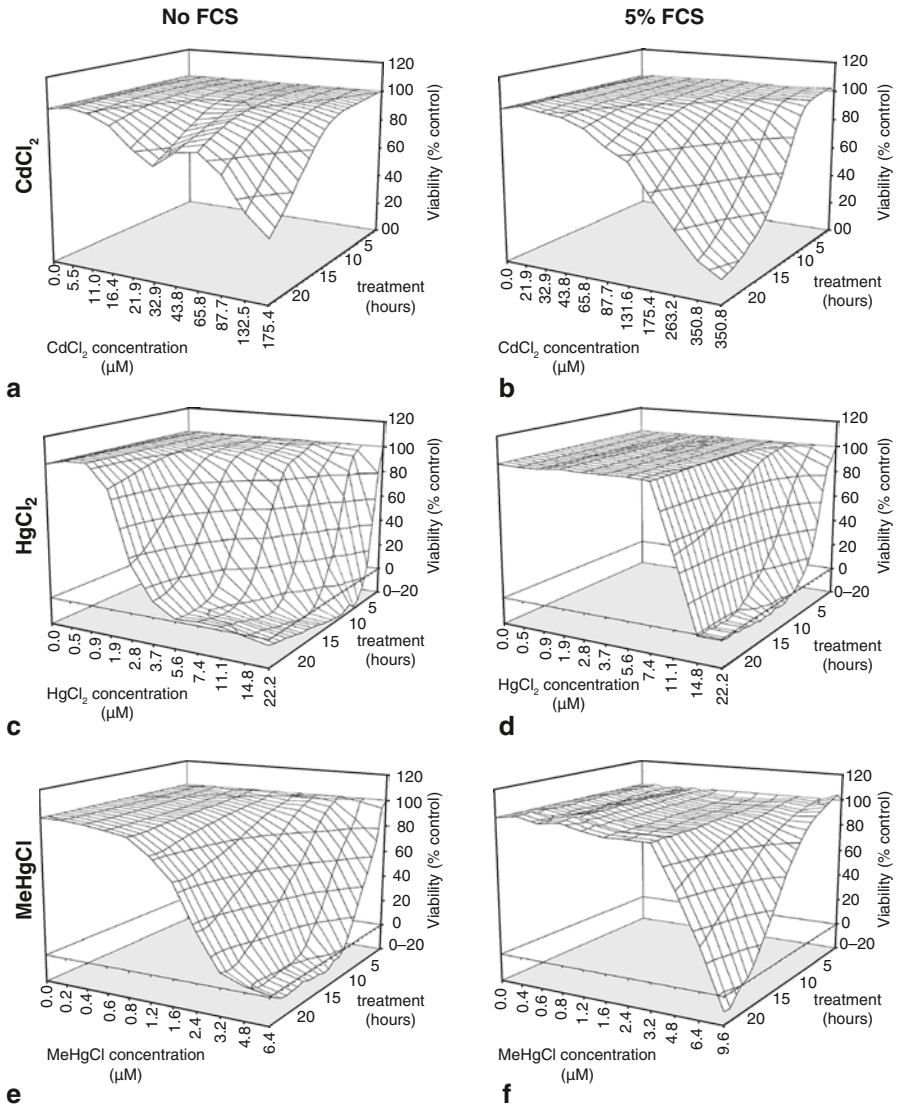


Fig. 5.1 The effect of CdCl₂ (**a**, **b**), HgCl₂ (**c**, **d**), and MeHgCl (**e**, **f**) on cell viability in *Aedes albopictus* C6/36 cultures. Toxicity was assayed in the absence (**a**, **c**, **e**) and presence (**b**, **d**, **f**) of FCS in the medium. Mean standard deviations were 3.0, 6.7, 5.0, 5.7, 9.8, and 11.2% for **a–f**, respectively. (Reproduced from Braeckman et al. 1997a with permission from Kluwer Academic Publishers)

Table 5.1 Lethal doses (LD) and inhibitory concentrations (IC) of heavy metals in the *Aedes albopictus* C6/36 cell line

FCS in the medium (%)	CdCl ₂		HgCl ₂		MeHgCl		CuSO ₄
	0	5	0	5	0	5	2.5
Cell viability: LD ₅₀	140.20	149.71	2.51	11.19	2.08	5.47	1030.00
FCS protection factor ^b	1.07		4.46		2.63		ND
Cell proliferation: IC ₁₀₀		13.83		27.70		2.08	ND
Cell proliferation: IC ₅₀		1.75		18.34		0.97	ND

^a All values in μM

^b The FCS protection factor was calculated as $\text{LD}_{50}^{5\% \text{FCS}} / \text{LD}_{50}^{0\% \text{FCS}}$

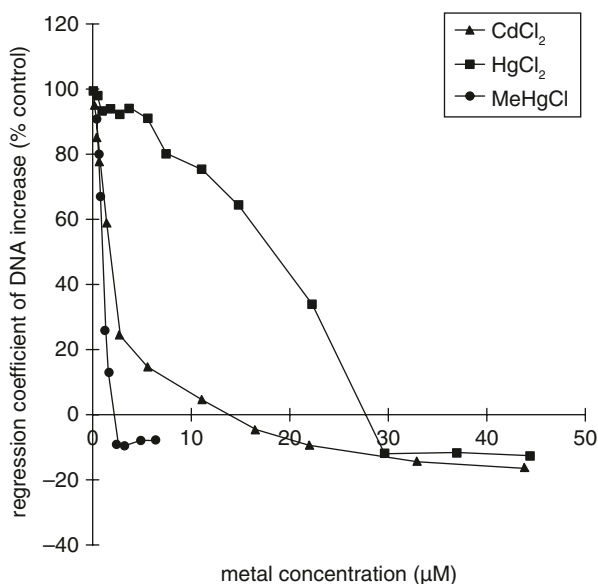
A separate test on CuSO₄ toxicity indicated that this metal is far less able to damage the membrane integrity compared to the other metals (Table 5.1). From our experiments, we cannot distinguish whether the disturbance of membrane integrity is a primary or secondary effect.

In most cases, we found classical sigmoid dose–response curves for heavy metal toxicity. However, one highly reproducible exception occurred: cells that were treated with CdCl₂ in serum-free MK medium showed a clear deviation from the expected sigmoid pattern. At low CdCl₂ concentrations (up to 32.9 μM), we observed the onset of a normal sigmoid viability decrease. In the concentration interval between 32.9 and 132.5 μM CdCl₂, viability levels were higher than expected from the sigmoid model, however. This hormesis-like pattern suggests the induction of a defense system, decreasing Cd toxicity to a considerable extent. Several Cd detoxification systems maybe responsible such as glutathione, metallothioneins and larger detoxification molecules of the heat shock protein family (Bauman et al. 1993; Chin and Templeton 1993; Singhal et al. 1987). More detailed information on this phenomenon is described in the section “Cadmium-induced molecular defense mechanisms”.

Proliferation Assays

We tested long-term toxicity of CdCl₂, HgCl₂ and MeHgCl by monitoring cell proliferation in the presence of these metals. We observed continuous cell proliferation in the control cultures during the 18-day test period. For the three metal species tested, inhibition of proliferation was concentration-dependent (Fig. 5.2). Although membrane integrity tests showed that high cadmium concentrations did not interfere with cell viability (LD₅₀=150 μM), cell proliferation was extremely sensitive to CdCl₂ (IC₅₀=1.75 μM , Table 5.1). This remarkable discrepancy may be due to the fact that Cd²⁺ may enter the cell without disrupting the membrane. Once inside the cell, this heavy metal may interfere with several intracellular processes such as mitosis and Ca²⁺ signaling, resulting in severe inhibition of cell proliferation.

Fig. 5.2 The effect of CdCl₂, HgCl₂ and MeHgCl on proliferation rates of *Aedes albopictus* C6/36 cell cultures. Cell proliferation is measured as the increase of DNA content in the culture and expressed as % control rate. (Reproduced from Braeckman et al. 1997a with permission from Kluwer Academic Publishers)



Although the effect of HgCl₂ and MeHgCl on membrane integrity is fairly similar ($LD_{50}^{HgCl_2} = 11.2 \mu M$ vs. $LD_{50}^{MeHgCl} = 5.5 \mu M$), their inhibitory effects on cell proliferation is widely different ($IC_{50}^{HgCl_2} = 18.3 \mu M$ vs. $IC_{50}^{MeHgCl} = 0.97 \mu M$). MeHg proved to be potent inhibitor of cell proliferation whereas Hg permitted proliferation within a large concentration range. Similar effects were described by Repetto and co-workers (1993) and Thrasher and Adams (1972). Specific inhibition of cell proliferation by MeHg may arise from its property to disrupt microtubules *in vivo* at very low concentrations which in turn inhibits mitotic spindle formation (Thrasher and Adams 1972; Miura et al. 1978). It was also reported that MeHg can cause DNA damage and inhibits DNA synthesis (Roy et al. 1991). The relatively low potency of HgCl₂ to inhibit cell proliferation was also found by Miura et al. (1979). It is remarkable that we found that acute membrane disruption by HgCl₂ occurred at lower concentrations than proliferation inhibition ($LD_{50}^{HgCl_2} = 11.2 \mu M$ vs. $IC_{50}^{HgCl_2} = 18.3 \mu M$). This seems odd as dead cells with disrupted membranes are not able to proliferate anymore. However, in a culture, dead cells and cellular debris may bind Hg²⁺ very tightly, thereby decreasing the availability of free Hg²⁺ in such a way that surviving cells may continue to proliferate. In contrast, MeHg⁺ and Cd²⁺ can readily shift between thiol groups and therefore they may retain their bioavailability.

In conclusion, the viability and proliferation assays showed that there are clear differences among the toxicities of Cd, Hg and MeHg which reflect differences of their mechanisms of action. Hg and MeHg proved to be the most potent membrane-disrupting agents while MeHg and Cd were the strongest inhibitors of cell proliferation. We have no comparable data for CuSO₄.

General Cell Morphology (Light Microscopy)

Aedes albopictus C6/36 cells have a similar morphology to insect hemocytes (Fig. 5.3a). They have a fibroblast-like shape and produce cellular extensions that rarely exceed the length of a cell body diameter. These extensions seem to be randomly placed and oriented. Also sheet-like lamellipodia with microspikes (short and stiff protrusions) were observed. When cells were treated with sublethal doses of CdCl₂, HgCl₂ or CuSO₄ for a few hours, their morphology changed dramatically, showing long neurite-like extensions. CdCl₂ and HgCl₂-treated cells showed many of these long processes that were randomly distributed around the cell body (Fig. 5.3b) while the CuSO₄-exposed cells showed mostly uni- or bipolar extensions (Fig. 5.3c). MeHgCl-treated cells did not show a neuron-like morphology at all (Fig. 5.3d). The appearance of long slender neurite-like extensions may reflect a general stress response, rather than a specific effect of the heavy metals as this particular morphology was also obtained when cells were treated with 20-OH ecdysone (Smagghe et al. 2003) and the F-actin poison cytochalasin B (Fig. 5.3e). The formation of these extensions is new to heavy metal literature although similar extensions have been described in other fields of insect cell research. First, the observed cellular morphology strikingly matches the effect of 20-OH ecdysone in *Drosophila*, *Malacosoma* and *Choristoneura* cells (Courgeon 1972; Cherbas et al. 1977, 1980; Berger et al. 1978; Wing 1988; Peel and Milner 1992; Sohi et al. 1995). Secondly, epidermal feet are known to be induced by oxygen deficiency and they help to drag tracheoles towards hypoxic regions in the insect body (Wigglesworth 1977). It is plausible that Cd and Hg cause epidermal feet in *Aedes albopictus* cells as these metals are known to target the respiratory system (Weinberg et al. 1982; Reddy and Bhagyalakshmi 1994).

The cytoplasmic feet are supported by microtubules. We studied the cytoskeletal support of the long extensions induced by CdCl₂ and HgCl₂ by treating the cells with 100 µM colchicin or 10 µM cytochalasin B. Colchicin inhibits the polymerization of tubulin by binding specifically on free dimers. Cytochalasin B inhibits actin polymerization by capping the positive pole of a growing filament. When *Aedes* cells were pretreated with colchicine and subsequently exposed to CdCl₂ or HgCl₂, they did not develop the characteristic long extensions, suggesting that these are supported by microtubules. Once these extensions had been formed by metal treatment, they could not be removed by colchicine post-treatment, suggesting that the microtubules were stabilized. Microtubular support of the extensions was also confirmed by immunostaining (Fig. 5.3f) and electron microscopy (Fig. 5.3g) (Raes et al. 2000). Cytochalasin B treatment resulted in a severe clustering of cellular F-actin as shown by BODIPY®-phalloidin staining (Fig. 5.3h) and the formation of long processes (Fig. 5.3e), clearly indicating that these long neurite-like structures were not supported by actin. Cytochalasin B-treated cells had a flatter appearance and processes were somewhat thicker compared to the metal-stressed cells. Post-treatment of HgCl₂ and CdCl₂-exposed cells with cytochalasin B did not alter the shape of the cells.

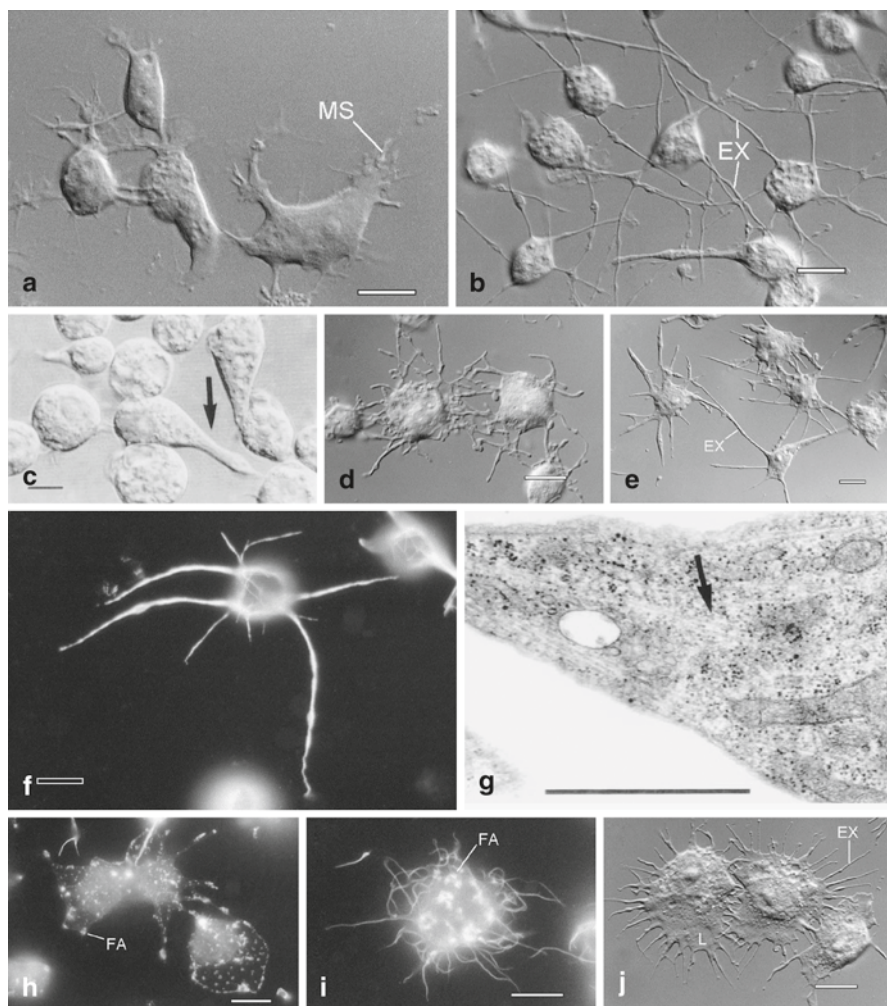


Fig. 5.3 **a** Untreated *Aedes albopictus* C6/36 cells (MS:microspike). **b** Outgrowth of long extensions (EX) after a 3 h treatment with 44 μM CdCl₂. **c** Cells treated with 1.5 mM CuSO₄ for 4 h show stiff monopolar extensions (*arrow*). **d** Multiple short extensions were observed in *Aedes* cells treated with 2 μM MeHgCl for 3 h. **e** Cytochalasin B treatment (10 μM for 3 h) induced long extensions (EX) as well. **f** *Aedes* cells, treated with 3.7 μM HgCl₂ for 3 h and immunostained for α -tubulin, show high fluorescence in the metal-induced extensions. **g** Electron micrograph of the base of a CuSO₄-induced extension (0.75 mM for 6 h) which is supported by parallel microtubules (*arrow*). **h** Cytochalasin B treatment (10 μM for 3 h) induced condensation of actin into distinct foci (FA: F-actin aggregation). **i** MeHgCl-treated cells (2 μM for 3 h) showed many short F-actin-supported extensions and some F-actin aggregation (FA) in the cell body. **j** When MeHgCl-treated cells (2 μM for 3 h) were post-treated with cytochalasin B (10 μM for 3 h), the cell body flattened and showed short, radially oriented extensions (EX). Bars are 10 μm (except g: bar is 1 μm). (Reproduced from Braeckman et al. 1997b (a, b, d, e, f, h, i, j) and Raes et al. 2000 (c, g) with permission from Academic Press and Wiley-Liss, Inc.)

Interestingly, MeHgCl-treated cells did not show the characteristic long extensions that were induced by all other stressing situations (Fig. 5.3d). However, MeHg is known to be a strong inhibitor of microtubule polymerization (Imura et al. 1980; Sager et al. 1983), which easily explains the absence of any microtubule-supported extensions. MeHgCl treatment induced large numbers of actin-supported filopodia (Fig. 5.3i) the reason of which remains unclear. Post-treatment of MeHg-exposed cells with cytochalasin B could not induce the long extensions as seen in cells treated with cytochalasin B alone. This observation shows that the cytochalasin B-induced processes are probably also supported by microtubules. During post-treatment, the cytochalasin B kept its cell-flattening effect resulting in round flat cells with short radial filopodia (Fig. 5.3j).

In conclusion, short 3-h treatment of *Aedes albopictus* cells with sublethal doses of CdCl₂ and HgCl₂ induced abnormal microtubular polymerization giving the cells a neuron-like appearance. In accordance with its microtubule-disrupting activity, MeHgCl was not able to induce such long neurite-like processes. Instead, it gave rise to many short F-actin-supported filopodia.

Ultrastructural Effects (Electron Microscopy)

After studying Cd and Hg toxicity and the effects of these metals at the light microscopical level, we wanted to gather further information on their subcellular targets in *Aedes albopictus* C6/36 cells. Heavy metal treatment was based on the LD_{50/24h} values obtained in the membrane integrity tests (Fig. 5.1). Cells were treated for 6 and 24 h with 66 μM CdCl₂, 9.3 μM HgCl₂ or 5.5 μM MeHgCl. In a separate experiment, cells were treated with 750 μM CuSO₄ (LD_{5/24h}) to visualize its apoptotic effect. We will focus on the Cu-induced effects at the end of this section.

Untreated *Aedes albopictus* cells resembled typical insect hemocytes and showed phagocytotic properties. Their nucleus had a rounded shape or was slightly irregular, the chromatin was homogeneously distributed with few chromatin apposed to the nuclear envelope and the nucleolus was well-developed (Fig. 5.4a). In general, only few RER profiles could be detected and in some cases they were organized in concentric whorls. Also some small SER patches were observed but the Golgi system was poorly developed. The cytoplasm showed many lysosomes containing myelin-like membrane structures. The mitochondria had an electron-dense matrix with electron-lucent cristae (Fig. 5.4b) and they often showed electron-dense granules.

A 6-h cadmium treatment did not result in any ultrastructural changes while for both mercury species several morphological alterations could already be observed. Cells that were treated for 24 h either with cadmium or mercury showed the most clear-cut intracellular effects. Many of these alterations occurred in all metal-treated cells, independent of the nature of the heavy metal and thus may represent a general stress response. The nuclei often showed irregular indentations (Fig. 5.4c), an increased nucleolar volume, slight chromatin clumping and appearance of electron-lucent spaces in the nucleoplasm. Nuclear indentations were also reported in cad-

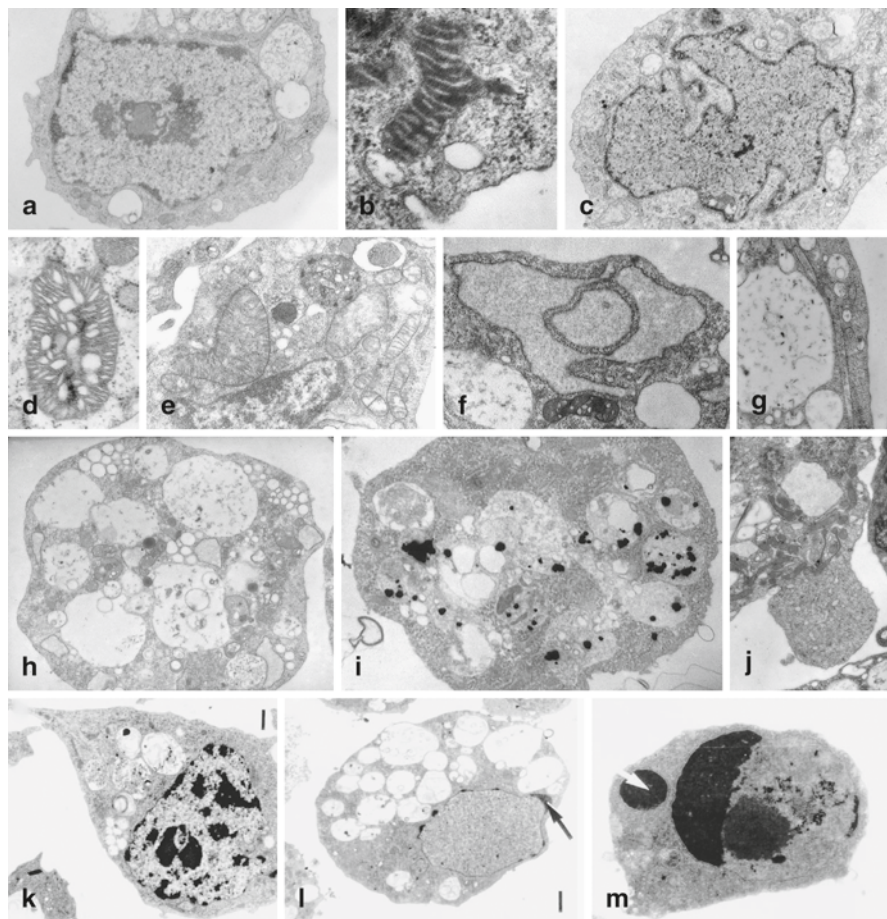


Fig. 5.4 Transmission electron micrographs of control and metal-treated *Aedes albopictus* C6/36 cells. **a** Untreated cell. **b** Mitochondrion of a control cell. **c** Nuclear indentations in a CdCl₂-treated cell (66 μM for 24 h). **d** CdCl₂ treatment (66 μM for 24 h) caused mitochondrial condensation. Metal-treated cells also showed mitochondrial dilatation (**e**, 9.3 μM HgCl₂ for 6 h) and severe swelling of the RER cisternae (**f**, 9.3 μM HgCl₂ for 24 h). **g** MeHgCl-treated cells (5.5 μM for 24 h) typically showed tube-like structures that possibly consist of RER membranes. **h** HgCl₂-treated cell (9.3 μM for 24 h) with expanded lysosomal system and clusters of small vesicles. **i** When mercury-treated cells (3 μM HgCl₂ for 24 h) were stained by autometallography, silver grains were predominantly found in the lysosomes. **j** Blebs, devoid of major cell organelles were observed in MeHgCl-treated *Aedes* cells (5.5 μM for 24 h). **k** After a 6-h treatment with 0.75 mM CuSO₄·5H₂O, *Aedes* cells were polarized with a vacuole localized at one pole. After 18 h of copper treatment, cells also showed first signs of chromatin clumping along the nuclear envelope (*arrow*), typical for apoptosis (**l**). **m** At longer treatment times, cells showed severe chromatin clumping and nuclear budding (*arrow*). Bars are 1 μm. (Reproduced from Braeckman et al. 1999a (d), Braeckman and Raes 1999 (a, f, g, j) and Raes et al. 2000 (k, l, m) with permission from Harcourt Brace & Co. Ltd. and Wiley-Liss Inc.)

mium- and mercury-treated hepatocytes (Hirano et al. 1991; Bucio et al. 1995). The mitochondria became pleomorphic: in some cells they were inflated with dense material while in others there were accumulations of numerous small dividing mitochondria. Some mitochondria showed matrix condensation (Fig. 5.4d) and sometimes the first signs of necrotic degeneration could be observed (Fig. 5.4e). Mitochondrial swelling was most common in Cd-treated cells and only found to a lesser extent in Hg-treated cells. Mitochondrial pleomorphy is a pre-necrotic event due to the disturbance of respiration and of mitochondrial growth and replication (Trump et al. 1978). Metal-induced mitochondrial alterations have been reported frequently before (Hawkins 1980; Seidman et al. 1986; Kawahara et al. 1990; Pawert et al. 1996). In many cases, inflated RER cisternae, filled with a proteinaceous material occurred (Fig. 5.4f); similar swellings were found in the nuclear envelope. Also cells with a dark cytoplasm showing increased ribosomal content were observed. These may be signs of activated protein synthesis and this issue will be dealt with in more detail in the last section. The number and the diameter of the lysosomes were increased although their general appearance was similar to that of the control cells (Fig. 5.4h). A dilated lysosomal system has been described by many authors (Ferri and Macha 1980; Hawkins 1980; Morselt et al. 1983; Hemelraad et al. 1990) and may reflect enhanced turnover of intracellular components or enlarged endocytotic activity. Autometallography is a histochemical technique that visualizes hotspots of mercury accumulation in cells or tissues. Individual mercury atoms bound to proteins cannot be visualized with this method. Electron micrographs of mercury-treated *Aedes* cells stained with autometallography showed that lysosomes were the primary accumulation sites in the cell (Fig. 5.4i). This confirms earlier observations in invertebrate animals (Ballan-Dufrançais et al. 1980; Jeantet et al. 1980; Raes and De Coster 1991; Marigómez et al. 1996) and vertebrate cells and tissues (Baatrup and Danscher 1987; Danscher et al. 1994; Christensen 1996). Mercury accumulations were also detected near the plasma membrane corroborating the observation of Endo et al. (1995) that the non-internalized fraction of mercury, bound to the plasma membrane, is much greater than the internalized fraction. We found a striking heterogeneity in the amount of mercury accumulation among cells. This corroborates with the heterogeneity found in the ultrastructural pathology discussed above. Lysosomal accumulation of mercury was already detected after a 30-min incubation time. We have no data on intracellular Cd storage sites as the autometallographical procedure is not sensitive to cadmium.

Besides these general ultrastructural effects, we also observed a few metal-specific alterations in the treated *Aedes* cells. Although mitochondrial dilation was induced by cadmium as well as mercury, it occurred earlier and more strikingly in CdCl₂-treated cells, suggesting that mitochondrial function is very sensitive to Cd²⁺. HgCl₂-treated cells specifically showed typical clusters of small electron-lucent vesicles in the vicinity of a dictyosome, suggesting that these may be primary lysosomes (Fig. 5.4h). The cells treated with MeHgCl showed blebbing of the plasma membrane (Fig. 5.4j) and nuclear indentation that was generally stronger than in CdCl₂- and HgCl₂-treated cells indicating disruption of the cytoskeleton. In the cytosol of MeHg-treated cells, remarkable tube-like structures were found to which

many ribosomes were attached (Fig. 5.4g). They are reminiscent to cytoplasmic inclusions found in the oenocytes of *Calpodes ethlius* (Locke 1969). The etiology and significance of these structures remains to be elucidated.

Unlike CdCl₂, HgCl₂ and MeHgCl, CuSO₄ caused massive apoptosis in the *Aedes* cell culture. The only common morphological feature that occurred in the Cu-treated cells is the formation of long, microtubule-supported neurite-like extensions. However, these were not randomly spread but tend to show a bipolar orientation. None of the aforementioned intracellular alterations occurred in *Aedes* cells treated with 750 μM CuSO₄. Morphology of the mitochondria, lysosomes, and endoplasmic reticulum seemed to be unaffected, although clustering of the vacuome at one side of the cell has been observed (Fig. 5.4k). After 6 h of Cu treatment, some cells already showed smooth chromatin clumps along the nuclear envelope, which is a first sign of apoptosis (Fig. 5.4l). At longer treatment times, severe chromatin clumping, nuclear budding and formation of apoptotic bodies occurred (Fig. 5.4m). The copper-induced apoptosis was confirmed by gel electrophoresis, which showed the typical laddering pattern caused by inter-nucleosomal DNA cleavage (Fig. 5.5a) At higher CuSO₄ concentrations, the proportion of necrotic cells rose while apoptosis decreased (Fig. 5.5b). Literature on Cu²⁺-induced apoptosis is very scarce; this phenomenon has been described *in vivo* in some vertebrates (Haywood et al. 1996; King and Bremmer 1979; Fuentalba and Haywood 1988) but for invertebrate cells, no information is available. More recently, Xia et al. (2005) described Zn²⁺-induced apoptosis in *Spodoptera* larval hemocytes. In our mercury-treated cells no apoptotic cells could be detected. However, in CdCl₂-treated cells, a few apoptotic cells

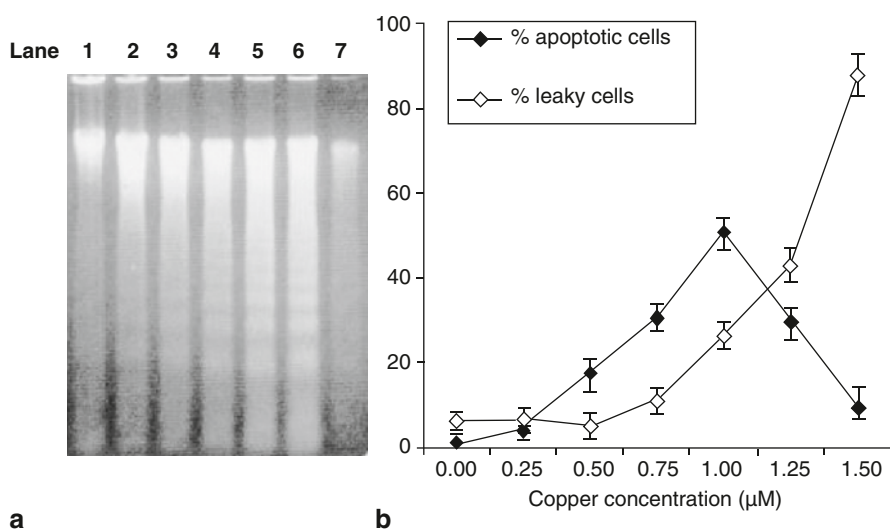


Fig. 5.5 **a** DNA laddering pattern of *Aedes* cells treated with CuSO₄·5H₂O. Lanes 1–7 control, 0.25, 0.50, 0.75, 1.00, 1.25, and 1.50 mM, respectively. **b** Fraction of apoptotic and leaky cells as a function of CuSO₄ concentration in the medium. (Reproduced from Raes et al. 2000 with permission from Wiley-Liss, Inc.)

Table 5.2 Overview of the most prominent ultrastructural changes observed in cadmium- and mercury-treated cells

Ultrastructural effect	CdCl ₂	HgCl ₂	MeHgCl
Chromatin condensation	***	**	**
Irregular indentations of the nucleus	**	**	***
Dilatation of the perinuclear cisternae	**	*	*
Dilatation of the RER by proteinaceous material	***	***	**
Increase of RER-associated ribosomes	***	**	**
Increase of free ribosomes	**	*	*
Expansion of the Golgi apparatus		*	
Clusters of small vesicles		**	
Expansion of the lysosomal system	**	*	*
Lipid vacuoles		**	
Cytoplasmic tubular structures			**
Mitochondrial dilation (osmotic swelling)	***	*	*
Mitochondrial dilation (due to electron-dense material)		**	**
Condensation of the mitochondrial matrix	***	***	***
Flocculent substance in the mitochondrial matrix	*	**	**
Mitochondrial fission		*	*
Blebbing of the plasma membrane			**

Asterisks indicate the severity of the morphological effect: ()=no effect, (*)=moderate, (**)=clear, (***)=strong

could be found. The pronounced apoptotic effect of CuSO₄ may be related its free radical-generating properties (Hockenberry et al. 1993; Stohs and Bagchi 1995). An overview of the most prominent ultrastructural changes in cadmium- and mercury-treated *Aedes* cells can be found in Table 5.2.

Metal Uptake

It is very conceivable that heavy metals exert their toxic effects by interaction with intracellular processes. In order to interact with intracellular components, heavy metals need to enter the cell by passive diffusion, carrier or channel-mediated uptake or by endocytosis. We analytically quantified Cd and Hg uptake by atomic absorption and atomic fluorescence spectrometry, respectively. We followed metal uptake kinetics and studied the effects of temperature and inhibitors to identify the routes of intake. The sublethal metal concentrations used in this series of experiments were based on short term viability assays (Table 5.1).

Immediately after administration, metals are readily taken up in the cells and subsequently, gradual saturation of the intracellular metal concentration occurs (Fig. 5.6). CdCl₂ accumulates quickly (T_{1/2}=25 min at 131 μM) (Fig. 5.6a) while the dose-accumulation curve (24 h of CdCl₂ treatment) showed a hyperbolic rela-

tion between dosage and intracellular metal accumulation in the sublethal concentration range (Fig. 5.6d). These data indicate that cadmium is taken up by (saturable) mediated transport, probably through ion channels. Indeed, at least part of the Cd uptake occurs through verapamil-sensitive Ca²⁺-channels (Fig. 5.6j). The role of Ca²⁺-channels in Cd uptake has been shown by several authors (Blazka and Shaikh 1991; Borowitz and McLaughlin 1992; Souza et al. 1997). The mitochondrial uncoupler DNP had no effect on Cd uptake in *Aedes* cells, showing that this process is ATP-independent which in turn confirms the importance of facilitated diffusion (Fig. 5.6k). However, in the literature, conflicting data exists on the energy dependency of cellular cadmium uptake (Roesijadi and Unger 1993; Pigman et al. 1997; Garty et al. 1986; Endo and Shaikh 1993). We found that both cadmium toxicity and uptake significantly increase with temperature (Fig. 5.6g) which is in agreement with the proposed mediated uptake mechanisms.

For both mercury species, dose accumulation curves are linear in the sublethal dose range (Fig. 5.6e, f) indicating that diffusion maybe the major way of entry into the cell. Kinetic experiments show that inorganic mercury ($T_{1/2}=130$ min at 0.9 μ M) accumulates much more slowly than methylmercury ($T_{1/2}=18.5$ min at 0.6 μ M) (Fig. 5.6b, c). This agrees well with the fact that a lipid bilayer is not a significant barrier for the lipophilic MeHg (Lakowicz and Anderson 1980; Nakada and Imura 1982) while it is for inorganic ionic Hg²⁺. Accumulation of HgCl₂ increases with temperature while HgCl₂ toxicity is temperature independent (Fig. 5.6h). The latter effect may be explained by the fact that the plasma membrane is the major target of HgCl₂ (Passow and Rothstein 1960, Nakada and Imura 1982; Miura et al. 1984; Aleo et al. 1992; Repetto et al. 1993). If the inorganic mercury would disrupt the plasma membrane by direct attack from outside the cell, its toxicity (measured as membrane integrity) would be independent of temperature, uptake rate or intracellular mercury levels. On the other hand, temperature-dependent membrane fluidity may facilitate mercury uptake by passive diffusion to some extent (Foulkes and Bergman 1993; Endo et al. 1995), explaining increased accumulation at higher temperatures. Furthermore, HgCl₂ uptake was found to be insensitive to DNP-pretreatment (Fig. 5.6k), showing that this process does not require ATP.

Opposite to HgCl₂, the toxicity of MeHgCl is temperature dependent while its uptake is not (Fig. 5.6i). Probably, due to its lipophilic character, MeHgCl readily penetrates the plasma membrane, independently from its fluidity, resulting in a temperature independent accumulation. However, MeHgCl toxicity increases with temperature, suggesting that MeHgCl interferes with temperature-sensitive cellular processes. Cell membrane permeation may be a secondary effect caused by deregulation of these cellular processes. MeHgCl accumulation in *Aedes* cells doubled after DNP pretreatment (Fig. 5.6k). This surprising effect may be related to the unusual uptake kinetics (Fig. 5.6c). After about 1 h of MeHgCl treatment, intracellular mercury levels decrease to a plateau level, suggesting that MeHgCl is actively removed out of the cell. This would explain why DNP-treated cells, that have low ATP levels and cannot actively pump MeHgCl out of the cell, would accumulate higher mercury levels. Fujiyama et al. (1994) showed that the efflux of a

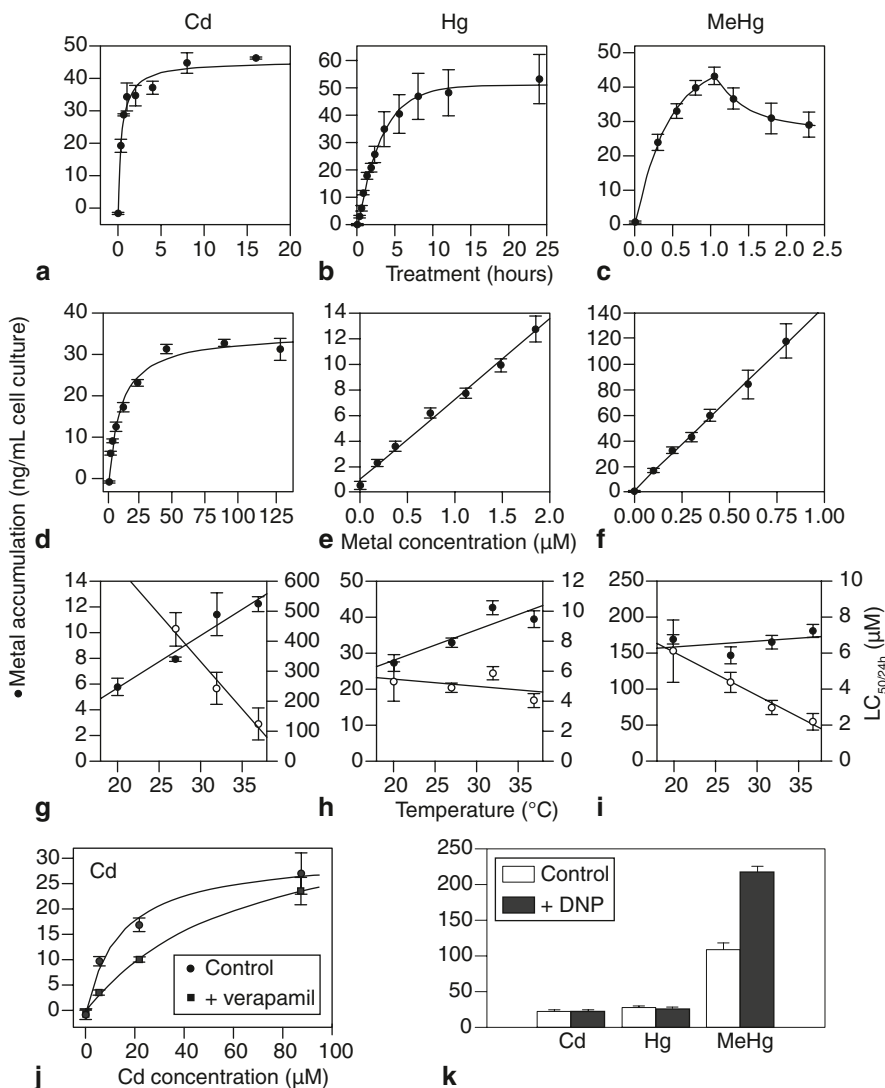


Fig. 5.6 The uptake of CdCl_2 , HgCl_2 and MeHgCl in *Aedes albopictus* C6/36 cells: uptake kinetics of CdCl_2 (**a**), HgCl_2 (**b**) and MeHgCl (**c**); dose-dependent uptake of CdCl_2 (**d**), HgCl_2 (**e**), MeHgCl (**f**) after a 24 h treatment. Comparison of metal uptake and toxicity ($\text{LC}_{50/24\text{h}}$): CdCl_2 (**g**), HgCl_2 (**h**), MeHgCl (**i**); the following metal concentrations and incubations times were used for the uptake experiments: CdCl_2 , 33 μM for 1 h, HgCl_2 and MeHgCl , 0.6 μM for 2 h. **j** Inhibition of cadmium uptake in *Aedes* cells by a 30 min 500 μM verapamil pre-treatment. Cells were exposed to CdCl_2 for 12 h. **k** The effect of 100 μM DNP on the accumulation of CdCl_2 , HgCl_2 , and MeHgCl . All metal treatments were 0.6 μM for 2 h. (Reproduced from Braeckman et al. 1998 (b, c, e, f, h, i, k), Braeckman et al. 1999b (g, j, k) with permission from Academic Press)

MeHg–glutathione complex in astrocytes is mediated by an organic acid transporter. For some of these transporters it was shown that they are ATP-dependent (Steinberg et al. 1987; Ballatori and Truong 1995).

Mitochondrial Impairment and Anaerobic Metabolism in Cd-Treated Cells

The ultrastructural pathologies, viability curves and proliferation patterns of cadmium-treated *Aedes* cells required more detailed investigation. Under normal growth, we expect a straight correlation between cell proliferation rate and medium acidification, i.e. more cells will lead to faster acidification of the medium. We observed such a pattern in mercury-treated *Aedes* cells (Fig. 5.7b, c) but not in Cd-treated cells (Fig. 5.7a). In the latter, we found that low cell numbers correlated to strong

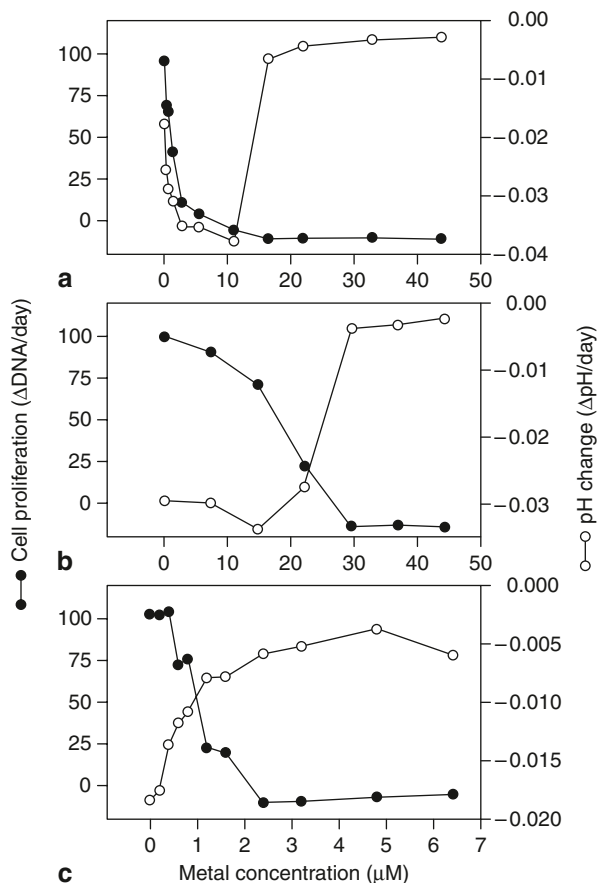
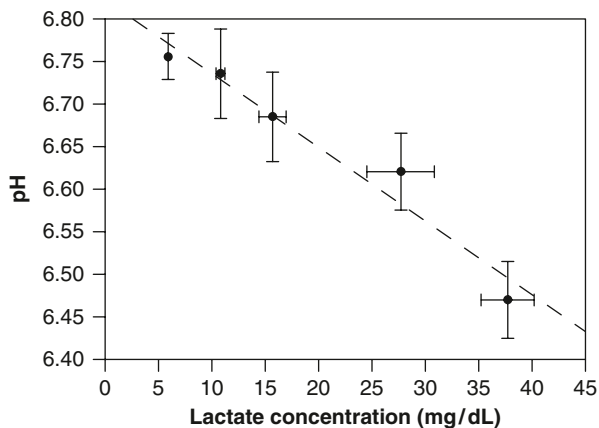


Fig. 5.7 Comparison between metal-induced inhibition of cell proliferation (expressed as change in DNA content per ml medium per day) and medium acidification (expressed as pH change per day in the medium). **a** CdCl₂, **b** HgCl₂, **c** MeHgCl

Fig. 5.8 Correlation between medium pH and lactate levels of medium from *Aedes albopictus* cultures treated with CdCl₂ for 18 days. The correlation coefficient (R^2) of the linear best fit was 0.955. (Reproduced from Braeckman et al. 1999a with permission from Harcourt Brace & Co. Ltd.)



medium acidification in the Cd concentration range up to 11 μM . At higher Cd levels, medium pH remained stable, probably because nearly all cells were dead. The cadmium-induced medium acidification suggests mitochondrial impairment and activation of compensatory anaerobic pathways (such as lactate production). In several vertebrate as well as invertebrate studies, mitochondria were described as important target organelles for cadmium (Jay et al. 1991; Miccadei and Floridi 1993; Reddy and Bhagyalkshmi 1994). Moreover, in our ultrastructural studies, we observed mitochondrial swelling in cadmium-treated cells. The Cd-induced switch to anaerobic pathways was confirmed by the increased lactate levels we found in the medium of cadmium-treated cultures. Furthermore, medium pH correlated very well to lactate levels (Fig. 5.8), suggesting that the cadmium-induced medium acidification was caused by lactate accumulation and mitochondrial impairment.

Cadmium-Induced Molecular Defense Mechanisms

The viability curve of Cd-treated *Aedes* cell cultured in serum-free medium deviated substantially from the standard sigmoid curve (Fig. 5.1a). We wondered whether this peculiar curve shape would reflect a dose-dependent trigger of a stress response. *Aedes* cells were treated for 24 h with a CdCl₂ gradient (11–175 μM) after which cell viability and protein analysis was performed. In the range of 33–110 μM CdCl₂, a clear deviation of the sigmoid viability curve occurred which coincided with a raise of protein density in the culture (Fig. 5.9). Equal amounts of proteins (10 $\mu\text{g}/\text{lane}$) of a selected number of the Cd-treated and control cultures were loaded on SDS-gel for separation. Cadmium clearly induces a set of proteins in the 70-kDa range (71, 75 and 78 kDa) of which the 78-kDa protein is most strongly expressed (Fig. 5.10). Quantification of this protein band over the cadmium concentration range perfectly matched the viability deviation sug-

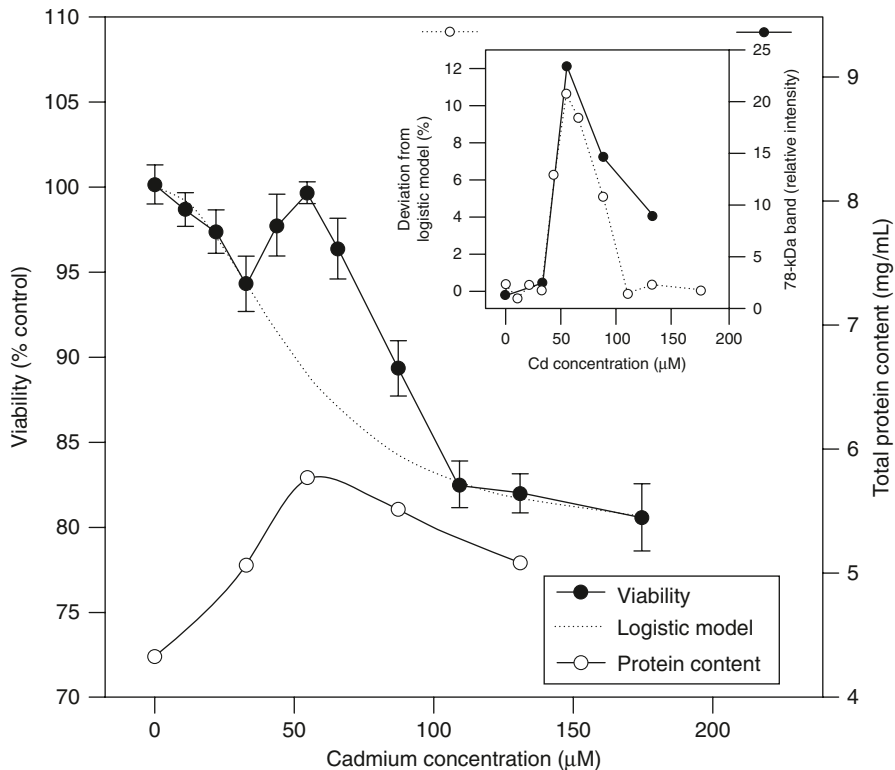
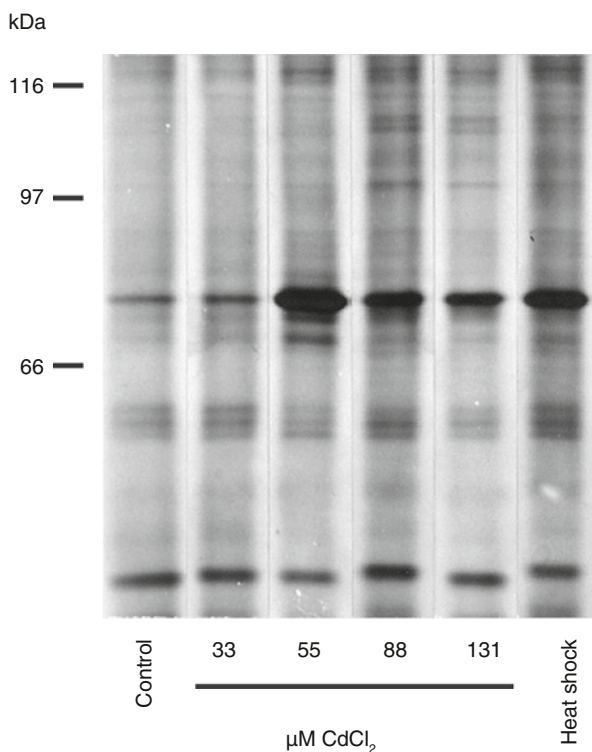


Fig. 5.9 Comparison of the viability (*closed circles*) and total protein content (*open circles*) of *Aedes albopictus* cells treated with CdCl₂ for 24 h (the *dotted line* shows the expected viability trend according to a logistic model). Inset: comparison of the deviation of viability from the logistic model and the relative intensity of a 78-kDa protein band in CdCl₂-treated cells. (Reproduced from Braeckman et al. 1999b with permission from Academic Press)

gesting a protective role for the 78-kDa protein (Fig. 5.9 inset). This protein was also highly induced in a heat-stressed sample (30 min 40°C), suggesting that this may be a member of the HSP family. It has been shown previously that Cd can induce several HSPs in insect cells (Courgeon et al. 1984; Veldhuizen-Tsoerkan et al. 1990; Sonoda et al. 2007). Although we could not identify the 78-kDa protein in this series of experiments, it may represent the insect ortholog of Grp78 (glucose-regulated protein)/BiP (Binding immunoglobulin protein). This stress-inducible molecular chaperone has an important function in the solubilization of aggregates of misfolded proteins in the RER (unfolded protein response). This correlates very well with the heavily loaded and dilated RER cisternae observed in Cd-treated *Aedes* cells (Fig. 5.4f). Besides the proteins in the 70-kDa range, some larger proteins were also induced at the highest Cd concentrations tested (98, 108, 110, and 120 kDa Fig. 5.10). While the 98 kDa protein may represent an ortholog

Fig. 5.10 Silver-stained SDS-PAGE of *Aedes* cells treated for 24 h with CdCl₂ or heat-shock (40°C for 30 min). (Reproduced from Braeckman et al. 1999b with permission from Academic Press)

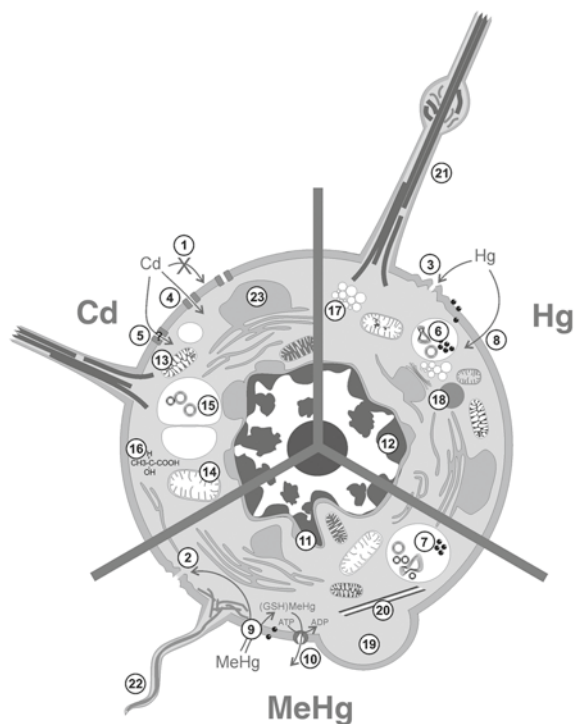


to the mammalian Grp94 stress protein (Goering et al. 1993), the others probably belong to the HSP110 family.

Conclusions

Cadmium and mercury are among the most toxic heavy metals and a threat to all life forms. As a consequence, these metals have received much attention and numerous studies have been carried out on vertebrate models. The knowledge about the cellular toxicity of cadmium and mercury on invertebrates *in vivo* is fragmentary, but *in vitro*, it is almost non-existent. This exploratory study in the *Aedes albopictus* C6/36 cell line shows that the cellular uptake of, and response to, cadmium, mercury and copper is widely divergent (Fig. 5.11). Cadmium and methylmercury strongly affected cell proliferation rather than membrane integrity indicating that these metal species enter the *Aedes* cells without disrupting the membrane. At high concentrations membrane disruption was found but may be as a secondary effect (Fig. 5.11 numbers 1, 2). For HgCl₂-treated cells, membrane disruption and inhibition of cell proliferation was found in the same concentration range, suggesting that the plasma

Fig. 5.11 Uptake and ultra-structural effects of CdCl₂, HgCl₂, and MeHgCl in the *Aedes albopictus* C6/36 cell line. The numbers in the diagram are referred to in the conclusions section



membrane may be a primary target of this metal species (3). The uptake of cadmium occurred largely through verapamil-sensitive Ca²⁺ channels (4), although at high concentration a different ATP-independent, temperature-sensitive route became more important (5). Mercury was taken up by the cells through simple diffusion (8, 9) and the metals accumulated in the lysosomes (6, 7). MeHg was taken up more quickly than inorganic Hg. Apparently, intracellular MeHg was exteriorized by an ATP-dependent process (10). The heavy metal-treated cells showed some general ultrastructural pathologies, usually referred to as preneurotic alterations: nuclear indentation (11) with peripheral chromatin condensation (12). Mitochondrial condensation (13) indicates a first reversible step towards decreased function while osmotic dilatation represents a more advanced stage of mitochondrial disruption (14). Also increased lysosomal profiles were seen in Cd-(15) and Hg-treated (6, 7) cells. Metal-specific effects were few and they were mostly quantitative rather than qualitative. Mitochondrial dilatation was most severe in Cd-treated cells. This was paralleled by increased medium acidification by lactate (16). HgCl₂-treated cells showed typical clusters of small vesicles adjacent to the dictyosome (17) that may be primary lysosomes. These cells also contained lipid droplets (18). MeHg caused blebbing of the plasma membrane (19) and nuclear deformation (11) to a greater extent than Cd and Hg, which indicated disruption of the cytoskeleton. In the cytosol of MeHg-treated cells, we found remarkable tubular structures (20) of which

the significance remains to be elucidated. The most striking phenomenon of CdCl_2 , HgCl_2 and CuSO_4 -treated cells was the formation of long, microtubule-supported extensions (21). This reaction was also seen in other insect cells after application of a wide range of stressors. These neurite-like processes were absent in MeHg-treated cells as this metal specifically inhibits microtubule polymerization. MeHg induced high numbers of short F-actin-supported filopodia (22). Cadmium and mercury-treatment resulted in dilatation of the RER by proteinaceous material (23). This effect was most noticeable in Cd-treated cells. This observation may indicate RER-stress and the induction of large amounts of chaperones. Indeed, SDS-PAGE analysis of Cd-treated *Aedes* cells revealed the strong induction of a 78-kDa protein (probably the *Aedes* ortholog of the RER chaperone Grp78/BiP) and some larger proteins. The induction pattern overlapped completely with an unusual viability pattern that was observed in the sublethal cadmium concentration range, indicating the induction of an efficient cellular defense system.

Contrary to Cd and Hg, CuSO_4 induced massive apoptosis in *Aedes* cells as was shown by chromatin condensation, formation of apoptotic bodies and DNA laddering. At high Cu concentrations, cells died necrotically.

Acknowledgements I want to acknowledge H. Raes for introducing me into the wonderful world of scientific research and her excellent promotorship during my metal-related research activities. I also acknowledge R. Dams, L. Mees and M. Helsen for help with the atomic spectrometry, G. Criel and T. McRae for support with the antibody staining, G. Smagge for running the SDS-PAGES, L. De Ridder and J. Quatacker for the use of the transmission electron microscopes, and J. R. Vanfleteren for helpful discussions. This study was granted by the Belgian Fund for Medical Scientific Research (3.9001.92).

References

- Aleo MD, Taub ML, Kostyniak PJ (1992) Primary cultures of rabbit renal proximal tubule cells. III. Comparative cytotoxicity of inorganic and organic mercury. *Toxicol Appl Pharm* 112:310–317
- Baatrup E, Danscher G (1987) Cytochemical demonstration of mercury deposits in trout liver and kidney following methyl mercury intoxication: differentiation of two mercury pools by selenium. *Ecotox Environ Safe* 14:129–141
- Ballan-Dufrançais C, Ruste J, Jeantet AY (1980) Quantitative electron probe microanalysis on insects exposed to mercury. I Methods. An approach on the molecular form of the stored mercury. Possible occurrence of metallothionein-like proteins. *Biol Cell* 39:317–324
- Ballatori N, Truong AT (1995) Multiple canalicular transport mechanisms for glutathione S-conjugates. *J Biol Chem* 270:3594–3601
- Bauman JW, Liu J, Klaassen CD (1993) Production of metallothionein and heat-shock proteins in response to metals. *Fund Appl Toxicol* 21:15–22
- Berger E, Ringler R, Alahiotis S, Frank M (1978) Ecdysone-induced changes in morphology and protein synthesis in *Drosophila* cell cultures. *Dev Biol* 62:498–511
- Blazka ME, Shaikh ZA (1991) Differences in cadmium and mercury uptakes by hepatocytes: role of calcium channels. *Toxicol Appl Pharm* 110:355–363
- Blum H, Beier H, Gross HJ (1987) Improved silver staining of plant proteins, RNA and DNA in polyacrylamide gels. *Electrophoresis* 8:93–99

- Borowitz JL, McLaughlin JL (1992) Evidence for calcium channels in brine shrimp: diltiazem protects shrimp against cadmium. *B Environ Contam Toxicol* 48:435–440
- Bradford MM (1976) A rapid and sensitive method for the quantitation of microgram quantities of protein utilizing the principle of protein-dye binding. *Anal Biochem* 72:248–254
- Braeckman BP, Raes H (1999) The ultrastructural effect and subcellular localization of mercuric chloride and methylmercuric chloride in insect cells (*Aedes albopictus* C6/36). *Tissue Cell* 31:223–232
- Braeckman BP, Raes H, Van Hoye D (1997a) Heavy metal toxicity in an insect cell line. Effects of cadmium chloride, mercuric chloride and methylmercuric chloride on cell viability and proliferation in *Aedes albopictus* cells. *Cell Biol Toxicol* 13:389–397
- Braeckman BP, Simoens C, Rzezniak U, Raes H (1997b) Effect of sublethal doses of cadmium, inorganic mercury and methylmercury on the cell morphology of an insect cell line (*Aedes albopictus*, C6/36). *Cell Biol Int* 21:823–832
- Braeckman BP, Cornelis R, Rzezniak U, Raes H (1998) Uptake of HgCl₂ and MeHgCl in an insect Cell Line (*Aedes albopictus* C6/36). *Environ Res* 79:33–40
- Braeckman BP, Brys K, Rzezniak U, Raes H (1999a) Cadmium pathology in an insect cell line: ultrastructural and biochemical effects. *Tissue Cell* 31:45–53
- Braeckman BP, Smaghe G, Brutsaert N, Cornelis R, Raes H (1999b) Cadmium uptake and defense mechanism in insect cells. *Environ Res* 80:231–243
- Bucio L, Souza V, Albores A, Sierra A, Chávez E, Cárabez A, Gutiérrez-Ruiz MC (1995) Cadmium and mercury toxicity in a human fetal hepatic cell line (WRL-68 cells). *Toxicology* 102:285–299
- Cherbas P, Cherbas L, Williams C-M (1977) Induction of acetylcholinesterase activity by b-ecdysone in a *Drosophila* cell line. *Science* 197:275–277
- Cherbas L, Yonge C-D, Cherbas P, Williams C-M (1980) The morphological response of Kc-H cells to ecdysteroids: hormonal specificity. *Wilhelm Roux Arch* 189:1–15
- Chin TA, Templeton DM (1993) Protective elevations of glutathione and metallothionein in cadmium-exposed mesangial cells. *Toxicology* 77:145–156
- Christensen M (1996) Histochemical localization of autometallographically detectable mercury in tissues of the immune system from mice exposed to mercuric chloride. *Histochem J* 28:217–225
- Corrigan A-J, Huang P-C (1981) Cellular uptake of cadmium and zinc. *Biol Trace Elem Res* 3:197–216
- Courgeon A-M (1972) Action of insect hormones at the cellular level. Morphological changes of a diploid cell line of *Drosophila melanogaster*, treated with ecdysone and several analogues *in vitro*. *Exp Cell Res* 74:327–336
- Courgeon A-M, Maisonhaute C, Best-Belpomme M (1984) Heat shock proteins are induced by cadmium in *Drosophila* cells. *Exp Cell Res* 153:515–521
- Danscher G, Stoltenberg M, Juhl S (1994) How to detect gold, silver and mercury in human brain and other tissues by autometallographic silver amplification. *Neuropath Appl Neuro* 20:454–467
- Endo T, Shaikh ZA (1993) Cadmium uptake by primary cultures of rat renal cortical epithelial cells: influence of cell density and other metal ions. *Toxicol Appl Pharm* 121:203–209
- Endo T, Sakata M, Shaikh ZA (1995) Mercury uptake by primary cultures of rat renal cortical epithelial cells. *Toxicol Appl Pharm* 132:36–43
- Fang SC, Fallin E (1976) The binding of various mercurial compounds to serum proteins. *Bull Environ Contam Toxicol* 15:110–117
- Ferri S, Macha N (1980) Lysosomal enhancement in hepatic cells of a teleost fish induced by cadmium. *Cell Biol Int Rep* 4:357–363
- Foulkes EC, Bergman D (1993) Inorganic mercury absorption in mature and immature rat jejunum: transcellular and intercellular pathways *in vivo* and in everted sacs. *Toxicol Appl Pharm* 120:89–95
- Fuentalba IC, Haywood S (1988) Cellular mechanisms of toxicity and tolerance in the copper loaded rat: I. Ultrastructural changes in the liver. *Liver* 8:372–380
- Fujiyama J, Hirayama K, Yasutake A (1994) Mechanism of methylmercury efflux from cultured astrocytes. *Biochem Pharmacol* 47:1525–1530

- Garty M, Bracken WM, Klaassen CD (1986) Cadmium uptake in red blood cells. *Toxicology* 42:111–119
- Goering PL, Fisher BR, Kish CL (1993) Stress protein synthesis induced in rat liver by cadmium precedes hepatotoxicity. *Toxicol Appl Pharm* 122:139–148
- Hawkins WE, Tate LG, Sarphe TG (1980) Acute effects of cadmium on the spot *Leiostomus xanthurus* (Teleostei): tissue distribution and renal ultrastructure. *J Toxicol Env Health* 6:283–295
- Haywood S, Fuentealba IC, Foster J, Ross G (1996) Pathobiology of copper-induced injury in Bedlington terriers: ultrastructural and microanalytical studies. *Anal Cell Pathol* 10:229–241
- Hemelraad J, Herwig HJ, van Donselaar EG, Holwerda DA, Zandee DI (1990) Effects of cadmium in freshwater clams. II. Ultrastructural changes in the renal system of *Anodonta cygnea*. *Arch Environ Contam Toxicol* 19:691–698
- Hirano T, Ueda H, Kawahara A, Fujimoto S (1991) Cadmium toxicity on cultured neonatal rat hepatocytes: Biochemical and ultrastructural analyses. *Histol Histopathol* 6:127–133
- Hockenberry DM, Oltvai ZN, Yin X, Milliman CL, Korsmeyer SJ (1993) Bcl-2 functions in an antioxidant pathway to prevent apoptosis. *Cell* 75:241–251
- Igarashi A (1978) Isolation of a Singh's *Aedes albopictus* cell clone sensitive to dengue and chikungunya viruses. *J Gen Virol* 40:531–544
- Imura N, Miura K, Inokawa M, Nakada S (1980) Mechanism of methylmercury cytotoxicity: by biochemical and morphological experiments using cultured cells. *Toxicology* 17:241–254
- Jay D, Zamorano R, Munoz E, Gleason R, Boldu JL (1991) Study of the interaction of cadmium with membrane-bound succinate dehydrogenase. *J Bioenerg Biomembr* 23:381–389
- Jeantet AY, Ballan-Dufrançais C, Ruste J (1980) Quantitative electron probe microanalysis on insects exposed to mercury. II Involvement of the lysosomal system in detoxification processes. *Biol Cell* 39:325–334
- Kawahara A, Yoshizuka M, Hirano T, Ohsato K, Fujimoto S (1990) Cadmium toxicity in perinatal rat hepatocytes: electron microscopy, X-ray microanalysis, and morphometric analysis. *Exp Mol Pathol* 53:180–190
- King TP, Bremmer I (1979) Autophagy and apoptosis in liver during the prehaemolytic phase of chronic copper poisoning in sheep. *J Comp Pathol* 89:515–530
- Kitamura S (1966) The *in vitro* cultivation of tissues from mosquitoes. *Kobe J Med Sci* 12:63–70
- Kushida H (1966) Staining of thin sections with lead acetate. *J Electron Microsc* 15:93
- Labarca C, Paigen K (1980) A simple, rapid and sensitive DNA assay procedure. *Anal Biochem* 102:344–352
- Lakowicz JR, Anderson CJ (1980) Permeability of lipid bilayers to methylmercuric chloride: quantification by fluorescence quenching of a carbazole-labeled phospholipid. *Chem Biol Interact* 30:309–323
- Locke M (1969) The ultrastructure of the oenocytes in the molt/intermolt cycle of an insect. *Tissue Cell* 1:103–154
- Marigómez I, Soto M, Kortabitarte M (1996) Tissue-level biomarkers and biological effect of mercury on sentinel slugs, *Arion ater*. *Arch Environ Contam Toxicol* 31:54–62
- McGeoch MA (1998) The selection, testing and application of terrestrial insects as bioindicators. *Biol Rev* 73:181–201
- Miccadei S, Floridi A (1993) Sites of inhibition of mitochondrial electron transport by cadmium. *Chem-Biol Interact* 89:159–167
- Miura K, Suzuki K, Imura N (1978) Effects of methylmercury on mitotic mouse glioma cells. *Environ Res* 17:453–471
- Miura K, Nakada S, Suzuki K, Imura N (1979) Ultrastructural studies on the cytotoxic effects of mercuric chloride on mouse glioma. *Ecotox Environ Safe* 3:352–361
- Miura K, Inokawa M, Imura N (1984) Effects of methylmercury and some metal ions in microtubule networks in mouse glioma cells and *in vitro* tubulin polymerization. *Toxicol Appl Pharm* 73:218–231
- Morselt AFW, Copius Peereboom-Stegeman JHJ, Puvion E, Maarschalkerweerd VJ (1983) Investigation of the mechanism of cadmium toxicity at cellular level. II. An electron microscopical study. *Arch Toxicol* 52:99–108

- Nakada S, Imura N (1982) Uptake of methylmercury and inorganic mercury by mouse glioma and mouse neuroblastoma cells. *Neurotoxicology* 3:249–258
- Nakada S, Inoue K, Nojuma S, Imura N (1978) Change in permeability of liposomes caused by methylmercury and inorganic mercury. *Chem Biol Interact* 22:15–23
- Nieminen AL, Gores GJ, Bond JM, Imberti R, Herman B, Lemasters J (1992) A novel cytotoxicity screening assay using a multiwell fluorescence scanner. *Toxicol Appl Pharm* 115:147–155
- Passow H, Rothstein A (1960) The binding of mercury by the yeast cell in relation to changes in permeability. *J Gen Physiol* 43:621–633
- Pawert M, Triebkorn R, Gräff S, Berkus M, Schulz J, Köhler H-R (1996) Cellular alterations in collembolan midgut cells as a marker of heavy metal exposure: ultrastructure and intracellular metal distribution. *Sci Total Environ* 181:187–200
- Peel D-J, Milner M-J (1992) The response of *Drosophila* imaginal disc cell lines to ecdysteroids. *Roux's Arch Dev Biol* 202:23–35
- Pigman AE, Blanchard J, Laird HE (1997) A study of cadmium transport pathways using the Caco-2 cell model. *Toxicol Appl Pharm* 142:243–247
- Raes H, De Coster W (1991) Storage and detoxication of inorganic and organic mercury in honeybees: histochemical and ultrastructural evidence. *Prog Histochem Cytoc* 23:316–320
- Raes H, Braeckman BP, Criel GRJ, Rzeznik U, Vanfleteren JR (2000) Copper induces apoptosis in *Aedes C6/36* cells. *J Exp Zool* 286:1–12
- Reddy P-S, Bhagyalakshmi A (1994) Changes in oxidative metabolism in selected tissues of the crab (*Scylla serrata*) in response to cadmium toxicity. *Ecotox Environ Safe* 29:255–264
- Repetto G, Sanz P, Repetto M (1993) *In vitro* effects of mercuric chloride and methylmercury chloride on neuroblastoma cells. *Toxicol In vitro* 7:353–357
- Roesijadi G, Unger ME (1993) Cadmium uptake in gills of the mollusc *Crassostrea virginica* and inhibition by calcium channel blockers. *Aquat Toxicol* 24:195–206
- Roy C, Prasad KVS, Reuhl KR, Little JE, Valentine BK, Brown DL (1991) Taxol protects the microtubules of concanavalin A-Activated Lymphocytes from Disassembly by Methylmercury but DNA-synthesis is still inhibited. *Exp Cell Res* 195:345–352
- Sager PR, Doherty RA, Olmsted JB (1983) Interaction of methylmercury with microtubules in cultured cells and *in vitro*. *Exp Cell Res* 146:127–137
- Seidman LA, Bergtrom G, Gingrich DJ, Remsen CC (1986) Accumulation of cadmium by the fourth instar larva of the fly *Chironomus thummi*. *Tissue Cell* 18:395–405
- Singh KRP (1967) Cell cultures derived from larvae of *Aedes albopictus* (Skuse) and *Aedes aegypti* (L.). *Curr Sci India* 19:506–508
- Singhal RK, Anderson ME, Meister A (1987) Glutathione, a first line of defense against cadmium toxicity. *Faseb J* 1:220–223
- Smaghe G, Braeckman BP, Huys N, Raes H (2003) Cultured mosquito cells *Aedes albopictus* C6/36 (Dip., Culicidae) responsive to 20-hydroxyecdysone and non-steroidal ecdysone agonist. *J Appl Entomol* 127:167–173
- Sohi SS, Palli SR, Cook BJ, Retnakaran A (1995) Forest insect cell lines responsive to 20-hydroxyecdysone and two nonsteroidal ecdysone agonists, RH-5849 and RH-5992. *J Insect Physiol* 41:457–464
- Sonoda S, Ashfaq M, Tsumuki H (2007) A comparison of heat shock protein genes from cultured cells of the cabbage armyworm, *Mamestra brassicae*, in response to heavy metals. *Arch Insect Biochem Physiol* 65:210–222
- Souza V, Bucio L, Gutiérrez-Ruiz MC (1997) Cadmium uptake by a human hepatic cell line (WRL-68 cells). *Toxicology* 120:215–220
- Steinberg TH, Newman AS, Swanson JA, Silverstein SC (1987) Macrophages possess probenecid-inhibitable organic anion transporters that remove fluorescent dyes from the cytoplasmic matrix. *J Cell Biol* 105:2695–2702
- Stohs SJ, Bagchi D (1995) Oxidative mechanisms in the toxicity of metal ions. *Free Radic Biol Med* 18:321–336
- Thrasher JD, Adams JF (1972) The effect of four mercury compounds on the generation time and cell division in *Tetrahymena pyriformis*, WH14. *Environ Res* 5:443–450

- Trump BF, Jesudason ML, Jones RT (1978) Ultrastructural features of diseased cells. In: Trump BF, Jones RT (eds) Diagnostic electron microscopy, vol 1. Wiley, New York, pp 1–88
- Veldhuizen-Tsoerkan MB, Holwerda DA, van der Mast CA, Zandee DI (1990) Effects of cadmium exposure and heat shock on protein synthesis in gill tissue of the sea mussel *mytilus edulis* L. Comp Biochem Phys C 96:419–426
- Weinberg JM, Harding PG, Humes HD (1982) Mitochondrial bioenergetics during the initiation of mercuric chloride-induced renal injury. J Biol Chem 257:60–67
- Wigglesworth VB (1977) Structural changes in the epidermal cells of *Rhodnius* during tracheole capture. J Cell Sci 26:161–174
- Wing KD (1988) RH 5849, a nonsteroidal ecdysone agonist: effects on a *Drosophila* cell line. Science 241:467–469
- Woods A, Sherwin T, Sasse R, MacRae TH, Baines AJ, Gull K (1989) Definition of individual components within the cytoskeleton of *Trypanosoma brucei* by a library of monoclonal antibodies. J Cell Sci 93:491–500
- Xia Q, Sun HX, Hu XJ, Shu YH, Gu DX, Zhang GR (2005) Apoptosis of *Spodoptera litura* larval hemocytes induced by heavy metal zinc. Chin Sci Bull 50:2856–2860

Part IV
Genotoxic Effects of Heavy Metals

Chapter 6

Cellular Changes in Mammalian Cells Induced by Cadmium

Gáspár Bánfalvi

Abstract This chapter describes the cellular effects of low concentrations of CdCl₂ (0.5–5 μM) causing biochemical (strand breaks, carcinogenic indicator, DNA replication, DNA repair) and morphological (chromatin) changes in CHO and murine preB cells. Low Cd concentration (0.5–1 μM) interferes with both replicative and repair DNA synthesis. The replicative DNA synthesis is gradually inhibited, but this inhibition is less than the increment of repair DNA synthesis and the overall rate of DNA synthesis in damaged cells will be higher than in normal cells. This hormesis-like effect suggests the induction of an active DNA repair system. A low level of cell cycle-dependent fluctuation of spontaneous strand breaks was observed in control cells, which was 10–40-times higher in S phase upon Cd treatment. The oxidative DNA damage product 8-oxodeoxyguanosine was induced at low (0.5 μM) CdCl₂ concentration. Among the interphase chromatin damages the most characteristic feature was the appearance of holes and disruptions in nuclei which are regarded as typical diagnostic symptoms of cadmium toxicity.

Introduction

Oxydative DNA Damage Caused by Heavy Metals

Ionic heavy metals all contribute to the formation of free radicals, which are atoms or chemical compounds with odd number of electrons in their outer orbital. Cells are constantly exposed to low levels of free radicals in the process known

G. Bánfalvi (✉)

Department of Microbial Biotechnology and Cell Biology, University of Debrecen, 1 Egyetem Square, 4010 Debrecen, Hungary

Tel.: +36-52-512-900

Fax: +36-52-512-925

e-mail: bgaspar@delfin.klte.hu

as aging. Free radicals among them reactive oxygen species (ROS) pick up electrons from other atoms and convert them into secondary free radicals generating a chain reaction causing random biological damages in the cell. The incomplete one-electron oxydation of oxygen generates molecules and ions known as reactive oxygen species (ROS). These intermediates include the singlet oxygen (O_2^-), hydroperoxyl radical ($\bullet HO_2$), hydrogenperoxide (H_2O_2), superoxide ($\bullet O_2^-$), the most dangerous hydroxyl radical ($\bullet OH$), hydroxyl ion (HO^-) and hypochlorite ion (OCl^-). Most of the reactive oxygen species are thought to be generated through the Fenton chemistry and by the Haber-Weiss reaction and are supposed to be the major cause of metal carcinogenesis (Kasprzak 1995 and Chap. 11). According to this view the incidence of cancer increases with age, with an elevated basal metabolic rate and oxidative damage to DNA (Shigenaga et al. 1989; Ames et al. 1993). A corollary of this hypothesis is that heavy-metal-induced oxidative stress can lead to different types of DNA damages as a consequence of multiple steps of incomplete O_2 reduction in cells, ultimately producing water. Common types of oxidative structural changes in DNA involve alterations in nucleotide bases, cross-links, strand breaks, formation of bulky DNA adducts, etc. Low levels DNA damages temporarily suppress DNA replication at checkpoints to avoid mutagenic changes being perpetuated in the genome of the next generation of cells (Hartwell and Weinert 1989; Murray 1992). A comparison of cell cycle profiles of replicative and repair DNA synthesis in cells showed opposite trends. The fluctuating rates of repair synthesis and replication turned out to be inversely correlated (Banfalvi et al. 1997b).

In this chapter the biochemical and morphological damages caused by the heavy metal Cd^{2+} ions are dealt with. Cadmium reduces replicative, and increases repair DNA synthesis during cell cycle. Change in DNA synthesis upon Cd treatment can be expressed as a general toxicity ratio of replication/repair synthesis. Cd induced DNA strand breaks and the carcinogen indicator 8-deoxyguanosine were measured. Cellular DNA tightly packed in the nucleus by histone and non-histon proteins can bind metal ions with high affinity. There is now a general consensus that proteins are the primary targets of heavy metal ions. Notable exceptions are Cr, Ni and Pt which interact directly with DNA. Metal- such as Cd-driven redox reactions are likely to exhaust the cellular antioxidant defense systems, induce the inhibition of major antioxidant enzymes and will increase the level of endogenous oxidants toxic to DNA (Kasprzak 1996; Myers et al. 2008). Nuclear damages caused by metal binding and redox reactions, affecting DNA repair and gene expression regulator proteins, may be involved in carcinogenesis through epigenetic mechanisms (see Kasprzak in Chap. 11). Heavy metal binding to nuclear proteins will affect the chromatin structure in each step of the condensation process. This chapter visualizes morphological chromatin changes in a cell-cycle-dependent manner. Characteristic chromatotoxic morphological changes induced by Cd were visible at the end of S phase, in G and M phases manifested as large holes and disruptions in the nuclear membrane.

Methods

Chemicals

The isotopes [3H]-thymidine 5'-triphosphate (3.03 TBq mmol⁻¹) and [3H]-thymidine (2.86 TBq/mmol) were purchased from ICN Isotope and Nuclear Division (Irvine, CA). Nucleotides, propidium iodide and diazobicyclo-(2,2,2)-octane were from Sigma-Aldrich Chemie GmbH (Munich, Germany). The 2,6-diamino-2-phenylindole (DAPI) was the product of Braunschweig Chemie (Braunschweig, Germany). Dextran T-150 was purchased from Pharmacia-Biochemicals (Gaithersburg, MD). Growth media and sera were obtained from Invitrogen (Carlsbad, CA).

Solutions

Antifade medium consisted of 90% glycerol, 2% (w/w) 1,4-diazobicyclo-(2,2,2)-octane, 20 mM Tris-Cl (pH 8.0), 0.02% sodium azide, and 25 ng/ml DAPI for blue fluorescent total staining of DNA or of 0.2 µg/ml propidium iodide for red DNA staining.

Isotonic buffer for DNA synthesis contained 140 mM sucrose, 60 mM potassium chloride (KCl), 10 mM HEPES (pH 7.4), 5 mM KPO₄ buffer (K₂HPO₄ and KH₂PO₄), 5 mM magnesium chloride (MgCl₂), and 0.5 mM calcium chloride.

Hypotonic buffer for reversible permeabilization contained 9 mM HEPES (pH 7.8), 5.8 mM dithiothreitol, 4.5% dextran T-150, 1 mM EGTA, and 4.5 mM MgCl₂. Swelling buffer consisted of 50 mM KCl, 10 mM magnesium sulfate, 3 mM dithiothreitol, and 5 mM sodium phosphate (Na₂HPO₄/NaH₂PO₄) buffer, pH 8.0.

Swelling Buffer consisted of 50 mM KCl, 10 mM MgSO₄, 3 mM dithiothreitol and 5 mM NaPO₄, pH 8.0.

Cell Growth

The epithelial-like Chinese hamster ovary cells (CHO-K1, ATCC, Rockville, MD, #CCL61) were grown in F-12 Ham's medium supplemented with 10% heat-inactivated bovine serum (Gacsi et al. 2005).

Human K562 cells were cultured in RPMI-1640 medium supplemented with 10% fetal bovine serum (FBS). The continuous cell line K-562 was established from the pleural effusion of a 53-year-old female with chronic myelogenous leukemia in terminal blast crises (Lozzio and Lozzio 1975).

The murine pre-B-cell line 70Z/3-M8 (Offer et al. 2001) was grown in suspension culture at 37°C in RPMI 1640 medium supplemented with 10% fetal bovine serum, 2 µg/ml mycophenolic acid, 150 µg/ml xanthine, and 15 µg/ml hypoxanthine

and 2×10^{-5} M β -mercaptoethanol. The cell line 70Z/3-M8 is a stable clone derived by transfection of pSVLMP53, a p53 mutant cDNA with an alternatively spliced C-terminus, and drug resistant *gpt* gene (Offer et al. 2001). The typical chromosome number (modal number) in murine pre-B-cell line is twenty.

HaCaT cells are human skin cells (keratinocytes) that have been transformed (mutated) to be immortal with an unlimited growth potential, but unlike other immortal cell lines they are not tumorigenic. The HaCaT cell line mimics many of the properties of normal epidermal keratinocytes and can differentiate under appropriate experimental conditions (Boukamp et al. 1988).

Heavy Metal Treatment

Cells were treated with various concentrations of heavy metals after they have been recultured for 9 h. Cells were grown for an additional 15 h in the presence of the heavy metal before being harvested.

Cell Cycle Synchronization

Suspension cultures of cells were grown for 24 h to a final concentration of $2\text{--}4 \times 10^5$ cells/ml and fractionated by counterflow centrifugal elutriation. Cells were harvested by centrifugation at 600 g for 5 min at 5°C and resuspended in medium containing 1% fetal bovine serum. Large particles originating from medium and from cell aggregates were removed by passing the cell suspension through a 100 mesh stainless-steel sieve. Synchronized cell fractions were obtained by counter-streaming centrifugation performed (Banfalvi 2008). Elutriation was performed at a temperature of 20°C and cells were eluted in F12 medium containing 1% fetal bovine serum. The fraction collected during loading was discarded. This fraction contained unloaded and dead cells. Fractions (100 ml each) were collected at increasing flow rates. Cells were separated at lower resolution into eight, or at higher resolution into 12 or 16 elutriation fractions. Each fraction was routinely monitored by light microscopy. Fractions contained single cells, which increased in size with each fraction elutriated. Cells were counted with a Coulter Counter and the increase in cell size was monitored by a Coulter Channelizer. Cell number was also assessed in a Burkert chamber, and viability (>98%) was determined by trypan blue dye exclusion on each elutriated fraction.

Flow Cytometry

The quality of cell synchronization was analyzed by flow cytometry after staining of cells with 50 μ g/ml propidium iodide in 0.1 M ammonium citrate for 15 min at

0°C, followed by the addition of an equal volume of 70% ethanol at 0°C. The cells were analyzed by a FACScan flow cytometer (Becton Dickinson) using the Cell-Quest (Becton Dickinson) software as described (Offer et al. 2001).

Reversible Permeabilization of Cells

This method enables the cell membrane to be permeabilized and resealed while maintaining viability during the cell cycle. The method was originally developed for the reversible permeabilization of murine lymphocytes (Banfalvi et al. 1984), and adapted to other mammalian cells. Briefly, 1 ml of Hypotonic Buffer was added to 5×10^7 cells in the presence of Dextran T-150 as a molecular coat to prevent cells from disruption. Permeabilization lasted for 2 min at 0°C. For reversal of permeabilization, the hypotonic solution was diluted with 20 ml growth medium containing 10% fetal bovine serum. Cells were sealed after permeabilization by incubation in a CO₂ incubator at 37°C and 5% CO₂ for 3 h to avoid their stickiness, but allowing them to open any time during the cell cycle.

DNA Synthesis in Reversibly Permeabilized Cells

The measurement of DNA synthesis is based on the fact that intact cells are able to incorporate thymidine, but permeable cells cannot utilize them only deoxyribonucleoside triphosphates (dNTPs). ATP dependent replicative and ATP-independent repair DNA synthesis were measured in permeable cells as described (Banfalvi et al. 1997b; Ujvarosi et al. 2007). The efficiency of reversal of permeabilization was tested by [³H]-thymidine incorporation. After reversal of permeabilization the recovery of 5×10^5 cells was measured by incubation in the presence of 37 kBq [³H]-thymidine at 37°C for 30 min.

The reaction of DNA synthesis was terminated by the addition of an equal volume of 1 M perchloric acid. After centrifugation the precipitate was washed three times with cold 0.5 M perchloric acid. The precipitate was hydrolyzed in 0.5 M perchloric acid at 90°C for 30 min and the radioactivity was determined.

DNA Isolation

High-molecular-mass DNA was isolated by the standard protocol of Ausubel et al. (1994) from 10⁶ cells of each elutriated fraction. The amount of DNA was determined with a DyNA Quant fluorimeter (Hofer) using Hoechst 33258 dye, which binds to the minor groove of double-stranded DNA. This bound dye was excited with long-UV light at 365 nm and its fluorescence was measured in triplicate samples at 458 nm, with calf thymus DNA serving as DNA standard.

Random Oligonucleotide-Primed Synthesis (ROPS) Assay

In healthy, untreated cells most of the 3'-OH pre-existing breaks in DNA come from Okazaki fragments during DNA replication. Further DNA strand breaks are generated during isolation of DNA and caused by DNA damage. The 3'-OH moieties were labeled by the random primed oligonucleotide synthesis as described earlier (Banfalvi et al. 2000).

Analysis of 8-hydroxy-2'-deoxyguanosine

Purified DNA was digested to nucleotides with nuclease P1 and alkaline phosphatase, and 8-hydroxy-2'-deoxyguanosine (8-OHdG) was analyzed as previously described (Mikhailova et al. 1997; Banfalvi et al. 2000). The level of 8-OHdG was expressed per 10^5 dG.

Isolation of Nuclei

After reversal of permeabilization cells were washed with phosphate buffered saline (PBS) and incubated at 37°C for 10 min in Swelling Buffer, followed by centrifugation at 500 g for 5 min. Nuclear structures were isolated by the slow addition of 20 volumes of the standard Clarks's Fixative (methanol:glacial acetic acid, 3:1). Nuclei were then centrifuged at 500 g for 5 min, washed twice in Fixative and resuspended in 1 ml of Fixative. The Clark's fixative keeps cells in a "swollen" state, achieved after hypotonic treatment. The fixative solution elutes some of the membrane lipids and proteins and makes the membrane more fragile and suitable for spreading flat on the slide when subjected to the drying techniques (Henegariu et al. 2001). Cellular and nuclear volumes and nuclear diameter were determined with Multisizers.

Spreads of Nuclear Structures

Preparation of nuclei for spreads of chromatin structures used the method developed for metaphase chromosomes. Nuclei in Fixative stored at 4°C for 1–7 days were spread over glass slides dropwise from a height of approximately 30 cm. Dropping helps to distribute nuclei evenly on the slide surface (Henegariu et al. 2001). Slides were air dried, stored at room temperature overnight, rinsed with PBS and dehydrated using increasing concentrations of ethanol (70, 90, 95 and 100%).

Visualization of Chromatin Structures

Experiments employed the DNA fluorochrome DAPI for fluorescent staining. Different shades of the blue colour of DAPI fluorescence indicate the degree of chromatin compactness. Regarding chromatin staining, it is important to mention that

DAPI binds specifically to A–T rich sequences in the minor groove of DNA (Parolin et al. 1995).

Dehydrated slides containing chromatin structures were mounted in 35 μ l Anti-fade Medium under 24 \times 50 mm coverslips. Blue fluorescence of DAPI was monitored with Olympus AX70 fluorescence microscope or Axioplan Universal microscope (Carl Zeiss, Oberkochen, Germany), equipped with HBO 50 microscope illuminator, MC 100 spot camera, Sonny 3CCD Video Camera (DXC-930 P), Sonny camera adapter and Sonny Trinitron Color Video Monitor. Magnification of ocular (10 \times) and immersion object (100 \times) lenses was 1000 \times . The refractive indexes of condenser and objective lenses were 1.515. Homogeneous path for light was obtained by filling the air gaps with Cargille immersion oil (n_D^{25} :1.515) (Cargille-Sacher Inc., Cedar Grow, NJ).

Results

Cellular Effects of Cadmium

Effect of Cd on Replicative and Repair Synthesis

The change in the rate of replicative and repair synthesis was followed throughout the S phase in synchronized populations of cells before and after 0.5 μ m CdCl₂ treatment. Synchrony of fractions was confirmed by the simultaneous measurement of cell size in a Coulter Channelizer, by flow cytometry and by the determination of DNA content in each fraction. The flow cytometric profiles in fractions of untreated and Cd-treated cells are shown in Fig. 6.1a, b. A comparison of the cell number in control and in Cd-treated cells shows that 0.5 μ m CdCl₂ prevents cell cycle progression, cell growth lagging behind the control by more than 60%. Cd treatment shifted the growth profile of CHO cells towards larger cell size (Fig. 6.1c, d). The increase in cell size was also visible under the microscope.

In elutriated fractions, similar to the situation in unseparated cells, the overall rate of DNA replication was decreased by more than 70% in Cd-treated cells, with some of the smaller peaks almost invisible (Fig. 6.1e, f). Elutriation resolved five replicative and five repair peaks. Compared with the replication profile, an inverse correlation was observed for repair synthesis. Cd treatment increased the rate of repair synthesis. The overall rate of repair synthesis was three times higher in cells after Cd treatment (Fig. 6.1g, h).

DNA Strand Breaks and Oxidative DNA Damage Generated by Cd

The level of spontaneous strand breaks indicates the number of free ends in control cells, which is regarded as a reflection of short replication intermediates in the oligonucleotide size range such as early replication intermediates, elongated

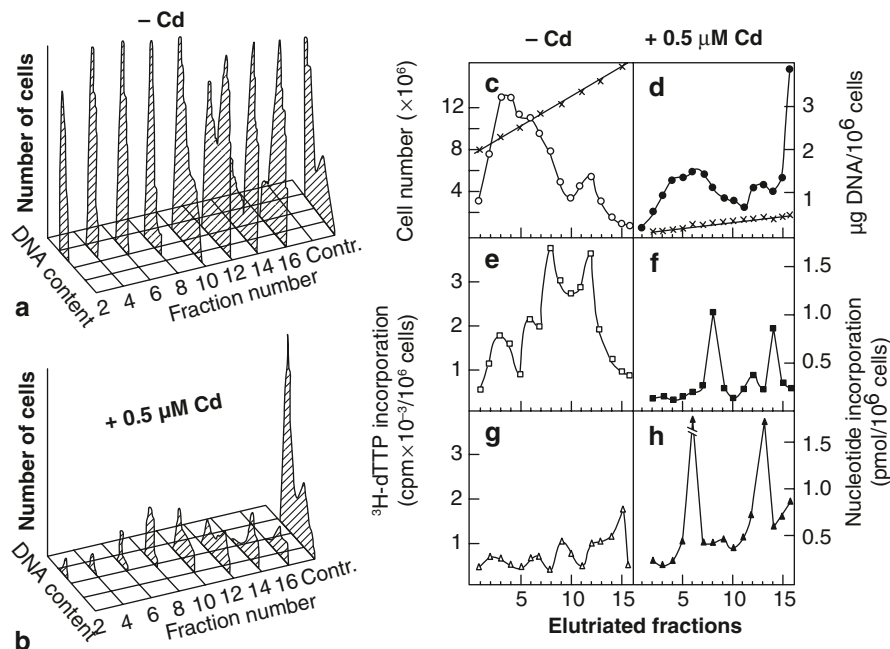


Fig. 6.1 The elutriation profiles after cadmium treatment showing the viability of CHO cells, the DNA content, the replicative and repair DNA synthesis. Cells were treated with $0.5 \mu\text{M CdCl}_2$ at $4 \times 10^5/\text{ml}$ density and subjected to elutriation as described in the Methods. **a** Control cells, **b** Cd-treated cells. The same experiment was carried out showing **c** Cell number in elutriated fractions of control cells (o-o) and DNA content (x-x). **d** Cell number in Cd-treated cells (●-●) and DNA content (x-x). **e** Replicative DNA synthesis in control cells (□-□). **f** DNA replication in Cd treated cells (■-■). **g** Repair DNA synthesis in control cells (Δ-Δ), and **h** repair synthesis in Cd-treated cells (▲-▲). (Redrawn by permission Bánfalvi et al. 2000)

intermediates of intermediate size such as Okazaki fragments, and the accumulation of long fragments at the end of S phase. After Cd treatment, the number of strand breaks was increased by more than an order of magnitude, 10–40 times greater than control throughout the cell cycle (Fig. 6.2).

The presence of the oxidative DNA damage product, 8-OHdG, was followed in elutriated fractions. 8-OHdG levels were low in controls and 30–60 times higher in cells treated with $0.5 \mu\text{M CdCl}_2$. There was only a relatively small reduction in the 8-OHdG content in early S phase, and a gradual decrease to 50% was observed from the middle to the end of S phase (Fig. 6.2).

Chromatin Changes Induced by Cd

Intermediates of chromatin condensation during the cell cycle of untreated cells are shown in Fig. 6.3. Cadmium induced apoptotic changes have been visualized in a

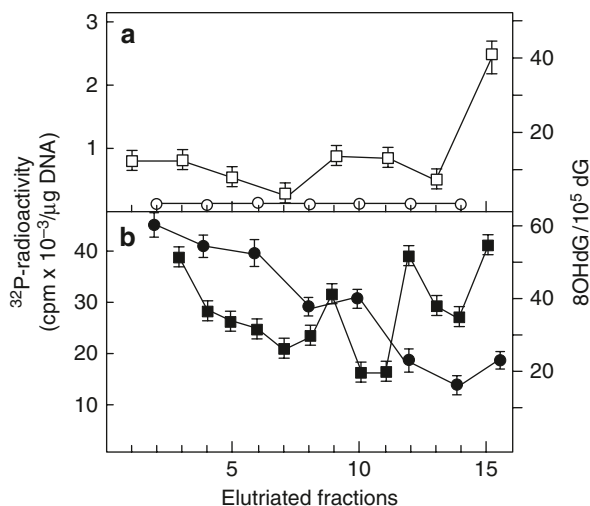


Fig. 6.2 DNA fragmentation and level of carcinogenic indicator upon cadmium treatment of CHO cells. Elutriation was carried out as in Fig. 6.1. **a** DNA fragmentation in control cells (\square – \square), 8-oxo-2'-deoxyguanosine content relative to 10^5 deoxyguanosine (8OHdG/ 10^5 dG) in control cells (\circ – \circ). **b** DNA fragmentation after $0.5 \mu\text{M CdCl}_2$ treatment (\blacksquare – \blacksquare), 8OHdG/ 10^5 dG content (\bullet – \bullet). Electrochemical detection of the intrinsic mutagenic indicator 8OHdG was by HPLC. (Redrawn by permission Banfalvi et al. 2000)

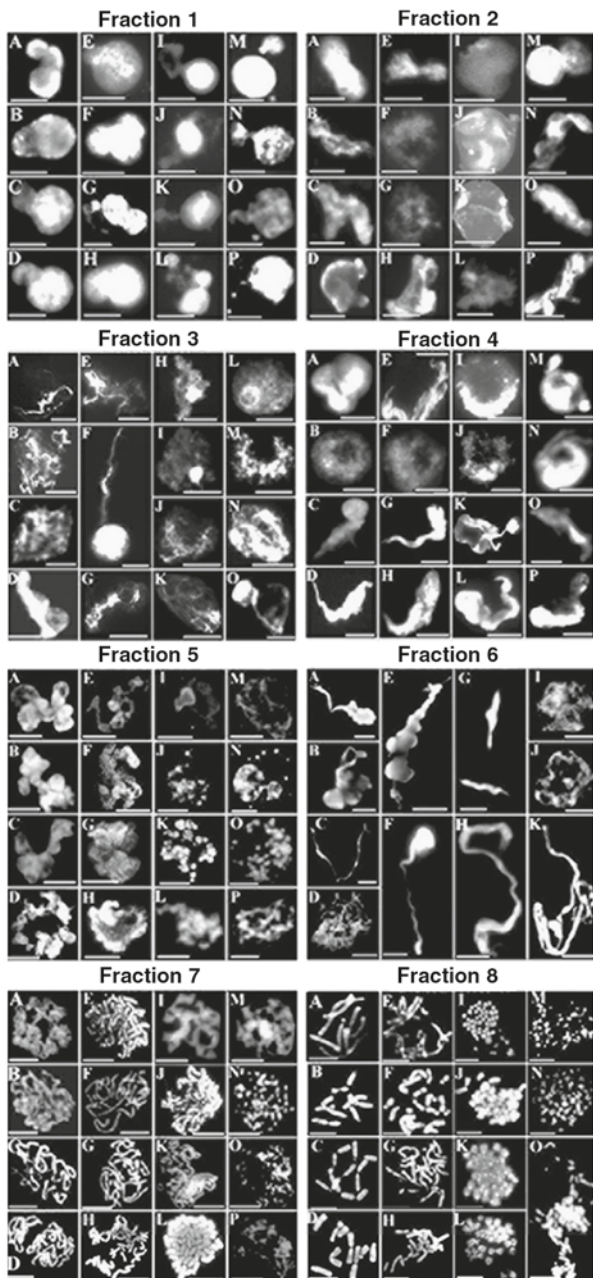
cell cycle-dependent manner. Among these structures the absence of decondensed veil-like structures, and premature chromatin condensation as apoptotic bodies, the absence of fibrous structures, the lack of supercoiled chromatin in mid-S phase were observed and visualized (Banfalvi et al. 2005).

Here only the Cd induced rejection of some of the chromatin bodies, intranuclear inclusions and the formation of clusters of large sized perichromatin granules are shown in elutriation fraction 7 (late S phase) (Fig. 6.4, left panels). Most severe losses and disruptions of the nuclear membrane were observed in elutriation fraction 8 (late S, G2, M) (Fig. 6.4, right panels). The disruption of the nuclear membrane did not lead to distinguishable intermediates, rather it obscured the picture (Fig. 6.4a–e, right panels) resulting in large nuclei with big holes and sticky elongated and condensed chromosomal forms (Fig. 6.4f, right panels).

Growth Inhibition by Cd in Murine PreB Cells

To determine which stage of the cell cycle is most vulnerable to heavy metal treatment two concentrations of cadmium (1 and $5 \mu\text{M}$) have been chosen. Cell cultures of 1.2×10^5 cells/ml were grown in the absence and in the presence of 1 and $5 \mu\text{M CdCl}_2$. Significantly higher inhibitory effect of cadmium on cell growth was measured in mid-S phase (Table 6.1). An overall 38 and 66% cell growth inhibition

Fig. 6.3 Intermediates of chromatin condensation during the cell cycle. Indian muntjac (IM), Chinese hamster ovary (CHO), murine preB (preB) and human erytroleukemia (K562) cells at different stages of the cell cycle were obtained by centrifugal elutriation. Eight fractions were collected. Nuclei from each fraction were isolated stained with DAPI and visualized by fluorescent microscopy. Typical images were selected to illustrate the temporal order of condensation of interphase chromatin in nuclei of IM (a–d), CHO (e–h), preB (i–l) and K562 (m–p) cells. Bar, 5 μ M each. (With permission of Bánfalvi et al. 2006)



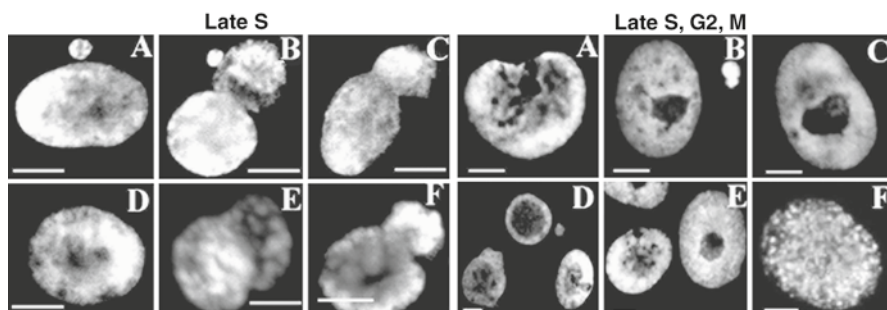


Fig. 6.4 Cadmium induced chromatin changes in late S, G2 and M phases. CHO cells were treated with Cd, synchronized and 8 fractions were collected. Chromatin structures were isolated as described in the Methods. Chromatin structures in elutriation fraction 7 (late S) with expelled chromatin bodies (a, b), elongated nuclei with disrupted membranes (b, c), intra-nuclear inclusions (a, d–f), large-sized perichromatin granules (e, f). Elutriation fraction 8 (late S, G2, M): disrupted nuclear membrane with large holes (A–E), sticky, elongated chromosomal forms (F). Bars 5 μm each. (Reproduced with the permission of Banfalvi et al. 2005)

was registered after treatment with 1 and 5 μM CdCl₂, respectively. Most dramatic reduction in cell number occurred in elutriation fraction 6, corresponding to mid S phase. In this subpopulation (fraction 6) also significant changes in chromatin structure were observed.

Chromatin Changes Induced by Cd in Murine PreB Cells

Interphase chromatin structures in murine control pre-B-cells have been described in Fig. 6.3 (I–L panels of each fraction) at lower resolution of centrifugal elutriation by collecting eight fractions (Banfalvi et al. 2006). When higher resolution was used (13 fractions collected) the same chromatin structures were visualized after DAPI staining. These structures included veil-like nuclear material with some polarization of the chromatin in early S phase, fibrous structures in early mid S phase, chromatin bodies in mid S phase, chromatin ribbon later in mid S phase, precondensed chromosomes in late S, G2 and M phases corresponding to those seen in Fig. 6.3. The flow cytometric profiles of elutriated fractions show that after Cd treatment the virtual DNA content is significantly increased in mid and late S phases (Fig. 6.5).

The chromatin changes seen in murine preB cells also correspond to those seen in CHO cells after Cd treatment. Most typical changes of cadmium treatment are the severe disruptions of the nuclear membrane observed from the mid S phase (Fig. 6.6, elutriation fractions 6–8) till the end of S phase, in G2 and M phases (Fig. 6.6, fractions 10–12, late S). These disruptions did not allow to distinguish among the final stages of chromatin condensation, resulting in nuclei with big holes inside them and sticky imperfectly condensed chromosomes (Fig. 6.6, fraction 12, panel D)

Table 6.1 Elutriation of control and Cd treated murine preB cells. (Reproduced with the permission of Bánfalvi et al. 2007)

Fraction number	Cell cycle phase	Elutriated		1 μM CdCl ₂		5 μM dCl ₃	
		Control $\times 10^6$ cells	%	$\times 10^6$ cells	%	$\times 10^6$ cells	%
1	Discarded	5.5	2.54	5.1	2.36	2.2	1.01
2	Early S	6	2.78	12.5	5.78	5.2	2.41
3	Early S	36	16.67	22	10.19	20.3	9.39
4	Early mid S	36.5	16.90	30.3	14.02	11.8	5.46
5	Early mid S	30	13.68	17.5	8.10	7.5	3.47
6	Mid S	28	12.96	13.5	6.25	5.2	2.41
7	Mid S	18	8.33	12	5.56	4.8	2.22
8	Late mid S	16	7.41	12.5	5.78	4.8	2.22
9	Late mid S	14	6.48	11	5.09	4.0	1.85
10	Late S	12	5.56	10.5	4.86	3.8	1.76
11	Late S, G2, M	5	2.31	7.5	3.47	2.4	1.11
12	Late S, G2, M	8	3.70	6	2.78	2.0	0.93
13	Late S, G2, M	1	0.46	0.5	0.23	0.2	0.09
Elutriated total:		216 $\times 10^6$	100%	160.9 $\times 10^6$	61.9%	74.2 $\times 10^6$	34.4%

Loaded control population (2.16×10^8) was taken as 100%

Percentage of cell number in each fraction is expressed as % of the total population

Control cells subjected to elutriation: 2.2×10^8

Loss during manipulation: 4×10^6 (1.8%)

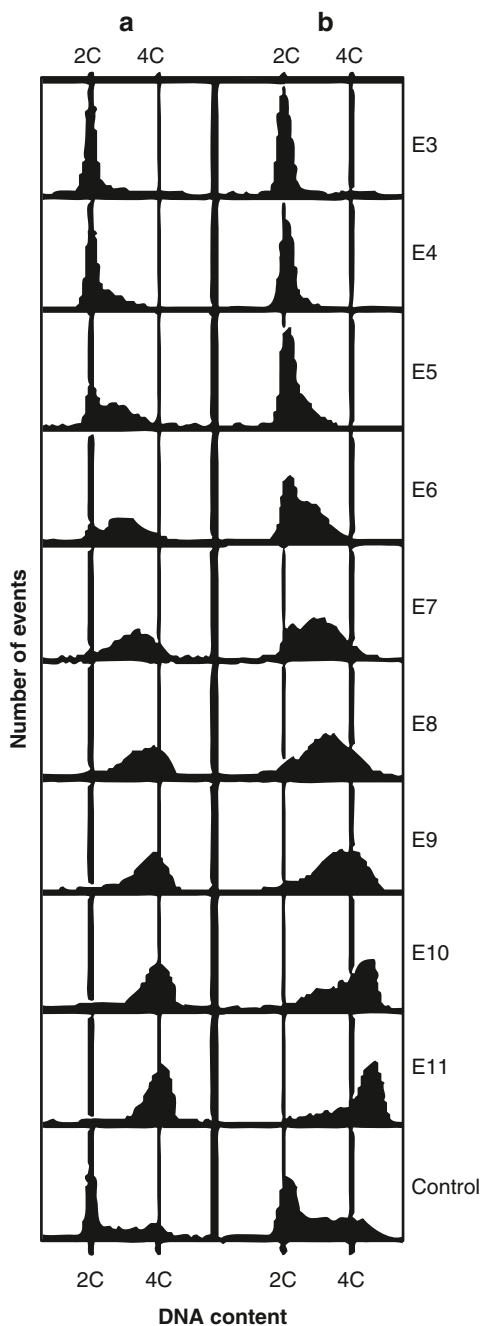
Cadmium treated cells (1 μM) subjected to elutriation: 1.7×10^8

Loss of Cd treated (1 μM) cells during manipulation: 9.1×10^6 (5.4%)

Cadmium treated cells (5 μM) used for elutriation: 8×10^7

Loss of Cd treated (5 μM) cells during manipulation: 5.8×10^6 (7.3%)

Fig. 6.5 Flow cytometry of elutriation elutriated murine preB cells before (a) and after (b) 1 μ M CdCl₂ treatment. The DNA content of each elutriation fraction is indicated as haploid genome content (C-value) on the abscissa and cell number is given on the ordinate. Controls are representing unelutriated cells before and after cadmium treatment. (Reproduced with permission of Banfalvi et al. 2007)



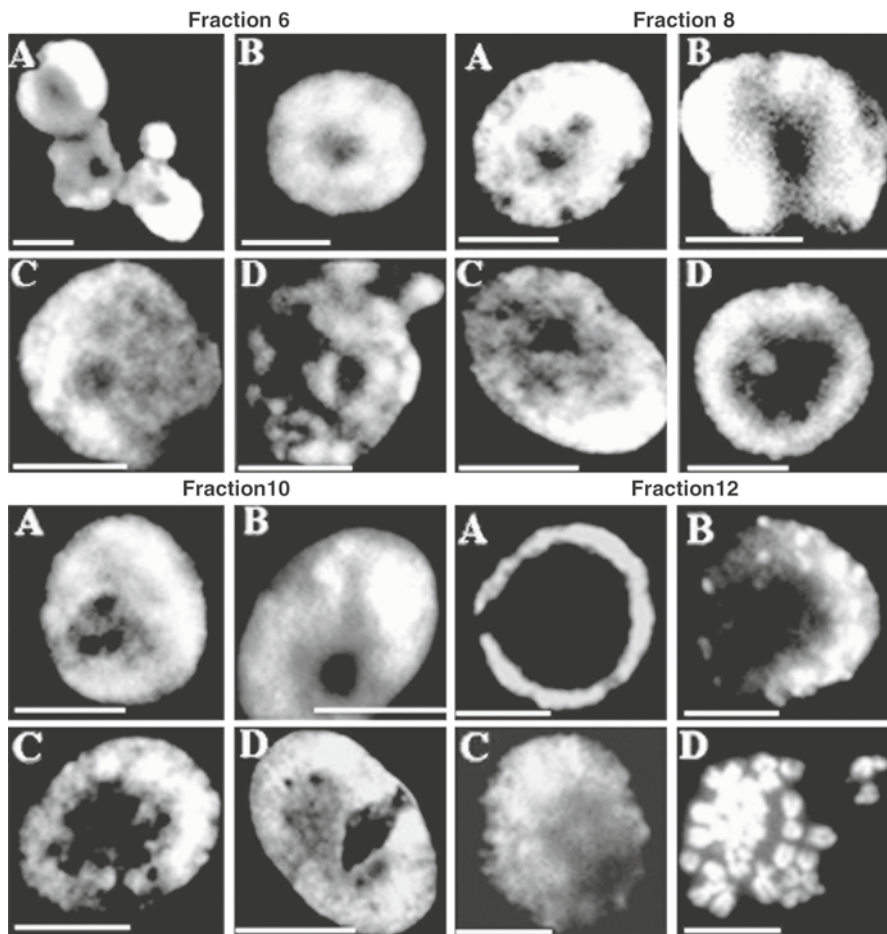


Fig. 6.6 Cadmium induced chromatin changes in mid S phase (Elutriation Fraction 6–8) and at the end of S phase nuclei of murine preB cells (Elutriation Fraction 10–12). Cells were treated and chromatin structures were isolated as described in the Methods. Fraction 6–8: large-sized perinuclear granules and holes in the middle of the nucleus (a–d). Elutriation fraction 10: disrupted nuclear membrane with large holes (a–d). Elutriation fraction 12: linear arrangement of condensing chromosomes (a–c), sticky precondensed chromosomes. (d) Bars 5 μm each. (With permission of Bánfalvi et al. 2007)

Discussion

DNA damage caused by heavy metals (Cd, Zn, Hg, Ni, Zn) can be traced back to oxidative DNA damage, the main products of which are 4,6-diamino-4-hydroxy-5-formamidopyrimidine and 8-oxo-2'-deoxyguanosine (8OHdG) (Breimer 1990). Here only the toxic cellular effects exerted by Cd are discussed. Flow cytometry revealed increased cellular and nuclear sizes after Cd treatment. We have measured

a 30–60-fold increase of the carcinogenic indicator 8OHdG and a 20–40-fold increase in strand breaks after 0.5 μM CdCl_2 treatment. The level of carcinogenic indicator after this Cd treatment was highest in G1 and early S phase and showed a gradual decline towards the end of S phase. To the contrary the profile of DNA fragmentation showed fluctuation during S phase, indicating that various subphases of the cell cycle have different susceptibility to Cd induced DNA strand breakage.

The natural oscillation of replicative and repair DNA synthesis during S phase in control cells is related to the existence of several replication and repair subphases which do not coincide, but follow each other in a sinusoid-alike pattern (Banfalvi et al. 1997a). Cd treatment affected both replicative and repair DNA synthesis. DNA replication was suppressed and in contrast repair synthesis increased. The maximum and minimum values of these S-phase checkpoints varied in agreement with the notion that different types of DNA damages affect different S subphase replication and repair checkpoints. The most characteristic effect of Cd was observed at the level of chromatin condensation seen as large extensive disruptions and holes in the nuclear membrane and sticky incompletely folded chromosomes both in CHO and in murine pre B cells. The fact that we have seen the same transitory forms of chromatin condensation in different mammalian cells (Banfalvi et al. 2006) and that genotoxic changes generated by Cd were similar in CHO and murine preB cells point to: (a) a general mechanism of chromatin condensation at least in mammalian cells and (b) due to the common mechanism of condensation, the same genotoxic agent will exert the same toxic effect. These observations indicate that typical chromatin damages could be distinguished and categorized based on the assesment of injury-specific chromatin changes. The next chapters will focus primarily on genotoxic chromatin changes evoked by other heavy metals such as Ni, Cr, Ag.

References

- Ames BN, Shigenaga MK, Hagen TM (1993) Oxidants, antioxidants and degenerative diseases of aging. *Proc Natl Acad Sci U S A* 90:7915–7922
- Ausubel FM, Brent R, Kingston RE, Moore DD, Seidman JG, Smith JA, Struhl K (eds) (1994) *Current protocols in molecular biology*. v. 2nd edn. Greene Publishing Association, John Wiley and Sons, New York
- Banfalvi G (2008) Cell cycle synchronization of animal cells and nuclei by centrifugal elutriation. *Nature Protocols* 3:663–673
- Banfalvi G, Sooki-Toth A, Sarkar N, Csuzi S, Antoni F (1984) Nascent DNA chains synthesized in recersibly permeable cells of mouse thymocytes. *Eur J Biochem* 139:553–559
- Banfalvi G, Mikhailova M, Poirier LA, Chou MW (1997a) Multiple subphases of DNA replication in CHO cells. *DNA Cell Biol* 16:1493–1498
- Banfalvi G, Poirier LA, Mikhailova M, Chou MW (1997b) Realtionship of repair and replicative DNA synthesis to cell cycle in Chinese hamster ovary (CHO-K1) cells. *DNA Cell Biol* 16:1155–1160
- Banfalvi G, Littlefield N, Hass B, Mikhailova M, Csuka I, Szepessy E, Chou WM (2000) Effect of cadmium on the relationship between replicative and repair DNA synthesis in synchronized CHO cells. *Eur J Biochem* 267:6580–6585

- Bánfalvi G, Gacsi M, Nagy G, Kiss BZ, Basnakian AG (2005) Cadmium induced apoptotic changes in chromatin structure and subphases of nuclear growth during the cell cycle in CHO cells. *Apoptosis* 10:631–642
- Bánfalvi G, Nagy G, Gacsi M, Roszser T, Basnakian AG (2006) Common pathway of chromosome condensation in mammalian cells. *DNA Cell Biol* 25:295–301
- Bánfalvi G, Ujvarosi K, Trencsenyi G, Somogyi C, Nagy G, Basnakian AG (2007) Cell culture density dependent toxicity and chromatin changes upon cadmium treatment in murine pre-B cells. *Apoptosis* 12:1219–1228
- Boukamp P, Petrussevska RT, Breitkreut D, Hornung J, Markham A, Fusenig NE (1988) Normal keratinization in a spontaneously immortalized aneuploid human keratinocyte line. *J Cell Biol* 106:761–771
- Breimer LH (1990) Molecular mechanisms of oxygen radical carcinogenesis and mutagenesis: the role of DNA base damage. *Mol Carcinogen* 3:188–197
- Gacsi M, Nagy G, Pinter G, Basnakian AG, Bánfalvi G (2005) Condensation of interphase chromatin in nuclei of Chinese hamster ovary (CHO-K1) cells. *DNA Cell Biol* 24:43–53
- Hartwell LH, Weinert TA (1989) Checkpoints: controls that ensure the order of cell cycle events. *Science* 246:629–634
- Henegariu O, Heerema NA, Lowe Wright L, Bray-Ward P, Ward DC, Vance GH (2001) Improvements in cytogenetic slide preparation: controlled chromosome spreading, chemical aging and gradual denaturing. *Cytometry* 43:101–109
- Kasprzak KS (1995) Possible role of oxidative damage in metal-induced carcinogenesis. *Cancer Invest* 13:411–430
- Kasprzak KS (1996) Oxidative DNA damage in metal-induced carcinogenesis. In: Chang LW (ed) *Toxicology of Metals*. CRC Lewis Publishers, Boca Raton
- Lozzio CB, Lozzio BB (1975) Human chronic myelogenous leukemia cell-line with positive Philadelphia chromosome. *Blood* 45:321–334
- Mikhailova MV, Littlefield NA, Hass B, Poirier LA, Chou MW (1997) Cadmium induced 8-hydroxydeoxyguanosine formation, DNA strand breaks and antioxidant activities in lymphoblastoid cells. *Cancer Lett* 115:141–148
- Murray AW (1992) Creative blocks: cell-cycle checkpoints and feedback controls. *Nature (London)* 359:599–604
- Myers JM, Antholine WE, Myers CR (2008) Hexavalent chromium causes the oxidation of thioredoxin in human bronchial epithelial cells. *Toxicology* 246:222–233
- Offer H, Zurer I, Bánfalvi G, Rehak M, Falcovitz A, Milyavsky M, Goldfinger N, Rotter V (2001) p53 modulates base excision activity in a cell cycle-specific manner after genotoxic stress. *Cancer Res* 61:88–96
- Parolin C, Zanotti G, Palu G (1995) A model for the sequence-dependent DNA binding of 40,6-diamidino-2-phenylindole (DAPI). *Biochem Biophys Commun* 208:332–338
- Shigenaga MK, Gimeno CJ, Ames BC (1989) Urinary 8-hydroxy-20-deoxyguanosine as a biological marker of *in vivo* oxidative DNA damage. *Proc Natl Acad Sci U S A* 86:9697–9701
- Ujvarosi K, Hunyadi J, Nagy G, Pocsi I, Bánfalvi G (2007) Preapoptotic chromatin changes induced by ultraviolet B irradiation in human erythroleukemia K562 cells. *Apoptosis* 12:2089–2099

Chapter 7

Chromatin Toxicity of Ni(II) Ions in K562 Erythroleukemia Cells

Gábor Nagy, Diána Laza, Kinga Ujvárosi and Gáspár Bánfalvi

Abstract Utilizing time-lapse video microscopy, the chapter describes the effect of Ni(II) on chromatin changes and survival of K562 cells. Differential effects on chromatin organization are reported relative to dose and duration of Ni(II) incubation, with gradation of apoptotic to necrotic changes manifested as the dosage increases. Ni(II) generated cytotoxic effects in K562 cells at low concentration with an estimated IC₅₀ value of 2 μM . Chromatotoxicity was also visualized by time-lapse video microscopy designed to follow the motility of single cells under physiological and genotoxic conditions. Ni-treated cells moved faster than control cells, but this motion was less intense than the so called “apoptotic dance” preceding cell death observed after the Pb-treatment of HaCaT cells. Low (0.2–0.5 μM) concentrations of Ni(II) caused the polarization and the rejection of apoptotic bodies. In addition 1 μM NiCl₂ generated larger apoptotic chromatin circles. At 5 μM NiCl₂ the slight expansion of nuclei and the continuous chromatin ribbon became visible. At 10 μM Ni(II) most of the nuclear material condensed prematurely, the rest remained in highly decondensed fibrillary stage. Necrotic changes took place at ≥ 50 μM NiCl₂ with less fibrillary chromatin, with moderately increased and round shaped nuclei.

Introduction

By the chemical definition of Chap. 1 the density of heavy metals exceeds 3 g/cm³. From biological point of view heavy metal microelements can be divided to essential (Co, Cr, Cu, Ni, Zn) and toxic (Ag, Cd, Hg, Pb) heavy metals. Although, nickel is among the essential heavy metals, its function in the human body has not been clarified. The healthy human body contains 5–8 g nickel that is thought to be

G. Bánfalvi (✉)

Department of Microbial Biotechnology and Cell Biology, University of Debrecen, 1 Egyetem Square, 4010 Debrecen, Hungary

Tel. +36-52-512-900

Fax: +36-52-512-925

e-mail: bgaspar@delfin.klte.hu

involved primarily in the regulation of liver function. Nickel seems to be involved in the activation and inhibition of enzymes, but so far no enzymes containing nickel have been found. Further benefits of nickel are related to normal growth, skin and bone structure, iron absorption and metabolism and red blood cell production. Ni is also required for the metabolism of glucose, lipids, hormones and cell membrane.

Increasing concentrations of heavy metals including nickel are likely to generate cytotoxic, genotoxic effects. Environmental pollution and human exposure to nickel occurs in natural and human activities. Electroplating process is a typical source of metal pollution induced by human activity. Workers exposed to nickel contact and inhalation of nickel fumes during nickel-plating process had a consistent effect on hepatic inflammatory function (Babu et al. 2006). Exposure to nickel compounds in occupationally exposed workers has been clearly associated with increased incidence of respiratory cancers. Nickel compounds are also potent inducers of tumors in experimental animals (Sunderman 1982).

Considerable evidence has been accumulated that nickel ions bind to and damage DNA. Administration of nickel ions *i.p.* to rats induced single-strand breaks, DNA-DNA and DNA-protein cross-links in tissues that had accumulated the highest intranuclear concentrations of nickel ion (Ciccarelli and Wetterhahn 1984). Treatment of cultured CHO cells with Ni(II) induced repairable single-strand breaks and DNA-protein cross-links that persisted up to 24 h after removal of the nickel (Patierno and Costa 1985). DNA-protein cross links induced by NiCl₂ were both concentration and time dependent and preferentially occurred in cells in the late S phase of the cell cycle (Patierno et al. 1985). Treatment of Chinese hamster ovary (CHO) cells with nickel chloride (NiCl₂) decreased the amount of DNA in the magnesium-insoluble fraction but increased the amount of DNA in the fast-sedimenting chromatin fraction indicating that nickel induced widespread alterations in chromatin conformation (Patierno et al. 1987).

Ni(II) genotoxicity in cells may be aggravated through the generation of reactive oxygen species (ROS). Free radicals bind to DNA and as such are rather mutagenic, catalyse the formation of covalent cross-links of proteins and amino acids (Kasprzak et al. 2003). The selective binding of Ni ions to proteins and amino acids has been reported to be by several orders of magnitude higher than for DNA. Consequently, Ni(II) interacted with chromatin because of the protein present, not because of its reactivity with DNA (Costa et al. 1994). The major hypothesis regarding the carcinogenic action of Ni has involved the ability to deliver high concentrations of Ni intracellularly entering the nucleus and interacting with chromatin, selectively damaging heterochromatin, and silencing the expression of genes located near the heterochromatin by inducing a loss of histone H4 and H3 acetylation and DNA hypermethylation (Costa et al. 2003).

The major aim of our work is to explore the relationship between chromatin changes and apoptosis versus necrosis generated by heavy metals, different types of irradiation and chemicals. Originally we have traced large scale chromatin condensation in healthy mammalian cell lines and have found that the pattern of chromatin condensation follows a common pathway (Banfalvi et al. 2006). Differences in chromosome condensation were found between the higher arthropod (*Drosophila*) and mammalian cells (Indian muntjac, CHO, murine preB and human K562) (Banfalvi et al. 2006, 2008). Apoptotic chromatin changes were induced by Cd²⁺, Hg²⁺

and Pb²⁺ ions (Banfalvi et al. 2005; Farkas et al. 2010; Nagy et al. 2010). The apoptotic effect exerted by Cd on chromatin structure has been visualized in Chap. 6.

The binding of heavy metals to DNA and/or chromatin constituents may adversely affect gene structure and function. These xenobiotics including Ni(II) ultimately may initiate carcinogenesis (Kasprzak et al. 2003). However, large-scale chromatin changes induced by Ni(II) have not been studied. This chapter describes how Ni(II) ions influence the cellular motility and how chromatin structures are distorted in a dose-related manner.

Materials and Methods

Chemicals and Reagents

Nickel chloride (NiCl₂) was obtained from Sigma-Aldrich (Budapest, Hungary). A stock solution of nickel chloride was prepared in distilled water and filter sterilized (pore size 0.22 μm) prior to addition to cell-culture media.

Growth media and sera were obtained from Invitrogen (Carlsbad, CA, USA), 6-diamidino-2-phenylindole dihydrochloride (DAPI), 1,4-diazabicyclo-(2,2,2)-octane (DABCO) and other reagents were purchased from Sigma-Aldrich (Budapest, Hungary). Antifade Medium contained 90% glycerol, 2% (w/w) 1,4-diazobicyclo-(2,2,2)-octane, 20 mM Tris-Cl, pH 8.0, 0.02% sodium azide, and 25 ng/ml DAPI. Swelling Buffer consisted of 50 mM KCl, 10 mM MgSO₄, 3 mM dithiothreitol, and 5 mM NaPO₄, pH 8.0. Hypotonic Buffer for reversible permeabilization contained 9 mM HEPES, pH 7.8, 5.8 mM dithiothreitol, 4.5% dextran T-150, 1 mM EGTA and 4.5 mM MgCl₂. Fixative solution contained methanol:glacial acetic acid (3:1).

Cell Growth

Human erythroleukemia K562 cells were chosen for these experiments as in their suspension culture the cellular motion of individual could be followed much better by time-lapse video microscopy than in monolayer cells. The reason that we did not use the earlier preferred CHO-K1 cells was the observation of Fletcher et al. (1994) that AS52 cells derived from CHO-K1 were much less sensitive to NiCl₂. K562 cells were cultured in RPMI-1640 medium supplemented with 10% fetal bovine serum (FBS). The continuous cell line K-562 was established by Lozzio and Lozzio from the pleural effusion of a 53-year-old woman with chronic myelogenous leukemia in terminal blast crises (Lozzio and Lozzio 1975).

Treatment with Nickel Chloride

Subcultured K562 cells were grown for 9 h and then treated with Ni(II) chloride (1–100 μM NiCl₂). Cells were grown for an additional 15 h in the presence of the

heavy metal before being harvested, unless otherwise noted. Data are averages of three replicate experiments. As a quantitative measure of cytotoxic effects we determined the inhibition concentration for a 50% reduction of the cell number per culture (IC50) (Halle and Göres 1987).

Cells for chromatin monitoring were grown in plastic TC flasks (75 cm²). Heavy metal ion concentrations were applied using concentration ranges for NiCl₂ between 0.2 and 100 µM. Cells were incubated with each toxin concentration for 15 h. Toxicity was estimated by the cell viability test and during the immunofluorescence visualization of the chromatin structure. Simultaneously, control experiments were carried out in the same way, but in the absence of Ni(II).

Reversible Permeabilization of Cells

Based on the technique of reversible permeabilization, nuclei of cells could be opened to visualize large scale chromatin changes. This method, originally developed for the reversible permeabilization of lymphocytes isolated from the murine thymus (Banfalvi et al. 1984), was adapted to K562 erythroleukemia cells. Briefly, 1 ml of Hypotonic Buffer was added to 10⁶ cells in the presence of Dextran T-150 as a molecular coat to prevent cells from disruption. Permeabilization lasted for 2 min at 0°C. For reversal of permeabilization, the hypotonic solution was replaced by RPMI 1640 medium containing 10% fetal bovine serum, and the cells were incubated in a CO₂ incubator at 37°C and 5% CO₂ for 3 h.

Isolation of Nuclei

Due to the cyclic character of chromatin unfolding and chromosome condensation, isolated cell populations were treated with colcemid to prevent cells from entering a new cell cycle. Cells (10⁶) were resuspended in growth medium after reversal of permeabilization and treated with 0.1 µg/ml colcemid for 2 h at 37°C under 5% CO₂. Cells were centrifuged (5 min 600 g), washed twice with PBS.

Determination of viable cell number: Cells were resuspended in 5 ml PBS and 50 µl cell suspension was given to 50 µl 0.5% trypan blue dissolved in PBS. Viable cells that did not take up trypan blue were counted in a Bürker chamber. Once cell number/ml was determined, 10⁶ cells were taken for osmotic swelling.

Osmotic cell swelling: Cells (10⁶) were washed twice with PBS and incubated at 37°C for 10 min in Swelling Buffer. Swelling was followed by centrifugation at 500 g for 5 min.

Isolation of nuclei: After swelling nuclei were isolated from the pellet of cells by the slow addition under constant stirring of 14 ml Fixative Solution. Nuclei were then centrifuged at 500 g for 5 min and washed twice in Fixative.

Spreads of Nuclear Structures

Preparation of nuclei for spreads of chromatin structures used the method developed for metaphase chromosomes. Nuclei washed in Fixative were centrifuged at 500 g for 5 min and resuspended in 1 ml Fixative. Nuclei were spread over glass slides dropwise from a height of approximately 30 cm. Slides were air dried, stored at room temperature overnight, rinsed with PBS and dehydrated using increasing concentrations of ethanol (70, 90, 95 and 100%).

Visualization of Large Scale Chromatin Structures

Dehydrated slides containing normal, apoptotic or necrotic chromatin structures were mounted in 35 μ l Antifade Medium under 24 \times 50 mm coverslips. Images were assessed by observing chromatin changes visualized after staining with DAPI by fluorescence microscopy (Nikon Eclipse E800 Nikon Corporation, Tokyo). All images were acquired using constant camera settings to allow for comparative analysis of staining intensities.

Time-Lapse Photography

Two inverse microscopes were placed in CO₂ incubator equipped with high sensitivity video cameras, connected to a custom-built dual image acquisition computer system. Custom-built illumination was developed to minimize heat- and phototoxicity. Operation of the spectrally cold-white light emitting diodes were synchronized with image acquisition periods. Cell cultures in T flasks were placed on inverse microscopes. The screen of the computer was divided in two portions showing side-by-side the morphological changes of the control and the treated cells. Photographs of K562 cells were taken every minute. The time of exposure was indicated in each frame. Exposures were converted to videofilms by speeding up the projection to 30 exposures/sec. Individual K562 cells of suspension cultures were selected for further analysis. Individual photographs were chosen shown in the figures. Time-lapse photography of individual cells allows us to determine the growth profile of individual cells grown in both monolayer and suspension cultures. Genotoxicity specific growth profiles of cell death could be clearly distinguished after Pb(II) treatment of HaCaT cells (Nagy et al. 2010).

Results

Cellular Toxicity of NiCl₂

Concentration dependent stoichiometry of cellular toxicity is shown by growing eight cell cultures starting at 10⁶ cells/ml in the presence of 0.2–100 μ M Ni(II) chlo-

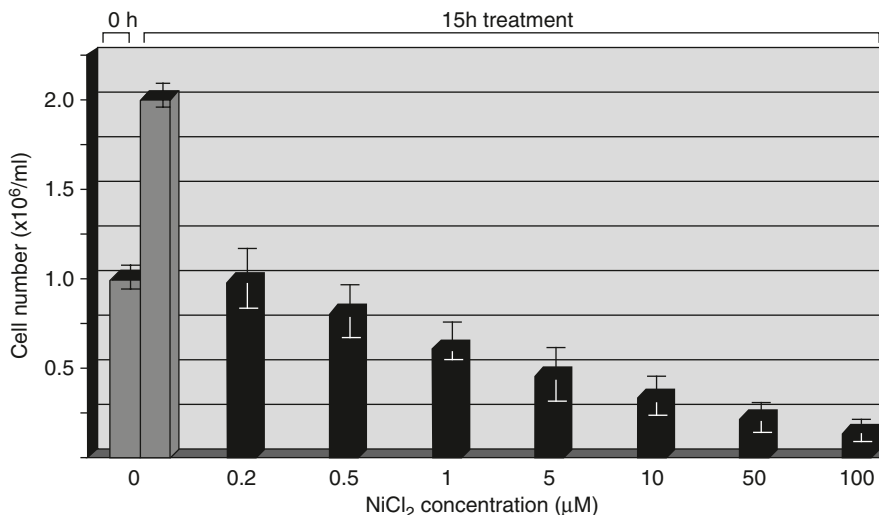


Fig. 7.1 Inhibition of cell growth at different nickel concentrations. The growth of eight cell cultures was started at 10^6 cells/ml in the presence of 0.2, 0.5, 1, 5, 10, 50 and 100 μM NiCl_2 , respectively. The control sample (grey) was not treated. After treatment the cell number was counted in each population. In the representation the abscissa is showing the nickel concentration and the ordinate the cell number. Error bars indicate standard errors of three replicates

ride for 15 h at 37°C and 5% CO_2 (Fig. 7.1). The control culture was not subjected to NiCl_2 treatment. Subtoxic levels of Ni(II) ($\leq 0.1 \mu\text{M}$) did not cause noticeable changes in viability (not shown). The growth rate was tested at increasing concentrations in the presence of 0.2, 0.5, 1, 5, 10, 50 and 100 μM NiCl_2 resulting in cell loss corresponding to 3, 20, 37, 53, 66, 78 and 87%, respectively. From the data of survival we have estimated the 50% inhibition (IC_{50}) of K562 cell growth that corresponded to 2 μM (0.26 $\mu\text{g/ml}$ NiCl_2 , equivalent to 0.12 $\mu\text{g/ml}$ Ni(II)).

Chromatin Structures of Normal Untreated Cells

The common pathway of chromosome condensation was followed during the normal cell cycle including several intermediate chromosomal structures (Banfalvi et al. 2006). These forms have been described earlier and are presented here only to demonstrate that these physiological chromatin forms shown in Fig. 7.2 differ from those isolated from cells subjected to NiCl_2 treatment.

Density Changes in Chromatin Structures at Low (0.2 and 0.5 μM) Concentrations of Ni(II)

Prior to the isolation of chromatin structures from reversibly permeabilized cells, K562 cultures were treated with low concentrations (0.2–0.5 μM) of nickel chloride (Fig. 7.3).

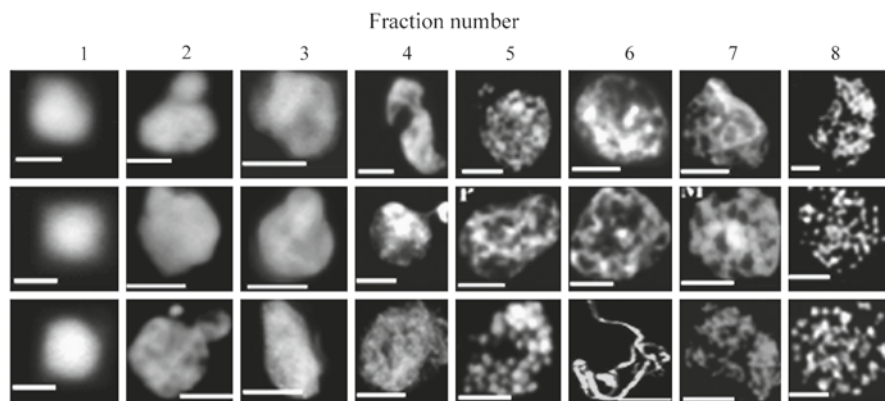


Fig. 7.2 Intermediates of chromatin condensation in synchronized fractions of untreated cells. Permeabilization of cells was followed by the restoration of membrane structures, colcemid treatment and isolation of chromatin structures as described in the Methods. Regular structures seen under fluorescent microscope after DAPI staining: decondensed chromatin (*fraction 1*), extrusion of coiled chromatin (*fraction 2*), fibrous chromatin (*fraction 3*), ribboned supercoiled chromatin (*fraction 4*), chromatin bodies (*fraction 5*), early bent chromosomes (*fraction 6*), elongated pre-chromosomes (*fraction 7*) metaphase chromosomes (*fraction 8*). Bar 5 μm each

1. At 0.2 μM Ni(II) the uneven condensation of chromatin was indicated by the polarization of dense fluorescent chromatin patches (seen throughout Fig. 7.3a–k, left panel),
2. Condensed chromatin was often rejected as apoptotic bodies at 0.5 μM Ni(II) concentration (Fig. 7.3c, g, j, k, right panel).

Apoptotic Chromatin Changes at Elevated (1–5 μM) Concentrations of Nickel Chloride

Upon treatment of K562 cells with higher (1–5 μM) nickel chloride the gradual aggravation of apoptosis could be visualized with increasing number of apoptotic bodies and moderate nuclear shrinkage. In the presence of 1 μM concentration of nickel chloride the major apoptotic changes were:

1. reduced nuclear size (Fig. 7.4a–k, left panel),
2. polarization of chromatin (Fig. 7.4a, c, d, e, g, j, left panel),
3. formation of apoptotic chromatin circles (Fig. 7.4a–e, left panel),
4. formation and rejection of apoptotic bodies (Fig. 7.4b, g, h, j, k, left panel).

In the chromatin structures of nuclei isolated after treatment with a somewhat higher Ni(II) chloride concentration (5 μM) (Fig. 7.4, right panel) the number of apoptotic bodies was significantly reduced. The nucleus started to expand (Fig. 7.4a, b, d, g, right panel) and most of the nucleus gradually opened making visible the two ends of the chromatin ribbon (Fig. 7.4f–k, right panel).

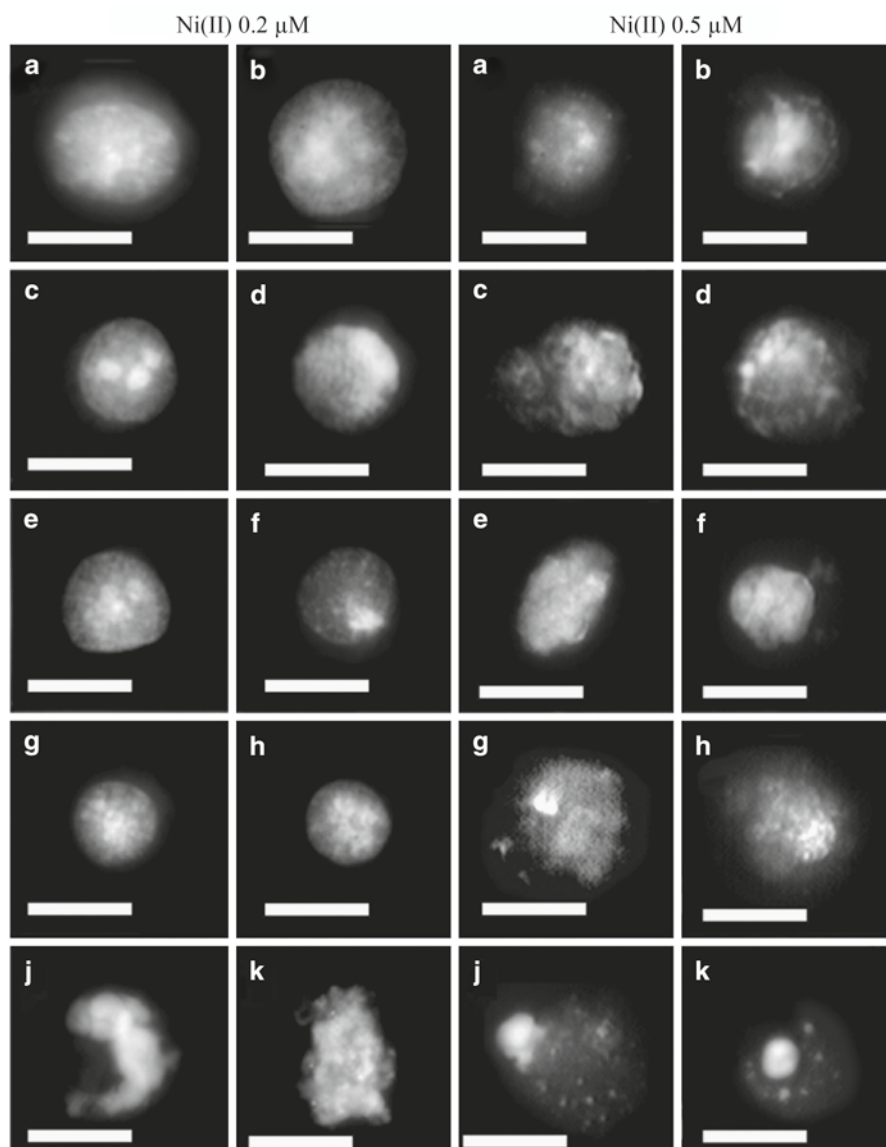


Fig. 7.3 Chromatin monitoring at low cellular concentrations of nickel. Cells were treated with 0.2 or 0.5 μM NiCl₂, reversibly permeabilized, subjected to colcemid treatment and isolation of chromatin structures as described in Sect. 2. Chromatin structures were visualized after DAPI staining. Bar 5 μm each

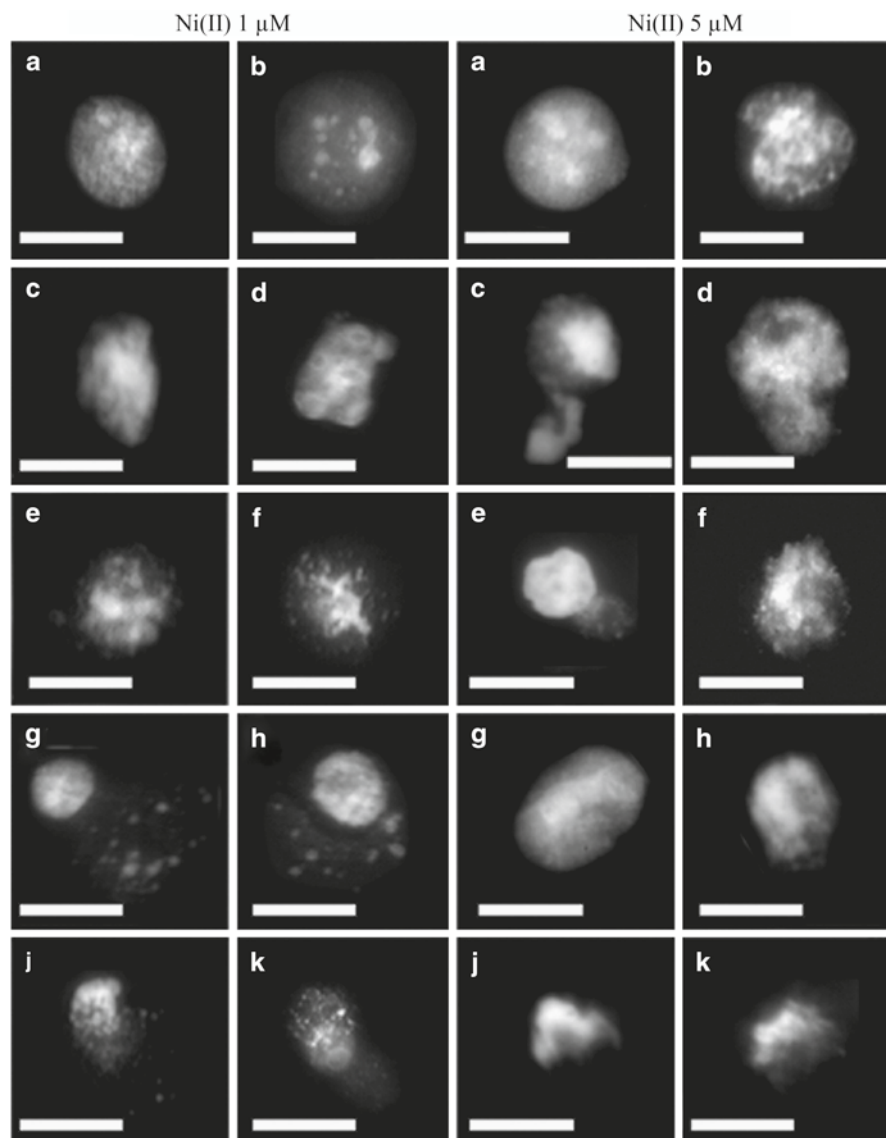


Fig. 7.4 Chromatin changes at higher cellular concentrations of nickel. Cells were treated with 1 or 5 μM NiCl_2 , reversibly permeabilized, subjected to colcemid treatment, and isolation of chromatin structures as described in Sect. 2. Chromatin structures were visualized after DAPI staining. Bar 5 μm each.

Chromatin Changes at Higher (10 μ M) Nickel Chloride Concentration

The apoptotic cellular effect of 10 μ M Ni(II) chloride is seen in Fig. 7.5 (left panel).

1. Fluorescence intensities of chromatin indicate that most of the nuclear material is highly condensed, while the rest of it remains in highly decondensed fibrillary stage (Fig. 7.5a–k, left panel)
2. Fibrillary chromatin is often rejected as a comet tail containing less condensed apoptotic chromatin circles (Fig. 7.5f–k, left panel).

Necrotic Chromatin Changes at High (50 μ M) Nickel Chloride Concentration

When 50 μ M Ni(II) concentration was applied, necrotic changes took place that manifested in the reduction of the fibrillary chromatin, in a moderately increased nuclear size and in the preservation of the relatively round shaped nuclei (Fig. 7.5a–k, right panel). Similar chromatotoxic tendency was observed at higher (100–200 μ M) Ni(II) concentrations (not shown).

Cellular Motion After 100 μ M NiCl₂ Treatment

Recently we have followed the motility of single cells with time-lapse video microscopy in control HaCaT cells and after subjecting them to 50 μ M Pb(NO₃)₂ incubation. Their vigorous movement known as apoptotic dance was monitored (Nagy et al. 2010). The K562 cells were also photographed every minute with our long-term scanning device and the cellular motion of individual cells was followed for 24 h. After subjecting cells to relatively high (10–50 μ M) concentrations of NiCl₂ we did not observe intense apoptotic agitation. However, the motion of cells was temporarily higher after 100 μ M concentration of Ni(II) exposure. The transiently elevated cellular motility is indicated by the changing position of cells up to 100 min incubation time (Fig. 7.6). The increase in cell number between 0 and 100 min is explained by the sedimentation and temporary trajectory of the suspension cell culture of K562 cells. After 5 h the motion of cells slowed down, cells aggregated and tended to stick together (Fig. 7.6). Worthy to mention that the cell size even at this high Ni(II) concentration decreased only slightly at the beginning of the treatment that would have reflected apoptosis, and the small increase in cell size after longer incubation was not a general tendency that would have pointed to necrosis.

The unusual finding that necrotic concentrations of Ni(II) did not cause drastic changes in cellular size and induced only a moderate nuclear size increase prompted us to follow the fate of those cells which were disrupted after exposure to high

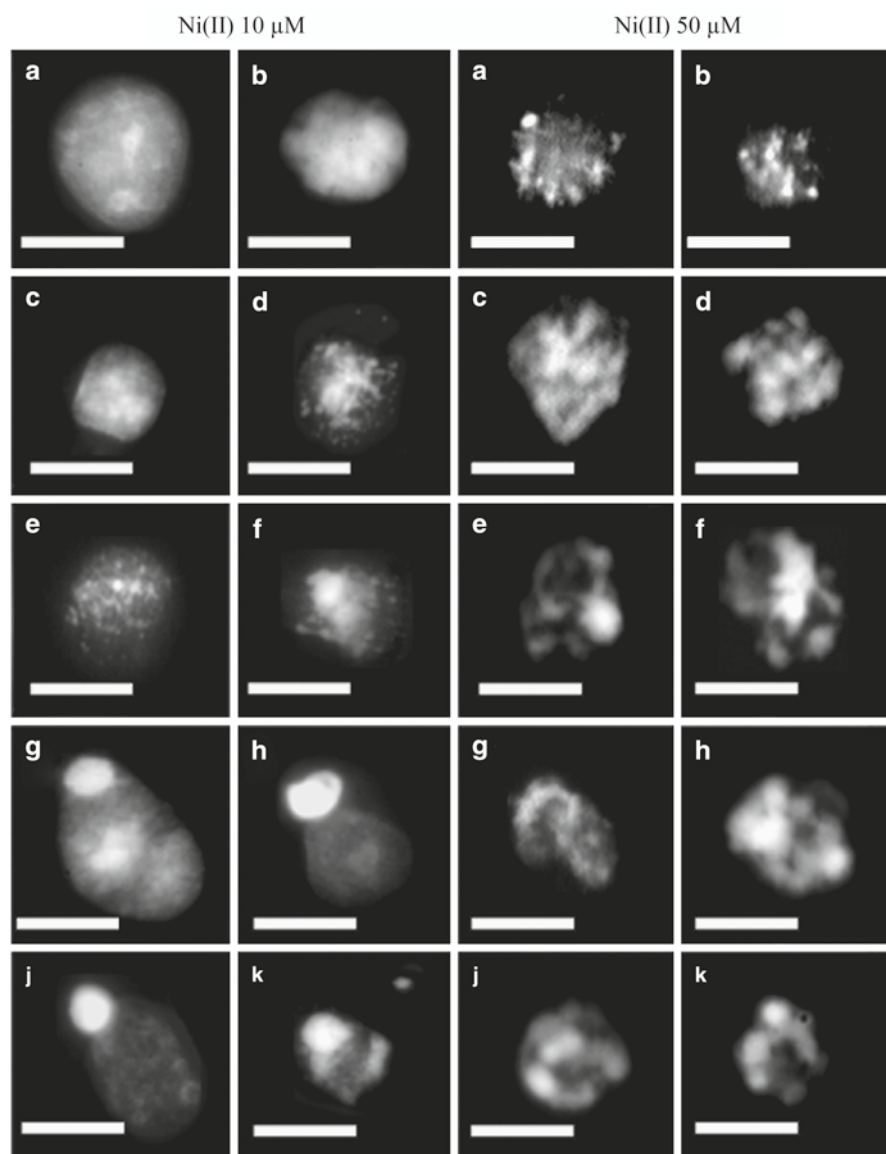
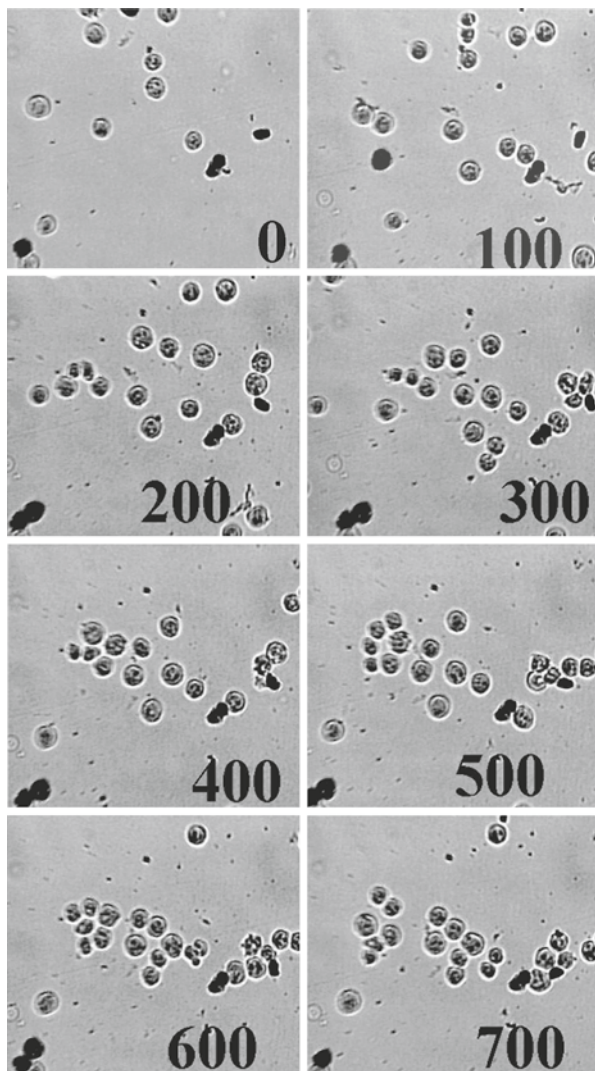


Fig. 7.5 Apoptotic chromatin changes at 10 μM, necrotic changes at 50 μM Ni(II) chloride treatment. Cells were treated as in Fig. 7.3. Isolation and visualization of chromatin structures were the same as described in Fig. 7.3. Bar 5 μm each

Fig. 7.6 Monitoring cellular motion after 100 μM Ni(II) treatment in the time-lapse photography system. Cells were grown in 25 ml T-flasks and treated with Ni(II) as in Fig. 7.3 and placed on reverse microscope sitting in a carbondioxide incubator. Photographs were taken every minute by custom built video camera attached to the microscope and connected to the computer. The motion of cells is indicated by their changing position. *Black numbers* indicate the time of photography in minutes after heavy metal treatment



(100 μM) Ni(II) concentration. Figure 7.7 (left side) shows the fate of a necrotic cell from the beginning of treatment (0 min) up to more than 10 h (611 min), with the black arrows pointing to the necrotic cell. The tendency of cell aggregation and sticking together seen in Fig. 7.6 is also evident. The disrupted necrotic cell has been selected for closer scrutiny and its negative image is shown in the right panel of Fig. 7.7. The necrotic chromatin condensation of this cells is best viewed after 212 min of Ni(II) treatment (upper right corners of both panels in Fig. 7.7), where the chain of prematurely condensed chromosomes of the selected necrotic cell is clearly distinguishable.

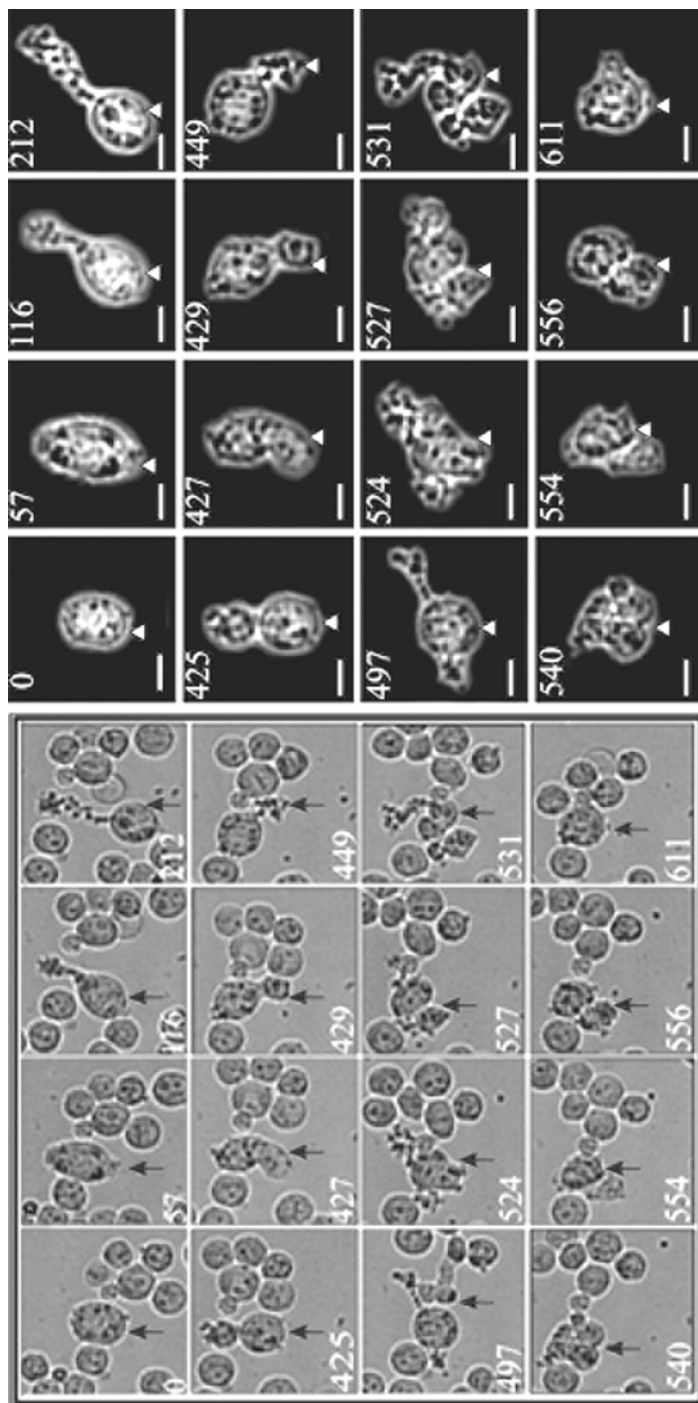


Fig. 7.7 Long-term scanning of a necrotic cell after the treatment of K562 cells with 100 μM NiCl_2 , as in Fig. 7.6. *Left panel:* The necrotic cell inside a small population of undisturbed cells is indicated by the *black arrows*. *White numbers* indicated the time of photography in minutes from the beginning of heavy metal treatment. *Right panel* shows the same cell which has been processed by the drawing function of Adobe Photoshop 5.0 program. *White numbers* indicate the time of photography in minutes after heavy metal treatment. Bar, 5 μm each. A more detailed view of long-term scanning after this 100 μM NiCl_2 treatment is seen in the slideshow. (Video film is available at <http://etox.net/videos/videofig7/Ni.wmv>)

Discussion

As far as the cellular, including morphological, effects of Ni(II) ions are concerned, there are only sporadic references available. We summarize this literature before comparing it with our results. Morphological transformation studies in Syrian hamster cells revealed that of the 12 metal salts tested, acceptable evidence for human carcinogenicity was found only for arsenic, beryllium, chromium, cadmium and nickel (DiPaolo and Casto 1979). Carcinogenic, transforming water-insoluble Ni compounds including NiCl₂ are phagocytized by cells; and undergo dissolution inside the cell, releasing Ni ions that interact with chromatin, producing highly selective damage to heterochromatin (Costa et al. 1994). Nickel(II) ions involved in heterochromatinization of chromatin within regions of the genome, will inhibit any further molecular interactions with underlying genes. Heterochromatinization with nickel(II) ions through the condensation of chromatin took place to a greater extent than by the natural divalent cation of the cell, magnesium ion (Mg²⁺) (Ellen et al. 2009). The alteration of gene expression supported the emerging theory that nickel(II) exerted its epigenetic carcinogenic effect by enhanced DNA methylation and compaction, rather than by mutagenic mechanism (Lee et al. 1995). In mammalian cells not all metals induced breakage of DNA (DiPaolo et al. 1978). Nonlethal concentrations of arsenic and cadmium caused breaks, while beryllium or nickel did not produce breaks even at concentrations that caused 100% cell death (Casto et al. 1976; DiPaolo et al. 1978). Nickel(II) induced only a slight increase in DNA strand breaks at high (≥ 250 μM) concentrations (Dally and Hartwig 1997). Heavy metal ions (Pb, Au, Co, Cr, Cu, Zn) influenced the *in vitro* nitric monoxide production of murine macrophages. To the opposite Cd, Hg and Ni ions did not exert any significant effect on NO production and that the toxicity of lead, cobalt and nickel was caused by different mechanisms. By accepting the view that heavy metals are very broad in their activity and that the resulting cytotoxicity is due to a number of different mechanisms, one would expect that the pathway leading to cell death could occur in many ways and characteristic nuclear changes are reflected in the pattern of chromatin condensation.

We have found that NiCl₂ causes cell death at low concentration (IC₅₀: 2 μM , 0.26 $\mu\text{g/ml}$) in human K562 erythroleukemia cells. Others have described that the IC₅₀ of NiCl₂ in AS52 cells was significantly higher, corresponding to 45–60 $\mu\text{g/ml}$ (346–461 μM) NiCl₂ (Fletcher et al. 1994). As already mentioned AS52 cells have been derived by the modification of CHO-K1 cells. Our data show that K562 cells are much more sensitive to NiCl₂ than the modified AS strain of CHO-K1 cell. However, there were no significant changes in cell size even when cells were treated with high concentrations (100 μM) of NiCl₂. Slight apoptotic shrinkage of nuclei could be visualized at 1 μM Ni(II) that turned gradually to nuclear enlargement and disruption of some of the nuclei at higher than 5 μM concentrations. These cellular changes manifested at the chromatin level are in conformity with the finding of others that (a) the primary target of Ni(II) is the nucleus, primarily the chromatin (DiPaolo and Casto 1979), (b) Ni(II) causes chromatin condensation through

heterochromatization (Costa et al. 1994), (c) Ni(II) replaces the natural divalent cation, magnesium ion (Mg^{2+}) (Ellen et al. 2009), (d) Ni(II) exerts its epigenetic carcinogenic effect by enhanced DNA methylation and compaction, rather than by mutagenic mechanism (Lee et al. 1995).

In normal cells that have not been subjected to Ni(II) treatment we have shown typical interphase chromatin structures that corresponded to those found in other mammalian cells (Banfalvi et al. 2006). Although, the transformations of Ni(II) are known to induce heterochromatization, earlier studies did not deal with large-scale chromatin changes. To summarize these Ni-induced chromatin changes:

1. Low (0.2–0.5 μM) concentrations of Ni(II) induced the polarization of dense fluorescent chromatin patches and the rejection of apoptotic bodies.
2. 1 μM $NiCl_2$ caused polarization, rejection of smaller apoptotic bodies and the formation of larger apoptotic chromatin circles.
3. At 5 μM $NiCl_2$ nuclear expansion made the two ends of the chromatin visible, suggesting that the folding process was blocked in the chromatin ribbon stage.
4. At 10 μM Ni(II) most of the nuclear material was highly condensed, while the rest remained in highly decondensed fibrillary stage.
5. Necrotic changes at 50 μM $NiCl_2$ manifested in the reduction of the fibrillary chromatin, moderate increase in nuclear size and preservation of the relatively round shaped nuclei.
6. High (50–100 μM) $NiCl_2$ concentrations on cellular motility, was not as paralyzing as Hg(II) (Farkas et al. 2010) and caused much less agitation of cells than the “apoptotic dance” provoked by Pb(II) (Nagy et al. 2010). Cells tended to aggregate and stuck together contributing to the gradual reduction of cellular motion.

Conclusions

The human K562 erythroleukemia cell line turned out to be a proper choice to test the cellular toxicity of Ni(II) due to its sensitivity expressed by the low, 2 μM IC50 value. The K562 suspension cell culture was successfully applied for the long-term scanning of individual cells. The cell size varied only slightly upon treatment of a wide range (0.2–100 μM) of $NiCl_2$ concentration. To summarize the Ni(II) induced chromatin changes: (a) one of the most important function, the cell motility is not significantly impaired, (b) the nuclear effect, namely heterochromatization is dominating the picture after Ni(II) treatment, (c) the chromatotoxic effect is manifested as retarded condensation at different stages of the chromatin folding process, and (d) the multiple forms of chromatin structures retarded by Ni(II) depend on the concentration of the heavy metal and the duration of incubation.

Acknowledgement This work was supported by Hungarian Scientific Research Fund (OTKA grant) T 42762 grant to G.B.

References

- Babu K, Rajmohan RH, Rajan KB (2006) Assessment of functional integrity of liver among workers exposed to soluble nickel compounds during nickel plating. *Ind J Occup Environ Med* 10:78–81
- Banfalvi G (2008) Chromatin fiber structure and plectonemic model of chromosome condensation in *Drosophila* cells. *DNA Cell Biol* 27:65–70
- Banfalvi G, Sooki-Toth A, Sarkar N, Csuzi S, Antoni F (1984) Nascent DNA synthesized reversibly permeable cells of mouse thymocytes. *Eur J Biochem* 139:553–559
- Banfalvi G, Gacsi M, Nagy G, Kiss ZB, Basnakian AG (2005) Cadmium induced apoptotic changes in chromatin structure and subphases of nuclear growth during the cell cycle in CHO cells. *Apoptosis* 10:631–642
- Banfalvi G, Nagy G, Gacsi M, Roszer T, Basnakian AG (2006) Common pathway of chromosome condensation in mammalian cells. *DNA Cell Biol* 25:295–301
- Casto BC, Pieczynski WJ, Nelson AL, DiPaolo JA (1976) *In vitro* transformation and enhancement of viral transformation with metals. *Proc Am Assoc Cancer Res* 17:12
- Ciccarelli RB, Wetterhahn KE (1984) Nickel-bound chromatin, nucleic acids, and nuclear proteins from kidney and liver of rats treated with nickel carbonate *in vivo*. *Cancer Res* 44:3892–3897
- Costa M, Salnikow K, Cosentino S, Klein CB, Huang X, Zhuang Z (1994) Molecular mechanisms of nickel carcinogenesis. *Environ Health Perspect* 102(3):127–130
- Costa M, Yan Y, Zhao D, Salnikow K (2003) Molecular mechanisms of nickel carcinogenesis: gene silencing by nickel delivery to the nucleus and gene activation/inactivation by nickel-induced cell signaling. *J Environ Monit* 5:222–223
- Dally H, Hartwig A (1997) Induction and repair inhibition of oxidative DNA damage by nickel(II) and cadmium(II) in mammalian cells. *Carcinogenesis* 18:1021–1026
- DiPaolo JA, Casto BC (1979) Quantitative studies of *in vitro* morphological transformation of Syrian hamster cells by inorganic metal salts. *Cancer Res* 39:1008–1013
- DiPaolo JA, Nelson RL, Casto BC (1978) *In vitro* neoplastic transformation of Syrian hamster cells by lead acetate and its relevance to environmental carcinogenesis. *Br J Cancer* 38:452–455
- Ellen TP, Kluz T, Harder ME, Xiong J, Costa M (2009) Heterochromatinization as a potential mechanism of nickel-induced carcinogenesis. *Biochemistry* 48:4626–4632
- Farkas E, Ujvarosi K, Nagy G, Posta J, Banfalvi G (2010) Apoptogenic and necrogenic effects of mercuric acetate on the chromatin structure of K562 human erythroleukemia cells. *Toxicol In vitro* 24:267–275
- Fletcher GG, Rossetto FE, Turnbull JD, Nieboer E (1994) Toxicity, uptake, and mutagenicity of particulate and soluble nickel compounds. *Environ Health Perspect* 102(3):69–79
- Halle W, Göres E (1987) Prediction of LD50 values by cell culture. *Pharmazie* 42:245–248
- Kasprzak KS, Sunderman FW Jr, Salnikow K (2003) Nickel carcinogenesis. *Mutat Res* 533:67–97
- Lee YW, Klein CB, Kargacin B, Salnikow K, Kitahara J, Dowjat K, Zhitkovich A, Christie NT, Costa M (1995) Carcinogenic nickel silences gene expression by chromatin condensation and DNA methylation: a new model for epigenetic carcinogens. *Mol Cell Biol* 15:2547–2557
- Lozzio CB, Lozzio BB (1975) Human chronic myelogenous leukemia cell-line with positive Philadelphia chromosome. *Blood* 45:321–334
- Nagy G, Pinter G, Kohut G, Adam A, Trencsenyi G, Hornok L, Banfalvi G (2010) Time-lapse analysis of cell death in mammalian and fungal cells. *DNA Cell Biol* 29:249–259
- Patierno SR, Costa M (1985) DNA-protein crosslinks induced by nickel compounds in intact cultured mammalian cells. *Chem-Biol Interact* 55:75–91
- Patierno SP, Sugiyama M, Basilion JP, Costa M (1985) Preferential DNA-protein cross-linking by NiCl₂ in magnesium-insoluble regions of fractionated Chinese hamster ovary cell chromatin. *Cancer Res* 45:5787–5794
- Patierno SR, Sugiyama M, Costa M (1987) Effect of nickel(II) on DNA-protein binding, thymidine incorporation, and sedimentation pattern of chromatin fractions from intact mammalian cells. *J Biochem Toxicol* 2:13–23
- Sunderman FW Jr (1982) Recent research on nickel carcinogenesis. *Environ Health Perspect* 40:131–141

Chapter 8

Genotoxic Chromatin Changes in *Schizosaccharomyces Pombe* Induced by Hexavalent chromium (CrVI) Ions

Gábor Papp, Gábor Nagy, István Pócsi, Miklós Pesti and Gáspár Bánfalvi

Abstract Based on their MIC50 values Cr(VI) turned out to be 15-times more toxic than Cr(III) in *S. pombe* estimated to be 15 and 225 μM , respectively. Major focus of this chapter is placed on large-scale chromatin structures of fungal nuclei, isolated from protoplasts of the fission yeast *Schizosaccharomyces pombe* and visualized for the first time by fluorescence microscopy. Although, the pattern of chromosome condensation was similar to mammalian cells, but less compact and resembled more to that of *Drosophila*. *S. pombe* cells were treated with hexavalent chromate ions (CrVI) in a concentration-dependent manner and chromatin structures were analysed. Results show that subtoxic levels of Cr(VI) ($<1 \mu\text{M}$) did not cause significant chromatin changes. Early signs of apoptotic cytotoxicity were observed at 10 μM Cr(VI) concentration. Nuclear changes caused by Cr(VI) in the concentration range between 10 and 50 μM were characterized by apoptosis seen as broken nuclei and apoptotic bodies. High concentration of Cr(VI) ions (75–200 μM) initiated necrotic nuclear changes, with focal condensation of chromatin and the formation of extremely enlarged nuclei that were in a highly decondensed fibrillary state. The necrotic enlargement of fibrillary nuclei was dependent on the Cr(VI) concentration.

Introduction

The extensive distribution of anthropogenic hexavalent chromate (CrVI) in soil and groundwater originating from metal processing, chromeplating, resistant alloys, refractory industry, wood treatment, leather tanneries, pigment and dye productions (Bailar 1997; United States Environmental Protection Agency 1998; Ryan et al. 2002) is a world-wide problem. The Cr(VI) can be detoxified by reduction to tri-

G. Bánfalvi (✉)

Department of Microbial Biotechnology and Cell Biology, University of Debrecen,

1 Egyetem Square, 4010 Debrecen, Hungary

Tel.: +36-52-512-900

Fax: +36-52-512-925

e-mail: bgaspar@delfin.klte.hu

valent chromium (Cr(III)) and removed from freshwater. Chromium exposure takes place through breathing, eating and drinking of chromium containing compounds that are present in low concentrations in air and water. The metal form of chromium (Cr) is of low toxicity. Cr(III) in low concentrations is essential for health, shortages cause disruptions in sugar and fat metabolism (Cefalu et al. 2002). Food that contains Cr(III) is the main route of chromium uptake, as Cr(III) occurs naturally in the food, particularly in vegetables, fruits and meat (<http://www.lenntech.com/periodic/elements/cr.htm>).

Contaminated water containing the toxic Cr(VI) is dangerous for those, who work in the steel and textile industry. Tobacco smoking is another source of Cr(VI) exposure. Although, Cr is an essential trace element for living organisms (Bailar 1997), higher than allowed levels of Cr(VI) in drinking water ($50\text{--}100\ \mu\text{g l}^{-1}$, $\sim 1\text{--}2\ \mu\text{M}$) are of increasing concern, eliciting environmental and health problems (Petrilli and Flora 1977; Sharma et al. 1995), mutagenicity (Nishioka 1975) and carcinogenicity (Venitt and Levy 1974).

Under physiological conditions Cr(VI) reacts with intracellular reductants (primarily ascorbate and glutathione) to produce short-lived intermediates such as Cr(V) and/or Cr(IV), free radicals and the end-product Cr(III) (Costa 2003; Xu et al. 2004, 2005). As far as the genotoxic effect is concerned Cr(VI) was studied in calf thymus nuclei, but no binding of Cr was detected after incubation up to 0.5 mM Cr(VI) concentration. Cr(III) turned out to be the genotoxic agent after chromate uptake by living cells (Köster and Beyersmann 1985). The metabolism of Cr(VI) takes place in specific cellular fractions (mitochondria, microsomal and soluble components) with glutathione being the primary oxidizing agent in the reduction (Wiegand et al. 1984). The reduced Cr(III) induces DNA crosslinks and strand breaks in nuclei (Fornance et al. 1981). The mutagenic effect of Cr(III) has been demonstrated in the Ames test with *Salmonella typhimurium* (Warren et al. 1981).

As far as the the number and estimated size of chromosomes is concerned among the *Ascomycetes* of fungi, *S. pombe* seems to be an ideal model organism to study large scale chromatin structure with an estimated 12.5 Mbp genome and its three chromosomes of 3.5–5.7 Mbp. Other fungi either contain many DNA molecules or too small chromosomes. For fungi analyzed electrophoretically the numbers of DNA molecules ranged between 3 to 21 with size ranges between 0.2 and 12 Mbp (Mills and McClusky 1990). Five histone bands are commonly seen on electrophoresis of histones in plant, animal and most filamentous fungi. H1 histone serves as a bridge between adjacent nucleosomes. However, the yeasts *S. cerevisiae* and *S. pombe* and the oomycete *Achlya* lack histone H1 (Newlon 1988; Munz et al. 1989; Pekkala and Silver 1990). The lack of H1 histone in maintaining tertiary structure of DNA was assumed to have implications for the packaging of chromatin and lack the ability to condense chromosomes (Newlon 1988).

Contrary to the absence of H1 histone, *Achlya* turned out to be able to form condensed chromatin (Pekkala and Silver 1990). Nevertheless, one would expect that the lack of H1 histone would reduce the compaction of the chromosomes. The chromatin structure of fungi has not been studied extensively; consequently the large-scale chromatin condensation pattern of fungi is not known. As neither have data

related to chromatin structure of fission yeast been published, nor the relatively old observations of Cr(VI) genotoxicity been explained at chromatin level, our aim was to clarify what kind of modifying effects the hexavalent chromium ions exert on the chromatin structure of fission yeasts. Here we describe that in nuclei isolated from the protoplasts of the fission yeast *S. pombe* the basic pattern of chromatin folding is similar to that of the mammalian nucleus, but does not reach the compaction of mammalian chromosomes. Low, subtoxic concentrations of Cr(VI) (10–50 μM) induced apoptosis, while higher concentrations (75–200 μM) generated necrogenic alterations in the chromatin structure of *S. pombe*.

Materials and Methods

Materials and Solutions

The metal salt potassium dichromate ($\text{K}_2\text{Cr}_2\text{O}_7$) of analytical grade was purchased from Reanal, Budapest, Hungary. A stock solution of potassium dichromate was freshly prepared in distilled water and filter sterilized (pore size 0.22 μm) prior to addition to cell-culture media. 6-diamidino-2-phenylindole dihydrochloride (DAPI), 1,4-diazabicyclo-(2,2,2)-octane (DABCO) and other reagents were purchased from Sigma–Aldrich (Budapest, Hungary). Antifade medium consisted of 90% glycerol, 2% (w/w) 1,4-diazobicyclo-(2,2,2)-octane, 20 mM Tris–Cl, pH 8.0, 0.02% sodium azide, and 25 ng/ml DAPI. Swelling buffer consisted of 50 mM KCl, 10 mM MgSO_4 , 3 mM dithiothreitol, and 5 mM NaPO_4 ($\text{Na}_2\text{HPO}_4/\text{NaH}_2\text{PO}_4$) buffer, pH 8.0. Fixative solution contained methanol:glacial acetic acid (3:1). The protoplasting solution that was filter sterilized consisted of 0.6 M KCl.

Cell Growth

The fission yeast *S. pombe* auxotrophic and heterothallic strain (lys1-131, h^+) designated CW-6 and later *6chr*⁺ was used (Pesti et al. 1981; Czakó-Vér et al. 1999). It is a well characterized *6chr*⁺ strain of *S. pombe*. The main characteristics of the *6chr*⁺ strain are: generation time 2.24 h, minimal inhibitory concentrations of CrO_4^{2-} , Cd^{2+} , Cu^{2+} , Zn^{2+} and Ni^{2+} were relatively high, 225, 1250, 3500, 2500, and 750 μM , respectively. 65% of $^{51}\text{CrO}_4^{2-}$ was taken up within 30 min from the surrounding solution which contained 75 μM Cr(VI), and 750 $\mu\text{g/g}$ dry biomass of total Cr was accumulated within 8 min. The organically bound chromium was 250 $\mu\text{g/g}$ dry biomass within 2 h in lysine starved medium (Czakó-Vér et al. 2004). It does not exhibit adaptation processes to Cr(VI); glutathione (GSH) content is 58 ± 11.0 nmol (mg protein)⁻¹. Specific activity of its antioxidant enzymes and quantity of reactive oxygen species under uninduced conditions have been published (Pesti et al. 2002; Gazdag et al. 2003).

S. pombe cells were cultured in a 3.33-Hz incubator shaker at 30°C in complete liquid medium (YEL). The medium contained 0.5% yeast extract, 3% glucose, 175 $\mu\text{g ml}^{-1}$ lysine, pH 5.6. Medium was solidified with 2% agar (YEA) (Moreno et al. 1991).

Toxicity of Cr (VI) on S. Pombe

The cells were precultured overnight in YEL medium (resulting in exponential-phase culture and washed twice by centrifugation (600 g, 5 min). They were recultured in fresh YEL medium. The cells were started at a density sufficient to produce an OD_{595} of 0.05 and cultivated for 12 h. These mid-log-phase cells were used to determine the survival rates of cells exposed to the $\text{K}_2\text{Cr}_2\text{O}_7$ (1–500 μM) as estimated according to Lee et al. (1995).

Preparation of Protoplasts

Mid-log-phase cells were collected by centrifugations and washed twice with 0.6 M KCl solution. For protoplast formation, the suspensions were incubated for 20 min at 30°C in protoplasting solution that contained 10 mg/ml lyophilized enzyme prepared from *Trichoderma harzianum* (Sigma-Aldrich, Budapest, Hungary) in 0.6 M KCl as osmotic stabilizer. After incubation the protoplasts were washed twice in stabilizer solution and were treated with $\text{K}_2\text{Cr}_2\text{O}_7$ (0, 1, 10, 50, 75, 100, 200 μM) for 24 h.

Isolation and Visualization of Large Scale Chromatin Structures

Details of these procedures have been described in the Methods of Chap. 6 as: Isolation of Nuclei, Spreads of Nuclear Structures, and Visualization of Chromatin Structures.

Results

Visualization of Interphase Chromatin Structures of S. Pombe

Originally we used reversibly permeabilized mammary cells to visualize interphase chromatin structures. By reversing permeabilization, it was possible to confirm the existence of a flexible chromatin folding pattern through a series of

transient geometric forms referred to as decondensed fibrillar, supercoiled ribboned forms, chromatin bodies, thin and thick fibers and elongated chromosomes (Gacsi et al. 2005). It was confirmed that chromatin condensation in nuclei of exponentially growing mammalian cells (Indian Muntjac, CHO, murine preB, K562 erythroleukemia) started with the polarization of the nuclear material (Banfalvi et al. 2006).

To visualize chromatin structures in untreated yeast cells, DAPI staining showed the oval shaped nucleus (Fig. 8.1Cn). Overexposure revealed the shape of the same *S. pombe* cell (Fig. 8.1Ch). Chromatin structures were isolated from protoplasts of exponentially growing *S. pombe*. Although, in these experiments most of the cells were in S phase, they represented different stages of chromatin compaction (Fig. 8.1a–q). The elongated shape of the nucleus (Fig. 8.1a, b) gradually rounded up and became polarized, with increased fluorescent intensity indicating local condensation of the fibrillary chromatin veil (Fig. 8.1c, d). Supercoiling of the veiled chromatin led to the formation of chromatin ribbon (Fig. 8.1e–h) with large coils corresponding to individual chromosomes, referred to as chromatin bodies (Fig. 8.1g, h). That chromatin is a continuous structure is reflected by Fig. 8.1j–m, with two ends (Fig. 8.1l, m). The linear forms of condensed structures resemble mammalian chromosomes, but their compaction did not reach that of the metaphase chromosomes of mammalian cells (Fig. 8.1n–q). The images of chromatin condensation observed in Fig. 8.2 indicate that this process is more simple in *S. pombe* cells than in mammalian cells. No forms resembling highly-condensed mammalian metaphase chromosomes are observed. This is not surprising in regard to the evolutionary distance in molecular phylogenetics of the organisms in question.

Cellular Toxicity of Cr(VI)

To prove the concentration dependent cellular toxicity two mid-log-phase cell cultures were grown starting at 10^7 cells/ml in the presence of 225 and 500 μM $\text{K}_2\text{Cr}_2\text{O}_7$ at 30°C . Triplicate samples (10^6 each) were taken from cultures at 0, 20, 40 and 60 min to reach about 90% inhibition of growth. The survival rate of *S. pombe* can be seen in Fig. 8.2a.

In the next series of experiments cells were incubated in the presence of 1–500 μM $\text{K}_2\text{Cr}_2\text{O}_7$ for 60 min. The control culture was not subjected to Cr treatment. Subtoxic levels of dichromate (<1 μM) did not cause noticeable changes in viability (not shown). Thus the growth rate was tested at higher concentrations in the presence of 1, 10, 50, 100, 200 and 500 μM $\text{K}_2\text{Cr}_2\text{O}_7$ resulting in cell loss corresponding to 22, 41, 63, 76, 79 and 91%, respectively (Fig. 8.2b). From these data the estimated MIC50 concentration of $\text{K}_2\text{Cr}_2\text{O}_7$ is 15 μM , a clear indication that dichromate (Cr(VI)) is much more toxic than chromate (Cr(III)) with an estimated 225 μM MIC50 for K_2CrO_4 .

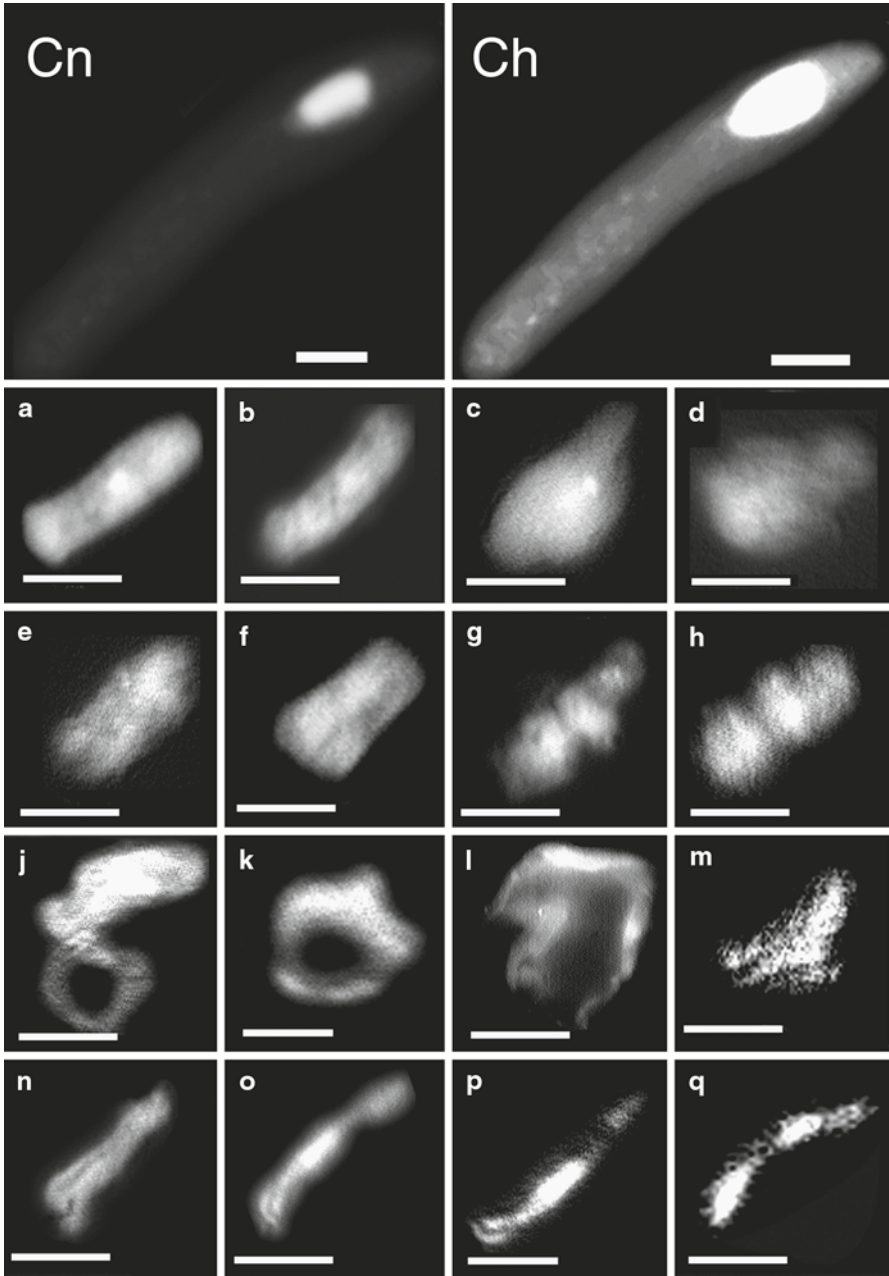


Fig. 8.1 Intermediates in the condensation of *S. pombe* chromatin. Protoplasts were prepared from exponentially growing cells. **Cn** Control nucleus is a *S. pombe* cell stained with DAPI. **Ch** Control hypha, the same *S. pombe* cell overexposed to visualize the whole cell. Nuclei were isolated from protoplasts, spread over glass slides and stained with DAPI. The images of frequently seen patterns were selected to illustrate: **a, b** decondensed chromatin that maintained the oval shape of the nucleus in the cell. **c, d** Rounded up and polarized chromatin. **e–h** Chromatin ribbon formation. **g, h** Chromatin bodies, the earliest visible forms of interphase chromosomes. **j–m** Early elongated chromosomal forms. **n–q** Bent and linear forms of condensed chromosomes. Bar, 10 μ m each

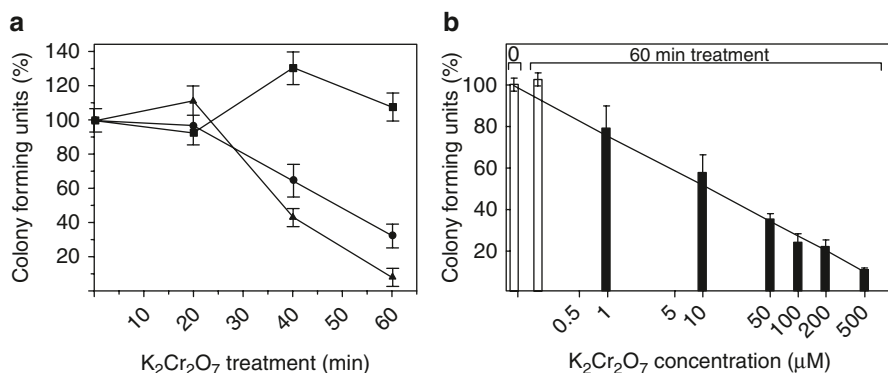


Fig. 8.2 Dose-dependent loss in viability of *S. pombe* upon treatment with Cr(VI). **a** Colony forming units of control cells (■-■) and after treatment with 225 (●-●) and 500 μM (▲-▲) Cr(VI). **b** The growth of seven cell cultures was started at 10^6 cells/ml, one in the absence and six cultures in the presence of 1, 10, 50, 100, 200 and 500 μM, respectively. The control sample (*white columns*) represented the untreated cell population at 0 and 60 min. After treatment with Cr(VI) (*black columns*) at different concentrations the cell number was counted in each population. In the representation the abscissa is showing the Cr(VI) concentration and the ordinate the colony forming units. The 0 h control was taken as 100%

Apoptotic Chromatin Changes at Low Cr(VI) Concentration (10–50 μM)

Density changes in chromatin structure at subtoxic concentration (1 μM) of Cr(VI) were observed occasionally, but these changes occurred infrequently and are therefore not presented.

Apoptotic chromatin changes at low concentrations (10 or 50 μM) of Cr(VI) were observed and the gradual aggravation of apoptosis could be seen. In the presence of 10 μM concentration of Cr(VI) three major changes took place (Fig. 8.3, left panels): (a) the polarization and disintegration of the nuclear material (Fig. 8.3, left panels a–d, and g–h), (b) the expansion of the fibrillary chromatin with a few small apoptotic bodies inside (Fig. 8.3, left panels e and f), and (c) the formation of large apoptotic bodies (Fig. 8.3, left panels, h–k). Due to the stickiness of the nuclear material it did not fall apart to apoptotic bodies upon treatment with 50 μM Cr(VI), only the shrinkage of nuclei could be observed (Fig. 8.3, right panels a–k).

Necrotic Chromatin Changes at Higher Cr(VI) Concentration

The necrotic nuclear effect of 75, 100 and 200 μM Cr(VI) seen in Fig. 8.4 represents the first morphological visualization of yeast chromatin changes upon ne-

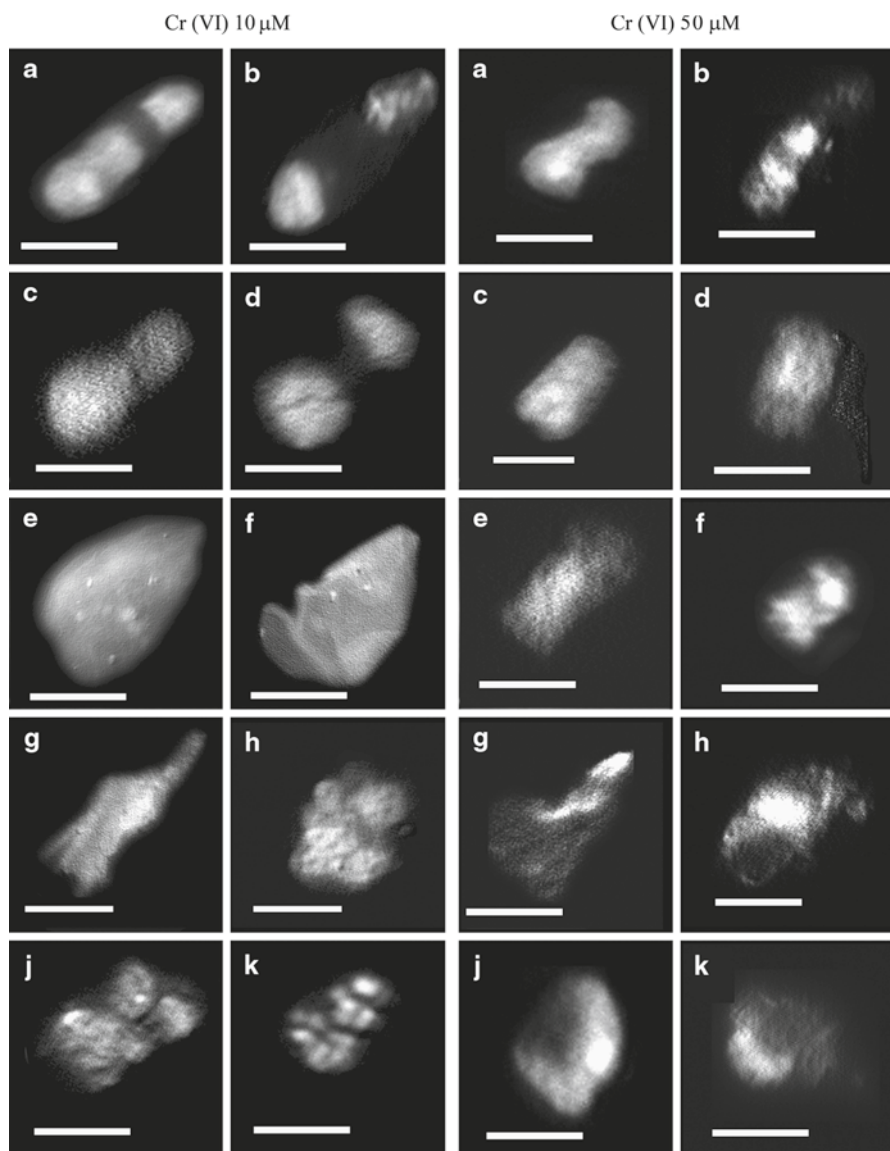


Fig. 8.3 Appearance of apoptotic chromatin bodies upon treatment of 10 and 50 μ M potassium dichromate. The Cr(VI) treatment was followed by preparation of protoplast and isolation of nuclei. Chromatin structures were stained with DAPI and visualized as described in the Methods. Bar 10 μ m each

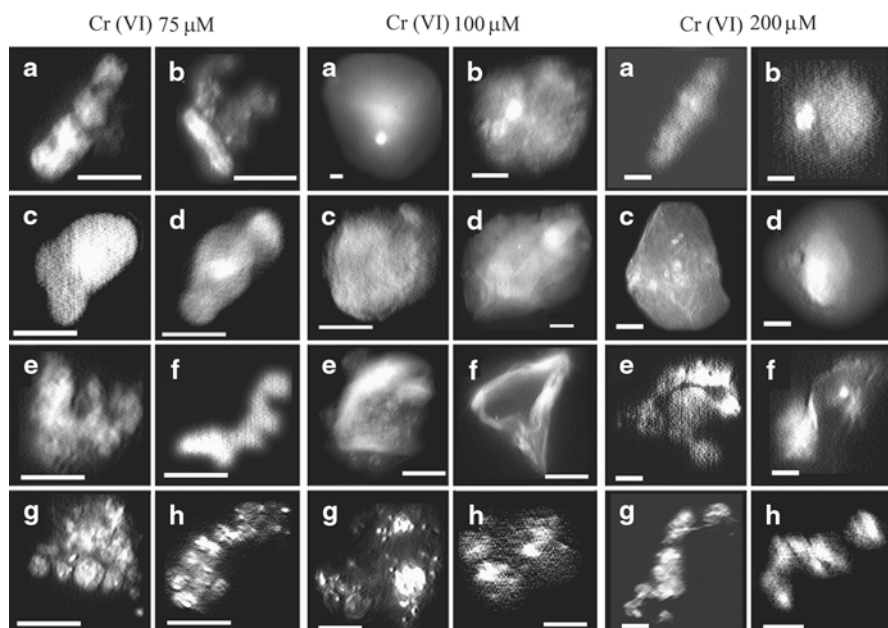
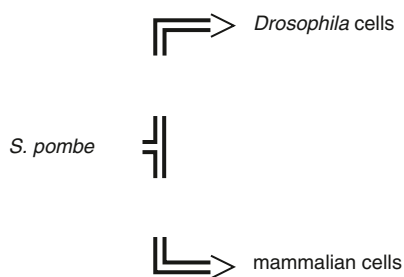


Fig. 8.4 Enlargement of nuclei after treatment with necrotic concentration of Cr(VI). Cells were treated with 75, 100 and 200 μM potassium dichromate. The rest of the procedures were the same as given in Fig. 8.2 and detailed in the Methods. Bar 10 μm each

crotic treatment. Figure 8.4 (left panels, a–d) demonstrates that the enlargement upon 75 μM Cr(VI) was due to the generation of fibrillary chromatin inside the nucleus. The nucleus did not fall apart and maintained its structure. The opening of the nucleus revealed that the nuclear material has two ends and the chromatin is a continuous structure (Fig. 8.4, left panels e, f). Occasionally the chromatin was fragmented to large apoptotic bodies (Fig. 8.4, left panels g, h), reflecting a mixed (apoptotic-necrotic) type of cell death. At higher (100 μM Cr(VI)) concentration high focal density of chromatin and simultaneously the extremely enlarged fibrillar chromatin formation dominated the picture (Fig. 8.4, middle panels a–f). The three chromosomes of *S. pombe* can be distinguished in the middle panels (Fig. 8.4g, h), but highly condensed structures resembling metaphase chromosomes of mammalian cells could not be seen. At 200 μM Cr(VI) concentration the same necrotic tendency was observed (Fig. 8.4, right panels) with extremely enlarged fibrillar chromatin and the lack of highly condensed chromosomes. Some compaction is seen in the right panels of Fig. 8.4e–g. Highest compaction of the three chromosomes of *S. pombe* is seen in the lower right corner of Fig. 8.4h. None of the chromosomes seen in control cells or after Cr(VI) treatment reached the compaction of metaphase mammalian cells.

Discussion

Morphological chromatin studies of fungal cells including the fission yeast *S. pombe* are missing. Our goals were to visualize large-scale chromatin structures of interphase *S. pombe* cells and to clarify whether these structures are similar to those seen in mammalian (Banfalvi et al. 2006), and in *Drosophila* nuclei (Banfalvi 2008) and how these structures are modified upon Cr(VI) treatment. Experiments revealed that the intermediates of chromatin condensation are similar to mammalian cells involving the fibrillary chromatin veil, the formation of chromatin ribbon and the earliest visible interphase chromosomes referred to as chromatin bodies, elongated linear chromosomes and condensed chromosomes. It is worthy of mention that compact chromosomes that would correspond to the metaphase chromosomes of mammalian cells were not seen, indicating that the pattern of chromosome condensation differs to some extent from the common pathway of chromosome condensation in mammalian nuclei (Banfalvi et al. 2006). In the higher arthropod eukaryote *Drosophila* the presence of many small subchromosomal particles indicated that chromosomes of *Drosophila* cells consisted of smaller units called rodlets, providing flexibility to condensing chromosomes (Banfalvi 2008). Such small chromosomal subunits were not visible in *S. pombe*. These differences in chromatin condensation point to an evolutionary tendency:



indicating that *Drosophila* and mammalian chromosome folding went in different directions.

The chromatin structures found in control, untreated *S. pombe* cells were compared to those seen after genotoxic treatment with increasing concentrations of Cr(VI) ions. The oxidation states of chromium range from Cr(II) to Cr(VI), with the trivalent and hexavalent states being the most stable and common in terrestrial environments (Katz and Salem 1994). That Cr(VI) is about 15-times more toxic than Cr(III) in *S. pombe* can be seen from their MIC50 values estimated to be 15 and 225 μM , respectively. As the biosorption of Cr(VI) by the cell wall and plasma membrane of yeasts and fungi is likely to be accompanied by its reduction ($\text{Cr(VI)} \rightarrow \text{Cr(V)} \rightarrow \text{Cr(IV)} \rightarrow \text{Cr(III)}$), the uptake of Cr(VI) is also the most important step in the detoxification of the most toxic dichromate. Cr(VI) is not only more toxic than Cr(III) but also a potent carcinogen that causes most adverse health effects (National Institute of Occupational Safety and Health 1975; Tandon 1982; Bianchi et al. 1983; IARC 1990; Cervantes et al. 2001; Dayan and Paine 2001). In cells, the complex forming Cr(III) ions interact with microfilaments, mitochondria, lysosomes and nucleus and interfere with signalling path-

ways through the inducement of oxidative stress. The intracellular Cr(VI) reduction results in Cr(V/VI) complexes and various organic radicals which are all potential DNA-damaging agents. The three electron transfer steps from Cr(VI) to Cr(III) generates reactive oxygen species quite effectively via depleting of GSH and inducing hydroxyl radicals, superoxide anions and H₂O₂ during re-oxidation processes. The electron transfer taking place through the Fenton-type Haber–Weiss reactions is initiating a chain-reaction, which has been proposed as the probable cause of multiple cellular damages underlying complex toxicity and carcinogenicity of heavy metals including Cr(VI). Cr(VI) is known to accumulate mainly in the cytosolic compartment (Ksheminska et al. 2005; Ghareeb and Gadd 1998) and causes cellular changes on the cell surface (Mutter et al. 2001). The genomic consequences of the oxidative stress caused by Cr(VI) are not known, yet. The final outcome of cellular toxicity of Cr(VI) was in some cases apoptosis, but more often necrosis (Rudolf and Cervinka 2003; Poljsak et al. 2010). We confirm this observation, treatment with lower concentrations of Cr(VI), that was expected to induce apoptosis, did not generate many small, rather fewer and larger apoptotic bodies.

As far as the effect of Cr on chromatin structure is concerned, it was reported to bind to DNA, nuclear proteins, and ribonucleoproteins in liver and kidney cells. A much smaller proportion of the Cr bound to chromatin was associated with the DNA after treatment with Cr(III) than with Cr(VI) (Cupo and Wetterhahn 1985). Preferential binding of Cr to guanine has been observed upon incubation of Cr(VI) with homopolyribonucleotides in the presence of a microsomal-metabolizing system (Tsapakos et al. 1983). The interaction of Cr with the phosphate groups of nucleotides is believed to be electrostatic. The nature of the chromium:guanine interaction has not been determined. DNA damage was found only after Cr(VI) treatment and only certain types of Cr-DNA complexes formed after administration of Cr(VI) produced lesions in the DNA that were detectable, suggesting that not all types of Cr-DNA complexes produce DNA lesions (Tsapakos and Wetterhahn 1983). The electrostatic interactions of Cr(VI) with nucleotides would indicate that the cross-linking could be reversible. That this might be the case is reflected by experiments on chick embryo hepatocytes treated with Cr(VI) at concentrations that did not affect cell viability. Reversible cross-linking might be the cause that in low concentration of Cr(VI), corresponding to the tolerable levels of Cr(VI) in water (1 μM) this heavy metal did not change significantly the viability of cells and the chromatin structure was also similar to the control cells. In conformity with these observations DNA strand breaks and interstrand cross-links were completely repaired. Little or no DNA damage remained in the liver 10–24 h after Cr(VI) injection into chick embryos (Hamilton and Wetterhahn 1986), while DNA-protein crosslinks in the kidney of rats persisted for a somewhat longer period (40 h) of time (Tsapakos et al. 1983). The sequential recruitment and cooperation of mismatch repair proteins in processing of Cr-DNA cross-links is regarded as the main cause of double-strand breaks and chromosomal breakage at low and moderate Cr(VI) doses (Reynolds et al. 2009).

Recent data provided evidence for a three-step cross-linking mechanism involving the reduction of Cr(VI) to Cr(III), the Cr(III)-DNA binding, and the protein

capture by DNA-bound Cr(III) generating protein-Cr(III)-DNA cross-links (Macfie et al. 2010). Cr cross-links histone deacetylase 1-DNA methyltransferase 1 complexes to *Cyp1a1* promoter chromatin and inhibits histone marks (Schnekenburger et al. 2007). Cross-linking of proteins is likely to perturb normal chromatin structure regulation and remodeling, causing the disruption of gene expression regulatory patterns (Shumilla et al. 1999; Majumder et al. 2003; O'Brien et al. 2003; Reynolds et al. 2004). The protein cross-linking of Cr(VI) is expected to expand the nuclear structure and this could be reflected in the chromatin structure upon Cr(VI) treatment. In conformity with this idea we have seen the enlargement of the fibrillary chromatin in nuclei of *S. pombe* cells exposed to Cr(VI) in a concentration-dependent manner between 75–200 μM $\text{K}_2\text{Cr}_2\text{O}_7$. Although, the enlargement of the nuclear material reflected necrosis, the fine fibrillary structure may be due to the cross-linking of Cr(VI) or its reduced species and the non-standard apoptotic changes at lower Cr(VI) concentrations. The final outcome of chromatin changes is that the chromatotoxic effect of Cr(VI) is neither a typical apoptotic- nor a necrotic-type of cell death.

Conclusions

To summarize the morphological effects of Cr(VI), the similarities with the necrotic agent Hg^{2+} at 100 μM concentration and apoptotic ultraviolet irradiation are pointed out. Upon mercury treatment of K562 human erythroleukemia cells: (a) the cellular and nuclear size increased, (b) the enlargement of the nucleus was due to the generation of large holes, (c) the nucleus did not fall apart, its round structure was maintained (d) the opening of nuclei resembling horseshoes demonstrated that the nuclear material has two ends and the chromatin maintained its continuous structure (Farkas et al. 2010).

One could argue that there are only two major types of cell deaths and they are classified based on one criterion only, which is nuclear morphology highly similar regardless of genotoxic agent applied. However, interphase chromatin structures have not been analysed earlier. We have found that different genotoxic agents affect chromatin condensation and cause various topological DNA changes. These alterations are potential indicators of cytotoxicity and cell death can be categorized by the type of the genotoxic agent. The data on chromatotoxicity upon cadmium, gamma treatment and ultraviolet light irradiation (Banfalvi 2009), mercury (Farkas et al. 2010) and cyanotoxin treatment (Gacsi et al. 2009) and experiments presented in this chapter support the notion that: (a) similar to multicellular organisms, the cells of fission yeast also die in many ways, (b) apoptotic and necrotic events may overlap depending on cell type and genotoxic concentration, and (c) genotoxic agents can be categorized by fingerprinting the injury-specific chromatin changes.

Acknowledgement This work was supported by the OTKA grant T042762 (G.B.).

References

- Bailar JC (1997) Chromium. In: Parker SP (ed) McGraw-Hill Encyclopedia of science and technology, vol 3, 8th edn. McGraw-Hill, New York
- Banfalvi G (2008) Chromatin fiber structure and plectonemic model of chromosome condensation in *Drosophila* cells. DNA Cell Biol 27:65–70
- Banfalvi G (2009) Chapter V. Apoptotic chromatin changes. Apoptotic chromatin changes. Springer Science, Heidelberg, pp 293–364
- Banfalvi G, Nagy G, Gacsi M, Roszer T, Basnakian AG (2006) Common pathway of chromosome condensation in mammalian cells. DNA Cell Biol 25:295–301
- Bianchi V, Celotti L, Lanfranchi G, Majone F, Marin G, Montaldi A, Sponza G, Tamino G, Venier P, Zantedeschi A, Levis AG (1983) Genetic effects of chromium compounds. Mutat Res 117:279–300
- Cefalu WT, Wang ZQ, Zhang XH, Baldor LC, Russell JC (2002) Oral chromium picolinate improves carbohydrate and lipid metabolism and enhances skeletal muscle Glut-4 translocation in obese, hyperinsulinemic (JCR-LA corpulent) rats. J Nutr 132:1107–1114
- Cervantes C, Campos-García J, Devars S, Gutiérrez-Corona F, Loza-Tavera H, Torres-Guzmán JC, Moreno-Sánchez R (2001) Interactions of chromium with microorganisms and plants. FEMS Microbiol Rev 25:335–347
- Costa M (2003) Potential hazards of hexavalent chromium in our drinking water. Toxicol Appl Pharmacol 188:1–5
- Cupo DY, Wetterhahn KE (1985) Binding of chromium to chromatin and DNA from liver and kidney of rats treated with sodium dichromate and chromium(III) chloride *in vivo*. Cancer Res 45:1146–1151
- Czakó-Vér K, Batie M, Raspor P, Sipiczki M, Pesti M (1999) Hexavalent chromium uptake by sensitive and tolerant mutants of *Schizosaccharomyces pombe*. FEMS Microbiol Letts 178:109–115
- Czakó-Vér K, Koósz Z, Antal J, Rác T, Sipiczki M, Pesti M (2004) Characterization of chromate-sensitive and -tolerant mutants of *Schizosaccharomyces pombe*. Folia Microbiol 49:31–36
- Dayan AD, Paine AJ (2001) Mechanisms of chromium toxicity, carcinogenicity and allergenicity: review of the literature from 1985 to 2000. Hum Exp Toxicol 20:439–451
- Farkas E, Ujvarosi K, Nagy G, Posta J, Banfalvi G (2010) Apoptogenic and necrogenic effects of mercuric acetate on the chromatin structure of K562 human erythroleukemia cells. Toxicol in vitro 24:267–275
- Fornace AJ, Seres DS, Lechner JF, Harris CC (1981) DNA-protein cross-linking by chromium salts. Chem Biol Interact 36:345–354
- Gacsi M, Nagy G, Pinter G, Basnakian AG, Banfalvi G (2005) Condensation of interphase chromatin in nuclei of Chinese hamster ovary (CHO-K1) cells. DNA Cell Biol 24:43–53
- Gacsi M, Antal O, Vasas G, Mathe C, Borbely G, Saker LM, Gyori J, Farkas A, Vehovszky A, Banfalvi G (2009) Comparative study of cyanotoxins affecting cytoskeletal and chromatin structures in CHO-K1 cells. Toxicol in vitro 23:710–718
- Gazdag Z, Pócsi I, Belágyi J, Emri T, Blaskó Á, Takács K, Pesti M (2003) Chromate tolerance caused by reduced hydroxyl radical production and decreased glutathione reductase activity in *Schizosaccharomyces pombe*. J Basic Microbiol 43:96–103
- Ghahrehab MM, Gadd GM (1998) Evidence for the involvement of vacuolar activity in metal(loid) tolerance: vacuolar-lacing and -defective mutants of *Saccharomyces cerevisiae* display higher sensitivity to chromate, tellurite and selenite. BioMetals 11:101–106
- Hamilton JW, Wetterhahn KE (1986) Chromium (VI)-induced DNA damage in chick embryo liver and blood cells *in vivo*. Carcinogenesis 7:2085–2088. <http://www.lenntech.com/periodic/elements/cr.htm#ixzz0TG3y1SQj>
- International Agency for Research on Cancer (IARC) (1990) IARC monograph on the evaluation of carcinogenic risk to humans from chromium, nickel and welding. Lyon, France

- Katz A, Salem H (1994) The biological and environmental chemistry of chromium. VCH Publishers, New York
- Köster A, Beyersmann D (1985) Chromium binding by calf thymus nuclei and effects on chromatin. *Toxicol Environ Chem* 10:307–313
- Ksheminska H, Fedorovych D, Babyak L, Yanovych D, Kaszycky P, Koloczek H (2005) Chromium(III) and (VI) tolerance and bioaccumulation in yeast: a survey of cellular chromium content in selected strains of representative genera. *Process Biochem* 40:1565–1572
- Lee J, Dawes IW, Roe JH (1995) Adaptive response of *Schizosaccharomyces pombe* to hydrogen peroxide and menadione. *Microbiol* 141:3127–3132
- Macfie A, Hagan E, Zhitkovich A (2010) Mechanism of DNA-protein cross-linking by chromium. *Chem Res Toxicol* 23:341–347
- Majumder S, Ghoshal K, Summers D, Bai S, Datta J, Jacob ST (2003) Chromium(VI) down-regulates heavy metal-induced metallothionein gene transcription by modifying transactivation potential of the key transcription factor, metal-responsive transcription factor 1. *J Biol Chem* 278:26216–26226
- Mills D, McCluskey K (1990) Electrophoretic karyotypes of fungi: the new cytology. *Mol Plant-Microb Interact* 3:351–357
- Moreno S, Klar A, Nurse P (1991) Molecular genetic analysis of fission yeast *Schizosaccharomyces pombe*. *Methods Enzymol* 194:795–826
- Munz P, Wolf K, Kohli J, Leupold V (1989) Genetics overview. In: Nasim A, Young P, Johnson BF (eds) *Molecular Biology of Fission Yeast*, Academic, New York, pp 1–30
- Mutter O, Patmalnieks A, Rapoport A (2001) Interrelation of the yeast *Candida utilis* and Cr(VI): metal reduction and its distribution in the cell and medium. *Proc. Biochem* 36:963–970
- National Institute of Occupational Safety and Health (1975) Biological effects of exposure. Criteria for a recommended standard: Occupational exposure to chromium VI. Washington DC, U.S. Department of Health, Education and Welfare, pp 23–121
- Newlon CS (1988) Yeast chromosome replication and segregation. *Microbiol Rev* 52:568–601
- Nishioka H (1975) Mutagenic activities of metal compounds in bacteria. *Mutat Res* 31:185–189
- O'Brien TJ, Ceryak S, Patierno SR (2003) Complexities of chromium carcinogenesis: role of cellular response, repair and recovery mechanisms. *Mutat Res* 533:3–36
- Pekkala DH, Silver JC (1990) Characterization and nucleosomal-core localization of *Achlya* histones involved in stress-induced chromatin condensation. *Exp Cell Res* 187:16–24
- Pesti M, Novak EK, Ferenczy L, Svoboda A (1981) Freeze fracture electron microscopical investigation of *Candida albicans* cells sensitive and resistant to nystatin. *Sabouraudia* 19:17–26
- Pesti M, Gazdag Z, Emri T, Farkas N, Koós Z, Belágyi J, Pesti M (2002) Chromate sensitivity in fission yeast is caused by increased glutathione reductase activity and peroxide overproduction. *J Basic Microbiol* 42:408–419
- Petrilli FL, Flora SD (1977) Toxicity and mutagenicity of hexavalent chromium on *Salmonella typhimurium*. *Appl Environ Microbiol* 33:805–809
- Poljsak B, Pócsi I, Pesti M (2010) Interference of chromium with cellular functions. *J Basic Microbiol* 50:21–36
- Reynolds M, Peterson E, Quievryn G, Zhitkovich A (2004) Human nucleotide excision repair efficiently removes chromium-DNA phosphate adducts and protects cells against chromate toxicity. *J Biol Chem* 279:30419–30424
- Reynolds ME, Peterson-Roth EC, Bepalov IA, Johnston T, Gurel VM, Menard HL, Zhitkovich A (2009) Rapid DNA double-strand breaks resulting from processing of Cr-DNA cross-links by both MutS dimers. *Cancer Res* 69:1071–1079
- Rudolf E, Cervinka M (2003) Chromium(III) produces distinct type of cell death in cultured cells. *Acta Med* 46:139–146
- Ryan MP, Williams DE, Chater RJ, Hutton BM, McPhail DS (2002) Why stainless steel corrodes? *Nature (London)* 415:770–774
- Schnekenburger M, Talaska G, Puga A (2007) Chromium cross-links histone deacetylase 1-DNA methyltransferase 1 complexes to chromatin, inhibiting histone-remodeling marks critical for transcriptional activation. *Mol Cell Biol* 27:7089–7101

- Sharma DC, Chatterjee C, Sharma CP (1995) Chromium accumulation and its effects on wheat (*Triticum aestivum* L. cv. HD 2204) metabolism. *Plant Sci* 111:145–151
- Shumilla JA, Broderick RJ, Wang Y, Barchowsky A (1999) Chromium(VI) inhibits the transcriptional activity of nuclear factor-kappaB by decreasing the interaction of p65 with cAMP-responsive element-binding protein-binding protein. *J Biol Chem* 274:36207–36212
- Tandon SK (1982) Organ toxicity of chromium in animals. In: Langard S (ed) *Nucleoli of normal-land regenerating rat liver with special reference to the different biological and environmental aspects of chromium*. Elsevier/North-Holland Biomedical Press, Amsterdam, pp 209–220
- Tsapakos MJ, Wetterhahn KE (1983) The interaction of chromium with nucleic acids. *Chem Biol Interact* 46:265–277
- Tsapakos MJ, Hampton TH, Wetterhahn KE (1983) Chromium(VI)-induced DNA lesions and chromium distribution in rat kidney, liver, and lung. *Cancer Res* 43:5662–5667
- United States Environmental Protection Agency (US EPA) (1998) *United States Environmental Protection Agency (US EPA), Toxicological review of hexavalent chromium (CAS No. 18540-29-9)*. US EPA, Washington DC
- Venitt S, Levy LS (1974) Mutagenicity of chromates in bacteria and its relevance to chromate carcinogenesis. *Nature (London)* 250:493–495
- Warren G, Schultz P, Bancroft D, Bennett K, Abbott EH, Rogers S (1981) Mutagenicity of a series of hexacoordinate chromium (III) compounds. *Mutat Res* 90:111–118
- Wiegand HJ, Ottenwalder H, Bolt HM (1984) The reduction of chromium(VI) to chromium(II) by glutathione: an intracellular redox pathway in the metabolism of the carcinogen chromate. *Toxicology* 33:341–348
- Xu XR, Li HB, Gu J-D (2004) Reduction of hexavalent chromium by ascorbic acid in aqueous solutions. *Chemosphere* 57:609–613
- Xu XR, Li HB, Gu J-D, Li XY (2005) Kinetics of the reduction of chromium (VI) by vitamin C. *Environ Toxicol Chem* 24:1310–1314

Chapter 9

Chromatin Changes upon Silver Nitrate Treatment in Human Keratinocyte HaCaT and K562 Erythroleukemia Cells

Gábor Nagy, Melinda Turáni, Katalin Éva Kovács and Gáspár Bánfalvi

Abstract Inhibition of cellular growth of silver nitrate was tested in two different mammalian cell lines: in HaCaT keratinocyte and K562 erythroleukemia cell cultures resulting in 6.4 and 3.5 μM AgNO_3 MIC50 values, respectively. Fluorescent microscopic visualization of large-scale chromatin structures revealed that after AgNO_3 treatment at low concentrations ($<1 \mu\text{M}$), regarded earlier as subtoxic levels, chromatin changes were early signs of cytotoxicity especially with K562 cells. Typical nuclear changes induced by silver nitrate involved (a) the polarization of precondensed and the extrusion of decondensed chromatin seen as chromatin tails, (b) the tail (“comet”) formation was dependent on silver nitrate concentration, (c) K562 erythroleukemia cells were more susceptible to silver nitrate (0.5–5 μM) treatment, than HaCaT cells, (d) elevated silver nitrate concentrations (10–15 μM) caused nuclear shrinking with an infrequent formation of apoptotic bodies, (e) higher Ag^+ concentrations (20–50 μM) allowed the expansion of the nuclear material without necrotic disruptions. The chromatin tail formation could be accounted for by a decrease in chromatin supercoiling related to a dose dependent reduction of ATP content, cell viability and increased production of reactive oxygen species.

Introduction

The administration of dilute solutions of silver nitrate in the drinking water of rodents was tolerated for months with no visible signs of toxicity. After several months of treatment due to the affinity of silver to cell membranes, tissues became laden with silver and deposited permanently as silver sulfide in many tissues and organs (Westhofen and Schafer 1986). Similarly, industrial workers exposed to

G. Bánfalvi (✉)

Department of Microbial Biotechnology and Cell Biology,
University of Debrecen, 1 Egyetem Square, 4010 Debrecen, Hungary
Tel.: +36-52-512-900
Fax: +36-52-512-925
e-mail: bgaspar@delfin.klte.hu

chronic ingestion, inhalation, or dermal absorption of silver developed argyria, a gray or blue-gray, permanent discoloration of the skin. Silver nitrate is darkened by sunlight or contact with organic matter such as the skin. This discoloration has been exploited by using silver nitrate as a vital stain, to mark cells in order to follow their subsequent migration by the colored inclusions. The medical use of silver nitrate made it a powerful antimicrobial agent on the one hand. Despite the intensive use of AgNO_3 in commercial products, there is a serious lack of information concerning the toxicity and cellular responses to silver nitrate. In contrast, the toxic accumulation of silver in cells degraded silver nitrate to a Janus-faced molecule. This dichotomy initiated further investigations into the role of silver nitrate in mammalian cell toxicology to consider both sides of the coin.

Not only the *in vitro* germicidal testing and standardization of silver compounds remains to be solved (Chopra 2007). The *in vitro* toxicity of silver ions on eukaryotic cells is equally contradictory. It was shown that silver nitrate inhibited the growth of fibroblasts (Liedberg and Lundeberg 1989), hepatocytes (Baldi et al. 1988), and lymphocytes (Hussain et al. 1992). The cytotoxicity caused approximately 76% fibroblast growth inhibition at 40 μM AgNO_3 concentration and contact time of 2 h. Lower (4–20 μM) silver nitrate concentrations were also cytotoxic to human dermal fibroblasts (Hidalgo et al. 1998; Hidalgo and Domínguez 1998). In contrast anodically generated silver ions had no impact on mammalian cells in culture (Hall et al. 1988). Others made similar observations and did not find tissue toxicity in clinical evaluations (Cooms and Wan 1992). Similarly, no evidence was provided that would have linked silver ions to toxicity (Demling and DeSanti 2001). These conflicting observations necessitated further investigations with respect to the *in vitro* cellular toxicity of silver nitrate on mammalian cells.

Cadmium as one of the most toxic heavy metals affected both replicative and repair DNA synthesis. DNA replication was suppressed and in contrast repair synthesis increased. The maximum and minimum values of these S-phase checkpoints varied in agreement with our notion that different types of DNA damages affect different S subphase replication and repair checkpoints (Banfalvi et al. 2000). The most sensitive and characteristic effect of Cd was observed at the level of chromatin condensation seen as large extensive disruptions and holes in the nuclear membrane and sticky incompletely folded chromosomes both in CHO and in murine pre B cells (Banfalvi et al. 2005, 2007; Chap. 6). The fact that Cd generated typical transitory forms of chromatin condensation in different mammalian cells (Banfalvi et al. 2006), but differed from the chromatotoxic effect of Hg (Farkas et al. 2010) indicated that different genotoxic agents are specific to the heavy metal. Based on this working hypothesis the aim of this chapter is to test, whether or not silver nitrate (i) has *in vitro* toxicity on mammalian (HaCaT, K562) cells, (ii) exerts chromatotoxicity, and if it does, (iii) whether these chromatin changes are characteristic to Ag^+ . Here we describe that AgNO_3 treatment initiates chromatin decondensation without characteristic signs of apoptosis or necrosis and blocks the condensation process at the stage of chromatin ribbon formation. The chapter confirms the notion that the genotoxic effect of heavy metals can be distinguished and categorized based on the assessment of injury-specific chromatin changes.

Materials and Methods

Chemicals and Reagents

Silver nitrate (AgNO_3) was obtained from Sigma-Aldrich (Budapest, Hungary). A stock solution of silver nitrate, was prepared in distilled water and filter sterilized (pore size 0.22 μm) prior to addition to cell-culture media.

Growth media and sera were obtained from Invitrogen (Carlsbad, CA, USA), 6-diamidino-2-phenylindole dihydrochloride (DAPI), 1,4-diazabicyclo-(2,2,2)-octane (DABCO) and other reagents were purchased from Sigma-Aldrich (Budapest, Hungary). Antifade Medium consisted of 90% glycerol, 2% (w/w) 1,4-diazabicyclo-(2,2,2)-octane, 20 mM Tris-Cl, pH 8.0, 0.02% sodium azide, and 25 ng/ml DAPI. Swelling Buffer consisted of 50 mM KCl, 10 mM MgSO_4 , 3 mM dithiothreitol, and 5 mM NaPO_4 , pH 8.0. Hypotonic Buffer for reversible permeabilization contained 9 mM HEPES, pH 7.8, 5.8 mM dithiothreitol, 4.5% dextran T-150, 1 mM EGTA and 4.5 mM MgCl_2 . Swelling Buffer consisted of 50 mM KCl, 10 mM MgSO_4 , 3 mM dithiothreitol and 5 mM NaPO_4 , pH 8.0. Fixative solution contained methanol:glacial acetic acid (3:1).

Cell Culture and Silver Nitrate Exposure

Human erythroleukemia K562 and human skin keratocyte HaCaT cells were cultured in RPMI-1640 medium (Sigma) containing 100 IU penicillin/ml, 50 μg streptomycin sulfate/ml, 2 mM L-glutamine and 5% fetal bovine serum (FBS) (Hyclone, Logan, UT). Subculturing was performed after treating the cells with 0.05% trypsin/EDTA solution. The continuous cell line K-562 was from the pleural effusion of a 53-year-old woman with chronic myelogenous leukemia in terminal blast crises (Lozzio and Lozzio 1975). The HaCaT cell line is derived from human skin keratinocytes that spontaneously transformed *in vitro* during long term incubation (Boukamp et al. 1988, 1990).

Recultured K562 and HaCaT cells were grown for 9 h and then treated with AgNO_3 (0.5–50 μM). Cells were grown for an additional 15 h in the presence of the heavy metal before being harvested, unless otherwise noted.

Isolation and Visualization of Large Scale Chromatin Structures

Details of these procedures have been described in the Methods of Chap. 6 as: Reversible Permeabilization of Cells, Isolation of Nuclei, Spreads of Nuclear Structures, and Visualization of Chromatin Structures. Reversible permeabilization was originally developed for murine thymocytes (Banfalvi et al. 1984).

Time-Lapse Photography

Two inverse microscopes sitting in the CO₂ incubator were equipped with high sensitivity video cameras, connected to a custom-built dual image acquisition computer system (Farkas et al. 2010). Briefly, custom-built illumination was developed to minimize heat- and fototoxicity. Operation of the spectrally warm-white light emitting diodes were synchronized with image acquisition periods. Cell cultures in 25 ml T flasks were placed on inverse microscopes. The screen of the computer was divided in two portions showing side-by-side the morphological changes of the control and the treated cells. Photographs of cells were taken every minute. The time of exposure was indicated in each frame. Exposures were converted to video-films by speeding up the projection to 30 exposures/s. Individual cells of suspension cultures were selected for further analysis. Individual photographs were chosen as panels shown in the figures. Time-lapse photography of individual cells allows us to determine the growth profile of individual cells grown both in monolayer and in suspension cultures. Genotoxic specific growth profiles of cell death are expected to be distinguished.

Changes in Chromatin Structure upon Silver Nitrate Exposure

Cells for chromatin monitoring were grown in plastic TC flasks (75 cm²) under the same condition, as described above. Heavy metal ion concentrations were applied using concentration ranges for silver nitrate between 0.5 and 50 µM. Cells were incubated with each AgNO₃ concentration for 15 h. Toxicity was estimated by the cell viability test, and during the immunofluorescence investigation of chromatin structure. Simultaneously, control experiments were carried out in the same way, but in the absence of Ag²⁺.

Results

Cell Viability After AgNO₃ Treatment

We have used two cell lines to test the *in vitro* damaging effect of different concentrations of silver nitrate on cell growth. Immortalized human skin keratinocytes (HaCaT) have been chosen, as silver nitrate solutions are highly irritating to the skin, mucous membranes, and eyes (Stokinger 1981). K562 human erythroleukemia cells bear some proteomic resemblance to both undifferentiated granulocytes (Klein et al. 1976) and erythrocytes (Andersson et al. 1979). K562 cells were chosen as the major abdominal pain caused in workers exposed to silver nitrate and silver oxide dusts correlated significantly with blood silver levels (Rosenman et al. 1979).

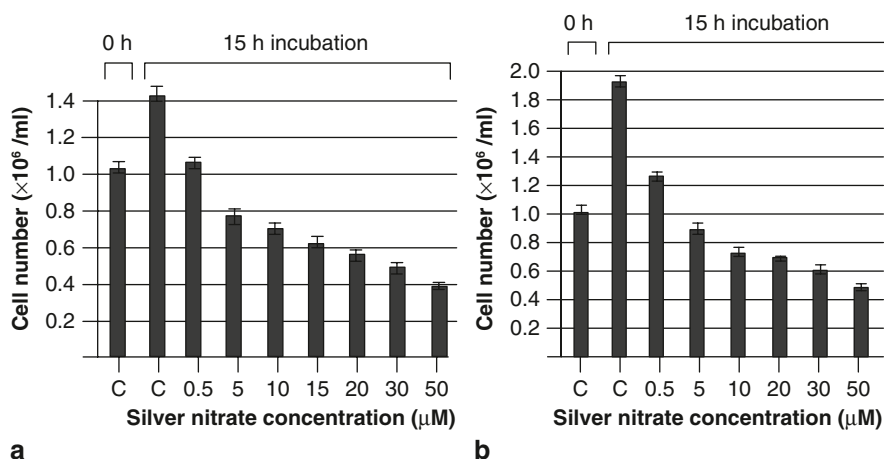


Fig. 9.1 Inhibition of HaCaT and K562 cell growth at different silver nitrate concentration. **a** The growth of nine HaCaT cell cultures was started at 10^6 cells/ml in the presence of 0.5, 5, 10, 15, 20, 30 and 50 μM AgNO_3 , respectively. **b** Similarly, eight K562 cell cultures were initiated at 10^6 cells/ml in the presence of 0.5, 5, 10, 20, 30 and 50 μM AgNO_3 , respectively. The control samples (C) were not treated. After 15 h treatment the cell number was counted in each population. In the representation the abscissa is showing the silver ion concentration and the ordinate the cell number

HaCaT cells were grown in 25 ml T-flasks and cell growth of individual cells was visualized by our long-time scanning system placed in a CO_2 incubator. Cell growth of viable cells was measured by counting the number of trypan blue excluding cells before starting the experiments and 15 h later (Fig. 9.1). In the control population the number of dead cells taking up trypan blue was less than 3% (not shown).

The concentration dependent cellular toxicity of silver nitrate on HaCaT cells is shown in Fig. 9.1a. The control was not subjected to AgNO_3 treatment. Subtoxic levels of silver nitrate (≤ 0.1 μM) did not cause measurable toxicity (not shown). Noticeable changes in growth rate were found in the presence of 0.5, 5, 10, 15, 20, 30 and 50 μM Ag corresponding to cell losses of 28, 47, 52, 58, 62, 67 and 75%, respectively relative to the growth rate of the 15 h control HaCaT cell population. Worthy to mention that after 0.5 μM AgNO_3 treatment the cell number was higher than in the 0 h control, indicating some cell growth. Minimum inhibitory concentration required to inhibit the growth of 50% of HaCaT cells (MIC50) was 6.4 μM AgNO_3 .

Higher growth inhibition was observed when K562 cells were treated with silver nitrate (Fig. 9.1b). The growth rate of K562 cells in the presence of 0.5, 5, 10, 15, 20, 30 and 50 μM Ag was inhibited by 32, 54, 60, 64, 69, 72 and 77%, respectively. Subtoxic (0.5 μM) concentration of AgNO_3 treatment did not cause loss of K562 cells, in fact it was significantly higher than the 0 h control. The minimum inhibitory concentration to cause 50% growth inhibition of K562 cells (MIC50) was 3.5 μM AgNO_3 , indicating that K562 cells were more susceptible to silver nitrate than HaCaT cells.

Time-Lapse Analysis of Cell Death

Time-lapse video microscopy was designed to follow the movement, shape and growth of individual cells for an unlimited period of time under physiological conditions in a carbon dioxide incubator. The long-term scanning of control HaCaT cells lasted for two days and the initial cell density viewed under the area the camera was monitoring increased from 70 to 90% confluency (Fig. 9.2). In the presence of $0.5 \mu\text{M AgNO}_3$ a reduced growth of HaCaT cells was observed without significant morphologic changes (Fig. 9.3). Long-term scanning revealed that the typical elongated HaCaT cells gradually rounded up and within 100 min of $10 \mu\text{M AgNO}_3$ treatment apoptotic signs were clearly distinguishable and after 900 min (15 h) most of the cells suffered apoptosis (Fig. 9.4). At high AgNO_3 concentration ($50 \mu\text{M}$) the time of apoptotic shrinkage of cells took only 10 min (Fig. 9.5). Necrotic swelling of cells was not observed.

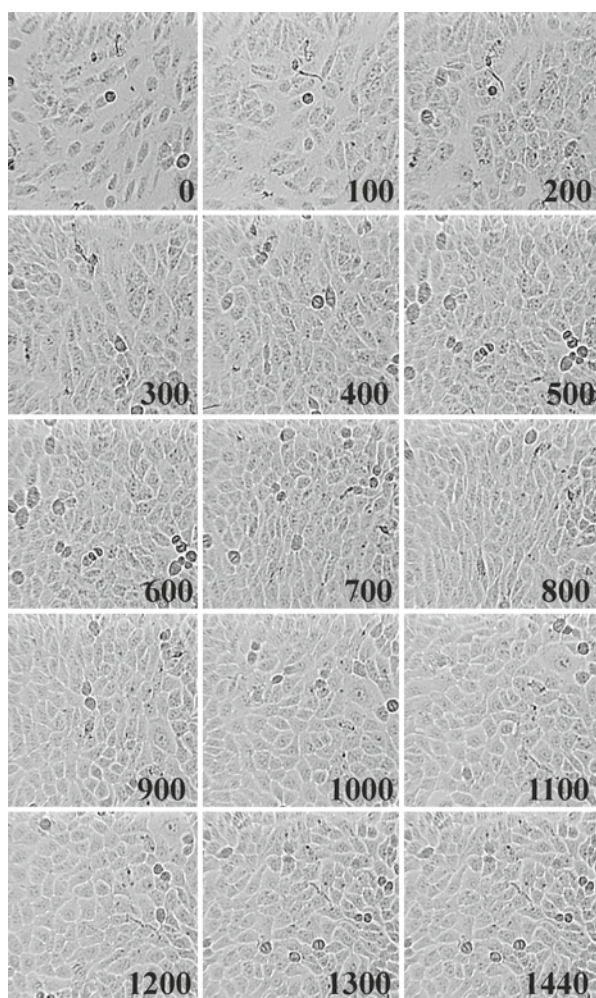


Fig. 9.2 Monitoring cell growth in the time-lapse photography of HaCaT cells. Cells were grown as described in the Materials section. Dividing round cells are in the foreground, and monolayer cells near confluence in the background. Black numbers at the bottom of each panel show the time passed in minutes from the recording. Images were brightness- and contrast-balanced, freed of interlacing and flickering, and gradient equalized and subjected to histogram equation as described. (Farkas et al. 2010)

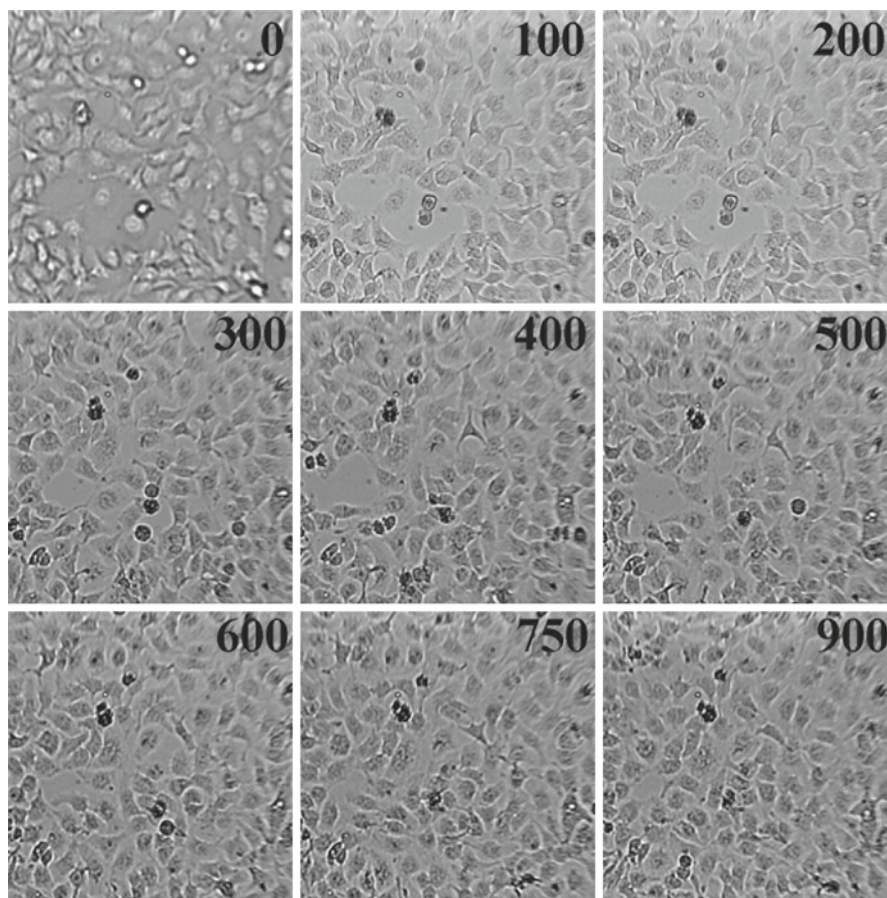


Fig. 9.3 Monitoring reduced HaCaT cell growth in the presence of $0.5 \mu\text{M AgNO}_3$. Cells were grown as described in the Materials section and under Fig. 9.2. Black numbers at the top of each panel show the time passed in minutes from the recording

A similar experiment was carried out with K562 cells. Cells grown in 25 ml T-flasks were visualized by long-time scanning system in CO_2 incubator. Cell growth of viable cells was measured by counting the number of viable cells before and 15 h after the experiment. Observations were similar to those shown with HaCaT cells (results not presented).

Chromatin Structures in Control HaCaT Cells and After Subtoxic ($0.5 \mu\text{M}$) Concentration of Silver Nitrate Treatment

Reversible permeabilization of cells was used to open the nucleus during any stages of the cell cycle and to visualize large scale chromatin condensation in the pres-

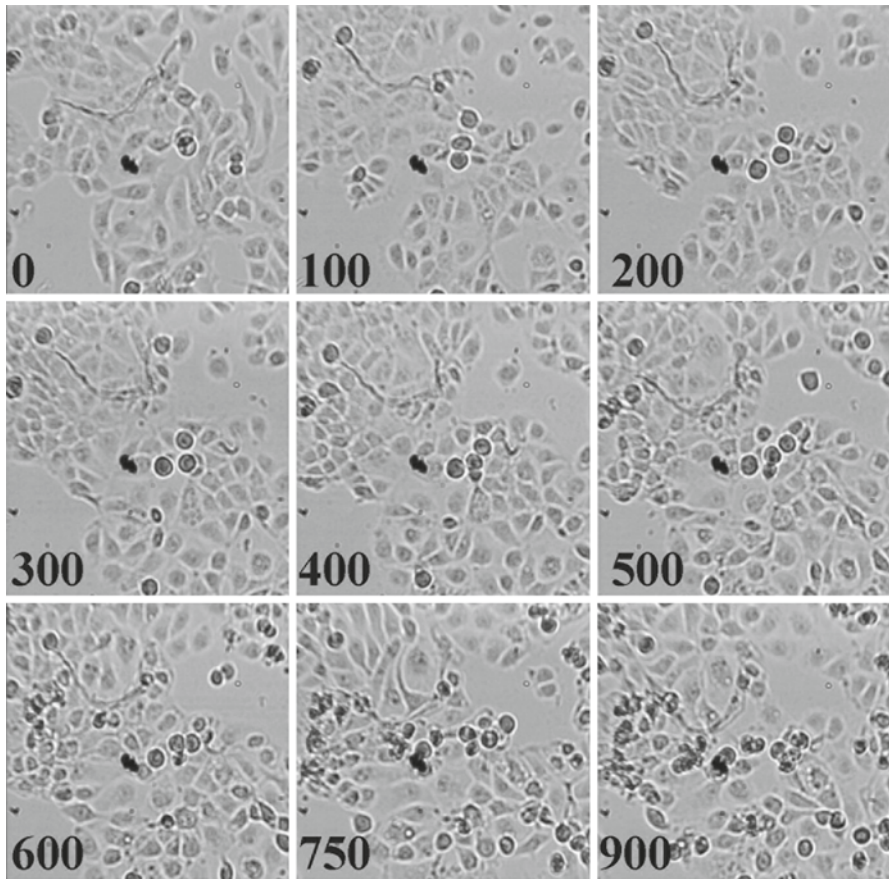


Fig. 9.4 Monitoring apoptotic HaCaT cell death in the presence of 10 μM AgNO_3 . Cells were grown as described in the Materials section and in Fig. 9.2. Black numbers at the bottom of each panel show the time passed in minutes from the recording

ence and in the absence of genotoxic materials. By using this approach we have described earlier the common intermediates of large scale chromatin folding in control, untreated mammalian (CHO, Indian muntjac, murine preB, K562) cells (Banfalvi et al. 2006). The veil-like chromatin in early S phase turned to fibrous and negatively supercoiled chromatin ribbon in mid-S phase was followed by the formation of chromatin bodies, referred to as the earliest visible interphase chromosomes, and by elongated and condensed form of chromosomes in the second half of the S phase.

The upper panels of Fig. 9.6 show typical chromatin structures in control HaCaT cells, involving decondensed veil-like chromatin (Fig. 9.6a, b), fibrous

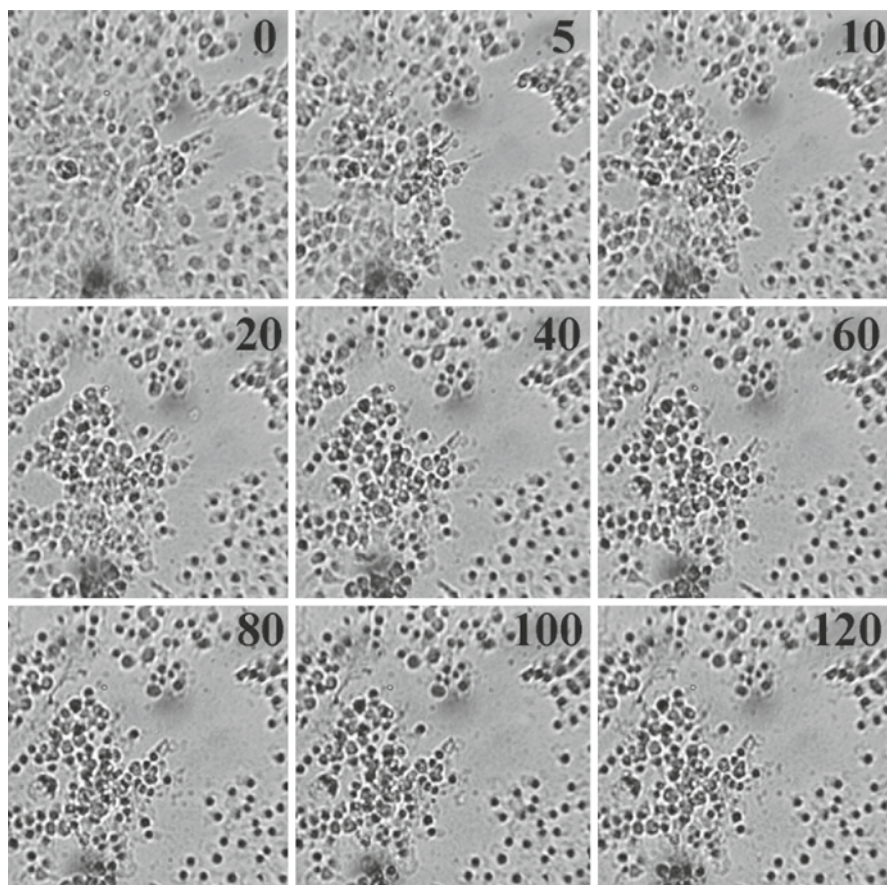
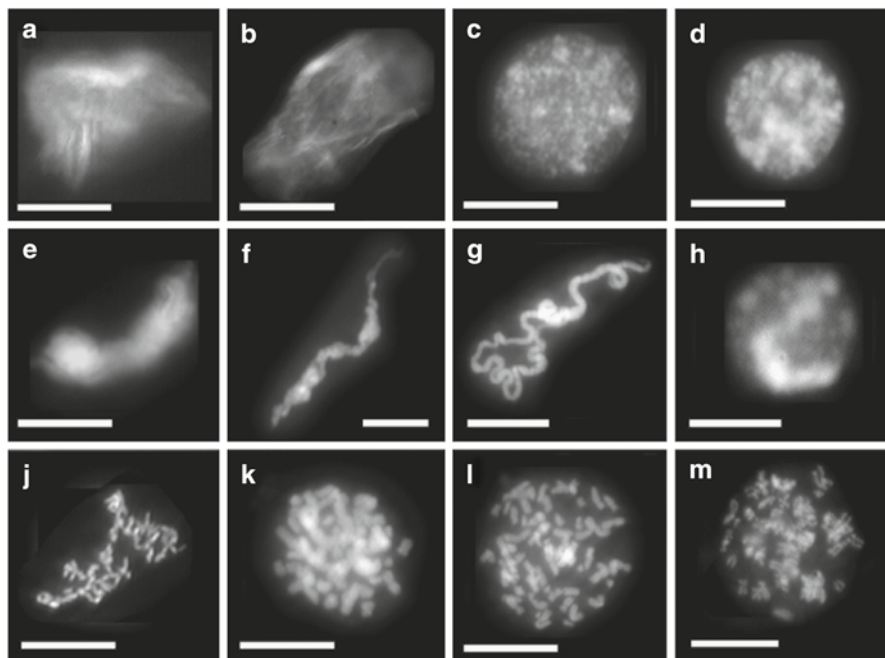
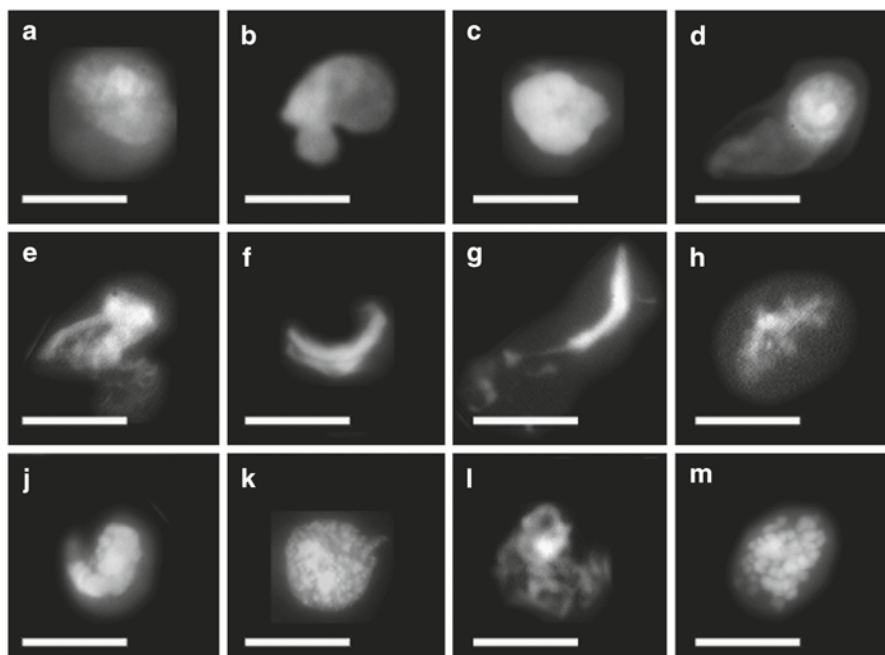


Fig. 9.5 Monitoring apoptosis of HaCaT cells in the presence of $50 \mu\text{M AgNO}_3$. Cells were grown as described in the Materials section and in Fig. 9.2. Black numbers at the top of each panel show the time passed in minutes from the recording

chromatin (Fig. 9.6c, d), ribboned chromatin (Fig. 9.6e–h), prechromosomes (Fig. 9.6j, k), condensed chromosomes approaching metaphase (Fig. 9.6l, m). Similar forms isolated from nuclei of HaCaT cells shown in the upper panels of Fig. 9.6 have been presented earlier and serve to demonstrate how these physiological chromatin forms differ from those isolated from cells subjected to silver nitrate treatment.

In the presence of $0.5 \mu\text{M}$ concentration of silver nitrate (Fig. 9.6, lower panels) changes in chromatin structure were seen as: (i) polarization of chromatin (Fig. 9.6a, d, e, g, h, l, m), (ii), appearance of fibrous chromatin tails around the nucleus (Fig. 9.6a, b, c, e, h, j, l) and (iii) incomplete condensation of metaphase chromosomes (Fig. 9.6h, k, l, m), (iv) decrease in nuclear size (Fig. 9.6a–m).

HaCaT control

HaCaT 0.5 μM AgNO₃

Chromatin Changes at Low (5–10 μM) Concentrations of Silver Nitrate in Nuclei of HaCaT Cells

In the presence of 5 μM concentration of silver nitrate (Fig. 9.7, upper panels), beside the polarization of chromatin, the most typical nuclear change was the appearance of chromatin ribbons and fibrous chromatin tails around the nucleus. A similar tendency was observed when HaCaT cells were grown in the presence of 10 μM concentration of AgNO_3 (Fig. 9.7, lower panels). The moderate decrease in nuclear size, was not associated with the formation of apoptotic bodies.

Chromatin Changes at Elevated (15–20 μM) Concentrations of Silver Nitrate in Nuclei of HaCaT Cells

The chromatin structures of nuclei isolated after somewhat higher concentration of silver nitrate (15–20 μM) exposure (Fig. 9.8) resembled those chromatin changes that were presented in Fig. 9.7. It is noteworthy to mention that the cellular and nuclear size decreased during these chromatin changes. Apoptotic body formation, known as the most characteristic morphological feature of apoptosis, was not observed even after treatment with higher silver nitrate concentrations.

Chromatin Changes at Higher (30–50 μM) Concentrations of Silver Nitrate in Nuclei of HaCaT Cells

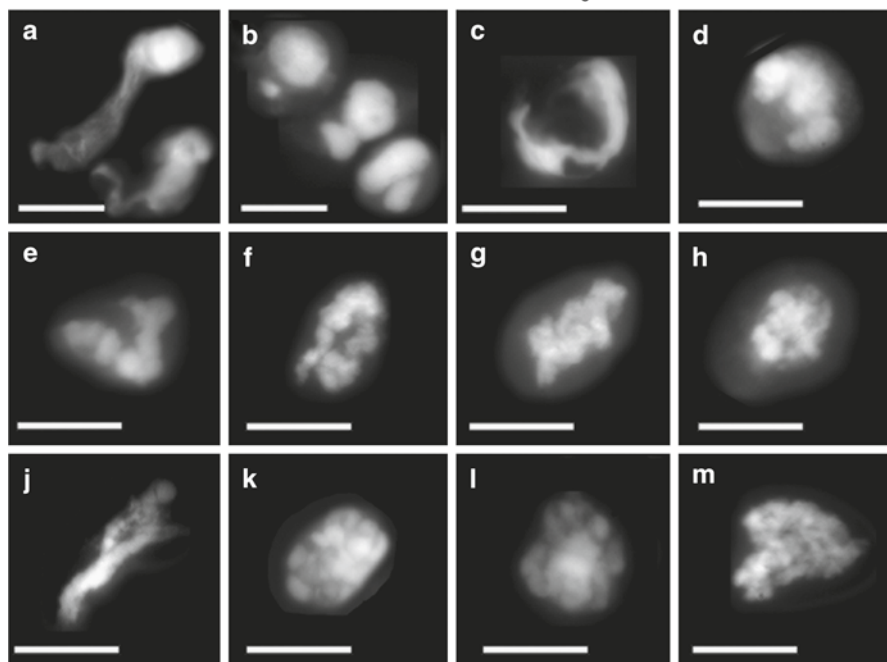
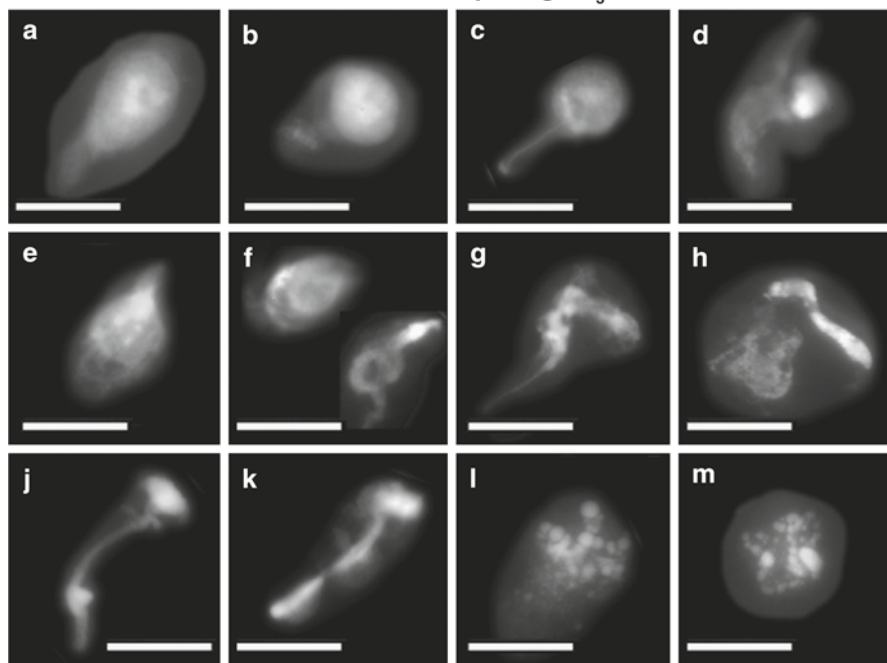
High silver nitrate concentration (30 and 50 μM) resulted not only in the formation of comet-like chromatin structures, but caused the nuclear material to unwind seen as ribboned structures (Fig. 9.9). The unwinding of chromatin structures points to the possibility that silver nitrate affects the supercoiling process of chromatin condensation.

Chromatin Structures of Normal Untreated K562 Cells

We have used reversible permeabilization to open the nuclei of K562 cells to visualize large scale chromatin changes similarly to those described for HaCaT cells. Using this

←

Fig. 9.6 Intermediates of chromatin condensation in control HaCaT cells and after treatment with subtoxic (0.5 μM) concentration of silver nitrate. Permeabilization of cells was followed by the restoration of membrane structures, colcemid treatment and isolation of chromatin structures as described in the Methods. *Upper panels:* Intermediates of chromatin condensation in untreated cells. *Lower panels:* nuclear structures isolated after treatment with 0.5 μM AgNO_3 . Bar, 5 μm each

HaCaT 5 μM AgNO_3 HaCaT 10 μM AgNO_3 

approach the shape and the density change from veil-like chromatin to fibrous and supercoiled chromatin to the mid-S phase was followed by chromatin bodies, elongated and condensed form of chromosomes in the second half of the S phase (Fig. 9.10). We have described recently these forms in healthy K562 cells (Farkas et al. 2010).

Chromatin Changes at Low (0.5–5 μM) Concentrations of Silver Nitrate in Nuclei of K562 Cells

The chromatin structures of K562 nuclei isolated at low silver nitrate concentration (0.5 and 5 μM) (Fig. 9.11) resembled those changes seen in HaCaT cells, with the notable difference that “comet formation” manifested already at the lowest (0.5 μM) concentration. This is taken as a clear indication that (a) K562 cells are more vulnerable to Ag^+ than HaCaT cells and (b) that chromatin changes are sensitive indicators detecting chromatin damages at low concentrations where the cell number did not decrease and some cell growth still occurred.

Shrinkage and Expansion of Nuclear Structures of K562 Cells at Elevated (10–50 μM) Ag^+ Concentrations

The reduction of nuclear size was observed after 10 μM AgNO_3 treatment in nuclei of K562 cells. This would indicate apoptosis if apoptotic bodies were present. Although, the size of the nuclei did not increase, the isolated nuclear material was enlarged at 20 and 50 μM AgNO_3 concentrations without nuclear disruption (Fig. 9.12). The nucleus did not fall apart but its round size became elongated with the expulsion of the less condensed chromatin. The elongation of the nucleus revealed that the structure of the nuclear material became less tense, but more relaxed. The lack of both apoptotic bodies and disruptions argue equally against apoptotic and necrotic cell death.

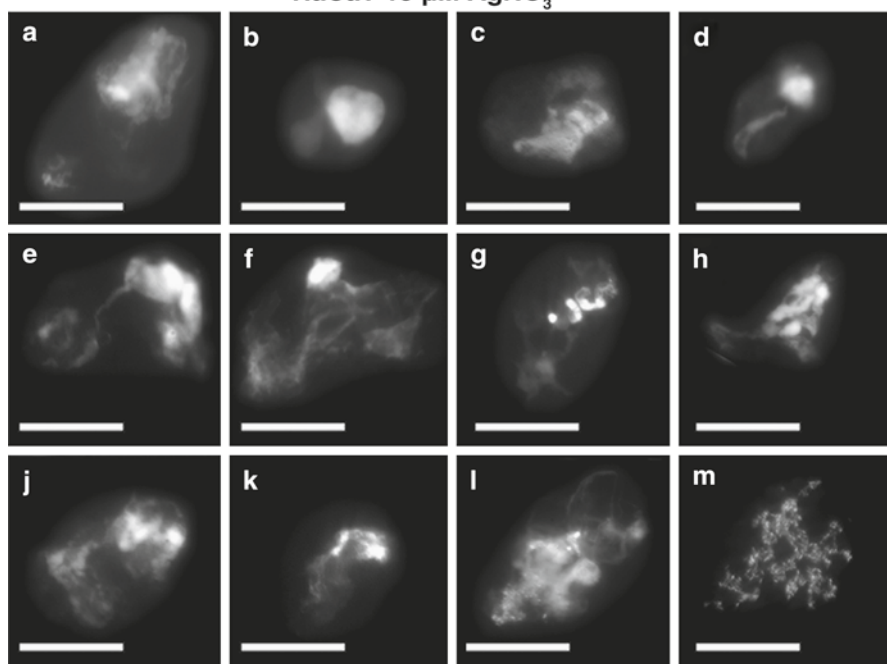
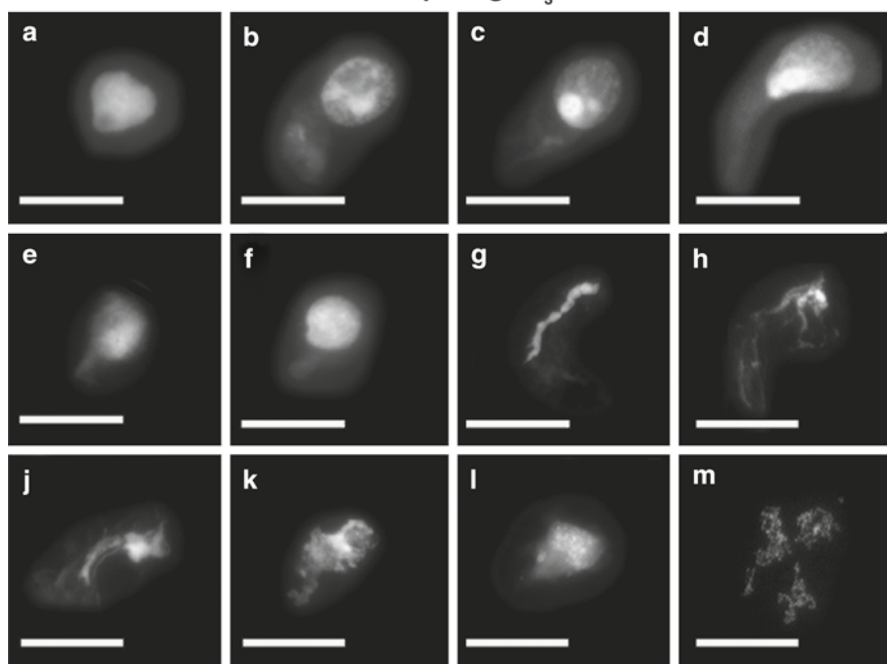
Discussion

Biological Effects of Metallic Silver

Only four heavy metals are highly toxic and cause damaging effects at very low ($< \mu\text{M}$) concentrations: lead (Pb), cadmium (Cd), mercury (Hg), and inorganic arse-



Fig. 9.7 Chromatin changes induced by low cellular concentration of silver nitrate. Cell were treated either with 5 μM (*upper panels*) or 10 μM AgNO_3 (*lower panels*), reversibly permeabilized, subjected to colcemid treatment and isolation of chromatin structures as described in the Methods. Chromatin structures were visualized after DAPI staining. Bar, 5 μm each

HaCaT 15 μM AgNO_3 HaCaT 20 μM AgNO_3 

nic (As). Other heavy metals—such as cobalt (Co), copper (Cu), iron (Fe), manganese (Mn), molybdenum (Mo), vanadium (V), strontium (Sr), and zinc (Zn)—are essential to health as trace elements. None of the noble (precious) metals (gold, silver, platinum) are considered essential. The Silver Safety Committee (<http://www.silversafety.org/>) announced that metallic or colloidal forms of noble metals are harmless. Silver metal has been used as a historical antimicrobial agent, as at those times there were few other choices. The only advantage of silver over antibiotics is that it is also effective at killing antibiotic-resistant bacterial strains. The Food and Drug Administration (FDA) proposed banning silver in over-the counter products in 1997 and issued a final rule in 1999. It is now believed that silver in any form is a bio-accumulative toxic heavy metal, like mercury, lead, and arsenic. Metallic silver is listed in the 1979 Registry of Toxic Effects as causing cancer in animals.

Toxic Effects of Silver Ions

Similarly to other heavy metal ions, silver ions (Ag^+) can bind to negatively-charged organic molecules to form complexes and display toxic reactions *in vitro* and *in vivo*. Silver compounds show toxic effects to some bacteria, viruses, algae and fungi, but unlike other heavy metal ions are less toxic to humans. Silver nitrate earned its worldwide fame as the building block of silver halide production, the cornerstone of the multi-billion dollar industry of photography. It has equally versatile applications in silver plating, making mirrors and in medical application. The medical application of silver nitrate dates to 1884 (Grier 1983) and has been used as 1% solution to treat the eyes of neonates against ocular infections and blindness. It was used to remove warts, prevent bleeding, bacterial infections and is one of the most popular agents for wound infections, especially in burned patients (Bader 1966).

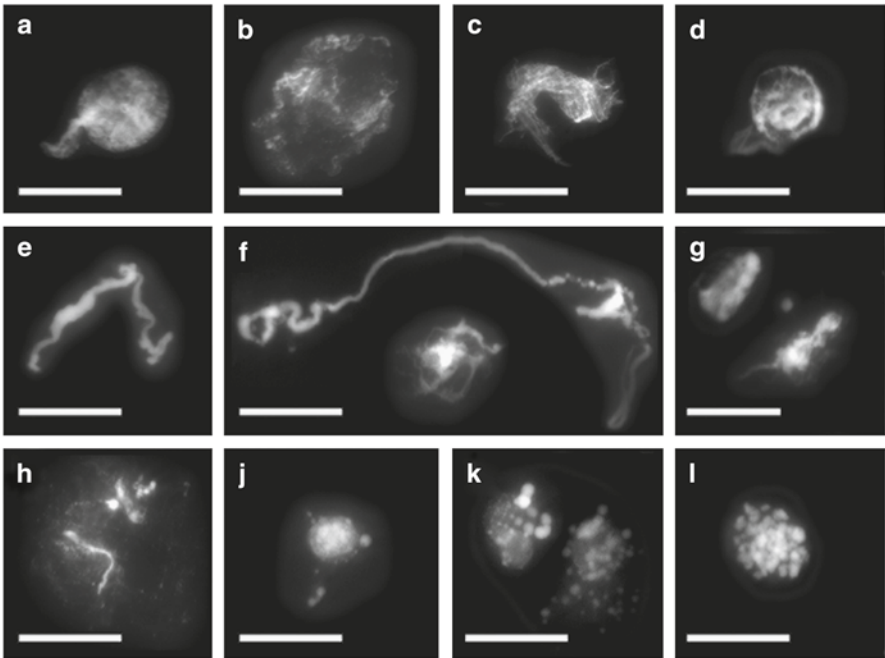
Cellular Effect of Silver Nitrate on Eukaryotic Cells

Chronic *per os* administration of inorganic silver nitrate caused cellular alterations in nuclear and cytoplasmic morphology, the disappearance of the endoplasmic reticulum; the transformation in mitochondrial morphology, and the increase in the number of irregularly shaped smooth walled cytoplasmic densities, that were assumed to be lipid granules (Hadek 1966). The cellular effects of silver nitrate on

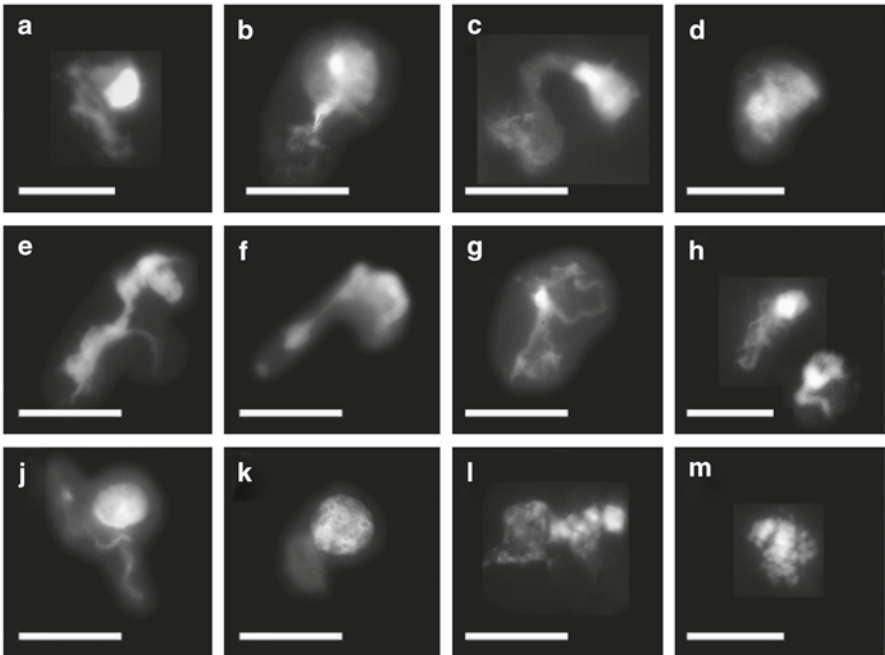


Fig. 9.8 Chromatin changes in HaCaT cells generated by elevated concentrations of silver nitrate. Cells were treated either with 15 μM (*upper panels*) or 20 μM AgNO_3 (*lower panels*), reversibly permeabilized, subjected to colcemid treatment and isolation of chromatin structures as described in the Methods. Chromatin structures were visualized after DAPI staining. Bar, 5 μm each

HaCaT 30 μM AgNO_3



HaCaT 50 μM AgNO_3



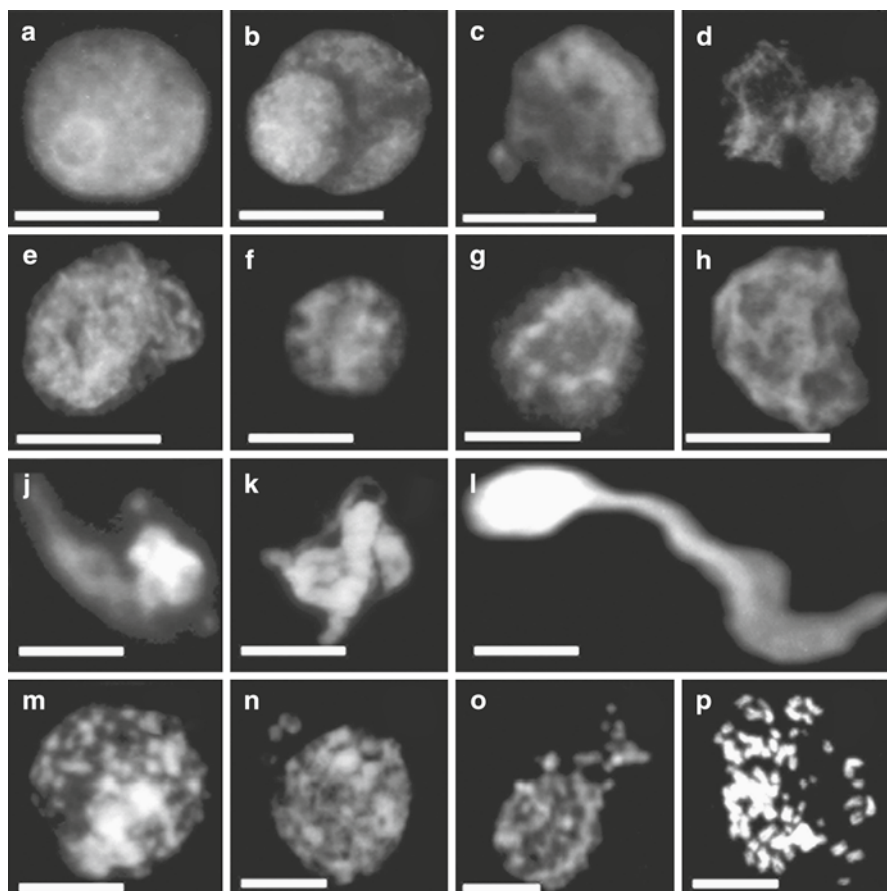


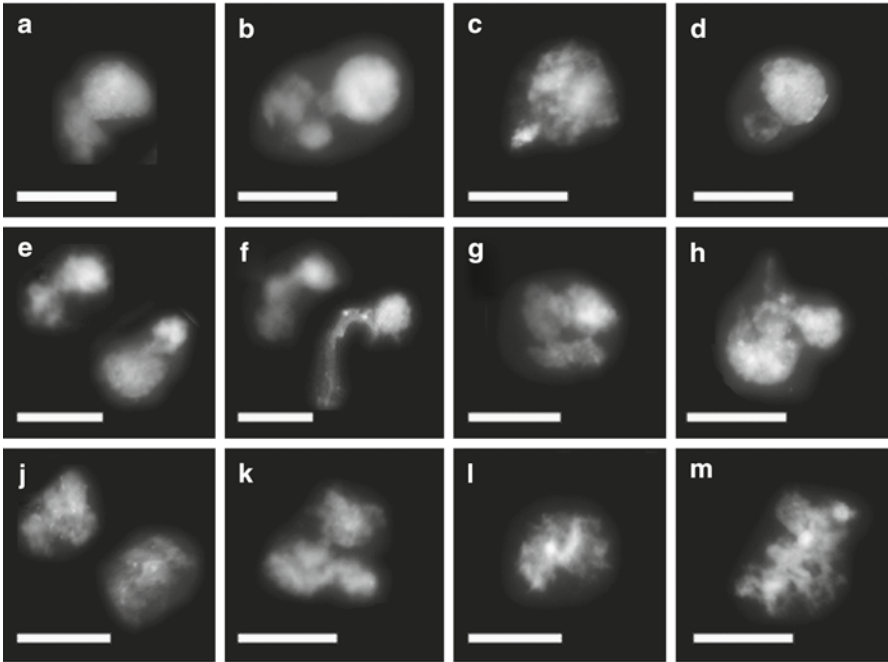
Fig. 9.10 Intermediates of chromatin condensation in untreated K562 cells. Permeabilization of cells was followed by the restoration of membrane structures, colcemid treatment and isolation of chromatin structures as described in the Methods. Regular structures seen under fluorescent microscope after DAPI staining: decondensed chromatin (**a**), extrusion of spherical chromatin (**b**), fibrous chromatin (**c** and **d**), chromatin bodies (**e**), ribboned supercoiled chromatin (**f**–**l**), prechromosomes (**m**–**o**), metaphase chromosomes (**p**). Bar, 5 μm each. (With permission of Farkas et al. 2010)

mammalian cells remained poorly characterized for several decades. Studies have demonstrated the cytotoxicity of silver ions *in vitro*, but the data from these reports did not lead to definitive conclusions (Wataha et al. 2000). The viability of human acute monocytic leukemia (THP-1) cells exposed to 25 μM AgNO_3 was less than 20% after 6 h suggesting that cell death at this dose was a rapid process (Foldbjerg et al. 2009). For the inhibition of cell growth by Ag^+ we have selected a concentra-

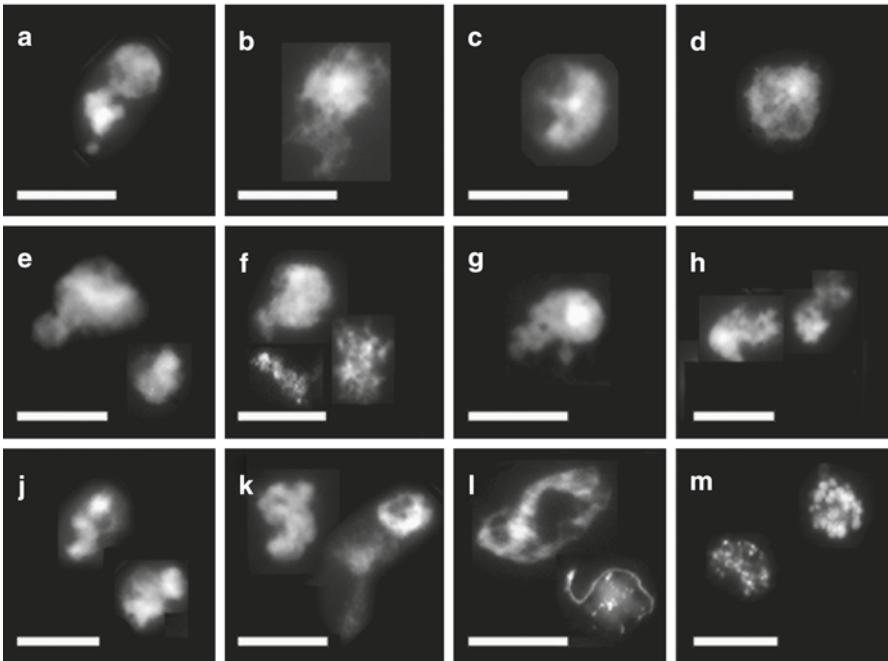


Fig. 9.9 Chromatin changes induced by high concentrations of silver nitrate. Cell were treated with 30 μM (*upper panels*) or with 50 μM AgNO_3 (*lower panels*), reversibly permeabilized, subjected to colcemid treatment and isolation of chromatin structures as described in the Methods. Chromatin structures were visualized after DAPI staining. Bar, 5 μm each

K562 0.5 μM AgNO_3



K562 5 μM AgNO_3



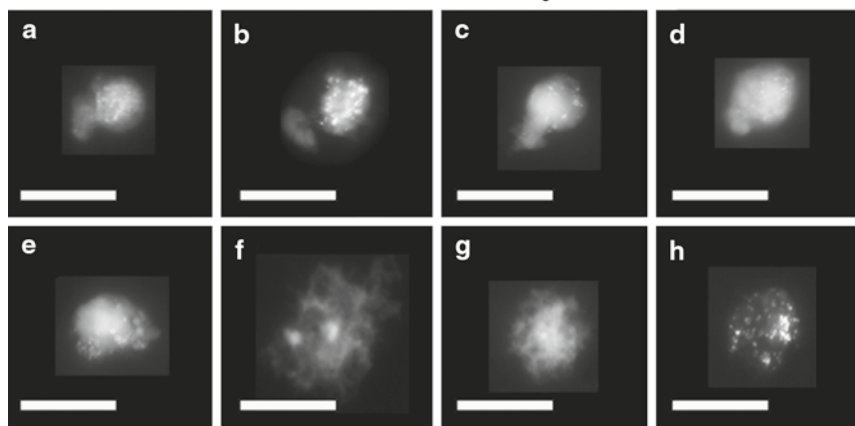
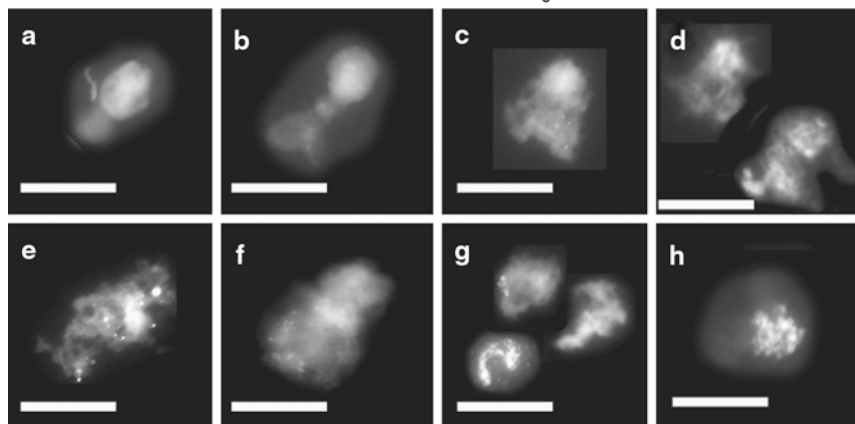
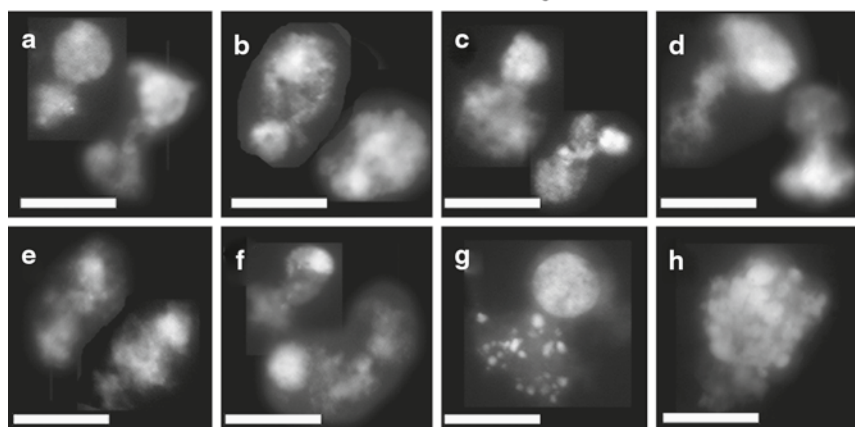
tion range between 0.5 and 50 μM AgNO_3 . Comparable results were obtained in our viability tests with MIC50 values of 6.4 and 3.5 μM AgNO_3 in HaCaT and K562 cells, respectively after 15 h treatment.

Metal ions affected yeast cell growth with a toxicity ranked in decreasing order as follows: $\text{Hg} > \text{Ag} > \text{Au} > \text{Cu}$, Ni, Co, Zn (Yang and Pon 2003). Since most toxic metal ions induced oxidative stress on cells through the mitochondrial respiratory chain, mitochondria became suspicious to be targets of metal toxicity. Indeed, Ag ions caused morphological changes in mitochondria, respiration-deficient cells appeared to be resistant to Ag ion, but not to Hg. This led Yang and Pon (2003) to the conclusion that the oxidation activity in mitochondria may play a role in acute toxicity of silver ion. This idea has been confirmed by a recent study that reported the cytotoxicity of silver in normal IMR 90 human lung fibroblasts and in U251 human glioblastoma cells (AshaRani et al. 2009). These authors have measured drastically reduced ATP content, cell viability, metabolic activity and increased production of reactive oxygen species (ROS) in a dose dependent manner. The DNA damage was also dose dependent and more prominent in the U251 cancer cell line. Moreover, the silver treatment of the same authors caused cell cycle arrest in G₂/M phase due to the repair of damaged DNA. Annexin-V propidium iodide (PI) staining showed no massive apoptosis or necrosis. To the contrary increased cellular ROS levels have been shown to be associated with the induction of apoptotic and necrotic cell death in cell cultures (Ott et al. 2007; Ueda et al. 2002). This process is mediated by the mitochondrial death pathway. Ag induced generation of ROS, depletion of antioxidant GSH and reduction of mitochondrial function were measured in BRL 3A rat liver cells and rat alveolar macrophages (Carlson et al. 2008; Hussain et al. 2005). Furthermore, Ag depleted GSH in human skin carcinoma and human fibrosarcoma cell lines and this depletion was associated with markers of apoptosis (Arora et al. 2008). Similarly to Ag many mitochondrial processes are targeted by arsenicals (Vujcic et al. 2007; Ralph 2008; Thorsen et al. 2009). Moreover, As is also known to inhibit ATP synthesis in yeast mitochondria (Cortes et al. 2000).

The effects of silver and silver ions on large-scale chromatin structures have not been studied earlier. The reduced ATP level caused by silver may have implications for the chromatin structure. Moreover, the mutagenic/carcinogenic effect of silver nitrate inducing DNA repair could also affect chromatin condensation. We have tested this possibility in two different cell lines (HaCaT, K562) and have concluded that the presence of silver nitrate is likely to reduce the unwinding of chromatin structures and to prevent chromatin condensation both at lower (0.5–5 μM) and at higher silver nitrate (10–50 μM) concentrations. These changes may be related to the decreased ATP level and point to the possibility that silver nitrate reduces the



Fig. 9.11 Chromatin changes induced at low cellular concentration of silver nitrate. K562 cells were treated either with 0.5 μM (*upper panels*) or with 5 μM AgNO_3 (*lower panels*). Cells were subjected to reversibly permeabilization, subjected to colcemid treatment and isolation of chromatin structures as described in the Methods. Chromatin structures were visualized after DAPI staining. Bar, 5 μm each

K562 10 μM AgNO_3 K562 20 μM AgNO_3 K562 50 μM AgNO_3 

ATP energy-dependent negative supercoiling process of chromatin condensation resulting in more relaxed chromatin structures, primarily in the formation of ribboned chromatin, that may still be compact enough to prevent the nucleolytic degradation of DNA.

Conclusions

The fact that after silver nitrate treatment we did not see metaphase chromosomes can be explained by the mutagenic (carcinogenic) effect of silver causing cell cycle arrest in G₂/M phase possibly due to repair of damaged DNA. In contrast to the effect of other heavy metals on mammalian cells that we have tested so far (Cd, Hg, Ni) (Banfalvi et al. 2007; Farkas et al. 2010; Chap. 7), the moderate decrease in nuclear size upon treatment with lower silver nitrate concentration (10 μM), was not associated with the formation of apoptotic bodies. The increased repair activity after silver nitrate treatment points to the cellular effort to rescue damaged cells (Asha-Rani et al. 2009) and can be accounted for the lack of apoptotic bodies. Our experiments carried out at low silver nitrate concentrations are in agreement with the finding that apoptotic staining did not show apoptotic or necrotic cell death (AshaRani et al. 2009). Higher (10–50 μM) silver nitrate concentrations caused the expansion of the nuclear material primarily as the opening of the round nucleus forming elongated structures, resembling ribboned chromatin, without the necrotic explosion of the nucleus. Depending on the dose, we have detected mixed signs of morphological changes with both apoptotic and necrotic cell death in conformity with the hierarchical oxidative stress model in which low levels of ROS activate cellular defense mechanisms and survival, whereas high levels activate cell death (Nel et al. 2006).

All these observations are compatible with the fact that silver is causing cancer in animals. Although, certain forms of the heavy metals are considered human carcinogens and act through different pathways, the carcinogenic mechanism of silver ions remains to be clarified. Finally, we came to the conclusion that chromatin changes induced by different heavy metals are not uniform. Rodriguez et al. (1997) suggested that the metal ion-dependent hydrogen peroxide induced DNA damage is more sequence specific than metal specific. However, this idea does not exclude the possibility that other types of oxidative nuclear damages and/or protein binding of heavy metals could not have a more specific effect on chromatin structure. Regarding the specificity the protein binding of heavy metals is of primary interest. This notion is supported by the fact that protein (enzyme) activation and the inhibi-

←
Fig. 9.12 Chromatin shrinking and enlargement of nuclear material of K562 cells caused by elevated concentrations of silver nitrate. K562 cells were treated with 10 μM (*upper panels*) causing shrinkage, 20 μM (*middle panels*) and 50 μM AgNO₃ inducing enlargement of the nuclear material. Cells were subjected to reversibly permeabilization, followed by colcemid treatment and isolation of chromatin structures as described in the Methods. Chromatin structures were visualized after DAPI staining. Bar, 5 μm each

tory redox potential of heavy metals depend on different affinities of metal cations for various side-chain donors in proteins and coordination modes of the complexes formed. The extent and character of the damage may strongly depend on the metal (Kasprzak Chap. 11).

Acknowledgements This work was supported by Hungarian Scientific Research Fund (OTKA grant) T 42762 grant to G.B.

References

- Andersson LC, Nilsson K, Gahmberg CG (1979) K562—a human erythroleukemic cell line. *Int J Cancer* 23:143–147
- Arora S, Jain J, Rajwade JM, Paknikar KM (2008) Cellular responses induced by silver nanoparticles: *in vitro* studies. *Toxicol Lett* 179:93–100
- AshaRani PV, Low Kah Mun G, Hande MP, Valiyaveetil S (2009) Cytotoxicity and genotoxicity of silver nanoparticles in human cells. *ACS Nano* 3:279–290
- Bader KF (1966) Organ deposition of silver following silver nitrate therapy for burns. *Plast Reconstr Surg* 37:550–551
- Baldi C, Minoia C, DiNuici A, Capodaglio E, Manzo L (1988) Effects of silver in isolated rat hepatocytes. *Toxicol Lett* 41:261–268
- Banfalvi G, Sooki-Toth A, Sarkar N, Csuzi S, Antoni F (1984) Nascent DNA synthesized reversibly permeable cells of mouse thymocytes. *Eur J Biochem* 139:553–559
- Banfalvi G, Littlefield N, Hass B, Mikhailova M, Csuka I, Szepessy E, Chou WM (2000) Effect of cadmium on the relationship between replicative and repair DNA synthesis in synchronized CHO cells. *Eur J Biochem* 267:6580–6585
- Banfalvi G, Gacsi M, Nagy G, Kiss BZ, Basnakian AG (2005) Cadmium induced apoptotic changes in chromatin structure and subphases of nuclear growth during the cell cycle in CHO cells. *Apoptosis* 10:631–642
- Banfalvi G, Nagy G, Gacsi M, Roszer T, Basnakian AG (2006) Common pathway of chromosome condensation in mammalian cells. *DNA Cell Biol* 25:295–301
- Banfalvi G, Ujvarosi K, Trencsenyi G, Somogyi C, Nagy G, Basnakian AG (2007) Cell culture dependent toxicity and chromatin changes upon cadmium treatment in murine pre-B cells. *Apoptosis* 12:1219–1228
- Boukamp P, Petrussevska RT, Breitkreutz D, Hornung J, Markham A, Fusenig NE (1988) Normal keratinization in a spontaneously immortalized aneuploid human keratinocyte cell line. *J Cell Biol* 106:761–771
- Boukamp P, Stanbridge EJ, Foo DY, Cerutti PA, Fusenig NE (1990) c-Ha-ras oncogene expression in immortalized human keratinocytes (HaCaT) alters growth potential *in vivo* but lacks correlation with malignancy. *Cancer Res* 50:2840–2847
- Carlson C, Hussain SM, Schrand AM, Braydich-Stolle LK, Hess KL, Jones RL, Schlager JJ (2008) Unique cellular interaction of silver nanoparticles: size-dependent generation of reactive oxygen species. *J Phys Chem B* 112:13608–13619
- Chopra I (2007) The increasing use of silver-based products as antimicrobial agents: a useful development or a cause for concern? *J Antimicrob Chemother* 59:587–590
- Cooms C, Wan A (1992) Do burn patients have a silver burning? *Burns* 18:179–184
- Cortes P, Castrejon V, Sampedro JG, Uribe S (2000) Interactions of arsenate, sulfate and phosphate with yeast mitochondria. *Biochim Biophys Acta* 1456:67–76
- Demling RH, DeSanti L (2001) Effects of silver on wound management. *Wounds* 13(1 suppl A):5–14

- Farkas E, Ujvarosi K, Nagy G, Posta J, Banfalvi G (2010) Apoptogenic and necrogenic effects of mercuric acetate on the chromatin structure of K562 human erythroleukemia cells. *Toxicol In vitro* 24:267–275
- Foldbjerg R, Olesen P, Hougaard M, Dang DA, Hoffmann HJ, Autrup H (2009) PVP-coated silver nanoparticles and silver ions induce reactive oxygen species, apoptosis and necrosis in THP-1 monocytes. *Toxicol Lett* 190:156–162
- Grier N (1983) Silver and its compounds. In: Block SS (ed) *Disinfection, sterilization and preservation*, 3rd edn. Lea and Febiger, Philadelphia, PA, pp 375–389
- Hadek R (1966) Preliminary report on the cellular effect of intravital silver in the mouse ovary. *J Ultrastruct Res* 15:66–73
- Hall RE, Bender G, Marquis RE (1988) *In vitro* effects of low intensity direct current generated silver on eukaryotic cells. *J Oral Maxillofac Surg* 46:128–133
- Hidalgo E, Domínguez C (1998) Study of cytotoxicity mechanisms of silver nitrate in human dermal fibroblasts. *Toxicol Lett* 98:169–179
- Hidalgo E, Bartolomé R, Barroso C, Moreno A, Domínguez C (1998) Silver nitrate: antimicrobial activity related to cytotoxicity in cultured human fibroblasts. *Skin Pharmacol Appl Skin Physiol* 11:140–151
- Hussain S, Anner RM, Anner BM (1992) Cysteine protects Na, K-ATPase and isolated human lymphocytes from silver toxicity. *Biochem Biophys Res Commun* 189:144–149
- Hussain SM, Hess KL, Gearhart JM, Geiss KT, Schlager JJ (2005) *In vitro* toxicity of nanoparticles in BRL 3A rat liver cells. *Toxicol In vitro* 19:975–983
- Klein E, Ben-Bassat H, Neumann H, Ralph P, Zeuthen J, Polliack A, Vánky F (1976) Properties of the K562 cell line, derived from a patient with chronic myeloid leukemia. *Int J Cancer* 18:421–431
- Liedberg H, Lundeberg T (1989) Assessment of silver-coated urinary catheter toxicity by cell culture. *Urol Res* 32:359–360
- Lozzio CB, Lozzio BB (1975) Human chronic myelogenous leukemia cell-line with positive Philadelphia chromosome. *Blood* 45:321–334
- Nel A, Xia T, Madler L, Li N (2006) Toxic potential of materials at the nanolevel. *Science* 311:622–627
- Ott M, Gogvadze V, Orrenius S, Zhivotovsky B (2007) Mitochondria, oxidative stress and cell death. *Apoptosis* 12:913–922
- Ralph SJ (2008) Arsenic-based antineoplastic drugs and their mechanisms of action. *Met Based Drugs* 2008:260146
- Rodriguez H, Holmquist GP, D'Agostino R Jr, Keller J, Akman SA (1997) Metal ion-dependent hydrogen peroxide-induced DNA damage is more sequence specific than metal specific. *Cancer Res* 57:2394–2403
- Rosenman KD, Moss A, Kon S (1979) Argyria: clinical implications of exposure to silver nitrate and silver oxide. *J Occup Med* 21:430–435
- Stokinger HE (1981) Silver. In: Clayton GD, Clayton E (eds) *Patty's industrial hygiene and toxicology*, vol 2A. Wiley, New York, pp 1881–1894
- Thorsen M, Perrone GG, Kristiansson E, Traini M, Ye T, Dawes IW, Nerman O, Tamás MJ (2009) Genetic basis of arsenite and cadmium tolerance in *Saccharomyces cerevisiae*. *BMC Genom* 10:105
- Ueda S, Masutani H, Nakamura H, Tanaka T, Ueno M, Yodoi J (2002) Redox control of cell death. *Antioxid Redox Signal* 4:405–414
- Vujcic M, Shroff M, Singh KK (2007) Genetic determinants of mitochondrial response to arsenic in yeast *Saccharomyces cerevisiae*. *Cancer Res* 67:9740–9749
- Wataha JC, Lockwood PE, Schedle A (2000) Effect of silver, copper, mercury, and nickel ions on cellular proliferation during extended, low-dose exposures. *J Biomed Mater Res* 52:360–364
- Westhofen M, Schafe H (1986) Generalized argyria in man: neurological, ultrastructural and X-ray microanalytical findings. *Arch Otorhinolaryngol* 243:260–264
- Yang HC, Pon LA (2003) Toxicity of metal ions used in dental alloys: a study in the yeast *Saccharomyces cerevisiae*. *Drug Chem Toxicol* 26:75–85

Part V
Chemical Carcinogenesis Induced by
Heavy Metals

Chapter 10

Heavy Metal-Induced Carcinogenicity: Depleted Uranium and Heavy-Metal Tungsten Alloy

John F. Kalinich

Abstract Continued development of novel munitions for the battlefield opens the possibility of wounds containing embedded fragments of metals or metal mixtures whose toxicological properties may not as yet be well-understood. This chapter reviews what is currently known about two recent additions to many nations' arsenals: depleted uranium and heavy-metal tungsten alloy. The toxicological and genotoxic properties of these materials, derived from both *in vitro* and *in vivo* studies, will be discussed, as will the health effects of known human exposures. Finally, areas requiring further research will be detailed.

Introduction

Advances in weapon design and the expanding terroristic use of Improvised Explosive Devices have opened the possibility of human exposure to metals or metal mixtures whose toxicological properties and physiological effects are not known. In this chapter, two of the more recent additions to the weapons arena, depleted uranium and heavy-metal tungsten alloy, will be discussed. The known toxicological properties of uranium and tungsten will be addressed with respect to a variety of human exposure scenarios, including inhalation, ingestion, and embedded fragments. The influence of depleted uranium and heavy-metal tungsten alloy on gene expression and signal transduction pathways leading to carcinogenicity will be considered and finally, areas requiring further research will be detailed.

J. F. Kalinich (✉)
Armed Forces Radiobiology Research Institute, 8901 Wisconsin Avenue, Bethesda MD
20889-5603, USA
Tel.: +1-301-295-9242
Fax: +1-301-295-1731
e-mail: kalinich@afri.usuhs.mil

Table 10.1 Uranium characteristics

Chemical symbol	U
Atomic number	92
Atomic weight	238.029
Category	Actinide
Group/series/block	n.a./7/f
Melting point	1135°C
Common oxidation states	+4, +5, +6
Density	18.95 gm/cm ³

Depleted Uranium (DU)

Uranium was first identified by Klaproth in 1789 and named after the planet Uranus. However, it was not until over 100 years later that the radioactive properties of uranium were described by Becquerel. Uranium is a naturally occurring element widely spread in the environment. It is normally found at low levels (parts per million) in soil, water, plants, and animals, including humans (ATSDR 1999). Average daily uranium intake in humans is approximately 3 µg, primarily through food and drinking water. Uranium, as found in nature, is slightly radioactive and consists predominantly of three isotopes, ²³⁴U, ²³⁵U, and ²³⁸U (Table 10.1). Although all three isotopes are radioactive, ²³⁴U and ²³⁵U have a much higher specific activity than ²³⁸U. Natural uranium consists largely of ²³⁸U (99.274%) with smaller amounts of ²³⁴U (0.006%) and ²³⁵U (0.72%). The processing of uranium for use in nuclear reactors and nuclear weapons involves increasing the percentages of the high specific activity isotopes with respect to ²³⁸U. This process is known as “enrichment” and results in the production of two different uranium fractions. The “enriched” fraction consists of approximately 97.010% ²³⁸U, 0.03% ²³⁴U, and 2.96% ²³⁵U. The “depleted” fraction consists of approximately 99.745% ²³⁸U, 0.005% ²³⁴U, and 0.25% ²³⁵U. Although radiologically different, both fractions remain identical chemically.

Depleted uranium has several commercial applications including shielding for radioactive material and as counterweights in aircraft and ships. However, it is because of its military applications that depleted uranium has received much of its attention. Because it is extremely dense, with a density second only to tungsten, depleted uranium is used for shielding for tanks and vehicles and as kinetic-energy armor-penetrating munitions. The use of DU munitions presents the greatest chance of human exposure. Although the toxicological hazards of uranium have been recognized for over a 100 years, many of these adverse effects were ascribed to radioactivity. Depleted uranium is approximately 40% less radioactive than natural uranium; thus, although radiation may play a role in the induction of cellular damage, the chemical properties of DU are also of paramount concern. In addition, metals such as titanium or molybdenum are often added during production of DU-containing munitions to provide specific metallurgic properties. The original uranium source from which DU was processed can also add minor contaminants to the final product. For example, DU obtained from reprocessed nuclear fuel can have small amounts of fission products and transuranics present, including strontium,

cesium, plutonium, and americium. Also, the normal radioactive decay pathways of uranium can introduce additional contaminants (e.g., thorium) in the final product. Therefore, when evaluating the cellular effects of DU exposure, the presence of contaminants introduced as a result of processing, as well as those resulting from normal radioactive decay, cannot be discounted. As noted above, one of the main military uses of DU is in the production of kinetic-energy armor-penetrating munitions. The first widespread use of these munitions was in the 1991 Persian Gulf War. DU munitions were also used by NATO forces in the recent conflicts in Bosnia and Kosovo. Because of concern over the health and environmental effects of the use of DU munitions there has been a movement toward the use of alternative materials and the heavy-metal tungsten alloys are one of these.

Heavy-Metal Tungsten Alloy

Tungsten was first identified in 1758 by the Swedish chemist Cronstedt. The word tungsten is Swedish for “heavy stone” and is a tribute to its density; the highest of any naturally occurring element (Table 10.2). Tungsten is found in varying concentrations in air, water, and soil. In soil, tungsten is found as a mineral mixture, primarily as wolframite or scheelite (van der Voet et al. 2007). Weathering and dissolution of rocks and soil result in tungsten being released into the air or entering the groundwater. Environmental tungsten levels are generally very low, except in areas of tungsten mines or natural deposits (ATSDR 2005). As such, uptake levels are usually insignificant, with occupational exposure being the most likely route of tungsten internalization in humans.

Because of its density and high melting point, tungsten is used in a variety of commercial applications including light bulb filaments, counterweights, radiation shields, and thermocouples. It is also found, as tungsten carbide, in cutting blades and drill bits. Tungsten has also been used as replacement for lead in small-caliber ammunition. In 1991, the U.S. Fish and Wildlife Service banned the use of lead shot for the hunting of waterfowl and advocated the use of ammunition formulations that were not toxic when ingested by wildlife. Many of the subsequently approved ammunitions contain varying amounts of tungsten in combination with other metals such as nickel, tin, iron, copper, and bismuth. In addition, a formulation of tungsten with a polymer matrix has also been approved for use. Toxicity testing has shown

Table 10.2 Tungsten characteristics

Chemical symbol	W
Atomic number	74
Atomic weight	183.85
Category	Transition Metal
Group/series/block	6/6/d
Melting point	3422°C
Common oxidation states	+6
Density	19.25 gm/cm ³

no adverse health effects of these materials (Kraabel et al. 1996; Kelly et al. 1998; Mitchell et al. 2001a, b, c; Brewer et al. 2003).

Military applications of tungsten also include the use of tungsten-based composites, primarily tungsten/tin and tungsten/Nylon, as replacements for lead in small-caliber ammunition. As noted earlier, widespread public concern over the health and environmental impact of the continued use of depleted uranium has led many countries to replace depleted uranium with various tungsten alloys in their arsenals of armor-penetrating munitions. In many of these formulations, tungsten is combined with two or more of the following transition metals: nickel, cobalt, iron, and copper. Although these materials are referred to as “tungsten alloys”, they are in fact two-phase composites, due to the extremely high melting point of tungsten. During manufacturing, powders of the appropriate metals are mixed and heated. Heating occurs at temperatures below the melting point of tungsten, but above the melting points of the transition metals. The melted transition metals dissolve a small amount of tungsten; however, most of the tungsten powder remains intact. The result is a material consisting of pure tungsten grains surrounded by a “binder matrix” composed of tungsten and the added transition metals. In contrast, additional material added during the processing of depleted uranium results in a true alloy because of the similar melting points of the components.

Routes of Exposure

Depleted uranium and tungsten alloys can be internalized by three primary routes: inhalation, ingestion, or wound contamination via embedded fragments. Regardless of the route of exposure, several factors govern the eventual health effects induced by the internalized metals. Clearly, the amount of material internalized plays a major role in the end-result of any exposure. Equally important however are the chemical and physical properties of the metal. These properties include solubility characteristics (particularly in biological fluids), particle size, speciation, and chemical reactivity (Yokel et al. 2006). For inhalation exposures, the size of the inhaled particle as well as its solubility will determine its ultimate fate. Approximately 25% of inhaled particles are immediately exhaled (International Commission on Radiological Protection 1966). Of the remaining 75%, particles less than 5 μm in diameter can reach the alveolar space while particles greater than 10 μm tend to remain in upper areas of the lung (Morrow et al. 1967). Once deposited in the lung, the solubility of the particle is of importance. Soluble metals are rapidly dissolved and enter the circulatory system. Less soluble metals will eventually be removed through the process of phagocytosis by the alveolar macrophages. Larger inhaled particles, unable to access the alveolar space, will be removed from the lung via mucocilliary clearance. However, many of the particles, once cleared, will be swallowed and thus enter the gastrointestinal tract. In addition to swallowing after mucocilliary clearance, metals can be ingested through contaminated food or liquids. Once ingested, absorption of the metals will depend upon the chemical form and solubility. Both uranium and tungsten are usually poorly absorbed by the gastrointestinal tract (Leggett 1997;

Leggett and Pellmar 2003). Wound contamination can occur as a result of metals entering open wounds (e.g., as dust or liquid) or as embedded fragments. As with other routes of exposure, the physicochemical properties of the metal are of prime importance when determining its fate *in vivo*. Research with intramuscularly injected metallic radionuclides has shown that even those considered insoluble can be solubilized *in vivo* (Bistline et al. 1972; Lloyd et al. 1974; Dagle et al. 1985). This fact was dramatically shown in studies investigating the health effects of embedded fragments of depleted uranium where solubilization and urinary excretion of the uranium was found within 48 h after implantation of the solid metal into the leg muscles of laboratory rodents (Pellmar et al. 1999).

Regardless of the route of internalization, several different cell types could potentially be affected by exposure to metals. The epithelial cells of the gastrointestinal tract and the mesenteric lymph nodes have been shown to accumulate depleted uranium after chronic ingestion (Dublineau et al. 2006). Inhalation results in the exposure of epithelial cells and alveolar macrophages (Schins and Borm 1999; Monleau et al. 2006). As noted earlier, the alveolar macrophages play a key role in both particle clearance and retention in the lung (Tasat and De Ray 1987). Wound contamination and embedded fragments present a far more complex situation because of the wide variety of cell types and mediators involved in wound healing. Briefly, the process of wound healing can loosely be divided into three phases: inflammation, proliferation, and remodeling (Broughton and Janis 2006; Tsirogianni et al. 2006; Li et al. 2007). Immediately after a wound is suffered, platelets arrive to begin the process of clot formation to maintain hemostasis. Neutrophils and macrophages are the next cell types to arrive at the wound site and are responsible for eliminating foreign organisms and debris, including nonviable tissue. Macrophages are also capable of phagocytizing small metal particulates and can concentrate these metals in the phagolysosomal vesicles before exiting through the lymphatic system (Berry et al. 1997; Lizon and Fritsch 1999). However, the most important role of the macrophage is the secretion of numerous cell mediators that lead to the proliferation phase of wound healing. In the proliferation phase, fibroblasts migrate to the wound site to produce the extracellular matrix and granulation tissue required for proper wound healing. Maturation of the extracellular matrix occurs during the remodeling phase and, depending upon the type of wound, can take up to a year to complete. In many cases, the specific response of the macrophages to the internalized metals will determine the ultimate outcome of the exposure, including the induction of cancer (Sica et al. 2008).

In Vitro Studies

Depleted Uranium

Cell culture systems have been used for many years to model potential adverse health effects from exposure to metals. Macrophage, kidney, lung, and neuronal cell lines have all been utilized to assess metal toxicity, as well as genomic and proteomic changes occurring as a result of exposure. Treatment of Chinese hamster

ovary cells with depleted uranium resulted in decreased cell viability and increased chromosomal aberrations (Lin et al. 1993). Cellular damage, evidenced by an increase in the release of lactate dehydrogenase, was observed in LLC-PK1 kidney cells after uranium treatment (Furuya et al. 1997; Mirto et al. 1999). Several studies have also shown that the mouse macrophage cell line, J774, is capable of internalizing extracellular depleted uranium (Kalinich and McClain 2001). Once internalized, the DU can induce cell death, via apoptosis, in a concentration-dependent manner (Kalinich et al. 2002). Not all cultured cell lines appear capable of internalizing DU. When assessed colorimetrically using the method of Kalinich and McClain (2001), Molt-4, a human T-cell leukemia line, and Reh, a human B-cell lymphoma line, did not appear to internalize DU added to the extracellular medium. In addition, these cell lines were far less susceptible to the cytotoxic effects of DU exposure, showing no significant change in viability compared to untreated cells (Fig. 10.1).

Peritoneal macrophages and splenic T-cells isolated from mice then exposed to varying concentrations of DU also demonstrated that macrophages are much more sensitive to the cytotoxic effects DU than other immune system cells (Wan et al. 2006). Treatment of cultured human osteoblast cells with either soluble or insoluble forms of DU transformed the cells to a neoplastic phenotype. These transformed cells also formed tumors when injected into immunocompromised mice (Miller et al. 1998; McClain and Miller 2007). As noted earlier, although DU is 40% less radioactive than natural uranium, it is still radioactive and that characteristic also has the

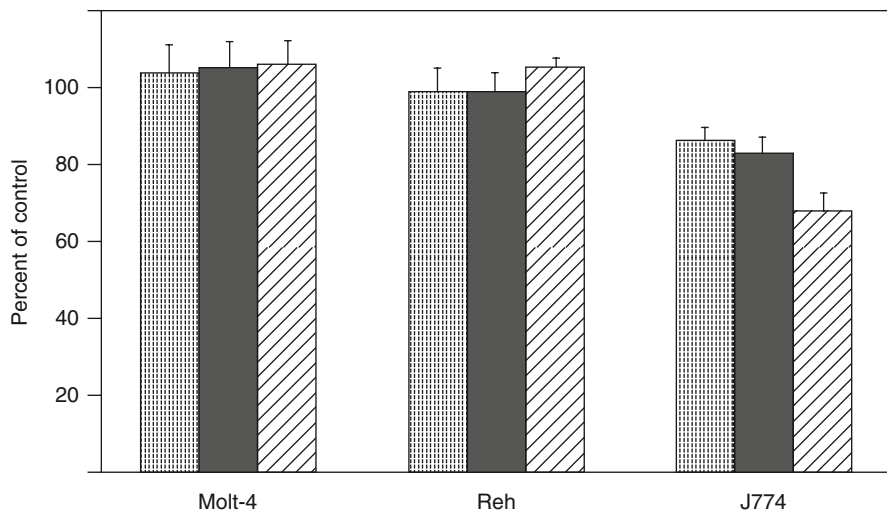


Fig. 10.1 Cell viability assessment of Molt-4, Reh, and J774 cells treated with depleted uranium-uranyl chloride for 24 h at 37°C. Viability was determined using the MTT assay and data normalized to values from untreated cells and are the mean of 6 independent experiments. Error bars represent standard error of the mean. The *stippled bars* represent a uranium concentration of 1 µg/ml, the *black bars* represent a uranium concentration of 10 µg/ml, and the *slanted-line bars* represent a uranium concentration of 100 µg/ml

potential to induce significant cellular damage. The question of whether the chemical or radiological property is primarily responsible for the cellular damage inflicted by DU is still open to debate. At present, it appears that the chemical characteristics of DU are predominantly responsible for the observed cellular damage, with the radiological component playing a smaller role (Miller et al. 2002a, b, 2003).

Along with inducing genotoxic effects *in vitro*, low-level DU exposure can also alter gene expression patterns in many cell types. In NR8383 cells, a rat alveolar macrophage cell line, DU has been shown to induce secretion of tumor necrosis factor α (TNF- α), as well as activate the c-Jun N-terminal kinase (JNK) and p38 mitogen-activated protein kinase (p38 MAPK) pathways (Gazin et al. 2004). This work suggests that macrophages exposed to uranium, either through inhalation or wound contamination, can secrete elevated amounts of TNF α , a major proinflammatory cytokine. Because of the central role TNF α plays in regulating the release of secondary inflammation mediators (Cromwell et al. 1992), any perturbation can have far reaching consequences for the organism. DU can also induce a number of stress-related genes in HepG2 cells, a human liver carcinoma cell line. In this assay, HepG2 cells, stably transfected with chloramphenicol acetyltransferase under the transcriptional control of a variety of stress-gene regulatory sequences, were treated with insoluble DU (Miller et al. 2004). Several categories of promoters were affected in a dose-dependent manner including transcription factor binding sites (FOS, NF κ BRE, CRE, p53RE, and RARE), cell cycle regulation sites (GADD45, GADD153), transport proteins (GRP78, HSP70), and the promoter for metallothionein IIA (HMTIIA). These data indicate that DU can activate gene expression through a variety of signal transduction pathways, including many that are involved in the carcinogenic process. Using microarray technology, Prat and colleagues (Prat et al. 2005), demonstrated that exposure of cultured HEK292 cells, a human embryonic kidney cell line, to DU resulted in both up- and down-regulation of numerous genes including many involved in signal transduction and trafficking pathways. Microarray technology was also used to assess the effect of DU exposure on gene expression patterns in mouse peritoneal macrophages and CD4⁺ T cells (Wan et al. 2006). Again, DU was shown to alter gene expression profiles with genes responsible for signal transduction pathways, chemokines, and interleukins affected the greatest. As a result of these findings, Wan et al. (2006) postulated the potential for cancer development as a consequence of DU exposure.

Heavy-Metal Tungsten Alloy

There have been far fewer studies on the toxicological and genotoxic properties of the heavy-metal tungsten alloys. There are several reports investigating the toxicity of tungsten alone. The cytotoxicity of degrading tungsten coils used medically for vascular occlusions was assessed in cultured human smooth muscle, endothelial, vascular, and fibroblast cells. Cytotoxicity was observed only at tungsten concentrations above 50 μ g/ml (Peuster et al. 2003). *In vitro* studies with

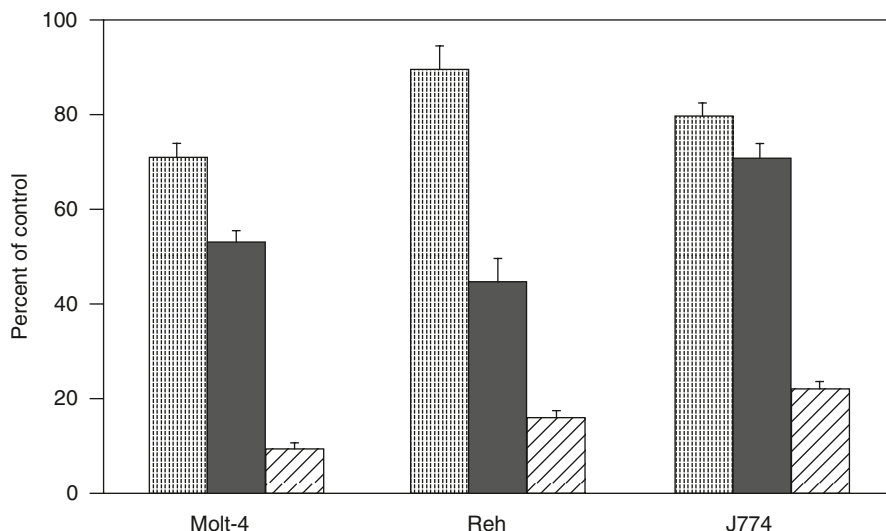


Fig. 10.2 Cell viability assessment of Molt-4, Reh, and J774 cells treated with heavy-metal tungsten alloy (91% tungsten, 6% nickel, 3% cobalt) for 24 h at 37°C. Viability was determined using the MTT assay and data normalized to values from untreated cells and are the mean of 6 independent experiments. *Error bars* represent standard error of the mean. The *stippled bars* represent an alloy concentration of 1 µg/ml, the *black bars* represent an alloy concentration of 10 µg/ml, and the *slanted-line bars* represent an alloy concentration of 100 µg/ml

J774, Molt-4, and Reh cells have shown that, unlike DU, exposure to a heavy-metal tungsten alloy composed of tungsten (92%), nickel (5%), and cobalt (3%) resulted in decreased viability of all three cell lines in a concentration-dependent manner (Fig. 10.2). The same tungsten alloy mixture, as well as one composed of tungsten (92%), nickel (5%), and iron (3%), was found to transform cultured human osteoblast (HOS) cells to a neoplastic phenotype (Miller et al. 2001). The individual metals comprising the alloys were also able to transform the HOS cells, but at a frequency far lower than the mixtures. In fact, when the transformation frequency data from the individual metals are compared with those of the alloys, it appears that there is synergistic effect between two or more of the metals, leading to increased transformation (Miller et al. 2002c). While both tungsten alloys (WNiCo and WNiFe) and all individual component metals could transform HOS cells, only those cells transformed by the tungsten alloys developed tumors when injected into immunocompromised mice (Miller et al. 2001). The tungsten/nickel/cobalt alloy was also capable of inducing the expression of several genes when assayed using chloramphenicol acetyltransferase-transfected HepG2 cells (Miller et al. 2004). As with DU, tungsten alloy had the ability to induce gene promoters in several categories including transcription factor binding sites (FOS, NFκBRE, CRE, and p53RE), transport proteins (HSP70), and the promoter for metallothionein IIA (HMTIIA). Surprisingly, tungsten alloy exposure had no effect on either

of the cell cycle regulation promoters tested (GADD45, GADD153) in contrast to DU. When tested individually, the metals comprising the alloy were also able to induce the promoters affected by the alloy, but did so at a much lower level. Again, a synergistic effect of the metals in the alloy on gene induction was observed (Miller et al. 2004).

In Vivo Studies

Depleted Uranium

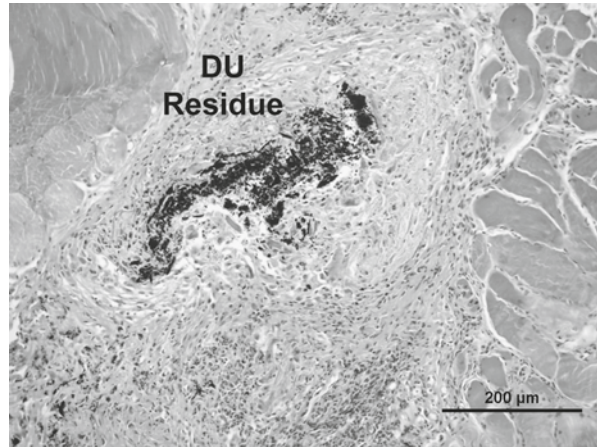
During the Persian Gulf War of 1991, several individuals suffered wounds containing embedded DU fragments. Concern, both chemical and radiological, over the long-term health effects of this unique material led to several studies investigating the toxicological and carcinogenic properties of embedded DU fragments. Development and validation of a rodent model system to study the biological effects of embedded fragments was undertaken at the Armed Forces Radiobiology Research Institute (Castro et al. 1996). This model system involves surgically implanting small pellets of test material into the leg muscles to mimic shrapnel wounds. An x-ray of the location of several 1×2 mm cylindrical pellets is shown in Fig. 10.3. Sprague Dawley rats, implanted with up to 20 DU pellets (1×2 mm cylinders) for periods up to 2 years, exhibited no overt adverse health effects. No tumors were observed at the pellet implantation sites for either DU or tantalum, an inert negative control metal (Pellmar et al. 1999).

The DU pellets degrade rapidly *in vivo*, with significant uranium levels measured in the urine as early as 2 days post-implantation. Some of the DU pellet material is not immediately solubilized and can be found at the pellet implantation site



Fig. 10.3 Radiograph of rat showing location of depleted uranium pellets (1×2 mm cylinders) surgically implanted in the gastrocnemius muscles of the rear legs

Fig. 10.4 Histopathological examination of a hematoxylin-and-eosin-stained section of leg muscle from a F344 rat implanted with depleted uranium pellets for 3 months. DU residue is visible at pellet implantation site. Scale bar=200 μ m



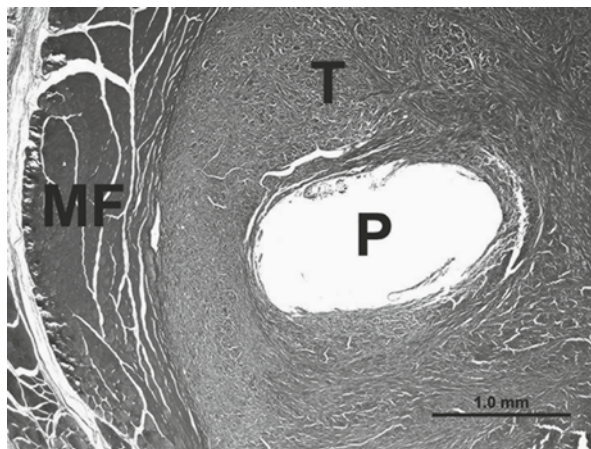
upon histopathological examination (Fig. 10.4). Over time, as more of the pellet degrades, DU can be found in a variety of tissues including kidney, liver, brain, testes, and lymph nodes (Pellmar et al. 1999). Similar results were reported by Hahn and colleagues using Wistar rats (Hahn et al. 2002). When DU was implanted as 1×2 mm cylindrical pellets, no tumors were observed. However, when embedded as squares ($2.5 \times 2.5 \times 1.5$ mm or $5 \times 5 \times 1.5$ mm), DU induced soft-tissue sarcomas at the implantation sites. Rats implanted with tantalum did not develop tumors indicating that the observed DU effects were not the result of foreign-body carcinogenesis (Brand et al. 1975, 1976). As with the Pellmar study, the DU material began to degrade shortly after implantation. Taken together these studies indicate that once a certain mass is reached, DU fragments are capable of inducing neoplastic changes resulting in soft-tissue sarcomas in laboratory rats.

Embedded DU fragments also induced gene changes in the muscle tissue surrounding the metal. Using Northern blot analysis, Miller et al. (2000) demonstrated elevated mRNA levels of p53, k-ras, and bcl-2 in muscle tissue adjacent to embedded DU pellets. Utilizing immunohistochemical techniques, Hahn (2007) showed increased p53 protein levels in tissue surrounding the implanted DU. However, MDM2, c-myc, and p21 levels were found to be no different than control.

Heavy-Metal Tungsten Alloy

Thus far only one study has been published in the peer-reviewed literature describing the health effects of embedded tungsten alloy. F344 rats implanted with a tungsten alloy comprised of tungsten (91.1%), nickel (6.0%), and cobalt (2.9%) developed highly aggressive rhabdomyosarcomas at the pellet implantation sites (Kalinich et al. 2005). The tumors grew rapidly and metastasized to the lungs requiring euthanasia of the animals. Tumor incidence was 100%. Rats implanted with nickel, a known carcinogen, also developed tumors, but did so at a slower rate

Fig. 10.5 Histopathological examination of a Gomori trichrome-stained section of leg muscle and tumor from a F344 rat implanted with heavy-metal tungsten alloy pellets (91.1% tungsten, 6% nickel, 2.9% cobalt) for 6 months. “P” indicates site of pellet implantation. “T” denotes the tungsten alloy-induced tumor (rhabdomyosarcoma). “MF” shows area of normal muscle fibers. Scale bar = 1.0 mm



than those rats treated with the tungsten alloy. Rats implanted with tantalum did not develop tumors. As with DU, the metals comprising the tungsten alloy rapidly solubilized and were found in the urine at an order of magnitude higher than control values (Kalinich et al. 2008). However, in contrast to DU, no particulate material was observed at the pellet implantation site upon histopathological examination (Fig. 10.5). Significant hematological changes were observed as early as 1 month after implantation; well before any neoplastic changes had occurred. Whether these changes are attributable to an individual metal in the alloy or a synergistic effect between two or more components is not yet known.

Human Exposures

Depleted Uranium

As noted above, the first widespread use of DU was in the 1991 Persian Gulf War. During this conflict several individuals were wounded with DU fragments. United States military personnel with retained DU fragments have been followed clinically by the Veterans Affairs Medical Center in Baltimore, Maryland. After 16 years of follow-up surveillance, there has been no indication of any clinically significant DU-related health effects (McDiarmid et al. 2000, 2001, 2004, 2006, 2007a, b, 2009; Dorsey et al. 2009). However, there is some indication of a weak genotoxic effect as a result of the embedded DU fragments. This was determined by fluorescent in-situ hybridization (FISH) analysis of the hypoxanthine-guanine phosphoribosyl transferase (HPRT) locus in peripheral blood lymphocytes (McDiarmid et al. 2007a, b). As a result of these findings, the authors have recommended continued surveillance of these individuals.

Heavy-Metal Tungsten Alloy

A variety of tungsten-based munitions have been proposed as replacements for DU in armor-penetrating shells and for lead in small-caliber ammunition. As yet, there have been no reports on whether there are individuals with retained fragments of these materials and, further, that these fragments are resulting in adverse health effects. There are several reports in the literature describing adverse health effects due to exposure to tungsten and tungsten-based materials. As part of an initiation rite, a French artillery soldier drank 250 ml of a beer and wine mixture that had been used to rinse a gun barrel. Shortly after, he suffered seizures and was comatose for 24 h (Marquet et al. 1996). Extremely high levels of tungsten were found in his blood and urine and persisted for 2 weeks (Marquet et al. 1997). Although his malady was blamed on tungsten intoxication, there are some who believe the organic residue left in the gun barrel as a result of the explosive charge of the shell was actually to blame for his condition (Lison et al. 1997). There have also been two reports in the literature of granuloma formation as a result of embedded metal from a lawn mower blade (Saruwatari et al. 2009) and a chain saw blade (Osawa et al. 2006), respectively. In both cases, metal analysis of the excised fragment showed that it was composed primarily of tungsten with smaller amounts of other metals.

Conclusions

Little is known about metal-induced gene expression changes and carcinogenicity especially with respect to militarily-relevant metals. Improvement in weapons design and the terroristic use of Improvised Explosive Devices will continue to increase the possibility of embedded fragment injuries with metals or metal mixtures whose toxicological properties are not fully understood. The metals discussed in this chapter, depleted uranium and heavy-metal tungsten alloy, are only two such examples. In this final section, areas requiring additional research in order to enhance our understanding of heavy metal carcinogenicity will be discussed.

Although *in vivo* exposure scenarios may differ, the common factor in most is the presence of the macrophage. Macrophages are not only capable of phagocytizing small metal particulates (Berry et al. 1997; Lison and Fritsch 1999), but have also been shown to interact with and modify the surface composition of metal alloys through the production of reactive chemical species (Thomsen and Gretzer 2001; Lin and Bumgardner 2004). The critical role the macrophage plays in wound repair, as well as its postulated regulatory link between inflammation and cancer induction (Sica et al. 2008), makes this cell type key in understanding heavy metal-induced carcinogenicity.

In vitro studies have demonstrated that macrophage viability is affected by both DU and heavy-metal tungsten alloy. In addition, gene expression patterns are perturbed by both treatments. No consensus has been reached on an exact list of specific up- and down-regulated genes by metal exposure primarily due to experimental design differences between the published studies. However, there is a pattern of up-regulation of those genes involved in transcription regulation and signal transduc-

tion, as well as those coding for the interleukins and transport proteins. Areas that require further research include an investigation of gene induction by insoluble as well as soluble metals and alloys. As seen with DU, even though a fragment begins to rapidly degrade once implanted (as determined by urine uranium levels), substantial particulate material is still found at the implantation site. As yet unknown is whether exposure to the insoluble DU will result in a similar pattern of gene induction as for the soluble material. Exposure to heavy-metal tungsten alloy raises similar concerns and may be more difficult to decipher because of the number of metals comprising the alloy and their proposed synergism with respect to biological effects (Miller et al. 2004). Again, a detailed investigation of the alloy, as well as the individual metal components, in both soluble and insoluble forms will greatly enhance our knowledge of metal-induced gene expression.

Although *in vitro* studies will provide a foundation for our understanding of heavy metal-induced carcinogenicity, *in vivo* models will be necessary to definitively determine if embedded fragments of these materials have the potential to cause cancer. In addition, recent advances in laser microdissection and microarray techniques will be crucial in elucidating metal-induced gene-expression changes in the tissue immediately adjacent to the embedded fragment. Not only will this information allow correlation of *in vitro* and *in vivo* findings, but it will be critical if changes in treatment strategies, either surgically or pharmacologically, are required in order to maintain the health and well-being of wounded individuals.

Acknowledgements The views expressed here are strictly those of the author and not those of the Armed Forces Radiobiology Research Institute, the Uniformed Services University, or the United States Department of Defense. Mention of any commercial reagents or devices does not constitute endorsement by the United States Government. Dr. Kalinich has been supported in part by grants from the U.S. Army Medical Research and Materiel Command (Award #: DAMD17-01-1-0821) and the U.S. Army Peer-Reviewed Medical Research Program (Award #: W81XWH-06-2-0025). The author would like to thank Dr Steven Mog, DVM for obtaining histopathological images.

References

- ATSDR (Agency for Toxic Substances and Disease Registry), Public Health Service, U.S. Department of Health and Human Services (1999) Toxicological profile for uranium
- ATSDR (Agency for Toxic Substances and Disease Registry), Public Health Service, U.S. Department of Health and Human Services (2005) Toxicological profile for tungsten
- Berry JP, Zhang L, Galle P, Ansoborlo E, Henge-Napoli MH, Donnadieu-Claraz M (1997) Role of the alveolar macrophage lysosomes in metal detoxification. *Microsc Res Tech* 36:313–323
- Bistline RW, Watters RL, Lebel JL (1972) A study of translocation dynamics of plutonium and americium from simulated puncture wounds in beagle dogs. *Health Phys* 22:829–831
- Brand KG, Buoen LC, Johnson KH, Brand T (1975) Etiological factors, stages, and the role of the foreign body in foreign-body tumorigenesis: a review. *Cancer Res* 35:279–286
- Brand KG, Johnson KH, Buoen LC (1976) Foreign body tumorigenesis. *CRC Crit Rev Toxicol* 4:353–394
- Brewer L, Fairbrother A, Clark J, Amick D (2003) Acute toxicity of lead, steel, and an iron-tungsten-nickel shot to mallard ducks (*Anas platyrhynchos*). *J Wild Dis* 39:638–648
- Broughton G, Janis JE (2006) The basic science of wound healing. *Plast Reconstr Surg* 117 (Suppl):12S–34S

- Castro CA, Benson KA, Bogo V, Daxon EG, Hogan JB, Jacocks HM, Landauer MR, McBride SA, Shehata CW (1996) Establishment of an animal model to evaluate the biological effects of intramuscularly embedded depleted uranium fragments. Armed Forces Radiobiology Research Institute. Bethesda, MD, Technical Report 96-3
- Cromwell O, Hamid Q, Corrigan CJ, Barkans J, Meng Q, Collins PD, Kay AB (1992) Expression and generation of interleukin-8, IL-6 and granulocyte-macrophage colony-stimulating factor by bronchial epithelial cells and enhancement by IL-1 beta and tumor necrosis factor. *Immunology* 77:330–337
- Dagle GE, Lebel JL, Phemister RD, Watters RL, Gomez LS (1985) Translocation kinetics of plutonium oxide from the popliteal lymph nodes of beagles. *Health Phys* 28:395–398
- Dorsey CD, Engelhardt SM, Squibb KS, McDiarmid MA (2009) Biological monitoring for depleted uranium exposure in US veterans. *Environ Health Perspect* 117:953–956
- Dublineau I, Grison S, Grandcolas L, Baudelin C, Tessier C, Suhard D, Frelon S, Cossonnet C, Claraz M, Ritt J, Paquet P, Voisin P, Gourmelon P (2006) Absorption, accumulation and biological effects of depleted uranium in Peyer's patches of rats. *Toxicology* 227:227–239
- Furuya R, Kumagai H, Hishida A (1997) Acquired resistance to rechallenge injury with uranyl acetate in LLC-PK1 cells. *J Lab Clin Med* 129:347–355
- Gazin V, Kerdine S, Grillon G, Pallardy M, Raoul H (2004) Uranium induces TNF α secretion and MAPK activation in a rat alveolar macrophage cell line. *Toxicol Appl Pharmacol* 194:49–59
- Hahn FF (2007) Carcinogenesis of depleted uranium: studies in animals. In: Miller AC (ed) *Depleted uranium: properties, uses, and health consequences*. CRC Press, Boca Raton, FL
- Hahn FF, Guilmette RA, Hoover MD (2002) Implanted depleted uranium fragments cause soft tissue sarcomas in the muscles of rats. *Environ Health Perspect* 110:51–59
- International Commission on Radiological Protection (1966) Deposition and retention models for internal dosimetry of the human respiratory tract. Task group on lung dynamics. *Health Phys* 12:173–207
- Kalinich JF, McClain DE (2001) Staining of intracellular deposits of uranium in cultured murine macrophages *Biotech Histochem* 76:247–252
- Kalinich JF, Ramakrishnan N, Villa V, McClain DE (2002) Depleted uranium-uranyl chloride induces apoptosis in mouse J774 macrophages. *Toxicology* 179:105–114
- Kalinich JF, Emond CA, Dalton TK, Mog SR, Coleman GD, Kordell JE, Miller AC, McClain DE (2005) Embedded weapons-grade tungsten alloy shrapnel rapidly induces metastatic high-grade rhabdomyosarcomas in F344 rats. *Environ Health Perspect* 113:729–734
- Kalinich JF, Vergara VB, Emond CA (2008) Urinary and serum metal levels as indicators of embedded tungsten alloy fragments. *Mil Med* 173:754–758
- Kelly ME, Fitzgerald SD, Aulerich RJ, Balander RJ, Powell DC, Stickle RL, Stevens W, Cray C, Tempelman RJ, Bursian SJ (1998) Acute effects of lead, steel, tungsten-iron, and tungsten-polymer shot administered to game-farm mallards *J Wild Dis* 34:673–687
- Kraabel BJ, Miller MW, Getzy DM, Ringelman JK (1996) Effects of embedded tungsten-bismuth-tin shot and steel shot on mallards (*Anas platyrhynchos*). *J Wild Dis* 32:1–8
- Leggett RW (1997) A model of the distribution and retention of tungsten in the human body. *Sci Total Environ* 206:147–165
- Leggett RW, Pellmar TC (2003) The biokinetics of uranium migrating from embedded DU fragments. *J Environ Radioact* 64:205–225
- Li J, Chen J, Kirsner R (2007) Pathophysiology of acute wound healing. *Clin Dermatol* 25:9–18
- Lin H-Y, Bumgardner JD (2004) Changes in the surface oxide composition of Co-Cr-Mo implant alloy by macrophage cells and their released reactive chemical species. *Biomaterials* 25:1233–1238
- Lin RH, Wu LJ, Lee CH, Lin-Shiau SY (1993) Cytogenetic toxicity of uranyl nitrate in Chinese hamster ovary cells. *Mut Res* 319:197–203
- Lison D, Buchet JP, Hoet P (1997) Toxicity of tungsten. *Lancet* 349:58–59
- Lizon C, Fritsch P (1999) Chemical toxicity of some actinides and lanthanides toward alveolar macrophages: an *in vitro* study. *Int J Radiat Biol* 75:1459–1471
- Lloyd RD, Atherton DR, Mays CW, McFarland SS, Williams JL (1974) The early excretion, retention and distribution of injected curium citrate in beagles. *Health Phys* 27:61–67

- Marquet P, Francois B, Vignon P, Lachatre G (1996) A soldier who had seizures after drinking quarter of a litre of wine. *Lancet* 348:1070
- Marquet P, Francois B, Lotfi H, Turcant A, Debord J, Nedelec G, Lachatre G (1997) Tungsten determination in biological fluids, hair and nails by plasma emission spectrometry in a case of severe acute toxication in man. *J Forensic Sci* 42:527–530
- McClain DE, Miller AC (2007) Depleted uranium biological effects: introduction and early *in vitro* and *in vivo* studies. In: Miller AC (ed) *Depleted uranium: properties, uses, and health consequences*. CRC Press, Boca Raton
- McDiarmid MA, Keogh JP, Hooper FJ, McPhaul K, Squibb K, Kane R, DiPino R, Kabat M, Kaup B, Anderson L, Hoover D, Brown L, Hamilton M, Jacobson-Kram D, Burrows B, Walsh M (2000) Health effects of depleted uranium on exposed Gulf War veterans. *Environ Res* 82:168–180
- McDiarmid MA, Squibb K, Engelhardt S, Oliver M, Gucer P, Wilson PD, Kane R, Kabat M, Kaup B, Anderson L, Hoover D, Brown L, Jacobson-Kram D (2001) Surveillance of depleted uranium exposed Gulf War veterans: health effects observed in an enlarged “friendly fire” cohort. *J Occup Environ Med* 43:991–1000
- McDiarmid MA, Engelhardt S, Oliver M, Gucer P, Wilson PD, Kane R, Kabat M, Kaup B, Anderson L, Hoover D, Brown L, Handwerker B, Albertini R, Jacobson-Kram D, Thorne CD, Squibb KS (2004) Health effects of depleted uranium on exposed Gulf War veterans: a ten-year follow-up. *J Toxicol Environ Health—Part A—Curr Issues* 67:277–296
- McDiarmid MA, Engelhardt SM, Oliver M, Gucer P, Wilson PD, Kane R, Kabat M, Kaup B, Anderson L, Hoover D, Brown L, Albertini RJ, Gudi R, Jacobson-Kram D, Thorne CD, Squibb KS (2006) Biological monitoring and surveillance results of Gulf War I veterans exposed to depleted uranium. *Int Arch Occup Environ Health* 79:11–21
- McDiarmid MA, Engelhardt SM, Oliver M, Gucer P, Wilson PD, Kane R, Cernich A, Kaup B, Anderson L, Hoover D, Brown L, Albertini R, Gudi R, Jacobson-Kram D, Squibb KS (2007a) Health surveillance of Gulf War I veterans exposed to depleted uranium: updating the cohort. *Health Phys* 93:60–73
- McDiarmid MA, Squibb K, Engelhardt S, Gucer P, Oliver M (2007b) Surveillance of Gulf War I veterans exposed to depleted uranium: 15 years of follow-up. *Euro J Oncol* 12:235–242
- McDiarmid MA, Engelhardt SM, Dorsey CD, Oliver M, Gucer P, Wilson PD, Kane R, Cernich A, Kaup B, Anderson L, Hoover D, Brown L, Albertini R, Gudi R, Squibb KS (2009) Surveillance results of depleted uranium-exposed Gulf War I veterans: sixteen years of follow-up. *J Toxicol Environ Health—Part A—Curr Issues* 72:14–29
- Miller AC, Blakely WF, Livengood D, Whittaker T, Xu J, Ejnik JW, Hamilton MM, Parlette E, St John T, Gerstenberg HM, Hsu H (1998) Transformation of human osteoblast cells to the tumorigenic phenotype by depleted uranium-uranyl chloride. *Environ Health Perspect* 106:465–471
- Miller AC, Xu J, Stewart M, Emond E, Hodge S, Matthews C, Kalinich J, McClain DE (2000) Potential health effects of the heavy metals, depleted uranium and tungsten, used in armor-piercing munitions: comparison of neoplastic transformation, mutagenicity, genomic instability, and oncogenesis. In: Centeno JA, Coltery PH, Vernet G, Finkelman RB, Gibb H, Etienne JC (eds) *Metals in biology and medicine*, vol 6. John Libbey Eurotext, Paris
- Miller AC, Mog S, McKinney L-A, Luo L, Allen J, Xu J, Page N (2001) Neoplastic transformation of human osteoblast cells to the tumorigenic phenotype by heavy metal-tungsten alloy particles: induction of genotoxic effects. *Carcinogenesis* 22:115–125
- Miller AC, Stewart M, Brooks K, Shi L, Page N (2002a) Depleted uranium-catalyzed oxidative DNA damage: absence of significant alpha particle decay. *J Inorg Biochem* 91:246–252
- Miller AC, Xu J, Stewart M, Brooks K, Hodge S, Shi L, Page N, McClain D (2002b) Observation of radiation-specific damage in human cells exposed to depleted uranium: dicentric frequency and neoplastic transformation as endpoints. *Radiat Protec Dosim* 99:275–278
- Miller AC, Xu J, Stewart M, Prasanna PGS, Page N (2002c) Potential late health effects of depleted uranium and tungsten used in armor-piercing munitions: comparison of neoplastic transformation and genotoxicity with the known carcinogen nickel. *Mil Med* 167(Suppl 1):120–122

- Miller AC, Brooks K, Stewart M, Anderson B, Shi L, McClain D, Page N (2003) Genomic instability in human osteoblast cells after exposure to depleted uranium: delayed lethality and micronuclei formation. *J Environ Radioact* 64:247–259
- Miller AC, Brooks K, Smith J, Page N (2004) Effect of the militarily-relevant heavy metals, depleted uranium and heavy metal tungsten-alloy on gene expression in human liver carcinoma cells (HepG2). *Mol Cell Biochem* 255:247–256
- Mirto H, Henge-Napoli MH, Gibert R, Ansoborlo E, Fournier M, Cambar J (1999) Intracellular behavior of uranium (VI) on renal epithelial cell in culture (LLC-PK1): influence of uranium speciation. *Toxicol Lett* 104:249–256
- Mitchell RR, Fitzgerald SD, Aulerich RJ, Balander RJ, Powell DC, Tempelman RJ, Cray C, Stevens W, Bursian SJ (2001a) Hematological effects and metal residue concentrations following chronic dosing with tungsten-iron and tungsten-polymer shot in adult game-farm mallards. *J Wild Dis* 37:459–467
- Mitchell RR, Fitzgerald SD, Aulerich RJ, Balander RJ, Powell DC, Tempelman RJ, Stevens W, Bursian SJ (2001b) Reproductive effects and duckling survivability following chronic dosing with tungsten-iron and tungsten-polymer shot in adult game-farm mallards. *J Wild Dis* 37:468–474
- Mitchell RR, Fitzgerald SD, Aulerich RJ, Balander RJ, Powell DC, Tempelman RJ, Stickle RL, Stevens W, Bursian SJ (2001c) Health effects following chronic dosing with tungsten-iron and tungsten-polymer shot in adult game-farm mallards. *J Wild Dis* 37:451–458
- Monleau M, De Meo M, Paquet F, Chazel V, Dumenil G, Donnadieu-Clarz M (2006) Genotoxic and inflammatory effects of depleted uranium particles inhaled by rats. *Toxicol Sci* 89:287–295
- Morrow PE, Gibb FR, Gazioglu KM (1967) A study of particulate clearance from the human lungs. *Am Rev Respirat Dis* 96:1209–1221
- Osawa R, Abe R, Inokuma D, Yokota K, Ito H, Nabeshima M, Shimizu H (2006) Chain saw blade granuloma: reaction to a deeply embedded metal fragment. *Arch Dermatol* 142:1079–1080
- Pellmar TC, Fuciarelli AF, Ejnik JW, Hamilton M, Hogan J, Strocko S, Emond C, Mottaz HM, Landauer MR (1999) Distribution of uranium in rats implanted with depleted uranium pellets. *Toxicol Sci* 49:29–39
- Peuster M, Fink C, von Schnakenburg C (2003) Biocompatibility of corroding tungsten coils: *in vitro* assessment of degradation kinetics and cytotoxicity on human cells. *Biomaterials* 24:4057–4061
- Prat O, Berenguer F, Malard V, Tavan E, Sage N, Steinmetz G, Quemener E (2005) Transcriptional and proteomic responses of human renal HEK293 cells to uranium toxicity. *Proteomics* 5:297–306
- Saruwatari H, Kamiwada R, Matsushita S, Hashiguchi T, Kawai K, Kanekura T (2009) Tungsten granuloma attributable to a piece of lawn-mower blade. *Clin Exp Dermatol* 34:e268–e269
- Schins RP, Borm PJ (1999) Mechanisms and mediators in coal dust induced toxicity: a review. *Ann Occup Hygiene* 43:7–33
- Sica A, Allavena P, Mantovani A (2008) Cancer related inflammation: the macrophage connection. *Cancer Lett* 264:204–215
- Tasat DR, De Ray BM (1987) Cytotoxic effect of uranium dioxide on rat alveolar macrophages. *Environ Res* 112:1628–1635
- Thomsen P, Gretzer C (2001) Macrophage interactions with modified material surfaces. *Curr Opin Solid State Mater Sci* 5:163–176
- Tsirogianni AK, Moutsopoulos NM, Moutsopoulos HM (2006) Wound healing: immunological aspects. *Injury* 37S:S5–S12
- van der Voet GB, Todorov TI, Centeno JA, Jonas W, Ives J, Mullick FG (2007) Metals and health: a clinical toxicological perspective on tungsten and review of the literature. *Mil Med* 172:1002–1005
- Wan B, Fleming JT, Schultz TW, Sayler GS (2006) *In vitro* immune toxicity of depleted uranium: effects on murine macrophages, CD⁺ T cells, and gene expression profiles. *Environ Health Perspect* 114:85–91
- Yokel RA, Lasley SM, Dorman DC (2006) The speciation of metals in mammals influences their toxicokinetics and toxicodynamics and therefore human health risk assessment. *J Toxicol Environ Health Part B* 9:63–85

Chapter 11

Role of Oxidative Damage in Metal-Induced Carcinogenesis

Kazimierz S. Kasprzak

Abstract This chapter presents and discusses evidence of possible mechanistic involvement of oxidative DNA and protein damage in metal-induced carcinogenesis. Carcinogenic metals, e.g., Be, Cd, Cr, Co, Ni, and the metalloid As, are capable of generating various kinds of active oxygen and other reactive species in direct redox reactions with O_2 , $O_2^{\bullet-}$, H_2O_2 , organic peroxides, and other cellular or tissue substrates, and/or indirectly—by inducing inflammation or unleashing physiological redox-active metals, Fe and Cu. The reactive species may damage all cell components, including DNA, RNA, free triphosphonucleosides, proteins, and lipids, and exhaust cellular antioxidant defenses, e.g., deplete ascorbate. The damage may be aggravated by metal-assisted inhibition of DNA repair and histone demethylation systems. The association of oxidative damage with carcinogenesis is strongly supported by mutagenicity of DNA base products, strand breaks, apurinic sites, cross-links, and adducts typical for the attacking reactive species (oxygen-, carbon-, or sulfur-centered radicals), originating from oxidized amino acids and proteins, and 4-hydroxynonenal, a lipid oxidation product. Oxidative damage to nuclear proteins affects chromatin structure and gene expression, whereas such damage to regulatory proteins disturbs cell cycle and apoptosis. Thus, oxidative DNA damage may assist in the initiation while RNA and protein damage may facilitate the promotion and progression of cancer.

Introduction

Certain transition metals, including beryllium, cadmium, chromium, cobalt, and nickel, and the metalloid arsenic, are carcinogenic to humans. The same metals and several more (lead, copper, platinum, iron, tungsten, and uranium) have been found

K. S. Kasprzak (✉)

Laboratory of Comparative Carcinogenesis, National Cancer Institute at Frederick, Bldg. 538, Room 205E, Frederick MD 21702-1201, USA

Tel.: +1-301-846-5738

Fax: +1-301-846-5946

e-mail: kasprzak@mail.nih.gov

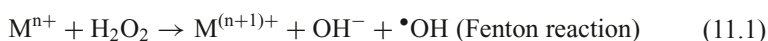
to induce cancer in laboratory or domestic animals (Wei et al. 1985; Kalinich et al. 2005; Kasprzak and Salnikow 2007; Miller and McClain 2007; Beyersmann and Hartwig 2008; Wild et al. 2009). The underlying molecular mechanisms stem from the rich coordination chemistry and redox chemistry of these metals. They include pathogenic effects resulting directly from adventitious binding of carcinogenic metal ions to cellular components at sites designated to carry physiological metal ions and other sites, especially those in the cell nucleus or, indirectly, from redox activity of the metals in the intra- and extra-cellular environment. The binding may affect the structure and function of a biomolecule, while the redox activity of the metal gives rise to chemical reactions that generate very reactive radical intermediates. Such intermediates will attack and damage cell components that ultimately leads to a variety of detrimental effects, ranging from a sudden death to the slow, multi-stage process of cellular transformation to neoplastic phenotype.

It is believed that neoplastic transformation of cells results from mutations, i.e., heritable alterations in the genetic code. Therefore, it has been presumed that the ultimate target of chemical carcinogens is the DNA molecule to which they bind and thus impair its correct replication, leading to mutations. From this point of view, DNA having abundance of phosphate anions as well as nitrogen and oxygen metal coordination centers looks like an ideal partner for binding metal cations (Wu and Davey 2010). However, cellular DNA is tightly packed in the nucleus by the histone proteins that can bind metal ions as well and with even stronger affinity. Due to the abundance of thiol groups, some other types of nuclear proteins, e.g., zinc-fingers and metallothioneins, may also be expected to bind metals other than zinc (Nordberg 1998; Kroncke and Klotz 2009; Ngu and Stillman 2009; Chiaverini and De Ley 2010; Klug 2010). Therefore, it is not surprising that following *in vitro* and *in vivo* exposures of cells metals have been found in cell nuclei as well as at other cellular sites (Bryan 1981). However, metal distribution between the DNA and protein moieties in the nuclei of living cells remains largely unknown. The same is true for mitochondrial DNA. Nevertheless, we may assume that proteins are important providers of transition metal binding sites in the cell nucleus. And, most importantly, at least some of those proteins can assist in the generation of reactive intermediates in redox reactions of the bound metal with cellular oxidants and reducing (anti-oxidant) molecules. The damage resulting from metal binding and redox reactions, especially that affecting DNA repair and gene expression regulating proteins, may be involved in carcinogenesis through epigenetic mechanisms. Thus, in addition to having the capacity to initiate carcinogenesis through genotoxic insults on DNA, the metals also can promote and assist in progression of carcinogenesis through epigenetic toxicity.

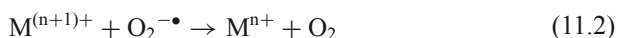
In this chapter, we will consider mostly the effects related to the generation of reactive intermediates by the ingested metal derivatives (both, particulate and soluble metal compounds) and their possible mechanistic involvement in carcinogenesis. Less attention will be devoted to strictly conformational effects of metal binding on the function of their bioligands unless that function is critical to the fidelity of gene replication and expression (e.g., DNA repair and signaling molecules).

Basic Redox Biochemistry of Carcinogenic Metals

In the cellular/tissue environment, the ingested metal derivatives are likely to react with ambient oxygen (O_2) and the metabolic intermediates, superoxide ($O_2^{\bullet-}$) and hydrogen peroxide (H_2O_2), present in cell nucleus and cytoplasm (Kukielka and Cederbaum 1990). The major chemical mechanisms involve the Fenton/Haber–Weiss reactions and autoxidation:



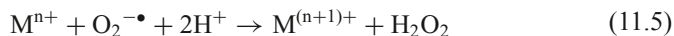
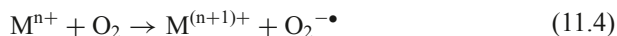
The metal cation, just oxidized, may be turned back to reaction 11.1 by reduction with $O_2^{\bullet-}$:



The balance of these two reactions is:



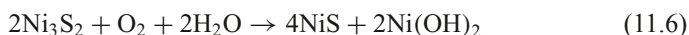
Thus, the two oxidation states of a metal cation (M^{n+} and $M^{(n+1)+}$) constitute a catalytic electron transfer (redox) couple. In the absence of chelators, the Fenton reaction is driven by Cu(I), Fe(II), Co(II), Ti(III), and Cr(V) ions. Besides metabolism, the substrates for the Fenton/Haber–Weiss chemistry may also be generated through autoxidation of metal ions:



The yield of $O_2^{\bullet-}$ and/or H_2O_2 in reactions 11.4 and 11.5 depends on pH and the presence or absence of ligands (chelators). Equations 11.2 and 11.5 indicate that, depending on the reaction conditions, $O_2^{\bullet-}$ may serve as either reductant or oxidant of a metal ion. Metal compounds interacting with H_2O_2 produce not only free $\bullet OH$ radicals but also other strong oxidants, such as singlet oxygen, and metal-centered -oxo and -peroxo species, all capable of damaging DNA and proteins. The formation of the latter oxidants “caged” at the metal binding sites provides an explanation for the often observed site specificity of metal-mediated oxidative damage (Klein et al. 1991; Standeven and Wetterhahn 1991; Kasprzak 1996; Bal et al. 1997a, b; Landolph 1999; Kasprzak and Buzard 2000; Sugden and Stearns 2000). The ligand complexing the metal cation strongly affects the above reactions (Bartosz 1995; Landolph 1999; Kasprzak and Buzard 2000). It may either enhance or inhibit them. For example, autoxidation of Fe(II) is enhanced by EDTA and nitrilotriacetic acid (NTA) (Hamazaki et al. 1989), but inhibited by o-phenanthroline and deferoxamine (Loeb et al. 1988; Nassi-Calò et al. 1989). NTA enables Fe(III) to react with H_2O_2 and generate $\bullet OH$ (Inoue and Kawanishi 1987). Deferoxamine inhibits free radical generation by Cr(V) (Shi et al. 1992). At physiological pH range, Ni(II) aquo-cation reacts with H_2O_2 only very slowly (Sigel 1974). However, its reactivity toward

H_2O_2 and O_2 may be greatly accelerated by specific bioligands (see below). Likewise, Co(II) aqua-cation, stable under air, becomes sensitive to oxidation with O_2 in the presence of organic ligands. The same ligand may enhance redox activity of one metal but suppress that of another metal (Fig. 11.2). Chelator may participate in the redox reaction and become itself a source of radical intermediates (Kasprzak 1996; Landolph 1999; Kasprzak and Buzard 2000).

Redox chemistry may also be involved in the mechanisms of oxidative damage inflicted by particulate metal carcinogens composed of metal sulfides, pure metals, metal alloys and sinters (Kalinich et al. 2005), and asbestos (Kasprzak 1996; Landolph 1999; Xu et al. 1999; Kasprzak and Buzard 2000). The sulfides usually display higher carcinogenic activity than other derivatives of the same metals. One possible reason for this is the potential of both the metal and the sulfur moieties to undergo oxidation and thus activate O_2 or other oxygen species. In aqueous media the reactions are as follows:



Reactions 11.6 and 11.7 show only the end products, which had been first identified in test tube experiments (Kasprzak and Sunderman 1977). However, the generation of reactive intermediates, such as SO_3^{2-} and Ni_7S_6 , in the course of these reactions was later found in cells exposed to Ni_3S_2 (Oskarsson et al. 1979; Lee et al. 1982) and *in vitro* (Shi et al. 1994).

The W–Co hard metal particles release carcinogenic cobalt to the cellular milieu due to redox reactions driven by the tungsten/cobalt galvanic interaction with likely participation of and damage to various components of the surrounding biological “electrolyte” (De Boeck et al. 2003; Lison et al. 1995; Francia et al. 2007). In addition, particulate metal carcinogens, deposited in animal tissues through inhalation or ingestion, trigger inflammatory response that results in infiltration of the affected tissue by macrophages and other phagocytes with all their secretory and intrinsic oxidants, including H_2O_2 and hypochlorous acid, both known to yield $\bullet\text{OH}$ in the presence of certain transition metal ions (Klein et al. 1991; Kasprzak 1996; Kasprzak and Buzard 2000). Macrophages also release nitric oxide, NO, a multifunctional signaling radical species that readily interacts with thiol groups in proteins to form S-nitrosothiols. NO, reacting with $\text{O}_2^{\bullet-}$, forms peroxynitrite. Transition metals rapidly decompose S-nitrosothiols to NO and disulfides (thus causing thiol oxidation) that may dysregulate the signaling functions of NO. They also decompose peroxynitrite and promote protein nitration (reviewed in Buzard and Kasprzak 2000; Petit et al. 2006).

Transition metals have been found in numerous experiments to promote lipid peroxidation in living cells. The metals are capable of doing this through initiation (e.g., by generation of $\bullet\text{OH}$ from metabolic H_2O_2) and/or extension of the peroxidation process caused by other factors, e.g., lipoxygenase. In the latter case, metal ions would react with naturally produced lipid peroxides to generate alkoxy- and

peroxy-radicals and other reactive products. Overall, the chemistry underlying the complex processes of lipid peroxidation in the presence of metals encompasses the formation of highly reactive radical intermediates and end products such as hydroxyaldehydes and aldehydes, malondialdehyde and 4-hydroxynonenal being the best known of them (Sunderman 1986; Bartosz 1995). They are capable of producing promutagenic DNA adducts (Nair et al. 1999). Enhancement of lipid peroxidation was observed in cultured cells and experimental animals exposed to Cd(II), Co(II), Hg(II), Ni(II), Pb(II), Sn(II), V(V) (Sunderman 1986; Kasprzak 1996; Landolph 1999; Kasprzak and Buzard 2000) and Fe(III) (Hartwig et al. 1993) compounds.

Since nickel and chromium are the two most potent carcinogenic metals, their redox biochemistry is worthy of a few more words (Lancaster 1988; Klein et al. 1991; Standeven and Wetterhahn 1991; Kasprzak 1996; Landolph 1999; Sugden and Stearns 2000; Salnikow and Zhitkovich 2008; Beyersmann and Hartwig 2008). At physiological pH range, redox effects of nickel depend on its ability to form the Ni(II)/Ni(III) redox couple. This, however, is possible only when Ni(II) is chelated by certain peptides and proteins in a square-planar arrangement; octahedral Ni(II) complexes are devoid of redox activity (Bal et al. 2000a). These complexes reacting with O₂ or H₂O₂ generate not only •OH (or an oxo-cation NiO²⁺), but also other oxygen-, carbon-, and sulfur-centered radicals originating from the ligands (Kasprzak 1996, 2002; Landolph 1999; Kasprzak and Buzard 2000). Redox biochemistry of chromium is richer. This metal is much more toxic and carcinogenic when administered as Cr(VI) (chromate or dichromate) than as Cr(III) that reflects a substantial difference in their cellular uptake. The MIC₅₀ values show that Cr(VI) is about 15-times more toxic than Cr(III) at least in *S. pombe* (see Chap. 8). Intracellular Cr(VI) is reduced by ascorbate, GSH, GSH reductase, carbohydrates, and other reductants (e.g., cysteine) to Cr(V), Cr(IV), and ultimately Cr(III). The reactive intermediates of the Cr(VI) reduction include singlet oxygen, •OH, and oxygen- and sulfur-centered radicals. Hence, the ability of Cr(VI) to oxidatively damage DNA and proteins depends on its gradual reduction coupled with generation of reactive oxygen and other radical species (Wetterhahn et al. 1989; Shi et al. 1993; Salnikow and Zhitkovich 2008).

The metal-driven redox reactions may exhaust cellular antioxidant defense systems. This, in concert with metal-induced inhibition of major antioxidant enzymes, catalase, superoxide dismutase, GSH peroxidase and thioredoxins, will increase the level of endogenous metabolic DNA oxidants (reviewed in Kasprzak 1996; Myers et al. 2008). Deprivation of cells of one such antioxidant, ascorbate, is particularly dangerous because it impairs the activity of some of the DNA repair enzymes, alkyl-DNA dioxygenases (e.g., human ABH2 and ABH3) (Sedgwick 2004), gene expression-regulating factor HIF1- α , and histone demethylases (Salnikow and Kasprzak 2005; Mosammaparast and Shi 2010). The latter effects, in addition to metal inhibition of other DNA repair enzymes through various mechanisms (reviewed in Bal et al. 2010; Beyersmann and Hartwig 2008) may greatly contribute to the overall level of promutagenic DNA damage and aberrant gene expression essential for cancer induction and growth.

The above is a brief summary of what the metals can do. However, what they really do in terms of oxidative damage in cultured cells and multicellular organisms, and how that damage relates to cell transformation and cancer is presented and discussed below.

Oxidative DNA Damage

DNA Base Damage

The nature of products of metal-mediated oxidation of DNA bases clearly indicates the involvement of the $\bullet\text{OH}$ radical, either free or metal-centered, in the reaction mechanism. Relevant DNA base products are depicted in Fig. 11.1. Many of them have been found in chromatin of cultured cells exposed to H_2O_2 plus Co(II), Cu(II), Ni(II), or Fe(III) (Nackerdien et al. 1991; Dizdaroglu et al. 1991). Ni(II) also generated these products under ambient O_2 , but only in chromatin, not in pure DNA, indicating possible facilitation of nickel redox activity by chromatin proteins. Chapter 7 describes the effect of Ni(II) on large-scale chromatin structures and survival of K562 cells. Subsequently, amino acid binding domains for Ni(II) and Cu(II) were identified in core histones H3, H2A, and H4 and in human protamine P2. Metal complexes with peptides modeling some of these domains did, in fact, promote DNA base oxidation in test tube experiments (Bal et al. 1997a, b, 2010; Zoroddu et al. 2000). Oxidative base damage formation was found in pure DNA exposed to Cr(VI) plus H_2O_2 , GSH, and GSH reductase (Klein et al. 1991; Standeven and Wetterhahn 1991; Kasprzak 1996; Bal et al. 1997a, b; Landolph 1999; Kasprzak and Buzard 2000; Sugden and Stearns 2000), Fe(II) or Fe(III) plus H_2O_2 , $\text{O}_2^{\bullet-}$, and to neutrophils (reviewed in Kasprzak 1996; Landolph 1999; Kasprzak and Buzard 2000). Some types of iron-rich asbestos mediated oxidative DNA base damage proportionally to their iron contents (Xu et al. 1999; Aust and Eveleigh 1999). Very importantly, following *in vivo* exposure to Ni(II) and Co(II), elevated amounts of at least one damaged DNA base were found in organs of F344 rats and BALB/c mice (Kasprzak et al. 1991, 1992, 1994b; Misra et al. 1993). Oxidative DNA base damage was detected in animals treated with Co(II), Fe(III), Cd(II), or As(III) (Umemura et al. 1990, 1991; Kasprzak et al. 1994, 1996; Bialkowski et al. 1999; Kinoshita et al. 2007). It was also detected in humans exposed to cadmium and arsenic (Engstrom et al. 2010).

Oxidative damage may also be inflicted upon the free nucleotide pool. Here, the damaged nucleobases have the potential of causing mutations through mispairing during DNA and RNA synthesis. To prevent such mutations from occurring, cells have been equipped with specific “sanitizing” enzymes, such as bacterial MutT and mammalian MTH1, which specifically hydrolyze oxidatively damaged nucleoside triphosphates, 8-oxo-dGTP, 8-oxo-dATP, 2-OH-dATP, 8-oxo-GTP, and 2-OH-ATP (Nakabeppu 2001; Fujikawa et al. 2001; Nakamura et al. 2010). The

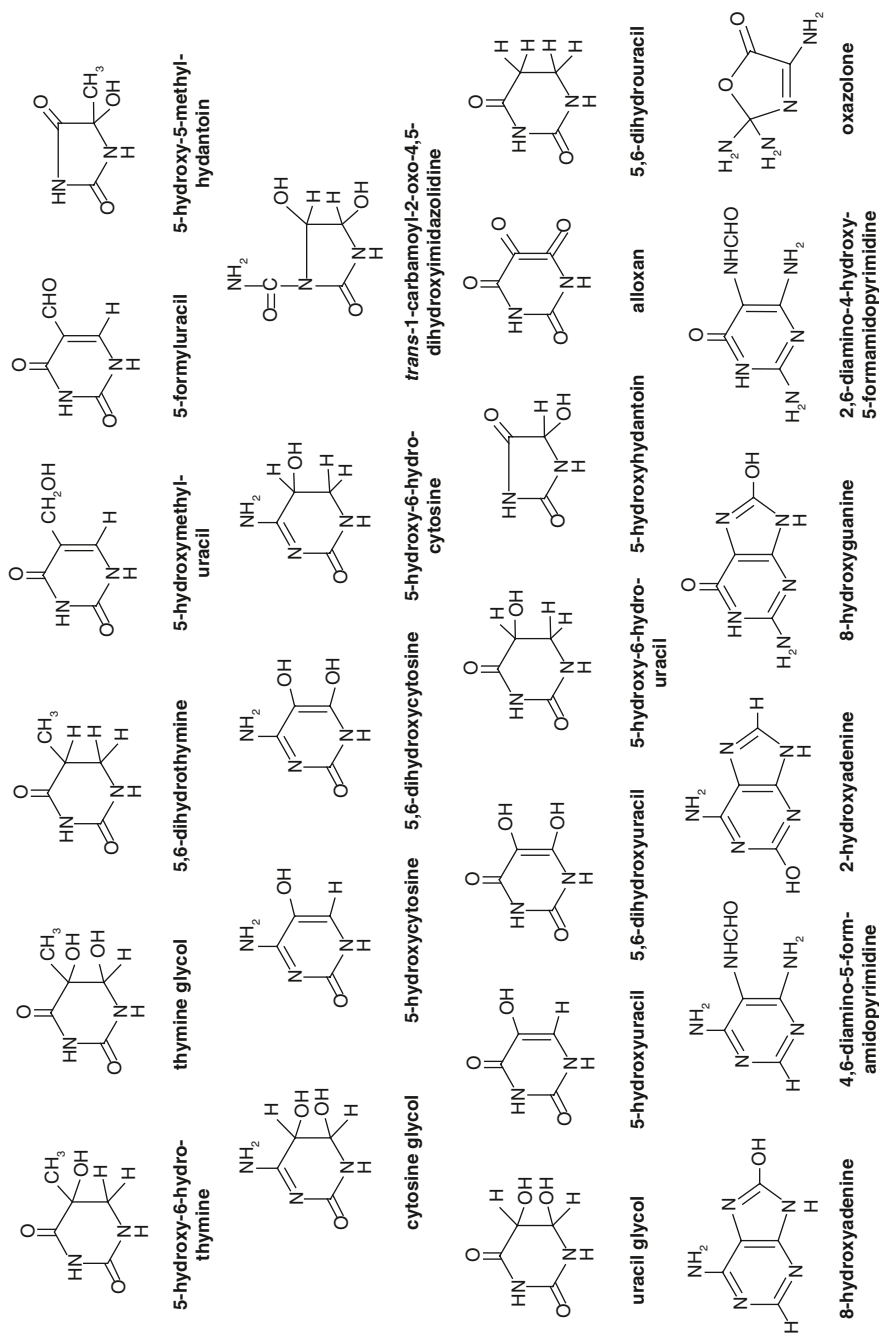


Fig. 11.1 Major products of oxidative damage to the DNA bases. (Reprinted with permission from Evans et al. 2004)

high hydrolytic activity of these enzymes toward damaged RNA substrates raises an intriguing question about possible significance of oxidative RNA damage to cell transformation. The mechanisms of oxidative damage to RNA, and the associated pathogenic consequences of this damage have been reviewed recently by Kong and Lin (2010).

Cross-Linking

DNA–protein and DNA–amino acid cross-linking is the most common effect of toxic metals exposure on chromatin. It results in the formation of “bulky DNA adducts”. This effect was observed in both *in vitro* and *in vivo* experiments (Chang et al. 1993; Randerath et al. 1996; Salnikow and Zhitkovich 2008). Metals can generate the cross-links by forming mixed DNA/protein ligand complexes, or by inducing the formation of strong covalent bonds directly between DNA and the proteins as a result of free radical attack on chromatin. Cross-links of the first type may be broken by external chelators or increased ionic strength, whereas those of the second type do not break under these conditions (Singh et al. 1998). The formation of strong covalent DNA–protein cross-links was observed in isolated nuclear chromatin exposed to Fe(II) in the presence of H₂O₂ and EDTA. Tetraglycine facilitated DNA–protein cross-linking by Ni(II) under ambient O₂ in isolated calf thymus nucleohistone; protein–protein cross-linking among histones was also observed (Kasprzak and Bare 1989). In cells treated with Cr(VI), besides DNA–protein cross-links, DNA adducts with GSH and cysteine were also identified (Wetterhahn et al. 1989; Borges and Wetterhahn 1989). Increased levels of DNA–protein cross-linking in lymphocytes have been proposed as a potential biomarker of genotoxic effects of several metals. DNA–protein cross-links were generated by Pt(II), Cu(II), Cr(VI), and As(III), but not by Mn(VII), Hg(II), Pb(II), Cd(II), Al(III), or Mg(II) (Chválová et al. 2007; reviewed in Landolph 1999; Kasprzak 1996, 2002; Kasprzak and Buzard 2000).

In view of the fact that transition metals promote lipid peroxidation it may be expected that the abundant lipid peroxidation product 4-hydroxynonenal, known to avidly form promutagenic DNA adducts (Nair et al. 1999; Fernandes et al. 2003; Feng et al. 2003; West and Marnett 2005), should be yet another substrate for cross-linking mediation by the metals. The formation of 4-hydroxynonenal–DNA adducts was, indeed, observed in livers of dietary iron-overloaded rats; but possible role of these adducts in hepatic tumors causation was not studied (Asare et al. 2009).

Relatively little is known about site specificity of the covalent cross-links induction by particular metals. In nucleohistone, •OH generated by ionizing radiation induced the formation of covalent bonds between DNA pyrimidines and tyrosine, glycine, alanine, valine, leucine, isoleucine, threonine, and lysine residues (Dizdaroğlu 1994). The metal-generated •OH would be expected to be more site specific. However, in chromatin treated *in vitro* with H₂O₂ in the presence of Fe(III) or

Cu(II), the formation of covalent cross-links was detected only between thymine and tyrosine (Dizdaroglu 1992) despite dissimilar coordination chemistries of these metal ions. This may indicate that the accessibility of metal binding sites in chromatin is limited to a few chromatin sites that are able to accommodate different metal ions (Rodriguez et al. 1997).

Free radicals also have been known to generate intra- and inter-strand cross-linking between DNA bases, but the influence of metals on these types of cross-linking requires further exploration. Current evidence of such influence is sparse and mostly indirect. For example, formation of cross-links between two cytosines or two thymines in the same strand, typical of DNA damage caused by free radicals generated by γ - and UV-radiation, results in tandem dinucleotides CC \rightarrow TT transition mutations; and these were observed in isolated DNA exposed to Fe(III), Ni(II), or Cu(II) plus oxidant (Tkeshelashvili et al. 1993).

The formation of cross-links in chromatin manifests itself in morphologic aberrations of chromosomes. Such aberrations were observed in lymphocytes of workers exposed to nickel and chromium compounds (reviewed in Kasprzak 1996, 2002; Landolph 1999; Kasprzak and Buzard 2000). In cultured Chinese hamster ovary cells, chromosomal alterations caused by Ni(II) were predominantly localized in the protein-rich, heterochromatic region of the X chromosome (Huang et al. 1995).

Strand Scission

DNA strand scission was found in organs of experimental animals administered with Cd(II) and Ni(II) (Saplakoğlu et al. 1997; Valverde et al. 2000). Likewise, cells cultured with Cd(II), Ni(II), or Fe(III)-NTA complex, had their nuclear DNA fragmented to a significant extent (Cai and Zhuang 1999; Robbiano et al. 2006; Knöbel et al. 2007). In test tube experiments, single-strand breaks were produced in DNA by Cr(VI) in the presence of H₂O₂ or GSH plus ambient O₂, and by Cu(II) and Ni(II) plus H₂O₂ (reviewed in Kasprzak 1996, 2002). The frequency of DNA single strand breaks was enhanced for Ni(II), but inhibited for Cu(II), by a pentadecapeptide containing the N-terminal metal binding motif of human protamine P2 (Bal et al. 1997b; Liang et al. 1999). Thus, the same peptidic ligand may exert opposite effect on the capability of different metals to mediate DNA strand scission (Fig. 11.2). This difference might be due to dissimilar rearrangement of the peptide conformation by each metal and the resulting different spatial interaction of the complexes with DNA (Bal et al. 1997a; Liang et al. 1999). Interestingly, for the Cu(II) plus H₂O₂ mixture, addition of the protamine P2-derived peptide HP2₁₋₁₅ that fully prevented strand scission did not abolish base oxidation in the same sample of DNA (Fig. 11.3) (Liang et al. 1999). Also, both metals directed oxidative damage toward the ligand itself (Fig. 11.4a). In pure DNA, Kawanishi et al. (1989) have found that Ni(II) promotes *in vitro* DNA cleavage by H₂O₂ in a site-specific way

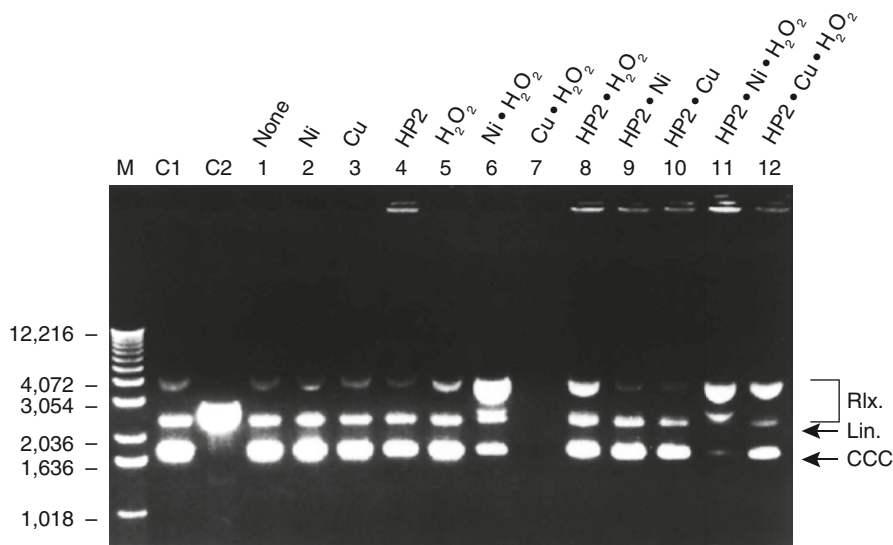


Fig. 11.2 Strand scission in covalently closed circular (CCC) pUC19 supercoiled plasmid DNA exposed for 16 h at 37°C, pH 7.4, to 1 mM H_2O_2 in the presence of equimolar concentrations of HP2₁₋₁₅ peptide (8 μ M) and Ni(II), or Cu(II) at combinations given on top of this figure. M, molecular weight markers; C1, pUC19 alone; C2, pUC19 linearized with *Pst*I restriction enzyme; Rlx., Lin., and CCC, relaxed, linearized, and circular forms of pUC19, respectively. The differences between lines 6 and 11 are indicative of HP2₁₋₁₅-induced enhancement of DNA strand scission (CCC disappearance) by Ni(II)+ H_2O_2 , while the differences between lines 7 and 12 indicate protective effect of HP2₁₋₁₅ against Cu(II)+ H_2O_2 -caused complete DNA degradation (disappearance of all fractions). (Liang et al. 1999)

characteristic for action of a reactive nickel–oxygen complex rather than free \bullet OH or singlet oxygen.

The site-specific character of metal-mediated DNA cleavage is even better pronounced for chromium. As also shown in a pioneering study by Kawanishi's group (Kawanishi et al. 1986), DNA fragments exposed to Cr(VI) and H_2O_2 were cleaved predominantly at the guanine sites. DNA cleavage mediation by O_2 and H_2O_2 in the presence of Ni(II), Cu(II), and Fe(III) complexes and ligand effects on the selectivity of that cleavage, was studied in detail by several laboratories (reviewed in Kasprzak 1996, 2002; Landolph 1999; Kasprzak and Buzard 2000).

Depurination

The spectrum of DNA damage by carcinogenic transition metals also includes depurination. For example, Cr(VI) and Cu(II) were found to release guanine and adenine, respectively, and Ni(II) appeared to release adenine from the DNA mol-

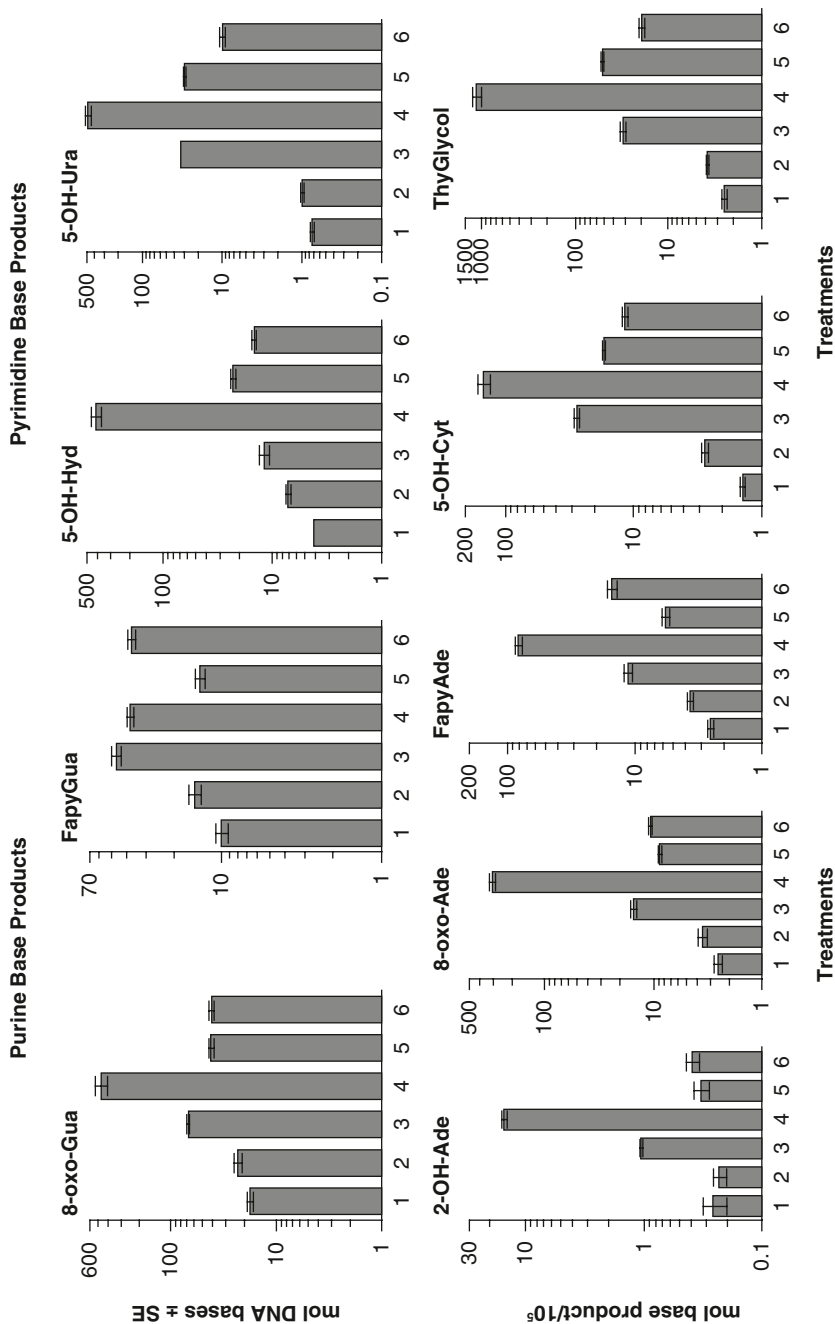


Fig. 11.3 DNA base oxidation in pUC19 plasmid DNA by 1 mM H₂O₂ (16 h, 37°C, pH 7.4) in the absence or presence of 8 μM Ni(II), Cu(II), and HP2₁₋₁₅ peptide. Treatments, pUC19 plus: 1, HP2₁₋₁₅; 2, H₂O₂ + HP2₁₋₁₅; 3, H₂O₂ + Ni(II); 4, H₂O₂ + Cu(II); 5, H₂O₂ + Ni(II) + HP2₁₋₁₅; 6, H₂O₂ + Cu(II) + HP2₁₋₁₅. (Liang et al. 1999)

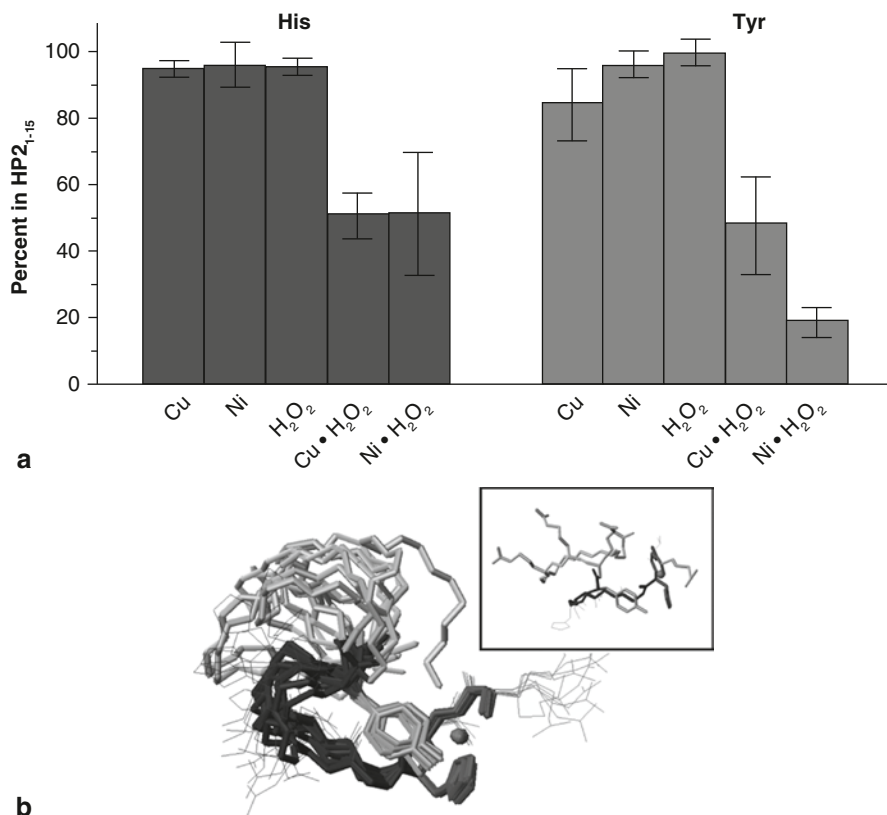


Fig. 11.4 **a** Relative changes in the histidine and tyrosine residues in 0.1 mM HP2₁₋₁₅ peptide incubated with equimolar concentrations of Ni(II) or Cu(II) and 1 mM H₂O₂ for 16 h at 37°C, pH 7.4, at combinations given under the bars (Bal et al. 1997b). **b** A structural family of the Ni(II) HP2₁₋₁₅ complex showing structuring effect on the linear peptide of Ni(II) cation coordinated by the N-terminal RTH-sequence (the imidazole-containing ring around Ni(II)) and interacting with tyrosine-8 phenol group (Bal et al. 2000b). The close proximity of this group to Ni(II) may explain relatively strong oxidation of tyrosine-8. The remaining amino acid residues in HP2₁₋₁₅ were not detectably affected except for arginine whose contents decreased by approximately 20% (Bal et al. 1997b). (Figure 11.4b has been reprinted with permission from Bal et al. 2000b, Copyright 2000, American Chemical Society)

ecule. The underlying mechanisms are thought to involve amino-imino tautomeric transitions and active oxygen attack (Bregadze et al. 2008). The depurination occurs concurrently with DNA strand scission and both effects can result from •OH insult on the DNA sugar moiety. Oxidatively modified sugars (reviewed in Dizdaroglu et al. 2002; Evans et al. 2004) constitute alkali-labile sites that have been frequently found in DNA isolated from metal-treated cells (Dizdaroglu 1994; reviewed in Kasprzak 1996, 2002; Landolph 1999; Kasprzak and Buzard 2000).

Oxidative Protein Damage

Oxidation of amino acids, peptides, and proteins as well as the involvement of transition metals in this process have been reviewed before (Requena et al. 2001a; Stadtman and Berlett 1991, 1997; Stadtman 1993). Along with the other types of oxidative damage, protein oxidation is believed to be mechanistically involved in a wide spectrum of pathologies, including cancer (Stadtman and Berlett 1997; Requena et al. 2001a, b). However its role in metal-induced carcinogenesis has not been studied in all necessary detail. The major targets for metal-promoted oxidation are the side chains of cysteine, histidine, arginine, lysine, and proline residues. The sulfhydryls are commonly oxidized to disulfides, but they may be turned into sulfino-, sulfeno-, and sulfono-derivatives, too. The latter is also true for the methionine residue. The histidine imidazole may be oxidized to yield aspartic acid, asparagine, or 2-OH-histidine. Arginine is oxidized to γ -glutamate-semialdehyde; lysine, to 2-amino-adipic-semialdehyde; and proline is turned into glutamic acid, pyroglutamic acid, γ -aminobutyric acid, and γ -glutamic-semialdehyde (Stadtman 1993). γ -Glutamic and amino adipic semialdehydes are the main carbonyl products of metal-catalyzed oxidation of proteins (Requena et al. 2001a). Deamidation of glutamine and oxidation of methionine residues, both effects known to be produced by oxygen radicals and nitric oxide (Ingrosso et al. 2002; Kong et al. 2006), were found in histone H2B isolated from Ni(II)-exposed cultured cells (Karaczyn et al. 2005).

The formation of radical intermediates in the oxidation processes of proteins results in protein fragmentation and intra- and inter-protein cross-linking. The protein-derived radicals may become cross-linked with DNA, as well (see above). The site-specificity of metal-mediated protein damage depends on the coordination of transition metal ions by proteins and peptides predominantly through the sulfhydryl, imidazole, and the deprotonated peptide bond and side chain nitrogens, followed by generation of metal-associated oxidizing species at these particular sites. Therefore, tyrosine, methionine, tryptophan, and phenylalanine, which do not bind metal cations under physiological conditions, seem to be less likely targets of metal-catalyzed oxidation (Stadtman 1993). They may, nonetheless, be damaged if they are located close to the metal binding site, either in the amino acid backbone or due to specific folding of the protein molecule. For example, when bound to a 15-mer peptide HP2₁₋₁₅ modeling the N-terminal sequence of human protamine P2 (Bal et al. 1997a), Ni(II) and Cu(II) catalyze oxidation by H₂O₂ of not only arginine-1 and histidine-3, which bind the metals directly, but also of tyrosine-8 located away from the metal-binding site (Fig. 11.4a). The reason for this was found in another study (Bal et al. 2000b) in which the solution structure of the Ni(II)-HP2₁₋₁₅ revealed a strong structuring effect of the metal on this peptide. This effect brought tyrosine-8 close to the metal center, and also positioned the positive arginine side chains on one side of the molecule (Fig 11.4b). Thus, by imposing conformational changes on its ligand, the bound metal directed oxidative damage to a particular residue (tyrosine-8), and also modulated the structure (and possibly function, e.g., DNA binding) of the ligand (Bal et al. 1997a, b, 2000b; Kasprzak 2002).

Because of different affinities of metal cations for various side-chain donors in proteins and different coordination modes of the resulting complexes, the extent and character of the damage may strongly depend on the metal. This was observed for Fe(II)- and Cu(II)-mediated oxidation of collagen by H_2O_2 (Hawkins and Davies 1997). The coordination mode was also the most likely cause of a profound difference in redox activity between two Ni(II) complexes originating from the 34-mer long C-terminal “tail” of histone H2A ($H2A_{34}$). Ni(II) is coordinated by $H2A_{34}$ through its ending –TESHHKAKGK amino acid sequence to form a redox-inactive octahedral complex (Bal et al. 1998). However, the binding causes hydrolysis of the ES peptide bond with liberation of the –SHHKAKGK peptide to which Ni(II) remains bound through the –SHH motif, yielding a redox-active square planar complex. Its reaction with H_2O_2 results in degradation of the serine and histidine residues (Bal et al. 2000a). It is noteworthy that the original –TESHHKAKGK sequence also coordinates Cu(II), though to different donor atoms than Ni(II), and forms a redox active copper complex (Mylonas et al. 2001).

In addition to mediation of oxidative damage to their protein ligands, the protein-bound metals may also promote oxidation of neighboring macromolecules (collateral damage). Relevant examples would include assistance in lipoprotein oxidation by ceruloplasmin-bound copper and promotion of DNA damage by copper/zinc superoxide dismutase and by nickel bound to isolated chromatin, nucleohistone, or to protamine- and histone-modeling peptides (Kasprzak 1996; Bal et al. 1997b; Liang et al. 1999; Landolph 1999; Kasprzak and Buzard 2000). And finally, through the assistance in lipid peroxidation, carcinogenic metals may indirectly enhance the generation of protein adducts of malondialdehyde, 4-oxononenal, and 4-hydroxynonenal that are believed to contribute mechanistically to the progress of many pathologic processes, including carcinogenesis (Jacobs and Marnett 2010).

Discussion

The results of numerous investigations suggest that the carcinogenic transition metals can be bound chemically by cellular components, including DNA, histones, protamines, and other proteins. The binding leads to structural and functional damage to these components. The damage may be direct owing to conformational changes imposed by the metal ion on its binding (coordinating) molecule, and/or indirect, caused by redox activity of the bound metal. In the latter case, the metal inflicts the damage through oxygen radical and other reactive intermediates arising from its reactions with O_2 , $O_2^{\cdot-}$, H_2O_2 , lipid peroxides, and/or other endogenous oxidants. The spatial range of oxidative damage may be focal or very broad, depending on the nature of the generated reactive species, and involve not only the metal-binding ligand but also neighboring molecules, e.g., DNA in chromatin. Proteins seem to be the primary sites for metal binding. They may either facilitate (promote) or inhibit redox activity of the metal, depending on the chemistry of a particular metal and structures of the resulting complexes.

The evidence for mechanistic involvement of oxidative damage in metal-induced carcinogenesis is particularly sound for two essential (but toxic when overdosed) metals, iron and copper, and three well-established human carcinogenic metals, nickel, chromium, and cadmium. Because of its relative abundance and thus high capacity to activate oxygen, iron displaced from a natural carrier (which controls its redox activity), e.g., by a competing transition metal or damaging insult on that carrier, has been considered as the ultimate carcinogen (Kon 1978; Toyokuni 2009). For copper, the mutant cinnamon (LEC) rat model looks like the best example of how efficiently a persistent oxidative stress due to metal accumulation in the liver leads to hepatitis and hepatic cancer (Marquez et al. 2007, Marquez-Quiñones et al. 2010). However, besides that of copper, mechanistic involvement of iron in the LEC rat carcinogenesis model has been postulated (Ma et al. 1997). Iron was also found to accelerate nickel-induced carcinogenesis in the rat kidney (Kasprzak et al. 1994). In the latter study, codon 12 of the K-ras oncogene in renal tumors contained the G to T transversion mutation typical for oxidation of the guanine residues in DNA (Higinbotham et al. 1992).

Experimental data indicate that physiologically non-redox active carcinogenic metals, cadmium and lead, promote oxidative damage, too. Such metals are likely to inflict the damage indirectly; for example, by triggering and promoting inflammation and lipid peroxidation, interfering with calcium, copper, and iron metabolism, or by inhibiting antioxidant defenses and DNA repair systems (Hartwig 1994, 1995; Valverde et al. 2001). Similar mechanisms may also be involved in arsenic-mediated oxidative damage and carcinogenesis (Kitchin and Conolly 2010).

The strongest association of oxidative damage with carcinogenesis comes from the promutagenic nature of many DNA base products and adducts resulting from the attack on DNA of active oxygen species and other reactive intermediates, e.g., malondialdehyde and 4-hydroxynonenal, generated in the presence of a transition metal (Kasprzak 1996; Valko et al. 2006; Marquez et al. 2007; Marquez-Quiñones et al. 2010). The mutations may occur during DNA replication and repair, as well as during transcription of genes on damaged DNA template (Hailer-Morrison et al. 2003). Also, the presence of the damaged guanine in DNA affects orderly methylation of the cytosine residues, thus affecting gene expression (Guz et al. 2008). Metal-induced DNA strand scission and depurination are mutagenic, too (Chiocca et al. 1991; Kanazawa et al. 2000; Bregadze et al. 2008; Brink et al. 2009).

Very importantly, certain carcinogenic metals (e.g., cadmium, lead, nickel) and arsenic inhibit DNA repair systems even at doses that are too low to induce detectable DNA lesions (Hartwig 1995). The metals may inhibit the activity of the ascorbate-dependent DNA dealkylating enzymes ABH2 and ABH3 (Sedgwick 2004) and the nucleotide pool sanitizing enzyme MTH1 (an analog of bacterial MutT) (Porter et al. 1997; Białkowski and Kasprzak 1998; Białkowski et al. 1999; Kasprzak et al. 2001). This inhibition will further increase the frequency of errors (mutations) during both DNA replication and repair processes. Carcinogenic metals are thus capable of augmenting promutagenic DNA lesions induced by themselves and/or other insults, e.g., by DNA methylating (alkylating) agents (reviewed in Beyersmann and Hartwig 2008; Bal et al. 2010). Altogether, the emergence of these lesions in DNA may be considered as a tumor-initiating event.

Reactive oxygen species serve as physiological signal transduction messengers in controlling expression of genes, including oncogenes, tumor suppressor genes, and many others (reviewed in Kasprzak and Buzard 2000; Buzard and Kasprzak 2000; Salnikow and Costa 2000). It seems likely, therefore, that the redox reactions driven by adventitious cellular metals disturb the timely and orderly generation of these messengers and affect the oxidation status of redox-dependent regulatory proteins, such as NF- κ B, AP-1, p53, K-ras, Bcl-2, ATF-1, HIF-1 α , and others. These effects must be detrimental to proper progression of the cell cycle and/or apoptosis (Rana 2008). In addition to a direct attack of reactive oxygen on the transcription factors, proper function of the latter may be disturbed by damage to upstream effectors. For example, the lipid peroxidation product 4-hydroxynonenal was found to form a covalent adduct to I κ B kinase and thus inhibit activation of the NF- κ B transcription factor (Ji et al. 2001). Metal binding and oxidation damage to regulatory proteins not belonging to the redox signaling network may, too, affect their structures and functions, including gene expression regulation. To this juncture, oxidation of the sulfhydryl groups of zinc fingers, especially those in DNA repair proteins, has been proposed to be a crucial step in carcinogenesis (Witkiewicz-Kucharczyk and Bal 2006). A similar mechanism may be responsible for metal-mediated inhibition of the tumor suppressor FHIT protein (Kowara et al. 2002, 2004). Also, the metal-induced oxidative stress leads to the destruction of cellular ascorbate and in a consequence to inactivation of various cellular ascorbate-dependent dioxygenases. Besides facilitating DNA dealkylation, mentioned above, the dioxygenases regulate activity of the HIF transcription factor and thus HIF-dependent genes expression (Salnikow et al. 2004; Salnikow and Kasprzak 2005, 2007; Kaczmarek et al. 2007), and histone demethylation (Mosammamarast and Shi 2010). All these kinds of protein damage are believed to promote carcinogenesis through epigenetic mechanisms. Unfortunately, the wide diversity of the protein oxidation products and the enormous complexity of the protein- and other molecule-dependent redox signaling network make it impossible at this moment to understand all aspects of the mechanistic role of protein damage in the lengthy multi-stage process of tumor induction and growth.

Conclusion

Reactions of the carcinogenic transition metals with cell components as well as with molecular oxygen and its metabolic intermediates lead to generation of highly reactive oxidants, which are capable of damaging cellular genetic material and regulatory proteins in a way facilitating the initiation, promotion and progression of cancer.

Acknowledgments Author would like to thank Dr. Yih-Horng Shiao for critical reading of the manuscript. This project was supported by the Intramural Research Program of the NIH, National Cancer Institute, Center for Cancer Research. The content of this publication does not necessarily reflect the views or policies of the Department of Health and Human Services, nor does mention of trade names, commercial products, or organizations imply endorsement by the U.S. Government.

References

- Asare GA, Kew MC, Mossanda KS, Paterson AC, Siziba K, Kahler-Venter CP (2009) Effects of exogenous antioxidants on dietary iron overload. *J Clin Biochem Nutr* 44:85–94
- Aust AE, Eveleigh JF (1999) Mechanisms of DNA oxidation. *Proc Soc Exp Biol Med* 222:246–252
- Bal W, Lukszo J, Jezowska-Bojczuk M, Kasprzak KS (1997a) Binding of nickel(II) and copper(II) to the N-terminal sequence of human protamine HP2. *Chem Res Toxicol* 10:906–914
- Bal W, Lukszo J, Kasprzak KS (1997b) Mediation of oxidative DNA damage by nickel(II) and copper(II) complexes with the N-terminal sequence of human protamine HP2. *Chem Res Toxicol* 10:915–921
- Bal W, Lukszo J, Bialkowski K, Kasprzak KS (1998) Interactions of nickel(II) with histones: interactions of Ni(II) with CH₃COThr-Glu-Ser-His-His-Lys-NH₂, a peptide modeling the potential metal binding site in the “C-tail” region of histone H2A. *Chem Res Toxicol* 11:1014–1023
- Bal W, Liang R, Lukszo J, Lee SH, Dizdaroglu M, Kasprzak KS (2000a) Nickel(II) specifically cleaves the C-terminal tail of the major variant of histone H2A and forms oxidative damage-mediating complex with the cleaved-off octapeptide. *Chem Res Toxicol* 13:616–624
- Bal W, Wojcik J, Maciejczyk M, Grochowski P, Kasprzak KS (2000b) Induction of a secondary structure in the N-terminal pentadecapeptide of human protamine HP2 through Ni(II) coordination. An NMR study. *Chem Res Toxicol* 13:823–830
- Bal W, Protas AM, Kasprzak KS (2010) Genotoxicity of metal ions: chemical insights. In: Sigel A, Sigel H, Sigel RKO (eds) *Metal ions in life sciences, vol 8: metal ions in toxicology: effects, interactions, interdependencies*. Royal Society of Chemistry Press, Cambridge
- Bartosz G (1995) *Druga twarz tlenu*. PWN, Warszawa
- Beyersmann D, Hartwig A (2008) Carcinogenic metal compounds: recent insight into molecular and cellular mechanisms. *Arch Toxicol* 82:493–512
- Bialkowski K, Kasprzak KS (1998) A novel assay of 8-oxo-2'-deoxyguanosine 5'-triphosphate pyrophosphohydrolase (8-oxo-dGTPase) activity in cultured cells and its use for evaluation of cadmium(II) inhibition of this activity. *Nucl Acids Res* 26:3194–3201
- Bialkowski K, Bialkowska A, Kasprzak KS (1999) Cadmium(II), but not nickel(II), inhibits 8-oxo-dGTPase activity and increases 8-oxo-dG levels in DNA of the rat testis, a target organ for cadmium(II) carcinogenesis. *Carcinogenesis* 20:1621–1624
- Borges KM, Wetterhahn KE (1989) Chromium cross-links glutathione and cysteine to DNA. *Carcinogenesis* 10:2165–2168
- Bregadze VG, Gelagutashvili ES, Tsakadze KJ, Melikishvili SZ (2008) Metal-induced point defects in DNA: model and mechanisms. *Chem Biodivers* 5:1980–1989
- Brink A, Richter I, Lutz U, Wanek P, Stopper H, Lutz WK (2009) Biological significance of DNA adducts: comparison of increments over background for various biomarkers of genotoxicity in L5178Y tk(+/-) mouse lymphoma cells treated with hydrogen peroxide and cumene hydroperoxide. *Mutat Res* 678:123–128
- Bryan SE (1981) Heavy metals in the cell's nucleus. In: Eichhorn GL, Marzilli LG (eds) *Metal ions in genetic information transfer*. Elsevier, New York
- Buzard GS, Kasprzak KS (2000) Possible roles of nitric oxide and redox cell signaling in metal-induced toxicity and carcinogenesis: a review. *J Environ Pathol Toxicol Oncol* 19:179–199
- Cai Y, Zhuang Z (1999) DNA damage in human peripheral blood lymphocyte caused by nickel and cadmium. *Zhonghua Yu Fang Yi Xue Za Zhi* 33:75–77
- Chang J, Watson WP, Randerath E, Randerath K (1993) Bulky DNA-adduct formation induced by Ni(II) *in vitro* and *in vivo* as assayed by 32P-postlabeling. *Mutat Res* 291:147–159
- Chiaverini N, De Ley M (2010) Protective effect of metallothionein on oxidative stress-induced DNA damage. *Free Radic Res* 44:605–613
- Chiocca SM, Sterner DA, Biggart NW, Murphy EC Jr (1991) Nickel mutagenesis: alteration of the MuSVts110 thermosensitive splicing phenotype by a nickel-induced duplication of the 3' splice site. *Mol Carcinog* 4:61–71

- Chválová K, Brabec V, Kaspárková J (2007) Mechanism of the formation of DNA–protein cross-links by antitumor cisplatin. *Nucleic Acids Res* 35:1812–1821
- De Boeck M, Hoet P, Lombaert N, Nemery B, Kirsch-Volders M, Lison D (2003) *In vivo* genotoxicity of hard metal dust: induction of micronuclei in rat type II epithelial lung cells. *Carcinogenesis* 24:1793–1800
- Dizdaroglu M (1992) Oxidative damage to DNA in mammalian chromatin. *Mutat Res* 275:331–342
- Dizdaroglu M (1994) Chemical determination of oxidative base damage in DNA by gas chromatography–mass spectrometry. *Methods Enzymol* 234:3–16
- Dizdaroglu M, Rao G, Halliwell B, Gajewski E (1991) Damage to the DNA bases in mammalian chromatin by hydrogen peroxide in the presence of ferric and cupric ions. *Arch Biochem Biophys* 285:317–324
- Dizdaroglu M, Jaruga P, Birincioglu M, Rodriguez H (2002) Free radical-induced damage to DNA: mechanisms and measurement. *Free Radic Biol Med* 32:1102–1115
- Engström KS, Vahter M, Johansson G, Lindh CH, Teichert F, Singh R, Kippler M, Nermell B, Raqib R, Strömberg U, Broberg K (2010) Chronic exposure to cadmium and arsenic strongly influences concentrations of 8-oxo-7,8-dihydro-2'-deoxyguanosine in urine. *Free Radic Biol Med* 48:1211–1217
- Evans MD, Dizdaroglu M, Cooke MS (2004) Oxidative DNA damage and disease: induction, repair and significance. *Mutat Res* 567:1–61
- Feng Z, Hu W, Amin S, Tang MS (2003) Mutational spectrum and genotoxicity of the major lipid peroxidation product, trans-4-hydroxy-2-nonenal, induced DNA adducts in nucleotide excision repair-proficient and -deficient human cells. *Biochemistry* 42:7848–7854
- Fernandes PH, Wang H, Rizzo CJ, Lloyd RS (2003) Site-specific mutagenicity of stereochemically defined 1,N2-deoxyguanosine adducts of trans-4-hydroxynonenal in mammalian cells. *Environ Mol Mutagen* 42:68–74
- Francia C, Bodoardo F, Penazzi N, Corazzari I, Fenoglio I (2007) Characterization of the electrochemical process responsible for the free radical release in hard metals. *Electrochim Acta* 52:7438–7443
- Fujikawa K, Kamiya H, Yakushiji H, Nakabeppu Y, Kasai H (2001) Human MTH1 protein hydrolyzes the oxidized ribonucleotide, 2-hydroxy-ATP. *Nucl Acids Res* 29:449–454
- Guz J, Foksinski M, Siomek A, Gackowski D, Rozalski R, Dziaaman T, Szpila A, Olinski R (2008) The relationship between 8-oxo-7,8-dihydro-2'-deoxyguanosine level and extent of cytosine methylation in leukocytes DNA of healthy subjects and in patients with colon adenomas and carcinomas. *Mutat Res* 640:170–173
- Hailer-Morrison MK, Kotler JM, Martin BD, Sugden KD (2003) Oxidized guanine lesions as modulators of gene transcription. Altered p50 binding affinity and repair shielding by 7,8-dihydro-8-oxo-2'-deoxyguanosine lesions in the NF-kappaB promoter element. *Biochemistry* 42:9761–9770
- Hamazaki S, Okada S, Li JL, Toyokuni S, Midorikawa O (1989) Oxygen reduction and lipid peroxidation by iron chelates with special reference to ferric nitrilotriacetate. *Arch Biochem Biophys* 272:10–17
- Hartwig A (1994) Role of DNA repair inhibition in lead- and cadmium-induced genotoxicity: a review. *Environ Health Perspect* 102(Suppl 3):45–50
- Hartwig A (1995) Current aspects in metal genotoxicity. *BioMetals* 8:3–11
- Hartwig A, Klyszcz-Nasko H, Schlegel L, Beyersmann D (1993) Cellular damage by ferric nitrilotriacetate and ferric citrate in V79 cells: interrelationship between lipid peroxidation, DNA strand breaks and sister chromatid exchanges. *Carcinogenesis* 14:107–112
- Hawkins CL, Davies MJ (1997) Oxidative damage to collagen and related substrates by metal ion/hydrogen peroxide systems: random attack or site-specific damage? *Biochim Biophys Acta* 1360:84–96
- Higinbotham KG, Rice JM, Diwan BA, Kasprzak KS, Reed CD, Perantoni AO (1992) GGT to GTT transversions in codon 12 of the *K-ras* oncogene in rat renal sarcomas induced with nickel

- sub sulfide or nickel subsulfide/iron are consistent with oxidative damage to DNA. *Cancer Res* 52:4747–4751
- Huang X, Kitahara J, Zhitkovich A, Dowjat K, Costa M (1995) Heterochromatic proteins specifically enhance nickel-induced 8-oxo-dG formation. *Carcinogenesis* 16:1753–1759
- Ingrosso D, Cimmino A, D'Angelo S, Alfinito F, Zappia V, Galletti P (2002) Protein methylation as a marker of aspartate damage in glucose-6-phosphate dehydrogenase-deficient erythrocytes: role of oxidative stress. *Eur J Biochem* 269:2032–2039
- Inoue S, Kawanishi S (1987) Hydroxyl radical production and human DNA damage induced by ferric nitrilotriacetate and hydrogen peroxide. *Cancer Res* 47:6522–6527
- Jacobs AT, Marnett LJ (2010) Systems analysis of protein modification and cellular responses induced by electrophile stress. *Acc Chem Res* 43:673–683
- Ji C, Kozak KR, Marnett LJ (2001) IkappaB kinase, a molecular target for inhibition by 4-hydroxy-2-nonenal. *J Biol Chem* 276:18223–18228
- Kaczmarek M, Timofeeva O, Karaczyn A, Malyguine A, Kasprzak KS, Salmikow K (2007) The role of ascorbate in the modulation of HIF-1 α protein and HIF-dependent transcription by chromium(VI) and nickel(II). *Free Radic Biol Med* 42:1246–1257
- Kalinich JF, Emond CA, Dalton TK, Mog SR, Coleman GD, Kordell JE, Miller AC, McClain DE (2005) Embedded weapons-grade tungsten alloy shrapnel rapidly induces metastatic high-grade rhabdomyosarcomas in F344 rats. *Environ Health Perspect* 113:729–734
- Kanazawa A, Sawa T, Akaik T, Maeda H (2000) Formation of abasic sites in DNA by t-butyl peroxy radicals: implication for potent genotoxicity of lipid peroxy radicals. *Cancer Lett* 156:51–55
- Karaczyn AA, Golebiowski F, Kasprzak KS (2005) Truncation, deamidation, and oxidation of histone H2B in cells cultured with nickel(II). *Chem Res Toxicol* 18:1934–1942
- Kasprzak KS (1996) Oxidative DNA damage in metal-induced carcinogenesis. In: Chang LW (ed) *Toxicology of metals*. CRC Lewis Publishers, Boca Raton
- Kasprzak KS (2002) Oxidative DNA and protein damage in metal-induced toxicity and carcinogenesis. *Free Radic Biol Med* 32:958–967
- Kasprzak KS, Bare RM (1989) *In vitro* polymerization of histones by carcinogenic nickel compounds. *Carcinogenesis* 10:621–624
- Kasprzak KS, Buzard GS (2000) The role of metals in oxidative damage and redox cell signaling derangement. In: Koropatnick J, Zalups R (eds) *Molecular biology and toxicology of metals*. Taylor and Francis, London
- Kasprzak KS, Salmikow K (2007) Nickel toxicity and carcinogenesis. In: Sigel A, Sigel H, Sigel RKO (eds) *Metal ions in life sciences: nickel and its surprising impact in nature*, vol. 2. Wiley, Chichester
- Kasprzak KS, Sunderman FW Jr (1977) Mechanisms of dissolution of nickel subsulfide in rat serum. *Res Commun Chem Pathol Pharmacol* 16:95–108
- Kasprzak KS, Misra M, Rodriguez RE, North SL (1991) Nickel-induced oxidation of renal DNA guanine residues *in vivo* and *in vitro*. *Toxicologist* 11:233
- Kasprzak KS, Diwan BA, Rice JM, Misra M, Riggs CW, Olinski R, Dizdaroglu M (1992) Nickel(II)-mediated oxidative DNA base damage in renal and hepatic chromatin of pregnant rats and their fetuses. Possible relevance to carcinogenesis. *Chem Res Toxicol* 5:809–815
- Kasprzak KS, Diwan BA, Rice JM (1994a) Iron accelerates while magnesium inhibits nickel-induced carcinogenesis in the rat kidney. *Toxicology* 90:129–140
- Kasprzak KS, Zastawny TH, North SL, Riggs CW, Diwan BA, Rice JM, Dizdaroglu M (1994b) Oxidative DNA base damage in renal, hepatic, and pulmonary chromatin of rats after intraperitoneal injection of cobalt(II) acetate. *Chem Res Toxicol* 7:329–335
- Kasprzak KS, Nakabeppu Y, Kakuma T, Sakai Y, Sekiguchi M, Ward JM, Diwan BA, Nagashima K, Kasprzak BH (2001) Intracellular distribution of the antimutagenic enzyme MTH1 in the liver, kidney and testis of F344 rats and its modulation by cadmium(II). *Exp Toxicol Pathol* 53:325–336
- Kawanishi S, Inoue S, Sano S (1986) Mechanism of DNA cleavage induced by sodium chromate(VI) in the presence of hydrogen peroxide. *J Biol Chem* 261:5952–5958

- Kawanishi S, Inoue S, Yamamoto K (1989) Site-specific DNA damage by nickel(II) ion in the presence of hydrogen peroxide. *Carcinogenesis* 12:2231–2235
- Kinoshita A, Wanibuchi H, Morimura K, Wei M, Nakae D, Arai T, Minowa O, Noda T, Nishimura S, Fukushima S (2007) Carcinogenicity of dimethylarsinic acid in Ogg1-deficient mice. *Cancer Sci* 98:803–814
- Kitchin KT, Conolly R (2010) Arsenic-induced carcinogenesis—oxidative stress as a possible mode of action and future research needs for more biologically based risk assessment. *Chem Res Toxicol* 23:327–335
- Klein CB, Frenkel K, Costa M (1991) The role of oxidative processes in metal carcinogenesis. *Chem Res Toxicol* 4:592–604
- Klug A (2010) The discovery of zinc fingers and their applications in gene regulation and genome manipulation. *Annu Rev Biochem* 79:213–231
- Knöbel Y, Weise A, Glei M, Sendt W, Claussen U, Pool-Zobel BL (2007) Ferric iron is genotoxic in non-transformed and preneoplastic human colon cells. *Food Chem Toxicol* 45:804–811
- Kon SH (1978) Biological autoxidation. I. Decontrolled iron: an ultimate carcinogen and toxicant: an hypothesis. *Med Hypotheses* 4:445–471
- Kong Q, Lin CL (2010) Oxidative damage to RNA: mechanisms, consequences, and diseases. *Cell Mol Life Sci* 67:1817–1829
- Kong L, Saavedra JE, Buzard GS, Xu X, Hood BL, Conrads TP, Veenstra TD, Keefer LK (2006) Deamidation of peptides in aerobic nitric oxide solution by a nitrosative pathway. *Nitric Oxide* 14:144–151
- Kowara R, Karaczyn A, Fivash MJ Jr, Kasprzak KS (2002) *In vitro* inhibition of the enzymatic activity of tumor suppressor *FHIT* gene product by carcinogenic transition metals. *Chem Res Toxicol* 15:319–325
- Kowara R, Salnikow K, Diwan BA, Bare RM, Waalkes MP, Kasprzak KS (2004) Reduced Fhit protein expression in nickel-transformed mouse cells and in nickel-induced murine sarcomas. *Mol Cell Biochem* 255:195–202
- Kroncke KD, Klotz LO (2009) Zinc fingers as biologic redox switches? *Antioxid Redox Signa* 11:1015–1027
- Kukielka E, Cederbaum AI (1990) NADPH- and NADH-dependent oxygen radical generation by rat liver nuclei in the presence of redox cycling agents and iron. *Arch Biochem Biophys* 283:326–333
- Lancaster JR Jr (1988) The bioinorganic chemistry of nickel. VCH, New York.
- Landolph JR (1999) Role of free radicals in metal-induced carcinogenesis. In: Sigel H, Sigel A (eds) *Metal ions in biological systems*, vol 36. M. Dekker, New York
- Lee JE, Ciccarelli RB, Jennette KW (1982) Solubilization of the carcinogen nickel subsulfide and its interaction with deoxyribonucleic acid and protein. *Biochemistry* 21:771–778
- Liang R, Senturker S, Shi X, Bal W, Dizdaroglu M, Kasprzak KS (1999) Effect of Ni(II) and Cu(II) on DNA interaction with the N-terminal sequence of human protamine P2: enhancement of binding and mediation of oxidative DNA strand scission and base damage. *Carcinogenesis* 20:893–898
- Lison D, Carbonnelle P, Mollo L, Lauwerys R, Fubini B (1995) Physicochemical mechanism of the interaction between cobalt metal and carbide particles to generate toxic activated oxygen species. *Chem Res Toxicol* 8:600–606
- Loeb LA, James EA, Waltersdorph AM, Klebanoff SJ (1988) Mutagenesis by the autoxidation of iron with isolated DNA. *Proc Natl Acad Sci U S A* 85:3918–3922
- Ma Y, Zhang D, Kawabata T, Kiriu T, Toyokuni S, Uchida K, Okada S (1997) Copper and iron-induced oxidative damage in non-tumor bearing LEC rats. *Pathol Int* 47:203–208
- Marquez A, Villa-Treviño S, Guéraud F (2007) The LEC rat: a useful model for studying liver carcinogenesis related to oxidative stress and inflammation. *Redox Rep* 12:35–39
- Marquez-Quiñones A, Cipak A, Zarkovic K, Fattel-Fazenda S, Villa-Treviño S, Waeg G, Zarkovic N, Guéraud F (2010) HNE-protein adducts formation in different pre-carcinogenic stages of hepatitis in LEC rats. *Free Radic Res* 44:119–127

- Miller AC, McClain D (2007) A review of depleted uranium biological effects: *in vitro* and *in vivo* studies. *Rev Environ Health* 22:75–89
- Misra M, Olinski R, Dizdaroglu M, Kasprzak KS (1993) Enhancement by l-histidine of nickel(II)-induced DNA–protein cross-linking and oxidative DNA base damage in the rat kidney. *Chem Res Toxicol* 6:33–37
- Mosammaparast N, Shi Y (2010) Reversal of histone methylation: biochemical and molecular mechanisms of histone demethylases. *Annu Rev Biochem* 79:155–179
- Myers JM, Antholine WE, Myers CR (2008) Hexavalent chromium causes the oxidation of thioredoxin in human bronchial epithelial cells. *Toxicology* 246:222–233
- Mylonas M, Malandrinos G, Plakatouras J, Hadjiliadis N, Kasprzak KS, Krezel A, Bal W (2001) Stray Cu(II) may cause oxidative damage when coordinated to the C-terminal tail of histone H2A. *Chem Res Toxicol* 14:1177–1183
- Nackerdien Z, Kasprzak KS, Rao G, Halliwell B, Dizdaroglu M (1991) Nickel(II)- and cobalt(II)-dependent damage by hydrogen peroxide to the DNA bases in isolated human chromatin. *Cancer Res* 51:5837–5842
- Nair J, Barbin A, Velic I, Bartsch H (1999) Etheno DNA-base adducts from endogenous reactive species. *Mutat Res* 424:59–69
- Nakabeppu Y (2001) Molecular genetics and structural biology of human MutT homolog, MTH1. *Mutat Res* 477:59–70
- Nakamura T, Meshitsuka S, Kitagawa S, Abe N, Yamada J, Ishino T, Nakano H, Tsuzuki T, Doi T, Kobayashi Y, Fujii S, Sekiguchi M, Yamagata Y (2010) Structural and dynamic features of the MutT protein in the recognition of nucleotides with the mutagenic 8-oxoguanine base. *J Biol Chem* 285:444–452
- Nassi-Calò L, Mello-Filho C, Meneghini R (1989) o-phenanthroline protects mammalian cells from hydrogen peroxide-induced gene mutation and morphological transformation. *Carcinogenesis* 10:1055–1057
- Ngu TT, Stillman MJ (2009) Metalation of metallothioneins. *IUBMB Life* 61:438–446
- Nordberg M (1998) Metallothioneins: historical review and state of knowledge. *Talanta* 46:243–254
- Oskarsson A, Andersson Y, Tjälve H (1979) Fate of nickel subsulfide during carcinogenesis studied by autoradiography and X-ray powder diffraction. *Cancer Res* 39:4175–4182
- Petit A, Mwale F, Tkaczyk C, Antoniou J, Zukor DJ, Huk OL (2006) Cobalt and chromium ions induce nitration of proteins in human U937 macrophages *in vitro*. *J Biomed Mater Res A* 79:599–605
- Porter DW, Yakushiji H, Nakabeppu Y, Sekiguchi M, Fivash MJ Jr, Kasprzak KS (1997) Sensitivity of *Escherichia coli* (MutT) and human (MTH1) 8-oxo-dGTPases to *in vitro* inhibition by the carcinogenic metals, nickel(II), copper(II), cobalt(II) and cadmium(II). *Carcinogenesis* 18:1785–1791
- Rana SV (2008) Metals and apoptosis: recent developments. *J Trace Elem Med Biol* 22:262–284
- Randerath K, Randerath E, Smith CV, Jian C (1996) Structural origins of bulky oxidative DNA adducts (type II I-compounds) as deduced by oxidation of oligonucleotides of known sequence. *Chem Res Toxicol* 9:247–254
- Requena JR, Chao C-C, Levine LR, Stadtman ER (2001a) Glutamic and amino adipic semialdehydes are the main carbonyl products of metal-catalyzed oxidation of proteins. *Proc Natl Acad Sci U S A* 98:69–74
- Requena JR, Groth D, Legname G, Stadtman ER, Prusiner SB, Levine RL (2001b) Copper-catalyzed oxidation of the recombinant Sha(29–231) prion protein. *Proc Natl Acad Sci U S A* 98:7170–7175
- Robbiano L, Baroni D, Novello L, Brambilla G (2006) Correlation between induction of DNA fragmentation in lung cells from rats and humans and carcinogenic activity. *Mutat Res* 605:94–102
- Rodriguez H, Holmquist GP, D’Agostino R Jr, Keller J, Akman SA (1997) Metal ion-dependent hydrogen peroxide-induced DNA damage is more sequence specific than metal specific. *Cancer Res* 57:2394–2403
- Salnikow K, Costa M (2000) Epigenetic mechanisms of nickel carcinogenesis. *J Environ Pathol Toxicol Oncol* 19:307–318

- Salnikow K, Kasprzak KS (2005) Ascorbate depletion: a critical step in nickel carcinogenesis? *Environ Health Perspect* 113:577–584
- Salnikow K, Kasprzak KS (2007) Nickel-dependent gene expression. In: Sigel A, Sigel H, Sigel RKO (eds) *Metal ions in life sciences: nickel and its surprising impact in nature*, vol 2. Wiley, Chichester
- Salnikow K, Zhitkovich A (2008) Genetic and epigenetic mechanisms in metal carcinogenesis and cocarcinogenesis: nickel, arsenic and chromium. *Chem Res Toxicol* 21:28–44
- Salnikow K, Donald S, Bruick R, Zhitkovich A, Phang J, Kasprzak KS (2004) Depletion of intracellular ascorbate by carcinogenic metals nickel and cobalt results in the induction of hypoxic stress. *J Biol Chem* 279:40337–40344
- Saplakoglu U, Işcan M, Işcan M (1997) DNA single-strand breakage in rat lung, liver and kidney after single and combined treatments of nickel and cadmium. *Mutat Res* 394:133–140
- Sedgwick B (2004) Repairing DNA methylation damage. *Nat Rev Mol Cell Biol* 5:148–157
- Shi XG, Sun XL, Gannett PM, Dalal NS (1992) Deferoxamine inhibition of Cr(V)-mediated radical generation and deoxyguanine hydroxylation: ESR and HPLC evidence. *Arch Biochem Biophys* 293:281–286
- Shi X, Dalal NS, Kasprzak KS (1993) Generation of free radicals of hydrogen peroxide and lipid hydroperoxides in the presence of Cr(III). *Arch Biochem Biophys* 302:294–299
- Shi X, Dalal NS, Kasprzak KS (1994) Enhanced generation of hydroxyl and sulfur trioxide anion radicals from oxidation of sodium sulfite, nickel(II) sulfite, and nickel subsulfide in the presence of nickel(II) complexes. *Environ Health Perspect* 102(Suppl 3):91–96
- Sigel H (1974) Metal ions and hydrogen peroxide. XXIX. On the kinetics and mechanism of the catalase-like activity of nickel(II) and nickel(II) amine complexes. *J Coord Chem* 3:235–247
- Singh J, Bridgewater LC, Patierno SR (1998) Differential sensitivity of chromium-mediated DNA interstrand crosslinks and DNA–protein crosslinks to disruption by alkali and EDTA. *Toxicol Sci* 45:72–76
- Stadtman ER (1993) Oxidation of free amino acids and amino acid residues in proteins by radiolysis and by metal-catalyzed reactions. *Annu Rev Biochem* 62:797–821
- Stadtman ER, Berlett BS (1991) Fenton chemistry: amino acid oxidation. *J Biol Chem* 266:17201–17211
- Stadtman ER, Berlett BS (1997) Reactive oxygen-mediated protein oxidation in aging and disease. *Chem Res Toxicol* 10:485–494
- Standeven AM, Wetterhahn KE (1991) Is there a role for reactive oxygen species in the mechanism of chromium(VI) carcinogenesis? *Chem Res Toxicol* 4:616–625
- Sugden KD, Stearns DM (2000) The role of chromium(V) in the mechanism of chromate-induced oxidative DNA damage and cancer. *J Environ Pathol Toxicol Oncol* 19:215–230
- Sunderman FW Jr (1986) Metals and lipid peroxidation. *Acta Pharmacol Toxicol* 59(Suppl 7):248–255
- Tkeshelashvili LK, Reid TM, McBride TJ, Loeb LA (1993) Oxidative damage in carcinogenesis. Nickel induces a signature mutation for oxygen free radical damage. *Cancer Res* 53:4172–4174
- Toyokuni S (2009) Role of iron in carcinogenesis: cancer as a ferrototoxic disease. *Cancer Sci* 100:9–16
- Umemura T, Sai K, Takagi A, Hasegawa R, Kurokawa Y (1990) Formation of 8-hydroxydeoxyguanosine (8-OH-dG) in rat kidney DNA after intraperitoneal administration of ferric nitrilotriacetate (Fe-NTA). *Carcinogenesis* 11:345–347
- Umemura T, Sai K, Takagi A, Hasegawa R, Kurokawa Y (1991) The effects of exogenous glutathione and cysteine on oxidative stress induced by ferric nitrilotriacetate. *Cancer Lett* 58:49–56
- Valko M, Rhodes CJ, Moncol J, Izakovic M, Mazur M (2006) Free radicals, metals and antioxidants in oxidative stress-induced cancer. *Chem Biol Interact* 160:1–40
- Valverde M, Fortoul TI, Díaz-Barriga F, Mejia J, del Castillo ER (2000) Induction of genotoxicity by cadmium chloride inhalation in several organs of CD-1 mice. *Mutagenesis* 15:109–114
- Valverde M, Trejo C, Rojas E (2001) Is the capacity of lead acetate and cadmium chloride to induce genotoxic damage due to direct DNA–metal interaction? *Mutagenesis* 16:265–270

- Wei H-J, Luo X-M, Yang SP (1985) Effects of molybdenum and tungsten on mammary carcinogenesis in SD rats. *J Natl Cancer Inst* 74:469–473
- West JD, Marnett LJ (2005) Alterations in gene expression induced by the lipid peroxidation product, 4-hydroxy-2-nonenal. *Chem Res Toxicol* 18:1642–1653
- Wetterhahn KE, Hamilton JW, Aiyar J, Borges KM, Floyd R (1989) Mechanisms of chromium(VI) carcinogenesis. Reactive intermediates and effect on gene expression. *Biol Trace Elem Res* 21:405–411
- Wild P, Bourgkard E, Paris C (2009) Lung cancer and exposure to metals: the epidemiological evidence. *Methods Mol Biol* 472:139–167
- Witkiewicz-Kucharczyk A, Bal W (2006) Damage of zinc fingers in DNA repair proteins, a novel molecular mechanism in carcinogenesis. *Toxicol Lett* 162:29–42
- Wu B, Davey CA (2010) Using soft X-rays for a detailed picture of divalent metal binding in the nucleosome. *J Mol Biol* 398:633–640
- Xu A, Wu L-J, Santella RM, Hei TK (1999) Role of oxyradicals in mutagenicity and DNA damage induced by crocidolite asbestos in mammalian cells. *Cancer Res* 59:5922–5926
- Zoroddu MA, Kowalik-Jankowska T, Kozłowski H, Molinari H, Salnikow K, Broday L, Costa M (2000) Interaction of Ni(II) and Cu(II) with a metal binding sequence of histone H4: AKRHRK, a model of the H4 tail. *Biochim Biophys Acta* 1475:163–168

Part VI
Cellular Responses to Heavy Metal
Exposure

Chapter 12

Non-native Proteins as Newly-Identified Targets of Heavy Metals and Metalloids

Sandeep K. Sharma, Pierre Goloubinoff and Philipp Christen

Abstract Heavy metal ions such as Cd^{2+} , Hg^{2+} and Pb^{2+} as well as metalloid arsenic(III) species very efficiently inhibit the refolding of chemically denatured proteins (IC_{50} values in nanomolar range). In their presence, the proteins misfold and aggregate. Denatured proteins appear to be much more susceptible to form high-affinity pluridentate complexes with heavy metals and metalloids than native proteins. In a denatured protein, the potential ligands of metal ions, the most important ones being cysteine and histidine residues, are more easily accessible for the toxic agents; moreover, denatured proteins with more flexible and motile backbones are more likely than folded native proteins to tolerate the formation of pluridentate protein–metal complexes with their defined geometry. In cells, the interference of metals with nascent and other non-native forms of proteins might manifest itself both in a quantitative deficiency of the affected proteins and the formation of proteotoxic aggregates. Possibly, the toxic effects of heavy metals and metalloids arise not only from their interaction with specific, particularly susceptible native proteins but also from a general derailing of protein folding. The toxic scope of heavy metals and metalloids thus could be more pleiotropic and extensive than assumed so far.

Introduction

Certain heavy metal ions and metalloids, e.g. iron, copper, manganese or zinc, act as cofactors of many proteins, enzymes in particular, and are essential components of living matter. However, these essential components in overdose as well as xenobiotic, i.e. non-essential, heavy metal ions and metalloids have proven to cause acute and chronic toxicoses in all forms of life (Hu 2005; Kosnett 2007), including carcinogenic effects (Waisberg et al. 2003) and prenatal and developmental defects

P. Christen (✉)
Department of Biochemistry, University of Zurich,
Winterthurerstrasse 190, 8057 Zürich, Switzerland
Fax: +41-44-635-6805
e-mail: christen@bioc.uzh.ch

(Bolin et al. 2006; Monnet-Tschudi et al. 2006; Wu et al. 2008). Environmental and occupational exposure of humans, in particular to cadmium, mercury, lead and arsenic, may entail severe health hazards. The very existence of this volume on *Cellular effects of heavy metals* testifies to the importance of heavy metal toxicity as a topic in medicine and public health. The interaction of heavy metal ions with living matter has also been medically exploited: organoarsenicals and mercury compounds were once used against syphilis and trypanosomiasis; calomel (Hg_2Cl_2) served as diuretic, laxative and antiseptic; sublimate (HgCl_2) and organic mercury compounds as antiseptic in the treatment of wounds and as conserving agent in certain vaccines. While these applications are now considered obsolete, other metal-containing compounds are still in medical use: bismuth subgallate is employed as internal deodorant and in cosmetic formulations, and a platinum complex (cisplatin) serves as a well established cytostatic agent. Recently, arsenic trioxide has been approved as a cytostatic against acute promyelocytic leukemia (Wang and Chen 2008).

While the general toxicity of heavy metals and arsenic is undisputed and their remarkably pleiotropic toxic effects are known in detail, the underlying molecular mechanisms are mostly unclear. General consensus holds that proteins are the prime targets of heavy metal ions and arsenicals; only few metals such as chromium, nickel and platinum are known to interact directly with DNA. Proteins have as yet been considered to be affected by metal ions in two different ways: the toxic metal ions either bind to free thiol and other functional groups of certain native proteins, or replace essential metal ions in metal-dependent proteins (Gurd and Wilcox 1956; Vallee and Ulmer 1972; Kägi and Hapke 1984; Fraústo da Silva and Williams 1993). Here, we review a third mode of how heavy metals and metalloids may interact with and impair cellular proteins. Folding proteins have proven much more susceptible to heavy metal ions and arsenicals than proteins that have reached their native state (Sharma et al. 2008; Ramadan et al. 2009). Heavy metal ions (at nanomolar concentration) and arsenic(III) compounds (at micromolar concentrations) have been found to inhibit the refolding of chemically denatured proteins. Conceivably, nascent proteins and other forms of non-native proteins in cells are affected by heavy metals and metalloids in the same way.

Principles of Protein Folding

The amino acid sequence of a protein determines its unique three-dimensional structure, which corresponds to the energetically most favorable spatial arrangement of the polypeptide chain (Anfinsen 1973). The refolding of chemically denatured proteins is initiated by abolishing the denaturing conditions, e.g. by dilution of the denaturing agent; thus, the total polypeptide chain simultaneously takes part in the refolding process. The intracellular folding of nascent proteins, however, appears to be co-translational, i.e. to start already in the first synthesized, amino-terminal segment before the synthesis of the polypeptide chain has been completed. Moreover, because of molecular crowding, the folding of many proteins

in cells is assisted by molecular chaperones, specialized proteins that improve the yield of folding and, in many cases, driven by ATP hydrolysis, rescue proteins, which are misfolded because of heat and other types of cellular stress. All major classes of molecular chaperones comprise heat-inducible members, their expression being markedly enhanced at elevated temperature and other conditions of cellular stress (for reviews, see Georgopoulos and Welch 1993; Sharma et al. 2009). Despite the apparently more complex mechanisms of intracellular protein folding as compared to *in vitro* protein folding, the general principle that a folding polypeptide chain spontaneously seeks to attain the conformation of lowest free energy still holds true.

Interaction of Heavy Metals with Functional Groups of Proteins

Heavy metal ions form monodentate and pluridentate complexes with S, N, O atoms in proteins. The most important ligands are the thiol groups of cysteine residues and the imidazole groups of histidine residues because they produce the most stable complexes (Table 12.1). The values of the dissociation equilibrium constants K'_d given in Table 12.1 are those for monodentate complexes; pluridentate (multidentate) complexes, in which the metal ion coordinates with more than one ligand in the same protein, are much more stable, their K'_d values roughly equating to the product of the K'_d values of the monodentate complexes of the individual ligands. Metalloproteins form such highly stable pluridentate complexes with their essential metal ions, most complexes having tetrahedral (with four ligands) or octahedral (six ligands) geometry (Gurd and Wilcox 1956; Vallee and Ulmer 1972; Kägi and Hapke 1984). Engagement of a folding protein in highly stable pluridentate protein–metal complexes has recently been found to interfere gravely with the formation of the native protein structure (Sharma et al. 2008; Ramadan et al. 2009). The reasons for folding proteins being more susceptible to heavy metals than native proteins seem obvious: the side chains in unfolded proteins are not only more exposed to the solvent but also more flexible and motile than in native folded proteins and thus more prone to be incorporated as ligands in pluridentate metal complexes.

Table 12.1 Monodentate complexes of functional groups in proteins with heavy metal ions: dissociation equilibrium constants and pK'_a values

	K'_d at pH 7			Approximate pK'_a in proteins
	Cd^{2+}	Hg^{2+}	Pb^{2+}	
Thiol group	2.5 μ M	0.063 nM	13 μ M	9.4
Imidazole group	2.0 mM	200 μ M	6.3 mM	6.5
Carboxyl group	16 mM	2.5 μ M	13 mM	4.6

K'_d is the apparent dissociation equilibrium constant at pH 7 of the reaction $ML \rightleftharpoons M+L$, where ML is the 1:1 complex of the metal ion M and ligand L (Kägi and Hapke 1984)

Interference of Heavy Metals with the Refolding of Chemically Denatured Proteins

Cd^{2+} , Hg^{2+} and Pb^{2+} at nanomolar concentrations have been found to inhibit the spontaneous refolding of chemically denatured luciferase (Fig. 12.1). The metal ions affect the refolding of the protein without apparent delay. In contrast, the native protein is much less affected by the metal ions under the same conditions, being inactivated only to a limited degree in a slow time-dependent process (Fig. 12.2).

The dose–response curves for refolding inhibition (Fig. 12.3a) reveal IC_{50} values in the two-digit nanomolar range (Table 12.2), whereas the dose–response curves for inactivation of native luciferase show less than 50% inhibition even at the highest concentration (500 nM) of Cd^{2+} and Pb^{2+} (Fig. 12.3b).

It is important to note that the concentration of luciferase was 350 nM (20 $\mu\text{g}/\text{ml}$) in all experiments; at lower concentrations, the reproducibility of the measurements had proven unsatisfactory. Therefore, the IC_{50} values had to be determined at metal ion concentrations considerably lower than the 350 nM concentration of the target protein and thus cannot serve for quantitatively estimating the stability of the protein–metal complexes underlying the folding inhibition. The IC_{50} values measured under these conditions (Table 12.2) perforce underestimate the folding-inhibitory effect of the metal ions, particularly that of Hg^{2+} .

Reduced glutathione and the chelating agent EDTA attenuate the inhibitory effect of Cd^{2+} . However, neither agent rescues protein that has become misfolded in the presence of cadmium ions (Sharma et al. 2008). The ATP-dependent Hsp70 molecular chaperone system (DnaK/DnaJ/GrpE of *Escherichia coli*) significantly reduces the refolding inhibitory effect of Cd^{2+} (Table 12.2). The cyclic action of this chaperone system includes the following steps: ATP-DnaK with fast binding and release kinetics binds the substrate, i.e. the non-native protein; DnaJ stimulates the hydrolysis of DnaK-bound ATP, thus converting ATP-DnaK to ADP-DnaK with slow kinetics and high affinity for the substrate (Palleros et al. 1993; Schmid et al. 1994); pulling action of tightly bound DnaK disentangles the misfolded substrate (De Los Rios et al. 2006; Sharma et al. 2009); GrpE exchanges DnaK-bound ADP with ATP, thus triggering the release of the substrate or its re-entry into the chaperone cycle (Siegenthaler and Christen 2006). Per cycle, one DnaK molecule hydrolyzes one ATP molecule, the rate of ATP hydrolysis thus corresponds to the rate of the chaperone cycle.

Measurement of ATP consumption clearly demonstrates an acceleration of the chaperone cycle, i.e. an increased engagement of the chaperone system, due to the metal-induced misfolding of luciferase (Fig. 12.4). The steady-state ATPase activity of DnaK/DnaJ/GrpE in the absence of denatured luciferase is relatively slow and not affected by Cd^{2+} . Denatured luciferase increases the ATPase activity through *cis*-activation of the DnaK-ATPase by DnaJ in ternary (ATP-DnaK)-luciferase-DnaJ complexes (Han and Christen 2003). The additional presence of Cd^{2+} increases the ATPase activity even more. Apparently, the perturbation of luciferase refolding by the metal ion almost doubles the chaperone load (Fig. 12.4).

Fig. 12.1 Inhibition of luciferase refolding by Cd^{2+} , Hg^{2+} and Pb^{2+} . Luciferase (17.5 μM) was chemically denatured in 6 M guanidine hydrochloride, 50 mM Tris acetate, 5 mM TCEP (Tris[2-carboxyethyl]phosphine, a non-thiol reducing agent), pH 7.5, for 30 min at 25°C. Spontaneous, unassisted refolding at 25°C was initiated through 1:50 dilution (final concentration of luciferase 350 nM) with refolding buffer (50 mM Tris acetate, 100 mM potassium perchlorate, 15 mM magnesium acetate, pH 7.5), containing the indicated concentrations of Cd^{2+} **a**, Hg^{2+} **b** and Pb^{2+} **c**. Luciferase activity was measured in samples of the refolding solution at the indicated times (for details, see Sharma et al. 2008). Error bars represent the SEM from three independent experiments

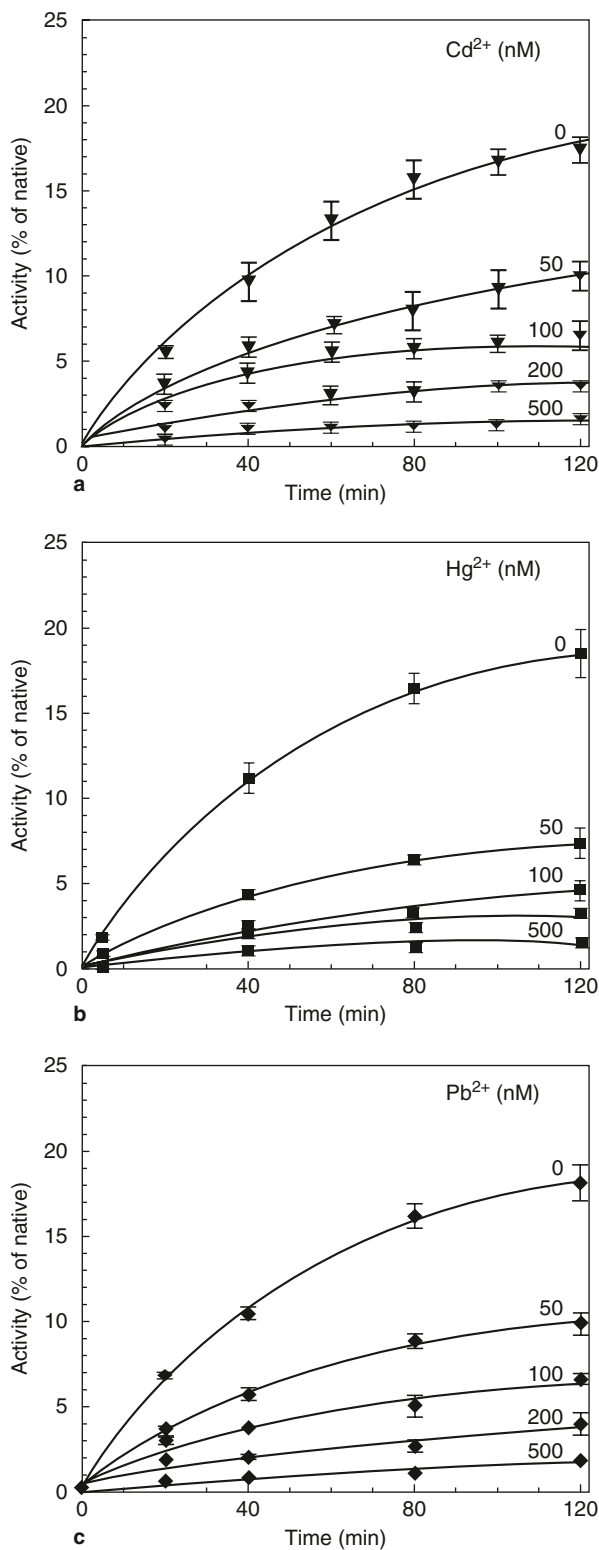


Fig. 12.2 Effect of metal ions on the enzymic activity of native luciferase. The effect of Cd^{2+} , Hg^{2+} and Pb^{2+} (100 nM) on the enzymic activity of native luciferase (350 nM) was tested in refolding buffer at 25°C under the same conditions as used for the refolding of chemically denatured luciferase (Fig. 12.1)

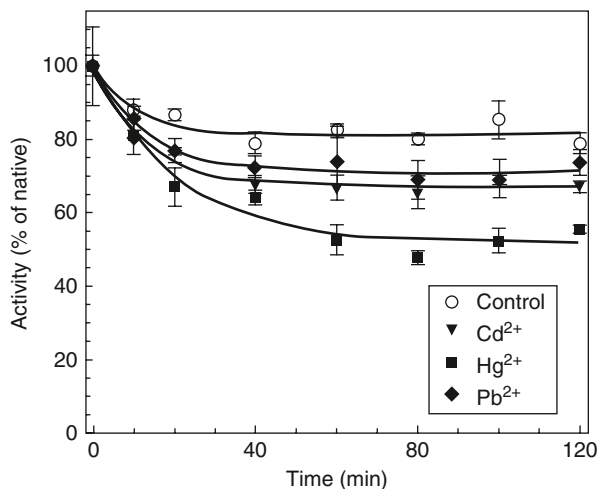


Fig. 12.3 Dose–response curves of Cd^{2+} , Hg^{2+} and Pb^{2+} for inhibition of refolding and inactivation of native enzyme. **a** Inhibition of spontaneous refolding of luciferase by Cd^{2+} , Hg^{2+} and Pb^{2+} . Chemically denatured luciferase (350 nM) was refolded at 25°C in the presence of increasing concentrations of metal ions. Luciferase activity was measured as a function of time, and the final yield of activity after 120 min (expressed as percentage of the yield in the absence of metal ion) plotted vs metal concentration. **b** Inactivation of native luciferase by Cd^{2+} , Hg^{2+} and Pb^{2+} . Luciferase (350 nM) was incubated for 120 min at 25°C with the indicated concentrations of metal ions. The residual activity after 120 min is plotted

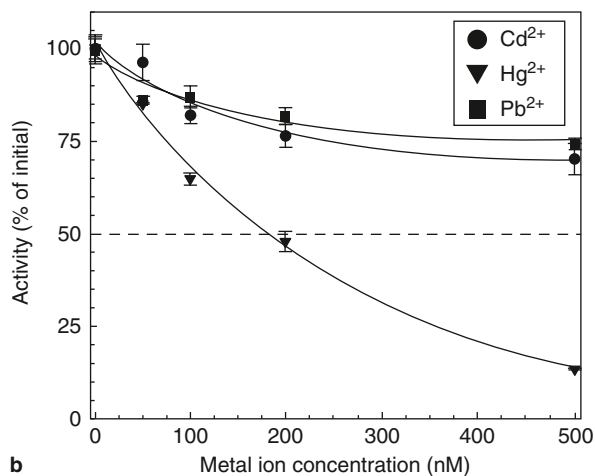
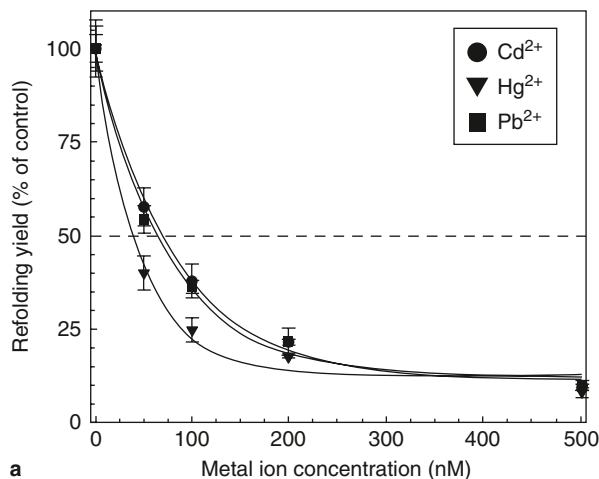
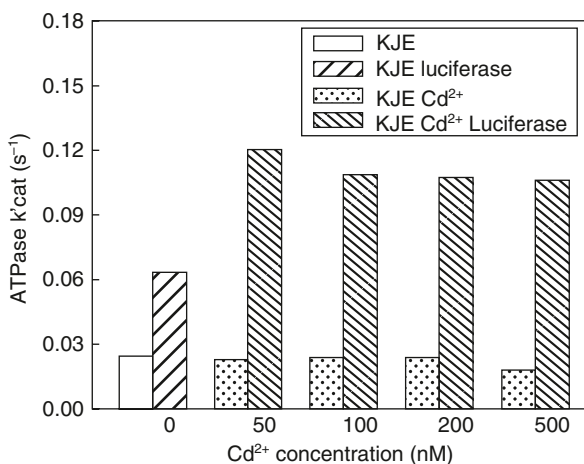


Table 12.2 IC_{50} values of Cd^{2+} , Hg^{2+} and Pb^{2+} for inhibition of protein refolding

	IC_{50} value (nM)			Cysteine residues (Number per protomer)
	Cd^{2+}	Hg^{2+}	Pb^{2+}	
<i>Luciferase</i>				4
spontaneous refolding	66 ± 11	40 ± 3	63 ± 6	
chaperone-assisted refolding	100 ± 5	53 ± 2	140 ± 11	
<i>Lactate dehydrogenase</i>				5
spontaneous refolding	68 ± 2	58 ± 6	74 ± 9	
<i>Malate dehydrogenase</i>				8
spontaneous refolding	300 ± 45	290 ± 16	520 ± 44	
<i>Glucose-6-phosphate dehydrogenase</i>				0
spontaneous refolding	340 ± 15	230 ± 18	> 600	

For chaperone-assisted refolding of luciferase, the refolding solution additionally contained $3.5 \mu M$ DnaK, $0.7 \mu M$ DnaJ, $1.4 \mu M$ GrpE and 5 mM ATP. The IC_{50} values with SEM were calculated from three independent experimental data sets

Fig. 12.4 Cd^{2+} increases the chaperone load due to luciferase refolding. The steady-state ATPase activity of the of DnaK/DnaJ/GrpE (KJE) molecular chaperone system in the presence of the indicated concentrations of Cd^{2+} was measured in the absence and presence of 350 nM refolding luciferase



The increased chaperone load is to be attributed to a higher incidence of misfolded polypeptide chains. An enhanced expression of cellular heat shock proteins, in particular of Hsp70, is indeed observed in cells exposed to heavy metal ions (Wagner et al. 1999; Han et al. 2007; Kusakabe et al. 2008; for reviews, see Hall 2002; Ahsan et al. 2009).

In addition to luciferase, we have tested with three other proteins whether their refolding was inhibited by metal ions (Table 12.2). Cysteine-containing lactate dehydrogenase proved as susceptible as cysteine-containing luciferase, while cysteine-containing malate dehydrogenase and cysteine-less glucose-6-phosphate dehydrogenase from *Leuconostoc mesenteroides* were somewhat less affected.

Mechanism of Folding Inhibition by Heavy Metal Ions

The efficiency of folding inhibition as expressed by the reciprocal of the IC_{50} values was $Hg^{2+} > Cd^{2+} > Pb^{2+}$ with all four proteins that have as yet been tested (Table 12.2). This order correlates with the relative stability of the monodentate complexes of these metal ions with thiol, imidazole and carboxylate groups in proteins (Table 12.1). However, the IC_{50} values of Cd^{2+} and Pb^{2+} (very tight binding Hg^{2+} , probably due to gross underestimating of its IC_{50} value as mentioned above, is an exception) are much lower than the dissociation equilibrium constants of the monodentate complexes. We infer from this discrepancy that the refolding-inhibitory protein–metal complexes are pluridentate rather than monodentate complexes, the metal ions being bound to several appropriately positioned liganding side chains of the denatured protein molecule. The possibility of metal ions interacting with two to six ligands and forming pluridentate complexes with their metal-specific geometry (Gurd and Wilcox 1956; Vallee and Ulmer 1972; Kägi and Hapke 1984; Fraústo da Silva and Williams 1993) is of course much higher in a denatured protein with its more flexible and motile polypeptide chain. The example of glucose-6-phosphate dehydrogenase (Table 12.2) shows that such chelate-like structures are even formed in proteins that are devoid of cysteine residues and apparently form stable pluridentate complexes exclusively with the more weakly binding imidazole and carboxylate ligands.

Xenobiotic heavy metals other than cadmium, mercury or lead as well as over-dosed essential heavy metals are of course also to be expected to perturb protein folding. Depending on the affected protein and the type of metal ion or metalloid, differential effects on the kinetics and thermodynamics of the folding trajectory of the protein will ensue.

Interference of As(III) Species with Oxidative Refolding of Disulfide Bond-Containing Proteins

Results very similar to those obtained with heavy metal ions have been reported by Ramadan et al. (2009) with three different arsenic(III) compounds, such as arsenite (arsenous acid, $As(OH)_3$) and monomethylarsenous acid ($CH_3As(OH)_2$) as inhibitors of oxidative protein refolding. Three different disulfide-bonded extracellular proteins were tested: lysozyme and ribonuclease A, each with four disulfide bridges, and riboflavin-binding protein with nine disulfide bridges. Low micromolar concentrations of the arsenicals efficiently inhibited the oxidative refolding of the chemically denatured proteins. The arsenicals bind rapidly and tightly to the cysteine residues of the reduced denatured proteins, three and two thiol groups coordinating with one molecule of arsenite and monomethylarsenous acid, respectively. Reduced glutathione (5 mM) weakens the inhibitory effect, which, however, still prevails. The interactions of the arsenic(III) compounds

with the reduced proteins are complex and not amenable to quantitative analysis, a tentative estimate by the authors of this review suggests IC_{50} values in the one-digit micromolar range.

In comparison with heavy metal ions, arsenicals thus seem somewhat less efficient in disturbing protein folding and their mode of inhibition, i.e. preventing the oxidative formation of structurally indispensable disulfide bonds, is different from that of heavy metal ions, which form pluridentate complexes comprising also protein side chains other than thiols. Despite these differences, the consequences of heavy metal ions and arsenicals interfering with protein refolding are in fact very similar: in both cases, aggregates of inactive misfolded proteins are produced with an increased propensity for binding thioflavin-T (Sharma et al. 2008; Ramadan et al. 2009), indicative of β -structured protein aggregates (LeVine 1999). Similar to heavy metals, arsenic induces the expression of heat-shock genes (Johnston et al. 1980; Levinson et al. 1980) and causes an accumulation of ubiquitinated cellular proteins (Kirkpatrick et al. 2003; Stanhill et al. 2006).

Possible Sequels of Protein Folding Inhibition in Cells

The results reviewed here indicate that the toxic scope of heavy metals and metalloids like arsenic might be greater than assumed as yet. Both groups of toxic agents might interact not only with specific native proteins that are particularly susceptible, but also, at least in principle, with any protein in non-native state. All nascent polypeptide chains are at least transitorily potential targets, and any proteins in other non-native states, e.g. proteins under heat or other cellular stress as well as natively unfolded (intrinsically unstructured) proteins (for a review, see Fink 2005), might also be affected. Denatured and other non-native proteins are indeed well known to be much more susceptible to proteolytic attack and to chemical modification, because the cleavable bonds and functional groups that are buried in the native protein become exposed upon denaturation (Means and Feeny 1971).

The susceptibility of proteins to folding inhibition by heavy metal ions or arsenicals may be assumed to depend on various structural features: first, on the number of cysteine and histidine residues and the distribution of such residues along the polypeptide chain, which determines their accessibility and the steric feasibility of forming pluridentate complexes; and second, the relative rates of complex formation and of attaining the native structure of the protein. In the completely folded protein most potentially liganding groups will be buried; moreover, the formation of pluridentate complexes with their specific geometry would require at least partial unfolding of the protein. Importantly, formation of protein–metal complexes, in contrast to proteolysis or chemical modification, is extremely fast, the rate constants of divalent metal ions for substitution of inner-sphere water of aquo ions being in the range of 10^7 – 10^9 s^{-1} (Fraústo da Silva and Williams 1993). The fast rate of complex formation may explain that even the folding of a fast-folder protein like ribonucleaseA is impaired by arsenic(III) species (Ramadan et al. 2009).

In the case of heavy metal and metalloid poisoning, the derailing of protein folding in general might not only lead to a loss of function, i.e. to a quantitative shortage of the affected proteins, but might manifest itself in the formation of toxic protein aggregates. Under these circumstances, cellular protein homeostasis might become imbalanced as observed in folding diseases (Chiti and Dobson 2006; Gidalevitz et al. 2006) and possibly in aging (Cohen et al. 2006).

Conclusions

We have clear-cut experimental evidence that heavy metals and metalloids very efficiently interfere with *in-vitro* protein refolding, and there is irrefutable evidence that these agents are highly toxic to all forms of life. However, there is a missing link between the *in-vitro* observation on the molecular level and the vast toxicological data stock. The missing link is experimental evidence that heavy metals and metalloids interfere with protein folding and induce formation of toxic protein aggregates not only *in vitro* but also in cells. There is correlative, but not cogent, evidence for this cause-and-effect relationship. Cells exposed to heavy metals and arsenicals invariably respond with an induction of heat shock proteins and an accumulation of ubiquitinated proteins (Johnston et al. 1980; Levinson et al. 1980; Wagner et al. 1999; Kirkpatrick et al. 2003; Othumpangat et al. 2005; Stanhill et al. 2006; Han et al. 2007; Kusakabe et al. 2008; for reviews, see Hall 2002; Ahsan et al. 2009).

The biological defense mechanisms against the sequels of heavy metal poisoning indeed are, in the order of their employment, reduced glutathione, the intracellular concentration of which being 5 mM or higher (Bánhegyi et al. 2007); ubiquitous metal-binding metallothioneins (Kägi and Schäffer 1988; Klaassen et al. 2009) and, additionally, in plants the enzymically synthesized phytochelatins (Freisinger 2008); the cellular chaperone network, in particular Hsp70 and Hsp60; and finally the gated proteases. If all these lines of defense fail, the deposition and compaction by aggresomes in less toxic inclusions, which may be degraded by lysosomal autophagy, provide a last resort (for reviews, see Hinault et al. 2006; Sharma et al. 2009). The *in-vivo Unfolded Protein Response* to heavy metal or metalloid poisoning might thus relate to the *in-vitro* observations that the refolding of proteins in the presence of a heavy metal ion results in an increased chaperone load (Fig. 12.4) and that folding inhibition by both heavy metals and arsenicals results in an accumulation of thioflavinT-binding aggregates (Sharma et al. 2008; Ramadan et al. 2009).

Future experimental efforts should focus on *in-vivo* experiments aimed at assessing the extent of the interference of heavy metals and metalloids with intracellular non-native proteins. The perturbation of the folding of cellular proteins in general, if existing, could contribute to explaining the pleiotropic, yet metal-specific, symptomatology of heavy metal poisoning (Waisberg et al. 2003; Hu 2005; Kosnett 2007). This mode of toxic action might not only be important in the pathogenesis of classic heavy metal poisoning, but also underlie so far unknown or inexplicable

consequences of exposure of living organisms to heavy metals, including certain protein folding diseases (Barnham et al. 2004; Chiti and Dobson 2006; Wu et al. 2008), autoimmune responses (Rowley and Monestier 2005), and subtle chronic impairments of health that are still undefined (Hu 2005; Cohen et al. 2006).

Acknowledgements This work was supported in part by a grant from the Swiss National Science Foundation (3100A0-109290) to PG. We thank J.H.R. Kägi for valuable discussions.

References

- Ahsan N, Renaut J, Komatsu S (2009) Recent developments in the application of proteomics to the analysis of plant responses to heavy metals. *Proteomics* 9:2602–2621
- Anfinsen CB (1973) Principles that govern the folding of protein chains. *Science* 181:223–230
- Bánhegyi G, Benedetti A, Csala M, Mandl J (2007) Stress on redox. *FEBS Lett* 581:3634–3640
- Barnham KJ, Masters CL, Bush AI (2004) Neurodegenerative diseases and oxidative stress. *Nat Rev Drug Discov* 3:205–214
- Bolin CM, Basha R, Cox D, Zawia NH, Maloney B, Lahiri DK, Cardozo-Pelaez F (2006) Exposure to lead and the developmental origin of oxidative DNA damage in the aging brain. *FASEB J* 20:788–790
- Chiti F, Dobson CM (2006) Protein misfolding, functional amyloid, and human disease. *Annu Rev Biochem* 75:333–366
- Cohen E, Bieschke J, Perciavalle RM, Kelly JW, Dillin A (2006) Opposing activities protect against age-onset proteotoxicity. *Science* 313:1604–1610
- De Los Rios P, Ben-Zvi A, Slutsky O, Azem A, Goloubinoff P (2006) Hsp70 chaperones accelerate protein translocation and the unfolding of stable protein aggregates by entropic pulling. *Proc Natl Acad Sci U S A* 103:6166–6171
- Fink AL (2005) Natively unfolded proteins. *Curr Opin Struct Biol* 15:35–41
- Fraústo da Silva JJR, Williams RJP (1993) The biological chemistry of the elements: the inorganic chemistry of life. Clarendon Press, Oxford
- Freisinger E (2008) Plant MTs—long neglected members of the metallothionein superfamily. *Dalton Trans* 47:6663–6675
- Georgopoulos C, Welch WJ (1993) Role of the major heat shock proteins as molecular chaperones. *Annu Rev Cell Biol* 9:601–634
- Gidalevitz T, Ben-Zvi A, Ho KH, Brignull HR, Morimoto RI (2006) Progressive disruption of cellular protein folding in models of polyglutamine diseases. *Science* 311:1471–1474
- Gurd FR, Wilcox PE (1956) Complex formation between metallic cations and proteins, peptides and amino acids. *Adv Protein Chem* 11:311–427
- Hall JL (2002) Cellular mechanisms for heavy metal detoxification and tolerance. *J Exp Bot* 53:1–11
- Han SG, Castranova V, Vallyathan V (2007) Comparative cytotoxicity of cadmium and mercury in a human bronchial epithelial cell line (BEAS-2B) and its role in oxidative stress and induction of heat shock protein 70. *J Toxicol Environ Health A* 70:852–860
- Han W, Christen P (2003) Mechanism of the targeting action of DnaJ in the DnaK molecular chaperone system. *J Biol Chem* 278:19038–19043
- Hinault MP, Ben-Zvi A, Goloubinoff P (2006) Chaperones and proteases: cellular fold-controlling factors of proteins in neurodegenerative diseases and aging. *J Mol Neurosci* 30:249–265
- Hu H (2005) Heavy metal poisoning. In: Kasper DL et al (eds) *Harrison's principles of internal medicine*, 16th edn. McGraw-Hill, New York, pp 2577–2580
- Johnston D, Oppermann H, Jackson J, Levinson W (1980) Induction of four proteins in chick embryo cells by sodium arsenite. *J Biol Chem* 255:6975–6980

- Kägi JHR, Hapke H-J (1984) Biochemical interactions of mercury, cadmium and lead. In: Nriagu JO (ed) Changing metal cycles and human health. Springer, Berlin, pp 237–250
- Kägi JHR, Schäffer A (1988) Biochemistry of metallothionein. *Biochemistry* 27:8509–8515
- Kirkpatrick DS, Dale KV, Catania JM, Gandolfi AJ (2003) Low-level arsenite causes accumulation of ubiquitinated proteins in rabbit renal cortical slices and HEK293 cells. *Toxicol Appl Pharmacol* 186:101–109
- Klaassen CD, Liu J, Diwan BA (2009) Metallothionein protection of cadmium toxicity. *Toxicol Appl Pharmacol* 238:215–220
- Kosnett MJ (2007) Heavy metal intoxication and chelators. In: Katzung BG (ed) Basic and clinical pharmacology, 10th edn. McGraw-Hill, New York, pp 945–957
- Kusakabe T, Nakajima K, Nakazato K, Suzuki K, Takada H, Satoh T, Oikawa M, Arakawa K, Nagamine T (2008) Changes of heavy metal, metallothionein and heat shock proteins in Sertoli cells induced by cadmium exposure. *Toxicol In vitro* 22:1469–1475
- LeVine H 3rd (1999) Quantification of beta-sheet amyloid fibril structures with thioflavin T. *Methods Enzymol* 309:274–284
- Levinson W, Oppermann H, Jackson J (1980) Transition series metals and sulfhydryl reagents induce the synthesis of four proteins in eukaryotic cells. *Biochim Biophys Acta* 606:170–180
- Means GE, Feeney RE (1971) Chemical modification of proteins. Holden-Day, San Francisco
- Monnet-Tschudi F, Zurich MG, Boschat C, Corbaz A, Honegger P (2006) Involvement of environmental mercury and lead in the etiology of neurodegenerative diseases. *Rev Environ Health* 21:105–117
- Othumpangat S, Kashon M, Joseph P (2005) Eukaryotic translation initiation factor 4E is a cellular target for toxicity and death due to exposure to cadmium chloride. *J Biol Chem* 280:25162–25169
- Palleros DR, Reid KL, Shi L, Welch WJ, Fink AL (1993) ATP-induced protein-Hsp70 complex dissociation requires K⁺ but not ATP hydrolysis. *Nature* 365:664–666
- Ramadan D, Rancy PC, Nagarkar RP, Schneider JP, Thorpe C (2009) Arsenic(III) species inhibit oxidative protein folding *in vitro*. *Biochemistry* 48:424–432
- Rowley B, Monestier M (2005) Mechanisms of heavy metal-induced autoimmunity. *Mol Immunol* 42:833–838
- Schmid D, Baici A, Gehrung H, Christen P (1994) Kinetics of molecular chaperone action. *Science* 263:971–973
- Sharma SK, Goloubinoff P, Christen P (2008) Heavy metal ions are potent inhibitors of protein folding. *Biochem Biophys Res Commun* 372:341–345
- Sharma SK, Christen P, Goloubinoff P (2009) Disaggregating chaperones: an unfolding story. *Curr Protein Pept Sci* 10:432–446
- Siegenthaler RK, Christen P (2006) Tuning of DnaK chaperone action by nonnative protein sensor DnaJ and thermosensor GrpE. *J Biol Chem* 281:34448–34456
- Stanhill A, Haynes CM, Zhang Y, Min G, Steele MC, Kalinina J, Martinez E, Pickart CM, Kong XP, Ron D (2006) An arsenite-inducible 19S regulatory particle-associated protein adapts proteasomes to proteotoxicity. *Mol Cell* 23:875–885
- Vallee BL, Ulmer DD (1972) Biochemical effects of mercury, cadmium, and lead. *Annu Rev Biochem* 41:91–128
- Wagner M, Hermans I, Bittinger F, Kirkpatrick CJ (1999) Induction of stress proteins in human endothelial cells by heavy metal ions and heat shock. *Am J Physiol* 277:L1026–1033
- Waisberg M, Joseph P, Hale B, Beyersmann D (2003) Molecular and cellular mechanisms of cadmium carcinogenesis. *Toxicology* 192:95–117
- Wang ZY, Chen Z (2008) Acute promyelocytic leukemia: from highly fatal to highly curable. *Blood* 111:2505–2515
- Wu J, Basha MR, Brock B, Cox DP, Cardozo-Pelaez F, McPherson CA, Harry J, Rice DC, Maloney B, Chen D, Lahiri DK, Zawia NH (2008) Alzheimer's disease (AD)-like pathology in aged monkeys after infantile exposure to environmental metal lead (Pb): evidence for a developmental origin and environmental link for AD. *J Neurosci* 28:3–9

Chapter 13

Cellular Mechanisms to Respond to Cadmium Exposure: Ubiquitin Ligases

Karin Flick and Peter Kaiser

Abstract Cadmium is increasingly used in industrial processes and is therefore becoming a mounting threat to the environment and human health. Ubiquitination has emerged as an important regulation mechanism in many processes, so it is no surprise that this protein modification plays a central role in the cellular response to cadmium exposure. The key enzymes in the process of ubiquitination are the E3 ubiquitin ligases due to their ability to confer substrate specificity. We present an overview of the roles of three such E3 ubiquitin ligases during cadmium stress in yeast and human cells. We discuss substrates and regulatory mechanisms of budding yeast SCF^{Met30}, fission yeast SCF^{Pof1}, and the mammalian Cul3/Keap1 ligase. The similarities and differences of these ubiquitin ligases that coordinate the cadmium stress response in yeast and human will be highlighted to describe the different mechanisms for cadmium sensing and detoxification.

Introduction

Ubiquitin System

Posttranslational modification of proteins with ubiquitin regulates many cellular and developmental processes. Ubiquitin is a small 76 amino acid protein, which is typically covalently attached to lysine residues or the amino terminus of the substrate proteins. Proteins may be ubiquitinated on one lysine or on multiple lysines with one ubiquitin (monoubiquitination), or a chain of ubiquitins (polyubiquitination) (Ciechanover et al. 2000; Hershko and Ciechanover 1998; Kerscher et al. 2006; Pickart 2004; Wilkinson 2000). Ubiquitin itself contains 7 lysine residues (K6, K11,

P. Kaiser (✉)

Department of Biological Chemistry, School of Medicine, University of California Irvine, 240D Med Sci I, Irvine, CA 92697-1700, USA

Tel.: +1-949-824-9442

Fax: +1-949-824-2688

e-mail: pkaiser@uci.edu

K27, K29, K33, K48 and K63), these lysines and ubiquitin’s amino terminal amino group can be used to form polyubiquitin chains (Meierhofer et al. 2008; Peng et al. 2003; Rahighi et al. 2009; Tokunaga et al. 2009). Dependent on which lysine of ubiquitin is used for chain elongation different types of linked chains can be formed. The linkage type of the ubiquitin chain is important and can define different functions of the ubiquitin chain, ranging from proteasome-dependent proteolysis to modulation of protein function, structure, assembly, and protein localization.

Attachment of ubiquitin to substrates is achieved by the E1-E2-E3 cascade of enzymes, which is composed of the E1 or ubiquitin activating enzymes, E2s or ubiquitin conjugating enzymes, and finally the E3 ubiquitin ligases (Fig. 13.1) (Hershko and Ciechanover 1998). The energy dependent activation of ubiquitin by an E1 is the first step in this cascade. Next the activated ubiquitin is transferred to the reactive cysteine in an E2. In the last step the ubiquitin is covalently linked to the lysine of the substrate, this step usually requires an E3 ubiquitin ligase. Ubiquitin ligases stimulate the catalytic activity of E2 enzymes and confer substrate specificity to the process, which makes the E3s the central players in the ubiquitination process. Similar to other posttranslational modifications, ubiquitination is reversible. Deu-

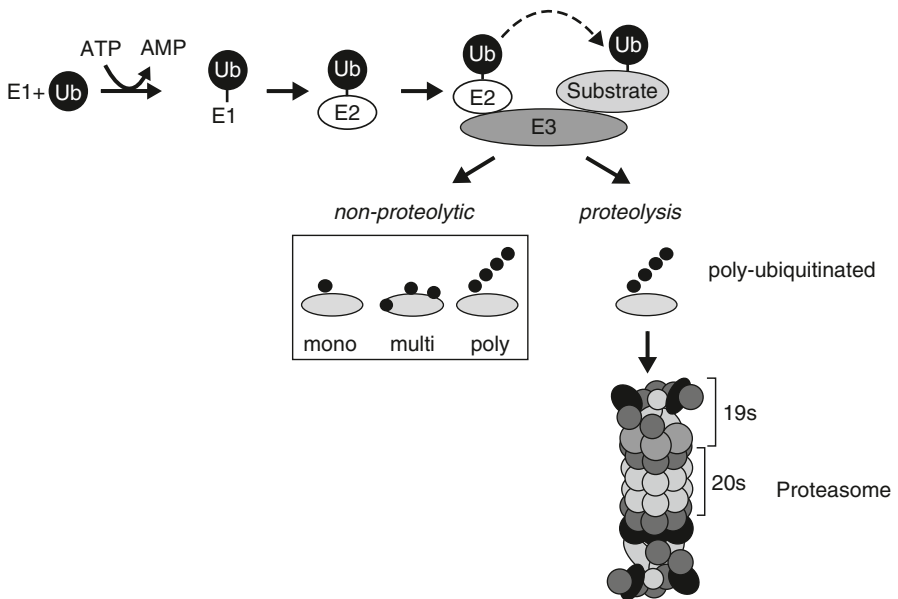


Fig. 13.1 The ubiquitin-proteasome system. Ubiquitin is activated by the E1 enzyme in an ATP-requiring reaction, transferred to one of many E2 enzymes, and finally conjugated to substrate proteins. The E3 ubiquitin ligases serve as substrate specificity factors in this process. Substrates can be mono, multi, or poly-ubiquitinated. Only poly-ubiquitination signals degradation by the 26S proteasome, which is composed of the 19S and 20S subcomplexes. Ubiquitin receptors are important for recognition and transfer of proteasome substrates to the 26S proteasome. All types of ubiquitination can have proteolysis-independent function and directly regulate localization or activity of proteins

biquitinating enzymes (DUBs) remove ubiquitin from proteins and disassemble polyubiquitin chains (Nijman et al. 2005; Wilkinson 2000). DUBs provide an additional layer of control to the ubiquitin system and are necessary for maintaining sufficient pools of free ubiquitin for ubiquitination reactions.

E3 Ubiquitin Ligases

The vital role of E3 ubiquitin ligases in substrate ubiquitination is highlighted by the diversity of E3s. While there are only 2 E1s and 38 E2s encoded in the human genome, an estimated 600–1000 E3s can be found in the human genome, surpassing the 518 protein kinase genes (Li et al. 2008).

Two main classes of E3 ubiquitin ligases have been defined based on the distinct mechanism of how they facilitate transfer of ubiquitin to substrates. HECT (Homologous to E6AP C-Terminus) -domain E3s play a more active role in the ubiquitin transfer since the activated ubiquitin is first transferred to a conserved cysteine residue in the HECT-domain before it is attached to the substrate (Kee and Huibregtse 2007). RING (Really Interesting New Gene)/U-box E3 ligases on the other hand never directly bind the activated ubiquitin but facilitate the direct transfer of ubiquitin to the substrate by allosteric activation of the E2 (Deshaies and Joazeiro 2009).

Cullin-Ring Ligases (CRLs)

A very large group within the RING domain class of E3 ligases are the cullin-based E3s (Cardozo and Pagano 2004; Petroski and Deshaies 2005). Cullins do not contain a RING-domain themselves, but bind to a small RING protein (ROC1, 2 (Ring Of Cullins), Hrt1/Rbx1) (Jackson et al. 2000). Cullin-RING ligases (CRLs) have attracted much attention because of their modular design, the diversity of processes they regulate, and their prominent role in cell cycle control. Cullins act as a scaffolding subunit, which binds directly or indirectly to one of many substrate specificity subunits. The cullin core thus provides a platform for interaction with an array of substrate adapters to target a large number of diverse proteins for regulated ubiquitination.

The SCF-Complex

The archetypical and best characterized E3 ligases belong to the CUL1 containing SCF (Skp1-Cul1-F-box) family of CRL ligases (Cardozo and Pagano 2004; Petroski and Deshaies 2005; Willems et al. 2004). In SCF-ligases CUL1 functions as a scaffold to interact with Skp1 and the RING protein Roc1/Rbx1/Hrt1 (Fig. 13.2). Skp1

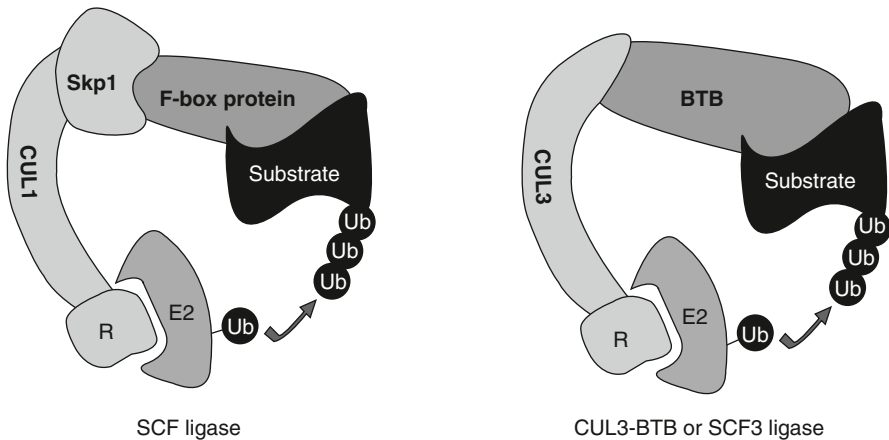


Fig. 13.2 CUL1 and CUL3 ubiquitin ligases. CUL1 and CUL3 ligases are multisubunit E3s with similar architecture. The RING-finger subunit (R), known as Roc1/Hrt1/Rbx1, binds and activates E2 enzymes. The substrate recruiting subunits are the F-box protein in SCF complexes, and BTB proteins in CUL3-BTB or SCF3 ligases

in turn binds a conserved protein motive, the F-box. This motive is found in many different proteins that, in addition to the F-box, usually contain protein-protein interaction domains that are crucial for substrate recruitment to SCF ligases.

Cadmium and Ubiquitin Ligases

Cellular Response to Cadmium Exposure

Heavy metals present a major environmental hazard. In many regions heavy metal exposure is raising due to increased use of heavy metals in various manufacturing processes. This is underscored by a recent recall of children's jewellery in the U.S., because of its high cadmium content. In addition heavy metals tend to bioaccumulate and thus enter the food chain in concentrated form (Goering et al. 1994). Despite the importance of heavy metals as environmental toxins, their biological effects are largely unknown.

When cells are exposed to heavy metals they induce a complex response to preserve cellular and genomic integrity. This response includes, induction of defense mechanisms to detoxify heavy metals, repair of damaged macromolecules, and if necessary degradation and replacement of damaged cellular components (Jamieson 1998; Perego and Howell 1997). In addition, the cell division cycle reacts to heavy metal exposure to prevent propagation of damaged macromolecules such as DNA, proteins, and lipids. In general, very little is known about how cells detect and signal heavy metal exposure. Comparatively more is known about the defense mechanisms cells have developed against heavy metals. Detoxification by chelation to glutathi-

one and sequestration by metallothioneins through their high cysteine content are the primary mechanisms (Hamer 1986; Mehra and Winge 1991; Meister and Anderson 1983; Perego and Howell 1997; Wu et al. 2004). In both plants and yeasts the chelated heavy metals are then transported into the vacuole by an energy-dependent process and stored there (Cobbett 2000; Li et al. 1997). In mammals the heavy metal cadmium is transported to the kidneys and accumulates there to significant levels because of its long biological half-life of 10–30 year (Goering et al. 1994; Hengstler et al. 2003). Liver, lung, pancreas, testis, placenta, and bone show also increased cadmium concentrations as compared to other tissues (Zalups and Ahmad 2003).

The biological effects of cadmium are perhaps better studied than that of other heavy metals. High affinity for sulfhydryl groups, competition with Zn (II) in proteins, non-specific interaction with DNA, generation of reactive oxygen species and depletion of glutathione have been shown to contribute to the toxicity of cadmium (McMurray and Tainer 2003; Stohs and Bagchi 1995; Zalups and Ahmad 2003). Recently it has been proposed that the genotoxic effects of cadmium are indirect (Jin et al. 2003; McMurray and Tainer 2003). Rather than by direct DNA damage, cadmium was suggested to lead to genome instability by inhibition of the DNA mismatch repair system through damage of sulfhydryl groups containing components (Jin et al. 2003). The damaging effect of cadmium on sulfhydryl groups containing proteins is also reflected by gene expression profiling experiments and proteome analyses in response to cadmium exposure (Fauchon et al. 2002; Vido et al. 2001). These experiments demonstrated up-regulation of proteins involved in the sulfur amino acid biosynthesis pathway, indicating the need to replace damaged proteins containing the sulfur amino acids methionine and cysteine. Notably, exposure of yeast cells to arsenic lead to similar changes in gene expression profiles (Haugen et al. 2004). Interestingly, similar studies that analyzed the response to hydrogen peroxide induced oxidative stress showed a small decrease of sulfur amino acid pathway components demonstrating a striking difference between the cadmium/arsenic and the oxidative stress response in this respect (Godon et al. 1998). Cadmium exposure of yeast also induces expression of several isozymes of the carbohydrate metabolism such as pyruvate decarboxylase, enolase and aldehyde dehydrogenase (Fauchon et al. 2002). All the cadmium-induced isozymes showed markedly reduced sulfur content, that is less methionine and cysteine residues as compared to the enzymes expressed under non-stress conditions. The physiological significance of this ‘sulfur sparing response’ has not been tested rigorously, but it has been proposed that it allows cells to devote their sulfur resources to the synthesis of glutathione for cadmium detoxification. In addition, the isozyme switch may protect the carbohydrate metabolism because the sulfur-poor isozymes are predicted to be less cadmium-sensitive than their sulfur-rich counterparts (Fauchon et al. 2002; Jamieson 2002).

The important role of the ubiquitin proteasome system in the cellular response to cadmium stress has been recognized a number of years ago and is evident from increased expression of ubiquitin and several E2 enzymes during cadmium exposure, as well as the cadmium hypersensitivity of E2 and proteasome mutants (Jungmann et al. 1993). These effects are probably related to the high demand for degradation of damaged proteins. More recently, a regulatory role of ubiquitination in addition

to the role for protein quality control during cadmium exposure has been recognized. Here we will discuss three E3 ubiquitin ligases that control and coordinate the cellular response programs required for protection from cadmium stress; the human KEAP1/CUL3, fission yeast SCF^{Pof1}, and budding yeast SCF^{Met30}. The cellular cadmium response seems to be conserved among eukaryotes, because like Met30 in budding yeast, the F-box protein Pof1, its fission yeast homolog, is also required for cadmium defense (Baudouin-Cornu and Labarre 2006; Harrison et al. 2005). In addition, Keap1 the substrate adapter of the SCF-type ubiquitin ligase SCF3^{Keap1} regulates the response to cadmium and arsenic exposure in mammals (Fig. 13.3) (He et al. 2006; Stewart et al. 2003). All these SCF-type ubiquitin ligases regulate activity of a bZIP transcription factor, which in turn initiates a cadmium-specific transcription program.

Saccharomyces Cerevisiae Transcription Factor Met4

Both isozyme switching and induction of sulfur amino acid synthesis pathway components in response to cadmium exposure have been shown to depend primarily on

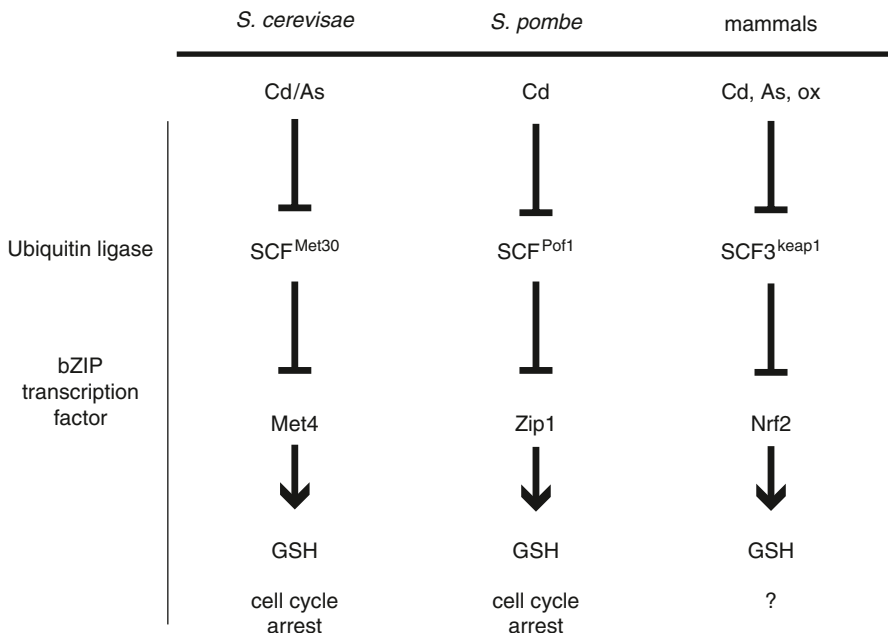


Fig. 13.3 Conservation of the cadmium response in budding yeast, fission yeast, and mammals. Cullin based ubiquitin ligases ubiquitinate and inactivate bZIP transcription factors. Cadmium stress blocks ubiquitination leading to activation of the transcription factors and induction of a stress response gene expression program

the transcription factor Met4 (Fauchon et al. 2002). Microarray analysis demonstrated that cadmium-dependent induction of over sixty genes was severely affected in *met4Δ* mutants (Fauchon et al. 2002). Consistent with these observations, *met4Δ* mutants are cadmium sensitive (Barbey et al. 2005; Wheeler et al. 2002; Yen et al. 2005). Thus, regulation of Met4 appears to be an important part of the cellular response to cadmium and arsenic (Yen et al. 2005).

The transcription factor Met4 is best known for its role in the regulation of genes involved in the sulfur assimilation pathway (Thomas and Surdin-Kerjan 1997). Several other transcription factors participate in this pathway. However, only Met4 has transactivating activity. Under normal conditions (i.e. enough sulfur amino acids in the medium) Met4 is in its inactive, ubiquitinated form, but when the intracellular S-adenosylmethionine (SAM) concentration drops below a certain threshold Met4 gets activated and leads to the transcription of genes involved in methionine synthesis (Thomas and Surdin-Kerjan 1997). SAM is the principal methyl-group donor in cells and is synthesized from methionine and ATP. Activation of Met4 involves its deubiquitination by so far unknown ubiquitin hydrolase(s). As soon as adequate SAM levels are restored Met4 is inactivated by ubiquitination by the ubiquitin ligase SCF^{Met30} together with the ubiquitin-conjugating enzyme Cdc34 (Flick et al. 2004; Kaiser et al. 2000; Rouillon et al. 2000).

Ubiquitinated Met4 is normally not subject to degradation by the proteasome, because an ubiquitin-binding domain (UIM) within Met4 protects Met4 from degradation (Flick et al. 2006). Therefore modification with ubiquitin plays a direct regulatory role in Met4 activity. This non-proteolytic regulation by ubiquitination allows for a very rapid activation of Met4 during cadmium stress without requirement of protein synthesis (Flick et al. 2006). However, under certain growth conditions that are most likely associated with physiological changes during entry into late-log phase, ubiquitinated Met4 gets degraded (Chandrasekaran et al. 2006; Kuras et al. 2002), and data not shown).

SCF^{Met30} and specifically the F-box protein Met30 are therefore the key regulators of Met4 activity. Full activation of Met4 induces a poorly understood cell cycle arrest that appears to be important to safeguard cellular integrity under conditions where SAM levels are low or during cadmium stress (Kaiser et al. 2006; Patton et al. 2000; Su et al. 2005). Consequently, the F-box protein Met30 is essential for cell cycle progression because it is required for ubiquitination and therefore inactivation of Met4.

In addition to regulation evoked by low SAM-levels, cadmium is also a potent regulator of Met4 ubiquitination (Barbey et al. 2005; Yen et al. 2005), as is arsenic, but no other heavy metals. Addition of cadmium leads to activation of Met4 resulting in the expression of *MET* genes and *GSH1*, a gene encoding the rate-limiting enzyme in the synthesis of glutathione. In addition, a cell cycle arrest is induced to allow for cadmium damage repair (Barbey et al. 2005; Kaiser et al. 2006; Yen et al. 2005). Activation of Met4 is initiated by inactivation of the ubiquitin ligase SCF^{Met30} followed by removal of the ubiquitin chain attached to Met4 by a so far unidentified deubiquitinating enzyme. Interestingly, deubiquitination is strongly activated during cadmium stress (Barbey et al. 2005).

Cadmium Exposure Leads to the Disassembly of SCF^{Met30}

Regulation of substrate ubiquitination by SCF type E3 ligases usually occurs at the level of substrate/F-box protein interaction. Frequently, phosphorylation of the substrate is the regulated step and creates a binding site for the F-box subunit. However, subcellular localization or relocation to a different compartment can also determine binding to the F-box protein and thus regulate substrate ubiquitination. Therefore it was very surprising when it was demonstrated that Met4 remains bound to the F-box protein Met30 during cadmium stress and that Met4 ubiquitination is blocked due to cadmium-induced dissociations of Met30 from the core ligase complex Cdc53/Skp1 (Barbey et al. 2005; Yen et al. 2005). SCF^{Met30} disassembly is a cadmium specific signal and not a default pathway for SCF^{Met30} regulation, because depletion of S-adenosylmethionine leads to loss of binding between Met30 and its substrate Met4, but has no effect on the Met30/Skp1 interaction (unpublished observation). Importantly, the cadmium signal specifically acts on SCF^{Met30} and does not affect the binding of other F-box proteins to Skp1 (Barbey et al. 2005).

Recently we found that Cdc48/p97 plays a significant role in inactivation of SCF^{Met30} during the cadmium response. Cdc48 is a chaperone-like ATPase, which is linked to the ubiquitin pathway. Intriguingly, Cdc48 can function as a ‘molecular wrench’ by segregating ubiquitinated substrates from unmodified partners (Jentsch and Rumpf 2007; Rape et al. 2001; Rumpf and Jentsch 2006; Shcherbik and Haines 2007).

Whether cadmium acts directly on any of the known components of the SCF^{Met30} system or whether an upstream signaling pathway is involved is still unclear. Experiments where cadmium was directly added to SCF^{Met30}/Met4 *in vitro* ubiquitination reactions didn’t lead to any measurable activity difference, suggesting that cadmium does not directly interfere with SCF^{Met30} activity and therefore a direct effect of cadmium on the ligase seems unlikely (Barbey et al. 2005).

The Schizosaccharomyces Pombe Transcription Factor Zip1

The ortholog of Met4 in *S. pombe* is the transcription factor Zip1, which like Met4 is a member of the bZIP (basic leucine zipper) transcription factor family (Harrison et al. 2005). However, Met4 is a transactivator devoid of intrinsic DNA binding ability and relies on its cofactors Met31, Met32 and Cbf1 to be directed to promoters (Thomas and Surdin-Kerjan 1997). In contrast, Zip1 has DNA binding activity. In addition, there is another major distinction between Met4 and Zip1 function. Met4 is essential for the sulfur metabolism in budding yeast and required for synthesis of sulfur containing amino acids like methionine and cysteine (Thomas and Surdin-Kerjan 1997). Zip1 on the other hand is only needed for the synthesis of methionine and cysteine in response to cadmium stress, but not during limiting nutrient conditions (Harrison et al. 2005). These differences in composition and function probably account for the divergence in regulation. Whereas, Met4’s ubiq-

ubiquitination leads to its direct inactivation without degradation, Zip1 is constantly ubiquitinated and targeted to the proteasome under non-stress conditions (Harrison et al. 2005). Direct inactivation of Met4 allows for a fast response to various conditions demanding different levels and specificity of Met4 activity (Flick et al. 2006). Zip1 activity on the other hand is only required under the very special situation of cadmium exposure. Accordingly, *zip1* mutants are cadmium sensitive and DNA microarray analysis showed dependence of 27 genes on Zip1, where 20 of these genes were induced in the response to cadmium stress. Remarkably, 15 of these 20 genes belong to a group of 32 genes that are uniquely induced by cadmium exposure and not under any other stress condition (Harrison et al. 2005). The fact that many of these genes solely rely on Zip1 strongly suggests that Zip1 is the major transcription factor in *S. pombe* regulating the defense against cadmium stress.

SCF^{Pof1} is Responsible for the Ubiquitination of Zip1

The fission yeast genome encodes for 18 F-box proteins, only two of them are essential. One of these essential F-box proteins is Pof1, which is the *S. pombe* counterpart to Met30. Pof1 forms the ubiquitin ligase SCF^{Pof1} by assembling with the cullin-1 Pcu1, the Skp1 homolog Psh1, and the small ring finger protein Pip1 (Harrison et al. 2005). Similar to budding yeast SCF^{Met30} and its key substrate Met4, the essential function of SCF^{Pof1} is the inactivation of Zip1, as deletion of *ZIP1* suppresses the lethality of *pof1*Δ mutations. Ubiquitination of Zip1 is constitutive under normal growth conditions, but upon cadmium exposure SCF^{Pof1} is inactivated by a yet to be determined mechanism. Binding of Zip1 by SCF^{Pof1} and therefore ubiquitination appears to be dependent on Zip1 phosphorylation by a so far unknown kinase (Harrison et al. 2005).

As it is the case for budding yeast Met30/Met4, Pof1 transcription is induced by activation of Zip1, which appears to be part of a feedback loop, by which cells prepare to inactivate the transcription factors once enough transcripts for the defense against cadmium stress have been produced.

Mammalian Transcription Factor Nrf2

As in budding and fission yeast a member of the bZIP-family of transcription factors, Nrf2 (Nuclear factor erythroid2-related factor 2) regulates the transcriptional response to coordinate defense against cadmium stress. But whereas oxidative stress does not trigger activation of either Met4 or Zip1, Nrf2 is best known for its role in protection against oxidative and electrophilic stress, and it is in this context that most studies have been done. Nrf2 is ubiquitously expressed in a wide range of tissues and cell types. Nrf2 is responsible for both inducible and constitu-

tive activation of gene expression via cis-acting responsive elements called ARE (Antioxidant-Responsive Element) or EpRE (Electrophile-Response Element) (Li and Kong 2009; Nguyen et al. 2009). Many aspects of Nrf2 regulation appear to be controversial, which might reflect diverse and stress-specific mechanisms of Nrf2 activation. Nevertheless, what appears to be generally accepted is that Nrf2 is regulated through ubiquitination, such that oxidative or heavy metal stress blocks Nrf2 ubiquitination and leads to its stabilization. The resulting accumulation of Nrf2 triggers its dimerization with a small Maf (musculoaponeurotic fibrosarcoma) protein, which also belong to the bZIP family of transcription factors and contain DNA binding activity but no discernable transactivation domain. The Nrf2/Maf heterodimer binds to ARE and EpRE elements and induces expression of genes important for survival under stress conditions.

KEAP1-CUL3 Ubiquitin Ligase is Responsible for the Ubiquitination of Nrf2

Nrf2 ubiquitination is catalyzed by the cullin-RING ligase SCF3^{KEAP1}. SCF3 ligase complexes are based on Cul-3 and are thus different from the Cul-1 based SCF ligases, but their general architecture is very similar (Petroski and Deshaies 2005; Willems et al. 2004) (Fig. 13.2). SCF3 ligases are characterized by the Bric-a-brac–Tramtrack–Broad complex (BTB) domain-containing proteins, which replace the F-box/Skp1 module. Indeed, the BTB-domain and Skp1 are structurally very similar and BTB-proteins can be viewed as single polypeptides that combine Skp1 and F-box protein functions. Accordingly, BTB-proteins are the substrate adaptor proteins in Cul-3 ligases, and Kelch-like ECH-associated protein 1 (KEAP1) is the specificity factor for Nrf2 ubiquitination (Zhang et al. 2004). KEAP1 contains a BTB as well as a Kelch-domain. Kelch-repeats in KEAP1 interact directly with Nrf2 for recruitment to the ligase. The Neh2 (Nrf2-ECH homology) domain is the interaction surface on Nrf2 that is required for recruitment by KEAP1. Similar to the substrate recruiting component Met30 in budding yeast and Pof1 in fission yeast, KEAP1 is an essential protein and its essential function is the down regulation of the transcription factor Nrf2. Consequently, inactivation of KEAP1 in mice leads to postnatal lethality due to constitutive Nrf2 activation (Wakabayashi et al. 2003).

There is no consensus about the dynamics of Nrf2 localization and the subcellular compartment for Nrf2 ubiquitination. Two models are suggested. The first model has Nrf2 anchored by KEAP1 binding and ubiquitination in the cytoplasm. Upon insult KEAP1 is inactivated by an unknown mechanism and Nrf2 is free to enter the nucleus to initiate transcription (reviewed in Li and Kong 2009). The opposing model suggests Nrf2 constitutively located in the nucleus and KEAP1 transiently shuttling into the nucleus (reviewed in Nguyen et al. 2009). During normal growth conditions SCF3^{KEAP1} seems to be constitutively active and ubiquitinates Nrf2 in an unregulated manner, as suggested by the fact that overexpression of KEAP1

leads to an increase in Nrf2 ubiquitination in cells (Nguyen et al. 2005; Zhang and Hannink 2003). However, both Nrf2 and KEAP1 have been reported to interact with cadmium and arsenic directly through specific cysteine thiol groups, and it was suggested that these cysteine residues mediate the heavy metal stress response (Dinkova-Kostova et al. 2002; Egger et al. 2005; He et al. 2008; Hong et al. 2005; Kobayashi et al. 2004; Yamamoto et al. 2008; Zhang and Hannink 2003). Furthermore, it has been suggested that this multipronged response where both proteins can function as sensors allows cells to fine tune its reaction to the nature and strength of the insult (He and Ma 2010).

Conclusions

Even though we are far from knowing all players and understanding the mechanisms of regulation that govern the cellular response to cadmium stress, it is evident from yeast to man that ubiquitin ligases play a key role. We have discussed ubiquitin ligases from budding yeast, fission yeast, and mammals with diverse mechanisms of regulation, but strikingly similar effects on protecting cells from cadmium exposure. At the heart of this conserved system is a bZIP transcription factor that is regulated through ubiquitination. These transcription factors, mammalian Nrf2, fission yeast Zip1, and budding yeast Met4, are responsible for expression of a set of genes that help cells to detoxify cadmium. Ubiquitination of the transcription factors serves different functions. In fission yeast and mammals the transcription factor is targeted for degradation by the proteasome, whereas ubiquitination of budding yeast Met4 can directly inhibit transactivation in a proteolysis-independent manner. These differences might reflect the diversity in transcription factor composition, because Met4 needs several cofactors for activity, and/or it might indicate a variation in how cells fine-tune the response. The ubiquitin ligases involved in these systems, SCF^{Met30} in budding yeast, SCF^{Pof1} in fission yeast, and mammalian SCF3^{KEAP1} are constitutively active, but are inactivated upon cadmium insult by a largely unknown mechanism. In the case of SCF^{Met30} inactivation involves disassembly of the SCF multi-protein complex (Barbey et al. 2005; Yen et al. 2005). A similar mechanism has been suggested for SCF3^{KEAP1} (Zhang et al. 2004), but remains controversial. Cysteine residues in both KEAP1 and Nrf2 have been reported to bind cadmium (and other inducers), suggesting that either of those proteins can sense the insult. A direct sensing mechanism through either the transcription factor or the ligase is a very appealing model and it will be of great interest to test similar direct effects of cadmium in the yeast systems.

Clearly, further studies in both mammals and yeast are required to show how cadmium is sensed and connected to ubiquitin ligase inhibition. All three ubiquitin ligases that coordinate the cadmium response are essential for cell viability, and their essential functions are deactivation of the transcription factor under non-stress conditions. Cell cycle arrest has been reported as a consequence of activation of both Met4 and Zip1. In the case of Met4 this cell cycle arrest happens both under

SAM-depletion and cadmium stress. Cells arrest predominantly in the G1-phase of the cell cycle and this checkpoint arrest presumably allows cells to repair and/or replenish essential components.

Studies on cellular cadmium stress response place E3 ubiquitin ligases at the center as coordinators for down-stream events such as detoxification, repair, replacement, and cell cycle response. However, our current understanding provides only a conceptual picture that lacks important details on how cadmium is sensed and signals are transmitted. Future studies will address these aspects of cellular cadmium response and are likely to extend the role ubiquitin ligases play during cadmium stress.

References

- Barbey R, Baudouin-Cornu P, Lee TA, Rouillon A, Zarzov P, Tyers M, Thomas D (2005) Inducible dissociation of SCF(Met30) ubiquitin ligase mediates a rapid transcriptional response to cadmium. *Embo J* 24:521–532
- Baudouin-Cornu P, Labarre J (2006) Regulation of the cadmium stress response through SCF-like ubiquitin ligases: comparison between *Saccharomyces cerevisiae*, *Schizosaccharomyces pombe* and mammalian cells. *Biochimie* 88(11):1673–1685
- Cardozo T, Pagano M (2004) The SCF ubiquitin ligase: insights into a molecular machine. *Nat Rev Mol Cell Biol* 5:739–751
- Chandrasekaran S, Deffenbaugh AE, Ford DA, Bailly E, Mathias N, Skowrya D (2006) Destabilization of binding to cofactors and SCFMet30 is the rate-limiting regulatory step in degradation of polyubiquitinated Met4. *Mol Cell* 24:689–699
- Ciechanover A, Orian A, Schwartz AL (2000) The ubiquitin-mediated proteolytic pathway: mode of action and clinical implications. *J Cell Biochem Suppl* 34:40–51
- Cobbett CS (2000) Phytochelatins and their roles in heavy metal detoxification. *Plant Physiol* 123:825–832
- Deshaias RJ, Joazeiro CA (2009) RING domain E3 ubiquitin ligases. *Annu Rev Biochem* 78:399–434
- Dinkova-Kostova AT, Holtzclaw WD, Cole RN, Itoh K, Wakabayashi N, Katoh Y, Yamamoto M, Talalay P (2002) Direct evidence that sulfhydryl groups of Keap1 are the sensors regulating induction of phase 2 enzymes that protect against carcinogens and oxidants. *Proc Natl Acad Sci U S A* 99:11908–11913
- Eggler AL, Liu G, Pezzuto JM, van Breemen RB, Mesecar AD (2005) Modifying specific cysteines of the electrophile-sensing human Keap1 protein is insufficient to disrupt binding to the Nrf2 domain Neh2. *Proc Natl Acad Sci U S A* 102:10070–10075
- Faucher M, Lagniel G, Aude JC, Lombardia L, Soularue P, Petat C, Marguerie G, Sentenac A, Werner M, Labarre J (2002) Sulfur sparing in the yeast proteome in response to sulfur demand. *Mol Cell* 9:713–723
- Flick K, Ouni I, Wohlschlegel JA, Capati C, McDonald WH, Yates JR, Kaiser P (2004) Proteolysis-independent regulation of the transcription factor Met4 by a single Lys 48-linked ubiquitin chain. *Nat Cell Biol* 6:634–641
- Flick K, Raasi S, Zhang H, Yen JL, Kaiser P (2006) A ubiquitin-interacting motif protects polyubiquitinated Met4 from degradation by the 26S proteasome. *Nat Cell Biol* 8:509–515
- Godon C, Lagniel G, Lee J, Buhler JM, Kieffer S, Perrot M, Boucherie H, Toledano MB, Labarre J (1998) The H₂O₂ stimulon in *Saccharomyces cerevisiae*. *J Biol Chem* 273:22480–22489
- Goering PL, Waalkes MP, Klaassen CD (1994) Toxicology of metals, biochemical effects. In: Goyer RA, Cherian MG (Eds) *Handbook of experimental pharmacology*, vol 115. Springer, New York, pp 189–214

- Hamer DH (1986) Metallothionein. *Annu Rev Biochem* 55:913–951
- Harrison C, Katayama S, Dhut S, Chen D, Jones N, Bahler J, Toda T (2005) SCF(Pof1)-ubiquitin and its target Zip1 transcription factor mediate cadmium response in fission yeast. *Embo J* 24:599–610
- Haugen AC, Kelley R, Collins JB, Tucker CJ, Deng C, Afshari CA, Brown JM, Ideker T, Van Houten B (2004) Integrating phenotypic and expression profiles to map arsenic-response networks. *Genome Biol* 5:R95
- He X, Ma Q (2010) Critical cysteine residues of Kelch-like ECH-associated protein 1 in arsenic sensing and suppression of nuclear factor erythroid 2-related factor 2. *J Pharmacol Exp Ther* 332:66–75
- He X, Chen MG, Lin GX, Ma Q (2006) Arsenic induces NAD(P)H-quinone oxidoreductase I by disrupting the Nrf2 x Keap1 x Cul3 complex and recruiting Nrf2 x Maf to the antioxidant response element enhancer. *J Biol Chem* 281:23620–23631
- He X, Chen MG, Ma Q (2008) Activation of Nrf2 in defense against cadmium-induced oxidative stress. *Chem Res Toxicol* 21:1375–1383
- Hengstler JG, Bolm-Audorff U, Faldum A, Janssen K, Reifenrath M, Gotte W, Jung D, Mayer-Popken O, Fuchs J, Gebhard S, Bienfait HG, Schlink K, Dietrich C, Faust D, Epe B, Oesch F (2003) Occupational exposure to heavy metals: DNA damage induction and DNA repair inhibition prove co-exposures to cadmium, cobalt and lead as more dangerous than hitherto expected. *Carcinogenesis* 24:63–73
- Hershko A, Ciechanover A (1998) The ubiquitin system. *Annu Rev Biochem* 67:425–479
- Hong F, Sekhar KR, Freeman ML, Liebler DC (2005) Specific patterns of electrophile adduction trigger Keap1 ubiquitination and Nrf2 activation. *J Biol Chem* 280:31768–31775
- Jackson PK, Eldridge AG, Freed E, Furstenthal L, Hsu JY, Kaiser BK, Reimann JD (2000) The lore of the RINGS: substrate recognition and catalysis by ubiquitin ligases. *Trends Cell Biol* 10:429–439
- Jamieson DJ (1998) Oxidative stress responses of the yeast *Saccharomyces cerevisiae*. *Yeast* 14:1511–1527
- Jamieson D (2002) Saving sulfur. *Nat Genet* 31:228–230
- Jentsch S, Rumpf S (2007) Cdc48 (p97): a “molecular gearbox” in the ubiquitin pathway? *Trends Biochem Sci* 32:6–11
- Jin YH, Clark AB, Slebos RJ, Al-Refai H, Taylor JA, Kunkel TA, Resnick MA, Gordenin DA (2003) Cadmium is a mutagen that acts by inhibiting mismatch repair. *Nat Genet* 34:326–329
- Jungmann J, Reins-H, Schobert C, Jentsch S (1993) Resistance to cadmium mediated by ubiquitin dependent proteolysis. *Nature* 361:369–371
- Kaiser P, Flick K, Wittenberg C, Reed SI (2000) Regulation of transcription by ubiquitination without proteolysis: Cdc34/SCF(Met30)-mediated inactivation of the transcription factor Met4. *Cell* 102:303–314
- Kaiser P, Su NY, Yen JL, Ouni I, Flick K (2006) The yeast ubiquitin ligase SCF-Met30: connecting environmental and intracellular conditions to cell division. *Cell Div* 1:16
- Kee Y, Huijbregtse JM (2007) Regulation of catalytic activities of HECT ubiquitin ligases. *Biochem Biophys Res Commun* 354:329–333
- Kerscher O, Felberbaum R, Hochstrasser M (2006) Modification of proteins by ubiquitin and ubiquitin-like proteins. *Annu Rev Cell Dev Biol* 22:159–180
- Kobayashi A, Kang MI, Okawa H, Ohtsuji M, Zenke Y, Chiba T, Igarashi K, Yamamoto M (2004) Oxidative stress sensor Keap1 functions as an adaptor for Cul3-based E3 ligase to regulate proteasomal degradation of Nrf2. *Mol Cell Biol* 24:7130–7139
- Kuras L, Rouillon A, Lee T, Barbey R, Tyers M, Thomas D (2002) Dual regulation of the met4 transcription factor by ubiquitin-dependent degradation and inhibition of promoter recruitment. *Mol Cell* 10:69–80
- Li W, Kong AN (2009) Molecular mechanisms of Nrf2-mediated antioxidant response. *Mol Carcinog* 48:91–104
- Li ZS, Lu YP, Zhen RG, Szczypka M, Thiele DJ, Rea PA (1997) A new pathway for vacuolar cadmium sequestration in *Saccharomyces cerevisiae*: YCF1-catalyzed transport of bis(glutathionato) cadmium. *Proc Natl Acad Sci U S A* 94:42–47

- Li W, Bengtson MH, Ulbrich A, Matsuda A, Reddy VA, Orth A, Chanda SK, Batalov S, Joazeiro CA (2008) Genome-wide and functional annotation of human E3 ubiquitin ligases identifies MULAN, a mitochondrial E3 that regulates the organelle's dynamics and signaling. *PLoS One* 3:e1487
- McMurray CT, Tainer JA (2003) Cancer, cadmium and genome integrity. *Nat Genet* 34:239–241
- Mehra RK, Winge DR (1991) Metal ion resistance in fungi: molecular mechanisms and their regulated expression. *J Cell Biochem* 45:30–40
- Meierhofer D, Wang X, Huang L, Kaiser P (2008) Quantitative analysis of global ubiquitination in HeLa cells by mass spectrometry. *J Proteome Res* 7:4566–4576
- Meister A, Anderson ME (1983) Glutathione. *Annu Rev Biochem* 52:711–760
- Nguyen T, Sherratt PJ, Nioi P, Yang CS, Pickett CB (2005) Nrf2 controls constitutive and inducible expression of ARE-driven genes through a dynamic pathway involving nucleocytoplasmic shuttling by Keap1. *J Biol Chem* 280:32485–32492
- Nguyen T, Nioi P, Pickett CB (2009) The Nrf2-antioxidant response element signaling pathway and its activation by oxidative stress. *J Biol Chem* 284:13291–13295
- Nijman SM, Luna-Vargas MP, Velds A, Brummelkamp TR, Dirac AM, Sixma TK, Bernards R (2005) A genomic and functional inventory of deubiquitinating enzymes. *Cell* 123:773–786
- Patton EE, Peyraud C, Rouillon A, Surdin KY, Tyers M, Thomas D (2000) SCF(Met30)-mediated control of the transcriptional activator Met4 is required for the G(1)-S transition. *Embo J* 19:1613–1624
- Peng J, Schwartz D, Elias JE, Thoreen CC, Cheng D, Marsischky G, Roelofs J, Finley D, Gygi SP (2003) A proteomics approach to understanding protein ubiquitination. *Nat Biotechnol* 21:921–926
- Perego P, Howell SB (1997) Molecular mechanisms controlling sensitivity to toxic metal ions in yeast. *Toxicol Appl Pharmacol* 147:312–318
- Petroski MD, Deshaies RJ (2005) Function and regulation of cullin-RING ubiquitin ligases. *Nat Rev Mol Cell Biol* 6:9–20
- Pickart CM (2004) Back to the future with ubiquitin. *Cell* 116:181–190
- Rahighi S, Ikeda F, Kawasaki M, Akutsu M, Suzuki N, Kato R, Kensche T, Uejima T, Bloor S, Komander D, Randow F, Wakatsuki S, Dikic I (2009) Specific recognition of linear ubiquitin chains by NEMO is important for NF-kappaB activation. *Cell* 136:1098–1109
- Rape M, Hoppe T, Gorr I, Kalocay M, Richly H, Jentsch S (2001) Mobilization of processed, membrane-tethered SPT23 transcription factor by CDC48(UFD1/NPL4), a ubiquitin-selective chaperone. *Cell* 107:667–677
- Rouillon A, Barbey R, Patton EE, Tyers M, Thomas D (2000) Feedback-regulated degradation of the transcriptional activator Met4 is triggered by the SCF(Met30) complex. *Embo J* 19:282–294
- Rumpf S, Jentsch S (2006) Functional division of substrate processing cofactors of the ubiquitin-selective Cdc48 chaperone. *Mol Cell* 21:261–269
- Shcherbik N, Haines DS (2007) Cdc48p(Npl4p/Ufd1p) binds and segregates membrane-anchored/tethered complexes via a polyubiquitin signal present on the anchors. *Mol Cell* 25:385–397
- Stewart D, Killen E, Naquin R, Alam S, Alam J (2003) Degradation of transcription factor Nrf2 via the ubiquitin-proteasome pathway and stabilization by cadmium. *J Biol Chem* 278:2396–2402
- Stohs SJ, Bagchi D (1995) Oxidative mechanisms in the toxicity of metal ions. *Free Radic Biol Med* 18:321–336
- Su NY, Flick K, Kaiser P (2005) The F-box protein Met30 is required for multiple steps in the budding yeast cell cycle. *Mol Cell Biol* 25:3875–3885
- Thomas D, Surdin-Kerjan Y (1997) Metabolism of sulfur amino acids in *Saccharomyces cerevisiae*. *Microbiol Mol Biol Rev* 61:503–532
- Tokunaga F, Sakata S, Saeki Y, Satomi Y, Kirisako T, Kamei K, Nakagawa T, Kato M, Murata S, Yamaoka S, Yamamoto M, Akira S, Takao T, Tanaka K, Iwai K (2009) Involvement of linear polyubiquitylation of NEMO in NF-kappaB activation. *Nat Cell Biol* 11:123–132
- Vido K, Spector D, Lagniel G, Lopez S, Toledano MB, Labarre J (2001) A proteome analysis of the cadmium response in *Saccharomyces cerevisiae*. *J Biol Chem* 276:8469–8474

- Wakabayashi N, Itoh K, Wakabayashi J, Motohashi H, Noda S, Takahashi S, Imakado S, Kotsuji T, Otsuka F, Roop DR, Harada T, Engel JD, Yamamoto M (2003) Keap1-null mutation leads to postnatal lethality due to constitutive Nrf2 activation. *Nat Genet* 35:238–245
- Wheeler GL, Quinn KA, Perrone G, Dawes IW, Grant CM (2002) Glutathione regulates the expression of gamma-glutamylcysteine synthetase via the Met4 transcription factor. *Mol Microbiol* 46:545–556
- Wilkinson KD (2000) Ubiquitination and deubiquitination: targeting of proteins for degradation by the proteasome. *Semin Cell Dev Biol* 11:141–148
- Willems AR, Schwab M, Tyers M (2004) A hitchhiker's guide to the cullin ubiquitin ligases: SCF and its kin. *Biochim Biophys Acta* 1695:133–170
- Wu G, Fang YZ, Yang S, Lupton JR, Turner ND (2004) Glutathione metabolism and its implications for health. *J Nutr* 134:489–492
- Yamamoto T, Suzuki T, Kobayashi A, Wakabayashi J, Maher J, Motohashi H, Yamamoto M (2008) Physiological significance of reactive cysteine residues of Keap1 in determining Nrf2 activity. *Mol Cell Biol* 28:2758–2770
- Yen JL, Su NY, Kaiser P (2005) The yeast ubiquitin ligase SCF^{Met30} regulates heavy metal response. *Mol Biol Cell* 16:1872–1882
- Zalups RK, Ahmad S (2003) Molecular handling of cadmium in transporting epithelia. *Toxicol Appl Pharmacol* 186:163–188
- Zhang DD, Hannink M (2003) Distinct cysteine residues in Keap1 are required for Keap1-dependent ubiquitination of Nrf2 and for stabilization of Nrf2 by chemopreventive agents and oxidative stress. *Mol Cell Biol* 23:8137–8151
- Zhang DD, Lo SC, Cross JV, Templeton DJ, Hannink M (2004) Keap1 is a redox-regulated substrate adaptor protein for a Cul3-dependent ubiquitin ligase complex. *Mol Cell Biol* 24:10941–10953

Chapter 14

Metals Induced Disruption of Ubiquitin Proteasome System, Activation of Stress Signaling and Apoptosis

Xiaozhong Yu, Rafael A. Ponce and Elaine M. Faustman

Abstract The ubiquitin proteasomal system (UPS) is a highly conserved cellular pathway that plays an important role in the selective degradation of cellular proteins, helping to regulate a variety of vital cellular functions. Disruption of this system, therefore, can have significant downstream effects on critical cellular functions, impacting susceptibility and development of disease. Our research focuses on the identification and characterization of cellular responses to environmental metal exposure and the relationship to the development of neurodegenerative diseases. Our studies have shown that metals can also disrupt the UPS system and that some of these responses are mediated through key cell stress pathways in a similar fashion to what is seen with model UPS inhibitors. Although the accumulation of high molecular weight polyubiquitinated protein conjugates (HMW-polyUb) induced by metals was similar to what was seen with UPS inhibitor MG132, metals were less effective at inhibiting proteasomal activity, suggesting that the metals disrupt the UPS through an alternate mechanism. Our integrative analysis of genome-wide gene expression and pathway mapping in the mouse embryonic fibroblast cells (MEFs) exposed to cadmium (Cd), methyl mercury (MeHg), and arsenic (AS) demonstrated an induction of oxidative stress, disruption of UPS and cell cycle regulation. Cd and MeHg treatment in MEFs cells induced significant alteration of UPS pathway genes. Our findings strongly support the hypothesis that metal-induced disruption of UPS function results in changes in critical cellular mechanisms such as cell cycle regulation and apoptosis. This disruption has a significant implication for the potential development and susceptibility of neurodegenerative disease.

E. M. Faustman (✉) · X. Yu
Department of Environmental Health, University of Washington
4225 Roosevelt Way NE, Suite 100, Seattle, WA 98105, USA
Fax: +1-206-685-4696
e-mail: faustman@uw.edu

Introduction

The Ubiquitin Proteasome System (UPS)

Protein degradation is a critical regulatory process that allows cells to rapidly respond to intracellular signals and changing environmental conditions by adjusting the levels of key effector proteins. The major proteolytic pathway in plants and animals is the ubiquitin proteasome pathway (UPS). This highly conserved system plays a major role in selective cellular protein degradation and regulates various cellular events within eukaryotic cells. It is a critical part of the cellular mechanism for protein catabolism and has roles in both housekeeping and the turnover of many regulatory proteins involved in DNA repair, cell cycle control, oncogenesis, antigen processing, transcription, neural and muscular degeneration, cellular differentiation, stress response and apoptosis as illustrated in Fig. 14.1 (Pines 1994; Morgan 1995; Murray 1995; Seufert et al. 1995; Lukas et al. 1999; Tomoda et al. 1999; Schulman et al. 2000; Hara et al. 2001; Yew 2001). The UPS consists of several components that act in concert in post-translational modification of proteins in these cellular pathways (Fig. 14.1) (Pines 1994; Morgan 1995; Murray 1995; Seufert et al. 1995; Lukas et al. 1999; Tomoda et al. 1999; Schulman et al. 2000; Hara et al. 2001; Yew 2001). Proteins degraded by the UPS are first covalently tagged with a molecule of ubiquitin (Ub), a highly conserved 76 amino acid protein found in all eukaryote cells (Wilkinson 1995). This conjugation involves three sequential enzymatic reactions (E1, E2 and E3). A polyubiquitin chain is then elaborated on the protein through the ligation of additional monomers of Ub in successive rounds of ubiquitination. Substrate proteins linked to polyubiquitin chains are recognized for proteolytic degradation by the proteasome. Ubiquitination of targeted substrates is a reversible process and is regulated by deubiquitination (DUB) enzymes (Wilkinson 1997; Kim et al. 2003; Wing 2003). DUB enzymes may “edit” the number of Ub moieties in the polyubiquitin chain of poorly or erroneously ubiquitinated proteins or generate free Ub from polyUb chains released after proteasomal activity. DUBs play several important roles by affecting the stability of ubiquitin-conjugated proteins and maintaining the steady-state levels of free ubiquitin (Wilkinson 1997; Kim et al. 2003; Wing 2003).

Conserved across evolution from yeast to man, eukaryotic ubiquitins share an identical sequence, is a stringent evolutionary conserved pathway across species (Ozkaynak et al. 1984; Wilkinson 1997, 2004; Wilkinson et al. 2005). Although absent in most prokaryotes including *Escherichia coli*, ubiquitin has been identified in all eukaryotes. This stringent evolutionary conservation of ubiquitin underscores the fundamental importance of the ubiquitin-proteasome pathway in basic cellular physiology. The UPS pathway in *Saccharomyces cerevisiae*, *Schizosaccharomyces pombe*, *Caenorhabditis elegans* and human has been initially compiled in the KEGG pathway database (<http://www.genome.jp/kegg/pathway/ko/ko04120.html>) and the Ortholog table of this UPS across species has been mapped (<http://www.genome.jp/kegg/ortholog/tab04120.html>). Based on updated research reports on this UPS pathway, we have further modified the above pathways for mice and

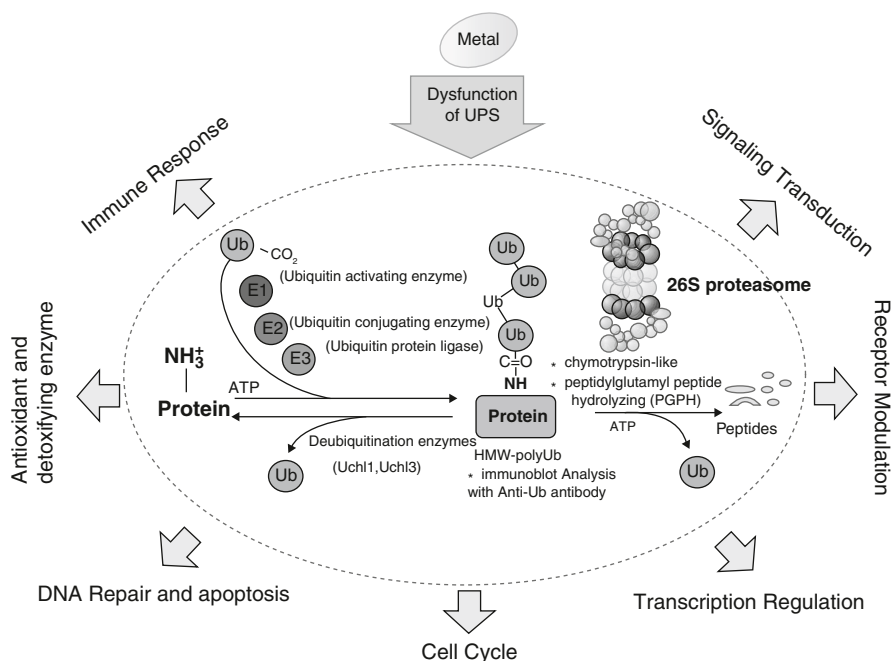


Fig. 14.1 Ubiquitin Proteasome System (UPS) and hypothesized molecular mechanism of metal-induced toxicity. This figure illustrates the complex components of the UPS. The center of this figure illustrates the UPS pathway where a ubiquitin-activating enzyme (E1) uses ATP to form a thioester bond between itself and ubiquitin (Ub) and it then transfers the activated Ub to a ubiquitin-conjugating enzyme (E2). Protein-ubiquitin ligation often requires the participation of a third component termed ubiquitin ligase (E3). Substrate proteins linked to polyUb chains are recognized for proteolytic degradation by the proteasome and recycling of Ub monomers by deubiquitination (DUB) enzymes. The complexity of this pathway implies multiple steps can be involved in the alteration of this pathway. In addition, this figure also shows two main approaches used to monitor the function of UPS (*). In summary, the UPS is the principal cellular mechanism for protein catabolism and alterations in this overall protein processing system have been shown to have serious impacts on many critical physiological systems. It represents a common hypothesized mechanistic pathway for explaining metal-induced neurotoxicity. (Figure is modified from Faustman et al. 2005)

human as illustrated in Fig. 14.1 for the pathway mapping of microarray data. The rapid degradation of numerous transcriptional regulators is essential for most signal transduction processes and responses to environmental cues. The selective and programmed degradation of cell-cycle regulatory proteins, such as cyclins, inhibitors of cyclin-dependent kinases, and anaphase inhibitors are essential rate controlling events in cell-cycle progression (Morgan 1995; Murray 1995; Lukas et al. 1999; Tomoda et al. 1999; Hara et al. 2001; Yew 2001). Impact to the UPS, therefore, can have far reaching effects on cellular processes. Inhibition of the proteasome can result in the accumulation of high molecular weight polyubiquitinated protein conjugates (HMW polyUb) of key regulatory proteins. The accumulation can lead to the induction of apoptosis (Blagosklonny et al. 1996; Maki et al. 1996; Michael

and Oren 2003). For example, the inhibition of the UPS with proteasomal inhibitors such as lactacystin and MG132, has been associated with accumulation of HMW-polyUb and subsequent apoptosis (Pasquini et al. 2000; Tenev et al. 2001; Meller et al. 2006).

UPS and Neurodegenerative Disease

There are strong indications that an altered UPS systems has a role in the development of neurodegenerative disorders (Wilkinson 2000). Several lines of evidence have suggested that defects in the UPS and protein processing underlie pathology in both familial and sporadic forms of the Parkinson's Disease (PD) (Leroy et al. 1998a, b). In support of this concept, mutations in α -synuclein that cause the protein to misfold and resist proteasomal degradation can cause familial PD (Ancolio et al. 2000; Marx et al. 2003). Similarly, mutations in two enzymes involved in the normal function of the UPS, parkin and Ub C-terminal hydrolase L1 (Uchl1) are also associated with hereditary PD (Wintermeyer et al. 2000; Burke 2004). Furthermore, structural and functional defects in 26/20S proteasome that are associated with the accumulation and aggregation of potentially cytotoxic abnormal proteins have also been identified in the patients with sporadic PD (Furukawa et al. 2002; McNaught et al. 2002). Thus, a defect in protein processing appears to be a common factor in sporadic and various familial forms of PD. This common mechanism can also account for the vulnerability in PD, why the disorder is age related (Dawson and Dawson 2003). A study using advance proteomic approach demonstrated that the protein level of Uchl1 is down-regulated in idiopathic PD as well as Alzheimer Disease (AD) brains (Choi et al. 2004). In addition, Barrachina et al. found that reduced Uchl1 expression was a contributory factor to the development of abnormal protein aggregation in dementia with Lewy bodies (DLB), and suggested Uchl1 as a putative therapeutic target in the treatment of dementia with DLB (Barrachina et al. 2006). Uchl1 is a member of a gene family whose products hydrolyze small C-terminal adducts of ubiquitin to generate the ubiquitin monomer. It is highly conserved across species (Fig. 14.2) and is predominantly expressed within neurons and testicular tissue (Doran et al. 1983; Mochida et al. 2004; Kwon et al. 2005). The Uchl1 enzyme was first defined in the context of familial and sporadic forms of the PD where it plays a pathological role in the formation of inclusions (Wintermeyer et al. 2000; Chung et al. 2003; Maraganore et al. 2004). A significant inverse association of the Uchl1 S18Y polymorphism with PD overall and in several strata has been observed, confirming its role as a susceptibility gene for PD (Maraganore et al. 2004; Facheris et al. 2005). Liu et al. found that within cultured cells Uchl1, especially variants linked to higher susceptibility to Parkinson disease, caused the accumulation of α -synuclein (Liu et al. 2002). Search on NCBI SNP found that more than 52 Uchl1 associated SNPs have been reported in humans (NCBI 2004). However, the functional significance of these SNPs has not been evaluated, and the relationship between these Uchl1 variants and susceptibility to metal-induced ad-

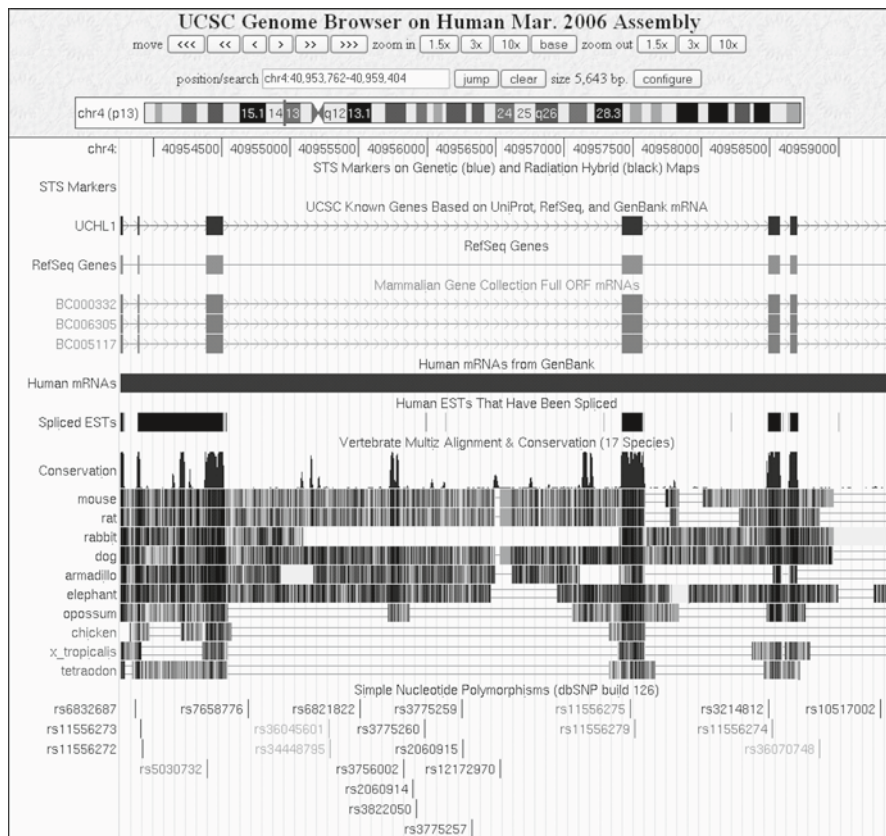


Fig. 14.2 Human Uchl1 gene and across species conservation. Uchl1 is located in human chromosome 4, and highly conserved across species, suggesting its critical role in ubiquitin dependent proteolysis. Expression of Uchl1 is highly specific to neurons and testicular tissue. Uchl1 is likely to play a pathological role in inclusion formation in Parkinson’s disease (PD) as well as Alzheimer (AD) disease. About 52 polymorphisms were found in human and Uchl1 S18Y polymorphism has been link to the development of PD. (Figure was generated using UCSC Genome browse <<http://genome.ucsc.edu/>> at March, 2006)

verse effects will provide valuable information on its role in the iteration of genetic gene and environmental exposure in ND development.

Environmental Metals Exposure and Neurodegenerative Disease

Environmental and occupational exposures to metals such as methyl mercury (MeHg) and cadmium (Cd) and arsenic (As) pose significant health risks to humans (EPA 2004). There is increasing evidence in a number of neurodegenerative diseases such as PD that metal-mediated abnormalities play a crucial role in disease

pathogenesis (Gorell et al. 1999; Carpenter 2001; Uversky et al. 2001; Levenson 2003; Powers et al. 2003). Heavy metals can exert their adverse effects through acute neurotoxicity or through slow accumulation during prolonged periods of life. Neurochemical, clinical and epidemiological studies have implicated several metals including iron, copper, manganese, lead, mercury, aluminum and zinc (Checkoway and Nelson 1999; Powers et al. 2003). Although still somewhat controversial, many epidemiological studies have established an association between increased risk for neurodegenerative diseases (ND) and exposure to metals and pesticides (Okuda et al. 1997; Carpenter 2001; Weiss et al. 2002). Developmental exposure of rats to the xenobiotic metal lead (Pb) resulted in a delayed over-expression of the amyloid precursor protein (APP) (Basha et al. 2005a, b). These data suggest that environmental influences occurring during brain development predetermine the expression and regulation of APP later in life, potentially influencing the course of amyloidogenesis, and argue for both an environmental trigger and a developmental origin of NDs.

The combination of the human health implications, the pervasiveness in the environment and the ability to bioaccumulate, has led to an increased concern about heavy metal exposures. In addition, while the effects of acute exposures are well known, the toxicity of many of these metals following chronic low level exposure are still being defined and characterized. MeHg is an environmental pollutant that acts as a neurotoxicant in humans, other primates, and rodents, and the developing central nervous system (CNS) is an important target of its toxicity (Clarkson 1987; Burbacher et al. 1990). While the lowest exposures that result in clinical manifestation of MeHg poisoning (paresthesia) are associated with MeHg concentrations in blood of 200 ppb, subtle neurodevelopmental deficits have been associated with human *in utero* MeHg exposure at lower concentrations (McKeown-Eyssen and Ruedy 1983; McKeown-Eyssen et al. 1990). As a result of an international ban on the use of mercurials as pesticides in the early 1970s, MeHg exposure in humans now occurs primarily through the consumption of fish and other marine species. Thus, populations that consume large amounts of these species are generally at greatest risk of adverse health (Mottet et al. 1985; Tollefson and Cordle 1986; Faustman et al. 2002). Cd is considered to be nephrotoxic and neurotoxic (Chang and Huang 1996) and has been classified as a human carcinogen by IARC (07/23/02). It is a ubiquitous contaminant, entering the environment through a number of sources including batteries, pigments, plastics, mining, smelting and cigarette smoke (Beyersmann and Hechtenberg 1997). Cadmium has an extensive biological half-life (>20 years) and can exhibit toxic insult on numerous tissues including the central nervous system (Goering et al. 1993, 2000). In addition, childhood exposure to Pb, even at relatively low levels (Canfield et al. 2003), results in a decline of cognitive function that persists into adulthood and that manifests as a continual lowering of IQ score plus alteration in behavior (Needleman et al. 1990). Each increase of 10 $\mu\text{g}/\text{dL}$ in the lifetime average blood lead concentration was found to be associated with a 4.6-point decrease in IQ (Schwartz et al. 2000). There appears to be no minimum threshold level below which lead does not cause brain injury (Canfield et al. 2003). Elevated lead levels in childhood have been associated with lower class standing in high school, lower vocabulary and grammatical-reasoning

scores, poorer hand-eye coordination, and self-reports of minor delinquent activity (Needleman et al. 1990).

Our lab has many years of experience investigating the molecular mechanism of metals induced effects on neurotoxicity, with an emphasis on the molecular mechanism associated with the cell proliferation, differentiation and cell cycle regulation (Ponce et al. 1994, 2001; Ou et al. 1999b; Miura et al. 1999; Faustman et al. 2002; Lewandowski et al. 2002, 2003a, b; Mendoza et al. 2002; Qu et al. 2003; Gribble et al. 2005; Sidhu et al. 2006). Our previous experiments found that within primary rodent embryonic neuronal cell (PNC) cultures, MeHg exposure lead to a time- and concentration-dependent inhibition of cell cycle progression and subsequent cell death (Ponce et al. 1994). The observed cell cycle arrest induced by MeHg was found to be associated with the altered expression of cell cycle regulatory genes Gadd 45, Gadd 153, p21 and p53 (Ou et al. 1997). Our studies with transgenic models also further demonstrated that MeHg's effects are dependent upon p21 and p53 genotype (Ou et al. 1999a; Gribble et al. 2003, 2005). These data are consistent with a hypothesis that altered expression of cell cycle regulatory genes contributes to the observed inhibition of cell proliferation, a mode of action for the selective effects on neurogenesis upon MeHg exposure. The objectives of our recent studies are to clarify the role of the UPS in cellular response to heavy metals and to identify the critical pathways that might influence susceptibility to the development of neurodegenerative diseases.

Results and Discussion

Recent studies highlight the critical role of the UPS in modulating metal-induced toxicity (Figueiredo-Pereira et al. 1998; Figueiredo-Pereira and Cohen 1999; Chen et al. 2002; Kirkpatrick et al. 2003; Stewart et al. 2003). By screening a yeast genomic DNA library, the over-expression of the ubiquitin-protein ligase CDC34 (E3) increased the cellular ubiquitinated protein levels and exhibited significant resistance to MeHg toxicity both in yeast and human cells (Furuchi et al. 2002; Hwang et al. 2002). The ubiquitinated conjugating activity of CDC34 is essential for the CDC34-mediated resistance to MeHg. This report suggested that MeHg induces the cellular accumulation of certain proteins that cause cell damage and that CDC34 is degraded after its ubiquitination in the proteasome (Furuchi et al. 2002; Hwang et al. 2002, 2005; Naganuma et al. 2002). The involvement of the UPS and HMW-polyUb accumulation has been linked to the cellular oxidative stress response in Cd-mediated toxicity (Figueiredo-Pereira et al. 1997). Other metals such as cobalt and arsenic have also been linked with the proteasomal inhibition, the accumulation of HMW-polyUb and subsequent apoptosis further implicating the UPS in metal-mediated toxicity. Additional studies have demonstrated that defects in the UPS sensitized cells to Cd-mediated impacts (Tsirigotis et al. 2001) and mutants in specific ubiquitin-conjugating enzymes are hypersensitive to Cd (Jungmann et al. 1993; Wagenknecht et al. 1999).

Our recent studies have shown that metals can also disrupt the UPS system and that some of these responses are mediated through key cell stress pathways in a similar fashion to what is seen with model UPS inhibitor MG132 (Faustman et al. 2005; Yu et al. 2008, 2010, 2011a, b). It has been demonstrated that a dysfunctional proteasome results in the accumulation of HMW-polyUb, which in turn leads to subsequent aberrant events (Orlowski 1999; Chen et al. 2000; Qui et al. 2000; Rideout et al. 2003). Inhibitions of the proteasome, as observed with the classic inhibitors lactacystin (Lac) and MG132, have been associated with alterations to the cell cycle, the activation of caspase-3, and the resulting induction of apoptosis (Pasquini et al. 2000). As shown in Fig. 14.1, the UPS pathway is complex and disruption can occur anywhere along the path. The final outcome of UPS disruption, however, is the same: an increase in HMW-polyUb. Proteasomal inhibition has been reported as the principal target in the disruption of UPS function. Several proteasome-specific protease inhibitors have been essential as model chemicals to investigate the UPS-dependent degradation pathway and the biological processes dependent on it (Wu et al. 2002; Zhang et al. 2002). In our previous studies, we selected MG132 and lactacystin, 26S proteasome-specific protease inhibitors, as model chemicals to serve as a comparison with metals. This methodology allowed us to test our hypothesis that the disruption of the UPS pathway is an important mechanism in metal-induced toxicity. To test this hypothesis, we investigated whether metal exposure increase the accumulation of HMW-polyUb, whether this metal-induced HMW-polyUb accumulation was related to the induction of cell stress signaling proteins and overall cytotoxicity and cell cycle arrest (Faustman et al. 2005). We treated cultures of MEFs with increasing concentrations of either Cd^{2+} (0.5–20 μM), MeHg (0.5–4 μM) or As^{3+} (0.5–20 μM). In order to further explore the relationship between the activation of the stress signaling pathway and the accumulation of HMW-polyUb, anisomycin (Anis), a classical inducer of chemical stress, was also included.

MeHg, Cd^{2+} , and As^{3+} Induced Alteration of the Proteasome Activity

Theoretically, steady-state levels of HMW-polyUb can be influenced by the rate of conjugation and the rate of ubiquitination loss, either through degradation by the proteasome or deubiquitination by isopeptidase. In order to clarify whether the inhibition of the proteasomal activity by the metals was the main mechanism leading to the accumulation of HMW-polyUb proteins, we measured two different proteasome activities as previously reported (Canu et al. 2000; Bobba et al. 2002; Rodgers and Dean 2003). Proteasomal activities included peptidylglutamyl peptide-hydrolyzing (PGPH) and chymotrypsin-like were measured after MeHg, Cd^{2+} and As^{3+} treatments (24 h) using the fluorogenic substrates Z-Leu-Leu-Glu-AMC or Suc-Leu-Leu-Val-Tyr-AMC. A dose-dependent inhibition of PGPH and chymotrypsin activities were observed following Cd^{2+} treatment with the maximum effect observed at

20 μM . MeHg treatment (2.5 μM) resulted in a limited induction of PGPH activity and a significant inhibition of chymotrypsin activity. Only seen at the highest concentration of 20 μM , As^{3+} treatment induced significant changes on both PGPH and chymotrypsin activity. MG132 and Lac significantly inhibited the chymotrypsin-like activity of the proteasome throughout the 24 h treatment, but exerted only marginal effects on the inhibition of PGPH activity. This initial observation suggests that at relatively high concentrations, the inhibition of the proteasomal activity by metals may contribute to the accumulation of HMW-polyUb, a response not significant at the low exposure levels. Since the proteasome has complex components, the limited measurement of just two kinds of activities cannot rule out the possibility of the effect of the metals on the other subunits of the proteasome.

MeHg, Cd^{2+} , and As^{3+} Induced Accumulation of HMW-polyUb

We measured the changes of HMW-polyUb by Western blot analysis after metals treatments (Sidhu et al. 2003; Faustman et al. 2005; Yu et al. 2011a, b). The representative Western blot images are shown in Fig. 14.3. Metal exposures induced accumulation of HMW-polyUb as observed with proteasome inhibitor MG132 and Lac. Cd^{2+} exposure resulted in a concentration-dependent accumulation of HMW-polyUb and significant at concentration above 5 μM Cd^{2+} (Fig. 14.3a). The maximal response was observed at a Cd^{2+} concentration of 10 μM , with attenuation evident at 20 μM , likely due to increased cytotoxicity. Cd^{2+} -associated accumulation of HMW-polyUb conjugates was qualitatively similar to the two proteasomal inhibitors, MG 132 and Lac (Fig. 14.3d), at concentrations associated with initial toxicological significance. Two prototypic inhibitors of proteasomal function, MG132 and lactacystin, induced significant accumulation of HMW-polyUb conjugates in MEFs (Fig. 14.3d). Aisomycin, a stress inducer, did not induce the accumulation of HMW-polyUb (Fig. 14.3d). These results demonstrated that Cd^{2+} treatment disrupts the UPS function, and that the accumulation of HMW-polyUb by Cd^{2+} seems to occur just below significant cellular toxicity. We found that MeHg exposure resulted in dose-dependent cytotoxicity and accumulation of HMW-polyUb conjugates was observed at a concentration of 0.5 μM (Fig. 14.3b), a concentration that did not cause a significant change in cytotoxicity. In contrast to Cd^{2+} and MeHg exposure (Fig. 14.3c), the increase in HMW-polyUb seen with As^{3+} exposure was limited to concentrations where significant cytotoxicity was observed (20 μM , 20% cell viability).

MeHg, Cd^{2+} , and As^{3+} Induced Activation of MAPK Signaling

Mitogen-activated protein kinases (MAPK) are a family of serine/threonine protein kinases that are involved in many cellular pathways such as cell proliferation, cell

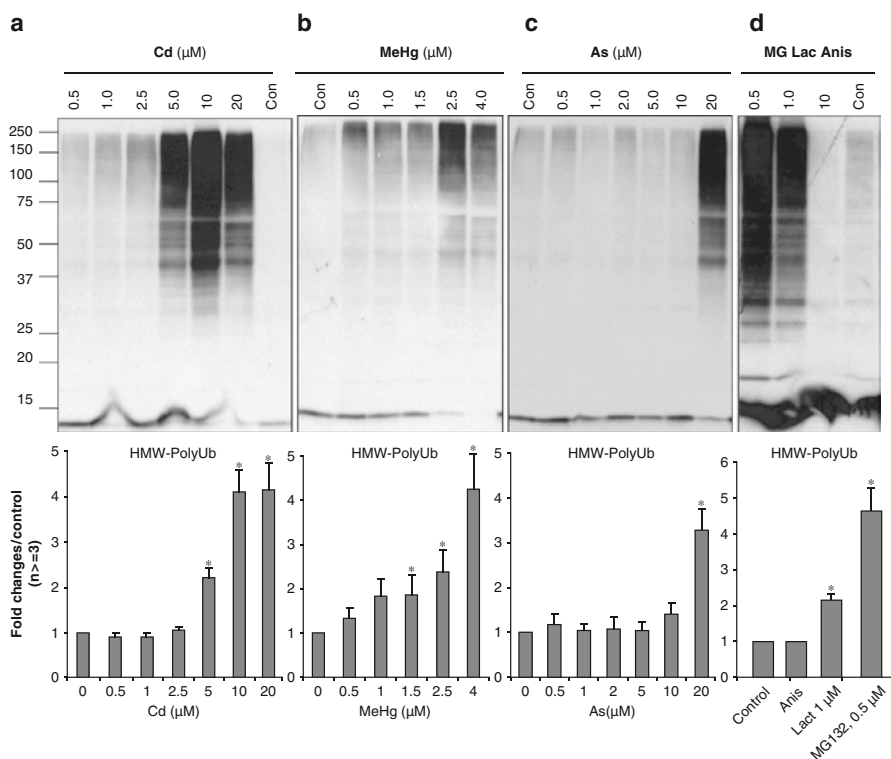


Fig. 14.3 Metal induced accumulation of high molecular weight ubiquitinated proteins (HMW-polyUb) 24 h after treatment with cadmium (Cd, **a**), methyl mercury (MeHg, **b**) and arsenic (As, **c**) in mouse embryonic fibroblast cells. Proteasome inhibitor MG132 and lactacystin as well as classic stress inducer anisomycin were also included (**d**). Cadmium (Cd, **a**), methyl mercury (MeHg, **b**) induced accumulations of HMW-polyUb in a similar manner as classic proteasomal inhibitors, MG 132 and lactacystin (**d**) while arsenic (**c**, As) only induced HMW-polyUb at high concentration (20 μM). Stress inducer anisomycin did not induce any change of HMW-polyUb. Data presented is the means of at least three independent experiments \pm SD. * $p \leq 0.05$. (Figures 14.3a–c are modified from Yu et al. 2011b; Sidhu et al. 2003; and Faustman et al. 2005, respectively)

differentiation, cell movement and cell death and have also activated in response to cellular stress. Previous studies have demonstrated that the disruption of the UPS, as observed with lactacystin and MG132, leads to significant activation of stress signaling, as well as alterations to other cellular pathways (Lopez Salon et al. 2000; Yang and Yu 2003). In addition, oxidative stress has been implicated in Cd-induced toxicity both *in vivo* or *in vitro* studies (Yang et al. 1997; Dong et al. 1998; Shaikh et al. 1999; Jurczuk et al. 2004). Major subfamilies of MAPKs have been described including extracellular signal-regulated kinase (ERK), c-Jun N-terminal kinase (JNK), and p38. In this study, we further examined whether possible association with the disruption of UPS and MAPK stress signaling (Sidhu et al. 2003; Faustman et al. 2005; Yu et al. 2011a, b). As shown in Fig. 14.4, treatment with Cd resulted in a dose-depen-

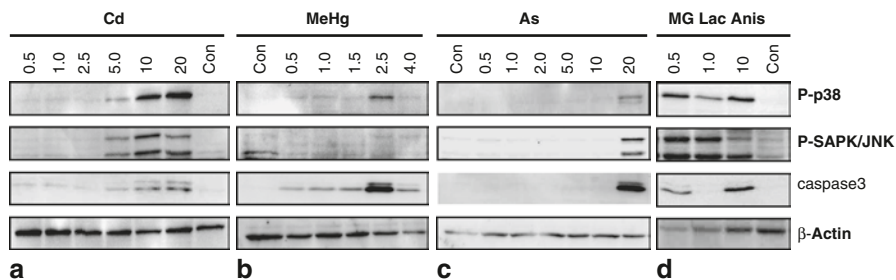


Fig. 14.4 Metal exposures induced alterations in stress signaling and apoptotic pathways. Treatment with cadmium (Cd, **a**), methyl mercury (MeHg, **b**) and arsenic (As, **c**) lasted for 24 h in mouse embryonic fibroblast cells. Proteasome inhibitor MG132 and lactacystin as well as classic stress inducer anisomycin were also included (**d**) Cd exposure resulted in a robust phosphorylation of p38 and SAPK/JNK, evident at a Cd concentration ≥ 5 μM . MeHg induced a dose-dependent modulation of p38 MAPK and caspase 3, significantly from dose of 2.5 μM . In contrast to Cd and MeHg exposure, As exposure caused significant increases in p38, p-SAPK/JNK and cleaved caspase 3 only at concentrations where significant cytotoxicity was observed. The dose dependent stimulation of p38 MAPK and SAPK/JNK phosphorylation induced by Cd and MeHg as well as proteasome inhibitors parallel corresponded to accumulation of HMW-polyUb conjugates. Representative bands from three independent experimental were shown. (Figures 14.4a–c are modified from Yu et al. 2011b; Sidhu et al. 2003; and Faustman et al. 2005, respectively)

dent up-regulation of the phosphorylated forms of SAPK/JNK and p38 (Fig. 14.4a). Significant activation of SAPK was observed at 10 μM Cd (24 h) and significant activation of p38 was observed at the dose of 5 μM , consistently paralleled with the dose dependent increase of caspase 3. This response paralleled the accumulation of HMW-polyUb and induction of apoptosis. The activation of SAPK/JNK and p38 have previously been associated with low-level Cd exposure and subsequent impacts on cell cycle progression and mitotic arrest (Ding and Templeton 2000; Iryo et al. 2000). To date, the relationship between MAPK activation and the accumulation of HMW poly-Ub induced by Cd is unclear. Our study links these two critical responses of Cd-induced toxicity, cellular stress and UPS disruption, as indicated by the accumulation of HMW-polyUb and the parallel activation of stress responses.

We found that MeHg treatment induced significant phosphorylation of cellular stress markers for both p38 and SAPK/JNK, two key intracellular signaling intermediates that are involved in mediating chemical stress (Fig. 14.4b). The stress response of p-p38 and cleaved caspase-3 increased significantly at concentrations of MeHg that were overtly cytotoxic (Fig. 14.4b). AS induced significant activation of p-p38, p-SAPK/JNK and cleaved caspase 3 only at concentration of 20 μM . MG132 (2.5 μM), lactacystin and anisomycin all up-regulated p-SAPK and JNK at the concentration tested. In contrast to metals, we did not observe an accumulation of HMW-polyUb with anisomycin at concentrations associated with its classical stress response effects (i.e. increase of p-p38, p-SAPK, and caspase 3 cleavage) (Fig. 14.4d).

In summary, Cd²⁺ and MeHg induced accumulations of HMW-polyUb in a qualitatively similar manner to the classic proteasomal inhibitors MG132 and Lac. In general, these responses occurred at concentrations that were lower than or paral-

leled what was required to see the activation of stress proteins and apoptosis. Increases in HMW-polyUb and stress responses as a result of As^{3+} exposure were limited to cytotoxic concentrations. Although the non-metal stress inducing agent Anis induced stress and apoptosis, it did not impact the UPS function. This suggests that the UPS might be the primary target of metals with a secondary activation of cellular stress signaling resulting in cell death. Our findings provide a novel mechanistic understanding of metal-induced cytotoxicity especially with the understanding of UPS dysfunction. These observations strongly suggest that exposures to metals such as MeHg and Cd^{2+} could increase cytotoxicity through their effect on the UPS. Because of the complexity of the UPS and its various protein targets, we designed a global gene expression study to identify the gene targets of the UPS affected by metal exposure (Yu et al. 2010).

Integrative Genomic Gene Expression Analysis and Pathway Mapping

Genomic gene expression profiling through microarray technology is a powerful approach to define comprehensive molecular mechanisms after chemical exposure. Furthermore, the integration of the genome-wide array data with knowledge-based pathway mapping facilitates the characterization of the molecular mechanism of metal-induced toxicity. We made significant progress in applying a genomic analysis method for our mechanistic study of metal induced toxicity utilizing the University of Washington's Functional Genomic and Proteomic Facility Cores (NIEHS Center for Ecogenetics and Environmental Health). We conducted gene expression array analysis by using the CodeLink Mouse UniSet 10K oligonucleotide-based platform to explore the gene alterations caused by metals (Yu et al. 2010). In this experiment, the classical proteasome inhibitor, MG132 (0.5 μM), was included to serve as a positive control and to help in the determination of whether the disruption of UPS is a critical mechanism of MeHg-induced toxicity. Furthermore, two additional heavy metals, cadmium (Cd^{2+}) and arsenic (As^{3+}), were included to define common and/or unique mechanisms in their toxicity. We treated MEFs with MeHg (2.5 μM), Cd^{2+} (5.0 μM) and As^{3+} (5.0 μM) for 24 h. Based on results of our previous studies, doses were selected where comparable minimal impacts were observed on stress signaling and apoptotic pathways (Sidhu et al. 2003; Faustman et al. 2005). Following normalization of the array data, we used multi-level analysis tools to explore the data, including group comparisons, cluster analysis, gene ontology analysis, and pathway analysis (GenMAPP) (Dahlquist et al. 2002; Doniger et al. 2003). Using these integrated approaches, we identified significant alterations in gene expression with the UPS pathway (Uchl1 and Ube2c), cell cycle regulation pathways (Cyclin B1 and Cdc25c), and antioxidant and phase II enzymes (Gsta2, Gsta4, and Noq1) with the metals and the proteasomal inhibitor, MG132 (Dahlquist et al. 2002; Doniger et al. 2003).

We initially applied two dimensional hierarchical clustering analysis organized by gene and treatment to identify genes that share common patterns of expression

across metal treatments (Yu et al. 2010). The gene expression pattern of 1,254 genes whose average intensities varied ≥ 2 -fold over control in at least one treatment and had a $p \leq 0.001$ (ANOVA) were included in this analysis. We found each treatment forms a distinctive gene expression patterns in response to each treatment. This analysis highlights common gene targets and similar changes in their expression between the metals and the classic proteasomal inhibitor. The array analysis determined that all three metals, in addition to MG132, induced significant impacts on specific gene clusters that include: (1) modulators of UPS functions such as deubiquitination (DUB) enzyme (Uchl1) and Ub conjugating enzyme (Ube2C), (2) antioxidant and phase II detoxifying enzyme genes such as glutathione S-transferase Gsta2, Gsta3, Gsta4, NADPH dehydrogenase quinone 1 (Noq1), and (3) cell cycle regulators such as cyclin B2, Cyclin A2, Cdc20, Cdkn3, Cdc20c, Nek2, Cdc3 and Cdc1. These findings are supportive of our hypothesis that the alteration of the UPS leads to changes in the degradation of key cell cycle regulators. Results from our cluster analysis suggest that the induction of genes in the antioxidant and detoxifying pathway, in combination with the disruption of genes involved in the UPS pathway, may be a critical and common mechanism in metal and MG132 induced cell cycle changes.

Interruptions of UPS Pathway

Function and pathway analysis is integral for evaluating microarray data in a biological context. To systematically examine the effects of metals as well as the proteasome inhibitor MG132 on cellular processes, we used GenMAPP and MAP-PFinder software packages to elucidate and visualize the effect of different metals on biological pathways (Yu et al. 2010). Gene Ontology analysis showed significant changes in the following important biological pathways including UPS, cell cycle regulation pathway, and antioxidant and phase II enzymes pathway. Figure 14.5 shows the effect of MG132, MeHg, As³⁺ and Cd²⁺, after 24 h exposure on the transcriptional response in genes within the UPS pathway. Both common and unique gene targets were observed across treatments. MG132, induced significant activation of proteasomal subunits of the 20S catalytic core and the 19s (PA700) regulatory complex (Fig. 14.5a). We observed up-regulation of deubiquitination enzymes Uchl1, Ufd1l and Usp14. Uchl1 plays a critical role in deubiquitination, reported to be implicated in PD and AD (Maraganore et al. 2004). Multiple Ub-protein ligases (E3), which recognize degradation motif on specific substrates and catalyze the transfer the Ub from E2 to target, were both up-regulated (Nedd4l, Fbxo6b, Skp1a, Skp2, Mdm2, ubr1, Rnf11) or down-regulated (Fbxl12, Siah1b, Siah2 and Lnx1). This suggests that a number of protein targets have been impacted by the treatment of MG132. For example, Mdm2 is critical for p53 stabilization (Li et al. 2002a, b). In Fig. 14.5b, MeHg induced significant activation of seven proteasome subunits of the 20S catalytic core and three subunits of the 19s (PA700) regulatory complex. MeHg also induced up-regulation of deubiquitination enzymes, Uchl1, USP38

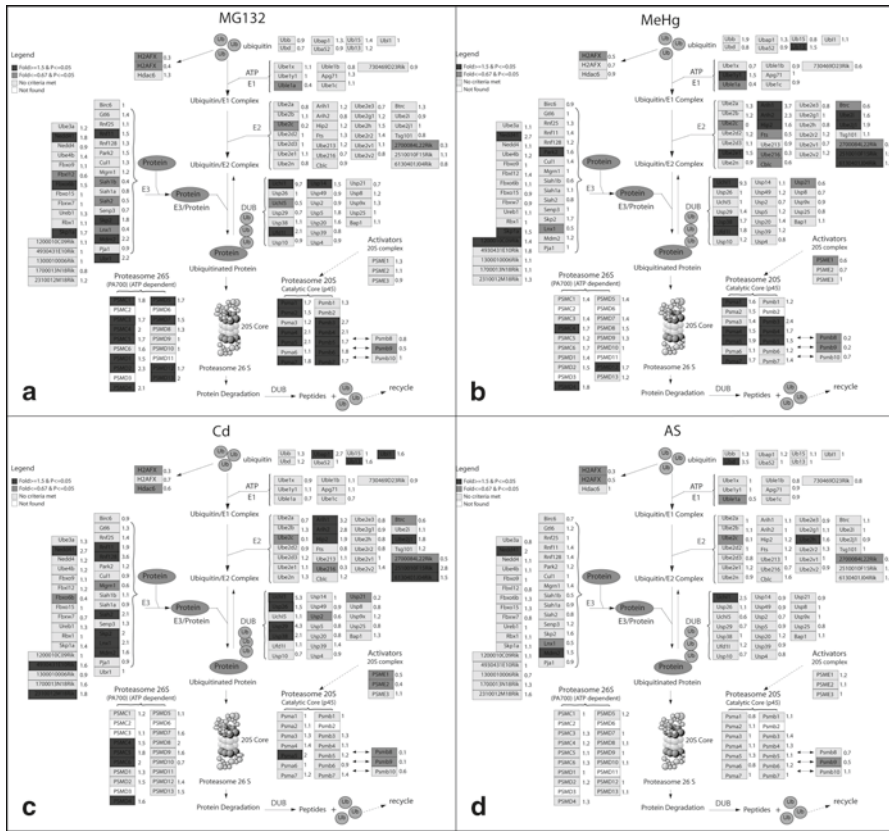


Fig. 14.5 Ubiquitin-proteasome pathway (UPS) in response to metals in treated mouse embryonic fibroblast cells. A knowledge based UPS pathway was built in GenMAPP program. Differential gene expression was based on treatment versus control expression change (1.5-fold and $p \leq 0.05$, t test). The comparison of the UPS pathway mapping among metals methyl mercury (MeHg, **b**), cadmium (Cd, **c**), and arsenic (As, **d**) and proteasome inhibitor MG132 (**a**) revealed both common and unique targets on the UPS in the MEF. Cd, MeHg and MG132 treatment in MEF cells induced significant up-regulation of proteasome regulatory complex 19s (PA700) and deubiquitination enzyme genes Uch11 and significant down-regulation of ubiquitin conjugating enzyme Ube2C, 2700084L22Rik. The comparison of the gene expression between the metals and proteasome inhibitor MG132 revealed both common and unique targets on the UPS and suggested the novel potential mechanism of metal induced toxicity. (Figures 14.5a–c are from Yu et al. 2010 and figure 14.5d is modified from Faustman et al. 2007)

and Ufd11, and also Ub E3 enzymes such as Nedd41, Skp1a, 4930431E10Rik, and Park2. In Fig. 14.5c, Cd^{2+} treatment in MEFs induced significant up-regulation of four subunits of the 19s (PA700) proteasome regulatory complex. Cd^{2+} also induced an increase in transcription of deubiquitination enzymes (Uch11, Usp29, Usp26 and Usp38) and Ub conjugating enzymes (Arlh1, Arih2, Hip2, Ube2j1, 2510010F15Rik, and 6130401J04Rik). Cd^{2+} also induced an increase in E3 enzymes such as Nedd41, 4930431E10Rik, 2310012M18Rik, Rnf11, Rnf128, Siah2,

Skp2, Mdm2 and Lnx1. In Fig. 14.5d, As³⁺ induced less impact on UPS pathway as compared with Cd²⁺, MeHg and MG132 did not show any significant impact on the proteasome subunits. As³⁺ did, however, significantly up-regulate DUB enzymes Uchl1, but to a lesser extent as compared to other metal treatments. It also significantly suppressed the E2 enzymes Ube2c and 2700084L22Rik, which were similar to the Cd²⁺, MeHg and MG132. Significant up-regulation of E3 enzymes such as Nedd4l, 2310012M18Rik, and Mdm2 were observed.

The comparison of resulting alterations in gene expression between these metals and the proteasomal inhibitor MG132 revealed both common and unique targets on the UPS in MEFs. These results strongly support our hypothesis that disruption of the UPS function is involved in metal-induced adverse effects, and demonstrate potential gene targets in this pathway. NDs have been reported to be associated with accumulation of ubiquitinated proteins in neuronal inclusions and also with signs of impairment of the UPS pathway that may contribute to this neurodegenerative process (Powers et al. 2003).

Conclusions

The overall objective of our studies is to examine the interaction between environmental metal exposure and disease development and susceptibility to identify critical mechanisms that facilitate neurodegenerative effects. The ubiquitin proteasomal system (UPS) is a highly conserved cellular pathway that plays an important role in the selective degradation of cellular proteins, helping to regulate a variety of vital cellular functions. Disruption of this system, therefore, can have significant downstream effects on critical cellular functions, impacting susceptibility and development of disease. Our research focuses on the identification and characterization of cellular responses to environmental metal exposure and the relationship to the development of neurodegenerative diseases. Our studies have shown that metals can also disrupt the UPS system and that some of these responses are mediated through key cell stress pathways in a similar fashion to what is seen with model UPS inhibitors. Although the accumulation of high molecular weight polyubiquitinated protein conjugates (HMW-polyUb) induced by metals was similar to what was seen with UPS inhibitor MG132, metals were less effective at inhibiting proteasomal activity, suggesting that the metals disrupt the UPS through an alternate mechanism. Our integrative analysis of genome-wide gene expression and pathway mapping in the mouse embryonic fibroblast cells (MEFs) exposed to cadmium (Cd), methyl mercury (MeHg), and arsenic (As) demonstrated an induction of oxidative stress, disruption of UPS and cell cycle regulation. Cd and MeHg treatment in MEFs cells induced significant alteration of UPS pathway genes. Our findings strongly support the hypothesis that metal-induced disruption of UPS function results in changes in critical cellular mechanisms such as cell cycle regulation and apoptosis. This disruption has a significant implication for the potential development and susceptibility of neurodegenerative disease.

Acknowledgements This work was supported in part by the National Institute of Environmental Health Sciences (NIEHS), the Environmental Protection Agency (EPA), and the National Science Foundation (NSF) through the following grants: Toxicogenomics (NIEHS: U10 ES 11387 and R01-ES10613) the Center for Children's Environmental Health Risks Research (NIEHS: 5-P01-ES009601 and EPA: RD-83170901), the Pacific Northwest Center for Human Health and Ocean Sciences (NIH/NIEHS: P50 ES012762 and NSF: OCE-0434087 and OCE-0910624) and the UW NIEHS Center for Ecogenetics and Environmental Health (NIEHS: 5 P30 ES07033). Its contents are solely the responsibility of the authors and do not necessarily represent the official views of the NIEHS, NIH, NSF or EPA.

References

- Ancolio K, Alves da Costa C, Ueda K, Checler F (2000) Alpha-synuclein and the Parkinson's disease-related mutant Ala53Thr-alpha-synuclein do not undergo proteasomal degradation in HEK293 and neuronal cells. *Neurosci Lett* 285:79–82
- Barrachina M, Castano E, Dalfó E, Maes T, Buesa C, Ferrer I (2006) Reduced ubiquitin C-terminal hydrolase-1 expression levels in dementia with Lewy bodies. *Neurobiol Dis* 22:265–273
- Basha MR, Murali M, Siddiqi HK, Ghosal K, Siddiqi OK, Lashuel HA, Ge YW, Lahiri DK, Zawia NH (2005a) Lead (Pb) exposure and its effect on APP proteolysis and Abeta aggregation. *Faseb J* 19:2083–2084
- Basha MR, Wei W, Bakheet SA, Benitez N, Siddiqi HK, Ge YW, Lahiri DK, Zawia NH (2005b) The fetal basis of amyloidogenesis: exposure to lead and latent overexpression of amyloid precursor protein and beta-amyloid in the aging brain. *J Neurosci* 25:823–829
- Beyersmann D, Hechtenberg S (1997) Cadmium, gene regulation, and cellular signalling in mammalian cells. *Toxicol Appl Pharmacol* 144:247–261
- Blagosklonny M, Sheng G, Omura S, El-Deiry W (1996) Proteasome-dependent regulation of p21 WAF1/CIP1 expression. *Biochem Biophys Res Commun* 227:564–569
- Bobba A, Canu N, Atlante A, Petragallo V, Calissano P, Marra E (2002) Proteasome inhibitors prevent cytochrome c release during apoptosis but not in excitotoxic death of cerebellar granule neurons. *FEBS Lett* 515:8–12
- Burbacher TM, Rodier PM, Weiss B (1990) Methylmercury developmental neurotoxicity: a comparison of effects in humans and animals. *Neurotoxicol Teratol* 12:191–202
- Burke RE (2004) Recent advances in research on Parkinson disease: synuclein and parkin. *Neurologist* 10:75–81
- Canfield RL, Kreher DA, Cornwell C, Henderson CR Jr (2003) Low-level lead exposure, executive functioning, and learning in early childhood. *Child Neuropsychol* 9:35–53
- Canu N, Barbato C, Ciotti MT, Serafino A, Dus L, Calissano P (2000) Proteasome involvement and accumulation of ubiquitinated proteins in cerebellar granule neurons undergoing apoptosis. *J Neurosci* 20:589–599
- Carpenter DO (2001) Effects of metals on the nervous system of humans and animals. *Int J Occup Med Environ Health* 14:209–218
- Chang CC, Huang PC (1996) Semi-empirical simulation of Zn/Cd binding site preference in the metal binding domains of mammalian metallothionein. *Protein Eng* 9:1165–1172
- Checkoway H, Nelson LM (1999) Epidemiologic approaches to the study of Parkinson's disease etiology. *Epidemiology* 10:327–336
- Chen F, Chang D, Goh M, Klibanov S, Ljungman M (2000) Role of p53 in cell cycle regulation and apoptosis following exposure to proteasome inhibitors. *Cell Growth Differ* 11:239–246
- Chen F, Zhang Z, Bower J, Lu Y, Leonard S, Ding M, Castranova V, Piwnicka-Worms H, Shi X (2002) Arsenite-induced cdc25c degradation is through the KEN-box and ubiquitin-proteasome pathway. *PNAS* 99:1990–1995
- Choi J, Levey AI, Weintraub ST, Rees HD, Gearing M, Chin LS, Li L (2004) Oxidative modifications and down-regulation of ubiquitin carboxyl-terminal hydrolase L1 associated with idiopathic Parkinson's and Alzheimer's diseases. *J Biol Chem* 279:13256–13264

- Chung KK, Dawson VL, Dawson TM (2003) New insights into Parkinson's disease. *J Neuro* 250(Suppl 3):III15–III24
- Clarkson TW (1987) Metal toxicity in the central nervous system. *Environ Health Perspect* 75:59–64
- Dahlquist KD, Salomonis N, Vranizan K, Lawlor SC, Conklin BR (2002) GenMAPP, a new tool for viewing and analyzing microarray data on biological pathways. *Nat Genet* 31:19–20
- Dawson TM, Dawson VL (2003) Molecular pathways of neurodegeneration in Parkinson's disease. *Science* 302:819–822
- Ding W, Templeton D (2000). Activation of parallel mitogen-activated protein kinase cascades and induction of c-fos by cadmium. *Toxicol Appl Pharmacol* 162:93–99
- Dong W, Simeonova PP, Gallucci R, Matheson J, Flood L, Wang S, Hubbs A, Luster MI (1998) Toxic metals stimulate inflammatory cytokines in hepatocytes through oxidative stress mechanisms. *Toxicol Appl Pharmacol* 151:359–366
- Doniger SW, Salomonis N, Dahlquist KD, Vranizan K, Lawlor SC, Conklin BR (2003) MAP-Finder: using Gene Ontology and GenMAPP to create a global gene-expression profile from microarray data. *Genome Biol* 4:R7
- Doran JF, Jackson P, Kynoch PA, Thompson RJ (1983) Isolation of PGP 9.5, a new human neuron-specific protein detected by high-resolution two-dimensional electrophoresis. *J Neurochem* 40:1542–1547
- EPA Common Chemicals Found at Superfund Sites (2004). <http://www.epa.gov/superfund/resources/chemicals.html>. Accessed 16 Mar 2004
- Facheris M, Strain KJ, Lesnick TG, de Andrade M, Bower JH, Ahlskog JE, Cunningham JM, Lincoln S, Farrer MJ, Rocca WA, Maraganore DM (2005) UCHL1 is associated with Parkinson's disease: a case-unaffected sibling and case-unrelated control study. *Neurosci Lett* 381:131–134
- Faustman EM, Ponce RA, Ou YC, Mendoza MA, Lewandowski T, Kavanagh T (2002) Investigations of methylmercury-induced alterations in neurogenesis. *Environ Health Perspect* 110(Suppl 5):859–864
- Figueiredo-Pereira M, Cohen G (1999) The ubiquitin/proteasome pathway: friend or foe in zinc-, cadmium-, and H₂O₂-induced neuronal oxidative stress. *Mol Biol Rep* 26:65–69
- Figueiredo-Pereira M, Yakushin S, Cohen G (1997) Accumulation of ubiquitinated proteins in mouse neuronal cells induced by oxidative stress. *Mol Biol Rep* 24:35–38
- Figueiredo-Pereira ME, Yakushin S, Cohen G (1998) Disruption of the intracellular sulfhydryl homeostasis by cadmium-induced oxidative stress leads to protein thiolation and ubiquitination in neuronal cells. *J Biol Chem* 273:12703–12709
- Furuchi T, Hwang GW, Naganuma A (2002) Overexpression of the ubiquitin-conjugating enzyme Cdc34 confers resistance to methylmercury in *Saccharomyces cerevisiae*. *Mol Pharmacol* 61:738–741
- Furukawa Y, Vigouroux S, Wong H, Guttman M, Rajput AH, Ang L, Briand M, Kish SJ, Briand Y (2002) Brain proteasomal function in sporadic Parkinson's disease and related disorders. *Ann Neurol* 51:779–782
- Goering PL, Fisher BR, Kish CL (1993) Stress protein synthesis induced in rat liver by cadmium precedes hepatotoxicity. *Toxicol Appl Pharmacol* 122:139–148
- Goering PL, Kuester RK, Neale AR, Chapekar MS, Zaremba TG, Gordon EA, Hitchins VM (2000) Effects of particulate and soluble cadmium species on biochemical and functional parameters in cultured murine macrophages. *In vitro Mol Toxicol* 13:125–136
- Gorell JM, Rybicki BA, Cole Johnson C, Peterson EL (1999) Occupational metal exposures and the risk of Parkinson's disease. *Neuroepidemiology* 18:303–308
- Gribble EJ, Mendoza A, Hong S, Sidhu J, Faustman EM (2003) Evaluation of cell cycle kinetics in p53 mouse embryonal fibroblasts: effects of methyl mercury. *Toxicol Sci* 72:67–67
- Gribble EJ, Hong SW, Faustman EM (2005) The magnitude of methylmercury-induced cytotoxicity and cell cycle arrest is p53-dependent. *Birth Defects Res A Clin Mol Teratol* 73:29–38
- Hara T, Kamura T, Nakayama K, Oshikawa K, Hatakeyama S (2001) Degradation of p27(Kip1) at the G(0)–G(1) transition mediated by a Skp2-independent ubiquitination pathway. *J Biol Chem* 276:48937–48943
- Hwang GW, Furuchi T, Naganuma A (2002) A ubiquitin-proteasome system is responsible for the protection of yeast and human cells against methylmercury. *Faseb J* 16:709–711

- Hwang GW, Sasaki D, Naganuma A (2005) Overexpression of Rad23 confers resistance to methylmercury in *Saccharomyces cerevisiae* via inhibition of the degradation of ubiquitinated proteins. *Mol Pharmacol* 68:1074–1078
- IARC (2002) Cadmium and cadmium compounds. <http://www-cie.iarc.fr/htdocs/monographs/vol58/mono58-2.html>. Accessed 23 July 2002
- Iryo Y, Matsuoka M, Wispriyono B, Sugiura T, Igisu H (2000) Involvement of the extracellular signal-regulated protein kinase (ERK) pathway in the induction of apoptosis by cadmium chloride in CCRF-CEM cells. *Biochem Pharmacol* 60:1875–1882
- Jungmann J, Reins H, Schobert C, Jentsch S (1993) Resistance to cadmium mediated by ubiquitin-dependent proteolysis. *Nature* 361:369–371
- Jurczuk M, Brzoska MM, Moniuszko-Jakoniuk J, Galazyn-Sidorczuk M, Kulikowska-Karpinska E (2004) Antioxidant enzymes activity and lipid peroxidation in liver and kidney of rats exposed to cadmium and ethanol. *Food Chem Toxicol* 42:429–438
- Kim JH, Park KC, Chung SS, Bang O, Chung CH (2003) Deubiquitinating enzymes as cellular regulators. *J Biochem (Tokyo)* 134:9–18
- Kirkpatrick D, Dale K, Catania J, Gandolfi A (2003) Low-level arsenite causes accumulation of ubiquitinated proteins in rabbit renal cortical slices and HERK293 cells. *Toxicol Appl Pharmacol* 186:101–109
- Kwon J, Mochida K, Wang YL, Sekiguchi S, Sankai T, Aoki S, Ogura A, Yoshikawa Y, Wada K (2005) Ubiquitin C-terminal hydrolase L-1 is essential for the early apoptotic wave of germinal cells and for sperm quality control during spermatogenesis. *Biol Reprod* 73:29–35
- Leroy E, Boyer R, Auburger G, Leube B, Ulm G, Mezey E, Harta G, Brownstein MJ, Jonnalagada S, Chernova T, Dehejia A, Lavedan C, Gasser T, Steinbach PJ, Wilkinson KD, Polymeropoulos MH (1998a) The ubiquitin pathway in Parkinson's disease. *Nature* 395:451–452
- Leroy E, Boyer R, Polymeropoulos MH (1998b) Intron–exon structure of ubiquitin c-terminal hydrolase-L1. *DNA Res* 5:397–400
- Levenson CW (2003) Iron and Parkinson's disease: chelators to the rescue? *Nutr Rev* 61:311–313
- Lewandowski TA, Pierce CH, Pingree SD, Hong S, Faustman EM (2002) Methylmercury distribution in the pregnant rat and embryo during early midbrain organogenesis. *Teratology* 66:235–241
- Lewandowski TA, Ponce RA, Charleston JS, Hong S, Faustman EM (2003a) Changes in cell cycle parameters and cell number in the rat midbrain during organogenesis. *Brain Res Dev Brain Res* 141:117–128
- Lewandowski TA, Ponce RA, Charleston JS, Hong S, Faustman EM (2003b) Effect of methylmercury on midbrain cell proliferation during organogenesis: potential cross-species differences and implications for risk assessment. *Toxicol Sci* 75:124–133
- Li M, Chen D, Shiloh A, Luo J, Nikolaev AY, Qin J, Gu W (2002a) Deubiquitination of p53 by HAUSP is an important pathway for p53 stabilization. *Nature* 416:648–653
- Li M, Luo J, Brooks CL, Gu W (2002b) Acetylation of p53 inhibits its ubiquitination by Mdm2. *J Biol Chem* 277:50607–50611
- Liu Y, Fallon L, Lashuel HA, Liu Z, Lansbury PT Jr (2002) The UCH-L1 gene encodes two opposing enzymatic activities that affect alpha-synuclein degradation and Parkinson's disease susceptibility. *Cell* 111:209–218
- Lopez Salom M, Morelli L, Castano EM, Soto EF, Pasquini JM (2000) Defective ubiquitination of cerebral proteins in Alzheimer's disease. *J Neurosci Res* 62:302–310
- Lukas C, Sorensen CS, Kramer E, Santoni-Rugiu E, Lindeneg C, Peters JM, Bartek J, Lukas J (1999) Accumulation of cyclin B1 requires E2F and cyclin-A-dependent rearrangement of the anaphase-promoting complex. *Nature* 401:815–818
- Maki CG, Huibregtse JM, Howley PM (1996) *In vivo* ubiquitination and proteasome-mediated degradation of p53. *Cancer Res* 56:2649–2654
- Maraganore DM, Lesnick TG, Elbaz A, Chartier-Harlin MC, Gasser T, Kruger R, Hattori N, Mellick GD, Quattrone A, Satoh J, Toda T, Wang J, Ioannidis JP, de Andrade M, Rocca WA (2004) UCHL1 is a Parkinson's disease susceptibility gene. *Ann Neurol* 55:512–521

- Marx FP, Holzmann C, Strauss KM, Li L, Eberhardt O, Gerhardt E, Cookson MR, Hernandez D, Farrer MJ, Kachergus J, Engelender S, Ross CA, Berger K, Schols L, Schulz JB, Riess O, Kruger R (2003) Identification and functional characterization of a novel R621C mutation in the synphilin-1 gene in Parkinson's disease. *Hum Mol Genet* 12:1223–1231
- McKeown-Eyssen GE, Ruedy J (1983) Prevalence of neurological abnormality in Cree Indians exposed to methylmercury in northern Quebec. *Clin Invest Med* 6:161–169
- McKeown-Eyssen GE, Ruedy J, Hogg S, Guernsey JR, Woods I (1990) Validity and reproducibility of a screening examination for neurological abnormality in persons exposed to methylmercury. *J Clin Epidemiol* 43:489–498
- McNaught KS, Belzair R, Jenner P, Olanow CW, Isacson O (2002) Selective loss of 20S proteasome alpha-subunits in the substantia nigra pars compacta in Parkinson's disease. *Neurosci Lett* 326:155–158
- Meller R, Cameron JA, Torrey DJ, Clayton CE, Ordenez AN, Henshall DC, Minami M, Schindler CK, Saugstad JA, Simon RP (2006) Rapid degradation of Bim by the ubiquitin-proteasome pathway mediates short-term ischemic tolerance in cultured neurons. *J Biol Chem* 281:7429–7436
- Mendoza MAC, Ponce RA, Ou YC, Faustman EM (2002) p21(WAF1/CIP1) inhibits cell cycle progression but not G2/M-phase transition following methylmercury exposure. *Toxicol Appl Pharmacol* 178:117–125
- Michael D, Oren M (2003) The p53-MDM2 module and the ubiquitin system. *Semin Cancer Biol* 13:49–58
- Miura K, Koide N, Himeno S, Nakagawa I, Imura N (1999) The involvement of microtubular disruption in methylmercury-induced apoptosis in neuronal and nonneuronal cell lines. *Toxicol Appl Pharmacol* 160:279–288
- Mochida K, Ohkubo N, Matsubara T, Ito K, Kakuno A, Fujii K (2004) Effects of endocrine-disrupting chemicals on expression of ubiquitin C-terminal hydrolase mRNA in testis and brain of the Japanese common goby. *Aquat Toxicol* 70:123–136
- Morgan DO (1995) Principles of CDK regulation. *Nature* 374:131–134
- Mottet NK, Shaw CM, Burbacher TM (1985) Health risks from increases in methylmercury exposure. *Environ Health Perspect* 63:133–140
- Murray A (1995) Cyclin ubiquitination: the destructive end of mitosis. *Cell* 81:149–152
- Naganuma A, Furuchi T, Miura N, Hwang GW, Kuge S (2002) Investigation of intracellular factors involved in methylmercury toxicity. *Tohoku J Exp Med* 196:65–70
- NCBI (2004) Uchl1 SNP. <http://www.ncbi.nlm.nih.gov/entrez/query.fcgi?CMD=Display&DB=snp>
- Needleman HL, Schell A, Bellinger D, Leviton A, Allred EN (1990) The long-term effects of exposure to low doses of lead in childhood. An 11-year follow-up report. *N Engl J Med* 322:83–88
- Okuda B, Iwamoto Y, Tachibana H, Sugita M (1997) Parkinsonism after acute cadmium poisoning. *Clin Neurol Neurosurg* 99:263–265
- Orlowski R (1999) The role of the ubiquitin-proteasome pathway in apoptosis. *Cell Death Differ* 6:303–313
- Ou YC, Thompson SA, Kirchner SC, Kavanagh TJ, Faustman EM (1997) Induction of growth arrest and DNA damage-inducible genes Gadd45 and Gadd153 in primary rodent embryonic cells following exposure to methylmercury. *Toxicol Appl Pharmacol* 147:31–38
- Ou YC, Thompson SA, Ponce RA, Schroeder J, Kavanagh TJ, Faustman EM (1999a) Induction of the cell cycle regulatory gene p21 (Waf1, Cip1) following methylmercury exposure *in vitro* and *in vivo*. *Toxicol Appl Pharmacol* 157:203–212
- Ou YC, White CC, Krejsa CM, Ponce RA, Kavanagh TJ, Faustman EM (1999b) The role of intracellular glutathione in methylmercury-induced toxicity in embryonic neuronal cells. *Neurotoxicology* 20:793–804
- Ozkaynak E, Finley D, Varshavsky A (1984) The yeast ubiquitin gene: head-to-tail repeats encoding a polyubiquitin precursor protein. *Nature* 312:663–666
- Pasquini L, Moreno MB, Adamo AM, Pasquini JM, Soto EF (2000) Lactacystin, a specific inhibitor of the proteasome, induces apoptosis and activates caspase-3 in cultured cerebellar granule cell. *J Neurosci Res* 59:601–611
- Pines J (1994) Cell cycle. Ubiquitin with everything. *Nature* 371:742–743

- Ponce RA, Kavanagh TJ, Mottet NK, Whittaker SG, Faustman EM (1994) Effects of methyl mercury on the cell cycle of primary rat CNS cells *in vitro*. *Toxicol Appl Pharmacol* 127:83–90
- Ponce RA, Wong EY, Faustman EM (2001) Quality adjusted life years (QALYs) and dose-response models in environmental health policy analysis—methodological considerations. *Sci Total Environ* 274:79–91
- Powers KM, Smith-Weller T, Franklin GM, Longstreth WT Jr, Swanson PD, Checkoway H (2003) Parkinson's disease risks associated with dietary iron, manganese, and other nutrient intakes. *Neurology* 60:1761–1766
- Qu H, Syversen T, Aschner M, Sonnewald U (2003) Effect of methylmercury on glutamate metabolism in cerebellar astrocytes in culture. *Neurochem Int* 43:411–416
- Qui JH, Asai A, Chi S, Saito N, Hamada H, Kirino T (2000) Proteasome inhibitors induce cytochrome c-caspase-3-like protease-mediated apoptosis in cultured cortical neurons. *J Neurosci* 20:259–265
- Rideout H, Wang Q, Park D, Stefanis L (2003) Cyclin-dependent kinase activity is required for apoptotic death but not inclusion formation in cortical neurons after proteasomal inhibition. *J Neurosci* 23:1237–1245
- Rodgers KJ, Dean RT (2003) Assessment of proteasome activity in cell lysates and tissue homogenates using peptide substrates. *Int J Biochem Cell Biol* 35:716–727
- Schulman BA, Carrano AC, Jeffrey PD, Bowen Z, Kinnucan ER, Finnin MS, Elledge SJ, Harper JW, Pagano M, Pavletich NP (2000) Insights into SCF ubiquitin ligases from the structure of the Skp1–Skp2 complex. *Nature* 408:381–386
- Schwartz BS, Stewart WF, Bolla KI, Simon PD, Bandeen-Roche K, Gordon PB, Links JM, Todd AC (2000) Past adult lead exposure is associated with longitudinal decline in cognitive function. *Neurology* 55:1144–1150
- Seufert W, Futcher B, Jentsch S (1995) Role of a ubiquitin-conjugating enzyme in degradation of S- and M-phase cyclins. *Nature* 373:78–81
- Shaikh ZA, Vu TT, Zaman K (1999) Oxidative stress as a mechanism of chronic cadmium-induced hepatotoxicity and renal toxicity and protection by antioxidants. *Toxicol Appl Pharmacol* 154:256–263
- Sidhu JS, Hong S, Erickson A, Baker A, Robinson J, Vliet P, Faustman EM (2003) Methyl mercury induces differential ubiquitin-conjugated protein levels in p53 variant mouse embryonal fibroblasts. *Toxicol Sci* 72:67
- Sidhu JS, Ponce RA, Vredevoogd MA, Yu X, Gribble E, Hong SW, Schneider E, Faustman EM (2006) Cell cycle inhibition by sodium arsenite in primary embryonic rat midbrain neuroepithelial cells. *Toxicol Sci* 89(2):475–484
- Stewart D, Killeen E, Naquin R, Alam S, Alam J (2003) Degradation of transcription factor Nrf2 via the ubiquitin-proteasome pathway and stabilization by cadmium. *J Biol Chem* 278:2396–2402
- Tenev T, Marani M, McNeish I, Lemoine NR (2001) Pro-caspase-3 overexpression sensitises ovarian cancer cells to proteasome inhibitors. *Cell Death Differ* 8:256–264
- Tollefson L, Cordle F (1986) Methylmercury in fish: a review of residue levels, fish consumption and regulatory action in the United States. *Environ Health Perspect* 68:203–208
- Tomoda K, Kubota Y, Kato J (1999) Degradation of the cyclin-dependent-kinase inhibitor p27Kip1 is instigated by Jab1. *Nature* 398:160–165
- Tsirigotis M, Zhang M, Chiu R, Wouters B, Gray D (2001) Sensitivity of mammalian cells expressing mutant ubiquitin to protein-damaging agents. *J Biol Chem* 276:46073–46078
- Uversky VN, Li J, Fink AL (2001) Metal-triggered structural transformations, aggregation, and fibrillation of human alpha-synuclein. A possible molecular link between Parkinson's disease and heavy metal exposure. *J Biol Chem* 276:44284–44296
- Wagenknecht B, Hermisson M, Eitel K, Weller M (1999) Proteasome inhibitors induce p53/p21-independent apoptosis in human glioma cells. *Cell Physiol Biochem* 9:117–125
- Weiss B, Clarkson TW, Simon W (2002) Silent latency periods in methylmercury poisoning and in neurodegenerative disease. *Environ Health Perspect* 110(Suppl 5):851–854
- Wilkinson KD (1995) Roles of ubiquitinylation in proteolysis and cellular regulation. *Annu Rev Nutr* 15:161–189

- Wilkinson KD (1997) Regulation of ubiquitin-dependent processes by deubiquitinating enzymes. *Faseb J* 11:1245–1256
- Wilkinson KD (2000) Ubiquitination and deubiquitination: targeting of proteins for degradation by the proteasome. *Semin Cell Dev Biol* 11:141–148
- Wilkinson KD (2004) Ubiquitin: a Nobel protein. *Cell* 119:741–745
- Wilkinson KD, Ventii KH, Friedrich KL, Mullally JE (2005) The ubiquitin signal: assembly, recognition and termination. Symposium on ubiquitin and signaling. *EMBO Rep* 6:815–820
- Wing SS (2003) Deubiquitinating enzymes—the importance of driving in reverse along the ubiquitin-proteasome pathway. *Int J Biochem Cell Biol* 35:590–605
- Wintermeyer P, Kruger R, Kuhn W, Muller T, Woitalla D, Berg D, Becker G, Leroy E, Polymeropoulos M, Berger K, Przuntek H, Schols L, Epplen JT, Riess O (2000) Mutation analysis and association studies of the UCHL1 gene in German Parkinson's disease patients. *Neuroreport* 11:2079–2082
- Wu HM, Chi KH, Lin WW (2002) Proteasome inhibitors stimulate activator protein-1 pathway via reactive oxygen species production. *FEBS Lett* 526:101–105
- Yang CF, Shen HM, Shen Y, Zhuang ZX, Ong CN (1997) Cadmium-induced oxidative cellular damage in human fetal lung fibroblasts (MRC-5 cells). *Environ Health Perspect* 105:712–716
- Yang Y, Yu X (2003) Regulation of apoptosis: the ubiquitous way. *FASEB J* 17:790–799
- Yew PR (2001) Ubiquitin-mediated proteolysis of vertebrate G1- and S-phase regulators. *J Cell Physiol* 187:1–10
- Yu X, Hong S, Faustman EM (2008) Cadmium-induced activation of stress signaling pathways, disruption of ubiquitin-dependent protein degradation and apoptosis in primary rat Sertoli cell-gonocyte cocultures. *Toxicol Sci* 104:385–396
- Yu X, Robinson JF, Sidhu JS, Hong S, Faustman EM (2010) A system-based comparison of gene expression reveals alterations in oxidative stress, disruption of ubiquitin-proteasome system and altered cell cycle regulation after exposure to cadmium and methylmercury in mouse embryonic fibroblast. *Toxicol Sci* 114:356–377
- Yu X, Sidhu JS, Robinson JF, Hong SW, Faustman EM (2011a) Arsenite induced p53-independent activation of cellular stress response, accumulation of high molecular weight ubiquitin-conjugated proteins (HMW-polyUb) *Toxicol Appl Pharmacol*. in press
- Yu X, Sidhu JS, Robinson JF, Hong SW, Faustman EM (2011b) Cadmium induced p53 dependent activation of stress signaling, accumulation of ubiquitinated proteins and apoptosis in mouse embryonic fibroblast cells *Toxicol Sci*. in press
- Zhang F, Monkkonen M, Roth S, Laiho M (2002) Proteasomal activity modulates TGF-ss signaling in a gene-specific manner. *FEBS Lett* 527:58–62

Part VII
Biomarkers

Chapter 15

Blood Lead Level (BLL, B-Pb) in Human and Animal Populations: B-Pb as a Biological Marker to Environmental Lead Exposure

Nelly Mañay, Adriana Cousillas and Teresa Heller

Abstract The use of biomarkers is widely spread in biological monitoring of susceptible human populations and is also applied to sensitive living species in the ecosystems. Lead, as one of the most toxic chemicals in the environment, can be absorbed and cause adverse health effects on living organisms. To assess its exposure toxicity risks in humans, it is necessary to determine the concentration of the chemical species that can produce such effects, and to measure the magnitude of them. Although the adverse effects of lead to the red blood cells have been used as biomarkers, whole blood is the main biological fluid used for assessment of lead exposure, both for screening and diagnostic purposes as for biomonitoring purposes in the long term. Blood lead level (BLL, B-Pb) is still the most reliable indicator of recent lead exposure. Animals can also suffer from diseases attributable to environmental pollution and may be even more susceptible to lead poisoning, presenting serious health problems before they occur in the human population. In human medicine, the recognition that animals can be “sentinels” of environmental health hazards is not yet widely spread and generally these data are not considered for medical intervention. This chapter reviews the main aspects of B-Pb as the predominant biological biomarker to environmental lead exposure in human and animal populations.

Introduction

Human environmental exposure to lead (Pb) may be through contaminated food, water, and house dust as well as through industrial activities such as minery, metal recycling and the electric accumulators industry. The use of lead-based paint, containing up to 50% lead, declined during the 1950s and to lesser amounts the interior

N. Mañay (✉)

Toxicology and Environmental Hygiene, Faculty of Chemistry, University of the Republic of Uruguay, Gral. Flores 2124, 11800 Montevideo, Uruguay

Tel.: +598-2-9241-809

Fax: +598-2-9241-906

e-mail: nmanay@fq.edu.uy

lead-based paint continued to be available until the mid-1970s in USA (CDC 1991). Besides, atmospheric concentrations of lead, have decreased significantly, as more countries have removed tetraethyllead from the gasoline during the past decades (Thomas et al. 1999).

The biomonitoring for human exposure to lead (Pb) reflects an individual's current body burden, which is a function of recent and/or past exposure. Thus, the appropriate selection and measurement of biomarkers of lead exposure is of critical importance for health care management purposes, public health decision making, and primary prevention (Barbosa et al. 2005). Out of several biomarkers, the blood lead concentration (B-Pb) or blood lead level (BLL) has been the most important biomarker used for biomonitoring of exposure in risk assessment as well as in environmental epidemiology (Bergdahl and Skerfving 2008).

The adverse effects of lead in animals are also extensively reported and, in general, provide support for observations in human studies, with some consistency in types of effects and B-Pb-effect relationships. However, animal data on lead toxicity are generally considered less suitable as the basis for health effects assessments than are the human data (ATSDR 2007a). There is no equivalent animal model for the effects of lead on humans, but the development of lead poisoning symptoms in household pets may lead to the identification of children with asymptomatic lead intoxication (Dowsett and Shannon 1994).

Aims

This chapter focuses on the importance of lead biomonitoring of human and animal populations and the use of appropriate biomarkers of environmental lead exposure. Lead effects on red blood cells interfering hem synthesis pathway are well described in the literature and have been used as “effect biomarkers” for exposure assessment. However, recent reports and studies were reviewed to support the lead concentration in whole blood (B-Pb) as the primary biological biomarker used to monitor human exposure to environmental lead. The need to share research and data of lead exposure from human and animal populations is also highlighted.

Methods

The following criteria were used for selecting relevant studies and reports to review:

- Biomonitoring and biomarkers' accepted definitions and main concepts.
- Human and animal environmental risk assessments.
- Lead toxicokinetics background and hematological effects.
- Lead exposure biomonitoring and whole blood lead concentration (B-Pb) as the main aim of discussion.

- Lead in plasma as biomarker for monitoring lead exposure.
- Lead risk assessments that combine data from animal toxicology and human-exposure- assessment-studies, focused on pets.

Biomonitoring and Biomarkers: Human and Animal Approach

Biological monitoring or biomonitoring is an important and useful tool for environmental human exposure assessment (NRC 2006). As defined by IUPAC, biomonitoring is the “continuous or repeated measurement of any naturally occurring or synthetic chemical, including potentially toxic substances or their metabolites or biochemical effects in tissues, secretata, excreta, expired air or any combination of these in order to evaluate occupational or environmental exposure and health risk by comparison with appropriate reference values based on knowledge of the probable relationship between ambient exposure and resultant adverse health effects” (IUPAC 2007).

The need for human biomonitoring data in public health risk assessment can play an important role in establishing a reliable causal relationship between a specific human health effect and a specific chemical exposure. The implementation strategies to monitor exposures and early health effects in human populations can prevent human disease due to environmental contaminants (Suk et al. 1996). Besides, the continuously increasing availability of analytical methodologies in combination with a constant decrease in detection limits has rendered biomonitoring both more accessible and more sensitive. As a consequence, biomonitoring is more and more frequently applied in various health settings. This leads primarily to an increase in the available knowledge on the extent of human exposure to chemical substances. In addition, it may create a number of opportunities for improving human health risk assessment (Boogaard and Money 2008). Although, several large reviews focused on various aspects of human biomonitoring and environmental risk assessment (WHO/IPCS 1999, 2001; NRC 2006), the health risks shared among human and animals as sentinels are scarcely considered.

Biological markers or biomarkers are general terms for specific measurements reflecting an interaction between a biological system and an environmental agent, which may be chemical, physical, or biological (WHO/IPCS 2001). IUPAC defines a biomarker as an “indicator signaling an event or condition in a biological system or sample and giving a measure of exposure, effect, or susceptibility and establishes that such an indicator may be a measurable chemical, biochemical, physiological, behavioral or other alteration within an organism” (IUPAC 2007). Biomarkers integrate exposure from all sources and take into account absorption, which may vary considerably due to a variety of factors including environmental characteristics, genetic predisposition, age, sex, ethnicity and/or lifestyle factors (WHO/IPCS 1999).

Biomarkers have been mainly referred to the measurements used in the diagnosis or risk assessment in the field of environmental health and three categories of bio-

markers have been defined in biomonitoring programmes for determining exposure and effects: biomarkers of exposure, biomarkers of effects and biomarkers of susceptibility (NRC 1987). A biomarker of exposure is the concentration of the chemical itself or its metabolite(s) in biological tissues or fluids (blood, urine, breath, hair, adipose tissue, etc.). A biomarker of effect is the biological effect that occurs as a result of human exposure to that chemical and a biomarker of susceptibility is the amount of a chemical or its metabolites bound to target molecules as indicators that the health of an organism is especially sensitive to the challenge of exposure to the chemical compound (NRC 1987; WHO/IPCS 1999).

In practice, most biomarkers are determined by laboratory tests or functional procedures. Therefore, most methodological issues including time of sampling, have to be validated for research and routine applications (WHO/IPCS 2001). Biomarkers commonly used in occupational health biomonitoring practice have been fully interpreted and validated in the scientific literature to be routinely applied (ICOH-SCOT 2010).

Risk assessments that combine data from animal toxicology and human-exposure assessment studies can also be used to interpret biomonitoring data within the results of the risk assessment. Animal toxicology study designs need to include the collection of relevant biomarker data to facilitate development of biomarker-response relationships for the purpose of extrapolating biomonitoring results to humans (NRC 2006).

However, there are still few data regarding levels of chemical agents in animals. A fair comparison of animal data with human data would seem to demand that internal levels in animals have also to be obtained (Paustenbach and Galbraith 2006). Both human and animal health professionals need to share research regarding environmental hazards and health outcomes in animal and human populations to prevent human diseases (Rabinowitz et al. 2009). The “One Health” approach is a transdisciplinary collaboration, linking human and animal health professionals exploring together the possibility that animals could be useful sentinels for human risks and perhaps, vice versa, to improve and promote both human and animal health (Rabinowitz et al. 2009; Conrad et al. 2009).

Toxicokinetics of Lead

For the general population, exposure to lead occurs primarily via the oral route, with some contribution by inhalation, whereas occupational exposure is primarily by inhalation with some contribution by oral intake. After entering the body, lead can travel along several pathways depending on its source and bioavailability. The fraction of Pb that is absorbed depends mainly on the physical and chemical form, especially particle size and the solubility of the specific compound. Other important factors are inherent to the exposed subject, such as age, sex, nutritional status and, possibly, genetic background (Barbosa et al. 2005).

According to the Agency for Toxic Substances and Disease Registry (ATSDR 2007a), inorganic lead can be absorbed by inhalation, oral, and dermal exposure, but the latter route is much less efficient than the first two. Submicron size particles can be almost completely absorbed through the respiratory tract, but larger particles may be swallowed. The extent and rate of absorption of lead through the gastrointestinal tract depend on characteristics of the individual and on physicochemical characteristics of the medium ingested. Children can absorb 40–50% of an oral dose of water-soluble lead compared to 3–10% for adults. Gastrointestinal absorption of inorganic lead occurs primarily in the duodenum by saturable mechanisms. The distribution of lead in the body is route independent and, in adults, approximately 94% of the total body burden of lead is in the bones compared to approximately 73% in children.

Physiologic differences between children and adults account for much of the increased susceptibility of small children to the deleterious effects of Pb: adults absorb about 10% of lead through the gastrointestinal route. However, studies in young children, showed that 40–50% of lead is absorbed, and that about one-half of the amount absorbed is retained. In adults, 94% of the Pb body burden is stored in bones and teeth, in children only 70%. Besides, the continuous growth process in young children implies constant bone remodeling for skeletal development due to the rate of turnover of lead in bone which is higher in children than in adults. As a consequence, Pb stored in bone is continually released back into the blood compartment, a process that has been described as “endogenous contamination” (Gulson et al. 1996). This process is particularly significant for pregnant women because pregnancy causes an increase in bone remodeling. The apparently limited success of various Pb hazard control measures in decreasing lead in blood levels (B-Pb) in exposed children and pregnant women may reflect a constant bone resorption process. Recently, quite different long-term Pb kinetics have been reported between men and women, with premenopausal women appearing to retain Pb more avidly and releasing Pb more slowly compared to postmenopausal women and to men (Télez-Rojo et al. 2004; Barbosa et al. 2005).

Lead in blood is contained mostly in red blood cells. During pregnancy, lactation, menopause, and osteoporosis there is an increased bone resorption and therefore increased level of lead in blood. Lead can be transferred from the mother to the fetus and also from the mother to infants through breast milk (Ettinger et al. 2004). The biotransformation of inorganic lead consists of formation of complexes with a variety of protein and nonprotein ligands.

Lead is excreted mainly in urine and feces. Minor routes of excretion include sweat, saliva, hair, nails, and breast milk. The elimination half-lives for inorganic lead in blood and bone are approximately 30 days and 27 years, respectively. Several kinetic models have been proposed to characterize such parameters as intercompartmental lead exchange rates, retention of lead in various tissues, and relative rates of distribution among the tissue groups. Some models are currently being used or are being considered for broad application in lead risk assessment (ATSDR 2007a). Barbosa et al. (2005) reviewed several toxicokinetic lead studies reported. The first one reported that lead is absorbed into the blood compartment and has a mean bio-

logical half-life of about 40 days in adult males. Afterwards, it was reported that the half-life in children and in pregnant women was longer, because of bone remodeling (Gulson et al. 1996). Lead from blood is incorporated into calcified tissues such as bone and teeth, where it can remain for years, with the half-life of Pb in bone (bone-Pb) ranging from 10 to 30 years. However, the use of the term “half-life” to describe the biological clearance of Pb from bone implicitly makes assumptions about the kinetics of the process by which Pb is released. From calcified tissue stores, Pb is released slowly, depending on bone turnover rates, which in turn are a function of the type of bone, whether compact (slow turnover) or trabecular (rapid turnover). The release rate of Pb from bone varies with age and intensity of exposure as well. Thus, the bone tissue does not represent a site or permanent sequestration of lead but rather a source of continuous internal exposure that may increase as a result of the changes in bone turnover observed at different life stages as reported in different studies by Gulson et al. (1995, 1996, 1998). In relation to exchange rates among compartments, the transfer of Pb from blood to other compartments is much faster than the 1-month estimate, with the overall clearance rate from blood (sum of rates from blood to cortical bone, to trabecular bone and to other tissue), implying a half-life of 10–12 days. This shows the difference between the overall clearance viewed from outside, when no allowance can be made for recirculation, and actual transfer rates.

Lead in blood (B-Pb) is representative of soft tissue lead, and most widely used as measure of body burden and absorbed doses of lead. The relationship between B-Pb and the concentration of lead in exposure sources is curvilinear. The half-life for lead in blood and other soft tissue is about 28–36 days. Blood lead is bound to the erythrocytes and seems to be in dynamic equilibrium with plasma lead. Plasma lead is more diffusible than erythrocyte lead and more important for evaluating the toxic effect of lead because the diffusible form exerts an influence on lead concentrations of other compartments and produces critical effects in the various organs (Sakai 2000; Barbosa et al. 2005). Levels of plasma lead (P-Pb) increase immediately with acute exposure, with a very short half-life of probably less than an hour. A sudden rise in P-Pb can indicate a very recent exposure, but it can also pass unnoticed because of its very short half-life (Sakai 2000). Lead is mobilized from bone back into blood when exposure to Pb is not excessive. In adults, 45–75% of the Pb in blood may have come from bone. For exposed children, the bone-Pb contribution to blood can be 90% or even more. Therefore, the decrease in B-Pb level after environmental Pb remediation may be partly neutralised by contributions from endogenous Pb sources (Barbosa et al. 2005).

Effects of Lead on Red Blood Cells

As it was aforementioned, most inorganic lead absorbed into the blood stream binds to hemoglobin in erythrocytes. These red blood cells rather behave as a depository for lead, which might produce some disturbances in erythrocyte metabolism such

as Na, K-ATPase, deltaaminolevulinic acid dehydratase (ALAD) and nicotinamide adenine dinucleotide synthetase (NADS) activity (Sakai 2000). The effects of lead on the haemopoietic system result in decreased haemoglobin synthesis, and may lead to anaemia, due to reduced haemoglobin production and shortened life-span of erythrocytes. Basophilic stippling commonly occurs due to the aggregation of ribonucleic acid in the cytoplasm of erythrocytes (WHO/IPCS 1995; HPA 2007)

Lead has a significant effect on haemoglobin synthesis by interfering with several enzymatic steps in the heme pathway. Lead inhibits δ -aminolevulinic acid dehydratase (ALAD) and ferrochelatase activity, thereby decreasing haem synthesis, which leads to an increase in δ -aminolevulinic acid synthase. The activity of ALAD may be inhibited at very low B-Pb concentrations with no threshold yet apparent. The reduced activity has been reported to be inversely correlated with BPb concentrations over the whole dose range (ATSDR 2007b; HPA 2007). Ferrochelatase, which catalyzes the insertion of iron into protoporphyrin IX, is quite sensitive to lead. A decrease in the activity of this enzyme results in an increase of the substrate, erythrocyte protoporphyrin (EP), in the red blood cells also found in the form of zinc protoporphyrin (ZPP—bound to zinc rather than to iron). Lead exposure also increases in blood and plasma δ -aminolevulinic acid (ALA) and free erythrocyte protoporphyrins (FEP) (ATSDR 2007b).

As described in ATSDR (2007b), lead can induce two types of anemia, often accompanied by basophilic stippling of the erythrocytes. Acute high-level lead exposure has been associated with hemolytic anemia. Frank anemia is not an early manifestation of lead exposure and is evident only when the B-Pb is significantly elevated for prolonged periods. In chronic lead exposure, lead induces anemia by both interfering with heme biosynthesis and by diminishing red blood cell survival. The anemia of lead intoxication is hypochromic, and normo- or microcytic with associated reticulocytosis. Inhibition of haemoglobin sufficient to cause clinically observable anaemia has been reported following exposure, with high concentrations of lead in blood. The heme synthesis pathway, on which lead has an effect, is involved in many other processes in the body including neural, renal, endocrine, and hepatic pathways. There is a concern about the meaning of and possible sequelae of these biochemical and enzyme changes at lower levels of lead (HPA 2007; ATSDR 2007b).

The effects of interactions of lead with some enzymatic processes responsible for heme synthesis can be used as lead biomarkers. Only to mention some of them, the inhibition of delta-aminolevulinic acid dehydratase (ALAD) and the variation in some metabolite concentrations (e.g. delta-aminolevulinic acid in urine (ALA-U), blood (ALA-B) or plasma (ALA-P), coproporphyrin in urine (CP), zinc protoporphyrin (ZP) in blood are considered lead biomarkers of effects. The activities of pyrimidine nucleotidase (P5'N) and nicotinamide adenine dinucleotide synthetase (NADS) in blood are also decreased in lead exposure, and nucleotide contents in blood is altered in lead exposure (Sakai 2000). These effects of lead on human, can be also useful as biomarkers of effects, but they are out of the scope of this chapter that focuses on lead concentration in whole blood (B-Pb) as the primary biological biomarker used for human exposure assessment.

Biomarkers of Lead Exposure

Lead body burden is a function of the recent and/or past exposure to Pb. The correct selection and measurement of lead biomarkers of exposure are of critical importance to health care management aims, public health interventions and primary prevention actions (Barbosa et al. 2005). The measurement of total lead body burden would be the ideal biomarker of lead exposure being biomarkers of lead exposure, the measurements of the total lead concentration in body fluids and tissues (ATSDR 2007a).

Owing to the fact that toxic effects of lead are the same regardless of the route of entry into the body, the most common way to measure the absorbed dose for lead has been the concentration of lead in whole blood (B-Pb), although other indices, such as lead in urine, bone, hair, or teeth are also available (ATSDR 2007a).

Blood Lead Concentration

For more than five decades, blood has been the most widely used specimen to assess the human body burden of lead as none of the current biomarkers of internal Pb dose have yet been accepted by the scientific community as a reliable substitute for a B-Pb measurement validated to be routinely used (Barbosa et al. 2005). Although, blood lead level is the primary biomarker used for exposure assessment of this metallic element, the Pb toxicokinetics aspects must be taken into account. Lead in blood measurements in general reflects only recent exposures due to the relatively short half-life of Pb in blood. Nevertheless, it may also indicate older exposures, because the lead stored and released from bones could be also an endogenous contribution to B-Pb (Gulson et al. 1996).

Blood lead concentration (B-Pb) is the most widely used biomarker and it is considered to be the most reliable for general clinical use and public health surveillance. Currently, blood lead measurement is the screening test of choice to identify children with elevated B-Pb (CDC 1991). Venous sampling of blood is preferable to finger prick sampling, which has a considerable risk of surface lead contamination from the finger if its cleaning is not carried out well (CDC 1991; ATSDR 2007a). As regards Pb distribution within the body compartments (blood, bone and soft tissues), the differentiation of low-level chronic exposure from a short high-level exposure is not possible on the basis of a single B-Pb measurement. Interpretation of B-Pb levels over a wide range of values must consider the relationship between total intake of lead and B-Pb concentrations, as well as the proportion of lead in plasma (WHO/IPCS 1995). As reported by ATSDR (2007a), the extensive use of blood lead reflects mainly the greater feasibility of incorporating blood lead measurements into clinical or epidemiological studies, compared to other potential dose indicators, such as lead in plasma, urine, or bone.

However, B-Pb measurements have several limitations. It was mentioned that the lead concentration in blood reflects the exposure history of the previous few

months and does not necessarily reflect the larger burden and the much slower elimination kinetics of lead in bone. The relationship between lead intake and B-Pb is curvilinear as the increment in B-Pb per unit of intake decreases with increasing B-Pb. Lead intake/blood lead relationships also varies with age as a result of age-dependency of gastrointestinal absorption of lead, and varies with diet and nutritional status. A practical outcome of the above mentioned characteristics of B-Pb is that it can change relatively rapidly (e.g. weeks) in response to changes in exposure; thus, B-Pb can be influenced by short-term variability in exposure that may have only minor effects on lead body burden (ATSDR 2007a). A single blood lead determination cannot distinguish between lower-level intermediate or chronic exposure and higher level acute exposure. Similarly, a single measurement may fail to detect a higher exposure that occurred (or ended) several months earlier. Time-integrated measurements of B-Pb may provide a means for accounting for some of these factors and thereby provide a better measure of long-term exposure (Roels et al. 1995).

Blood Lead Levels' Reference Values

Measurement of lead in whole blood is the most widely used biomarker for assessing lead exposure. Graphite Furnace Atomic Absorption Spectrometry (GFAAS) and Anode Stripping Voltametry (ASV) are the most widely used techniques for Pb-B in clinical laboratories for routine analysis. Inductively Coupled Plasma Mass Spectrometry (ICP/MS) is also a very powerful tool for trace analysis of lead and other metals. Although ICP/MS instruments are more costly than GFAAS instruments, their ability to analyze multiple metals from a single sample, low detection limits, reliability, and ease of use have increasingly made them popular for trace metal analysis (ATSDR 2007a).

Owing to the lead's importance as a cause of public health problems, international and national health agencies have issued advisory standards or enforceable regulations that set lead levels in different media (ATSDR 2007b). In 1997, the US CDC issued a new guidance on screening children for lead poisoning that recommends a systematic approach to the development of appropriate lead screening in USA states and communities (CDC 1997). The objective of the new guidelines is maximum screening of high-risk children and reduced screening of low-risk children, as contrasted with previous guidelines (CDC 1991), which recommended universal screening (ATSDR 2007a). As more information has emerged about the neurological, reproductive, and possible hypertensive toxicity of lead, and as parameters that are more sensitive are developed, the B-Pb levels of concern for lead exposure have been progressively lowered by US CDC. Since 1970, CDC understanding of childhood lead poisoning has changed substantially. As researchers have used more sensitive measurements and better study designs, the generally recognized level for lead toxicity has progressively descended. Before the mid-1960s, a level above 60 $\mu\text{g}/\text{dL}$ (micrograms/deciliter) was considered toxic. By 1978, the defined level of toxicity had declined 50% to 30 $\mu\text{g}/\text{dL}$. Since 1991 CDC has accepted 10 $\mu\text{g}/\text{dL}$

as the intervention level for children, an advisory level for environmental and educational intervention (CDC 1991). CDC case management guidelines are designed to keep children's B-Pb below 10 $\mu\text{g}/\text{dL}$ (CDC 2004). The World Health Organization also defined a B-Pb of 10 $\mu\text{g}/\text{dL}$ (0.48 $\mu\text{mol}/\text{L}$) as the threshold of concern in young children (WHO/IPCS 1995). Some studies have found neurobehavioral impairment in children with B-Pb below 10 $\mu\text{g}/\text{dL}$ (Canfield 2003; CDC 2004) and no blood lead threshold has been identified in children (ATSDR 2007a). Although, the B-Pb levels of U. S. populations have dropped markedly compared to 30 years ago, new concerns have been raised regarding those possible adverse health effects in children at B-Pb levels $<10 \mu\text{g}/\text{dL}$. Perhaps there is no safe threshold but, rather, a continuum of toxic effects. In light of all these health concerns, the CDC Advisory Committee on Childhood Lead Poisoning Prevention formed a working group to review the evidence for adverse health effects at B-Pb levels $<10 \mu\text{g}/\text{dL}$ in children (CDC 2004). Although this working group concluded that several studies in the literature had demonstrated a statistically significant association between B-Pb levels $<10 \mu\text{g}/\text{dL}$ and some adverse health effects in children, the effects could have been influenced by residual confounding factors. The working group's report called for further studies to examine the relationship between lower B-Pb levels and health outcomes to provide a more complete understanding of this issue (CDC 2004).

Elevated blood lead concentration (e.g., $>10 \mu\text{g}/\text{dL}$) is an indication of excessive exposure in infants and children (CDC 1991, 2005) as well as for women in child-bearing age. Those women of child bearing potential, whose B-Pb exceeds 10 $\mu\text{g}/\text{dL}$ are at risk of delivering a child with a blood lead over current Centers for Disease Control guideline of 10 $\mu\text{g}/\text{dL}$. The B-Pb of these children should be closely monitored and appropriate steps should be taken to minimize the child's exposure to environmental lead (ACGIH 2009). The report of CDC (2007), also recognized that a B-Pb of 10 $\mu\text{g}/\text{dL}$ did not define a threshold for the harmful effects of lead. Research conducted since 1991 has strengthened the evidence that children's physical and mental development can be affected at BLLs $<10 \mu\text{g}/\text{dL}$ as mentioned before (CDC 2004). This last report, identifies gaps in knowledge concerning lead levels in this range and outlines strategies to reduce childhood exposures to lead. It resumes scientific data relevant to counseling, blood lead screening, and lead exposure risk assessment. It also promotes further research to evaluate the effects of lead in blood at levels $<10 \mu\text{g}/\text{dL}$ and strategies to identify and reduce exposure or the potential for exposure to lead, including measures applied in medical offices and in homes (CDC 2007).

"Healthy People 2020" objectives are relevant to lead poisoning prevention and healthy homes. The proposed 2020 objective will be to reduce B-Pb in children by focusing on two sub-objectives: eliminate Elevated Blood Lead Level in children and reduce the mean B-Pb in children (CDC 2009). Since 1987, the National Institute for Occupational Safety and Health (NIOSH) of the Centers for Disease Control and Prevention (CDC) has sponsored the Adult Blood Lead Epidemiology and Surveillance (ABLES) program to track laboratory-reported blood lead levels (B-Pb) in adults (NIOSH 2004).

Elevated blood lead levels (B-Pb) in adults can damage the nervous, hematologic, reproductive, renal, cardiovascular and gastrointestinal systems. Most cases are

workplace-related. U. S. Department of Health and Human Services recommends that B-Pb among all adults be reduced to $<25 \mu\text{g}/\text{dL}$. The highest B-Pb acceptable by standards of the U. S. Occupational Safety and Health Administration is $40 \mu\text{g}/\text{dL}$. The geometric mean B-Pb of all adults in the United States is $<3 \mu\text{g}/\text{dL}$ (NIOSH 2004). The Biological Exposure Index (BEI) is a guidance value for assessing biological monitoring results in occupationally exposed adults and indicates exposure at the Threshold Limit Value (TLV) for workplace air. The biological exposure index (BEI) for lead in blood of exposed workers is $30 \mu\text{g}/\text{dL}$ (ACGIH 2009).

Alternative Biomarkers

As was described, the differentiation between lead exposure for years, i.e. low-level chronic exposure from a recent or short high-level lead exposure on the basis of a single B-Pb, is practically impossible owing to the complex kinetics of Pb distribution within the body (cycling among blood, bone, and soft tissues). Consequently, there is a renewed interest in alternative biomarkers that may aid diagnosis of the extent of Pb exposure. Such alternatives include Pb determinations in plasma/serum, saliva, bone, teeth, feces, and urine. However, none of these matrices has gained convincing acceptance as an alternative to B-Pb, due to data based on erroneous or dubious analytical protocols that do not consider the confounding variables (Barbosa et al. 2005).

Bergdahl and Skerfving (2008) reviewed the alternatives to whole-blood-lead for lead exposure biomarkers. The report focuses on a number of different qualities that are of importance in the evaluation of a biomarker's usefulness and performance. The best biomarker in most circumstances is blood lead level, but lead in bone or teeth (for past exposures), feces (for current gastrointestinal exposure), or urine (for organic Pb) are sometimes more useful. A remarkable feature is that no generally accepted biomarker exists for bioavailable Pb, though plasma, bone, teeth, urine, and hair have all been discussed. For monitoring lead workers' exposure, blood has shown a poor response to changes in exposure at high levels but the alternative of lead in plasma has not been sufficiently evaluated to be considered as another possible biomarker in occupational health services, although now it is not dependent on problems with current analytical methodologies. Authors suggested that urine may deserve more attention and that almost all biomarkers lack systematic data on variation within and between individuals. In this chapter only the plasma alternative is discussed in more detail.

Lead in Plasma/Serum

In recent years increased attention has been paid to monitoring the concentration of Pb in plasma (or serum). The development and use of more sensitive analytical instrumentation, especially inductively coupled plasma mass spectrometry (ICP-MS),

has resulted in determinations of Pb in plasma and serum specimens with much lower detection limits and with better accuracy taking care of the special conditions in the preanalytical phase (Schütz et al. 1996; Barbosa et al. 2005; ATSDR 2007a). Plasma lead (P-Pb) has an important role in lead metabolism, although the concentration is very low. Schütz et al. (1996), have shown plasma-Pb levels $<1.0 \mu\text{g/L}$ in nonexposed individuals based on ICP-MS methods. P-Pb is in equilibrium with the extra-cellular pool and is directly involved in all the movements of lead among different biological compartments (Sakai 2000). Lead in plasma represents a more relevant index of exposure to, distribution of, and health risks associated with Pb than does B-Pb. In regard to toxic effects of Pb, they could primarily be associated with plasma-Pb because this fraction is the most rapidly exchangeable one in the blood compartment as reviewed by Barbosa et al. (2005). According to the review of Sakai (2000), lead in plasma circulating in the body, affects the lead body burden and causes the toxicity of lead in some soft tissues, such as bone marrow, kidney, brain, etc. The levels of Pb-P are sharply elevated with a sudden intake or acute exposure to lead and rapidly diminished by time elapse from it, indicating that Pb-P is an index for very recent exposure. However, a significant gap in knowledge remains on the associations between plasma-Pb and toxicologic effects. Furthermore, the methodology to determine concentration of lead in plasma is still neither feasible for routine analysis nor validated (ATSDR 2007a).

Animal Populations

Sentinel animals can be used as early warning of potential health risks and to prevent the development of diseases in human populations. In several cases, the latency periods for development of the side effects are usually shorter in animals than in humans. In general, animals can be exposed to higher concentrations of pollutants and they may develop early signs of intoxication (Van der Schalie et al. 1999).

One possible application of sentinel species for environmental monitoring is to include exposure and adverse-effect-observations to support some of the stages of the risk assessment process. Although it is unlikely that data from sentinel species would be used as the sole determining factor in assessing risks to human health, they could be useful as a first basis for decisions on risk assessment and early warning in situations which require further studies, to suggest possible causes and effects and for monitoring the course of remedial activities as well. The need of critical research and interagency collaboration that could advance the use of sentinel species was also recognized (Van der Schalie et al. 1999).

The use of nonhuman organisms in early warning systems for human health risk is well-known for a long time as many toxic sentinel species examples have been reported in the late nineteenth century. The miner's canary that was used to warn of potentially lethal carbon monoxide concentrations in coal mines is perhaps the most widely known application of a sentinel animal system for monitoring, whereas the neurobehavioral symptoms displayed by cats that consumed methylmercury-con-

taminated fish from Minamata Bay in Japan in the 1950s provided a good example of an observation that had significance for human health. Despite recognition that animals could serve as “sentinels” for environmental risks to human health, there are no evidence-based guidelines for the use of animal sentinel data in human health decision making. Rabinowitz et al. (2009) performed a systematic review of the animal sentinel literature to assess the scientific evidence whether animals can serve as useful sentinels of environmental risks to human health. One of the main obstacles for the application of animal sentinels, is the difficulty to understand the mechanistic similarities and differences between toxicologic effects in sentinel species and in humans. Much attention was given to the impediments for the application of sentinel species and their acceptance in the scientific and relatory communities (Rabinowitz et al. 2009).

Biomonitoring in Pets

For some toxic substances including lead, the same biomarker of exposure can be used both for humans and animals, i.e. dogs, and similar toxic effects can be found. Furthermore, the conditions of exposure may be comparable, in some circumstances, for people and their pets. Dogs may show early symptoms of lead intoxication at statistically significant lower B-Pb than children. Moreover, dogs can also have significantly higher B-Pb than those in children when exposed and living in the same polluted area. Dogs may develop early clinical signs of lead toxicity such as neurologic (convulsions) and gastric symptoms (vomiting and diarrhoea). Young dogs are even more susceptible to lead poisoning as they are more likely to eat and chew lead materials, although adult dogs may also be affected. In contrast, lead poisoning is less frequently reported in cats. These can develop loss of appetite but neurologic signs are uncommon. Vomiting and diarrhoea occur occasionally. Cats with lead toxicity are usually adult but occasionally kittens may be also affected. Diagnosis of lead intoxication requires either a urine or a blood test. The diagnosis is sometimes difficult and two different tests may be required to confirm that lead poisoning is present, particularly in cats (Maddison and Hawke 1993).

Conclusions

Both human and animal lead exposure and health issues need to share research regarding environmental hazards and health effects that may develop in animal and human populations. Biomarkers are a general term for specific measurements reflecting an interaction between a biological system and an environmental agent, which may be chemical, physical, or biological. The biomarkers can be used for the diagnosis and also risk assessment of the toxic agents in environmental health studies.

As it was reviewed in this chapter, the concentration of lead in whole blood lead (B-Pb), is the best biomarker of exposure and the most widely used to measure the body burden and absorbed (internal) doses of lead and can be useful for lead exposure risk assessment, lead poisoning diagnosis, disease control and prevention.

Acknowledgements Prof. Cristina Alvarez for her invaluable work of correction and edition of the manuscript.

References

- ACGIH (2009) TLVs and BEIs. Threshold limit values for chemical substances and physical agents and biological exposure indices. American Conference of Governmental Industrial Hygienists, Cincinnati
- ATSDR, Agency for Toxic Substances and Disease Registry (2007a) Toxicological profile of lead. Health effects. <http://www.atsdr.cdc.gov/toxprofiles/tp13-c3.pdf>
- ATSDR, Agency for Toxic Substances and Disease Registry (2007b) Case studies in environmental medicine (CSEM) lead toxicity: what are the physiologic effects of lead exposure? WB 1105. <http://www.atsdr.cdc.gov/csem/lead/docs/lead.pdf>
- Barbosa F Jr, Tanus-Santos JE, Gerlach RF, Patrick J Parsons (2005) A critical review of biomarkers used for monitoring human exposure to lead: advantages, limitations, and future needs. *Environ Health Perspect* 113:1669–1674
- Bergdahl IA, Skerfving S (2008) Biomonitoring of lead exposure-alternatives to blood. *J Toxicol Environ Health A* 71:1235–1243
- Boogaard P, Money C (2008) A proposed framework for the interpretation of biomonitoring data. *Environ Health* 7:S12
- Canfield RL, Henderson CR, Cory-Slechta DA, Cox C, Juski TA, Lanphear BP (2003) Intellectual impairment in children with blood lead concentrations below 10 µg per deciliter. *N Engl J Med* 348:1517–1526
- CDC (1991) Preventing lead poisoning in young children, Atlanta: US Department of Health and Human Services, Public Health Service. <http://wonder.cdc.gov/wonder/Prevguid/p0000029/p0000029.asp>
- CDC, Centers for Disease Control and Prevention (1997) Screening young children for lead poisoning: guidance for state and local public health officials. Centers for Disease Control and Prevention. Atlanta, GA: U.S. Department of Health & Human Services. <http://www.cdc.gov/nceh/lead/publications/screening.htm>
- CDC, Centers for Disease Control and Prevention (2004) Work group of the advisory committee on childhood lead poisoning prevention. A review of the evidence of health effects of blood lead levels <10 µg/dL in children. Atlanta, GA. <http://www.cdc.gov/nceh/lead/ACCLPP/Meetings/Minutes/2005OctMinutes.pdf>
- CDC, Centers for Disease Control and Prevention (2005) Preventing lead poisoning in young children. Atlanta. <http://www.cdc.gov/nceh/lead/publications/PrevLeadPoisoning.pdf>
- CDC, Centers for Disease Control and Prevention (2007) Interpreting and managing blood lead levels <10 µg/dL in children and reducing childhood exposures to lead recommendations of CDC's Advisory committee on childhood lead poisoning prevention. November 2, 2007/56(RR08); pp 1–14,16
- CDC, Centers for Disease Control and Prevention (2009) Department of Health and Human Services National Center for Environmental Health/Agency for Toxic Substances and Disease Registry Lead Poisoning Prevention Branch. Advisory Committee on childhood lead poisoning prevention. ACCLPP Meeting Minutes. <http://www.cdc.gov/nceh/lead/ACCLPP/Meetings/Minutes/2009OctMinutes.pdf>. Accessed 21–22 Oct 2009

- Conrad PA, Mazet JA, Clifford D, Scott C, Wilkes M (2009) Evolution of a transdisciplinary “One Medicine–One Health” approach to global health education at the University of California Davis. *Prev Vet Med* 92:268–274 (Special section: Schwabe Symposium 2008)
- Dowsett R, Shannon M (1994) Childhood plumbism identified after lead poisoning in household pets. Effects of reducing lead in gasoline: an analysis of the international experience. *Environ Sci Technol* 33:3942–3948
- Ettinger AS, Téllez-Rojo MM, Amarasiriwardena C, Gonzalez-Cossio T, Peterson K, Aro A, Hu H, Hernández-Avila M (2004) Lead in breast milk in relation to maternal blood and bone lead levels at one-month postpartum. *Environ Health Perspect* 112:926–931
- Gulson BL, Mahaffey KR, Mizon KJ, Korsch MJ, Cameron MA, Vimpani G (1995) Contribution of tissue lead to blood lead in adult female subjects based on stable lead isotope methods. *J Lab Clin Med* 125:703–712
- Gulson BL, Mizon KJ, Korsch MJ, Horwarth D, Phillips A, Hall J (1996) Impact on blood lead in children and adults following relocation from their source of exposure and contribution of skeletal tissue to blood lead. *Bull Environ Contam Toxicol* 56:543–550
- Gulson BL, Mahaffey KR, Jameson CW, Mizon KJ, Korsch MJ, Cameron MA et al (1998) Mobilization of lead from the skeleton during the postnatal period is larger than during pregnancy. *J Lab Clin Med* 131:324–329
- HPA, Health Protection Agency (U.K.) (2007) Lead toxicological overview. Version 2. http://www.hpa.org.uk/web/HPAwebFile/HPAweb_C/1194947332124
- ICOH-SCOT (2010) Manno M, Viau C et al Biomonitoring for occupational health risk assessment (BOHRA). *Toxicol Lett* 192:3–16
- IUPAC (2007) International Union of Pure and Applied Chemistry and Human Health Division Glossary of terms used in toxicology. 2nd Edition (IUPAC recommendations 2007) prepared for publication by Duffus J, Nordberg M, Templeton D. *Pure Appl Chem* 79:1153–1344
- Maddison JE, Hawke CG (1993) Lead toxicity in dogs and cats. *LEAD Action News*, 4(4), ISSN 1324-6011, The journal of The LEAD (Lead Education and Abatement Design) Group Inc The University of Sydney. www.lead.org.au/lanv4n4/lanv4n4-21.html
- NIOSH (2004) Adult Blood Lead Epidemiology and Surveillance (ABLES) Program NIOSH Publication No. 2004-146. *Worker Health Chartbook 2004*. <http://www.cdc.gov/niosh/topics/ABLES/ables.html>
- NRC, National Research Council. Committee on Biological Markers (1987) Biological markers in environmental health research. *Environ Health Perspect* 74:3–9
- NRC, National Research Council (2006) *Human Biomonitoring for Environmental Chemicals*, National Academies Press, Committee on Human Biomonitoring for Environmental Toxicants ISBN 0-309-10272-3. http://www.nap.edu/catalog.php?record_id=11700
- Paustenbach D, Galbraith D (2006) Biomonitoring and biomarkers: exposure assessment will never be the same. *Environ Health Perspect* 114:1143–1149
- Rabinowitz P, Scotch M, Conti L (2009) Human and animal sentinels for shared health risks. *Vet Ital* 45:23–34
- Roels H, Konings J, Green S, Bradley D, Chettle D, Lauwerys R (1995) Time-integrated blood lead concentration is a valid surrogate for estimating the cumulative lead dose assessed by tibial lead measurement. *Environ Res* 69:75–82
- Sakai T (2000) Biomarkers of lead exposure. *Ind Health* 38:127–142
- Schütz A, Bergdahl IA, Ekholm A, Skerfving S (1996) Measurement by ICP-MS of lead in plasma and whole blood of lead workers and controls. *Occup Environ Med* 53:736–740
- Suk W, Collman G, Damstra T (1996) Human biomonitoring: research goals and needs. *Environ Health Perspect* 104:479–483
- Téllez-Rojo M, Hernández-Avila M, Lamadrid-Figueroa H, Smith D, Hernández-Cadena L, Mercado A, Aro A, Schwartz J, Hu H (2004) Impact of bone lead and bone resorption on plasma and whole blood lead levels during pregnancy. *Am J Epidemiol* 160:668–678
- Thomas V, Socolow R, Fanelli J, Spiro T (1999) Effects of reducing lead in gasoline: an analysis of the international experience. *Environ Sci Technol* 33:3942–3948

- Van der Schalie W, Gardner HS Jr, Bantle JA, De Rosa CT, Finch R, Reif J, Reuter RH, Backer L, Burger J, Folmar LC, Stokes W (1999) Animals as sentinels of human health hazards of environmental chemicals. *Environ Health Perspect* 107:309–315
- WHO/IPCS (1995) Biological indices of lead exposure and body burden. In: *IPCS Inorganic lead environmental health criteria* 165. WHO, Geneva, pp 114–118
- WHO/IPCS (1999) Principles for the assessment of risks to human health from exposure to chemicals, *Environmental Health Criteria* no. 210. Geneva, WHO. <http://www.inchem.org/documents/ehc/ehc/ehc210.htm>
- WHO/IPCS (2001) Biomarkers in risk assessment: validity and validation. *Environmental health criteria* 222. World Health Organization, Geneva, p 238. <http://www.inchem.org/documents/ehc/ehc/ehc222.htm>

Part VIII
Removal of Heavy Metals

Chapter 16

Removal of Heavy Metal Sulfides and Toxic Contaminants from Water

Gábor Szalóki, Ildikó Czégény, Gábor Nagy and Gáspár Bánfalvi

Abstract Precipitation of metal (Hg^{2+} , Ni^{2+} , Pb^{2+}) sulfides on Na_2S -impregnated bentonite was followed by the oxidation of residual Na_2S to insoluble sulfur. As a result an average of 97% nickel and 95% of lead was removed. The efficiency of removal of nickel was more than 99% at higher (10^{-3} g ion/L) concentration and somewhat less (93%) at lower (10^{-5} g ion/L) concentration. The same tendency was observed with 10^{-3} g ion/L lead ions (>99%) and a lower efficiency ($\approx 88\%$) of removal at 10^{-5} g ion/L Pb^{2+} concentration. The precipitate of heavy metal sulfides absorbed to bentonite was removed by filtration. The fine precipitate of HgS could not be removed completely. Additional chemical reactions converted the excess sodium sulfide to H_2S and oxidized it to sulfur using carbogen gas ($\text{O}_2\text{-CO}_2$) and aeration. Revitalization of water was confirmed by the guppy survival test.

Introduction

Environmental cyanide catastrophies prompted the elimination or at least the reduction of cyanide pollution of water (Cabrera et al. 1999; Simon et al. 2001; Soldan et al. 2001). That aeration of cyanide polluted water samples with carbogen gas (5% CO_2 and 95% O_2) followed by aeration could be one of the solutions, was confirmed by *in vivo* toxicity tests on fish (Bánfalvi 2000; Gacsi et al. 2005). Unfortunately, gold extraction with cyanide dissolves heavy metal ions. Studies have shown that dietary Ca^{2+} would be protective against the uptake of both waterborne and dietary Cd, as well as against the uptake of waterborne Zn^{2+} (Zohouri et al. 2001; Chowdhury et al. 2004; Baldisserotto et al. 2004, 2005; Alves and Wood 2006). Dietborne Ca not only reduced the uptake of Cd, but also altered how cells handled Cd intra-

G. Bánfalvi (✉)

Department of Microbial Biotechnology and Cell Biology, University of Debrecen, 1 Egyetem Square, 4010 Debrecen, Hungary

Tel.: 36-52-512-900

Fax: 36-52-512-925

e-mail: bgaspar@delfin.klte.hu

cellularly (Niyogi and Wood 2006). Nevertheless, high levels of heavy metal spills are unlikely to be counteracted by dietary Ca^{2+} , leaving the heavy metal removal from wastewater an unsolved problem.

To remove heavy metals effectively from metal-laden wastewater, engineers and scientists developed various physico-chemical processes, such as adsorption (Ng et al. 2009; Blanchard et al. 1984; Kapoor and Viraghavan 1998; Lee et al. 1998; Gharaibeh et al. 1998; Kim and Lim 1999; Yu et al. 2000; Meunier et al. 2003; Yavuz et al. 2003; Sekhar et al. 2003; Jang et al. 2005), ion-exchange (Korngold et al. 1996; Lacour et al. 2001), microfiltration (Bayhan et al. 2001), chemical precipitation (Eccles 1995), reverse osmosis and nanofiltration (Qdaisa and Moussab 2004). Our preliminary communication has described that the chemical removal of cadmium would be feasible by the addition of sodium sulfide to CdCl_2 solution and turning Cd^{2+} ions to CdS , adsorbing the highly insoluble cadmium sulfide precipitate to bentonite and removing it by filtration. This process was then followed by the release of the excess soluble sulfide as H_2S and finally oxidizing the hydrogen sulfide to sulfur (Banfalvi 2006). Industrial metal-sulfide precipitation was as an alternative to the metal-hydroxide precipitation chemistry for the removal of Cu, Ni, Pb, and Zn from automotive wastewater (Kim et al. 2002). The use of commercial sodium sulfide as an inexpensive sulfide source for the removal of high average zinc content from wastewater (Anotai et al. 1992) revealed no significant difference in heavy metal removal efficiency compared to other more expensive sulfur containing precipitants (Kim et al. 2002). The oxidation of the residual sodium sulfide generates highly poisonous H_2S . The metal-sulfide precipitation technology does not involve the removal of the excess sodium sulfide from the wastewater.

This chapter describes: (a) the precipitation of heavy metal ions (Ni, Pb, Hg) with sodium sulfide, (b) the absorption of heavy metal sulfides on the surface of bentonite powder, (c) the removal of heavy metal sulfides by filtration, (d) the conversion of excess sodium sulfide to H_2S by CO_2 treatment, (e) further oxidation of the released and extremely toxic H_2S to sulfur, (f) the removal of CO_2 from water by air flow and (g) control of remediation of water by the guppy survival test.

Methods

Chemicals and Reagents

Chemicals were purchased from Sigma-Aldrich (Budapest, Hungary). GF/C filter paper was the product of Glassworld Kft. (Jüllick Glass Holding Zrt., Szekesfehervar, Hungary). Commercial crude bentonite (aluminum silicate clay) which is 2,000-times less expensive than the pure montmorillonite surviving analytical purposes was bought as “Benti” (litter for cats). Benti was mixed with sodium sulfide wrapped in GF/C filter and suspended in heavy metal containing water. Carbogen gas (5% CO_2 , 95% O_2) was purchased from Messer Hungarogaz Kft., Budapest).

In most cases heavy metals dissolved in mining drainage are sulphates, but in our experiments nickel and mercuric chloride salts have been chosen. Lead was used

Table 16.1 Selection of heavy metal salts for precipitation with sodium sulfide

	Hg ²⁺	Ni ²⁺	Pb ²⁺
Sulfate	Turns to yellow basic sulfate and H ₂ SO ₄ *	Soluble in 1.4 parts of water	Soluble in 2,225 parts of water*
Chloride	Soluble in 1.5 parts of water [§]	Soluble in 1 part of water [§]	Soluble in 93 parts of water
Nitrate	At high dilution insoluble basic salt formation*	Soluble in 0.4 part of water	Soluble in 2 parts of water [§]

* Salts such as HgSO₄, PbSO₄, Hg (NO₃)₂ are either decomposed, or have a lower solubility, or form precipitate.

§ Salts of heavy metals were chosen, based on their high solubility

as its most soluble nitrate salt. To avoid the presence of insoluble, sparingly soluble or decomposable compounds, highly soluble heavy metal salts have been chosen for precipitation. As an example HgSO₄ is taken, when dissolved in water turns to yellow basic sulfate and H₂SO₄. The solubility of the heavy metal salts used for precipitation is given in Table 16.1.

Precipitation and Removal of Heavy Metals

The glass fiber filter (GF/C) bag containing the mixture of 1 g sodium sulfide and 5 g bentonite was placed into the heavy metal salt solution (200 ml). Precipitation of heavy metal sulfides and adsorption to bentonite was accelerated by stirring the solution with a magnetic stirrer.

Determination of Heavy Metal Content

After 5 min stirring the glass fiber, the filter paper bag containing the precipitated heavy metal sulfides and bentonite was removed and the concentration of the remaining heavy metal ion was determined in each dilution by an Atomic Absorption Spectrophotometer (AAS) using a Perkin-Elmer 800 Analyst and Zeeman background corrector (Banfalvi 2006).

Fish

Aquarium fish guppy (*Poecilia reticulata*) weighing 0.9–1.1 g (average 1.0 g) were randomly selected and kept in a 20 L polypropylene flow-trough, aerated glass tank. The aquarium was supplied with 0.1 L/min drinking water, pumped through the tank and fish were allowed to acclimate to ambient conditions (20°C, and pH 7.5–8.0) for one week prior to the start of the experiment. During the acclimation period no death occurred.

Two hours before the experiment groups of randomly selected fish (five in each group) were placed in 200 ml of drinking water in 500 ml beakers and were subjected to the guppy test upon toxic treatment or remediation of water. The time of fish survival was measured.

Guppy Ecotoxicity Test

The test was carried out using five fish in each experiment. Heavy metal concentrations between 10^{-6} and 10^{-4} M represent toxic but sublethal doses, therefore only the toxicity of 10^{-3} M solutions was tested. For the measurement of the lethal effect of Na_2S , 1 g was added to 200 ml drinking water. By choosing the aquarium fish guppy (*Poecilia reticulata*) we could avoid the use of large volumes of Na_2S and the potential danger of inhaling toxic amounts of H_2S . Experiments were carried out under ventilation. The nine treatment groups (five guppys each) included aqueous environments for the nominally heavy metal-free control, three groups were subjected to heavy metal (Hg, Ni or Pb) treatments, one group was subjected to Na_2S treatment. Three groups of fish were placed in water after removal of heavy metals and one group after detoxification of Na_2S with carbogen gas and air flow.

Treatment with Carbogen Gas and Air Flow

Carbogen gas (mixture of 5% CO_2 and 95% O_2) was bubbled with an aquarium aerator in water containing 1 g Na_2S /200 ml drinking water using a flow rate of 2 L/min. Carbogen treatment was followed by an airflow of 2 L/min for 30 min. After these treatments five fish were placed in water and the time of survival was measured.

Results

Analogy Between the Chemistry of Removing Cyanide and Heavy Metals

For the removal of cyanide from water we have used carbogen gas (5% CO_2 and 95% O_2) and airflow (Gacsi et al. 2005). The idea of detoxifying heavy metals is based on a series of analogous chemical reactions which can be divided in two groups: (a) precipitation of the metals as their sulfides on Na_2S impregnated bentonite, and (b) the detoxification of residual Na_2S .

(a) Metal sulfides will precipitate in the order of their increasing solubility products, starting with mercuric sulfide which has the lowest solubility ($K_{\text{sp}} 10^{-49}$ – 10^{-50}

at 18°C). The solubility product (K_{sp}) is deduced from the equilibrium constant of its sparingly soluble salt:

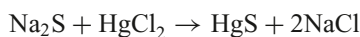
$$K_{eq} = \frac{[Hg^{2+}][S^{2-}]}{[HgS_{(s)}]}$$

where K_{eq} is the equilibrium constant and HgS is the sparingly soluble salt. The concentration of the pure solid $[HgS_{(s)}]$ is constant therefore the expression can be simplified by defining a new constant named solubility product (K_{sp}):

$$K_{eq}[HgS_{(s)}] = [Hg^{2+}][S^{2-}]$$

$$K_{sp} = K_{eq}[HgS_{(s)}] = [Hg^{2+}][S^{2-}]$$

The removal of Hg^{2+} ions is based on its precipitation to HgS :

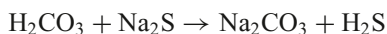


(b) After precipitation, adsorption and removal of the heavy metal sulfide by filtration, the next steps serve the purpose of releasing the excess sodium sulfide as H_2S with a stronger acid than hydrogen sulfide. To detoxify the excess sulfide ions in the Na_2S solution, the first reaction is the formation of carbonic acid from carbon dioxide dissolved in water. As indicated by its first dissociation constant (K_d) only a small portion of H_2CO_3 will dissociate spontaneously to protons and hydrocarbonate ions:

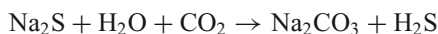


$$K_d = \frac{[H^+][HCO_3^-]}{[H_2CO_3]} = 4.3 \times 10^{-7}$$

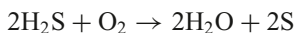
Although, H_2CO_3 is a weak acid ($K_d=4.3 \times 10^{-7}$ at 25°C), nevertheless stronger than hydrogen sulfide ($K_d=1.1 \times 10^{-7}$ at 25°C), consequently carbonic acid is able to release H_2S from the solution of its sodium sulfide salt:



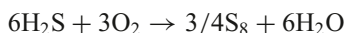
Summarizing the detoxification reactions:



The next step involves the oxidation of the dissolved hydrogen sulfide to sulfur:

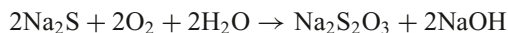


The formation of sulfur from hydrogen sulfide is similar to the Claus process which is faster, as it is catalyzed by $AlOOH$ and summarized as:

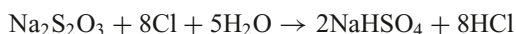


The production of polysulfide will not be favored since there is no catalyst present and the acidic environment provided by the presence of H_2CO_3 favors the decomposition of polysulfides to H_2S and insoluble sulfur.

Alternatively, the alkaline aqueous sodium sulfide solution (pH 10.6) upon staying in contact with air is oxidized slowly:



In this reaction the milder, but still toxic sodium thiosulfate is formed and the solution remains alkaline due to the presence of sodium hydroxide. The aqueous solution of sodium thiosulfate is nearly neutral. Additional reactions could serve the conversion of thiosulfate by exploiting the “antichlor” effect of sodium thiosulfate or to decrease the pH of the solution generated in the previous reaction:



However, these reactions would need a precise stoichiometry and alkaline titration. Rather the use of carbogen gas is recommended which favors the release of H_2S and decreases the pH approaching the physiological pH of natural drinking water.

Removal of Hg^{2+} , Ni^{2+} and Pb^{2+} as their Sulfides

A similar procedure applied for cadmium (Banfalvi 2006) is used for the removal of Hg^{2+} , Ni^{2+} and Pb^{2+} ions. The low solubility of the tested heavy metal sulfides allows their precipitation at very low concentrations (Hg^{2+} at $\approx 10^{-22}$, Pb^{2+} at $\approx 10^{-14}$ and Zn^{2+} at $\approx 10^{-11}$ g ion/L) and their removal by adsorption to bentonite. The mixture of 5 g bentonite and 1 g sodium sulfide placed into a glass fiber filter paper bag was plunged into 200 ml heavy metal ion containing solution. After stirring the solution with a magnetic stirrer the bag containing the precipitated heavy metal sulfide was removed and the remaining heavy metal ion was determined in each solution. Table 16.2 shows the removal of Ni^{2+} . Lower than 10^{-6} g ion/L concentrations of heavy metal ions could not be determined with AAS. The absorption to bentonite was more efficient at higher heavy metal concentrations in the range between 10^{-5} – 10^{-3} g ion/L.

Table 16.2 confirms that the higher the Ni^{2+} ion concentration, the more efficient was its removal. At 10^{-3} , 10^{-4} and 10^{-5} g ion/L Ni^{2+} concentrations the efficiency of removal was 99.6, 98.3 and 93.2%, respectively. Similar tendency was observed with Pb^{2+} (Table 16.3), at 10^{-3} , 10^{-4} and 10^{-5} g ion/L, the efficiency of removal was 99.4, 97.4 and 87.9%, respectively. At subtoxic levels of Pb^{2+} and Ni^{2+} concentrations (10^{-6} g ion/L or less) the removal of heavy metal sulfides could not be measured.

Table 16.2 Removal of nickel as NiS precipitate and absorption to bentonite

Ni ²⁺ (g ion/L)	Nickel concentration determined in				
	A (mg ion/L)	B (mg ion/L)	C (mg ion/L)	D (mg ion/L)	E (mg ion/L)
10 ⁻³	58.7	58.5	2.51	0.32	0.23 (0.4%)
10 ⁻⁴	5.871	5.68	1.23	0.12	0.10 (1.7%)
10 ⁻⁵	0.587	0.54	0.32	0.09	0.04 (6.8%)
10 ⁻⁶	0.058	0.06	0.06	0.05	0.04 (68.9%)
Average (%) 10 ⁻³ –10 ⁻⁵ (g ion/L)	100%	96.1%	26.6%	6.0%	3.0%

The experiment was carried out as described in the “Material and Methods”. A. Stock solution containing 237.7 mg NiCl₂·6H₂O (58.7 Ni²⁺) in 1000 ml distilled water corresponds to 10⁻³ g ion/L. Dilutions (10⁻⁴–10⁻⁶) were made from the stock solution. B. Determination of Ni²⁺ concentrations in stock solution and in dilutions by atomic absorption spectrometry (AAS). C. AAS of 200 ml Ni²⁺ solution containing 1 g sodium sulfide each. D. AAS after filtrating suspension containing 200 ml NiCl₂ stock or diluted solutions, 1 g sodium sulfide and 5 g bentonite, each. E. The same as D with the exception that the mixture of sodium sulfide and bentonite was in a filter bag and hanging in the solution containing NiCl₂. After mixing the filter bag was removed and the remaining Ni²⁺ in the solution was determined by AAS. Values are averages of three measurements

Table 16.3 Removal of lead as PbS by precipitation and absorption to bentonite

Pb ²⁺ (g ion/L)	Lead concentration determined in				
	A (mg ion/L)	B (mg ion/L)	C (mg ion/L)	D (mg ion/L)	E (mg ion/L)
10 ⁻³	207.2	207.6	3.28	1.40	1.24 (0.6%)
10 ⁻⁴	20.72	18.74	2.53	1.11	0.54 (2.6%)
10 ⁻⁵	2.07	2.03	0.54	0.40	0.25 (12.1%)
10 ⁻⁶	0.21	0.06	0.02	0.01	0.05 (23.8%)
Average (%) 10 ⁻³ –10 ⁻⁵ (g ion/L)	100%	96.1%	13.3%	8.4%	5.1%

The experiment was carried out as described in Table 16.2. The stock solution contained 331.23 mg lead nitrate corresponding to 207.2 mg Pb²⁺ g ion/L distilled water

Worthy to mention that although, precipitate formation was observed with HgS, the remaining mercuric ions left in the solution after filtration could not be determined. The fine and opalescent HgS precipitate diffused through the filter and clogged the electrode. Nevertheless, the ecotoxicity guppy test revealed that all fish remained alive proving that Hg²⁺ ions were also effectively precipitated and HgS removed.

Ecotoxicity Test of Heavy Metal Ions

The toxicity of heavy metals was demonstrated by physiological experiments. At 10⁻⁴ M or lower concentrations of heavy metal chlorides no fish death occurred (not

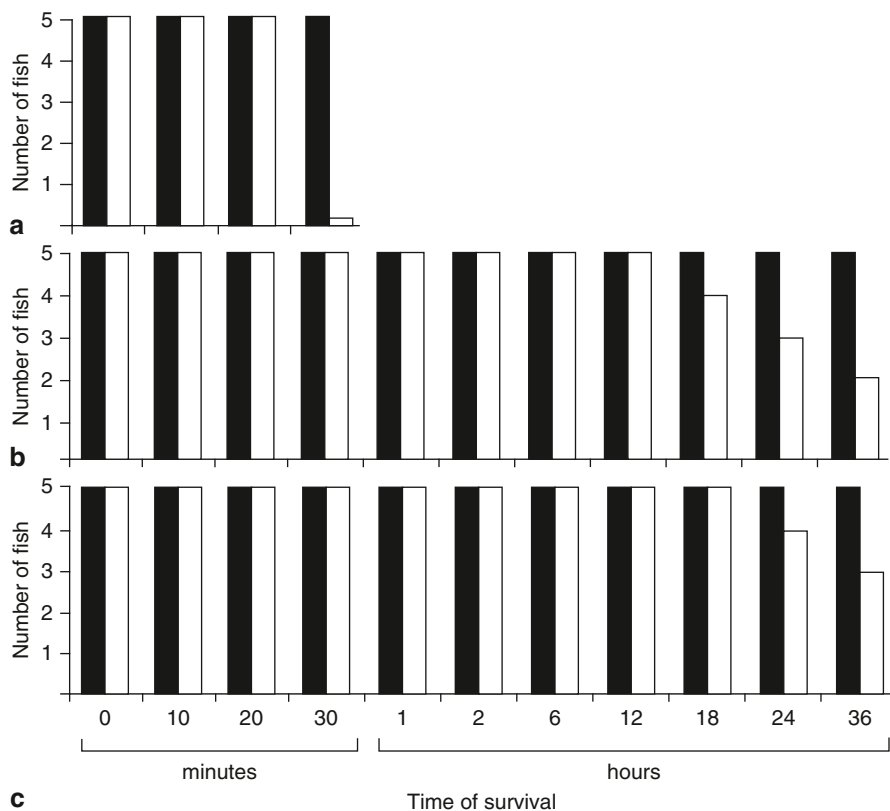


Fig. 16.1 Toxicity test of heavy metal ions. Guppy test using male guppies (five each, average weight 1 g) was carried out in heavy metal chloride containing drinking water as described in the Materials and Methods. The survival of fish was registered **a** in 10^{-3} M HgCl_2 solution and expressed in minutes, **b** in 10^{-3} M ZnCl_2 solution, and **c** in 10^{-3} M $\text{Pb}(\text{NO}_3)_2$ solution. Survival of fish: control (■), after heavy metal treatment (□)

shown). At 10^{-3} M as expected mercury turned out to be the most toxic, followed by Ni^{2+} and Pb^{2+} (Fig. 16.1). In the presence of 10^{-3} M HgCl_2 all fish (guppies) died within 30 min (Fig. 16.1a). To the contrary, lead and nickel ions had no imminent lethal effects. All five guppies survived 12 h, three of them 24 h and two remained alive after 36 h in the presence of 10^{-3} M NiCl_2 (Fig. 16.1b). Four of the five guppies survived the 24 h and three of them the 36 h 10^{-3} M PbCl_2 treatment (Fig. 16.1c).

Removal of Sodium Sulfide from Water

There is no doubt that the addition of Na_2S to mine tailings or in our experiments to drinking water containing heavy metal pollution and its oxidation would mean

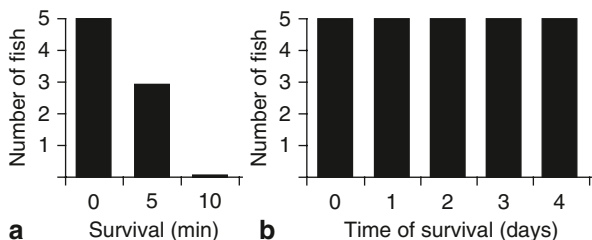


Fig. 16.2 Toxicity test and removal of Na_2S with carbogen gas. **a** Toxicity of sodium sulfide using male guppies (average 1 g, five each) was tested as described under Materials and Methods. **b** Sodium sulfide (1 g in 200 ml drinking water) was detoxified for 2 h by using carbon dioxide (5%) and oxygen (95%) mixture (carbogen gas). Carbogen gas was removed by aeration for 1 h. After detoxification fish (five guppies) were placed in water and their survival was registered

the production of H_2S which is even more toxic than the heavy metals. One could argue that the precipitation of heavy metals would be sufficient. However, the extreme toxicity of sodium sulfide (Fig. 16.2a) shows that this would not solve the problem and guppies died in the sodium sulfide solution within 10 min. To complete the answer to this objection: (a) precipitation of heavy metals in itself would not remove heavy metals, (b) sodium sulfide and cyanide can be effectively removed by the same procedure, namely by treatment with carbogen gas without additional manipulation. Consequently, the argument that precipitation of heavy metals would be sufficient is unacceptable due to the presence of heavy metal sulfides, which maintain a low, but constant level of heavy metal pollution defined by the solubility products of these sulfides. All three steps are important: (1) to precipitate, (2) to filtrate out heavy metal sulfides and (3) to decompose the excess sodium sulfide by CO_2 treatment and oxidation.

Figure 16.2b shows that sodium disulfide solution can be detoxified by carbogen gas (Fig. 16.2b). As a result of carbogen treatment none of the five fish died within four days. After these experiments guppies were placed back in the aquarium containing fresh drinking water and continued their regular life without further deaths.

pH Changes during Carbogen Treatment

Sodium sulfide solution is highly basic. The carbogen treatment generated carbonic acid which was beneficial as it lowered the pH of the solution. We have followed the decrease of pH upon carbogen treatment of the solution (1 g Na_2S in 200 ml) (Fig 16.3). Aeration alone did not influence significantly the pH. That the solution remained alkaline when only aeration was used is not surprising since the oxidation of Na_2S produces sodium hydroxide. Carbogen treatment for 2 h decreased the pH of sodium sulfide solution from 10.6 to 6.7. Aeration after carbogen treatment served: (a) the removal of carbon dioxide, (b) the oxygenization of water and (c)

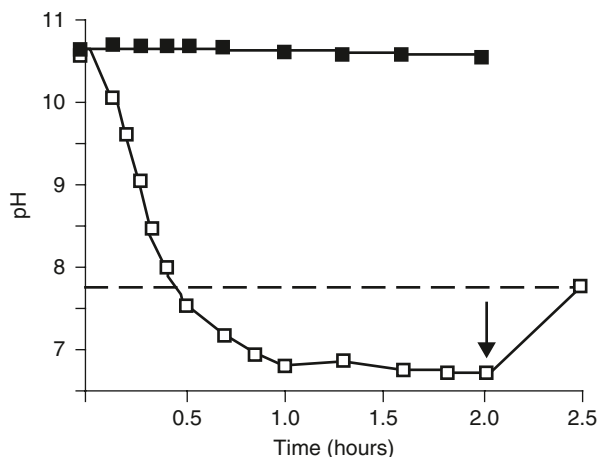


Fig. 16.3 The effect of aeration on the pH of sodium sulfide solution. Experiments were carried out under ventilated hood. 2×200 ml solutions of drinking water containing 1 g sodium sulfide each were prepared in two 500 ml beakers as described in the Methods. Air flow (2 L/min) was passed through one of the solutions for 2 h without significant change in the pH (■-■). Carbogen gas was bubbled through the second Na_2S solution with a speed of 2 L/min for 2 h (□-□). After 2 h, carbogen gas was replaced by air flow (black arrow). The pH of drinking water is indicated by the broken line (----)

the elevation of pH from 6.7 to 7.8 corresponding to the aerated aquarium pH value (Fig. 16.3).

Survival of Fish upon Removal of Heavy Metal and Sodium Sulfide

In these series of experiments heavy metal ions in drinking water (Ni^{2+} , Pb^{2+} , Hg^{2+} , 10^{-3} g ion/L each) were precipitated with sodium sulfide, adsorbed to bentonite and removed by filtration. Remediation with carbogen gas and aeration of water was followed by the adaptation of guppies to the remediated aqueous environment. The survival of fish was registered for four days. During these experiments there was no loss of fish (results are not shown). The survival of fish confirmed that the toxic effects of all three heavy metals and sodium sulfide were efficiently neutralized.

Discussion

As far as the environmental context is concerned cyanide pollution in waterways does not go alone, after the extraction of gold from leachate, the cyanide solution carries heavy metal contaminations. With respect to environmental health it is

of practical importance that we have established a simple cost efficient approach applicable for the detoxification of cyanide and for the removal of heavy metals in waterways (Hg^{2+} , Ni^{2+} , Pb^{2+}). It is advised to precipitate metal sulfides on the surface of an adsorbent and to remove the precipitate by filtration rather than left unattended, to prevent environmental precipitate formation on unicellular and multicellular organisms. The filtration of heavy metal sulfides has to be followed by the conversion of the extremely toxic soluble sulfide to sulfur. We have proved the feasibility of this detoxification method by the guppy test. In a broader sense this method allows not only the removal of heavy metals but more importantly the restoration of water quality for aqueous life.

The occurrence of heavy metals from the toxic spill of a pyrite mine in 1998 (Simon et al. 2001), the Baia Mare accident in 2000 and other smaller incidents indicated that further industrial accidents may occur in future (Soldan et al. 2001). Among the potential detoxification methods are those which emphasize the importance of stabilization of the heavy metals in aqueous environment. Sulfide species were recommended as a sink for mercury in lake sediments (Wolfenden et al. 2005). The application of an increased dosage of soluble sulfides has been suggested recently for the removal of cadmium and mercury (Banfalvi 2006; Piao and Bishop 2006). The immobilization of mercury ions by the addition of sodium sulfide indicated that after precipitation to HgS , mercury ion concentration could not be determined. This is explained by the formation of colloidal mercury sulfide that could not be removed completely by filtration and diffused through the filter and the fine precipitate clogged the electrode. Such phenomenon was observed neither with NiS nor with PbS nor earlier during the formation of CdS (Banfalvi 2006). Looking at the solubility products one would assume that the finest sulfide precipitate would be formed with that heavy metal which precipitates at the lowest ion concentration and produces the smallest colloidal particles. Indeed, mercury ions precipitate with sulfide ions at $\approx 10^{-23}$ – 10^{-24} g ion/L concentrations, followed by Pb^{2+} ($\approx 10^{-14}$ g ion/L), Ni^{2+} ($\approx 10^{-12}$ g ion/L), and Cd^{2+} ($\approx 10^{-5}$ g ion/L). Comparing the heavy metal ion concentrations with the average percentages obtained after the removal of heavy metal sulfides from their 10^{-3} – 10^{-5} g ion/L solutions we see a similar tendency. The fine precipitate of HgS (solubility product $\approx 10^{-49}$ – 10^{-53} depending on temperature) prevented the determination of the residual Hg^{2+} ions by atomic absorption spectrometry. Due to the fine precipitate formation the removal of HgS by filtration was probably less efficient than the removal of Ni^{2+} , Pb^{2+} , or Cd^{2+} . In conformity with the fine precipitate formation nickel sulfide and copper sulfide nanocrystal production was also reported (Ghezlbash and Korgel 2005). Three-dimensional, orthogonal lead sulfide (PbS) nanowire arrays and networks have also been published (Ge et al. 2005). The nanocrystal formation is of physiological importance and provides some explanation regarding the toxicity of the heavy metal nanocrystals. If heavy metal sulfides cannot be precipitated on the surface of an adsorbent *in situ nascendi*, the fine precipitate in water will cover other macroscopic and microscopic objects including living organism the ingestion of which may cause severe secondary heavy metal poisoning. To reduce the amount of nanocrystal formation, the *in situ* precipitation of heavy metal sulfides on the surface of an adsorbent such as bentonite offers a plausible solution.

To the question whether or not heavy metal sulfide formation and removal can be implemented and turned into practical solution, the explanation could be that the primary toxic effect of low concentrations of heavy metal pollution ($\leq 10^{-4}$ g ion/L) is a long lasting effect and does not cause immediate death in aqueous life. Based on toxicological experiments, an effective and harmless way to avoid the long-term poisonous effects of heavy metals after precipitation with sodium sulfide is their removal by filtration and the detoxification of residual sodium sulfide with carbogen gas (5% CO₂, 95% O₂) followed by the aeration to oxygenize water. After treatment of sodium sulfide with carbogen gas, a faint yellowish precipitate of sulfur sedimented at the bottom of the container, which did not influence the survival of fish.

Another objection to the precipitation could be that the Hg²⁺ ion concentration permitted in the drainage (0.05 ppm corresponding to somewhat less than 10^{-9} g ion/L) is much lower than what we have adopted (10^{-3} – 10^{-5} g ion/L) in the guppy test. The answer to this question is that at 10^{-3} g ion/L or lower concentrations of heavy metals (including Hg) no fish death occurred and the guppy test at these lower concentrations would not make sense. However, after environmental pollutions the concentration of heavy metals including Hg may mount to life threatening levels which justify our experiments at toxic concentrations.

Conclusions

Heavy metal pollutions can be stabilized by the precipitation of metal ions as their sulfide species that will behave as a sink especially in lake sediments (Wolfenden et al. 2005). The precipitation of heavy metal ions to lower their concentration in waterways is only a temporary solution and should be followed by the removal of the precipitate. The long term effects of heavy metal sulfides are: (1) different heavy metals will be precipitated at the same time, the cumulative physiological effects of which can be significant, (2) heavy metal sulfide sediments represents a low but constant metal ion reservoir which will be maintained as long as the precipitate is present, (3) the removal of polluted water and replacement with water free of contaminants would not solve the problem either as the presence of the precipitated sediment provides a metal ion reservoir, determined by the solubility product, (4) living species accumulate heavy metals dissolved in water, (5) metal sulfides precipitate on the surface of small corpuscles including small organisms and will be ingested.

The following solution is proposed to eliminate heavy metals from mine tailings and to prevent living organisms in waterways from the long-term effect of heavy metals and their sulfides: (1) precipitating the metals on Na₂S-impregnated fine powder of bentonite inside diffusible bags or other containers, (2) removing the heavy metal sulfides by filtration after their adsorption to bentonite i.e. the removal of bags containing the heavy metal sulfides adsorbed to bentonite, (3) oxidation of residual Na₂S to insoluble, non-toxic sulfur with carbon dioxide and reducing the

alkaline pH to physiological level, (4) aeration with air to remove carbon dioxide and to saturate water with oxygen.

Our experiments showed that sodium sulfide can be efficiently removed from water and the released hydrogen sulfide can be oxidized to sulfur. Although, the regeneration of water and the restoration of its physiological status was originally suggested for cyanide (Gacsi et al. 2005) it is also applicable to the removal of heavy metals from lakes and ponds in the vicinity of industrial and populated areas. One's first reaction to the proposal might be reluctance to add another toxin (Na_2S) to lakes, ponds and mine tailings, but since only the oxidation with carbogen and air is needed to decompose simultaneously both NaCN and Na_2S , this is not a valid objection. The proposed method can be used: (1) to handle the problem of gold and silver mine tailings, (2) to remove heavy metals from lakes and ponds as a potential way of dealing with a serious environmental problem.

Acknowledgements This work was supported by an OTKA T42762 grant obtained by GB. The technical assistance of Erzsebet Preczner and Zsolt Szeman is gratefully acknowledged. The studies involving experimental animals (fish) were conducted in accordance with national and international guidelines. For toxicological experiments, only the necessary lowest number of animals was used.

References

- Alves LC, Wood CM (2006) The chronic effects of dietary lead in freshwater juvenile rainbow trout (*Oncorhynchus mykiss*) fed elevated calcium diets. *Aquat Toxicol* 78:217–232
- Anotai J, Tontisirin P, Churod P (1992) Integrated treatment scheme for rubber thread wastewater: sulfide precipitation and biological processes. *J Hazard Mater* 141:1–7
- Baldisserotto B, Kamunde C, Matsuo A, Wood CM (2004) A protective effect of dietary calcium against acute waterborne cadmium uptake in rainbow trout. *Aquat Toxicol* 67:57–73
- Baldisserotto B, Chowdhury MJ, Wood CM (2005) Effects of dietary calcium and cadmium on cadmium accumulation, calcium and cadmium uptake from the water, and their interactions in juvenile rainbow trout. *Aquat Toxicol* 72:99–117
- Banfalvi G (2000) Removing cyanide from waterways. *Chem Innovat* 30:53–54
- Banfalvi G (2006) Removal of insoluble heavy metal sulfides from water. *Chemosphere* 63:1231–1234
- Bayhan YK, Keskinler B, Cakici A, Levent M, Akay G (2001) Removal of divalent heavy metal mixtures from water by *Saccharomyces cerevisiae* using cross-flow micro-filtration. *Water Res* 35:2191–2200
- Blanchard G, Maunay M, Martin G (1984) Removal of heavy metals from waters by means of natural zeolites. *Water Res* 12:1501–1507
- Cabrera F, Clemente L, Diaz Barrientos E, Lopez R, Murillo JM (1999) Heavy metal pollution of soils affected by the guadamar toxic flood. *Sci Total Environ* 247:117–129
- Chowdhury MJ, McDonald DG, Wood CM (2004) Gastrointestinal uptake and fate of cadmium in rainbow trout acclimated to sublethal dietary cadmium. *Aquat Toxicol* 69:149–163
- Eccles H (1995) Removal of heavy metals from effluent streams—why select a biological process? *Int Biodeterior Biodegrad* 1:5–16
- Gacsi M, Czegeny I, Nagy G, Banfalvi G (2005) Survival of fish upon removal of cyanide from water. *Environ Res* 97:293–299
- Ge JP, Wang J, Zhang HX, Wang X, Peng Q, Li YD (2005) Orthogonal PbS nanowire arrays and networks and their Raman scattering behavior. *Chemistry* 11:1889–1894

- Gharaibeh SH, Abu-El-Shar WY, Al-Kofahi MM (1998) Removal of selected heavy metals from aqueous solutions using processed solid residue of olive mill products. *Water Res* 32:498–502
- Ghezlbash A, Korgel BA (2005) Nickel sulfide and copper sulfide nanocrystal synthesis and polymorphism. *Langmuir* 21:9451–9456
- Jang A, Seo Y, Bishop PL (2005) The removal of heavy metals in urban runoff by sorption on mulch. *Environ Pollut* 133:117–127
- Kapoor A, Viraghavan T (1998) Removal of heavy metals from aqueous solutions using immobilized fungal biomass in continuous mode. *Water Res* 32:1968–1977
- Kim BS, Lim ST (1999) Removal of heavy metal ions from water by cross-linked carboxymethyl corn starch. *Carbohydr Polym* 39:217–223
- Kim BR, Gaines WA, Szafranski J, Bernath EF, Miles AM (2002) Removal of heavy metals from automotive wastewater by sulfide precipitation. *J Environ Eng* 128:612–623
- Korngold E, Belfer S, Urtizberea C (1996) Removal of heavy metals from drinking water by a cation exchanger. *Desalination* 104:197–201
- Lacour S, Bollinger JC, Serpaud B, Chantron P, Arcos R (2001) Removal of heavy metals in industrial wastewaters by ion-exchanger grafted textiles. *Anal Chim Acta* 428:121–132
- Lee SH, Jung CH, Chung H, Lee MY, Yang JW (1998) Removal of heavy metals from aqueous solution by apple residues. *Process Biochem* 33:205–211
- Meunier N, Laroulandie J, Blais JF, Tyagi RD (2003) Cocoa shells for heavy metal removal from acidic solutions. *Bioresour Technol* 90:255–263
- Ng TYT, Klinck JS, Wood CM (2009) Does dietary Ca protect against toxicity of a low dietborne Cd exposure to the rainbow trout? *Aquat Toxicol* 91:75–86
- Niyogi S, Wood CM (2006) Interaction between dietary calcium supplementation and chronic waterborne zinc exposure in juvenile rainbow trout (*Oncorhynchus mykiss*). *Comp Biochem Physiol C* 143:93–102
- Piao H, Bishop PL (2006) Stabilization of mercury-containing wastes using sulfide. *Environ Pollut* 139:498–506
- Qdaisa HA, Moussab H (2004) Removal of heavy metals from wastewater by membrane processes: a comparative study. *Desalination* 164:105–110
- Sekhar KC, Kamala CT, Chary NS, Anjaneyulu Y (2003) Removal of heavy metals using a plant biomass with reference to environmental control. *Int J Miner Process* 68:37–45
- Simon M, Martin F, Ortiz I, Garcia I, Fernandez J, Fernandez E, Dorronsoro C, Aguilar JC (2001) Soil pollution by oxidation of tailings from toxic spill of a pyrite mine. *Sci Total Environ* 279:63–74
- Soldan P, Pavonim M, Boucek J, Kokes J (2001) Baia Mare accident: brief ecotoxicological report of Czech experts. *Ecotoxicol Environ Saf* 49:255–261
- Wolfenden S, Charnock JM, Hilton J, Livens FR, Vaughan DJ (2005) Sulfide species as a sink for mercury in lake sediments. *Environ Sci Technol* 39:6644–6648
- Yavuz O, Altunkaynak Y, Guzel F (2003) Research note removal of copper, nickel, cobalt and manganese from aqueous solution by kaolinite. *Water Res* 37:948–952
- Yu B, Zhang Y, Shukla A, Shukla SS, Dorri KL (2000) The removal of heavy metal from aqueous solutions by sawdust adsorption-removal of copper. *J Hazard Mater* B80:33–42
- Zohouri MA, Pyle GG, Wood CM (2001) Dietary Ca²⁺ inhibits waterborne Cd uptake in Cd-exposed rainbow trout *Oncorhynchus mykiss*. *Comp Biochem Physiol C* 130:347–356

Index

A

accumulation, 116, 130, 133, 134, 136
Aedes albopictus, 116, 118, 122–129, 134, 136–139
animal, 316–318, 326, 327
antioxidative defense, 38, 40
apoptosis, 116, 120, 129, 131, 140, 164, 169, 172, 181, 185, 189, 196, 200, 205, 207, 213, 292–294, 297, 298, 301, 302, 305
arsenate, 88, 94, 95
arsenic, 264, 271, 297, 300–302, 304, 305
arsenite, 88, 94–96
atomic absorption spectrometry, 339, 343

B

bioaccumulation, 32, 36
Biomarker, 316–318, 321–323, 325, 327, 328
bioremediation, 38
Blood lead level, 316, 322, 324, 325
bZIP transcription factor, 280, 285

C

Cadmium, 118, 122, 124, 128, 130, 133, 134, 136, 138–140, 264, 266, 270, 275, 278–283, 285, 286, 295, 300–302, 304, 305
Carbogen gas, 333, 334, 336, 338, 341, 342, 344
carcinogenesis, 238, 249–252
carcinogenicity, 221, 232, 233
cell cycle regulation, 297, 302, 303, 305
cell proliferation, 116, 119, 124, 125, 135, 138
Cellular effects, 4, 11
Chromate, 60, 61, 63, 64, 66, 68, 69, 71–73
Chromatin structure, 148, 153, 157, 165–171, 173, 177, 180–183, 185, 188–190, 197, 198, 202, 205, 207, 213, 215
Chromium, 59, 60, 62–64, 66–76, 78, 180, 181, 188, 189

chromosome condensation, 188
Compartmentalization, 34
compatibility of bioelements, 6
copper, 129, 138
cullin, 277, 283, 284

D

Definition of Heavy Metals, 6
deletome, 32, 42–44
Depleted uranium, 221, 222, 224–226, 229, 230, 232
detection of heavy metals, 20, 22
DNA, 238, 239, 241–252

E

Elutriation, 150, 154–160
environmental exposure, 315, 317
environmental metal exposure, 305

F

fission yeast, 181, 188, 190
fluorescence microscopy, 153, 167
free radicals, 245

G

gene expression, 221, 227, 232
genetic engineering, 33, 35, 42, 45
Glutathione, 33, 40, 43, 44

H

heavy metal spill, 334
heavy metal toxicity, 264
heavy metals, 264, 265, 270–273
Human, 315–318, 321, 322, 325–327

I

interactome, 32, 42–44

L

lead, 264, 270, 272
 long-term scanning, 172, 175, 177, 200

M

Macrophage, 225–227, 232
 Mercury, 116–118, 121, 122, 128, 130, 133, 138, 264, 270
 metal chelators, 36
 metal transporters, 35
 metalloid detoxification, 97, 98
 metalloid tolerance, 91, 92, 94, 96, 101
 Metals, 237, 238, 240–242, 244–246, 249–252
 methylmercury, 116, 133, 138, 295, 300, 301, 304, 305
 molecular chaperones, 265

N

necrosis, 164, 172, 189, 190, 196, 213
 neurodegenerative disease, 295–297, 305
 nickel, 163–165, 168–171, 176

O

Oxidative damage, 239, 240, 242–245, 249–251
 oxidative stress, 36, 37, 39, 40, 43, 44, 60, 61, 64, 68, 70, 77, 297, 300, 305
 oxygen radicals, 249, 250

P

permeable cells, 151
 protein aggregates, 271, 272
 protein conjugates, 293, 305
 protein folding, 265, 270–273
 protein-metal complexes, 265, 266, 270, 271
 Proteins, 238–242, 244, 249, 250, 252
 proteome, 32, 42, 43
 protoplast, 181–184

R

radicals, 239, 241, 249
 Reversible permeabilization, 165, 166, 197, 201, 205
 Risk assessment, 60, 71, 74

S

SCF-ligase, 277
 siderophores, 38
 solubility products, 336, 337, 341, 343, 344
 strand breaks, 148, 152, 161
 stress pathways, 298, 305
 sulfide oxidation, 334

T

Toxicity, 60, 61, 63, 65, 67, 69, 71–73, 76–78, 223, 225, 227
 transcriptome, 32, 42–44
 tungsten alloy, 221, 228, 230–232

U

ubiquitin ligase, 276–278, 280, 281, 283, 285, 286
 ubiquitin proteasomal system (UPS), 305
 Ubiquitination, 276, 277, 279–285
 Ultrastructure, 117, 128, 130, 132, 135, 139
 UPS inhibitor, 298, 305
 Uptake, 116, 122, 132–134, 138, 139

V

Viability, 118, 119, 122–125, 132, 135–137, 140

Y

Yeast, 88–93, 95–98, 101, 103, 104